



Engineering homing properties of cancer-specific T lymphocytes in adoptive cell therapy

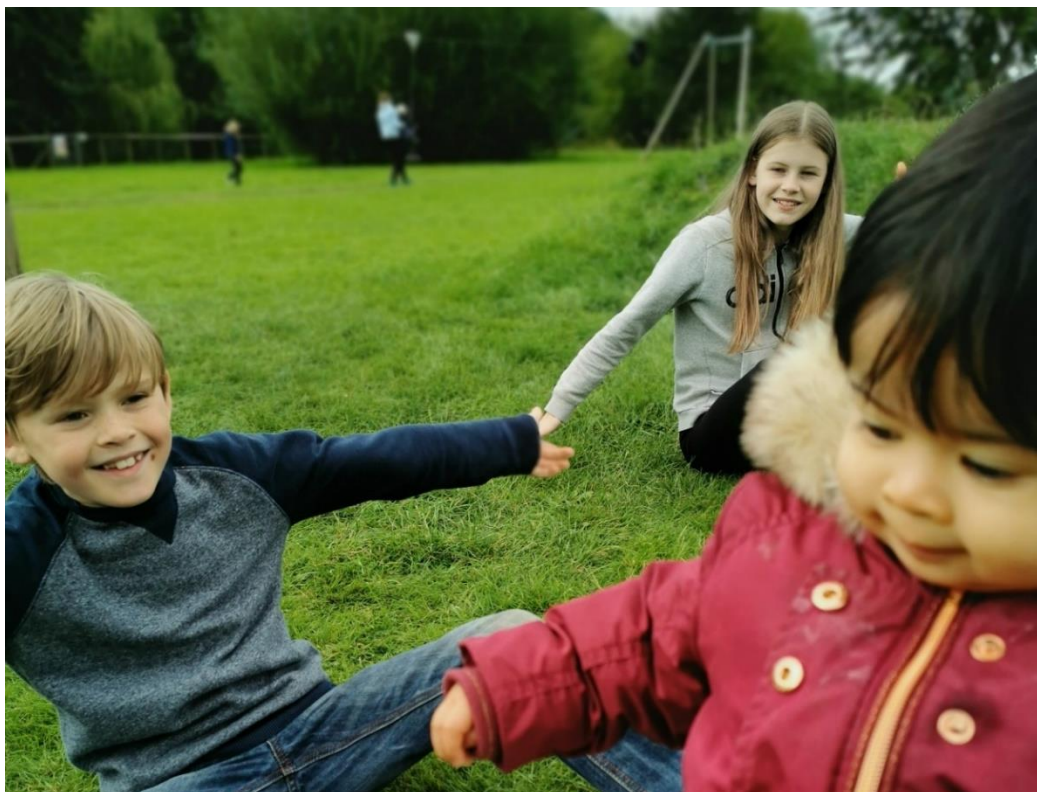
A thesis submitted to Cardiff University in candidature for the degree of Doctor of Philosophy.

Owen Rhys Moon

Institute of Infection and Immunity, School of Medicine
Cardiff University
October 2020

Acknowledgments

I dedicate this thesis to my wonderful nieces and nephew. I hope their futures are bright during this relatively bleak time in recent history.



Even though an individual may be the main driver behind a particular body of work, no one person is ever responsible for its success or completion. Therefore, I want to thank all those who have helped me both scientifically and personally throughout my PhD: my family, friends, colleagues and fantastic supervisors, Ann, David, and Vera.

Without their continued advice and support I could not have done this. Last but certainly no means least, I would like to thank my partner Katie who has listened to me talk about my thesis, and not much else, for the last few months, which must have been very dull indeed.

Lastly, to any PhD students currently reading this, I leave you with this quote from my favourite book:

“Ow! My brains!”

— Douglas Adams, *The Hitchhiker's Guide to the Galaxy*

COVID-19 impact on research and mitigation statement

The laboratories and animal facilities were closed to non-COVID-19 related research on 23rd of March 2020. The week prior to this I had conducted the imaging flow cytometry studies in 3.2.8 and 3.2.9 and the month before I had completed the preliminary *in vivo* study in 4.2.7 and mice were ready for further *in vivo* studies. We were advised by our animal facilities manager to place all colonies at minimal numbers including the L-selectin knockout colony used in this thesis. I kept enough of these mice to repeat a tricistronic vector transduction experiment as in 4.2.4 and conduct the studies described in 5.6.1. However, return to work was not granted, the mice had to be culled, and alternative experiments conducted.

My return to work status and laboratory access was approved on the 1st of August 2020 and I was granted a funded extension to my 3-year funded period for the month of October. Within my remaining 3 months, I generated the Molt3 cell line expressing L-selectin with a GFP tagged tail and conducted the studies in 3.2.6 to address hypotheses within this chapter. These cells were originally going to be used for live cell imaging alongside antigen presenting cells to address these same hypotheses as well as the further criticism that phorbol 12-myristate 13-acetate is not a physiological inducer of T cell activation and consequent L-selectin shedding. However, the appropriate microscope is located at the dementia research institute (Cardiff University) which has its own COVID-19 measures in place and currently training is difficult to co-ordinate.

During the suspension of non-COVID-19 related research activities I took the opportunities to compile my thesis for submission at the end of October 2020, contribute to a COVID-19 community journal club (from which manuscripts are being submitted for publication) and co-write a grant proposal for the Institutional Strategic Support Fund translational kick-starter award. This grant was awarded and as the co-lead applicant and named researcher the work proposed will be discussed as part of the future work in 5.6.2.

Abstract

Several cancer immunotherapies harness the ability of CD8 T cells to eradicate tumours. Adoptive cell transfer of cancer-specific T cells is an immunotherapy that has produced promising results for cancer patients. L-selectin is a membrane protein that enables T cell rolling on high endothelial cells and transendothelial migration into lymph nodes. During this process, and after T cell activation, the L-selectin ectodomain is proteolytically cleaved from the T cell surface by ADAM17. In pre-clinical melanoma models, adoptively transferred cancer-specific T cells, which expressed ectodomain shedding-resistant L-selectin, better controlled tumour growth than T cells bearing wildtype L-selectin. However, these adoptively transferred T cells were naïve and transgenic for a cancer-specific TCR and variants of L-selectin. This is a situation not reflected in the clinic. Here, I delivered a cancer-specific TCR, and variants of L-selectin, to T cells using a clinically relevant method. I further demonstrated that modified L-selectin variants affected CD8 T cell expression of CD25, Ki67, and PD-1 during cytotoxicity assays.

A lack of L-selectin ectodomain shedding has also been implicated in degranulation and killing by effector T cells, as well as naïve T cell activation-mediated upregulation of CD25 and consequent T cell proliferation. Recently, we demonstrated that ADAM17-dependent L-selectin ectodomain proteolysis generates a membrane-retained fragment (MRF) that undergoes γ -secretase proteolysis. The intracellular domain, or tail, of L-selectin interacts with several proteins, including PKC, grb-SOS, and Ick. Therefore, the L-selectin tail may perform signalling functions prior to, and following, γ -secretase proteolysis in T cells. I demonstrated that the MRF of L-selectin is lost from the cell membrane, either through degradation by the proteasome or further proteolysis by γ -secretase. Therefore, the altered phenotypes conferred by shedding-resistant L-selectin to cancer-specific T cells are likely due to retention of the tail of L-selectin at the cell surface and continued interaction with binding partners.

Abbreviations list

Elimination, equilibrium, and escape	3Es
Refinement, replacement, and reduction of animal use	3Rs
HIV gag (SLYNTVATL) reactive T cell receptor	868TCR
Abl kinase	Abl
A disintegrin and metalloprotease 17; tumour necrosis factor- α -converting enzyme	ADAM17
Adhesion and degranulation-promoting adapter protein	ADAP
APP intracellular domain released by γ -secretase proteolysis	AICD
A blocking ADAM17 antibody; D1(A12); Tape et al., 2011	anti-ADAM17
Antigen presenting cell	APC
Amyloid precursor protein	APP
Bafilomycin A1; autophagosome-lysosome fusion and ATPase inhibitor	BafA1
Bovine serum albumin	BSA
In-bred immune-competent strain of mice	C57BL/6
Calcium	Ca ²⁺
Chimeric antigen receptor	CAR
Casitas b lymphoma protein; an E3 ubiquitin ligase	Cbl
CC chemokine receptor	CCR
Cluster of differentiation	CD
α -chain of the IL-2 receptor	CD25
Complementarity determining region	CDR
Human carcinoembryonic antigen	CEA
Human carcinoembryonic antigen transgenic	CEAtg
Chemokine ligand	CCL
Chloroquine; autophagosome-lysosome fusion inhibitor	ChQ
CBF1, Su(h), LAG-1 family proteins	CSL
Cytotoxic T-lymphocyte-associated protein 4	CTLA-4
Diacylglycerol	DAG
Dendritic cell	DC

Lower affinity T cell receptor variant of DMF5	DMF4
Human melanoma reactive T cell receptor	DMF5
Dimethyl sulfoxide; used as a vehicle control	DMSO
ADAM17 active site inhibitor	DPC333
Ezrin, radixin and moesin	ERM
Fluorescence-activated cell sorting	FACS
Fas ligand	FasL
Four and a half lim domains 2	FHL2
Full-length	FL
Fluorescence minus one	FMO
Forkhead box protein O1	FOXO1
Fibroblastic reticular cell	FRC
Target cancer cells treated with Triton-x-100	Full lysis control
Green Fluorescent protein	GFP
Glycosylation-dependent cell adhesion molecule-1	GlyCAM-1
Human melanoma reactive T cell receptor	gp100(154)
Growth factor receptor-bound protein-son of sevenless	Grb2-SOS
Granzyme	gzm
Human embryonic kidney	HEK
High endothelial venule	HEV
Heterotrimeric $\alpha\beta\gamma$ complex	high affinity IL-2R
Hour	hr
Horseradish peroxidase	HRP
Incomplete Freund's adjuvant	IFA
interferon	IFN
Interleukin	IL
IL-2 receptor	IL-2R
IL-7 receptor	IL-7R
Immune checkpoint protein	Immune checkpoint
Inositol trisphosphate	IP ₃
Immunoreceptor tyrosine-based activation motif	ITAM

IL-2-inducible t-cell kinase	I κ B α
Human variant of L-selectin proposed to resist secondary proteolysis by γ -secretase	I Δ W L-selectin
Inhibitory binding partner of NF κ B	I κ B α
Janus kinase	JAK
Knock-out	KO
γ -secretase inhibitor	L-685
Lymphocyte activation gene-3	LAG-3
Linker of activation for t cells	LAT
Lymphocyte-specific protein tyrosine kinase	Lck
Lymph node	LN
Lymphotoxin α	LT α
Murine variant of L-selectin which resists ectodomain proteolysis	L Δ P L-selectin
Magnet-activated cell sorting	MACS
Major histocompatibility complex	MHC
Myeloid-derived suppressor cell	MDSC
Proteasomal inhibitor	MG132
Minute	min
A viral transfer vector based on Moloney murine leukaemia virus	MMLV
Membrane-retained fragment of L-selectin	MRF
MRT68921; prevents autophagy in cells by inhibiting ULK-1 and -2	MRT
Nuclear factor kappa-light-chain-enhancer of activated B cells	NF κ B
Notch intracellular domain released by γ -secretase proteolysis	NICD
Nitric oxide	NO
Non-obese diabetic, severe combined immune deficient, gamma-chain knockout	NSG
Non-signalling TGF β receptor	nsTGF β R
Ovalbumin peptide	OVA

Pepstatin and leupeptin; broad protease inhibitors	P&L
Phosphate buffered saline	PBS
PBS-TWEEN20	PBS-T
Polymerase chain reaction	PCR
Programmed cell death protein-1	PD-1
Phosphoinositide-dependent kinase-1	PK-1
Plasmacytoid dendritic cell	pDC
Programmed cell death protein -1 ligand	PDL
Phosphoinositide 3-kinase	PI3K
Phosphoinositide (3,4,5) trisphosphate	PIP ₃
Protein kinase C	PKC
Phospholipase	PLC
Phorbol 12-myristate 13-acetate	PMA
Peptide MHC	pMHC
pMHC class I	pMHCI
A viral transfer vector based on myeloproliferative sarcoma virus	pMP71
A viral transfer vector based on murine stem cell virus	pMSCV
Peripheral lymph node addressin	PNAd
M6P-rich mannan core	PPME
P-selectin ligand	PSGL-1/CD162
Phosphatase and tensin homolog	PTEN
Recombinant activating gene	RAG
Reactive oxygen species	ROS
Single chain variable fragment	scFv
Sialyl-lewis X	sLe ^x
SH2-domain-containing leukocyte protein of 76 kDa	Slp76
Tumour-associated macrophage	TAM
T central memory	T _{CM}
T cell receptor	TCR
Tumour draining inguinal lymph node	tdLN

T effector memory	T _{EM}
Transforming growth factor- α	TGF- α
T helper cell	T _H
T cell immunoreceptor with IG and ITIM domain	TIGIT
Tumour infiltrating lymphocyte	TIL
T-cell immunoglobulin and mucin domain-3	TIM-3
Tailless CD19 marker	tICD19
Tumour microenvironment	TME
Naïve CD8 T cell	T _N
Tumour necrosis factor- α	TNF- α
T regulatory cell	T _{REG}
T resident memory cell	T _{RM}
Tyrosinase-related protein	TRP
A T cell receptor which recognises the tyrosinase-related protein 2 (VYDFFVWL)	TRP2
Signal transducing protein	Vav
Vascular endothelial growth factor	VEGF
α 4 β 1 integrin	VLA-4
Wildtype	WT
ζ chain-associated protein kinase	ZAP-70
Various CD3 dimers	$\gamma\epsilon$, $\zeta\zeta$, $\delta\epsilon$
Δ M-N; human variant of L-selectin which resists ectodomain proteolysis	Δ MN L-selectin

Contents

Acknowledgments.....	ii
COVID-19 impact on research and mitigation statement.....	iii
Abstract.....	iv
Abbreviations.....	v
Content.....	x
Figures.....	xiv
Tables.....	xix
1.0.0. Chapter 1: Introduction.....	1
1.1.0. The cancer immunity cycle and tumour elimination, equilibrium, and escape.....	1
1.2.0. Transendothelial Migration and tumour HEV neogenesis.....	4
1.2.1. Naïve T cell trafficking to peripheral lymph nodes.....	4
1.2.2. HEV neogenesis in tumours and CD8 T cell infiltration.....	7
1.3.0. CD8 T cell activation and function.....	10
1.3.1. Naïve T cell trafficking to peripheral lymph nodes.....	10
1.3.2. CD8 T cell migration to sites of infection.....	11
1.3.3. CD8 T cell cytotoxic function.....	13
1.3.4. Clonal contraction and T cell memory formation.....	16
1.4.0. L-selectin.....	17
1.4.1. Function in CD8 T cells.....	17
1.4.2. Structure and relation to function.....	18
1.4.3. L-selectin expression and regulation.....	22
1.5.0. The tumour microenvironment and immunosuppression.....	27
1.5.1. Tumour vasculature.....	28
1.5.2. Dendritic cells.....	30
1.5.3. Tumour-associated macrophage.....	32
1.5.4. Myeloid-derived suppressor cells.....	32
1.5.5. T regulatory cells.....	34
1.6.0. T cell signalling and dysfunction in the tumour microenvironment.....	38
1.6.1. Functional T cell signalling.....	38
1.6.2. Dysfunctional T cell signalling.....	42
1.7.0. Cancer Immunotherapy.....	49
1.7.1. Cell-based immunotherapy.....	49

1.7.2.	Strategies to improve cell-based immunotherapies for solid tumours.....	57
1.7.3.	Harnessing or manipulating L-selectin for cell-based immunotherapies.....	58
1.8.0.	Hypotheses and aims.....	62
2.0.0.	Chapter 2: Materials and methods.....	65
2.1.0.	Molecular biology.....	65
2.1.1.	Polymerase chain reaction (PCR).....	65
2.1.2.	Restriction enzyme digestion.....	67
2.1.3.	Gel electrophoresis.....	67
2.1.4.	Ligation.....	67
2.1.5.	<i>E. coli</i> transformation and mini-prep.....	68
2.1.6.	Maxi-prep.....	69
2.1.7.	Western Blotting.....	69
2.2.0.	Tissue culture.....	72
2.2.1.	Adherent cells.....	73
2.2.2.	Suspension cells.....	74
2.2.3.	Cell treatments and activation.....	74
2.2.4.	Cryopreservation.....	75
2.3.0.	T cell transductions.....	76
2.3.1.	Lentivirus production for Molt3 T cell transductions.....	76
2.3.2.	Retrovirus production for primary murine CD8 T cell transductions.....	77
2.3.3.	Transduction.....	78
2.4.0.	Flow cytometry.....	79
2.4.1.	Extracellular staining.....	80
2.4.2.	Intracellular staining for conventional flow cytometry.....	81
2.4.3.	Intracellular staining for imaging flow cytometry.....	81
2.4.4.	Compensation and controls.....	84
2.5.0.	Cell sorting.....	84
2.5.1.	FACS.....	84
2.5.2.	MACS.....	84
2.6.0.	Cancer-specific T cell-mediated killing.....	85
2.6.1.	xCELLigence <i>ex vivo</i>	85
2.6.2.	B16.F10 subcutaneous tumour model <i>in vivo</i>	86
2.7.0.	Software.....	88
2.8.0.	Equipment.....	88
2.9.0.	Statistical analysis.....	88
3.0.0.	Chapter 3: Determining the fate of L-selectin's cytoplasmic tail following ADAM-17 dependent shedding.....	89
3.1.1.	Introduction.....	89
3.1.2.	Chapter aims.....	91
3.2.0.	Results.....	93

3.2.1.	Molt3 T cells can be transduced to express WT, Δ MN and Δ W L-selectin and the proteolysis of L-selectin induced by PMA.....	93
3.2.2.	Proteolysis of the ectodomain and cytoplasmic tail of L-selectin are inhibited by an anti-ADAM17 antibody and L-685, respectively.....	95
3.2.3.	L-selectin's ectodomain and cytoplasmic tail proteolysis can be limited by genetically modified Δ MN and Δ W L-selectin, respectively.....	99
3.2.4.	Defining parameters to assess the distribution of the tail of L-selectin using imaging flow cytometry.....	103
3.2.5.	The L-selectin tail is lost from the membrane following PMA-induced sequential proteolysis and does not co-localise with lysosomes or the nucleus.....	111
3.2.6.	Molt3 T cells expressing WT L-selectin with a cytosolic GFP tag lose GFP signal following PMA-induced L-selectin proteolysis.....	120
3.2.7.	Proteasomal inhibition of WT Molt3 T cells stabilises L-selectin's MRF following PMA-induced sequential proteolysis.....	125
3.2.8.	Proteasome Inhibition-induced accumulation of the MRF following PMA-induced sequential proteolysis of L-selectin could not be detected by imaging flow cytometry.....	127
3.2.9.	Of the L-selectin variants, only Δ MN L-selectin expressing Molt3 T cells retain the L-selectin tail at the membrane following PMA stimulation.....	132
3.3.0.	Discussion.....	137
4.0.0.	Chapter 4: Generation and use of cancer-specific murine CD8 T cells for adoptive immunotherapy of melanoma.....	143
4.1.1.	Introduction.....	143
4.1.2.	Chapter aims.....	147
4.2.0.	Results.....	149
4.2.1.	Isolated murine CD8 T cells can be activated <i>ex vivo</i> and transduced to express GFP.....	149
4.2.2.	Retroviruses using their 5' LTR promotor drive expression of a transgenic cancer-specific TCR.....	153
4.2.3.	Retroviruses using their 5' LTR promotor drive expression of transgenic human and murine L-selectin variants.....	157
4.2.4.	Retrovirus using the 5' LTR promotor drives co-expression of a transgenic cancer-specific TCR and human and murine L-selectin variants.....	163
4.2.5.	Retrovirally delivered L-selectin undergoes sequential proteolysis in transduced murine CD8 T cells.....	173
4.2.6.	TRP2-expressing T cells kill target cancer cells <i>in vitro</i>	177

4.2.7.	Murine CD8 T cells transduced to express TRP2 do not control tumour growth <i>in vivo</i>	197
4.3.0.	Discussion.....	201
5.0.0.	Chapter 5: General discussion.....	210
5.1.0.	Determining the sub-cellular distribution of the tail of L-selectin following γ -secretase proteolysis.....	210
5.2.0.	Fate of the cytoplasmic tail of L-selectin for human variants.....	213
5.3.0.	Impact of L-selectin variants on cancer-specific T cells <i>in vitro</i>	215
5.4.0.	<i>In vivo</i> evaluation of L-selectin variants in T cells.....	218
5.5.0.	Conclusion.....	220
5.6.0.	Future work.....	221
5.6.1.	Experiments not conducted due to the COVID-19 laboratory shut-down.....	221
5.6.2.	Proposed experiments to develop both the conducted experiments, and the studies not conducted due to the laboratory shutdown.....	223
	Reference list.....	226
	Appendix I: Supplementary figures.....	247
	Appendix II: Vector sequences.....	250

Figures

Figure 1.1. The cancer immunity cycle.....	2
Figure 1.2. Naïve T cells undergo transendothelial migration at high endothelial venules.....	7
Figure 1.3. Following transendothelial migration at high endothelial venules, naïve T cells are activated in peripheral lymph nodes.....	11
Figure 1.4. CD8 cytotoxic T cells mediate target cell apoptosis through several mechanisms.....	14
Figure 1.5. L-selectin structure and function.....	18
Figure 1.6. The potential signalling capacity of the tail of L-selectin.....	22
Figure 1.7. L-selectin undergoes sequential proteolysis following T cell activation.....	25
Figure 1.8. Direct and Indirect immunosuppressive functions of dendritic cells within the tumour microenvironment.....	31
Figure 1.9. Immunosuppressive functions of tumour associated macrophage.....	32
Figure 1.10. Immunosuppressive functions of myeloid-derived suppressor cells..	33
Figure 1.11. Immunosuppressive functions of T _{REGS}	36
Figure 1.12. Summary of CD8 T cell immunosuppression within the tumour microenvironment.....	37
Figure 1.13. CD8 T cells are activated through several signalling pathways.....	40
Figure 1.14. CD8 T cell signalling is abrogated by immune checkpoint ligation....	43
Figure 1.15. Overview of TCR/CAR T delivery.....	50
Figure 1.16. The chimeric antigen receptor has developed across several generations.....	52
Figure 2.1. ImageJ was used to quantify western blots.....	71
Figure 2.2. Suspension cell treatments.....	75
Figure 2.3. Overview of lenti- and retro- viral transduction protocols.....	76
Figure 2.4. Imaging flow cytometry can be used to derive whole cell and sub-cellular information.....	82
Figure 2.5. Representative images of different similarity scores for a nuclear stain (7-AAD) and a translocating protein (NFkB) in the IDEAS software	

package.....	83
Figure 2.6. RTCA Pro was used to process xCELLigence data.....	86
Figure 2.7. Overview of <i>in vivo</i> subcutaneous B16.F10 tumour model for adoptive transfer of cancer specific T cells.....	87
Figure 3.1. L-selectin undergoes sequential proteolysis following T cell activation.....	89
Figure 3.2. Molt3 T cells expressing the HIV-specific 868TCR can be transduced and enriched to express L-selectin variants which undergo ectodomain shedding following PMA treatment.....	94
Figure 3.3. L-selectin undergoes sequential proteolysis of its ecto- and intracellular domains following PMA treatment which can be abrogated by anti-ADAM17 and L-685 respectively.....	96
Figure 3.4. PMA induced L-selectin sequential proteolysis of its ecto- and intracellular domains is limited by genetic variants of L-selectin, Δ MN and I Δ W respectively.....	100
Figure 3.5. The cytoplasmic tail of L-selectin can be detected by imaging flow cytometry.....	104
Figure 3.6. Membrane associated fluorescence was used to define the membrane and intracellular masks of cells for imaging flow cytometry analysis..	107
Figure 3.7. Membrane and intracellular masks can be used to quantitate fluorophores.....	108
Figure 3.8. Intracellular spots can be counted by excluding membrane associated fluorescence.....	110
Figure 3.9. PMA induced sequential proteolysis of L-selectin's tail does not cause significant changes to L-selectin's tail median fluorescence intensity values across the whole cell.....	112
Figure 3.10. The median fluorescence intensity values across the whole cell for CD107a, CD69 or the tail of L-selectin did not change at any time points assayed.....	114
Figure 3.11. Following 15-minutes of incubation with PMA, the membrane similarity score between the membrane marker (CD69) and the L-selectin tail decreased.....	116

Figure 3.12. The similarity score between the tail of L-selectin, the lysosomal marker (CD107a) and the nucleus did not change at any time point following PMA treatment.....	117
Figure. 3.13. The number of spots per cell did not change at any timepoints following PMA treatment.....	118
Figure 3.14. PMA induces a decrease in L-selectin’s tail fluorescence intensity within the membrane mask.....	119
Figure 3.15. PMA induced a loss of L-selectin’s GFP-tagged tail fluorescence intensity.....	122
Figure 3.16. PMA induced a decrease in similarity between L-selectin’s GFP-tagged tail and the membrane marker.....	124
Figure 3.17. The proteasomal inhibitor MG132 stabilises the L-selectin MRF.....	126
Figure 3.18. The MG132 stabilised L-selectin MRF cannot be detected by imaging flow cytometry.....	129
Figure 3.19. The loss of similarity between the L-selectin tail and the membrane marker following PMA treatment is not affected by MG132.....	131
Figure 3.20. Δ MN but not Δ W L-selectin prevents the loss of L-selectin tail associated fluorescence intensity following PMA treatment.....	134
Figure 3.21. Δ MN but not Δ W L-selectin prevents the loss of similarity between the L-selectin tail and the membrane marker following PMA treatment.....	136
Figure 4.1. Solid tumour model used by Watson et al to demonstrate the benefits of Δ P in T cell mediated control of tumour growth.....	144
Figure 4.2. Solid tumour model used by Watson et al adapted to test the benefits of virally delivered CAR/TCR alongside L-selectin variants to mediate control of tumour growth.....	146
Figure 4.3. Isolation and activation of murine CD8 T cells.....	150
Figure 4.4. <i>In vitro</i> activated murine CD8 T cells were virally transduced to express GFP.....	152
Figure 4.5. <i>In vitro</i> activated murine CD8 T cells were retrovirally transduced to express human CEA-specific CAR.....	154
Figure 4.6. <i>In vitro</i> activated murine CD8 T cells were retrovirally transduced to express the melanoma-specific TRP2 TCR and enriched via MACS.....	156

Figure 4.7. Construction of MMLV retroviral vectors encoding human L-selectin variants.....	158
Figure 4.8. <i>In vitro</i> activated murine CD8 T cells were retrovirally transduced to express human L-selectin variants.....	159
Figure 4.9. Construction of pMSGV1 retroviral vectors encoding murine L-selectin variants.....	161
Figure 4.10. <i>In vitro</i> activated murine CD8 T cells were retrovirally transduced to express murine L-selectin variants.....	162
Figure 4.11. Quadcistronic constructs to deliver expression of TRP2, tICD19 marker and a L-selectin variant.....	163
Figure 4.12. Quadcistronic constructs deliver expression of TRP2 and murine L-selectin.....	164
Figure. 4.13. Quadcistronic constructs deliver expression of TRP2 and human L-selectin.....	166
Figure 4.14. Quadcistronic constructs deliver expression of tICD19 but not at the cell surface.....	168
Figure 4.15. Tricistronic constructs to deliver expression of TRP2 and a L-selectin variant.....	169
Figure 4.16. Tricistronic constructs deliver expression of TRP2 and murine L-selectin variants.....	170
Figure 4.17. Tricistronic constructs deliver expression on TRP2 and human L-selectin variants.....	172
Figure 4.18. Proteolysis of transgenic murine L-selectin was induced by PMA treatment in murine CD8 T cells.....	174
Figure 4.19. Sequential proteolysis of transgenic human L-selectin was induced by PMA treatment in murine CD8 T cells.....	176
Figure 4.20. TRP2 expressing murine T cells killed target tumour cells <i>in vitro</i>	179
Figure 4.21. Murine L-selectin expression has no effect on transient downregulation of TCR.....	181
Figure 4.22. Human L-selectin expression has no effect on transient tumour antigen induced downregulation of TCR.....	182
Figure 4.23. TRP2 and murine L-selectin variant expressing transduced T cells	

upregulate PD-1 during <i>in vitro</i> killing.....	185
Figure 4.24. TRP2 and human L-selectin variant expressing transduced T cells upregulate PD-1 during <i>in vitro</i> killing.....	186
Figure 4.25. Murine L-selectin levels continually rise whilst killing target cells.....	189
Figure 4.26. Human L-selectin levels continually rise whilst killing target cells.....	190
Figure 4.27. TRP2 mLΔP expressing transduced T cells have aberrant expression of CD25 prior to <i>in vitro</i> killing.....	193
Figure 4.28. Human IΔW L-selectin causes aberrant Ki67 expression whilst killing target cells.....	195
Figure 4.29. The number of live Vβ3+ T cells increases throughout <i>in vitro</i> cell culture from 8 to 12 days after the transduction protocol began.....	197
Figure 4.30. TRP2 expressing T cells are not able to control B16.F10 tumour growth in recipient tumour bearing mice.....	199
Figure 4.31. TRP2 expressing T cells are not elevated in recipient tumour bearing mice.....	201
Figure 5.1. The proposed pathways involved in proteolysis or degradation of WT L-selectin.....	211
Figure 5.2. The proposed pathways involved in proteolysis or degradation of WT and IΔW L-selectin following T cell treatment with PMA.....	215
Figure 5.3. L-selectin mRNA (<i>SELL</i>) expression correlates with patient survival in ovarian cancer.....	226

Tables

Table 1.1. T _{REGS} and their immunosuppressive functions.....	35
Table 1.2. Cytokines and their functions.....	47
Table 2.1. Primers used to generate transgene inserts.....	65
Table 2.2. PCR reaction mixes.....	66
Table 2.3. PCR conditions.....	66
Table 2.4. Primers used for sequence confirmation.....	69
Table 2.5. Composition of cell culture media used in this work.....	73
Table 2.6. Combination of retroviral vectors and packaging cell lines used in this work.....	78
Table 2.7. Antibodies and cell stains used for conventional- and imaging- flow cytometry.....	79
Table 4.1. The nomenclature of eGFP constructs used in this work.....	151
Table 5.1. The effects of L-selectin variant co-expression on cancer-specific T cells.....	216
Table 5.2. Proposed adoptive cell therapy treatment groups for B16.F10 melanoma-bearing mice.....	222
Table 5.3. Proposed adoptive cell therapy treatment groups for B16.F10 melanoma-bearing mice to evaluate L-selectin variants.....	223
Table 5.4. Proposed adoptive cell therapy treatment groups for NALM-6 engrafted NSG mice.....	225

1.0.0. Introduction

1.1.0. The cancer immunity cycle and tumour elimination, equilibrium, and escape

This thesis focuses on the modification of T cells to confer cancer specificity, which will enable them to recognise and destroy cancer cells. Upon the transfer of modified T cells to tumour-bearing hosts, these T cells should then be able to control tumour growth. This approach to cancer therapy is an 'adoptive cell transfer' immunotherapy and represents a strategy to restart the cancer immunity cycle outlined by Chen and Mellman (Chen and Mellman 2013). The cancer immunity cycle consists of 7 steps (Fig. 1.1) describing how tumour growth is controlled by T cells, namely: (1) release of cancer cell antigens (neoantigens); (2) neoantigen presentation; (3) priming and activation; (4) trafficking of T cells to tumours; (5) infiltration of T cells into tumours; (6) recognition of cancer cells by T cells; and (7) killing of cancerous cells (Chen and Mellman 2013). Each revolution of this cycle begets more T cell-mediated killing of cancerous cells and eventually leads to the eradication of the tumour (Chen and Mellman 2013). Adoptive cell transfer introduces a large amount of cancer-specific T cells, which have been activated *ex vivo* before administration (step 3) and then enter the cycle at step 4.

Several observations suggest that T cells play an important role in controlling cancer. In patients with ovarian carcinoma, the percentage of patients with progression-free and overall survival was greatly increased if their tumours contained CD4 and CD8 T cell infiltrates (Zhang et al., 2003). Similarly, T cell infiltration of colorectal tumours or the presence of T cells at the invasive edge improved disease free-survival significantly (Galon et al. 2006). Further, patients who did not have cancer recurrence had an increased immune cell number per tumour area analysed, which included CD8 T cells and granzyme B-positive cells (this is a marker of CD8 T cell effector function, covered in 1.3.3; Galon et al., 2006). Finally, in both oestrogen receptor-negative and -positive breast cancer, CD8 T cell infiltration of the tumour reduced the hazard of mortality by 21 % and 27 %, respectively (Ali et al. 2014). However, cancerous cells and immunosuppressive infiltrates within the tumour mediate the arrest of the cancer immunity cycle through several mechanisms

(covered in 1.5 and 1.6.2). Therefore, the goal of cancer immunotherapy is to restart this process without promoting autoimmunity (Chen and Mellman 2013).

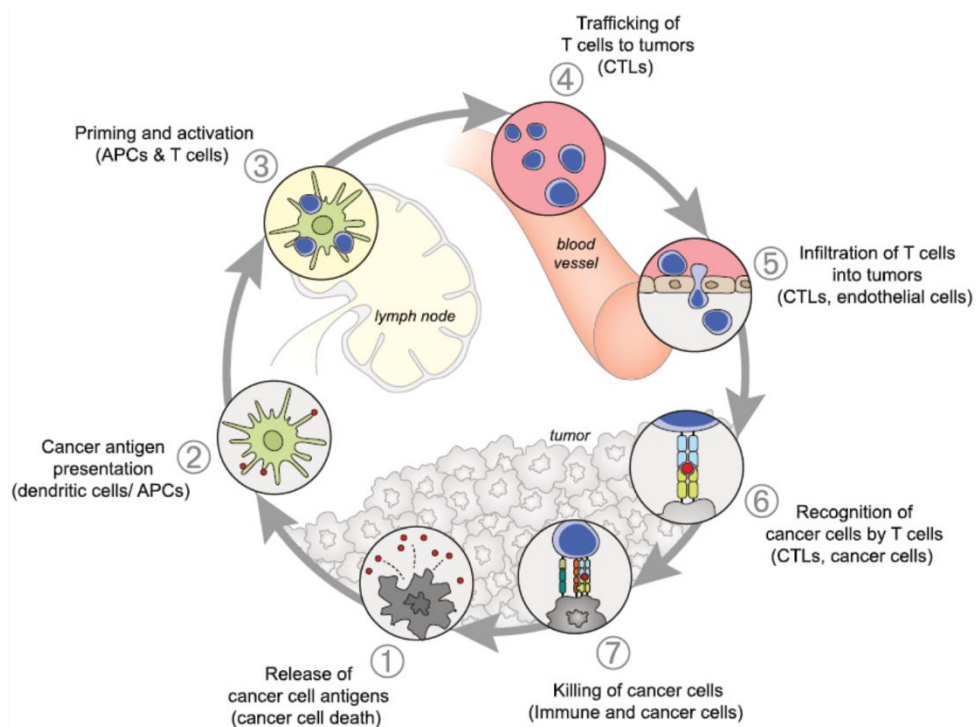


Figure 1.1. The cancer immunity cycle. The immune response to cancer proposed by Chen and Mellman. **(1)** Tumour associated antigens are released by cancer cells which are captured by peripheral dendritic cells. **(2)** The dendritic cells must process and cross-present neopeptides in a stimulatory context (TNF, IL-1, CD40/CD40L) rather than tolerogenic context (IL-4, IL-10, IL-13) either at the tumour or tumour draining lymph node. **(3)** cancer-specific T cells must recognise their cognate peptide MHC complex and be activated with proper co-stimulation (CD28, IL-2, IL-12) rather than inhibitory signals (PDL-1/PD-1, CTLA-4/CD28). **(4)** T cells must traffic to the tumour if activated in tumour draining lymph nodes by binding cancer associated chemokines (CCR2/CCL2; Craddock et al., 2010). **(5)** T cells must then effectively infiltrate the tumour (aided by HEV formation and hindered by the effects of VEGF). **(6)** T cells must then recognise the presented neopeptide on cancerous cells which can decrease expression of MHC1 (McGranahan et al., 2016). **(7)** Following TCR engagement, the T cells mediate cancer cell cytolysis which can be aided by upregulation of proteins within their lytic compartment and hindered by several mechanisms (immune checkpoints engagement and inhibitory soluble factors like TGF β and/or low concentrations of arginine). Figure modified from Chen and Mellman., 2013.

The mechanism by which the cancer immunity cycle is arrested and tumour growth is enabled has been proposed to develop in three stages alongside the immune response, namely: elimination, equilibrium and escape (3Es; Mittal et al., 2014). Elimination comprises complete revolutions of the cancer immunity cycle to eradicate neoplastic cells due to their inherent immunogenicity and recognition as non-self by T cells (Mittal et al. 2014). During equilibria, immunoediting occurs whereby T cell elimination of cancerous cells controls tumour growth but also acts as

a selective pressure, and neoplastic cells with the capability to evade immune detection survive (Mittal et al. 2014). The developing tumour may also recruit immunosuppressive components of the immune system to mediate arrest of the cancer cell cycle (Chen and Mellman 2013). Finally, through reduced cancer cell immunogenicity, resistance to cytolysis, and recruited or expressed immunosuppressive factors, tumours escape control by the immune system and their growth accelerates (Mittal et al. 2014).

Multiregional sequence analysis of early human non-small cell lung cancer biopsies for neoantigen load, combined with analysis of public databases for subclonal distribution of neoantigens throughout cancer progression, has provided support for the existence of tumour immunoediting in humans (McGranahan et al. 2016). This analysis found that if neoantigen burden was shared by the whole cancer, overall median survival was improved relative to samples where neoantigen burden was restricted to a subpopulation of cells, presumably due to immune escape in the absence of neoantigen expression (McGranahan et al. 2016). In support of this, two murine sarcoma cell populations (from methyl cholanthrene-induced tumours in T and B cell-deficient mice) were isolated and administered to immunocompetent mice and each had drastically different growth rates (Noguchi et al. 2017). One sarcoma was immunogenic due to widespread expression of a particular neoantigen, and the other had limited expression of that neoantigen (Noguchi et al. 2017). Phenocopying the human situation demonstrated by McGranahan, the murine tumours with widespread neoantigen showed spontaneous clearance while low neoantigen burdened tumours remained.

When further investigating the effect of neoantigen load on immune cell infiltrates, human lung tumours with shared neoantigen burden across the whole tumour had elevated levels of *CD8* and genes associated with T cell migration and effector function relative to those with subclonal neoantigen burden (McGranahan et al. 2016). However, immune checkpoint proteins (immune checkpoints; PD-1, LAG-3) and their ligands (PD-L1, PD-L2; molecules whose interactions limit CD8 T cell effector functions) were also elevated, indicating that these tumours could achieve

'escape' through a different mechanism (McGranahan et al. 2016). Again, this was mirrored in the murine model used by Noguchi et al, and murine tumours with widespread neoantigen expression had elevated levels of PD-L1 on cancer cells and tumour-associated macrophages, despite immune clearance of the tumour (Noguchi et al. 2017). However, if the tumour was modified to express even higher levels of PD-L1, clearance was prevented, demonstrating that tumour cell expression of PD-L1 can attenuate tumour rejection. In contrast, lower levels of PD-L1 were found on tumours without widespread neoantigen expression, which did not regress spontaneously (Noguchi et al. 2017). However, tumours with a low neoantigen burden did regress under PD-1 or PD-L1 immune checkpoint blockade or CRISPR knock-out (KO) of PD-L1, indicating that other immune responses could compensate for specific neoantigen loss (Noguchi et al. 2017). Importantly, in T and B cell-deficient mice, the tumour progressed despite being PD-L1-null, indicating a dependency on T cells and other, perhaps less immunogenic, neoepitopes in mediating control of tumour growth. In human lung squamous cell carcinoma samples, an alternate mechanism by which evasion of immune detection could be achieved was indicated by the observation that MHCI was expressed at low levels, impairing neoantigen presentation regardless of load or subclonal distribution (McGranahan et al. 2016).

Together, these frameworks for understanding the involvement of the immune system in tumour development, and the studies which support them, contextualise the current research into cancer immunotherapy, which seeks to kick-start the cancer immunity cycle.

1.2.0. Transendothelial Migration and tumour HEV neogenesis

1.2.1. Naïve T cell trafficking to peripheral lymph nodes

T cells recognise peptide antigens through their T cell receptor (TCR) when presented in the context of the major histocompatibility complex (MHC) on the surface of antigen presenting cells (APCs). Through positive and negative selection within the thymus, T cells bearing TCRs which tolerate peptide antigens derived from self-proteins but recognise those derived from neoplastic cells or pathogens (foreign)

are produced. These are naïve, or antigen in-experienced, and circulate throughout the body. The α/β TCR complex is made up of a heterodimer, in which variable regions define specificity for a particular peptide MHC (pMHC), and other CD3 dimers, which provide signalling moieties necessary for TCR complex signalling. The variable regions on the α and β chains are termed the complementarity determining regions (CDR) 1, 2, and 3. The variability of the CDR regions is generated by somatic V(D)J recombination of gene segments by the recombinant activating gene (RAG)-1 and RAG-2 enzymes (Jung and Alt 2004; Clambey et al. 2014). α/β T cells can be further classified according to their expression of the CD4 or CD8 co-receptor. The latter carry out direct cytotoxic function against cells presenting foreign peptides. To carry out this function, CD8 T cells must first be 'activated' by APCs. These cells must present the foreign peptide upon the CD8 T cell restricted MHC class I (pMHCI) alongside co-stimulatory ligands CD80 and CD86 within a cytokine milieu conducive to T cell activation. Importantly for this thesis, these cytotoxic cells are the primary mediators of tumour rejection (Waldman et al., 2020).

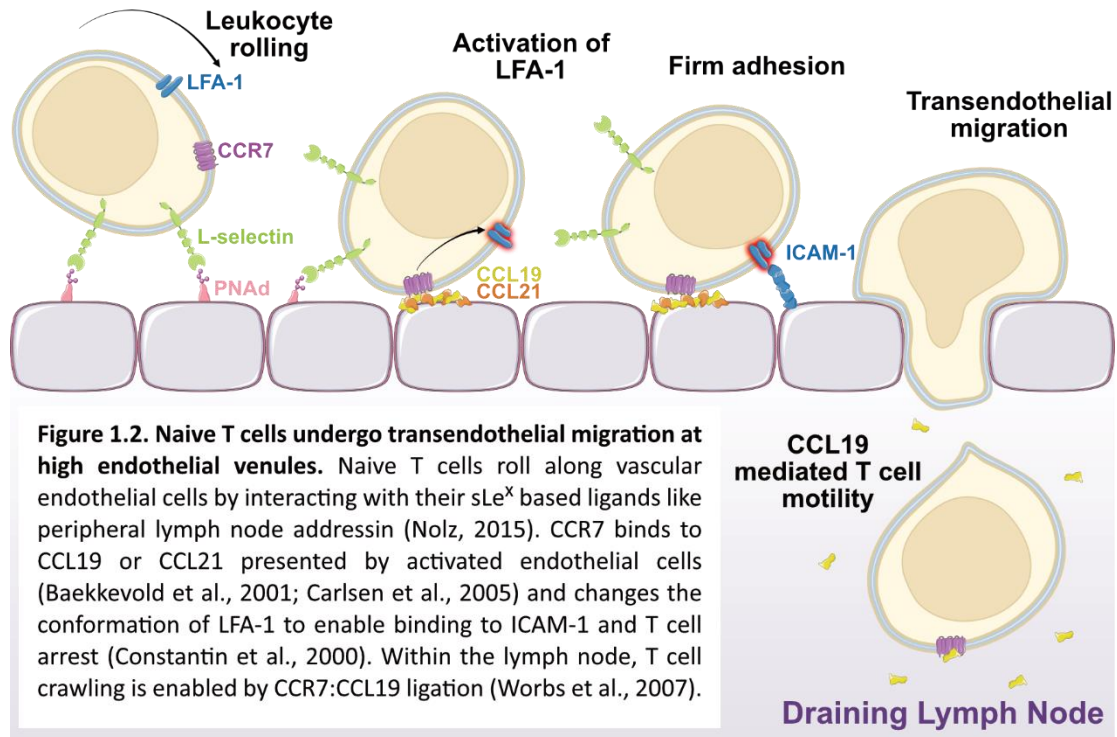
Naïve CD8 T cells (T_N) are characterised by their expression of L-selectin and CC chemokine receptor (CCR) 7, which allow T cells to roll along vascular endothelium and undergo transendothelial migration at high endothelial venules (HEVs) within lymph nodes (Fig. 1.2 ;Nolz, 2015). Here, they scan APCs for pMHCI which are cognate for their TCR before re-entry into the bloodstream via the efferent lymphatics (Nolz 2015). This repeating process is known as immunosurveillance. The importance of CCR7 was demonstrated using adoptive transfer of CCR7^{-/-} T cells into wildtype mice, where these T cells failed to accumulate in lymph nodes and remained in the peripheral blood (Förster et al., 1999). Similarly, competitive homing studies using T cells either sufficient or deficient in L-selectin surface expression showed that deficient T cells had impaired entry into lymph nodes and were enriched in the spleen (Arbonés et al. 1994).

The process of transendothelial migration begins with L-selectin interacting with its ligands, several of which are described under the term peripheral lymph node addressin (PNAd). Indeed, blockade of PNAd prevented lymphocyte homing to

peripheral lymph nodes similarly to L-selectin null T cells (Streeter et al. 1988; Nolz 2015). CCR7 then binds to both CC chemokine ligand (CCL) 19 and CCL21 presented by the endothelial cells of HEVs (Fig. 1.2; Nolz, 2015). Interestingly, *in situ* hybridisation and fluorescent antibody staining has revealed these chemokines are not expressed by the endothelial cells of human HEVs within secondary lymphoid organs, rather they are translocated from the lymph node paracortex to the luminal surface for presentation (Baekkevold et al. 2001; Carlsen et al. 2005). This interaction of chemokines with CCR7 enables a change in the conformation of the integrin LFA-1 (CD11a/CD18) to a higher affinity state, which caused lymphocytes to arrest on ICAM-1-coated surfaces during *in vitro* static adhesion and rolling assays (Fig. 1.2; Constantin et al., 2000).

Following this, T cells undergo transendothelial migration, and analysis of rat tissues revealed that L-selectin is lost from the T cell surface by proteolysis during this process and is recovered by the time T cells egress from the lymph node under steady-state conditions (Klinger et al. 2009; Rzeniewicz et al. 2015). In support of L-selectin proteolysis being important in transendothelial migration, *in vitro* adhesion assays to high endothelial cells revealed that unbound T cells retained high levels of L-selectin (79 % positive), whereas bound T cells had reduced levels (54 % positive) and transmigrated T cells had even further reduced levels of L-selectin (18 % positive; Klinger et al., 2009). Further, in competitive homing assays of T cells expressing L-selectin or cleavage-resistant forms of L-selectin, the latter have been observed to take longer to undergo transendothelial migration and accumulate near HEVs, although this does not affect the number of T cells recruited to peripheral lymph nodes (Galkina et al. 2003). The authors suggested this early proteolysis may enable T cells to transition from the lumen to the baso-lateral surface of high endothelial cells more rapidly, where L-selectin ligands are also present. Following entry into the lymph node, T cells again rely on CCR7 to interact with CCL19 to enable T cell motility (Fig. 1.2; Worbs et al., 2007) throughout the paracortex, where the chemokine is originally expressed (Baekkevold et al. 2001). This was demonstrated using two-photon imaging, which showed that CCL19 was localised

throughout the paracortical T cell area and that CCR7-deficient cells had poor motility relative to CCR7-sufficient T cells (Worbs et al. 2007). Although Worbs and colleagues used CD4 T cells, CD8 T cells also express CCR7, and likely use the same mechanism to navigate the peripheral interfollicular region (Fig.1.2; Hickman et al., 2008).



1.2.2. HEV neogenesis in tumours and CD8 T cell infiltration

PNAf-positive venules which are infiltrated by T cells have been identified in melanoma, lung, breast, colon and ovarian cancers (Martinet et al. 2011a). The authors refer to these as tumour HEVs. In 'HEV-high' breast cancer, significantly greater infiltration by total T cells and CD8 T cells was observed than in 'HEV-low' tumours. In support of T cell transmigration into breast cancer tissue via HEVs (Martinet et al. 2011a), T cells (including CD8 T cells) are seen around tumour HEVs in melanoma and their infiltration correlates with HEV density (Martinet et al. 2012). In freshly resected breast cancer tissue, HEV-high tumours also had an elevated number of several CD8 T cell subsets (effector CD8 T cells, T_N and T central memory; T_{CM}). Additionally, granzyme (gzm) A, gzm B and perforin (markers of CD8 T cell effector function; section 1.3.3) were observed. Correspondingly to T_N and T_{CM} infiltration, *SELL* (L-selectin gene) was upregulated in HEV-high tumours (Martinet et

al. 2011a). However, infiltrates were observed to be mostly T effector memory (T_{EM}), although some T_N cells were present. Interestingly, no correlation was observed between HEV density and the infiltration of immunosuppressive CD4 T cells known as T regulatory cells (T_{REGs} ; section 1.5; Martinet et al., 2012).

Importantly, when comparing overall disease-free and metastasis-free survival, HEV-high status conferred significantly greater survival for breast cancer patients (Martinet et al. 2011a). Further, PNA^d-positive HEVs were present in 152/225 melanoma sections and at higher densities within regressing melanomas, indicating it is prognostically favourable (Martinet et al. 2012). This was corroborated by chemically induced murine models of fibrosarcoma, where the area of total tumour analysed taken up by HEV inversely correlated with the tumour growth rate and correlated positively with the number of infiltrating CD8 T cells (Colbeck et al. 2017).

Given this prognostic favourability and correlation with T cell infiltration, these tumoural HEVs may provide the route via which T cells infiltrate the tumour to mediate cancer cell elimination and progress the cancer immunity cycle. As such, influencing HEV formation is of therapeutic interest and efforts have been made to understand HEV neogenesis. Martinet and colleagues found a correlation between the density of HEVs in melanoma lesions and their infiltration by dendritic cells. Further, clusters of these dendritic cells were significantly elevated in HEV-high tumours, and the authors suggested these cells may play a role in the development of HEV in the tumour microenvironment (TME; Martinet et al., 2012). Supporting this, when DCs were depleted in mice, peripheral lymph nodes lost expression of the enzymes which synthesise the L-selectin ligands PNA^d and GlyCAM-1, and consequently their expression was decreased in HEVs (Moussion and Girard 2011). This coincided with increased rolling velocity of lymphocytes, a decreased percentage of lymphocytes adhering and finally reduced recruitment of cells to the lymph node (Moussion and Girard 2011). Importantly, Moussion and Girard were able to tie this role for dendritic cells to their secretion of lymphotoxin α (LT α), a

molecule that when bound to its receptor is involved in lymphangiogenesis, through specific depletion of LT α -secreting dendritic cells *in vivo* (Moussion and Girard 2011).

In the TME, CD8 T cells rather than DCs have recently been implicated in HEV neogenesis. Following T_{REG} depletion in murine fibrosarcoma, PNA^d-positive tumour HEVs develop (although in this case without cuboidal morphology), which is not impacted by depletion of DCs (Colbeck et al., 2017). Conversely, CD8 T cell depletion abrogated HEV neogenesis induced by T_{REG} depletion (Colbeck et al. 2017). Further, specific blockade of TNF receptor signalling following T_{REG} depletion but not LT $\alpha\beta$ receptor signalling abrogated HEV neogenesis (Colbeck et al. 2017). Finally, tumour-infiltrating CD8 T cell expression of TNF correlated with HEV area within the tumour (Colbeck et al. 2017). Together, these findings indicate CD8 T cells may be the source of TNF-induced tumour HEV neogenesis once T_{REGS} are removed from the TME, rather than DCs as in the lymph node (Colbeck et al. 2017). Although, as the study by Martinet was conducted in melanoma, and the study by Colbeck et al in fibrosarcoma, both could be implicated in HEV neogenesis.

LT α is perhaps not the driver of tumour HEV formation, but despite this, an antibody-LT α chimera that targeted the protein to the TME was able to induce luminal PNA^d- and CCL21-positive HEVs infiltrated by L-selectin positive cells in melanoma-bearing mice, and their tumours were greatly reduced in size (Schrama et al. 2001). Recipient mice had greatly improved survival relative to control mice in a longitudinal study, and new T cell clones appeared in the tumour. This indicates that tumour HEVs can enable the recruitment of T_N tumour-reactive T cell populations which aid in tumour control (Schrama et al. 2001). Indeed, tumour infiltrating lymphocytes (TILs) reacted *in vitro* to the melanoma differentiation antigen tyrosinase related protein 2 (TRP2; Schrama et al. 2001). In the context of the cancer immunity cycle, this represents complete revolutions of the cycle. Due to the expression of PNA^d on high endothelial cells and infiltration by DCs at HEVs this

provides a mechanism by which T_N cells are activated, expanded and mediate effector function within the tumour, circumventing the need for repeated trafficking to the tumour and dilution of effector T cells in the blood stream. To this effect, direct manipulation of L-selectin expression on cancer-reactive T cells has been investigated to improve T cell efficacy, which will be introduced in 1.7.3.

1.3.0. CD8 T cell activation and function

Given the positive impact of CD8 T cell infiltration on ovarian, breast and colorectal cancer patient prognosis (Zhang et al. 2003a; Galon et al. 2006; Ali et al. 2014), and their proposed role in the cancer immunity cycle, (Chen and Mellman 2013), it is important to introduce CD8 T cell effector function, which has been most investigated using virus infection models.

1.3.1. Naïve CD8 T cell activation within the lymph node

Following transendothelial migration into the lymph node, T_N cells begin scanning dendritic cells for their cognate peptides presented by MHC (pMHC; Fig. 1.3A). Using intravital imaging, it has been demonstrated that inflammation causes low-level expression of CCR5 on T_N cells and that peptide-specific CD8 T cell clusters accumulate within the draining lymph node (Castellino et al. 2006). This depended upon the secretion of the CCR5-binding chemokines, CCL3 and CCL4, by CD4 T helper cells and DCs (Fig. 1.3B; Castellino et al., 2006). Interestingly, this was necessary for the long-term but not short-term proliferation and survival of CD8 T cells (Castellino et al. 2006), which highlights the important role of CD4 helper and DC priming of CD8 T cells. More recently, in a murine model of cutaneous herpes simplex virus infection, which takes into account the transfer of viral epitopes from tissue to the lymph, intravital imaging has revealed that lymph node-resident DCs receive peptide from skin-resident, migratory, DCs. Each population of DCs required contact from activated CD4 T helper cells to enable this transfer prior to CD8 T cell activation (Hor et al. 2015). Following these processes, CD8 T cells cluster in lymph nodes (Fig. 1.3B) within 48 hours and begin to upregulate CD69 (which indirectly enables retention of T cells in the lymph node for further activation) in response to type I interferons, and

proliferation is observed by 60 hours (Hor et al. 2015; Nolz 2015). During *in vitro* activation, naïve CD8 T cells secrete the pro-inflammatory cytokines TNF and IL-2 and upregulate the α -chain of the IL-2 receptor (CD25), which enables the formation of the high-affinity IL-2 receptor configuration (heterotrimeric $\alpha\beta\gamma$ complex; Cho et al., 1999; Pipkin et al., 2010). This enables autocrine IL-2-induced proliferation. Indeed, delayed expression of CD25 can consequently delay proliferation as measured by cell division index following *in vivo* and *in vitro* T cell activation (Mohammed et al. 2019). Further, this autocrine stimulation can also induce the secretion of IFN γ (Kasahara et al. 1983), which enables improved cytotoxicity by effector cells (section 1.3.3). Additionally, T_N cell activation induces a loss of L-selectin from the surface of T cells via ADAM17-mediated ectodomain proteolysis (section 1.4.3; Mohammed et al., 2019, 2016).

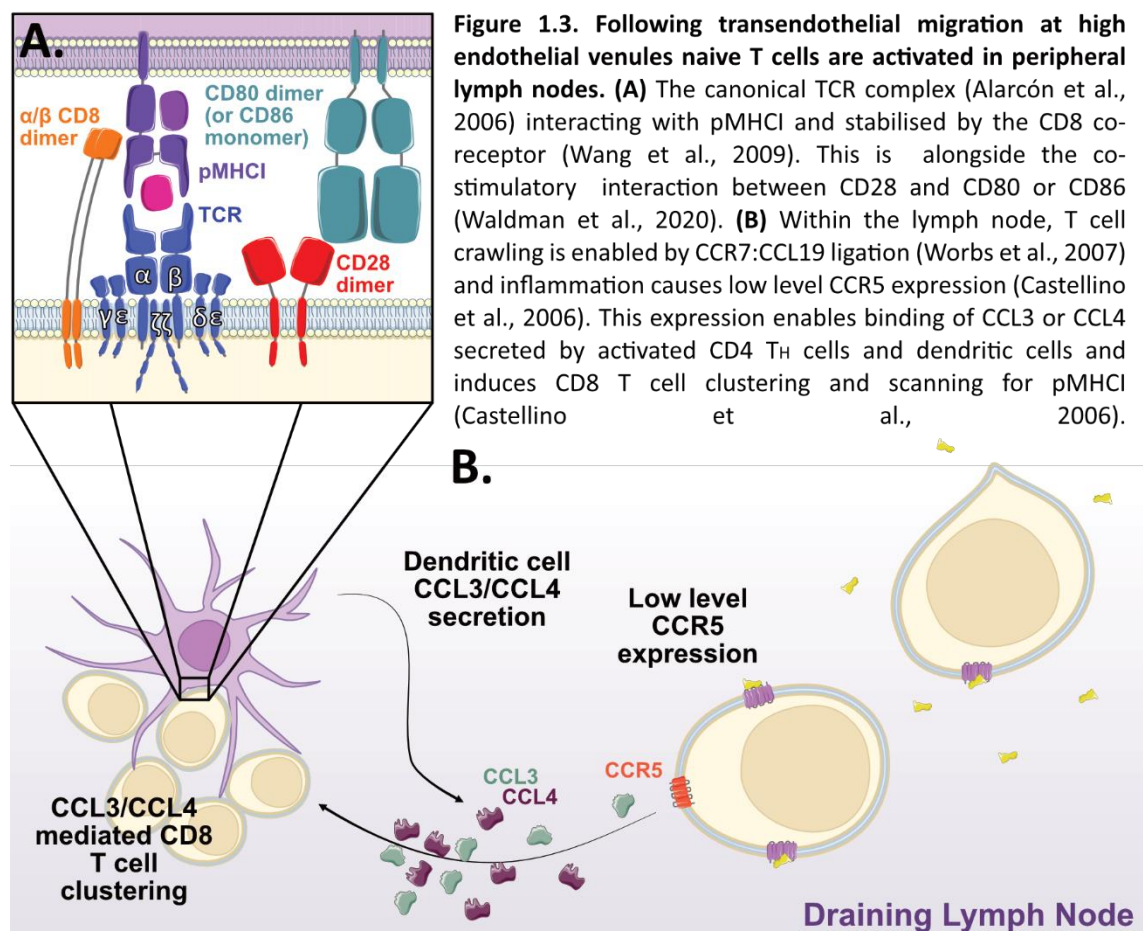


Figure 1.3. Following transendothelial migration at high endothelial venules naive T cells are activated in peripheral lymph nodes. (A) The canonical TCR complex (Alarcón et al., 2006) interacting with pMHC I and stabilised by the CD8 co-receptor (Wang et al., 2009). This is alongside the co-stimulatory interaction between CD28 and CD80 or CD86 (Waldman et al., 2020). **(B)** Within the lymph node, T cell crawling is enabled by CCR7:CCL19 ligation (Worbs et al., 2007) and inflammation causes low level CCR5 expression (Castellino et al., 2006). This expression enables binding of CCL3 or CCL4 secreted by activated CD4 T_H cells and dendritic cells and induces CD8 T cell clustering and scanning for pMHC I (Castellino et al., 2006).

1.3.2. CD8 T cell migration to sites of infection

Following clonal expansion, daughter cells are then capable of emigrating from the lymph node and homing to the site of viral infection, which relies upon a wide range

of cell surface molecules with co-ordinated ligand interactions with inflamed blood vessels. As demonstrated by intravital microscopy, where CD8 T cell expansion was preceded by CD4 expansion within draining lymph nodes, CD4 T cells are necessary for homing to sites of infection. Adoptive transfer of activated CD8 T cells from fully immunocompetent mice into CD4- and IFN γ -deficient mice demonstrated that CD4 secretion of IFN γ was necessary for accumulation of CD8 T cells at the site of infection (Nakanishi et al. 2009). This was dependent on CD8 T cell expression of CXCR3, that binds the inflammatory chemokines CXCL9 and CXCL10 secreted in response to IFN γ from CD4 T cells (Nakanishi et al. 2009).

Using peptide-pulsed, activated DCs and a variety of inoculation routes, Ferguson and Engelhard also demonstrated that CXCR3 was universally highly expressed by activated CD8 T cells, and CCRs 3, 4, 5, 6 and 9 were expressed on a subset of T cells. Further, CCR9 was elevated when primed in the mesenteric lymph node (Ferguson and Engelhard 2010). In addition to this, most CD8 T cells expressed $\alpha 4\beta 1$ integrin (VLA-4) and a P-selectin ligand (PSGL-1/CD162), whilst CD8 T cells primed in the peripheral axillary/brachial lymph nodes additionally expressed E-selectin ligands and those primed in the mesenteric lymph node expressed $\alpha 4\beta 7$ integrin (Ferguson and Engelhard 2010). These differential expression patterns may confer specific migratory patterns and homing abilities to activated effector T cells. In the Ferguson and Engelhard study, L-selectin expression was low and was not considered important for T cell homing. However, our own lab has demonstrated that L-selectin is also part of this process, whereby following L-selectin proteolysis during T cell activation, it is transiently re-expressed within the lymph node and peripheral blood 3 days post-infection (Mohammed et al. 2016). Further, recruitment into infected organs was abrogated if CD8 T cells were L-selectin deficient or L-selectin was blocked. Recruitment was enhanced if L-selectin expression was maintained on activated T cells using a proteolysis-resistant form of L-selectin (Mohammed et al. 2016). Together, these data demonstrate the requirement for CD4 T cell priming of the endothelium for transendothelial migration of activated effector CD8 T cells at the site of infection, which itself relies upon distinct combinations of chemokines, integrins and selectins.

1.3.3. CD8 T cell cytotoxic function

Following transendothelial migration into infected tissues and pMHC recognition, two-photon microscopy revealed greatly reduced track speeds and greatly increased turning angles of specific CD8 T cells (Halle et al. 2016). This demonstrates that TCR engagement can modulate T cell motility to increase the chances of repeated engagement with the infected target cell to mediate its cytolysis. Interestingly, the length of individual contacts between CD8 T cells and target cells did not affect target cell survival or induction of apoptosis (Halle et al. 2016). Rather, the cumulative number of contacts between several specific CD8 T cells and the target cell lead to enough contact time to significantly increase perforin dependent pore formation and consequent target cell apoptosis (Halle et al. 2016), indicating that multiple T cells or multiple interactions by a single T cell are required. Following initial T cell contact, target cell apoptosis typically occurred within 20–60 minutes and T cells could kill a median of 4.2 or 4.8 infected cells per day depending on whether the cells were infected with poxvirus or murine cytomegalovirus infection, respectively (Halle et al. 2016). Therefore, activated T cells contact several target cells several times per day to induce their apoptosis. This is supported using human effector T cells *in vitro*, which can control target cell growth when outnumbered up to 10 to 1 (Vasconcelos et al. 2015). However, Vasconcelos and colleagues revealed the capacity to kill target cells varies between clones of the same T cell population. In killing assays, 66 % of clonal T cells killed 2.8 target cells in 12 hours and the remaining 34 % of T cells killed 6.4 target cells across the same time period (Vasconcelos et al. 2015). The emergence of high-rate effector T cell killing depended on antigen density and IFN γ secretion (Vasconcelos et al. 2015). Therefore, the context of pMHC presentation is not just important for initial T cell activation and differentiation, but also their ability to mediate effector functions.

The cytokines secreted by activated T cells are part of this context and improve T cell mediated cytotoxicity. IL-2 can act as an autocrine stimulus and has been demonstrated to increased expression of the CD8 T cell effector molecules IFN γ , gzm A, gzm B , perforin and TNF (Fig. 1.4; Janas et al., 2005; Pipkin et al., 2010). Of these,

IFN γ and TNF have been demonstrated to mediate expression of Fas on target cells, which enables FasL-mediated T cell cytotoxicity (Böhm et al. 1998; Matsumura et al. 2000; Simon et al. 2000; Bhat et al. 2017). In addition, IFN γ can mediate the upregulation of MHC I on target cells (Böhm et al. 1998), presumably increasing the likelihood of recognition by TCRs on effector T cells. Further, IFN γ has been shown to increase T cell speed and net patrol area *in vivo* which would enable increased likelihood of detecting target cells (Bhat et al. 2017).

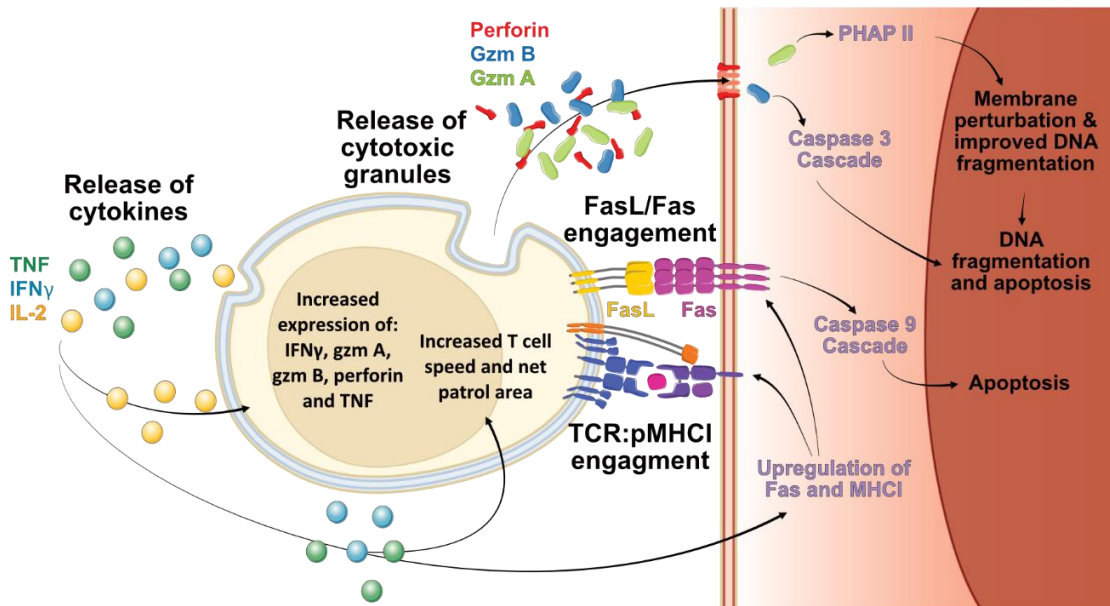


Figure 1.4. CD8 cytotoxic T cells mediate target cell apoptosis through several mechanisms. Following engagement of their TCR complex with pMHC I upon target cells, activated T cells secrete perforin and granzymes A and B from their cytotoxic granules (Law et al., 2010; Ebnet et al., 1995; Topham et al., 1997). These granzymes can cause DNA fragmentation and apoptosis (Goping et al., 2003; Beresford et al., 1999). In addition, CD8 cytotoxic T cells express FasL which can induce apoptosis of target cells expressing Fas (Topham et al., 1997). CD8 T cells also secrete soluble factors (TNF, IFN γ and IL-2) which augment their cytotoxic function (Simon et al., 2000; Janus et al., 2005; Böhm et al., 1998; Halle et al., 2016; Bhat et al., 2017). IL-2 increases expression of IFN γ , gzm A, gzm B, perforin and TNF (Janas et al., 2005; Pipkin et al., 2010). IFN γ and TNF can induce expression of Fas on target cells. IFN γ can also mediate the upregulation of MHC I, increase T cell speed and net patrol area (Böhm et al., 1998; Bhat et al., 2017).

As demonstrated by Halle *et al* using perforin-deficient mice, the ability of T cells to mediate apoptosis relies on their expression of perforin and its secretion from lytic granules to form pores on target cells (Halle et al. 2016). These pores enable secreted cytosolic factors from T cells to enter target cells and induce apoptosis (Fig. 1.4; Law et al., 2010). Several cytosolic factors exist within these granules, of which the gzm A and gzm B are the most well characterized. Gzm B is solely expressed in the granules of activated T cells, and activated T cells derived from gzm B-deficient

mice were unable to induce DNA fragmentation and target cell apoptosis (Heusel et al. 1994). Using human cell lines *in vitro*, treatment with gzm B alongside an agent capable of mediating its intracellular delivery, demonstrated gzm B acts on pro-caspase 3 and enables its' conversion to the catalytic subunits p20, p19 and p17, which lead to apoptosis via a caspase cascade (Fig. 1.4; Goping et al., 2003). In addition to gzm B, gzm A is also present in lytic granules, although gzm A-deficient murine effector T cells retain their cytolytic and DNA fragmentation functions *in vitro* (Ebnet et al. 1995). This indicates it is likely not a primary cause of T cell-mediated cytotoxic function. However, target cells treated *in vitro* with perforin and gzm B exhibited greater membrane perturbation and gzm B-mediated DNA fragmentation if also treated with gzm A (Fig. 1.4; Beresford et al., 1999). The role of gzm A was found to be independent of caspase 3 and acted on PHAP II downstream. This may infringe upon chromatin arrangement to aid gzm B-mediated DNA fragmentation (Beresford et al. 1999). Together, these data indicate that of the two granzymes, gzm B is dominant, but that gzm A may have a non-redundant role in mediating target cell apoptosis. However, despite similarity in the gzm sequences between mouse and human species, differences do exist. For example, human gzm B is at least 10-fold more cytotoxic than murine gzm B. Additionally, human gzm A was unable to mediate cell death alongside perforin as shown for its murine counterpart (Kaiserman et al. 2006).

Effector T cells also mediate target cell lysis by expressing Fas ligand (FasL), which upon binding Fas on target cells induce their apoptosis. This is exemplified by FasL antibody ligation-induced apoptosis of human cell lines *in vitro* which acts on caspase 9 downstream (Fig. 1.4; Goping et al., 2003). The importance of Fas-mediated cytotoxicity was demonstrated using *in vivo* influenza infection models, in which perforin-deficient T cells still cleared virus from mice, but if the virally infected mice were Fas deficient, the virus persisted (Topham et al. 1997). Together, perforin, granzymes and Fas ligation mediate target cell lysis.

1.3.4. Clonal contraction and T cell memory formation

Following elimination of virally infected cells, the now enriched clonal population of T cells contracts drastically, and what remains are T_{EM} (CCR7 and L-selectin negative) and T_{CM} (CCR7 and L-selectin positive) cells, the latter of which retain T_N cell lymph node homing properties (Nolz 2015). As such, whilst T_{CM} typically scan lymph nodes and undergo clonal expansion, T_{EM} are peripheral and act as rapid responders to reinfection (Nolz 2015). Within the T_{EM} subset are tissue-resident memory (T_{RM} ; CD103 and CD69 positive) cells, whose CD69 marker (with SIPR1) enables tissue residence (Nolz 2015). These memory populations together orchestrate CD8 immunological memory, but their origins are unclear. By using genetically barcoded thymocytes, naïve CD8 T cells specific for ovalbumin peptide (OVA) were used in adoptive transfer models of OVA-*Listeria Monocytogenes* and OVA-influenza A infections and showed that barcodes present during the effector and memory phases were highly correlated, indicating that these populations derive from the same clonal population of activated T cells (Gerlach et al. 2010). The avidity of the T cell receptor did not alter the ability of a given barcoded T cell clone to propagate T cell memory as had previously been theorised, rather this must be due to other factors.

It has been suggested that IL-2 and IL-12 drive the proliferation of short-lived effector and long-lived memory cells, respectively. During *in vitro* activation of CD8 T cells, it was demonstrated that cells cultured in low IL-2 lost expression of granzyme and perforin and the ability to mediate cytolysis of target cells, while gaining expression of the IL-7 receptor (IL-7R; Pipkin et al., 2010). Conversely, cells cultured in the presence of high concentrations of IL-2 did not express IL-7R, but retained granzyme and perforin expression, which enabled them to exert cytolytic function *in vitro* (Pipkin et al. 2010). When these cultured and activated cells were transferred into mice, competitive long-term engraftment demonstrated a reduced frequency in the periphery for T cells activated with high IL-2, indicating that it may skew T cell development toward short-lived effector cells (Pipkin et al. 2010). Immunoblotting showed all *in vitro* activated cells expressed the transcription factor T-bet, while cytolytic attributes were tied to the Blimp-1 and EOMES transcription factors. If

cultured in high IL-2 and then activated *in vitro* in the presence of IL-12, EOMES expression was lost and IL-7 receptor expression was gained, indicating that IL-12 and IL-7 may co-operate to confer greater potential for long-term survival and memory (Pipkin et al. 2010). These studies have implications for the work done in this thesis, because my *in vitro* activated and transduced cancer-specific T cells were cultured in a high concentration of IL-2 and were therefore likely to be short-lived effector T cells rather than long-lived memory cells (T_{EM} , T_{CM} or T_{RM} cells).

1.4.0. L-selectin

1.4.1. Function in CD8 T cells

Thus far, this introduction has implicated L-selectin in the recruitment of naïve and T_{CM} cells, both of which are L-selectin positive, to HEVs within lymph nodes for immunosurveillance (Streeter et al. 1988; Nolz 2015) and HEVs within tumours in mice and humans, where their presence improves survival and prognosis, respectively (Martinet et al., 2011; Schrama et al., 2001). I have also introduced proteolysis-mediated downregulation of L-selectin from the surface of T_N cells during transendothelial migration and activation, and the consequent re-expression by virus-specific T cells, which is crucial for T cell homing to infected tissues and viral clearance (Klinger et al. 2009; Mohammed et al. 2016).

Beyond homing, L-selectin has also been implicated in other effector functions of T cells. Using CD8 T cells expressing either L-selectin or a proteolysis-resistant form of L-selectin and HLA-matched target cells, it has been demonstrated that ectodomain shedding of L-selectin is necessary for degranulation and cytolysis of human effector CD8 T cells and target cell lysis (Yang et al. 2011). Another study, using an alternate version of shedding-resistant L-selectin, demonstrated that expression of CD25 (a sub-unit of the high affinity IL2-R) and proliferation of virus-specific murine T_N cells is delayed following *in vitro* and *in vivo* activation (Mohammed et al. 2019). Together, these studies indicate that L-selectin contributes to T cell function beyond homing.

1.4.2. Structure and relation to function

The human *SELL* gene was first identified in 1989 and was found to have an open reading frame of 1,181 base pairs encoding a protein of 372 amino acids (Tedder et al. 1989). The authors investigated mRNA expression and found it was expressed in blood lymphocytes, hence its name, leukocyte selectin. Sequence analysis predicted an extracellular domain (ECD) consisting of a C-type lectin binding domain, an epidermal growth factor like (EGF-like) domain, two short consensus repeat (SCR) domains and a 15 amino acid spacer that precedes the transmembrane domain (TMD; Tedder et al., 1989). Later, a short intracellular domain (ICD) of 12 amino acids was also predicted (Ord et al., 1990) and has since been confirmed to be 17 residues in length (Fig. 1.5; Killock et al., 2009).

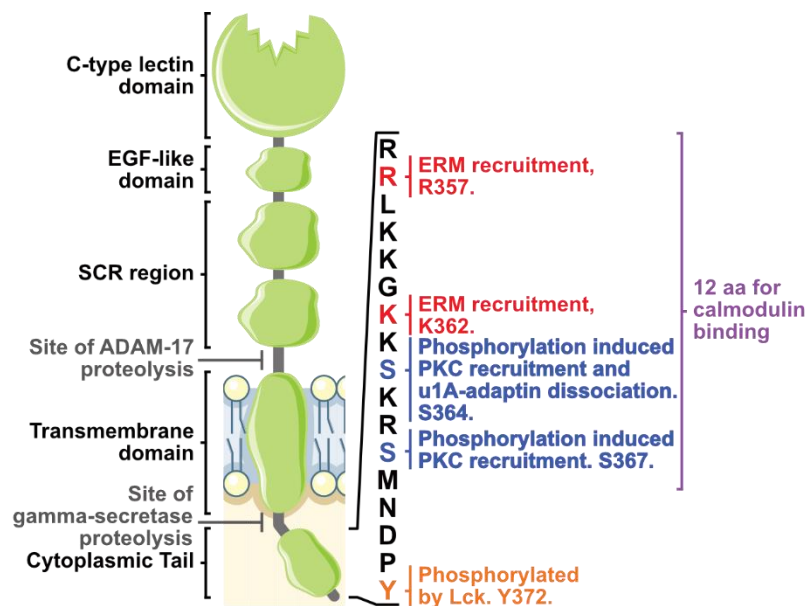


Figure 1.5. L-selectin structure and function. The predicted structure of L-selectin from sequence analysis (Tedder., 1989) of which the C-type lectin and EGF-like domain have been resolved by x-ray crystallography (Wedepohl et al., 2017) and cytoplasmic tail confirmed to be 17 amino acids (Killock and Ivetic., 2010). The membrane proximal ADAM-17 cleavage site was found to be between the SCR and transmembrane domains (Migaki et al., 1995) and the site of gamma-secretase cleavage is hypothesised to release the intracellular tail similarly to proteolysis of NOTCH (Schroeter et al., 1998) and APP (Kimberley et al., 2001). The first 13 residues of L-selectin's tail are required for calmodulin binding (Matala et al., 2001) whilst R357 and K362 are involved in ERM recruitment (Ivetic et al., 2002) and molecular simulations suggest they can be bound together (Killock and Ivetic., 2010). S364 and S367 phosphorylation can recruit PKC isoforms whilst phosphorylation of the former can cause dissociation of u1a-adaptin (Kilian et al., 2004; Dib et al., 2017). Y372 can be phosphorylated by Lck (Xu et al., 2008) following L-selectin cross-linking.

C-type lectin domain and EGF-like domain

L-selectin's ligands are based on Sialyl-Lewis X (sLe^x; Erbe et al., 1992), and it has been determined the entire C-type lectin domain is essential for Ca²⁺-dependent binding of M6P-rich mannan core (PPME) and fucodin, carbohydrates which simulate L-selectin's ligands (Kansas et al. 1991). As previously mentioned, several of these ligands are described as PNAd, which are characterised by the binding of the MECA-79 antibody and enable lymphocyte HEV rolling. PNAd are sLe^x O-linked proteins, including: CD34, GlyCAM-1, MAdCAM-1 (Baumheler et al., 1993; Berg et al., 1993; Mebius et al., 1993; Puri et al., 1995; Streeter et al., 1988).

Whilst it has been demonstrated that only the C-type lectin domain is necessary for ligand binding, there is evidence that this is modulated by the EGF-like domain (Kansas et al. 1991). To enable lymphocyte rolling, L-selectin at the leading edge of the cell must bind its ligands (catch), sustain this bond as the cell passes (and stress on the bond increases), and then release its ligand (slip) as the L-selectin ligand interaction is on the trailing edge of the cell. The C-type lectin and EGF domains are separated by a flexible 'hinge' and so can adopt an 'open' or 'closed' conformation, the latter of which is stabilised by an inter-domain hydrogen bond (Lou et al. 2006; Wedepohl et al. 2017). Without this hydrogen bond, neutrophils aggregated in flow assays indicating that the EGF-like domain limits the affinity of the C-type lectin domain at lower shear stresses which prevents leukocyte aggregates forming (Lou et al. 2006) and inappropriate arrest in venules with low (or without) shear flow.

L-selectin can be rapidly lost from the cell surface following ADAM-17 dependent proteolysis of the ectodomain (section 1.4.3). The EGF domain has also been linked to ectodomain proteolysis as mutants of the protein without it were not lost from the cell surface following potent stimulation of ADAM-17 activity (Zhao et al. 2001).

Sequence consensus repeat domain

There are variable numbers of short consensus sequence (SCR) domains within each selectin, with L-selectin having two. It has been suggested that these SCR regions are structural, acting to ensure L-selectin extends to the glycocalyx to enable the C-type

lectin domain to bind ligands on neighbouring cells (Kansas et al., 1991). However, like the EGF-like domain, they may have a role in modulating affinity, as IgG-L-selectin chimeras without them exhibit decreased immunohistochemical staining of peripheral lymph node endothelium (Watson et al., 1991). Zhao and colleagues also implicated the SCR regions in ectodomain proteolysis by ADAM-17 as proteolysis of L-selectin was completely abrogated in L-selectin mutants without these domains (Zhao et al. 2001).

Membrane proximal cleavage site

For human L-selectin, the site of ectodomain proteolysis has been determined to be the membrane proximal site between K321 and S322 (Fig. 1.5; Kahn et al., 1994; Migaki et al., 1995). Additionally, Kahn et al. were the first to demonstrate that ectodomain proteolysis left a membrane retained fragment following phorbol 12-myristate 13-acetate (PMA) stimulation (Kahn et al. 1994), which is investigated in this thesis. Ten of the residues between 318 and 332 are conserved between human, rat, and mouse. Alanine scanning mutagenesis revealed the sequence of this domain was not as important for proteolysis as the presence of the residues. Therefore, the spatial location and conformational arrangement of the ectodomain is important for L-selectin ectodomain proteolysis (Migaki et al. 1995).

Transmembrane domain

Electron microscopy revealed that L-selectin is topologically located on microvilli, whereas CD44 is located on the cell body. If the transmembrane and/or the intracellular domain were swapped, the topological location was also swapped. Therefore, the transmembrane domain of L-selectin is responsible for its location in microvilli (Buscher et al. 2010). This is particularly interesting, when considering both the signalling capacity of L-selectin's cytoplasmic tail (covered next), and the formation of L-selectin and TCR clusters detectable on the microvilli of T cells (Jung et al., 2016; supp. Fig. 11).

Cytoplasmic tail

The tail of L-selectin was also implicated in L-selectin cell topology by Buscher and colleagues. They demonstrated a decrease in the rolling flux of leukemic T cells in response to shear stress with a cytoplasmic domain replacement of L-selectin, which implicates the transmembrane domain and cytoplasmic tail of L-selectin in cellular location and the leukocyte's ability to roll under shear stress (Buscher et al. 2010). Therefore, this domain is clearly important for L-selectin's ability to mediate leukocyte rolling prior to transendothelial migration, and it appears to do so via a variety of binding partners (Fig. 1.5).

Using L-selectin pulldown assays, the tail of L-selectin was found to interact with ezrin in resting mouse T cells and moesin in PMA treated cells (Ivetic et al. 2002). Ezrin and moesin belong to the ezrin, radixin and moesin (ERM) group of proteins, which organise membrane proteins via interactions with the cell cytoskeleton. These interactions therefore link L-selectin's topological location to the cytoskeleton and to its function in leukocyte rolling (Ivetic et al. 2002). In support of this, the interaction depended on two basic residues, K362 and R357, in L-selectin's tail and alanine mutations of these residues relocated L-selectin to the cell body and reduced pre-B cell tethering to PSGL-1 in flow chamber assays (Ivetic et al. 2004). Together, this indicates that the interaction between the L-selectin tail and cell cytoskeleton is important for L-selectin's function.

Four further proteins (μ 1A-adaptin, complement component factor H, granulin and leucine rich repeat containing 48) were found to interact with L-selectin in pulldowns of PMA-activated macrophage cell lines. The association with μ 1A-adaptin was prevented when S364 was phosphorylated, or by removing one positive charge from the dibasic residues R356R357, K359K360 and K362K363 (Dib et al. 2017). The authors note intracellular co-localisation between the two proteins and suggest this is a reserve pool of L-selectin in the trans-Golgi network and μ 1a-adaptin facilitates rapid re-expression of L-selectin at the cell surface (Dib et al. 2017).

In addition to its role in L-selectin mediated rolling of T cells, L-selectin may alter T cell signalling following activation. The tail of L-selectin, can be phosphorylated at Y372 by Lck following anti-L-selectin mediated clustering of L-selectin (Brenner et al., 1996; Xu et al., 2008), which depended on Lck's SH2 domain (Fig. 1.5A; Xu et al., 2008). The earlier study by Brenner demonstrated that phosphorylated L-selectin co-precipitated with Grb2-SOS and could convert Ras to its active form (RasGTP; Fig. 1.6; Brenner et al., 1996) and signal via ERK which implicates L-selectin in the signalosome (section 1.6.1). Here, it may act via Grb2-SOS to mediate activation of Ras and signal via the ERK pathway. The more recent study by Xu et al demonstrated L-selectin-associated Lck acts downstream on Abl kinase (Abl) and ζ chain-associated protein kinase (Zap-70), following L-selectin ligand engagement, which may also modulate T cell signalling (Fig. 1.6; Xu et al., 2008). In addition, serine phosphorylation of the tail can recruit PKC isozymes (α , ι and θ ; Fig. 1.6) following CD3 cross-linking and can be prevented by replacing both S364 and S367 of L-selectin's tail with

alanine, although greater disruption was caused by replacing S364 rather than S367 (Kilian et al. 2004). This study highlights that not only is L-selectin's tail phosphorylated, it associates with PKC isoforms after T cell activation, which may induce phosphorylation of other interacting partners (Fig. 1.6).

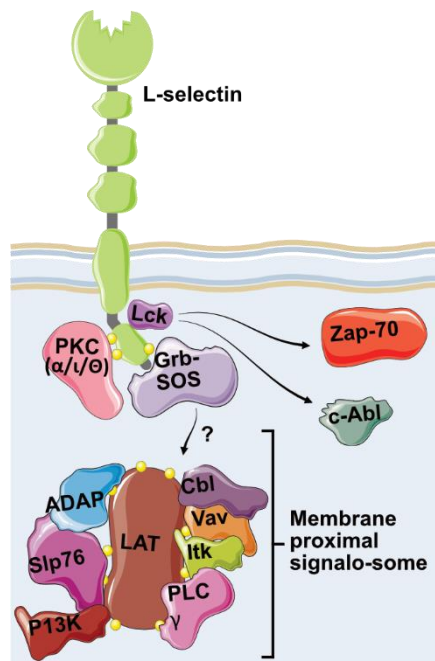


Figure 1.6. The potential signalling capacity of the tail of L-selectin. Pulldowns of L-selectin revealed Grb-SOS (Brenner et al., 1996) which forms part of the signalosome (Hwang et al., 2020) and Lck which acts on Zap-70 and c-Abl (Xu et al., 2008) as well as PKC isoforms (Kilian et al., 2004) which suggest L-selectin may have some capacity to influence T cell signalling prior to shedding.

1.4.3. L-selectin expression and regulation

L-selectin has several intracellular binding partners, is used as a marker of T_N and T_{CM} cells (Nolz 2015) and is implicated in T cell homing (Streeter et al. 1988; Klinger et al. 2009; Mohammed et al. 2016), IL-2-induced proliferation (Mohammed et al. 2019),

and degranulation of T cells and cytotoxic function (Yang et al. 2011). Therefore, it is important that L-selectin expression is tightly regulated.

Proteolytic control

Calmodulin is a protein which regulates many cellular binding partners through its ability to bind both them and Ca^{2+} , which can induce a conformational change in calmodulin, altering its ability to bind other proteins. L-selectin was found to interact with calmodulin both as a full-length protein and following ectodomain proteolysis, and this interaction was abrogated by treating L-selectin tail pulldowns with a chelating agent, indicating this interaction is regulated by Ca^{2+} (Matala et al. 2001). In the absence of bound calmodulin, soluble L-selectin extracellular domain increased in cell supernatants, indicating bound calmodulin limits ectodomain proteolysis (Matala et al. 2001). More recently, L-selectin clustered in the pseudopods of leukocytes undergoing transendothelial migration, following L-selectin phosphorylation and calmodulin dissociation. This highlights that ectodomain proteolysis during transendothelial migration is highly regulated by cytoplasmic tail interacting partners (Klinger et al. 2009; Rzeniewicz et al. 2015). Calmodulin interacts with first 13 residues of L-selectin cytoplasmic tail (Matala et al. 2001), which also bind ERM proteins (Fig. 1.5; Killock and Ivetić, 2010). This closely ties the binding partners of L-selectin's tail to L-selectin proteolysis and to cytoskeletal dependent capture of leukocytes in flowing blood.

Pharmacological inhibition of calmodulin promotes shedding of L-selectin from the surface of neutrophils. This can be prevented using a broad spectrum metalloprotease inhibitor (Kahn et al. 1994), demonstrating calmodulin acts in concert with a metalloprotease to mediate L-selectin shedding. During PMA- and TCR-induced proteolysis of L-selectin, the A disintegrin and metalloprotease-17 (ADAM-17; Fig. 1.7, Left; Mohammed et al., 2019) is responsible for cleavage, whereas spontaneous and constitutive release of soluble L-selectin ectodomain is mediated by a different metalloproteinase (Mohammed et al. 2019).

A potential regulatory mechanism involves the tetraspannin class of surface proteins, specifically tetraspannin CD9 and tetraspannin CD53. Tetraspanin 9, is broadly expressed on all peripheral blood mononuclear cells and has been demonstrated to co-localise with ADAM-17 (Tsukamoto et al. 2014). In a monocytic cell line, PMA-induced shedding of the ADAM-17 substrate LR11 was increased when CD9 was knocked down or blocked, and this could be abolished with metalloprotease inhibitors (Tsukamoto et al. 2014). In murine T cells, PMA-induced L-selectin ectodomain proteolysis was prevented with an ADAM-17 blocking antibody but only partially abrogated in CD53^{-/-} cells, indicating a role for this tetraspannin in modulating ADAM-17 shedding (Demaria et al. 2020). This mode of ADAM-17 substrate regulation may explain why ADAM-17 can be so promiscuous in cleavage site recognition, but have its activity tightly controlled.

In addition to the TCR in T cells, ADAM-17 is activated by several physiological stimuli in mouse fibroblasts. PMA, the most potent non-physiological activator is used in this thesis (Le Gall et al. 2010). Using PMA and an ADAM-17 active site inhibitor (DPC333), another regulatory mechanism for ADAM-17 has been proposed. By using DPC333 to bind the active site of ADAM17 on quiescent cells prior to washing excess inhibitor away, the authors found that PMA-induced shedding by ADAM-17 was not abrogated. They hypothesised that an endogenous active site inhibitor or inactive enzyme conformation prevents DPC333 binding prior to the active site of the enzyme and represents a mechanism of ADAM-17 regulation (Le Gall et al. 2010).

However, as ADAM-17 has more than 80 substrates, it is likely regulated by several mechanisms. Indeed, Canault and colleagues used a yeast-two-hybrid assay to identify 'four and a half LIM domains 2' (FHL2) as an interacting partner, which co-precipitated with actin and ADAM-17 in rat cardiomyocytes (Canault et al. 2006). Whilst these are fundamentally not immune cells, in peritoneal macrophages from FLH2^{-/-} mice, PMA-induced release of proteolytic substrates was reduced relative to wildtype counterparts (Canault et al. 2006), indicating localisation to actin via FLH2 may regulate ADAM-17 and substrate co-localisation. This is an attractive hypothesis when considering L-selectin interacts with ERM proteins (Ivetič et al. 2004). In

HEK293T and HeLa cells, large intracellular stores of ADAM-17 are present and PMA is able to induce maximal PKC mediated ADAM17 activity by transporting ADAM-17 to the cell surface within as little as one minute (Lorenzen et al. 2016). However, unlike a physiological ADAM-17 activator, PMA caused the internalisation and lysosomal degradation of mature ADAM17 after 90 minutes, which may be a regulatory mechanism for non-physiological levels of activation (Lorenzen et al. 2016).

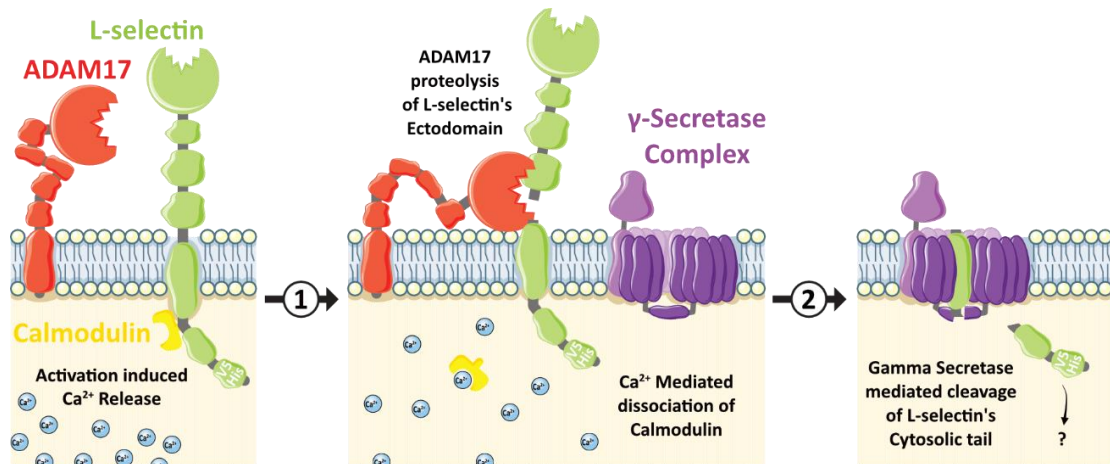


Figure 1.7. L-selectin undergoes sequential proteolysis following T cell activation. (Left) Following TCR mediated T cell activation or treatment with PMA released intracellular calcium binds calmodulin which dissociates from L-selectin hypothetically exposing it's ADAM17 cleavage site (Matala et al., 2001). **(Middle)** L-selectin undergoes ADAM17 mediated proteolysis to shed it's ectodomain (Kahn et al., 1994; Mohammed et al., 2019). **(Right)** γ -secretase recognises, and proteolyses, the ADAM17 membrane retained fragment of L-selectin to shed L-selectin's tail (Ager lab, unpublished observations).

In published work, γ -secretase has not been implicated in L-selectin proteolysis, although it has been demonstrated by members of our laboratory to further proteolyse the ADAM17 cleavage product (membrane retained fragment; Fig. 1.7, Middle and Right). Through the use anti-CD3/CD28 dynabeads, ectodomain proteolysis of L-selectin was induced in Molt-3 T cells, and an 8 kDa membrane retained fragment (MRF) could be observed 5 minutes after T cell activation by Western blotting, as was first observed by Kahn et al (Fig. 1.7, middle panel; Kahn et al., 1994). Detection of the MRF decreased 15 minutes after T cell activation and was lost by 60 minutes (Andrew Newman; PhD thesis). Detection of the accumulating MRF could be maintained by treating the T cells with the γ -secretase inhibitor L-685 during T cell activation, indicating γ -secretase proteolysis of the MRF (Andrew

Newman; PhD thesis). However, during these experiments, a γ -secretase product of L-selectin could not be reliably detected by Western blotting.

γ -secretase is a multicomponent complex made up of presenilin, nicastrin and anterior pharynx defective-1 and presenilin enhancer 1 or 2 (Fig. 1.7, middle and right). Each of these proteins are tightly regulated to control γ -secretase activity, which has more than 50 substrates (Beel and Sanders 2008). γ -secretase proteolysis is most studied in the context of amyloid precursor protein (APP) and NOTCH signalling as their processed fragments are implicated in Alzheimer's disease and cancer, respectively. Similarly to L-selectin's proteolysis by ADAM17 and γ -secretase, NOTCH is proteolysed by an ADAM and γ -secretase (Schroeter et al. 1998). Ligand binding induced intramembrane proteolysis of NOTCH which produces the NOTCH intracellular domain (NICD), which binds another CSL (CBF1, Su(H), Lag-1) family proteins to drive transcription of genes controlled by Hes-1 promoters (Schroeter et al. 1998). Additionally, nuclear fractionation of transfected cells expressing APP intracellular domain (the APP intracellular product of γ -secretase proteolysis; AICD) revealed that AICD is present in the nucleus and visible there by immunofluorescence if stabilised by its binding partner Fe65 (Kimberly et al. 2001). This thesis addresses the hypothesis that the γ -secretase cleavage product of L-selectin could have a similar role in transcriptional control and undergoes transport to the nucleus, which will be investigated by imaging flow cytometry.

Transcriptional control

As already covered, L-selectin is proteolysed following T cell activation and re-expressed prior to lymph node egress and arrival at the site of viral infection, after which expression is lost again (Mohammed et al. 2016). *In vitro* activation of CD8 T cells provides evidence that the first loss of L-selectin from the T cell surface is mediated by proteolysis, as described above, and recovery accompanied by an increased amount of mRNA transcript and translation as the rate of ectodomain proteolysis is unchanged (Day 1 post stimulation; Chao et al., 1997). The eventual loss of L-selectin expression by *in vitro*-activated CD8 T cells is accompanied by L-

selectin mRNA loss beginning at day 3 post-stimulation, which is completely lost by day 7 (Chao et al. 1997). More recently, the serine/threonine kinase Pak1 has been implicated in the control of L-selectin expression. T cells from Pak1-null mice showed reduced recruitment to the lymph node relative to their wildtype counterparts due to lower levels of L-selectin and CCR7 transcripts and surface expression (Dios-Esponera et al. 2019). This was mediated by JNK phosphorylation of FOXO1, a positive regulator of the Klf2 transcription factor which facilitates *Sell* transcription (Dios-Esponera et al. 2019). Conversely, peptide-specific T cell activation of T cells downregulates klf2 and L-selectin mRNA, and does so to a greater extent with higher affinity T cell receptors and at high concentrations of IL-2 (Preston et al. 2013). Therefore, control of L-selectin expression and T cell homing occurs at the transcriptional level and through proteolysis. When expression of L-selectin is delivered outside of endogenous promoters via retroviral and lentiviral vectors, as in this thesis, transcriptional control is circumvented.

1.5.0. The tumour microenvironment and immunosuppression

T cell tumour infiltration and the presence of tumour HEVs correlate with favourable patient outcomes, yet T cell infiltrates can still fail to clear tumours (Zhang et al. 2003a; Galon et al. 2006; Martinet et al. 2011a; Martinet et al. 2012; Ali et al. 2014). Primary and metastatic tumours are complex ecosystems made up of not just cancer cells but accessory cells within an extracellular matrix. These accessory cells include immune infiltrates, which play a role at every stage of cancer development (Gonzalez et al. 2018). Several innate and adaptive immune cell infiltrates correlate with worse patient prognosis, and act in opposition to the outlined CD8 T cell effector functions within the cancer immunity cycle (Gentles et al. 2015). My thesis focuses on improving cytotoxic T cell function for adoptive cell therapy of solid tumours, and so in this section, I will outline the 'key players' of immunosuppression within the primary TME (summarised in Fig. 1.12) and several of their mechanisms. Whilst not an exhaustive list, the exemplar modes of immunosuppression described give an indication of what tumour infiltrating T cells must overcome to exert their function.

1.5.1. Tumour vasculature

The first barrier to successful immunological control is arguably the tortuous, leaky blood vasculature in tumours. Tumour angiogenesis is induced in cancerous lesions by VEGF-A, which causes abnormal vasculature development. The blood vessels are subject to high interstitial pressure and altered blood flow. This presents a barrier to T cell transendothelial migration, as L-selectin ligand interactions depend on specific haemodynamic forces (Lou et al. 2006; Ager et al. 2016). Further, VEGF-A prevents ICAM-1 clustering, and *in vitro* adhesion assays demonstrate this severely limits human CD8 T cell adhesion on activated endothelial cells, providing another barrier to transendothelial migration at the tumour (Bouzin et al. 2007).

VEGF-A also directly promotes T cell dysfunction by inducing the expression of immune checkpoints on CD8 T cells. Immune checkpoints are surface proteins whose ligation can abrogate productive T cell signalling and therefore curb effector function and survival. Immune checkpoints include: PD-1, CTLA-4, TIM-3, LAG-3 and TIGIT and their mechanisms inhibiting T cell function are outlined in 1.6.2, Fig. 1.14. Treatment of VEGF-A-secreting murine colon carcinoma-bearing mice with a neutralising VEGF-A antibody reduced the proportion of PD-1 positive CD8 T cells and enhanced control of tumour growth (Voron et al. 2015). This was found to be a direct effect on the CD8 T cells, as *in vitro* activation of T cells in the presence of VEGF-A further increased expression of PD-1, CTLA-4, TIM-3, and LAG-3 (Voron et al. 2015). In CD8 positive TILs, the VEGF-A receptor 2 has been found to be upregulated relative to CD8 positive splenocytes from the same mice, and PD-1 expression on TILs could be reduced by blocking the VEGF receptor (Voron et al. 2015).

As the tumour develops, it outgrows the limited supply of nutrients and oxygen provided by the abnormal vasculature, resulting in hypoxia. Hypoxic conditions upregulate *CCL28* gene expression in several human ovarian cancer cell lines, which in chemotaxis assays recruits immunosuppressive T_{REGs} in a CCR10-dependent manner (Facciabene et al. 2011). Supporting this, when *CCL28* was over-expressed in ovarian cancer cells, *in vivo* tumour growth was faster than the parental ovarian tumours and had greater levels of VEGF-A, a higher density of tumour blood vessels

and T_{REG} infiltrates (Facciabene et al. 2011). T_{REG} or CCR10 positive cell depletion slowed tumour growth and lowered VEGF-A levels, closely tying together: tumour vasculature-induced hypoxia, CCL28 expression and T_{REG} recruitment (Facciabene et al. 2011). PD-1 ligand (PD-L1) induces T cell dysfunction upon binding PD-1 on activated T cells, and hypoxia has been demonstrated to increase PD-L1 expression and IL-6 and IL-10 secretion by splenic myeloid-derived suppressor cells (MDSCs; Noman et al., 2014). *In vitro* proliferation and CD8 T cell IFN γ production was limited by MDSCs only under hypoxic conditions (Noman et al. 2014). This was abrogated by PD-L1 blockade (Noman et al. 2014), indicating hypoxia enables MDSC immunosuppression via PD-L1 expression.

In addition to hypoxia-induced upregulation of immune checkpoint ligands on MDSCs, PD-L1 was upregulated on lymphatic endothelial cells in two syngeneic models of murine cancer: B16.F10 melanoma (overexpressing VEGF-C to promote lymphangiogenesis) and 4T1 breast cancer (Dieterich et al. 2017). CD4 and CD8 T cells were shown to interact with these lymphatic endothelial cells *in situ*, and expression of PD-L1 could be induced on these cells by IFN γ treatment *in vitro* (Dieterich et al. 2017). Together this suggests that lymphatic vessels in the TME may induce a negative feedback loop following T cell activation and IFN γ secretion.

Contrastingly, blood endothelial cells did not upregulate PD-L1 (Dieterich et al. 2017), but tissue microarrays revealed several cancers where endothelial cells expressed FasL, unlike healthy control tissue (Motz et al. 2014). Co-culture of human ovarian cancer endothelial cells with activated T cells induced T cell death that was preventable by FasL blockade, indicating that endothelial cells can limit T cell recruitment into tumours (Motz et al. 2014). In a similar assay using FasL-transduced endothelial cell lines, FasL could not mediate activated T_{REG} death, which may explain why FasL positive tumour blood vessels suppress CD8 T cell infiltration but not T_{REG} infiltration. Motz and colleagues demonstrated this *in vivo* and found FasL blockade induced a shift in CD8/T_{REG} ratio in favour of CD8 T cell infiltration, which was associated with decreased tumour volume (Motz et al. 2014). Together, these data demonstrate that for cancer-reactive cytotoxic T cells, the first barrier to overcome is

the tumour vasculature both directly, and in-directly as it recruits immunosuppressive cell populations.

1.5.2. Dendritic cells

DCs are professional antigen-presenting cells that can either activate or anergize T cells depending on the context of antigen presentation. CD11b and CD103 positive populations of DCs have been identified across murine models of breast cancer and melanoma (Broz et al. 2014). Both populations were able to uptake tumour antigen, but only CD103 positive DCs induced expression of the early activation marker CD69 on naïve and activated peptide-specific T cells (Broz et al. 2014). This related to the pH of CD103 positive DC endocytic compartments being more permissive to efficient cross-presentation and their secretion of IL-12, CXCL9 and CXCL10. These chemokines bind CXCR3 on CD8 T cells in tumours with high levels of CD8 T cell infiltration (Broz et al., 2014; Spranger et al., 2017). Conversely, CD11b positive DCs secrete immunosuppressive IL-10, express PD-L1 and are transcriptionally alike immunosuppressive tumour-associated macrophage (TAM; Broz et al., 2014). Supporting each DC populations opposing role in tumour immunity, human cancer TCGA datasets revealed overall survival was improved if the CD103 positive/negative DC ratio was high (negative consisting of CD11b DCs and TAMs).

Despite the capability of some tumour-associated DCs to promote revolutions of the cancer immunity cycle, DC functions are subverted to enable tumours to escape immune surveillance and therefore immune control. This was demonstrated in a p53/KRAS-driven model of ovarian carcinoma, which recapitulates DC populations from primary tumours (Scarlett et al. 2012). Scarlett and colleagues found whilst T cells were a large majority of hematopoietic cells within the tumour during the equilibrium phase, tumour escape and outgrowth was associated with an increased proportion of DCs (Scarlett et al. 2012). To demonstrate the role of DCs in the loss of T cell tumour control, Scarlett et al co-cultured CD3 T cells and either: DCs from the tumour-draining lymph nodes of tumours at equilibria with the immune system, or DCs from the draining lymph nodes of tumours escaping immune control. They demonstrated an inhibition of T cell proliferation by DCs from 'escaping' tumours but

not DCs from tumours at equilibria (Scarlett et al. 2012). This ties loss of immune control with a change in the context of antigen presentation by tumour-associated DCs. Indeed, tumour infiltrating DCs had higher levels of surface PD-L1, and lower levels of MHCII and CD40 at later stages. Further, they had increased arginase I activity which sequesters arginine from activated T cells curbing function (Scarlett et al. 2012). Therefore, they could directly induce CD8 T cell dysfunction and decrease presentation and co-stimulation to CD4 T helper cells. (Scarlett et al. 2012).

In addition to 'conventional' myeloid-like DCs, plasmacytoid DCs (pDC) have been identified in cutaneous melanomas and metastases, and a higher frequency of pDC infiltration in tumours significantly reduced patient survival (Aspord et al. 2013). pDC infiltration was also demonstrated in melanoma xenograft-bearing humanised mice, and both murine and human pDCs from tumour-draining lymph node could induce naïve CD4 T cell secretion of immunosuppressive cytokines (IL -5, -10 and -13) following *in vitro* stimulation. Patient tumour-derived pDCs expressed OX40L, and ICOSL and their blockade in the same assay significantly reduced IL- 5 and -13 or IL-10, respectively (Aspord et al. 2013). The authors reference tumour infiltrating T_{REG}s which express the ICOSL binding partner (ICOS), and suggest they facilitate plasmacytoid DC ICOSL ligation and consequent DC immunosuppression.

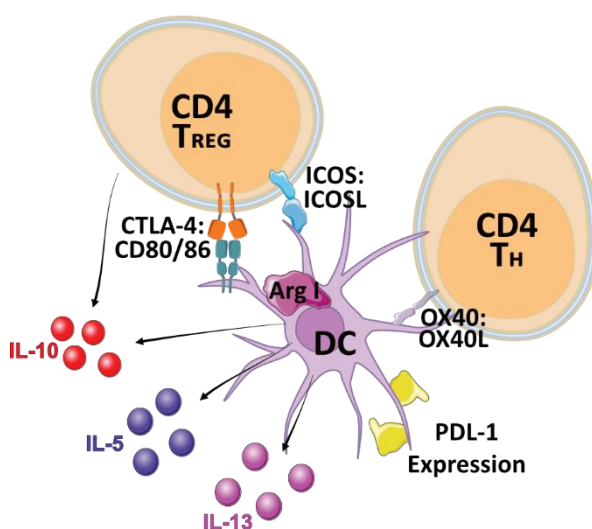


Figure 1.8. Direct and indirect immunosuppressive functions of dendritic cells within the tumour microenvironment. Through ICOS:ICOSL and CTLA-4:CD80/86 interactions T_{REG}s cause tumour infiltrating dendritic cells to secrete immunosuppressive cytokines (Aspord et al., 2013) and sequester and degrade stimulatory ligands (Kim et al., 2019; Wing et al., 2008), respectively. Similarly, CD4 T_H cells engage OX40L to induce tumour infiltrating dendritic cell secretion of immunosuppressive (IL-10) and pro-tumoural cytokines (IL-5 and IL-13 ;Aspord et al., 2013). Dendritic cells also express PDL-1 and arginase I which sequesters arginine from CD8 T cells (Scarlett et al., 2012).

1.5.3. Tumour-associated macrophages

In a recent meta-analysis of tumour-associated macrophage (TAM) in several cancer types, their infiltration correlated with worse overall survival in gastric, breast, bladder, ovarian, oral and thyroid cancers (Zhang et al. 2012). Within breast cancers, Broz and colleagues demonstrated that whilst murine TAMs have high levels of MHCII, CD80 and CD86 and the ability to take up antigen, they express PD-L1 and cannot sufficiently cross-present antigen and therefore cannot activate naïve antigen-specific CD8 T cells as measured by CD69 expression (Broz et al. 2014). Further, following the culture of peripheral blood macrophages in breast cancer cell line-conditioned media, macrophage differentiated to an immunosuppressive phenotype and produced higher levels of the pro-tumoural cytokines IL-6, IL-8 and IL-10 (table 1.2, Sousa et al., 2015). In several metastatic murine models of mammary carcinoma, two main myeloid populations were present within the lungs, namely TAMs and MDSCs, and elevated in number relative to control mouse lung tissue (Hamilton et al. 2014). Interestingly, whilst MDSCs were largely at the periphery of the tumour, the macrophages were found throughout the tumour (Hamilton et al. 2014). Isolated macrophages suppressed T cell IFN γ production and proliferation *in vitro* and were more inhibitory than tumour-derived MDSCs (Hamilton et al. 2014). Western blotting also revealed arginase I expression by TAMs but not by MDSCs (Hamilton et al. 2014), which may explain their enhanced suppressive ability. However, this is in disagreement with data from Liu et al., who demonstrated that MDSCs express arginase I in response to murine ovarian cancer cell line supernatant (Liu et al. 2009).

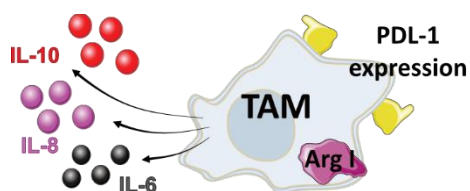


Figure 1.9. Immunosuppressive functions of tumour associated macrophage. TAM contribute to the pool of immunosuppressive IL-10 (Ruffell et al., 2014) and express PDL-1 (Broz et al., 2014) and arginase I, sequestering arginine from CD8 T cells (Hamilton et al., 2014).

1.5.4. Myeloid-derived suppressor cells

MDSCs are myeloid lineage progenitor cells, which are broadly categorised as polymorphonuclear and monocytic (Bronte et al. 2016). An ambitious study by Youn

and colleagues evaluated ten subcutaneous tumour mouse models, covering lung, breast, and colon cancer, as well as melanoma and sarcoma, and identified substantially elevated levels of polymorphonuclear MDSCs circulating in all mice (Youn et al. 2008). Further, slightly elevated levels of monocytic MDSCs were found in mice bearing thymoma, lung cell and mammary carcinoma relative to control mice, demonstrating that MDSCs are a pan-cancer feature of the TME (Youn et al. 2008). As indicated by hypoxia-induced PD-L1 expression and pro-tumoural cytokine secretion, MDSCs gain immunosuppressive function within the TME (Noman et al. 2014). Additionally, when co-cultured with peptide-pulsed splenocytes, monocytic MDSCs produced higher levels of nitric oxide (NO), whilst granulocytic MDSCs exhibited higher levels of reactive oxygen species (ROS) relative to one another (Youn et al. 2008). Both granulocytic and monocytic MDSC populations inhibited IFN γ production by peptide-pulsed splenocytes, which could be relieved by specific inhibitors of ROS or NO production, respectively (Youn et al. 2008), highlighting MDSC subpopulation-specific mechanisms that can mediate T cell inhibition. However, only circulating MDSCs and not tumour-derived MDSCs were studied. Although, tumour-derived MDSCs from metastatic melanoma-bearing mice also greatly limit splenocyte proliferation and IFN γ production relative to monocytic granulocytes from tumour-free mouse spleens (Hamilton et al. 2014).

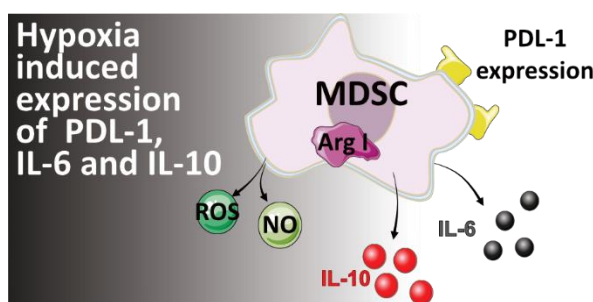


Figure 1.10. Immunosuppressive functions of myeloid derived suppressor cells. Hypoxia in the tumour microenvironment induces PDL-1 expression and the production of IL-6 and IL-10 by MDSCs (Noman et al., 2014). Other factors produced by MDSCs which hamper T cell function include: ROS and NO (Youn et al., 2008) and arginase I (Liu et al., 2009).

Martinet and colleagues demonstrated that patients with HEV-high tumours have a better prognosis, and HEVs are infiltrated by L-selectin expressing cells (Martinet et al., 2011). Schrama et al induced tumour HEV neogenesis by targeting LT α to the TME, which was associated with improved survival of tumour bearing mice and infiltration of new tumour reactive T cell clones (Schrama et al. 2001). Together,

these studies indicate that entry of L-selectin expressing T cells via tumour HEVs improve tumour control. Murine breast adenocarcinoma MDSCs can limit expression of L-selectin on non-activated CD4 and CD8 T cells *in vivo* (CD44 low T cells; Ku et al., 2016). L-selectin expression was partially rescued by partial MDSC depletion *in vivo*, and co-culture with MDSCs *in vitro* limited CD8 T cell L-selectin expression (Ku et al. 2016). Whilst L-selectin downregulation was suggested to be mediated by MDSC expression of trans-acting ADAM17, MDSC induced T cell L-selectin proteolysis has been shown to be independent of ADAM17 (Hanson et al. 2009; Ku et al. 2016). In lymph node trafficking experiments, adoptively transferred CD44 low CD8 T cells from control mice entered lymph nodes under homeostatic conditions, whilst CD8 T cells from tumour-bearing mice did not (Ku et al. 2016). In comparable experiments, in which peptide vaccination had also been administered, this inability to traffic to lymph node translated to a 70:1 ratio of activated CD8 T cells from control:tumour bearing mice in the draining lymph node (Ku et al. 2016). This study demonstrates that MDSC abrogation of L-selectin positive T cell priming at tumour-draining lymph nodes subverts the cancer immunity cycle and prevent spontaneous clearance of tumours.

1.5.5. T regulatory cells

In normal tissues, T_{REGs} suppress CD4 and CD8 effector function to ensure peripheral tolerance. By performing a similar role in the tumour, T_{REGs} mediate tumour escape of immune surveillance. Evaluation of stage IV non-small cell lung, gastric, colon and breast cancer patient tissues found malignant effusions had elevated frequencies of T_{REGs} relative to matched peripheral blood. Further, the frequency of T_{REGs} was elevated further still within the cancerous tissue relative to malignant effusions (Kim et al., 2019). Highlighting the significant role they play in cancer immunosuppression, T_{REG} infiltrates negatively correlated with overall survival and increased the risk of relapse in breast cancer patients (Bates et al. 2006). In addition, a low intraepithelial CD3/T_{REG} ratio determined in 101 biopsied tissues was associated with reduced disease free survival of colon carcinoma patients at a 5-year follow-up (Sinicrope et al. 2009), and a high intraepithelial CD8/T_{REG} ratio within ovarian cancer was also associated with improved median survival (Sato et al., 2005).

T_{REGs} have several modes of mediating immunosuppression, which are both contact - independent and -dependent, which are summarised in Table 1.1 and Fig. 1.11.

T _{REG} function	Effect	Experimental evidence
Contact independent		
Expression of the high affinity IL2-R	IL-2 enhances T _{REG} proliferation and sequesters IL-2 from CD8 T cells limiting proliferation	Assessment of antigen specific CD8 T cell numbers and IL-2 levels in immunised mice with and without T _{REG} depletion or IL-2R blockade (McNally et al. 2011).
Secretion of TGFβ (Duraismamy et al. 2013)	Binds the TGFβ receptor on CD8 T cells preventing control of tumour growth.	Adoptive transfer of cancer-specific CD8 T cells into tumour bearing mice controls tumour growth and no difference is observed if CD8 T cells express a non-signalling TGFβ receptor (nsTGFβR). Tumour control is curbed by adoptive transfer of T _{REGs} but not if CD8 T cells express the nsTGFβR (Chen et al. 2005).
Secretion of IL-10 and IL-35	Increased expression of immune checkpoints (PD-1, TIM-3, LAG-3, TIGIT) on CD8 TILs	Reduced expression of immune checkpoints (PD-1, TIM-3, LAG-3, TIGIT) on CD8 TILs from melanoma and thymoma bearing mice if T _{REGs} are IL-10 or IL-35 null. (Sawant et al. 2019).
Contact dependent		
T _{REG} PD-1 expression is elevated in the TME	Limited CD8 T cell IFNγ secretion and proliferation.	Lung cancer-derived murine T _{REGs} potently suppressed murine CD8 T cell proliferation and IFNγ production in vitro, which could be partially restored by pre-incubation of T _{REGs} with anti-PD-1 (Kim et al. 2019).
T _{REG} expression of gzm B	Limiting proliferation and inducing death of CD4 T helper (T _H) cells	Granzyme B-knockout T _{REGs} were less able to inhibit CD4 effector cell proliferation than wildtype T _{REGs} . T _{REGs} were also able to induce CD4 effector T cell death (Gondek et al. 2005).
T _{REG} expression of CTLA-4	Sequesters co-stimulatory ligands CD80 and CD86 and reduces their expression.	T _{REGs} reduced APC expression of CD80 and CD86 <i>in vitro</i> , specific knockdown of CTLA-4 in T _{REGs} mediated partial restoration of APC co-stimulatory ligand expression (Wing et al. 2008)

Table 1.1. T_{REGs} and their immunosuppressive mechanisms. The mechanisms by which T_{REG} cells limit anti tumoural effector function by T cells are summarised within this table and references cited within.

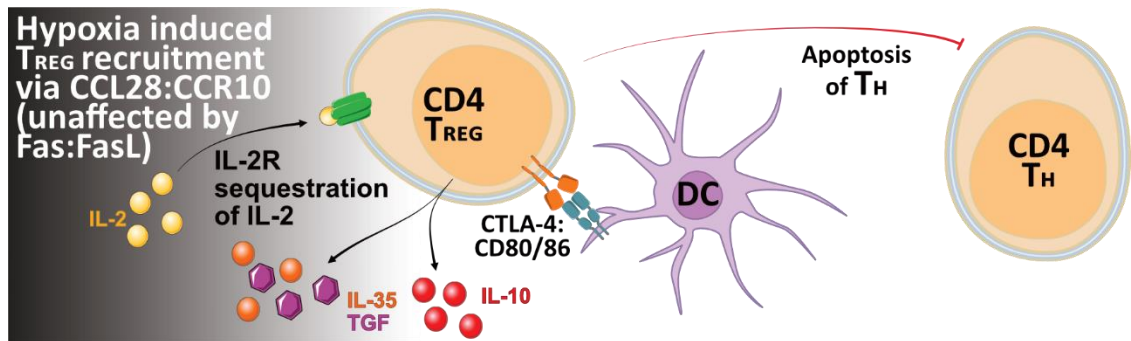


Figure 1.11. Immunosuppressive functions of TREGs. Hypoxia that preferentially recruit TREGs via CCL28:CCL10 (Facciabene et al., 2011) which is unaffected by FasL on tumour vascular endothelial cells (Motz et al., 2014). TREGs sequester IL-2 due to their constitutive expression of the high affinity IL-2 receptor (McNally et al., 2011), secrete TGF, IL-10 and IL-35 (Chen et al., 2005; Sawant et al., 2019) and induce apoptosis of CD4 TH cells (Gondek et al., 2005). Additionally, through CTLA-4:CD80/86 interactions TREGs sequester and degrade stimulatory ligands (Kim et al., 2019; Wing et al., 2008).

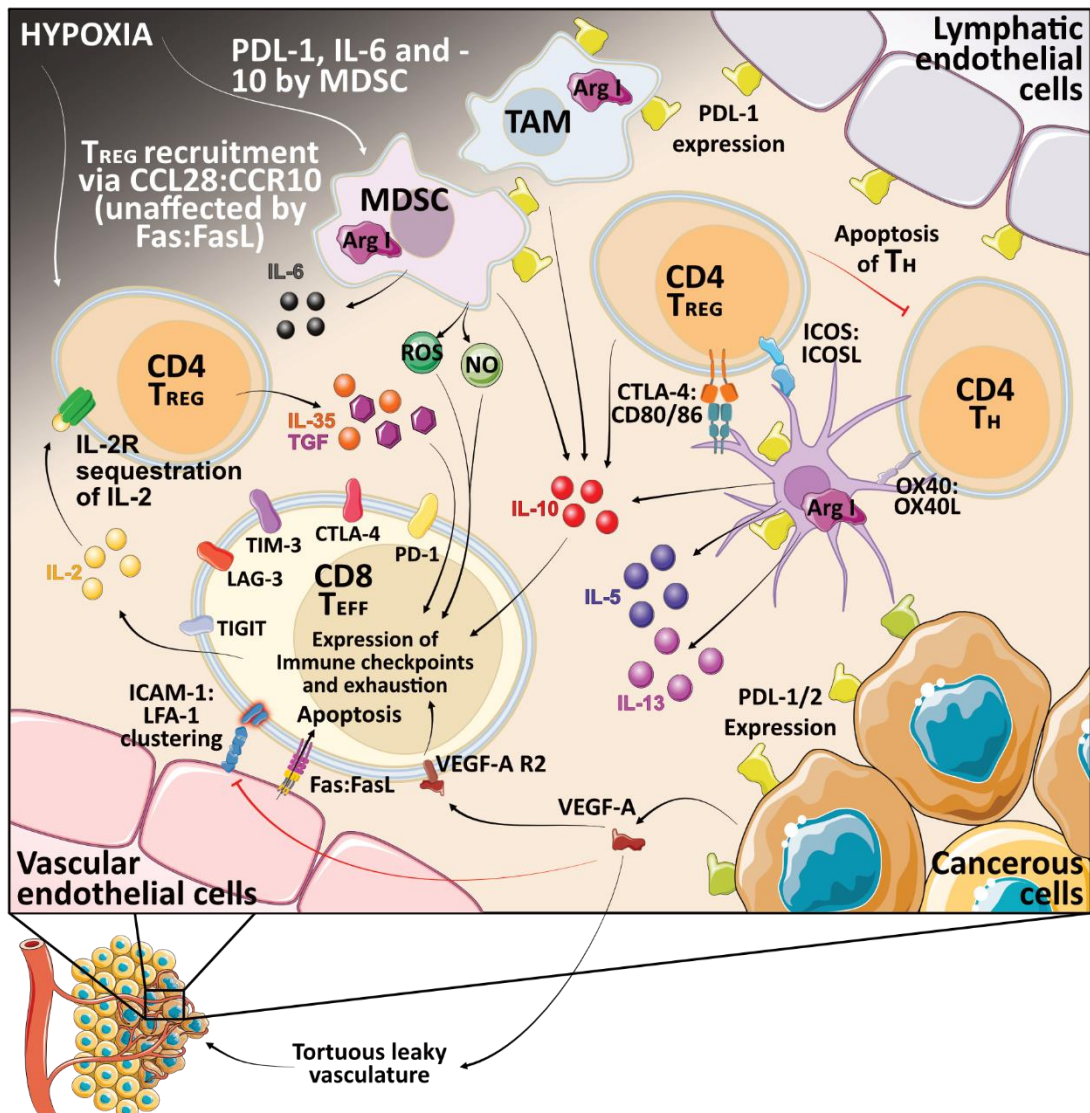


Figure 1.12. Summary of CD8 cytotoxic T cell immunosuppression within the tumour microenvironment. Cancerous tissues secrete VEGF-A which through angiogenesis promotes the development of a tortuous, leaky vascular network (Ager et al., 2016; Lou et al., 2006). This network produces regions of hypoxia that preferentially recruit TREGs via CCL28:CCL10 (Facciabene et al., 2011) and upregulate PDL-1 expression and the production of IL-6 and IL-10 by MDSCs (Noman et al., 2014). The recruitment of CD8 T cells is hampered by improper clustering of ICAM-1 and CD8 T cells binding VEGF-A via their VEGF-A receptor 2 promotes expression of immune checkpoint ligands (Bouzin et al., 2007; Voron et al., 2015). In addition, CD8 T cell expression of Fas in the microenvironment induces T cell apoptosis following ligation by FasL on tumour vascular endothelial cells which does not affect TREGs (Motz et al., 2014). These TREGs sequester IL-2 due to their constitutive expression of the high affinity IL-2 receptor (McNally et al., 2011), secrete TGF, IL-10 and IL-35 (Chen et al., 2005; Sawant et al., 2019) and induce apoptosis of CD4 TH cells (Gondek et al., 2005). Additionally, through ICOS:ICOSL and CTLA-4:B7.80/86 interactions TREGs cause tumour infiltrating dendritic cells to secrete immunosuppressive cytokines (Aspord et al., 2013) and sequester and degrade stimulatory ligands (Kim et al., 2019; Wing et al., 2008), respectively. Similarly, CD4 TH cells engage OX40L to induce tumour infiltrating dendritic cell secretion of immunosuppressive (IL-10) and pro-tumoural cytokines (IL-5 and IL-13; Aspord et al., 2013). TAM also contribute to the pool of IL10 (Ruffell et al., 2014). Other soluble factors which hamper T cell function include: arginase I, expressed by TAMs, (Hamilton et al., 2014), MDSCs (Liu et al., 2009) and dendritic cells (Scarlett et al., 2012) as well as ROS and NO which are produced by MDSCs (Youn et al., 2008). All the above soluble factors promote T cell exhaustion and expression of immune checkpoints that, if ligated, can dampen T cell function. Cancerous cells express the immune checkpoint ligands PDL-1 and PDL-2 whilst lymphatic endothelial cells (Dieterich et al., 2017), MDSCs (Noman et al., 2014), TAMs (Broz et al., 2014) and dendritic cells (Scarlett et al., 2012) express PDL-1.

1.6.0. T cell signalling and dysfunction in the tumour microenvironment

As discussed in 1.5.0, tumour-infiltrating DCs, TAMs, MDSCs and T_{REGS} express several immune checkpoint ligands and soluble factors, which curb T cell effector function and arrest the cancer immunity cycle at steps 5 and 6 (Fig. 1.1). The curbing of these functions depends on the immunosuppressive factors inducing dysfunctional T cell signalling.

1.6.1. Functional T cell signalling

For *in vitro* T cell culture, activation primarily relies upon the three-signal hypothesis: (1) recognition of the cognate pMHC by the TCR complex, (2) co-stimulation-mediated by CD28 ligation and (3) stimulatory cytokines. Within this thesis, to generate cancer-specific T cells, signal 1 and 2 were substituted with anti-CD3 and anti-CD28 binding, respectively, and IL-2 provided signal 3. Although, as discussed in 1.3.4 this may skew T cells towards short-lived T effector cells (Pipkin et al. 2010).

The TCR complex is made up of several components of which the α/β heterodimer has been determined responsible for T cell specificity through gene transfer experiments (Saito and Germain 1987) and CD3 dimers ($\gamma\epsilon$, $\zeta\zeta$, $\delta\epsilon$) for potentiating intracellular signals. Cross-linked chimeras containing ζ intracellular regions revealed these CD3 dimers possessed immunoreceptor tyrosine-based activation motifs (ITAMs; Romeo et al., 1992). When the CD3 ζ ITAMs were phosphorylated, they potentiated downstream activation signals within T cells (Letourneur and Klausner 1992). The arrangement of these transmembrane proteins on the cell surface is debated owing to the various detergents used to isolate them for analysis but for the typically presented arrangement see Fig. 1.3A (Alarcón et al., 2006).

To mediate naïve CD8 T cell activation, the pMHC I interacts not just with the specific TCR but also with the CD8 co-receptor, which crystallography of the murine structure has demonstrated stabilises the pMHC I and TCR interaction (Wang et al. 2009). For the human TCR and pMHC I interaction, the CD8 co-receptor stabilises this by approximately 2-fold (Wooldridge et al. 2005). Additionally, in T cell lines, immunoprecipitation of CD8 pulls down the tyrosine kinase Lck, which

phosphorylated CD8 and induced CD3 ITAM phosphorylation (Barber et al. 1989), indicating the TCR and CD8 co-receptor together potentiate downstream signalling. Using transfected cell lines, pulldowns revealed Lck phosphorylates ITAMs which enable Zap-70 association and consequent phosphorylation and activation by Lck. Zap-70 is then able to heavily phosphorylate linker of activation for T cells (LAT), which acts as a scaffold for protein recruitment (Zhang et al., 1998). Indeed, CD8 and LAT were recruited to the interface between target cells and cytotoxic T cells (the immune synapse) together within 2 minutes following TCR pMHC engagement (Purbhoo et al. 2004). By LAT pulldown in Jurkat cell lysates, TCR cross-linkage mediated the formation of a complex containing phospholipase (PLC) γ 1, Cbl, Vav, Slp76 (Zhang et al. 1998), which alongside phosphoinositide 3-kinase (PI3K), Grb2-SOS, ADAP and Itk, form a membrane-proximal signalosome (Smith-Garvin et al. 2009). This membrane-proximal signalosome is one of 4 major signalling pathways necessary for T cell activation, which are outlined here and summarised in Fig. 1.13.

The membrane-proximal signalosome

Downstream of the signalosome pathway, activated PLC γ 1 has been demonstrated as crucial for initiation of AP-1 and NFAT transcriptional programs (Zhang et al. 1998). PLC γ 1 hydrolyses of PIP₂ to release diacylglycerol (DAG) and inositol trisphosphate (IP₃), which each signal downstream via different mechanisms (Hwang et al. 2020). PMA is used within this thesis as a potent inducer of ADAM-17 proteolysis (section 1.4.3) and activates T cells by binding RasGRP (Roose et al. 2005). RasGRP converts RasGDP to its active form (RasGTP) to potentiate signalling via ERK-1, -2 and AP-1 (Roose et al. 2005). RasGRP relies upon binding by DAG (which PMA mimics) for its activity (Roose et al. 2005). In RasGRP KO cells, reintroduction of RasGRP revealed it is necessary for CD69 upregulation but not intracellular calcium release following CD3 ζ signalling (Roose et al. 2005). Early studies using a partially permeabilised T cell line treated with purified IP₃ demonstrated it released intracellular Ca²⁺ (Imboden and Stobo 1985) and the recent review by Hwang and colleagues implicates IP₃ in calmodulin-dependent NFAT nuclear translocation (Hwang et al., 2020). PMA also induces release of intracellular Ca²⁺ which enables

calmodulin to disassociate from L-selectin's tail enabling ectodomain proteolysis (Matala et al. 2001).

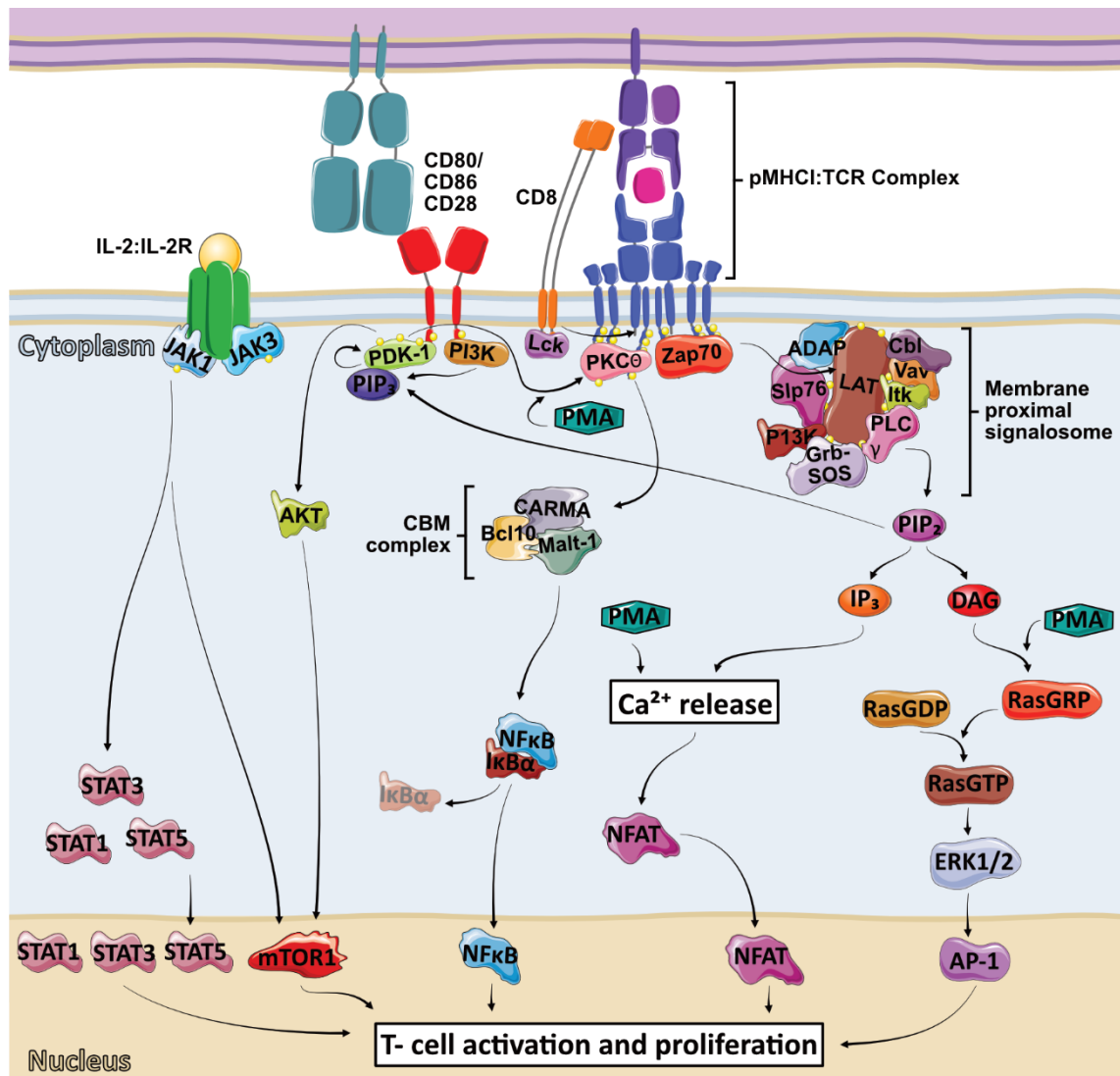


Figure 1.13. CD8 T cells are activated through several signalling pathways. T cells receive their activation signals through engagement of the TCR complex with its cognate pMHC, co-stimulation through CD28 interacting with its ligands CD80/86 and cytokines such as IL-2 (Waldman et al., 2020). The stabilising interaction with the CD8 co-receptor and MHC I recruits Lck kinase which phosphorylates CD3 signalling domains (Barber et al., 1989; Zhang et al., 1998; intracellular tyrosine activation motifs; ITAMs) enabling recruitment of PKCθ (Park et al., 2009) and ZAP70 (Zhang et al., 1998). ZAP70 phosphorylates linker for T cell activation (LAT) which enables the formation of the membrane proximal signalosome (Smith-Garvin et al., 2009). As part of this, PLCγ catalyses the degradation of PIP₂ to IP₃ and DAG which signal downstream via Ca²⁺ release and the RasGRP/ERK1/2 pathways, respectively (Imboden and Stobo, 1985; Roose et al., 2005; Hwang et al., 2020). Ligation of CD28 induces its phosphorylation and recruitment of PDK-1 (Park et al., 2009) and PI3K (Lu et al., 1998), the latter of which catalyses the conversion of PIP₂ to PIP₃ and PIP₃ recognition by PDK-1 (Park et al., 2009; Smith-Garvin et al., 2009). PDK-1 is then able to signal via the Akt/mTOR pathway and via PKAθ (Hwang et al., 2020) and the CBM complex to NFκB (Park et al., 2009). IL-2 binds to the IL-2R to signal via the JAK/STAT pathway (Miyazaki et al., 1994; Beadling et al., 1994; Ross et al., 2016).

PI3K, PDK-1 and PKC θ

The second pathway downstream of the phosphorylated ITAMs of the TCR complex relies upon recruitment of PKC θ . In a human T cell line, CD28 cross-linkage recruits PI3K, which catalyses PIP₃ formation (Lu et al., 1998). Using either anti-CD3, -CD28 or both, Park et al revealed PKC θ was recruited to the immunological synapse by anti-CD3 antibody binding, whilst CD28 binding recruits phosphoinositide-dependent kinase-1 (PDK-1; Park et al. 2009). PDK-1 recognises PIP₃, is autophosphorylated, and then can phosphorylate PKC θ which enables the formation of the trimolecular 'CBM' complex (Fig. 1.13; Smith-Garvin et al., 2009). Importantly, DAG (and therefore PMA) can also bind to and activate PKC θ (Hwang et al. 2020). CBM then mediates the degradation of the NF κ B regulatory domain I κ B α in the cytoplasm enabling NF κ B translocation to the nucleus where it mediates its role in T cell activation (Park et al. 2009; Smith-Garvin et al. 2009). These studies were the first to divulge why CD28 co-stimulation is necessary for T cell activation. In support of this, PDK-1 autophosphorylation was essential for CD69 and CD25 expression, IL-2 secretion, and proliferation during *in vitro* T cell activation (Park et al. 2009). The third pathway is also mediated by PDK-1 which signals via AKT and mTOR (Hwang et al. 2020).

IL-2 and the IL-2 receptor

The final pathway involves the IL-2 receptor, which has several configurations of its three subunits (α , β and γ), which vary in their affinity for IL-2 (Ross and Cantrell 2018). The intracellular domains of the IL-2 β and γ chains recruit Janus kinases (JAKs) -1 and -3 respectively (Miyazaki et al. 1994) within 5 minutes following human T cell treatment with IL-2, but not CD3 cross-linkage (Beadling et al. 1994). IL-2-R phosphorylation coincided with the IL-2-dependent binding of STAT transcription factors to target gene probes which were revealed to be STAT -1, -3 and possibly -5 (Beadling et al. 1994). Indeed, phosphoproteomic analysis of IL-2 signalling in IL-2 stimulated CD8 T cells revealed phosphorylation of STAT-5 and components of the mTOR signalling cascade, indicating that IL-2/IL-2 receptor signalling operates via several complex pathways in addition to the canonical JAK/STAT pathway (Ross et al. 2016). For example mTORC regulates both glucose metabolism (via Glut1 expression) on TCR/IL-2 stimulated CD8 cells and migration via expression of L-selectin and CCR7

(Finlay et al., 2012), whilst STAT5 is required for IL-2-induced proliferation of T cells (Moriggl et al., 1999). Ultimately, the transcription factors downstream of all four of these pathways co-operatively mediate the activation and proliferation of T cells.

1.6.2. Dysfunctional T cell signalling

Expression of immune checkpoints by tumour-infiltrating CD8 T cells

For immune checkpoint ligands to curtail tumour destruction, tumour-infiltrating T cells need to express immune checkpoints. This has been demonstrated in colon carcinoma and ovarian carcinoma murine models, where approximately one third of tumour-infiltrating CD8 lymphocytes were PD-1 positive, whilst another third were double positive for PD-1 and CTLA-4 (Duraiswamy et al. 2013). *In vitro* stimulation of a human TIL cell line with melanoma target cells induced greater expression of PD-1 upon T cells relative to peripheral blood T cells, indicating tumour-infiltrating CD8 T cells also more readily undergo immunosuppression (Blank et al. 2006). Importantly, the dysfunctional nature of TILs was increased by co-expression of PD-1 and CTLA-4 as *in vitro* stimulated double positive TILs showed reduced proliferation, L-selectin expression and produced less IFN γ , TNF, IL-2 and CD107a than those which were only PD-1 positive (Duraiswamy et al. 2013). This indicates these checkpoints act through distinct mechanisms which will be covered here and are summarised in Fig. 1.14. Further, if double positive for CTLA-4 and PD-1, they also expressed more of the emerging immune checkpoints TIM-3 and LAG-3.

Demonstrating the ability of immune checkpoints to limit T cell function, the proliferative potential of PD-1 positive TILs was restored by PD-1 blockade, but dual blockade was necessary if TILs were double positive for PD-1 and CTLA-4 (Duraiswamy et al. 2013). This may partly explain why dual checkpoint blockade benefited unresectable stage III melanoma patients over either single blockade in a phase III clinical trial. Here, median progression-free survival for those receiving blockade of PD-1, CTLA-4 or both was 6.9, 2.9 or 11.5 months, respectively (Larkin et al. 2015).

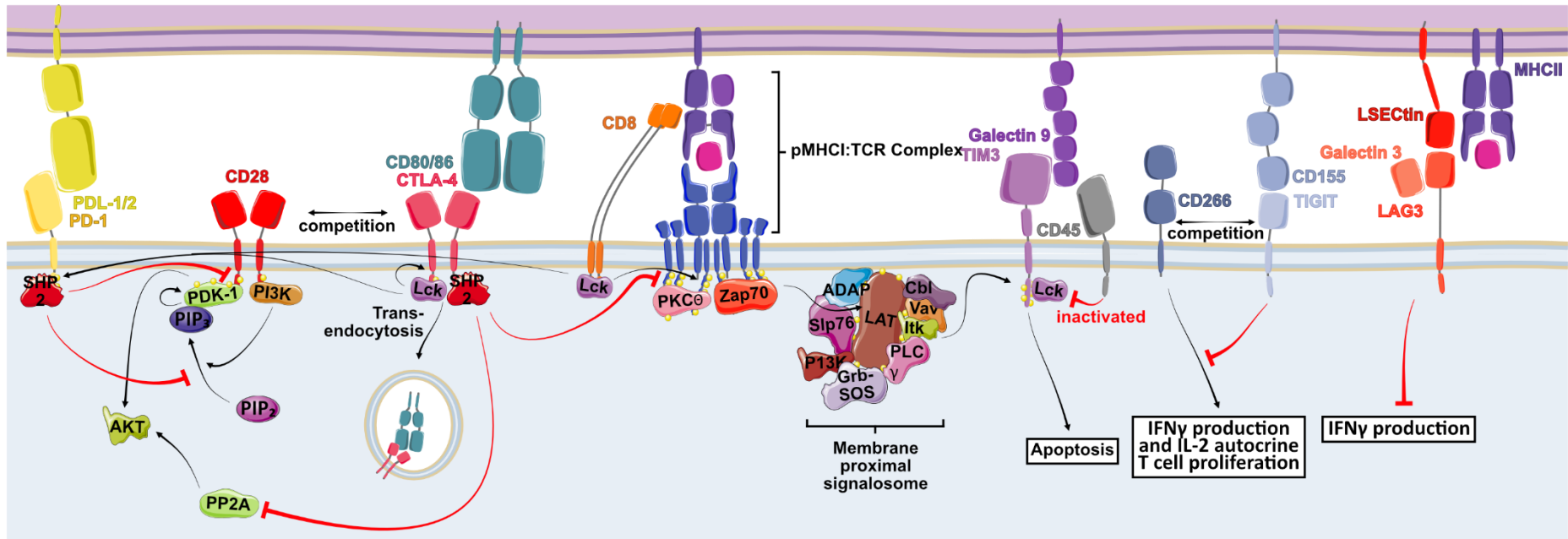


Figure 1.14. CD8 T cell signalling is abrogated by immune checkpoint ligation. T cells in the tumour microenvironment exhibit an exhausted phenotype and express the immune checkpoints: PD-1, CTLA-4, TIM-3, LAG-3 and TIGIT and those which express multiple exhibit greater dysfunction (Duraiwamy et al., 2013; Lozano et al., 2012) **(From left to right)** PDL-1/-2 ligation of PD-1 induces PD-1 intracellular domain phosphorylation and recruitment of SHP-2 which preferentially dephosphorylates CD28 (Hui et al., 2017) and prevents the formation of PIP₃ (Parry et al., 2005). CTLA-4 has a higher affinity for CD80/86 and competes with CD28 for ligand binding (Linsley et al., 1994) and once bound can undergo transendocytosis which together decrease the availability of the CD28 ligands (Qureshi et al., 2011). Additionally, CTLA-4 binds Lck and consequent phosphorylation enables the recruitment of SHP-2 that dephosphorylates the signalling ITAMs of the TCR complex curbing recruitment of downstream effectors (Chuang et al., 1999; Fraser et al., 1999) as well as dephosphorylating PP2A (Parry et al., 2005). Ligation of TIM-3 by its ligand galectin-9 causes its intracellular phosphorylation by Itk of the membrane proximal signalosome (van de Weyer et al., 2006) and association with CD45 which can inactivate Lck (Clayton et al., 2014). Phosphorylated TIM-3 associates with inactive Lck sequestering it from the active pool (Clayton et al., 2014). Further, ligation of Galectin-9 has been demonstrated to induce apoptosis (Kang et al., 2015). CD266 ligation induces T cell activation (IFN γ secretion and IL-2 autocrine T cell proliferation) and exists in a signalling axis with its ligand CD155 and its competitor TIGIT which limits CD266 function (Lozano et al., 2012). Whilst the downstream mechanism of LAG-3 is unknown, ligation by either of its ligands: galectin 3 or LSEctin curbs IFN γ production (Kouo et al., 2015; Xu et al., 2014).

CTLA-4 and PD-1

CTLA-4 is fully up-regulated as a homodimer on murine CD8 T cells 2 days following T cell activation *in vitro*, and blockade was able to augment T cell proliferation whilst CTLA-4 ligation prevented it (Walunas et al. 1994). These early results indicated CTLA-4 was a co-inhibitory receptor and further investigation found it utilises several mechanisms. Firstly, CTLA-4 competes with co-stimulatory CD28 for binding to CD80 and CD86 on APCs, which limits co-stimulatory signalling during T cell activation (Linsley et al. 1994). Furthermore, CTLA-4 is suggested to outcompete CD28 for these ligands as it has a 100-fold higher affinity for them (Linsley et al. 1994). Secondly, CTLA-4 ligation induces intercellular transfer of CD80 and CD86 from the surface of APCs to T cells. Qureshi et al demonstrated that trans-endocytosis of GFP-labelled CD86 into T cells occurs following CTLA-4 ligation *in vitro*, which can be prevented by CTLA-4 blockade (Qureshi et al. 2011). Finally, CTLA-4 possesses intracellular signalling domains, which modulate T cell signal transduction. CD3 cross-linkage dependent proliferation of T cells was prevented by CTLA-4 cross-linkage, but only if in close proximity to CD3 (Fraser et al. 1999). Mechanistically, in activated T cells, CTLA-4 co-precipitates with Lck and is tyrosine phosphorylated in its presence which recruits SHP-2 (Chuang et al. 1999). The SHP-2 phosphatase can then dephosphorylate signalling components of T cell activation. Indeed, luciferase reporters of downstream transcription factors AP-1, NFAT and NFκB were reduced in response to CTLA-4 cross-linking or ligation with a soluble Ig fusion protein (Fraser et al. 1999). In murine T cells, this resulted in decreased IL-2 production, decreased expression of CD25 and CD69 and mediated cell cycle arrest (Krummel and Allison 1996).

PD-1 is another immune checkpoint protein present on activated T cells which was detected in the thymus of mice following anti-CD3-induced cell death *in vivo* (Ishida et al. 1992). Similarly to the *in vitro* observations of CTLA-4 ligation, PD-1 ligation on CD3-crosslinked murine T cells curbed proliferation and limited IFNγ production (Freeman et al. 2000). Using a cell-free system and FRET, Hui and colleagues demonstrated that Lck phosphorylated the inhibitory signalling domain of PD-1, and this in turn also recruited SHP-2 (Hui et al. 2017). Interestingly, in this cell-free

system, CTLA-4 could not recruit SHP-2 which opposes earlier findings by Fraser et al indicating that other proteins may assist in CTLA-4 SHP-2 recruitment (Fraser et al. 1999; Hui et al. 2017). In this cell-free system, CD28 was the most sensitive to SHP-2 dephosphorylation of its tyrosine residues relative to CD3 (ζ) or any of its downstream signalling components. A human T cell line activated in the presence or absence of PD-L1 upon antigen presenting cells confirmed PD-1 preferential dephosphorylation of CD28 (Hui et al. 2017). Despite similar recruitment of SHP-2, CTLA-4 and PD-1 act on CD8 T cell function by different mechanisms. In a study by Parry et al, both inhibited phosphorylation and kinase activity of Akt. However, PD-1 did so by preventing the formation of the PI3K product, PIP₃, and CTLA-4 did so via the phosphatase, PP2A. Therefore, both checkpoints regulate Akt signal transduction, but via different mechanisms (Parry et al. 2005).

Emerging immune checkpoints

Beyond CTLA-4 and PD-1, several new immune checkpoints on T cells are beginning to be characterised in the context of the TME. Lymphocyte activation gene -3 (LAG-3) was originally identified in 1992 on *in vitro* activated human CD4 and CD8 T cells 24 hours following stimulation (Baixeras 1992). More recently, LAG-3 has been shown to be ligated by MHCII (MacLachlan et al. 2020), Fibrinogen-like protein 1 (Wang et al. 2019), LSEctin (Xu et al. 2014) and galectin-3 (Kouo et al. 2015). Galectin-3 and LSEctin were found to suppress TIL *in vivo* and tumour-draining lymph node T cell function *ex vivo*, respectively (as measured by IFN γ production; Kouo et al., 2015; Xu et al., 2014). However, the intracellular signalling mechanism of LAG-3 is unknown.

T-cell immunoglobulin and mucin domain-3 (TIM-3) is another upregulated immune checkpoint protein whose signalling capacity is currently being investigated. The TIM-3 intracellular domain contains a phosphorylatable tyrosine residue, which is phosphorylated by T cell kinase Itk following galectin-9 ligation (van de Weyer et al. 2006). TIM-3 expression is higher on TILs than on peripheral blood T cells isolated from colorectal cancer patients. Within the TIL population, TIM-3 expression on TILs correlates with Annexin V, suggesting that it has a role in inducing apoptosis (Kang et

al. 2015). This was confirmed in a comparable mouse model and importantly, *ex vivo* culture of TIL with recombinant galectin-9 increased annexin V binding which was abrogated using TIM-3 blockade (Kang et al. 2015). TIM-3 appears to mediate these effects by interfering with proximal TCR signalling, as it constitutively associates with Lck regardless of TIM-3 phosphorylation status. Conversely, during *in vitro* T cell activation, only in the presence of galectin-9 did CD45 (a phosphatase which inactivates Lck) co-precipitate TIM-3 and CD3. Therefore, TIM-3 constitutively associates with Lck but only following ligation by galectin-9, and consequent phosphorylation, does it associate with CD45. Lck is then inactivated by CD45 which abrogates TCR proximal signalling (Clayton et al. 2014).

Another upregulated checkpoint is T cell immunoreceptor with Ig and ITIM domains (TIGIT), which has been demonstrated upon CD4 T cells to have an immune axis based on ligand competition similar to CTLA-4, CD28 and their ligands (Lozano et al. 2012). By assessing T cell activation *in vitro*, a TIGIT agonist limited IL-2 production, CD25 expression and T cell proliferation (Lozano et al. 2012). To demonstrate the existence of an axis, blockade of either TIGIT's ligand on APCs, CD155, or its competitor on the T cell surface, CD226, curbed IFN γ production in TIGIT knockout cells (Lozano et al. 2012).

When taken together, immune checkpoint receptors all appear to impact on T cell signalling cascades by different mechanisms, and so it is unsurprising that their impacts on T cell dysfunction are cumulative (Duraiswamy et al. 2013).

Soluble immunosuppressive factors

Designation	Function
Stimulatory to T cells	
IL-2	Induces proliferation of T cells by autocrine signalling, is essential for T cell proliferation and skews T cell development toward effector T cell differentiation (Pipkin et al. 2010).
IL-7	Important for T cell homeostatic survival and proliferation.
IL-12	Development and maintenance of T _H 1 and dendritic cells which stimulate CD8 T cells. Enhances the cytotoxicity and IFN γ production by CD8 and NK T cells.
IL-18	Induces expression of IFN γ in the presence of IL-12, promotes CD4 T _H responses and enhances T cell cytotoxicity.
Pro-tumoural	
IL-4	CD4 cell differentiation to the T _H 2 subset, suppression of T cell proliferation <i>in vitro</i> (Mohammed et al. 2017), IFN γ related macrophage function and enhancer of pancreatic cancer cell growth (Prokopchuk et al. 2005).
IL-5	Induces growth, differentiation, and maturation of eosinophils as well as the differentiation and function of myeloid cells. Eosinophils are pro-metastatic and secrete CCL22 which recruits T _{REGS} to metastatic sites (Zaynagetdinov et al. 2015).
IL-6	Plays a role in acute inflammation and T cell proliferation during early infection. Described as a cytokine which 'cuts both ways' in the TME and can promote tumour cell survival and growth (Fisher et al. 2014).
IL-8	Chemoattractant for monocytes, macrophage, T cells and eosinophils as well as a stimulator of angiogenesis and elevated within several chronic inflammatory disorders.
IL-10	Inhibits macrophage function to mediate tissue homeostasis as well as downregulates CD28 signalling by SHP-2 recruitment in T cells. Induces expression of multiple immune checkpoints on CD8 T cells (Sawant et al. 2019)
IL-13	Signals through the chains common to the IL-4 receptor and activates the same signal transduction pathways. It has been demonstrated to reduce NKT cell mediated immunosurveillance (Terabe et al. 2000).
IL-35	Reduces effector T cell proliferation, increases T _{REG} proliferation and induces secretion of IL-10. Induces expression of multiple immune checkpoints on CD8 T cells (Sawant et al. 2019)

Table 1.2. Cytokines and their functions. Cytokines mentioned throughout this thesis as beneficial to T cell function or inhibitory and/or pro-tumoural are listed in this table and their pertinent roles in immunity are summarised (information adapted from Abbas and Lichtman and Akdis et al whilst additional tumour specific roles are cited within the table; Abbas and Lichtman, 2011; Akdis et al., 2016).

In addition to interleukins, which mediate CD8 T cell immunosuppression or are pro-tumoural (Table 1.2), several other soluble factors are secreted by tumour cell populations which curb cancer-specific T cell effector functions. Using murine

colorectal cancer models, knockdown of the TGF β receptor, Alk5, within CD8 T cells improved survival of tumour bearing mice, improved the number of TILs and their expression of granzyme B (Gunderson et al. 2020). Effector T cells express CXCR3 following activation, which can aid in tissue-specific homing (Ferguson and Engelhard 2010) and in homing assays, T cells without the capacity to signal via the TGF β receptor expressed CXCR3 and homed more effectively to tumours (Gunderson et al. 2020). Improved effector T cell tumour homing subsequently improved the survival of mice and this benefit was abrogated by CXCR3 blockade (Gunderson et al. 2020). Additionally, *in vitro* TGF β treatment downregulated CXCR3 expression during T cell activation indicating TGF β has a negative impact on T cell tumour homing (Gunderson et al. 2020). As well as defects in homing, the capacity of murine CD8 T cells to kill tumour cells *in vitro* is curbed in the presence of TGF β due to downregulation of FasL, perforin, granzyme A, granzyme B, IL-2 and IFN γ in T cells (Thomas and Massagué 2005).

The expression of arginase I by tumour-infiltrating immune populations can sequester arginine from tumour infiltrating CD8 T cells. When arginine is removed during *in vitro* culture of human T cell lines, the expression of CD3 ζ decreases progressively over time, beginning as early as 2 hours post-deprivation (Rodriguez et al. 2002). In addition, MDSCs produce high levels of NO, an arginine metabolite which has further detrimental effects on T cell proliferation (Youn et al. 2008). For example, splenocytes activated in the presence of MDSC-derived cell lines still produced IL-2, upregulated CD25 and CD69 but had their proliferation arrested (Mazzoni et al. 2002). Importantly, NO was produced in response to IFN γ , which is produced by activated T cells, and proliferation was restored if a NO synthase inhibitor was present during co-culture (Mazzoni et al. 2002). Together, this demonstrates NO is a potent mechanism by which MDSCs limit proliferation of activated TILs. In addition to NO, ROS are also produced by MDSCs, and this can have detrimental effects on TIL function (Youn et al. 2008). For example, TNF-induced NF κ B transcriptional activity was decreased in human T cell line if cells were pre-treated with ROS (Lahdenpohja et al. 1998). Further, ROS pre-treatment limited phosphorylation and transient degradation of the inhibitory binding partner of NF κ B

($\text{I}\kappa\text{B}\alpha$; Lahdenpohja et al., 1998), together demonstrating that chronic exposure to ROS can limit T cell activation-associated signalling pathways.

Here I have briefly covered some of the immunosuppressive mechanisms brought to bear on effector T cells within the TME and how these induce T cell dysfunction. Whilst this is not exhaustive, and does not consider the further complexity of differing populations in different tumour types and their cellular cross talk, it does outline the key obstacles to overcome for endogenously generated cancer-specific CD8 T cells to control the growth and progression of solid cancers.

1.7.0. Cancer immunotherapy

Arguably, the field of cancer immunotherapy began in 1891, when Coley's toxins were able to induce spontaneous remission of a patient's sarcoma. However, due to concerns regarding the injection of patients with pathogenic bacteria and the unknown mechanism of action, early immunotherapy was passed over in favour of radio- and chemo- therapy (Abbott and Ustoyev 2019). More recently, and what was my own introduction to cancer immunotherapy, was its naming as 'Scientific Breakthrough of the year' in 2013 owing to the success of immune checkpoint blockade in the treatment of metastatic melanoma (Hodi et al. 2010), for which it is now a first choice treatment for patients with stage III or IV melanoma. The discovery of perhaps the best known immune checkpoints, CTLA-4 and PD-1, and their implications in cancer therapy afforded Tasuku Honjo and James Allison the Nobel prize in 2018 (Huang and Chang 2019). Antibodies to these immune checkpoints block interactions which induce T cell dysfunction (section 1.7.2), but in doing so disrupt peripheral tolerance and cause drug-related adverse effects in up to 56.5 % of recipients (Wolchok et al. 2016).

1.7.1. Cell-based immunotherapies

More specific approaches of enhancing host T cell effector function consist of either expanding patient-derived tumour infiltrating T cells *ex vivo* and re-administering them (TIL therapy) or to take a patient's peripheral T cells and confer specificity for cancer cells to them before redelivering them (TCR and CAR-T therapy). TCR and

CAR-T cell therapies have been demonstrated to be successful in humans and mice, and the latter are used to study the underlying mechanisms of cell-based immunotherapies. For an overview of this process in each species, see Fig. 1.15.

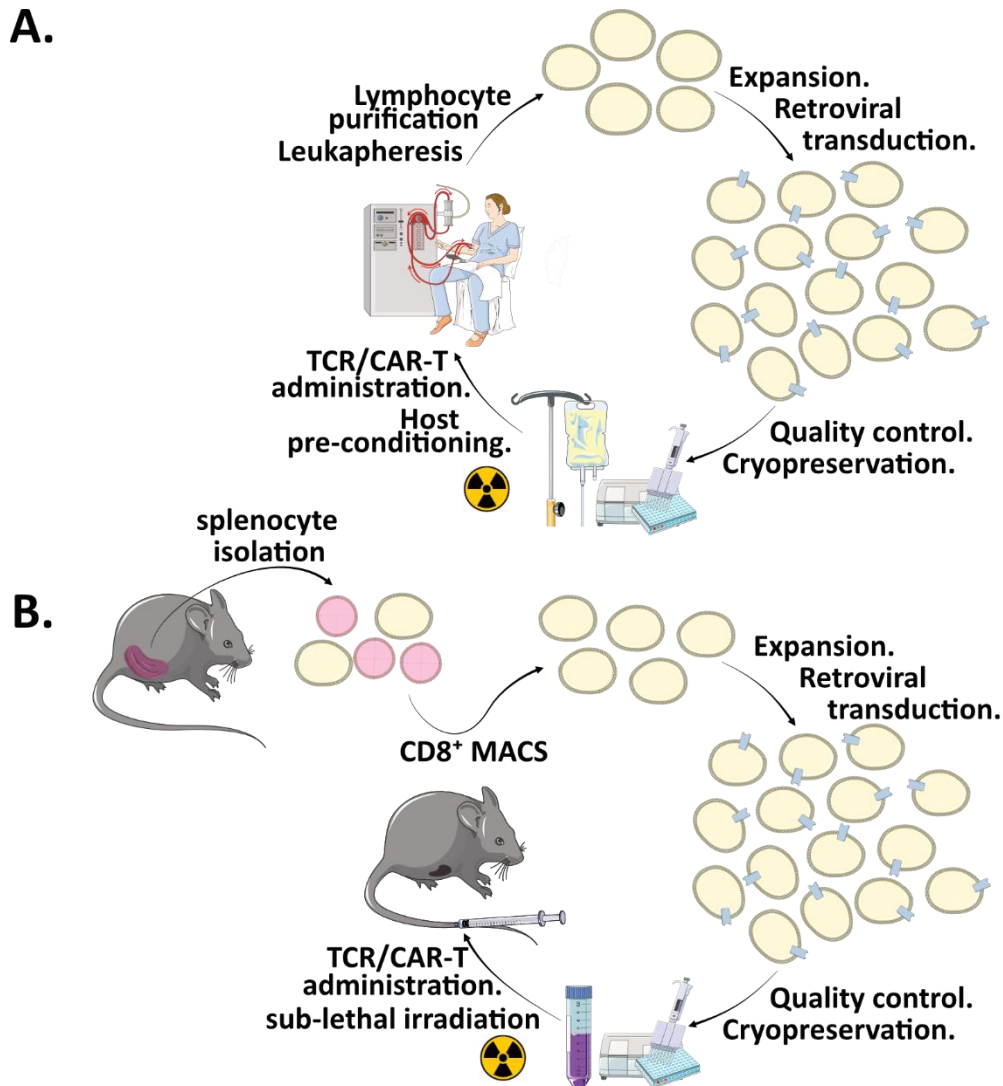


Figure 1.15. Overview of TCR/CAR T delivery. (A) In humans, T cells are isolated from patients peripheral blood before *in vitro* activation, modification by transduction, and expansion. Transduced T cells are then tested to ensure a high quality product (purity) and re-infused into the patient. The patient may or may not have received pre-conditioning with cyclophosphamide (information adapted from Zhao and Cao., 2019). **(B)** Within this thesis, a similar protocol is followed in the laboratory setting using splenocytes from donor mice as the source of lymphocytes from which CD8 T cells are purified. Mice undergo pre-conditioning in the form of sub-lethal total body irradiation.

Chimeric antigen receptor-engineered T cells

Chimeric antigen receptors (CARs) can redirect the T cell response to a specific protein expressed on the target cancer cell in a non-MHC restricted manner. Early attempts to generate chimeric antibody and T cell receptor based proteins capable

of conferring cancer specificity incorporated a single chain variable fragment (scFv) specific for a native tumour-associated epitope (target antigen), a hinge and transmembrane region of either CD3, CD8 or CD4, and the signalling domain of CD3 ζ (Rafiq et al. 2020). However, when this CAR was expressed in T_N transgenic mouse T cells, cross-linking this chimeric protein failed to induce T cell proliferation (Brocker and Karjalainen 1995). This indicated that a stimulatory signalling element was missing from these 1st generation CARs (Fig. 1.16). Maher and colleagues incorporated a CD28 costimulatory domain between the transmembrane domain and C-terminal CD3 ζ domain (Maher et al. 2002). When this second generation CAR construct was transduced into human peripheral blood T cells, this induced secretion of IL-2 and killing of target cells during co-culture experiments, which was not seen using T cells expressing constructs lacking the CD28 costimulatory domain (Maher et al. 2002). Importantly, secretion and killing could be mediated without the CD28 costimulatory domain if target cells expressed the CD28 ligand, CD80, indicating this domain is essential for T cell co-stimulation during recognition of target protein-expressing cells (Maher et al. 2002).

This is called a 2nd generation CAR (Fig. 1.16) and when 1st and 2nd generation CD19-targeting CAR T cells were administered to treat six non-Hodgkin's lymphoma patients, 2nd generation CARs had significantly higher persistence at 6-weeks post infusion and, importantly, appeared to be the only CAR-T cells at cutaneous lesions, clearly demonstrating the superiority of 2nd generation CARs for clinical use (Savoldo et al. 2011). Since then, a long-term follow up of 2nd generation CD19 CAR T cells used to treat acute lymphoblastic leukaemia patients in a phase I clinical trial showed that 83 % of patients had complete remission (Park et al. 2018). Those in remission with minimal residual disease had a median survival of 6.6 months, whilst those with undetectable disease had a median survival of 20.7 months. This is impressive considering patients treated with approved chemotherapeutics (Blinatumomab and Inotuzumab) had a median survival of only 7.7 months (Park et al. 2018).

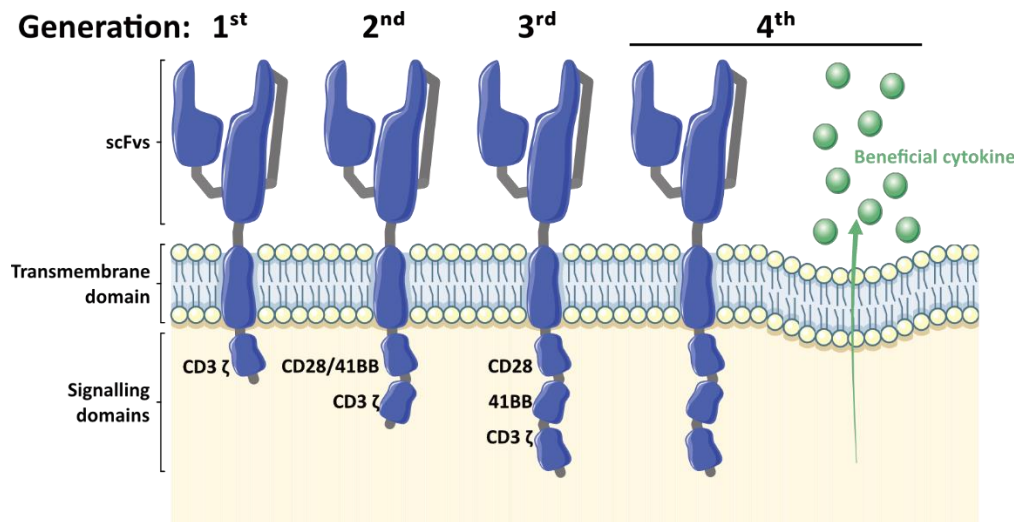


Figure 1.16. The chimeric antigen receptor has developed across several generations. Each generation of CAR within CAR-T cells has altered their efficacy and engraftment. The first generation of CAR constructs contained only the CD3 signalling domain and was unable to induce initial activation unless CD28 co-stimulation was also provided (Maher et al., 2002). Second generation CAR constructs did not have this limitation (Maher et al., 2002) and better engrafted in patients (Savoldo et al., 2011). Third generation constructs incorporate multiple beneficial signalling domains which improve engraftment in patients (Ramos et al., 2018) whilst fourth generation CAR-T cells possess an additional beneficial transgene (information adapted from Zhao and Cao., 2016).

2nd generation CARs have extended patient survival in the clinic, but when the scFv domain has been changed to different cancer targets, new issues have arisen. Human CAR T cells targeting the same human cancer via distinct scFv domains that bind to either a cancer antigen (GD2, a neuroblastoma and sarcoma-associated target) or to a transduced antigen (CD19), showed comparable killing of tumour cells *in vitro*. However, during an *in vivo* xenograft model, only the CD19 CAR T cells persisted in the spleen and tumour compartments and controlled tumour growth (Long et al. 2015). During *ex vivo* expansion using anti-CD3/CD28, T cells expressing the GD2-targeting CAR exhibited an exhausted phenotype (PD-1, TIM-3 and LAG-3 positive) and reduced secretion of pro-inflammatory cytokines (IL-2, TNF, IFN γ ; Long et al., 2015), whilst those expressing CD19 CAR did not. The exhausted phenotype was prevented by mutating the GD2-CAR CD3 ζ signalling domains to prevent their phosphorylation. This phosphorylation was found to be constitutive for the GD2 targeting CAR due to spontaneous cross-linking in the absence of CAR target ligation (Long et al. 2015). This is referred to as tonic signalling. Long et al demonstrated that by replacing the costimulatory domain of CD28 with that from 41BB, a late T cell activation co-stimulatory protein, exhaustion was mitigated. With this signalling

domain, GD2 CAR T cells had comparable TNF secretion and partial restoration of IL-2 and IFN γ secretion compared to CD19 CAR T cells with a CD28 signalling domain. Further, GD2 CAR T cells with the 41BB domain could control tumour growth *in vivo* (Long et al. 2015). CARs incorporating the 41BB signalling domain in place of CD28 are still considered to be 2nd generation CAR-T cells.

In a phase 1-2a trial using CD19 targeted CARs with a 41BB co-stimulatory domain to treat relapsed or refractory acute lymphoblastic leukaemia, 81 % of patients had complete remission with no residual disease and 76 % of patients survived at 12 months with CAR-T cells persisting in the peripheral blood for up to 20 months (Maude et al. 2018). Conclusions regarding efficacy cannot be drawn between Park et al (whose CD19 targeting CAR contained a CD28 costimulatory domain) and Maude et al, as different patient groups were treated, although CARs incorporating either CD28, 41BB or CD27 co-stimulatory domains have been compared *in vivo* (Song et al. 2012). Using a xenograft model of human ovarian cancer, and CARs targeting the folate receptor, Song and colleagues demonstrated that co-stimulation with any domain enabled CAR-T cells to comparably control tumour growth. However, only 2nd generation CARs with 41BB and CD27 costimulatory domains elevated CD4 and CD8 T cell counts in peripheral blood 3-weeks post administration (Song et al. 2012). It may be that this is increased *in vivo* persistence, but as the frequency of CAR positive events was significantly elevated on isolated peripheral cells in mice receiving the CAR with CD28 co-stimulation rather than CD27 or 41BB stimulation, no increased frequency of CAR positive T cells was observed in the blood between the co-stimulatory domains (Song et al. 2012). Thus, multiple 2nd generation CARs exist, and there is evidence that 41BB co-stimulation limits exhausted phenotypes *in vivo*, although 41BB CAR expression may be reduced relative to CD28 CARs, which may affect efficacy.

In the treatment of relapsing remitting non-Hodgkin's lymphoma using CARs incorporating either the CD28 or 41BB co-stimulatory domain, the CD28 domain group had more drastic side effects. In the study, one patient receiving a 41BB CAR experienced grade 3 neutropenia, which was the highest-grade side effect for that

treatment group. In contrast, for the CD28 CAR, one patient experienced grade 4 neutropenia, another grade 4 neurotoxicity, another grade 4 seizures, and another terminal grade 5 cytokine release syndrome, which resulted in termination of the CD28 CAR arm of the study (Ying et al. 2019). Thus, 2nd generation CAR-T cells incorporating 41BB rather than CD28 may be better tolerated in clinical use.

Due to the durable response rates and efficacy of CAR-T therapy for haematological malignancies, CD19 CAR-T was awarded 'breakthrough status' by the FDA in 2014. However, the attempted use of CAR T cells for solid tumours has not been so successful. A mesothelin-targeting CAR incorporating CD3 ζ , CD28 and 41BB signalling domains (3rd generation CAR; Fig. 1.16) was recently trialled in a single phase I study of malignant pleural mesothelioma, ovarian carcinoma and pancreatic ductal adenocarcinoma (Haas et al. 2019). Unlike CARs for haematological disease, which have seen success in treating acute lymphoblastic leukaemia (Park et al. 2018), the best outcome in this trial was stable disease at 28 days post-administration (11/15 patients) and median progression free survival was 2.1 months (Haas et al. 2019). In addition to the transient response to treatment, CAR-T cell persistence was low with CAR-T detection in the peripheral blood disappearing by 2 months post-administration (Haas et al. 2019). Interestingly, of the 5 patient cancerous lesion biopsies taken, three had detectable CAR-T cell DNA, but these levels were approximately 100-fold less than in the blood during expansion post administration (Haas et al., 2019) indicating that whilst trafficking was successful, perhaps improved trafficking could have improved tumour control. Indeed, intratumoural administration, which circumvents the need for homing, has been attempted using erbB-targeting CAR T cells to head and neck squamous cell carcinoma. Here, stable disease was similarly achieved for 11/15 treated patients at 6 weeks post-infusion, but one individual achieved a complete durable response that is currently ongoing (>3 years; Larcombe-Young et al., 2020).

TCR engineered T cells

In contrast to the CAR-T field, engineered TCR development has largely been focused on the treatment of solid tumours. Unlike CAR-T therapy, T cell specificity is MHC

restricted and can only recognise cancer-associated epitopes presented by MHC. However, as epitopes can arise from internal proteins in cancer cells, the potential number of targets on cancer cells is far greater. MART-1 and gp100 are melanoma-associated antigens which exhibit variable expression across melanoma lesions, between lesions and between patients (Marincola et al. 1996). Two $\alpha\beta$ TCRs, DMF5 and gp100(154), were detected either by screening melanoma patient TILs for MART-1-reactive TCRs or *in vivo* screening of HLA transgenic mice using gp100 peptide, residues 154 to 162, respectively (Johnson et al. 2009). Following expression in T cells, DMF5 and gp100(154) recognised melanoma-associated peptides MART-1 and gp(100), respectively, and killed cell lines expressing cognate peptide and produced IL-2 (Johnson et al. 2009). These TCR-bearing T cells were used to treat 36 patients with metastatic melanoma, with 20 receiving DMF5 T cells and 16 receiving gp100(154) T cells. Both T cells were detectable 1 month after administration in peripheral blood, but the frequency of tetramer-positive cells was variable in non-responder patients (Johnson et al. 2009). IL-2 peaked 5 days after administration in patient sera, and an objective partial response lasted between 3–17 months for 6/20 patients who received DMF5 T cells and 2/16 patients who received gp100(154) T cells. One gp100(154) recipient had a complete response (14 months ongoing at the time of publication; Johnson et al., 2009). However, significant on-target, off-tumour side effects were observed in 29/36 patients. These consisted of destruction of epidermal melanocytes and vitiligo, as well as damage to the eye and inner ear but were largely resolved by steroid application (Johnson et al. 2009). Of note, effects upon the eye and inner ear seen with the DMF5 TCR, were not seen with a lower affinity TCR variant (DMF4) in a prior study, highlighting the importance of optimising TCR affinity for therapy, given solid tumour targets are typically expressed by healthy tissues in lower amounts. The variable and transient response in this study is unsurprising when considering the heterogeneity of gp100 and MART-1 expression within and between patient lesions (Marincola et al. 1996).

In another TCR therapy study, a receptor able to recognise NY-ESO-1 cancer testis antigen was generated. NY-ESO-1 is not expressed in normal *adult* human tissues except the testis (which lack HLA class I), but is expressed by several cancers

including, breast, prostate, thyroid, synovial sarcoma, melanoma and ovarian cancer. Following transduction of the NY-ESO-1 TCR into patient's peripheral blood T cells, they were used to treat either melanoma or synovial cancer (Robbins et al. 2011). 5/11 melanoma patients had an objective response including two complete responses and one partial response. Of the sarcoma patients, 4/6 had an objective partial response but no complete responses (Robbins et al. 2011). Unlike CD19 CAR for haematological malignancies, persistence of TCR engineered T cells in peripheral blood detected by flow cytometry did not correlate with regression of the cancer (Robbins et al. 2011), possibly due to migration into cancerous lesions.

As highlighted by the TCR study targeting MART-1 and gp100, significant on-target, off-tumour side effects can be mediated by high-affinity TCR clones or CAR receptors. One study in particular highlights the dangers of this where the MAGE-A3 TCR was developed to treat myeloma and melanoma, but induced fatal and severe myocardial damage in the first two patients, due to cross-reactivity with an unrelated cardiac muscle tissue-derived peptide (Hodi et al. 2010). This highlights two important problems facing the fields of TCR and CAR-T therapy for their application in solid tumours. Whilst CD19 has near universal expression on B-cell related cancers, its presence on healthy cells results in their destruction. Fortunately, whilst long-term effects are currently unknown, B-cell aplasia is tolerated and can be mitigated by immunoglobulin replacement therapy (Kansagra et al. 2019). TCR or CAR-T mediated immune destruction of organs is not tolerated. Furthermore, solid tumours can be heterogenous, as demonstrated by the variable expression of MART-1 and gp100, which can promote cancer immune escape even if on-target, on-tumour effects are seen (Marincola et al. 1996). There are several strategies to mitigate these difficulties, such as, combinatorial 'Boolean AND-gated' antigen sensing CAR-T cells which require antigen signal 1 'AND' antigen signal 2 for CAR-T cell activation (Han et al., 2019), unconventional TCRs targeting cancerous metabolites which have the potential to target multiple different cancers (Crowther et al., 2020), and the removal of endogenous TCR chains via CRISPR to prevent mismatch pairing and unexpected off-target recognition (Legut et al. 2018). However, strategies to improve targeting stringency are not the topic of this thesis.

1.7.2. Strategies to improve the efficacy of cell-based immunotherapies for solid tumours

Each co-stimulatory domain used in 2nd generation CAR-T cells signals via different mechanisms and produces distinct RNA expression profiles, which confer different benefits to CAR-T cells (Long et al. 2015). Third generation CAR-T cells incorporating both CD28 and 41BB costimulatory domains alongside CD3 ζ have recently been generated to incorporate the benefits of both signalling domains. These were trialled alongside CD28 containing 2nd generation CD19-targeting CAR-T cell (Fig. 1.16; Ramos et al., 2018). Patients were simultaneously infused with both CD19-targeting CAR-T cell populations and 3rd generation CAR-T cells underwent greater expansion and maintained a higher level of engraftment up to 168 days post-infusion (Ramos et al. 2018). 4th generation CAR-T cells are currently being designed and tested in pre-clinical models to allow CAR-T cells to overcome the immunosuppressive TME. Typically, they consist of 2nd or 3rd generation CAR molecules co-expressed alongside another transgene, usually a cytokine. This is often referred to as 'armouring'. As this 'armour' is outside of the CAR construct itself, it can also be delivered alongside cancer-specific TCRs. An overview of the different generations of CAR constructs is shown in Fig. 1.16.

Several groups have sought to improve cancer-specific T cell efficacy by 'armouring' them with molecules that improve T cell homing to the tumour. For example, following poor infiltration of GD2-CAR T cells in human neuroblastoma, Craddock and colleagues sought to improve homing by co-expression of CAR with a chemokine receptor (Craddock et al. 2010). CCR2b was chosen as its ligand was secreted by neuroblastoma cell lines and primary tumour cells, and patient's CAR-T cells lacked CCR2b expression following *ex vivo* expansion (Craddock et al. 2010). T cells solely transduced with either CCR2b or control chemokine receptor (CCR7) transmigrated *in vitro* in response to their specific ligand in patient-derived neuroblastoma cell supernatants (Craddock et al. 2010). When CCR2-armoured GD2 CAR T cells were used to treat tumour cell xenografted mice, significantly elevated T cell and significantly lower tumour bioluminescence was observed compared to mice treated

with unarmoured CAR-T cells (Craddock et al. 2010). This indicates that, depending on the specific chemokine profile of a tumour, armouring can be performed to induce CAR T cell recruitment to the tumour site.

As an alternate approach, another group generated CAR-T cells which also express IL-7 and CCL19 to mimic fibroblastic reticular cells (FRCs). The authors cite the expression IL-7 and CCL19 by FRCs as being essential for maintenance of the T cell zone in lymph nodes. They demonstrated that IL-7 and CCL19 expression by CAR-T cells enhanced proliferation and migration *in vitro*, respectively. Each benefit could be abrogated by receptor blockade. Using mastocytoma and Lewis cell lung syngeneic carcinoma models, CAR-T cells armouring with IL-7 and CCL19 completely eradicated tumours, whilst non-armoured CAR-T cells induced modest control (Adachi et al. 2018). Adachi and colleagues conducted further comparative *in vivo* studies using CAR-T cells expressing both or either IL-7 or CCL19 (Adachi et al. 2018). These studies demonstrated limited control of tumour growth by CAR-T cells expressing either armouring transgene alone demonstrating both IL-7 and CCL19 were required for CAR-T efficacy. Prior to complete destruction of tumour, immunohistochemical analysis revealed CD3 positive cell infiltration throughout the tumour, which overlapped with DC staining in mice that received dual IL-7 and CCL19-armoured CAR-T cells (Adachi et al. 2018). In tumours from mice treated with conventional CAR-T cells, CD3 staining was restricted to the tumours edge (Adachi et al. 2018). This indicates that CAR-T cells designed to mimic fibroblast reticular cells can cause CD3 T cell and DC infiltration of the tumour centre and consequent tumour rejection (Adachi et al. 2018).

1.7.3. Harnessing or manipulating L-selectin for cell-based immunotherapies

Early work by Kjaergaard and Shu indicated that L-selectin expression by cancer-specific T cells caused their accumulation in the lymph nodes of tumour-bearing mice, but precluded them from both metastatic and subcutaneous tumour sites, as less than 5 % of T cell infiltrates were L-selectin positive (Kjaergaard and Shu 1999). The authors did not conduct longitudinal studies interrogating the kinetics of L-selectin expression, and so these cells may once have been L-selectin positive

(Kjaergaard and Shu 1999). In an effort to account for this, L-selectin negative and positive tumour-specific T cells isolated from lymph nodes of tumour-bearing mice were separated before adoptive transfer to mice with metastasis, and only the L-selectin negative cells mediated any tumour control (Kjaergaard and Shu 1999). This indicated that L-selectin deficiency is a prerequisite for tumour homing and control. However, the authors did not isolate CD8 T cells or exclude the possibility of immunosuppressive populations being adoptively transferred with each population.

More recently, the status of T cells as L-selectin positive has been demonstrated in a rhesus macaque model to confer elevated *in vivo* persistence to CD8 T cells. *In vitro*-activated CD8 T cells were sorted on L-selectin status (negative or positive) before transduction with differentiating markers. Following further *in vitro* expansion, both T cell populations were L-selectin negative, but following re-infusion into the original rhesus macaques, only 'L-selectin positive derived CD8 T cells' persisted in the blood past day 3 (Berger et al. 2008). Importantly, this could not be explained by L-selectin negative T cells being sequestered into tissues and *ex vivo* phenotypic analysis of 'L-selectin positive derived cells' indicated a sub-population of the transferred T cells persisted as T_{CM} cells (CCR7 and L-selectin positive; Berger et al., 2008). This indicates that L-selectin, or another cellular factor whose presence correlates with L-selectin status, confers the ability to persist *in vivo* and form a T_{CM} population, which could protect against tumour recurrence following initial destruction (Berger et al. 2008).

Different *in vitro* expansion protocols of murine CD8 T cells can generate T_{EM} (perforin and gzm B gene expression) and T_{CM} (CXCR3, CCR7 and L-selectin gene expression) cell populations of murine melanoma-specific T cells (Klebanoff et al. 2005). In support of the work by Berger and colleagues, adoptive transfer of these cancer-specific T cell populations into melanoma-bearing mice revealed that T_{CM} cells had a drastically greater ability to proliferate and clonally expand *in vivo* than the T_{EM} cells. Further, they better controlled tumour growth and improved survival of tumour-bearing mice relative to T_{EM} cells (Klebanoff et al. 2005). Another study, using the same cancer-specific T cells, demonstrated that weekly rounds of *in vitro*

peptide stimulation resulted in the progressive loss of L-selectin and CCR7 whilst gzm B and IFN γ expression was gained, alongside an increased ability to mediate cytolysis of peptide-pulsed target cancer cells *in vitro* (Gattinoni et al. 2005). However, during *in vivo* melanoma models, cancer-specific T cells which under went one round of stimulation, and had a more naïve like phenotype as they were L-selectin and CCR7 positive, were better able to control tumour growth than those more alike short lived effector cells, which had undergone four rounds of *in vitro* stimulation (Gattinoni et al. 2005). Further, the more naïve-like activated T cells were sorted into L-selectin negative and L-selectin positive populations, which were adoptively transferred into tumour bearing mice alongside a peptide vaccination, and only the L-selectin positive T cells could control tumour growth (Gattinoni et al. 2005). Together, these studies implicate L-selectin positive cells (often used to partially define T_{CM} cell populations) and T_{CM} populations as more efficacious cell types for cancer immunotherapy. However, other cellular factors which highly correlate with L-selectin status or designation as T_{CM} may be responsible for the perceived benefits.

To directly investigate the therapeutic benefit of L-selectin, rather than as a marker of a particular sub population of T cells like T_N or T_{CM} cells, several groups have performed studies with L-selectin sufficient or knockout cancer-specific T cells. In a comparable model to the previous experiment, Gattinoni et al backcrossed their cancer-specific mice to knockout L-selectin, and generated naïve-like activated T cells (Gattinoni et al. 2005). In melanoma-bearing mice, some control of tumour growth was seen in mice treated with L-selectin deficient T cells, but this was temporary, and T cell expansion in the blood was limited. Only L-selectin sufficient cancer-specific T cells eradicated tumours (Gattinoni et al. 2005). Further, Gattinoni and colleagues were able to demonstrate that L-selectin conferred tumour control relied on peptide vaccination and presentation of antigen by APCs (Gattinoni et al. 2005). In disagreement with this study, using the same cancer-specific populations of L-selectin null or sufficient cells, both were able to clear subcutaneous and metastatic tumours irrespective of L-selectin expression and reject tumours when rechallenged 35 days later (Díaz-Montero et al. 2013). This indicates that L-selectin status is not the sole mediator of the benefits observed by the aforementioned studies. However,

in this study, the adoptively transferred T cells were expanded in IL-12 rather than IL-2, which may improve the efficacy of both L-selectin -sufficient and -deficient cancer-specific T cells (Gattinoni et al. 2005; Díaz-Montero et al. 2013).

A different approach taken by our group, has been to utilise an L-selectin variant (ΔP) which does not undergo ectodomain proteolysis following T cell activation or during transmigration and is not under the transcriptional control of Klf2. This built on previous work which demonstrated that re-expression of L-selectin after activation of CD8 T cells was essential for homing to virus-infected organs. Moreover, activated T cell homing to these organs could be improved by preventing the downregulation of L-selectin that normally occurs during T cell differentiation to effector cells (Mohammed et al. 2016). It was hypothesised that maintaining L-selectin expression on activated cancer-specific T cells could be used to boost homing to solid tumours in adoptive transfer models. When tested, cancer-specific T cells which expressed the proteolysis-resistant form of L-selectin (ΔP) better controlled tumour growth of subcutaneously growing B16 tumours than T cells expressing endogenous wild type L-selectin, which is downregulated during the therapy. These ΔP -armoured cancer-specific T cells also controlled B16 growth in a lung metastasis model relative to untreated mice, and TILs contained more T cells exhibiting a T_{CM} phenotype (CD44 and CD27 positive) than those treated with cancer-specific T cells bearing WT L-selectin (Watson et al. 2019). Increased numbers of CD3 and CD8 T cells were detected in subcutaneous B16 tumours from mice treated with ΔP cancer-specific T cells in comparison with tumours treated with T cells expressing wild type L-selectin (Watson et al. 2019). However, these effects did not appear to be mediated by increased T cell homing as competitive homing studies revealed comparable levels of ΔP and L-selectin null TILs (Watson et al. 2019). *In vitro* activation of T_N cells revealed delayed activation-induced proliferation of ΔP T cells and elevated Ki67 expression relative to those expressing WT or no L-selectin (Watson et al. 2019).

As previously discussed in 1.4.1, if L-selectin proteolysis is prevented on CD8 T cells, CD25 expression and consequently proliferation, is delayed both *in vitro* and *in vivo*

(Mohammed et al. 2019). When taken together, the studies by Mohammed et al and Watson et al suggest that preventing L-selectin proteolysis may significantly alter the proliferation kinetics of ΔP T cells, delaying it until the T cells reach the tumour, where they can control tumour growth in greater number. However, these studies were conducted with T_N cells transgenic for each form of L-selectin and the cancer or virus specific TCR. This does not reflect the clinical approach to adoptive T cell therapy, where expression must be delivered by vector, which I attempted in this thesis.

1.8.0. Hypotheses and aims

The work in this thesis seeks to address the overarching hypothesis that the proteolytic processing of L-selectin can modulate the function of T cells for cancer immunotherapy in clinically relevant models.

To investigate this overarching hypothesis, two central hypotheses are investigated:

1. Following γ -secretase proteolysis of L-selectin in human T cells, the released cytoplasmic tail migrates to a sub-cellular compartment. This is based on work by Andrew Newman, who demonstrated that L-selectin is proteolysed sequentially by ADAM17 to release the ectodomain and then γ -secretase to release the cytoplasmic tail.

To address this hypothesis, the aims of chapter 3 were:

- a. Express appropriately tagged forms of L-selectin variants within a human T cell line.
- b. Develop an imaging flow cytometry methodology capable of distinguishing between membrane localised and intracellular L-selectin staining.
- c. Use the above methodology to:
 - i. determine the fate of L-selectin's intracellular tail by co-staining sub-cellular compartments and inhibiting degradation.

- ii. Evaluate mutants of L-selectin that are proposed to resist each step of sequential proteolysis of L-selectin.
2. Co-expression of cleavage-resistant human or murine L-selectin and a cancer-specific TCR by murine T cells delivered via a retroviral vector will recapitulate the phenotype of ΔP L-selectin and cancer-specific TCR transgenic mice in pre-clinical models of solid cancer immunotherapy. This is based on work by Watson et al, who found that ΔP L-selectin expressing naïve cancer-specific T cells better control tumour growth *in vivo* than cancer-specific T cells co-expressing wildtype L-selectin (Watson et al. 2019).

To address this hypothesis, the aims of chapter 4 were:

- a. Confer cancer specificity to murine T cells using clinically relevant methods i.e. retroviral transduction of transgenes encoding cancer specific TCR or CAR proteins.
- b. Co-express human and mouse variants of L-selectin alongside the protein conferring cancer specificity.
- c. Characterise these T cells *in vitro* to determine if:
 - i. L-selectin is proteolysed following T cell activation.
 - ii. T cells can mediate killing of tumour cells.
 - iii. Variants of L-selectin confer phenotypes to T cells.
- d. Characterise these T cells *in vivo* to determine if variants of L-selectin confer phenotypes which improve control of tumour growth.

2.0.0. Chapter 2: Materials and methods

2.1.0. Molecular biology

2.1.1. Polymerase chain reaction (PCR)

All PCR reactions were conducted using an Alpha thermocycler (PCR max) and used template vectors as depicted in their respective figures within the results chapters. Primers were designed using SnapGene and upon their arrival, suspended in RNase-free water (Qiagen), and stored with the rest of the PCR reagents at -20 °C.

To generate MMLV human L-selectin variant (WT, Δ MN or Δ W) vectors, the Hercul polymerase (Agilent) was used alongside the relevant primers (table 2.1) for human L-selectin amplification and T4 Ligase-mediated ligation as in 2.1.3. The reaction mix is detailed in Table 2.2, and the PCR conditions are detailed in Table 2.3.

To generate pMSGV1 murine L-selectin variant (WT or Δ P) vectors, the Platinum Blue PCR Supermix (Invitrogen, discontinued, 12580015) was used alongside the relevant primers (Table 2.1) for murine L-selectin amplification and InFusion ligation as in 2.1.3. The reaction mix is detailed in Table 2.2, and the PCR conditions are detailed in Table 2.3.

Designation	Sequence	Direction
MMLV-hLsel-F	GCTCCACCGCGGTGGGCCGCCACCATGGGCTGCAGA	Forward
MMLV-hLsel-R	CGCGGTACCGTCGACTTAATATGGGTCATTCACT	Reverse
pMSGV1-mLsel-F	AGCCCTCGAGAAGCTTGCCACCATGGTGTTCCATGGAGA	Forward
pMSGV1-mLsel-R	CCGCGGTACCGTCGACCTTAGTATGGATCATCCAT	Reverse

Table 2.1. Primers used to generate transgene inserts. The highlighted sequence within each primer correspond to either a restriction site or their overlapping region in the transgene or vector. Cyan = vector, red = transgene, magenta = restriction digestion site. Underlined sequences are Kozak sequences.

Herc II Polymerase		
Reagent	Volume (μL)	Final Concentration
Herc II Polymerase (50x)	1	1x
Herc II reaction buffer (5x)	10	1x
dNTP premix	0.5	25 mM each dNTP
Forward primer (10 μM)	1	0.2 μM
Reverse primer (10 μM)	1	0.2 μM
Template DNA	variable	0.1 ng μL^{-1} (5 ng)
Platinum Blue PCR Supermix		
Reagent	Volume (μL)	Final Concentration
Platinum Blue PCR Supermix (1x)	45	1x
Forward primer (10 μM)	1	0.2 μM
Reverse primer (10 μM)	1	0.2 μM
Template DNA	variable	0.1 ng μL^{-1} (5 ng)

Table 2.2. PCR reaction mixes. Due to variability in the volume required for the template DNA, RNase-free water (Qiagen) was used to make the volume up to 50 μL .

Herc II Polymerase		
Step	Temperature ($^{\circ}\text{C}$)	Time (s)
Initial denaturation	95	30
Cycle 1 (3x)	95	10
	47	10
Cycle 2 (25x)	72	40
	95	10
	68	10
Cycle 3 (2x)	72	40
	95	10
Hold	4	Indefinite
Platinum Blue PCR Supermix		
Step	Temperature ($^{\circ}\text{C}$)	Time (s)
Initial denaturation	95	60
Cycle 1 (40x)	95	20
	59	20
	68	80
Hold	4	Indefinite

Table 2.3. PCR conditions.

2.1.2. Restriction enzyme digestion

To digest DNA for either ligation or to determine if cloning was successful, double digests were performed using either: HindIII and Sall-HF or NotI-HF and Sall-HF (New England Biolabs). Briefly, 5 – 10 units of each enzyme was added per 50 µL reaction with 1 % bovine serum albumin (BSA; w/v), 10 µL of mini-prepped DNA or 2 µL of maxi-prepped DNA and appropriately diluted 10x 2.1 buffer (New England Biolabs). This was then incubated (overnight, 37 °C).

2.1.3. Gel electrophoresis

To cast gels, agarose in TBE (1 % agarose w/v in TBE buffer; 0.45 M Tris, 0.45 M boric acid, 10 mM EDTA, pH 8.0) was heated in a microwave and cooled to the point of not producing steam prior to the addition of ethidium bromide (Invitrogen) before casting in custom trays with ladder inserts (approx. 60 min, room temperature; RT). After setting, gels were submerged in TBE and loaded with 20 µL of each sample. Samples consisted of PCR products, digested PCR products, digested vector backbones and digested constructs which were diluted in 6x running buffer (New England Biolabs, B7025) and run (120 V, 30 – 60 min) alongside a quick load 1 kb plus DNA ladder (New England Biolabs, N0550S). To visualise and extract bands with a clean scalpel, a UV transilluminator was used (UVP, Upland, USA). Extracted DNA was purified using QIAquick gel purification kit (Qiagen) according to the manufacturer's protocol.

2.1.4. Ligation

To ligate transgene inserts into linearised, restriction digested, vector backbones, either T4 ligase (New England Biolabs), or the InFusion enzyme (Takara) was used. Both enzymes were used according to the manufacturer's protocol. Briefly, for T4 ligase, a 20 µL reaction consisting of digested vector (50 ng) and transgene insert (37.5 ng), T4 Ligase (1 µL) and appropriately diluted 10x T4 ligase buffer was incubated for 2 hr at RT. For the Infusion enzyme, a 10 µL reaction consisting of 3 µL of digested vector, 1 µL transgene insert, and appropriately diluted 5x Infusion HD enzyme premix was incubated (15 min, 50 °C). Regardless of enzyme, these ligation reactions were used directly to transform *E. coli* as in 2.1.5.

2.1.5. *E. coli* transformation and mini-prep

DH5 α competent *E. coli* (Thermo Fisher Scientific Scientific) were kept in 45 μ L aliquots (-80 $^{\circ}$ C) and thawed on ice. 5 μ L of the ligation reaction as in 2.1.4., was added to the bacteria prior to heat shock (30s, 42 $^{\circ}$ C) and incubation on ice (2 min). For selection of transformed colonies, bacteria were pelleted (1 min, RT, 10,062 g in a benchtop centrifuge), resuspended in pre-warmed (37 $^{\circ}$ C) 500 μ L SOC medium (Invitrogen), and incubated (60 min, 37 $^{\circ}$ C, shaking 220 rpm). Bacteria were then pelleted by centrifugation (1 min, RT, 10,062 g in benchtop centrifuge), 450 μ L of the supernatant was removed and the remaining 50 μ L used to resuspend bacteria. The bacterial suspension was then plated on pre-warmed (37 $^{\circ}$ C) 100 μ g/mL carbenicillin (Sigma-Aldrich-Aldrich) agar plates (1.5 % agar w/v in LB broth; LB broth is 1 % Tryptone and NaCl and 0.5 % Bacto-yeast w/v in ddH₂O; Sigma-Aldrich) and incubated (overnight, 37 $^{\circ}$ C).

To confirm insertion of transgenes into vectors via successful ligation and transformation, up to 5 single colonies were picked using a pipette tip and incubated in 5 mL 100 μ g/mL carbenicillin LB broth (overnight, 37 $^{\circ}$ C, shaking 220 rpm). The following day 4.5 mL of *E. coli* culture were mini-prepped using PureLink quick plasmid mini-prep kits (Invitrogen, K210010) and purified plasmids tested by restriction digestion for insertion of transgenes as in 2.1.2 and 2.1.3. Positive clones confirmed by restriction digestion were stored (-80 $^{\circ}$ C) after mixing 1:1 with 50 % glycerol (dilute in ddH₂O; Fisher Scientific). Following this, DNA was sequenced by Eurofins genomics using primers (Sigma-Aldrich; Table 2.4).

Designation	Sequence	Direction
AN37 Lsel Seq For	ATGGGCTGCAGAAGAAGACTAG	Forward
AN38 Lsel 206 seq Rev	CTGTGTAATTGTCTCGGCAG	Reverse
AN39 Lsel 504 seq For	TACACAGCTTCTTGCCAGCC	Forward
AN40 Lsel 623 seq Rev	CCTCCAAAGGCTCACACTGA	Reverse
AN41 Lsel 888 For	GCATGTACCTTCATCTGCTCAG	Forward
AN42 Lsel stop Rev	ATATGGGTCATTCATACTTC	Reverse
OM4 pMMLV rev	GACCACTGATATCCTGTCTTTAAC	Reverse
pMSGV1-mLsel-F1	CTCAAAGTAGACGGCATCGCAG	Forward
pMSGV1-mLsel-F2	ACTCTCACTAAAGAAGCAGAGAAC	Forward
pMSGV1-mLsel-F3	AGCCAATCTGCCAAGTGGTC	Forward
pMSGV1-mLsel-F4	AGCCAATCTGCCAAGTGGTC	Forward
pMSGV1-mLsel-R1	TTTGCTTGCAAACTTTCTAGC	Reverse
pMSGV1-mLsel-R2	CCCGTAATACCCTGCATCACAG	Reverse
pMSGV1-mLsel-R3	GAGCTCCTGGATTGTCAGTG	Reverse

Table 2.4. Primers used for sequence confirmation.

2.1.6. Maxi-prep

Glycerol stocks of transformed *E. coli*, which had been confirmed by restriction digestion and sequencing, were scraped whilst frozen using a pipette tip and used to inoculate 500 mL 100 µg/mL carbenicillin LB broth which was then incubated (overnight, 37 °C, shaking 220 rpm). *E. coli* were then maxi-prepped using the PureLink HiPure plasmid filter maxi-prep kit (Invitrogen, K210016) according to the manufacturer's protocol. DNA concentration and purity ($A_{260}/A_{280} > 1.8$) were tested using a ND-1000 Nanodrop spectrophotometer (Thermo Fisher Scientific).

2.1.7. Western Blotting

1 x10⁶ Molt3 T cells or tyrosinase-related protein (TRP) 2 reactive TCR (TRP2) positive primary murine CD8 T cells were added per well of a 96-well plate and following experimentation, washed in ice-cold PBS before lysis in 35 µL of ice-cold cell lysis buffer (35 min, 4 °C). This consists of 25 mM HEPES at pH 7.4, 150 mM sodium chloride, 10 mM magnesium chloride, 2 % glycerol, 1 % Triton X-100, 10 mM phenathroline, 1 mM sodium orthovanadate, 500 µL of 0.09 g 1,10-phenathroline in

2.5 mL ethanol and 1 protease inhibitor tablet per 10 mL of lysis buffer (Roche, Complete protease ULTRA). Cell lysates were centrifuged (5 min, 4 °C, 274 g) and the supernatants were collected and stored at -20 °C or used immediately.

Lysates were boiled to reduce viscosity (100 °C, 10 min) prior to the addition of a half-volume of 4 % reducing buffer (3.5 mL dH₂O, 1.25 mL of 0.5 M Tris-HCl at pH 6.8, 2.5 mL glycerol, 4 mL of 10 % SDS, 0.2 mL of 0.5 % bromophenol blue) with β -mercaptoethanol (add 50 μ L of β -mercaptoethanol to 950 μ L of reducing buffer prior to use) and centrifuged (30 min, 10,062 g) on a benchtop centrifuge. Lysates were then run (35 min, 200 V) using the X-cell module (Invitrogen; EI0002) alongside a SeeBlue pre-labelled protein ladder (Invitrogen; LC5625) using MES-SDS running buffer (Thermo Fisher Scientific; NP0002). Proteins were transferred to an activated PVDF Transfer Membrane (methanol, 30s, RT) with a pore size of 0.2 μ m (Thermo Fisher Scientific; 88520) for the capture of small proteins using the X-cell module (60 min, 30 V) according to the manufacturer's protocol with NuPage transfer buffer (Thermo Fisher Scientific; NP0006).

The PVDF membrane was kept in PBS-T (1 mL Tween-20 in 999 mL PBS) at 4 °C until use. The PVDF membrane was blocked with 5 % PBS-T (PBS-T with 5 % milk powder w/v; 60 min, RT, rocking) before staining for L-selectin's cytosolic tail (overnight, rocking, 4 °C) with antibody diluted in 5 % PBS-T. If tagged with V5/His, immunoblotting was done with an anti-V5 antibody (Thermo Fisher Scientific; R96025; 0.64/1000) and if not, the CA21 antibody was used (Kahn et al., 1994; 1/50). Alternatively, one western blot was performed for murine tICD19 (Thermo Fisher Scientific; PA5-85959; 1/2000). The following day, the PVDF membrane was washed 5x in PBS-T (5 min, RT, rocking) before addition of the secondary horseradish peroxidase (HRP) -conjugated antibody (Bio-Rad; 1706516; 1.6/1000 in 5 % PBS-T; 60 min, RT, rocking). The PVDF membrane was washed 5x in PBS-T (5 min, RT, rocking) before development of the membrane using a chemiluminescent substrate (Thermo Fisher Scientific; 34580) and imaged using a Syngene G:Box. Following imaging, PVDF membranes were stripped according to manufacturer's protocol (Thermo Fisher Scientific, 21059; 15 min, 37 °C) before washing 5x in PBS-T (5 min, RT, rocking),

blocking with 5 % PBS-T and re-probing for GAPDH. The re-probing followed the same protocol as blotting for L-selectin's tail but used the anti-GAPDH (abcam, ab9484, 0.32/1000 in 5 % PBS-T; 60 min, RT, rocking) primary antibody. For long-term storage, PVDF membranes were sealed in bags with PBS-T (4 °C).

Quantification of western blots was performed using ImageJ (National Institutes of Health, Bethesda). Briefly, the *rectangular selection tool* was used to outline bands of interest (Fig. 2.1A), and this was selected using *Analyze>gels>Select first lane* (Fig. 2.1B). The lanes were then plotted using *Analyze>gels>Plot lanes* (Fig. 2.1C), and the *wand tool* was used to attain the area of each peak (Fig. 2.1D), which corresponded to the blot intensity in the plotted lane.

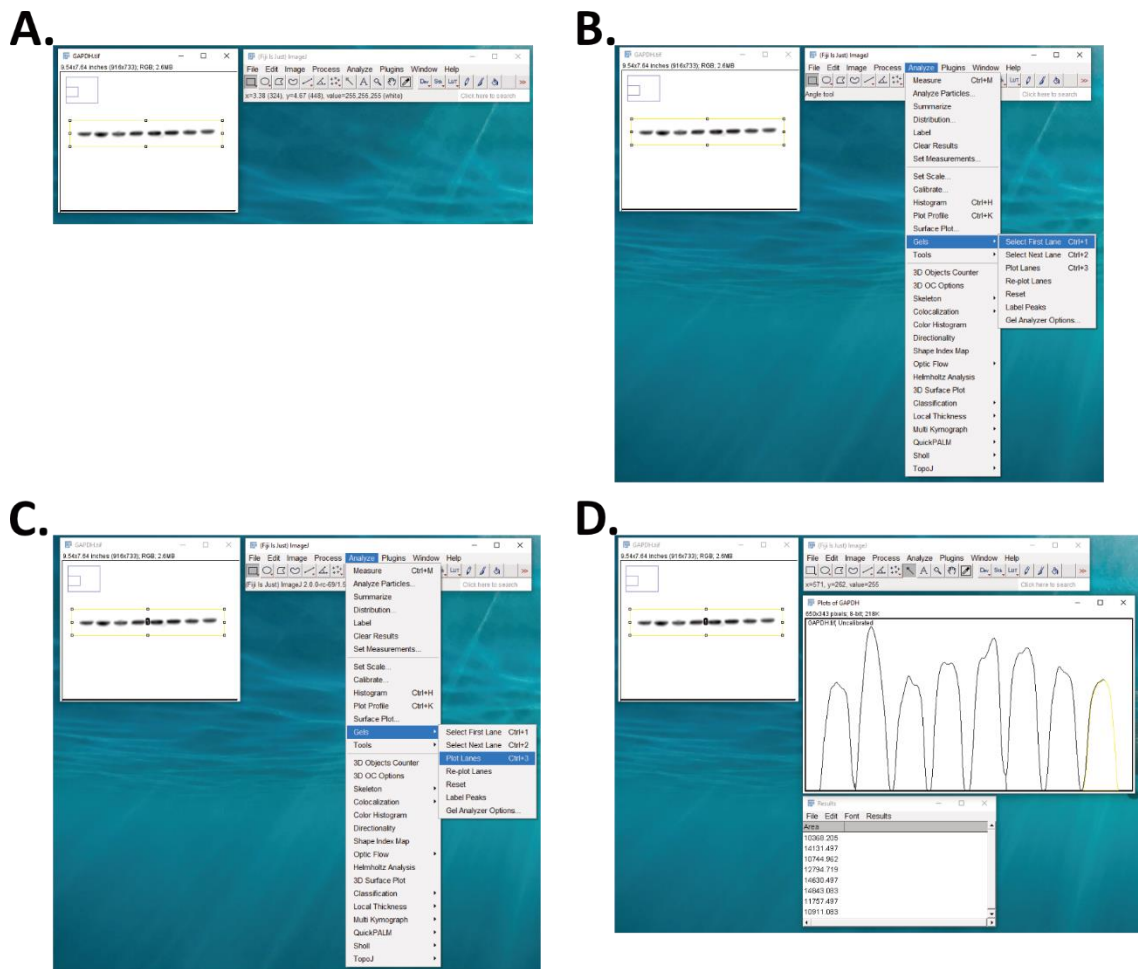


Figure 2.1. ImageJ was used to quantify western blots (A) The *rectangular selection tool* was used to outline bands of interest before (B) the *select first lane* and (C) *plot lanes* commands were used. (D) The *wand tool* was then used to to attain the area of each peak

These areas were normalised to control bands for presentation of quantified data using the following equations:

$$\text{Lane Normalisation Factor (LNF)} = \text{GAPDH}_{\text{Lane Intensity}} / \text{GAPDH}_{\text{Most Intense Lane}}$$
$$\text{Normalised Band of Interest Intensity} = \text{Band of Interest}_{\text{Lane Intensity}} / \text{LNF}$$

2.2.0. Tissue culture

All cell culture medium constituents were purchased from Thermo Fisher Scientific except fetal calf serum which was purchased from Gibco. Cell culture medium compositions are detailed in table 2.5. Cells were grown at 37 °C with 5 % CO₂ in a humidified incubator. HEK293T cells, Platinum-E cells (HEK293T derivative cell line containing viral gag-pol and ecotropic protein; Cell Biolabs) and Molt3 T-cells (ATCC; CRL-1552; Molt-3) expressing the 868TCR were kind gifts from Andrew Newman, Claire Bennett and John Bridgeman respectively. The 868TCR expressing Molt3 T cell line was received on a collaborative basis. The 868TCR recognises the HIV gag specific peptide (SLYNTVATL) and has been characterised elsewhere (Varela-Rohena et al. 2008) and 868TCR positive Molt3 T cells will hereafter be referred to as Molt3 T cells. To attain primary murine CD8 T cells, LselKO mice were culled according to schedule one practices (CO₂ asphyxiation followed by dislocation of neck), the spleen harvested and kept in 5 mL ice-cold PBS for transfer to tissue culture. In the tissue culture laboratory, spleens were mashed using the end of a 1 mL syringe through 70 µm cell strainers (VWR; 7340003) and the strainer washed through with 5 mL of ice-cold PBS. The cell suspension underwent RBC lysis according to the manufacturer's protocol (BioLegend; 420301) before negative isolation by magnetic activated cell sorting (MACS) for CD8 positive splenocytes according to the manufacturer's protocol (Stem Cell; 17953). The murine melanoma cell line B16.F10 was a kind gift from Awen Gallimore. Nunc cell culture dishes, plates and flasks were purchased from Thermo Fisher Scientific. Cells were counted using a LUNA-FL™ Dual Fluorescence Cell Counter either with 1:1 Trypan Blue or 1:10 AO/PI Cell viability reagent (Logos Biosystems; Thermo Fisher Scientific). Cell culture media are detailed in Table 2.5.

Medium	Composition	Use
R10	RPMI 1640 (4.5 g/L glucose), 10 % FCS, 2mM L-Glutamine, 100 IU penicillin, 100 µg/mL streptomycin and 1 mM sodium pyruvate	Culturing Molt3 T-cells and derived cell lines
R1	RPMI 1640 (4.5 g/L glucose), 1 % FCS, 2mM L-Glutamine, 100 IU penicillin, 100 µg/mL streptomycin and 1 mM sodium pyruvate	Used to culture Molt3 T-cells during T-cell activation protocols
Complete T cell media	R10 media, 1x MEM non-essential amino acids (Gibco; 11140050), 360 IU/ml hrIL2, 50 µM of β-mercaptoethanol (Gibco; 31350010)	Used to culture primary murine T cells
D10	DMEM (4.5 g/L glucose and 4 mM L-glutamine), 10 % FCS, 100 IU penicillin, 100 µg/mL streptomycin and 1 mM sodium pyruvate	Culturing HEK 293T cells
D0-7.1	49 mL DMEM and 1.25 mL 1 M HEPES. 5 M NaOH and 5 M HCl added dropwise to achieve pH 7.1	Used with viral plasmids and CaCl ₂ to create a transfection mixture
D10-7.9	49 mL D10 and 1.25 mL 1 M HEPES. 5 M NaOH and 5 M HCl added dropwise to achieve pH 7.9	Used to culture HEK 293T cells during overnight transfection
Freezing Media	DMSO, 90 % FCS	Used to freeze cells for liquid nitrogen storage

Table 2.5. Composition of cell culture media used in this work.

2.2.1. Adherent cells

Unless otherwise stated, adherent cells were cultured in D10 medium and passaged every 3 – 4 days upon reaching 80 % confluency. To passage, cells were washed once in PBS and incubated with 3 mL trypsin/EDTA (Gibco) per 75 cm² of tissue culture flask for 1 min at 37 °C with 5 % CO₂. To block trypsin, D10 medium was added at three times the volume of trypsin/EDTA added. Cells were centrifuged and re-plated in D10 at 3 x10⁵ cells per cm² (5 min, 20 °C, 274 g).

2.2.2. Suspension cells

Unless otherwise stated, Molt3 T-cells and derivative cell lines were seeded at 3×10^6 cells per T75, cultured in R10 and diluted 1:10 every two days. Depending on the yield of MACS isolation, $1 - 5 \times 10^6$ murine CD8 T cells were seeded in 2 mL complete T cell medium per well in a 12-well dish and the medium was changed every two days by replacing the top 1 mL without disturbing the suspended cells at the bottom of the well.

2.2.3. Cell treatments and activation

Suspension cells were seeded at 1×10^6 T-cells (or 1×10^6 TRP2 positive T cells) per well of a 96-well plate (U-bottom) and resuspended in 97 μ L R1 media. A variety of cellular inhibitors were used within this thesis and if used in an experiment, the above 97 μ L of R1 media was supplemented prior to incubation (37 °C, 5 % CO₂).

To inhibit PMA-induced proteolysis (paragraph below), R1 was supplemented with an ADAM-17 blocking antibody (D1(A12), 300 nM; Tape et al., 2011) or the γ -secretase inhibitor L-685 (10 μ M; Sigma-Aldrich) for 60 mins. Either human IgG or a DMSO solvent were used as controls, respectively. To investigate degradation of L-selectin's cytoplasmic tail following proteolysis, R1 was supplemented with either Chloroquine (20 μ M; Sigma-Aldrich; Pinazza et al., 2018), Bafilomycin A1 (100 nM; Sigma-Aldrich; Ishikura et al., 2016), MG132 (20 μ M; Sigma-Aldrich; Pinazza et al., 2018), MRT68921 (Sigma-Aldrich; Petherick et al. 2015) or Leupeptin (20 μ M; Sigma-Aldrich; Boland et al., 2010) with Pepstatin (20 μ M; Sigma-Aldrich; Boland et al., 2010) for 6 hr. In control wells, DMSO replaced each inhibitor as a supplement to R1 media.

To induce ADAM-17 activity, 3 μ L of 10 μ M PMA (Sigma-Aldrich) in DMSO (final PMA concentration of 300 nM) was added and incubated for up to 15 mins (37 °C, 5 % CO₂). PMA was added at 15, 10, 5, 0 mins before the reaction was arrested by washing the cells in 100 μ L ice-cold PBS and keeping the cells on ice until fixation or lysis. In control wells, DMSO replaced PMA as a supplement to R1 media.

Experimental outlines are displayed in Fig. 2.2.

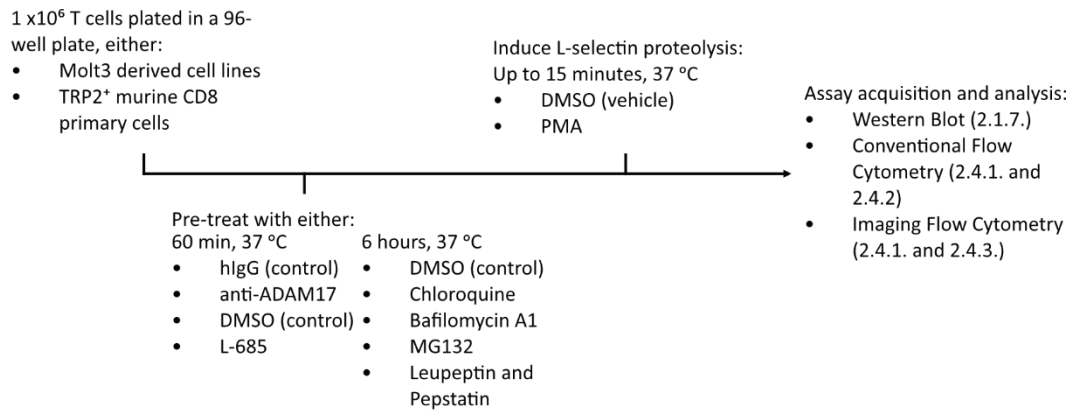


Figure 2.2. Suspension cell treatments.

2.2.4. Cryopreservation

For long-term storage, adherent cells were grown to 80 % confluency before trypsinisation, centrifugation (5 min, 20 °C, 274 g) and resuspension at a density of 3 x10⁶ cells ml⁻¹ in freezing medium (Table 2.5). Similarly, cultured suspension cells were centrifuged (5 min, 20 °C, 274 g) and resuspended at a density of 3x10⁶ cells ml⁻¹ in freezing medium. A 1 mL aliquot of cells suspended in freezing media was transferred per cryovial for overnight incubation in a MrFrosty (24 hr, -80 °C; Nalgene) before long-term storage in a liquid nitrogen (LN₂) Dewar.

2.3.0. T cell transductions

An overview of the transfection and transduction protocols used in this work is shown in Fig. 2.3. Details are provided in 2.3.1, 2.3.2 and 2.3.3.

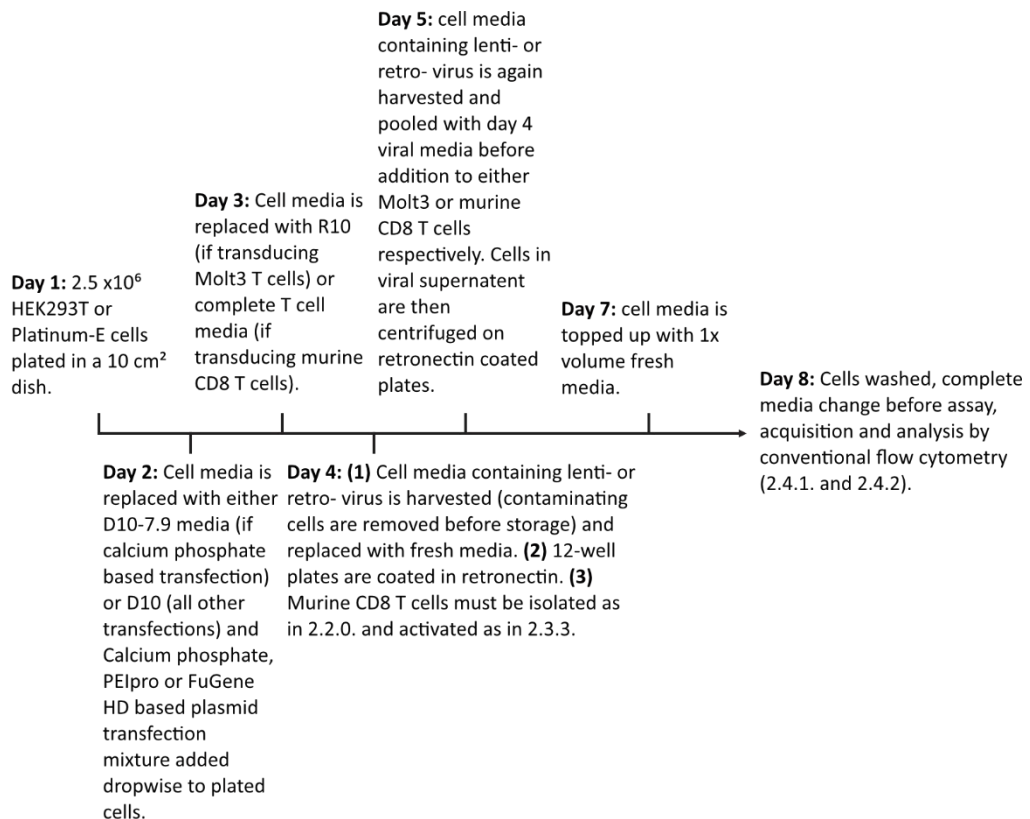


Figure 2.3. Overview of lenti- and retro- virus transduction protocols.

2.3.1. Lentivirus production for Molt3 T cell transduction

Using standard cell culture conditions, 2.5x10⁶ HEK293T cells were seeded in a 10 cm² cell culture grade petri dish and incubated overnight.

A second generation lentiviral transfer vector, pSxW (pLenti), was used with pMD29 and pCMVΔ8.91 to produce lentivirus in the HEK293T packaging cell line (Demaison et al. 2002; Yáñez-Muñoz et al. 2006). 15 μg of pLenti encoding either wildtype (pLenti-WT), ΔMN (pLenti-ΔMN; a 286 to 294 deletion mutant which resists ectodomain proteolysis called ΔM-N in the literature; Chen et al. 1995) or IΔW L-selectin (pLenti-IΔW; an I to W point mutation at amino acid residue 351 in the transmembrane domain) with a V5-His tagged intracellular tail was used to create a transfection mixture with 75 μL of 1M CaCl₂, 7.5 μg pMD29, 15 μg pΔ8.91 and 1.5 mL in D0-7.1. The transfection mixture was vortexed and incubated for 30 min at RT. Mock mixtures did not contain the transfer vector. The HEK293T cell medium was aspirated and replaced with 6 mL of D10-7.9. The transfection mixture was then added dropwise

across the plate. Alternatively, lentiviral backbone pHR'SIN-SEW containing a transgene encoding WT L-selectin tagged with GFP at its intracellular tail was used with pMD29 and pCMVΔ8.91 to produce lentivirus (Rzeniewicz et al. 2015). In this case, FuGene HD was used to produce a transfection mixture according to the manufacturer's protocol (Promega; E2311). Briefly, 10 μL of FuGene HD was mixed with 70 μL OptiMEM (Gibco). Separately, using the same vector amounts as stated previously, a 50 μL mixture was made with sterile ddH₂O. These were combined and vortexed to generate a transfection mixture, which was then incubated for 20 min at RT. Mock mixtures did not contain the transfer vector. The HEK293T cell medium was aspirated and replaced with 5 mL of D10. The transfection mixture was then added dropwise across the plate.

HEK293T cells were then incubated overnight under standard cell culture conditions. The medium was aspirated 24 hr later, replaced with 5 mL of R10, and incubated overnight under standard cell culture conditions. The medium containing lentivirus was harvested 24 hr later, contaminating cells pelleted (5 min, 4 °C, 274 g), and the supernatant stored (4 °C). Cell medium was replaced with R10. This was repeated the following day. The viral supernatants were pooled (10 mL lentivirus in R10) for long-term storage (snap-freeze 1 mL aliquots in LN₂ then store at -80 °C; long term storage drastically reduces viral titre) or used immediately.

2.3.2. Retrovirus production for primary murine CD8 T cell transduction

Using standard cell culture conditions, 2.5 x10⁶ platinum-E cells were seeded in a 10 cm² cell culture grade petri dish and incubated overnight.

2.6 μg of transfer vector and 1.5 μg packaging vector (Table 2.6) were mixed with sterile ddH₂O and used with FuGene according to manufacturer's protocol, and as briefly outlined above, to generate a transfection mixture. The exception to this was a single experiment for the vector encoding the CEACAR where either PEIpro (Polyplus) was used according to the manufacturer's instruction or calcium phosphate was used as in 2.3.1. with the packaging cell line being HEK293T cells. Mock mixtures did not contain the transfer vector. Virus-producing cell medium was aspirated and replaced with 5 mL D10 media. The transfection mixture was then added dropwise across the plate.

Virus-producing cells were then incubated overnight under standard cell culture conditions. 24 hr later, the medium was aspirated and replaced with 5 mL complete T cell medium and incubated overnight under standard cell culture conditions. The medium containing retrovirus was harvested 24 hr later, contaminating cells pelleted (5 min, 4 °C, 274 g), and the supernatant stored (4 °C). The media was then replaced with complete T cell medium. This was repeated the following day. The viral supernatants were pooled (10 mL retrovirus in complete T cell media) for long-term storage (snap freeze 1 mL aliquots in LN₂ then store at -80 °C; long term storage drastically reduces viral titre) or used immediately.

Transgene Vector	Packaging Vector(s)	Packaging cell line
pBullet-CMV-CEACAR-28z	pVPack-GagPol	HEK293T
	pVPack-Eco	
pMMLV-hL-selectin variants	pCL-Eco	Platinum-E
pMSGV1-mLselectin variants	pCL-Eco	Platinum-E
pMP71-TRP2 derived variants	pCL-Eco	Platinum-E

Table 2.6. Combination of retroviral vectors and packaging cell lines used in this work. Vectors encoding the human variants include WT, ΔMN or IΔW L-selectin and vectors encoding murine variants include WT or LΔP L-selectin. pCL-Eco and pMP71-TRP2 were kind gifts from Claire Bennett. The pBullet construct and pVPack vectors were kind gifts from Hinrich Abken. The pMSGV1 vector was from AddGene (#107226) and MMLV available in-house.

2.3.3. Transduction

The day prior to transduction, a 12-well plate was coated with retronectin according to manufacturer's instruction (Takara; T100B). Briefly, enough retronectin solution (0.02 mg ml⁻¹ in PBS) to cover the bottom of the well was added to each well used of a 12-well plate, sealed with parafilm, and incubated overnight (4 °C, rocking). If 1 transduced primary murine CD8 T cells, on the same day as retronectin was plated, 1 – 5 x10⁶ murine CD8 T cells were activated in complete T cell media supplemented with anti-CD3 (60 ng ml⁻¹; BD; 553057) and anti-CD28 (30 ng ml⁻¹; BD; 553294) before overnight incubation (standard tissue culture conditions).

After overnight incubation retronectin was removed and stored (it can be freeze/thawed and re-used up to 10x; -20 °C), before washing the wells twice with PBS. The plate was then blocked with BSA (2 % w/v in PBS and sterile filtered; Sigma-

Aldrich; 30 min, RT) before washing the wells twice with PBS. Either activated murine CD8 T cells or Molt3 T cells were washed in complete T cell medium (without activating antibodies) or R10 respectively before resuspension in 1 mL viral supernatant. The cell suspension was then added to a retronectin coated well. The plates were then centrifuged (90 min, 32 °C, 1188 g) prior to incubation under standard tissue culture conditions for 48 hr. The medium was topped up with 1 mL of complete T cell medium or R10 for activated murine CD8 T cells or Molt3 T cells, respectively. The transduced cells were assayed 72 hr later for transgene expression by flow cytometry.

2.4.0. Flow cytometry

Purified cells were stained with reagents as in table 2.7.

Target	Clone or RRID	Isotype	Fluorophore	µg test ⁻¹	Manufacturer
Anti-human					
L-selectin Ectodomain	DREG-56	Mouse IgG1	APC/Fire750	0.05	BioLegend
L-selectin Ectodomain	DREG-56	Mouse IgG1	PE	0.125	Invitrogen
Unknown (isotype control)	P3.6.2.8.1	Mouse IgG1	PE	0.125	Invitrogen
CD69	FN50	Mouse IgG1	PE	0.125	BioLegend
Unknown (isotype control)	MOPC-21	Mouse IgG1	PE	0.125	BioLegend
V5 epitope	AB2532221	Mouse IgG2a	AF647	0.025	Invitrogen
CD107a	eBioH4A3	Mouse IgG1	FITC	0.067	Invitrogen
Unknown (isotype control)	P3.6.2.8.1	Mouse IgG1	FITC	0.067	Invitrogen
TCR V beta 5 (a)	1C1	Mouse IgG1	FITC	1.000	Invitrogen
Unknown (isotype control)	MOPC-31C	Mouse IgG1	FITC	1.000	BD
58K Golgi protein	58K-9	Mouse IgG1, k	AF488	0.05	Abcam
Unknown (isotype control)	MOPC-21	Mouse IgG1	AF488	0.05	Abcam
γ-secretase (Pen-2 sub-unit)	EPR9200	Rabbit IgG	N/A	5	Abcam
Arthropod KLH (isotype)	EPR25A	Rabbit IgG	N/A	5	Abcam

Rabbit IgG (secondary)	Poly4064	Donkey Ig	BV421	0.25	BioLegend
Anti-mouse					
CD44	IM7	Rat IgG2b	FITC	0.025	BioLegend
LAG-3	C9B7W	Rat IgG1	PerCP/Cy5.5	0.2	BioLegend
CD69	H1.2F3	Hamster IgG	APC	0.2	BioLegend
L-selectin	Mel-14	Rat IgG2a	APC/Fire750	0.05	BioLegend
CD27	LG.3A10	Hamster IgG	Pacific Blue	0.5	BioLegend
CD8	53-6.7	Rat IgG2a	PerCP/Cy5.5	0.1	BioLegend
CD8	53-6.7	Rat IgG2a	BV711	0.1	BioLegend
CD25	3C7	Rat IgG2b	BV786	0.2	BD
Vβ3	KJ25	Hamster IgG2	PE	0.025	BD
PD1	J43	Hamster IgG	PE/eFluor610	0.2	eBiosciences
TIM-3	RMT3-23	Rat IgG2a	PE/Cy7	0.2	BioLegend
CD19	1D3	Rat IgG2a	PE/Cy7	0.25	eBiosciences
Ki67	16A8	Rat IgG2a	BV605	0.025	BioLegend
mIgG	AB_933619	Goat IgG	PE	0.5	Invitrogen
Label	Product			Volume test¹	Manufacturer
Live/Dead	Live/Dead fixable Aqua			100 μL (1:1000)	Invitrogen
Live/Dead	Live/Dead fixable Near-IR			100 μL (1:1000)	Invitrogen
Nucleus	NucBlue (Hoechst 33342)			15 μL (1 drop 500 μL ⁻¹)	Invitrogen

Table 2.7. Antibodies and cell stains used for conventional- and imaging- flow cytometry.

2.4.1. Extracellular staining

During all staining protocols, cells were protected from light. Between 1×10^5 – 1×10^6 cells of interest depending on availability were added to each well of a 96-well plate and centrifuged (5 min, 4 °C, 260 g) before flicking off supernatant. Cells were washed in 200 μL PBS before staining with Live/Dead reagents according to

manufacturer's protocol (Thermo Fisher Scientific). Preceding all consequent steps, cells were centrifuged, the supernatant discarded before resuspension in 50 μ L FACS buffer (2% FCS in PBS). Next, cells were incubated with 50 μ L of antibody diluted to optimal concentration for surface staining (30 min, RT).

If performing an extracellular stain, and cells were to be sorted to generate a pure population of marker positive cells, cells were then washed once in PBS and resuspended in 100 μ L FACS buffer. If cells were to undergo intracellular staining, the protocol differed depending on the type of flow cytometry analysis (see section below). If cells were to be analysed for surface expression of markers, cells washed once in PBS before being incubated in 4 % formaldehyde (2 mL formaldehyde in 50 mL PBS; 15 minutes, RT; Fisher Reagents; 10532955) before being washed once in PBS and resuspended in 100 μ L FACS buffer. Prior to analysis or sorting, cells were transferred to FACS tubes, wrapped in foil and stored (4 $^{\circ}$ C) until analysis or cell sorting. Data acquisition was conducted using a BD FACSCanto II.

2.4.2. Intracellular staining for conventional flow cytometry

For intracellular staining, surface-stained cells were washed once in PBS prior to fixation in 200 μ L eBio Fix/Perm (45 min, 4 $^{\circ}$ C; Invitrogen; 00-5523-00). Cells were then washed twice in 200 μ L eBio permeabilisation buffer before staining with 50 μ L of diluted antibody (again in permeabilisation buffer; 30 min, RT). Cells were then washed twice in 200 μ L eBio permeabilisation buffer before resuspension in 100 μ L FACS buffer. Prior to analysis or sorting, cells were transferred to FACS tubes, wrapped in foil and stored (4 $^{\circ}$ C) until analysis or cell sorting. Data acquisition was conducted using a custom BD LSR Fortessa.

2.4.3. Intracellular staining for imaging flow cytometry

For intracellular staining, surface-stained cells were washed once in PBS prior to fixation in 2 % fresh formaldehyde (2 % v/v in PBS; 60 mins, RT; Pierce; 28906). Following this, cells were washed three times in 200 μ L True Nuclear permeabilisation buffer (BioLegend; 424401) before staining with 50 μ L of diluted

antibody (again in permeabilisation buffer; 30 min, RT). Cells were then washed three times in 200 μ L True Nuclear permeabilisation buffer. For nuclear staining, cells were centrifuged (5 min, 4 $^{\circ}$ C, 274 g) and 15 μ L NucBlue (Invitrogen; R37605) was added to each sample (20 min, RT). Otherwise, cells were resuspended in 15 μ L FACS buffer. Prior to analysis or sorting, cells were transferred to eppendorf tubes, wrapped in foil and stored (4 $^{\circ}$ C) until analysis. Data acquisition was conducted at a 60x magnification using an ImageStream X Mark II imaging flow cytometer which can derive sub-cellular information (Fig. 2.4).

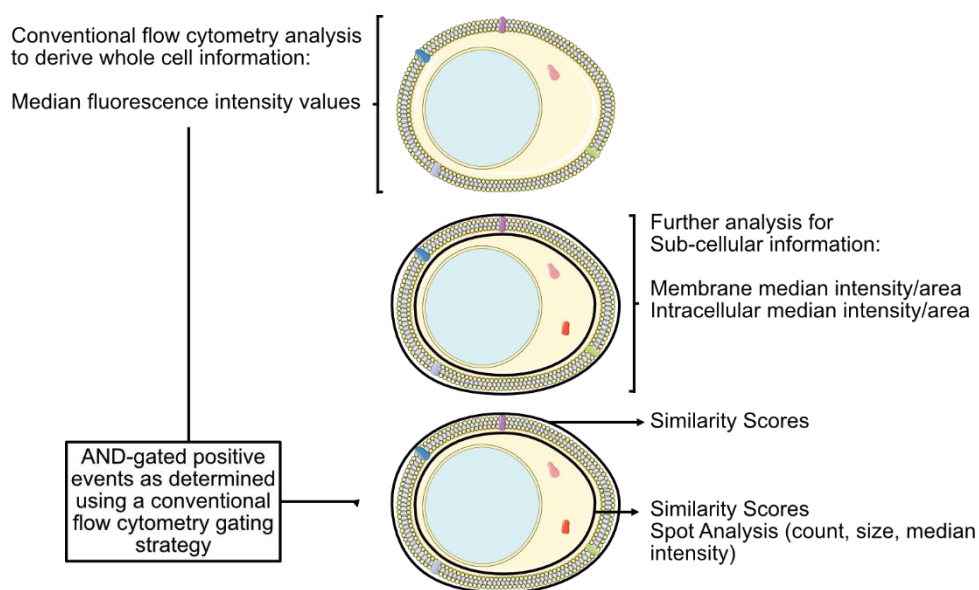


Figure 2.4. Imaging flow cytometry can derive whole cellular and sub-cellular information.

Median intensity values across the whole cell and median intensity values per unit area of sub-cellular regions were derived from live cells. The flow cytometry controls (e.g. isotype controls) were used to identify positive events by whole cell fluorescence intensity, and positive events were AND-gated for further analysis. Further analysis included assessment of similarity scores and spots.

Gating strategies and the analyses conducted are provided within each figure. The membrane and intracellular masks were generated as described in 3.2.4, and as such, varied depending on the antibodies and fluorophores used. As an example, for Molt3 T cells expressing V5/His tagged L-selectin and stained with anti-CD69/PE antibody and anti-V5/AF647 conjugated antibody, the membrane mask was defined as 'AdaptiveErode(M01, Ch01, 90) AND NOT AdaptiveErode(M01, Ch01, 80). The

intracellular mask was defined as 'AdaptiveErode(M01, Ch01, 90) AND NOT membrane mask'.

Within these masks similarity scores between fluorophore pairs were evaluated using the 'Similar Morphology' feature for similarity to the nucleus and 'Bright Detail Similarity R3' feature for any other cellular marker. An example of how the similarity score can vary, according to Luminex, is provided in Fig. 2.5.

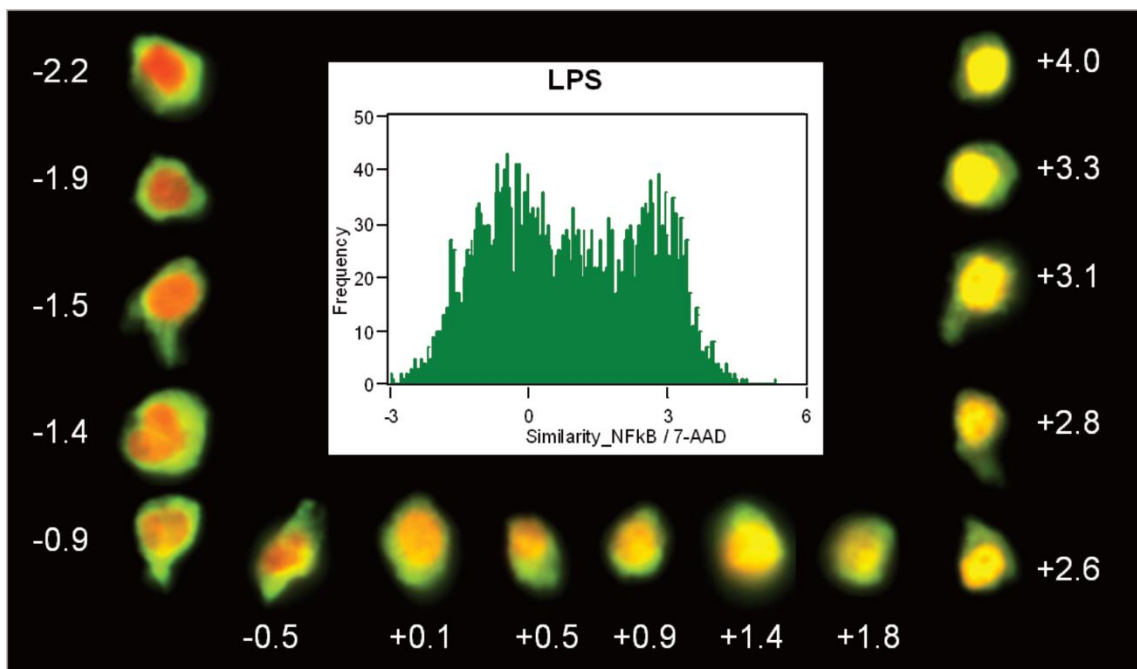


Figure 2.5. Representative images of different similarity scores for a nuclear stain (7-AAD) and a translocating protein (NFkB) in the IDEAS software package. The lower the similarity score the lower the degree of similarity between two fluorescent probes. Here, -2.2 demonstrates complete exclusion of NFkB from the nucleus and this persists up to the similarity score of +0.1. The higher the similarity score the greater the degree of similarity of two fluorescent probes. High similarity is evident from +1.4 to +4.0. Data reproduced from the IDEAS software package user manual.

Within the intracellular mask, spot counting was performed using the 'Spot Count' feature upon the 'spot mask'. Again, the spot mask parameters varied depending on the antibodies and fluorophores used. For example, for Molt3 T cells expressing V5/His tagged L-selectin the spots were defined as 'Intracellular mask AND (Spot(M11, Ch11, Bright, 4.93, 25, 0))'.

2.4.4. Controls and compensation

For conventional flow cytometry, UltraComp eBeads (Invitrogen; 01-2222-41) were stained individually with antibodies and for Live/Dead Aqua compensation, a V500-conjugated antibody (BD; 561391) was used as the Live/Dead stain cannot bind eBeads. Either isotype controls or fluorescence minus one (FMO) stains were used as controls and this is shown in the gating strategy of each experiment.

For imaging flow cytometry, single positive stains of each fluorophore on assayed cells were used and in the case of Live/Dead (Invitrogen) staining, cells were first killed (10 min, 58 °C) to ensure sufficient staining. Isotype controls were used for each experiment as shown in the gating strategy.

Compensation was performed using the BD FACSDiva software package if data was acquired using a BD flow cytometer. Experiments were compensated using the IDEAS software package if data was acquired using the ImageStream X Mark II.

2.5.0. Cell sorting

2.5.1. FACS

Transduced Molt3 T cells were stained as in 2.4.1. and sorted by Dr Kristin Ladell or Kelly Miners using a custom-modified FACS Aria II cytometer (BD). Cells were sorted into R10 media and then washed in R10 to remove azide (from the sheath fluid). Cells were cultured for 1 week prior to flow cytometry as in 2.4.1. to determine the purity of the sort relative to unsorted cells and isotype controls or FMOs.

2.5.2. MACS

Murine CD8 T cells were isolated by negative enrichment MACS as covered in 2.2.0. Once activated and transduced, cells were enriched for transgene expression using anti-mouse CD19 microbeads (Miltenyi Biotec, 130-121-301) and the AutoMACS (Miltenyi Biotec) according to the manufacturer's protocol. Cells were cultured for 1 week prior to flow cytometry as in 2.4.1. to determine the purity of the sort relative to unsorted cells and isotype controls or FMOs.

2.6.0. Cancer specific T cell-mediated killing

2.6.1. xCELLigence *ex vivo*

The RTCA SP real time cell analyser (ACEA) was programmed to test well conductivity (cell index) every 15 min for the duration of the experiment (up to 72 hr). B16.F10 target cells were counted and made up to a concentration of 50 cells μL^{-1} in complete T cell medium. 200 μL of the cell suspension was added to each well of a 96-well E-plate (ACEA; 300600910). The plate was loaded immediately onto the RTCA SP real time cell analyser (ACEA) for the initial scan to determine the background conductivity. Following this, the program was paused, and the plate was removed and incubated (45 min, RT) to allow cells to settle at the bottom of the well. The E-plate was then placed back on the analyser and the program was restarted. 12-18 hr later, once target cells had adhered and begun proliferating the programme was paused and treatments added. Treatments consisted of either 50 μL T cell medium (no treatment control), or the same volume containing transduced cancer-specific T cells, mock transduced T cells, or 0.5 % Triton-x-100 (Sigma-Aldrich; 1.25 μL ; full lysis control). The number of T cells added is indicated in the figure legend of the experiment. Following addition, the program was resumed.

During data analysis, the cell index was normalised using the following equation in the RTCA software package:

$$\text{Normalised } Cl_{ti} = Cl_{ti} / Cl_{nml_time}$$

Where Cl_{ti} = Cell index (CI) at a specific time point, and Cl_{nml_time} = CI at the time point prior to addition of T cells. This removes interwell variation in cell seeding attachment and growth.

Data were then further manipulated relative to the full lysis control to give % cytolysis:

$$\% \text{ Cytolysis}_{st} = [1 - (NCl_{st}) / (AvgNCl_{Rt})] \times 100$$

Where, NCI_{st} is the Normalised Cell Index for the sample and NCI_{Rt} is the average of Normalise Cell Index for the matching reference wells. This presents the cell indices as a % of the full lysis control. The process is summarised in Fig. 2.6.

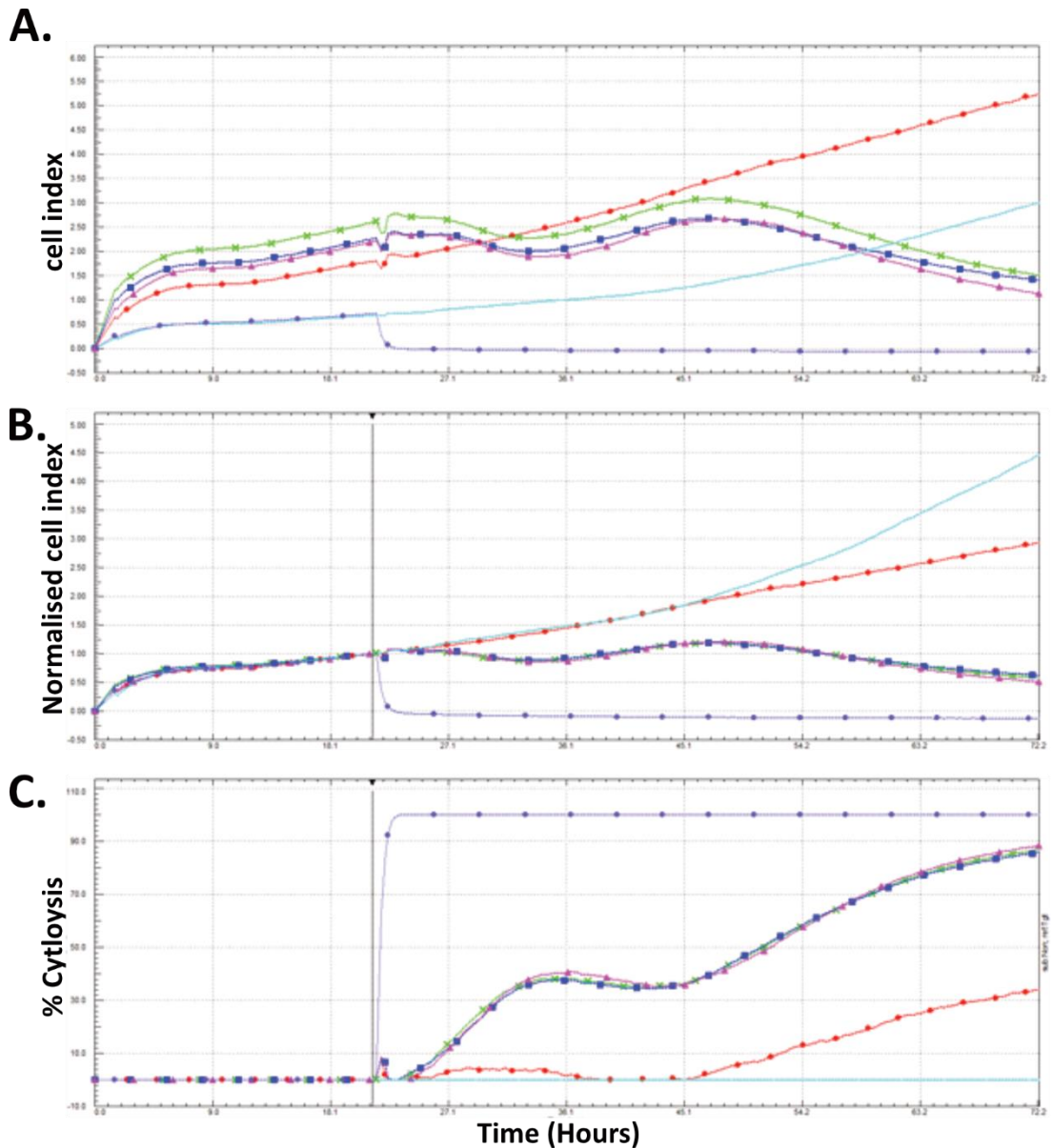


Figure 2.6. RTCA Pro was used to process xCELLigence data. The following variables were acquired, derived and plotted against time: **(A)** cell index, **(B)** normalised cell index and **(C)** % cytolysis.

2.6.2. B16.F10 subcutaneous tumour model *in vivo*

Thy1.1 and LselKO mouse colonies have been maintained by the Ager laboratory and were used for *in vivo* experiments within this thesis as tumour-bearing hosts and T cell donor mice, respectively. Animals were used according to UK Home Office

regulations under Ann Ager’s project licence (3003188) and the personal licence (I808ED7AB). Experimentation was performed during adulthood (3 – 6 months of age) during which mice were housed in open top cages within Cardiff University’s Heath Park Animal Unit. Mice were used if health screens of sentinel mice were negative.

On day 1, Thy1.1 male mice had their left flank shaved and were subcutaneously injected with 5×10^5 B16.F10 cells in 200 μ L PBS. Tumour growth was first assessed on day 3. On day 6 tumour size was again assessed before mice underwent total body sub-lethal irradiation 597cGy. On day 7, either 0.2×10^6 , 1×10^6 or 2×10^6 of donor TRP2 (V β 3 positive) T cells were administered intravenously. Donor T cells were taken from LN₂ storage and cultured 3 days prior to use. Calliper measurements of tumours were taken every 3 – 4 days and tumour volume calculated by:

$$Volume = (4/3) \times \pi \times (Length/2) \times (Width/2) \times (Depth/2)$$

At the termination of the study tumours were harvested, weighed and disaggregated using the gentleMACS according to the manufacturer’s protocol (Miltenyi Biotec) for Live/Dead cell counting and flow cytometry as covered in 2.4.1 to evaluate the presence of V β 3 positive TIL. The spleen and tdLN were also harvested and single cell suspensions generated as in 2.2.0. for Live/Dead counting and flow cytometry alongside the disaggregated tumour.

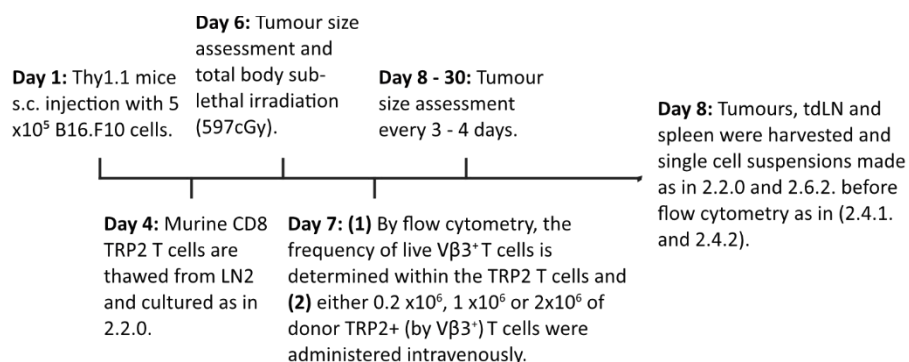


Figure 2.7. Overview of *in vivo* subcutaneous B16.F10 tumour model for adoptive transfer of cancer-specific T cells.

2.7.0. Software

For analysis, ImageJ (National Institutes of Health, Bethesda) was used to quantify western blots, FlowJo 10 (FlowJo LLC) was used to analyse conventional flow cytometry data (BD) and IDEAS (EMD Millipore) used to analyse imaging flow cytometry data. Primers and multi-cistronic vectors were designed using SnapGene (GSL Biotech LLC). To create figures, Affinity Designer (Serif Europe LLC) was used. This thesis was compiled in Microsoft word (Microsoft Corporation).

2.8.0. Equipment

Cells were centrifuged using a Heraeus Megafuge 4R (Thermo Fisher Scientific) and counted using a LUNA-FL™ Dual Fluorescence Cell Counter in a 1:1 ratio with Trypan Blue (Logos Biosystems; Thermo Fisher Scientific). Stained cells underwent FACS using a BD FACSAria III custom and were analysed using a BD FACSCanto II (BD), BD LSRFortessa or ImageStream X Mark II (EMD Millipore). To collect conventional- and imaging- flow cytometry data, BD FACSDIVA (BD) and INSPIRE (EMD Millipore) software packages were used, respectively. *In vitro* killing assays were performed using an ACEA RTCA SP real time cell analyser, and the corresponding RTCA Pro software package was used for data analysis.

2.9.0. Statistical analysis

All statistical analyses were conducted using GraphPad PRISM 8.2.1. Statistical tests were conducted on any experiment with $n \geq 3$. Replicate classifications are stated in the figure legends of chapter 3 whilst in chapter 4 all replicates were biological and tested in a single experiment. Data were tested for normality using the Shapiro-Wilk test. Parametric tests were used if the data were distributed normally, and non-parametric tests were used if the data were not distributed normally. The statistical tests used are presented in each figure legend. P-values < 0.05 were deemed significant. In each graph or plot, either the individual values and mean are shown, or the mean and standard deviation. Fisher's least significant difference test is abbreviated in figure legends as Fisher's LSD.

3.0.0. Determining the fate of L-selectin's cytoplasmic tail following ADAM-17 dependent shedding.

3.1.1. Introduction

Molt3 cells are a T lymphoblastic leukaemia cell line which lacks endogenous L-selectin expression. A prior member of the Ager laboratory (Andrew Newman) tagged L-selectin's intracellular tail with V5-His and delivered the gene in *trans* to Molt3 T cells via a lentiviral vector. Through western blotting, he showed that CD3/CD28 stimulation of wildtype (WT) L-selectin positive Molt3 T cells induced sequential proteolysis of L-selectin. First, the ectodomain was shed by tumour necrosis factor- α -converting enzyme (ADAM17; 5 minutes after activation), and then the membrane-retained fragment (MRF) began to be degraded (15 minutes after activation) unless the cells were pre-treated with a γ -secretase inhibitor (L-685 or DAPT), indicating sequential proteolysis (Fig. 3.1).

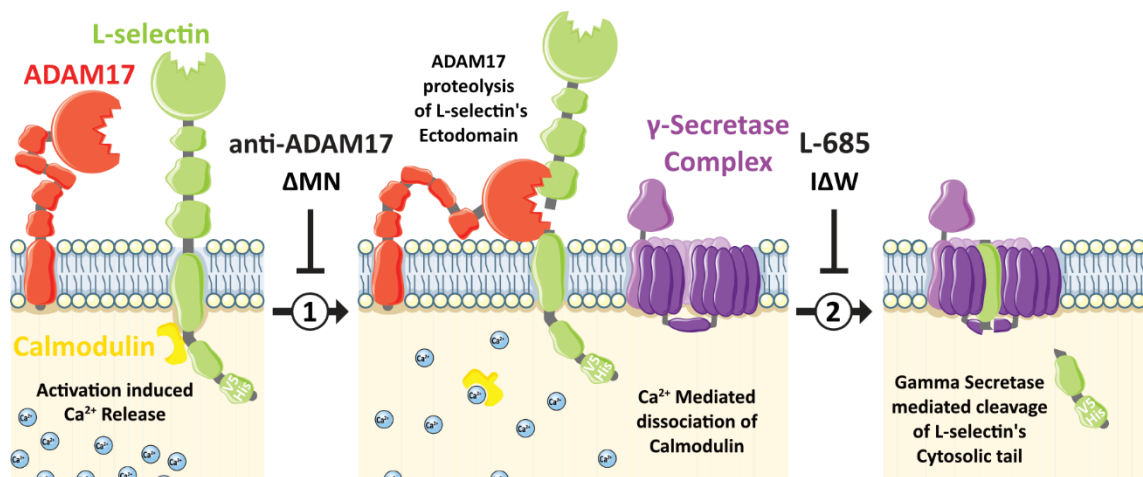


Figure 3.1. L-selectin undergoes sequential proteolysis following T cell activation. (Left) Following TCR mediated T cell activation or treatment with PMA released intracellular calcium binds calmodulin which dissociates from L-selectin exposing its' ADAM17 cleavage site (Matala et al., 2001). **(Middle)** L-selectin undergoes ADAM17 mediated proteolysis to shed it's ectodomain. This can be abrogated with blocking ADAM17 antibodies or truncation of L-selectin to exclude the cleavage site (Mohammed et al., 2019). **(Right)** γ -secretase recognises, and proteolyses, the ADAM17 membrane retained fragment of L-selectin to shed L-selectin's tail (Andrew Newman; unpublished observations).

Each proteolysis step can be abrogated using either enzyme inhibitors or genetic modification of L-selectin. Step 1 can be prevented by pre-treating cells with blocking anti-ADAM17 antibodies or truncation of L-selectin to remove the cleavage site (Δ MN L-selectin; Chen et al., 1995). Step 2 can be abrogated by pre-treating cells with the γ -secretase inhibitor, L-685, or by introducing a single point mutation into L-

selectin (IΔW L-selectin). The IΔW mutation is at amino acid residue 351 in the transmembrane domain and transforms an isoleucine (with a small hydrocarbon side chain) into a tryptophan (which possesses a bulky benzyl group containing side chain) whose side chain is proposed to sterically hinder a neighbouring phenylalanine residue (bulky indole ring containing side chain) disrupting L-selectin's tertiary structure. This disruption is proposed to prevent recognition of L-selectin's ADAM17 cleavage product by γ -secretase. However, this mutant has only been characterised by western blotting and requires imaging analysis to determine if the ADAM17 proteolysis product (MRF) of IΔW L-selectin remains at the membrane.

Cleavage-resistant L-selectin delays CD25 expression, which correlates with delayed proliferation *in vitro* and *in vivo* relative to WT L-selectin in murine T cells (Mohammed et al. 2019). Further, ectodomain cleavage (ADAM17)-resistant L-selectin expressing murine T cells controlled influenza and vaccinia virus infections (Mohammed et al. 2016) and the growth of solid and disseminated tumours better than T cells expressing wild-type L-selectin. Together, this indicates L-selectin may cause cell intrinsic differences that affect the kinetics of viral clearance and the control of tumour growth. I hypothesise this is due to the signalling capabilities of the L-selectin tail, either at the membrane prior to sequential cleavage or after release of the cytoplasmic tail, which can then act as a transcriptional regulator in a similar capacity to proteolysed NOTCH and amyloid precursor protein (APP; De Strooper et al., 1999; Gupta-Rossi et al., 2001; Kimberly et al., 2001).

The γ -secretase-released tail of APP has previously been difficult to detect, and to do so, it has been directly expressed in cells where it acts as a transcription factor (Kimberly et al. 2001). To induce maximal L-selectin proteolysis and therefore maximal release of the intracellular tail, I used a potent non-physiological activator of ADAM-17, namely phorbol 12-myristate 13-acetate (PMA; Lorenzen et al. 2016). To determine the fate of the L-selectin tail following T cell activation, I generated Molt3 T cells expressing either WT, ΔMN and IΔW L-selectin (WT, ΔMN and IΔW

Molt3 T cells respectively), validated the ADAM17 activator, PMA, as a reagent able to induce sequential proteolysis of L-selectin for imaging flow cytometry experiments. Imaging flow cytometry is best described as a flow cytometer in which every event recorded also has an image taken which can be consequently analysed like confocal images. Therefore, imaging flow cytometry overcomes the limitations of western blotting, which probes whole cell lysates and therefore cannot determine the subcellular distribution of L-selectin's cytoplasmic tail following ADAM17 mediated proteolysis. Additionally, the number of fluorophores which can be used in combination and the rate at which samples can be run make imaging flow cytometry higher throughput than confocal microscopy. Previous attempts by members of our laboratory to detect the γ -secretase-released tail of L-selectin by western blotting have been unsuccessful, and it was proposed this was due to migration to a sub-cellular compartment not soluble in the detergents used to generate cell lysates. I sought to use flow cytometry protocols and reagents capable of detecting cytoplasmic and nuclear proteins to overcome these limitations. In these experiments, I tracked the L-selectin tail following PMA treatment in the above cell lines.

3.1.2. Chapter aims

1. Generate WT, Δ MN and I Δ W L-selectin expressing Molt3 T cells and validate PMA as a reagent to induce sequential proteolysis of L-selectin for imaging flow cytometry experiments.
2. Following PMA-induced ADAM17 and γ -secretase proteolysis, use imaging flow cytometry to:
 - a. Determine the fate of L-selectin's tail.
 - b. Compare the sub-cellular distribution of the tail of L-selectin for each human variant: WT, Δ MN and I Δ W L-selectin.

3.2.0 Results

3.2.1. Molt3 T cells can be transduced to express WT, Δ MN and Δ W L-selectin and the proteolysis of L-selectin induced by PMA

Molt3 T cells were previously transduced by John Bridgeman to express the HIV-gag 868TCR (868TCR) which was gifted to the Ager lab on a collaborative basis. To express L-selectin, Molt3 868TCR positive T cells were transduced with a lentiviral vector encoding either WT, Δ MN or Δ W L-selectin and enriched by fluorescence-activated cell sorting (FACS) for 868TCR positive and L-selectin positive populations (Fig. 3.2A, B). The enriched populations were 96.8, 96.8 and 97.4 % L-selectin positive, respectively. Using WT Molt3 T cells and PMA, which is a known activator of ADAM17 (Lorenzen et al. 2016), concentrations of 300 nM PMA and above were found to induce maximal L-selectin ectodomain shedding after 15 minutes confirming Andrew Newman's unpublished observations. The number of L-selectin positive events were reduced by 21.7 % from 94.5 to 72.8 % (Fig. 3.2C). Thus, 300 nM of PMA was used in future shedding experiments.

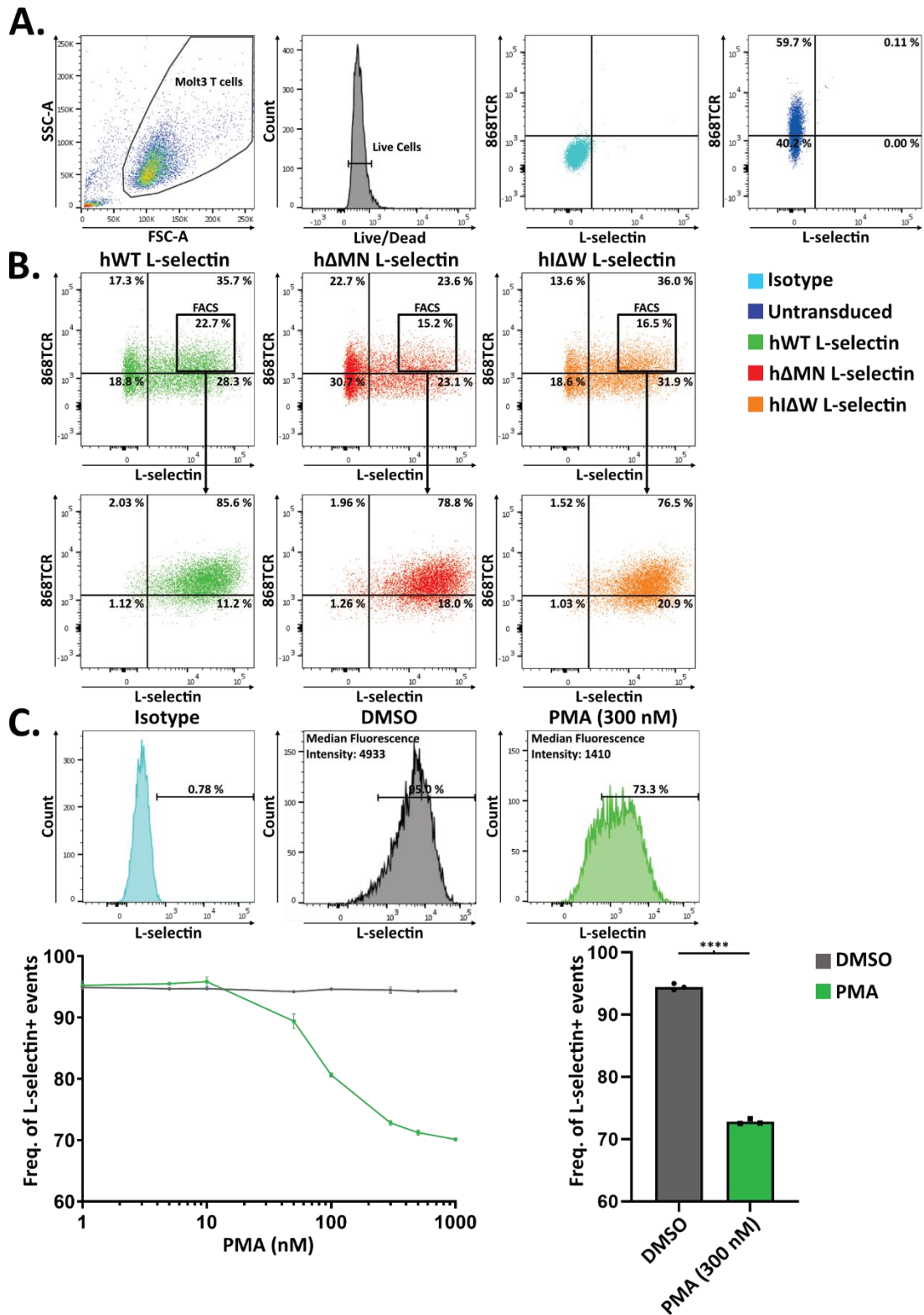


Figure 3.2. Molt3 T cells expressing the HIV-specific 868TCR can be transduced and enriched to express L-selectin variants which can undergo ectodomain shedding following PMA treatment. (A) The gating strategy by which 868TCR⁺ L-selectin⁺, live, Molt3 T cells were identified using isotype and fully stained untransduced controls **(B)** The high expressing 868TCR⁺ L-selectin⁺ cells enriched by FACS. **(C)** Sorted WT L-selectin⁺ Molt3 T cells were cryopreserved and after thawing and culture, titrated with PMA (15 min treatment) to determine the concentration capable of inducing maximal L-selectin ectodomain shedding. n = 3 technical replicates. Statistical Tests: Two-tailed, paired t-test was performed. **** = p < 0.0001.

3.2.2. Proteolysis of the ectodomain and cytoplasmic tail of L-selectin are inhibited by an anti-ADAM17 antibody and L-685, respectively

WT Molt3 T cells were pre-treated with either vehicle control (DMSO), L-685 (γ -secretase inhibitor), control IgG or a blocking anti-ADAM17 antibody (anti-ADAM17; Tape et al., 2011) for 1 hour prior to PMA-induced shedding in the presence of inhibitors. The blocking anti-ADAM17 antibody prevented PMA-induced L-selectin ectodomain shedding, whereas DMSO, L-685 and control IgG did not. Where ectodomain shedding occurred, it reduced the number of L-selectin positive events from approximately 85 % to 70 % (15 % reduction; Fig. 3.3A, B, C). The median fluorescence intensity decreased from approximately 5000 to 1400 (72 % reduction).

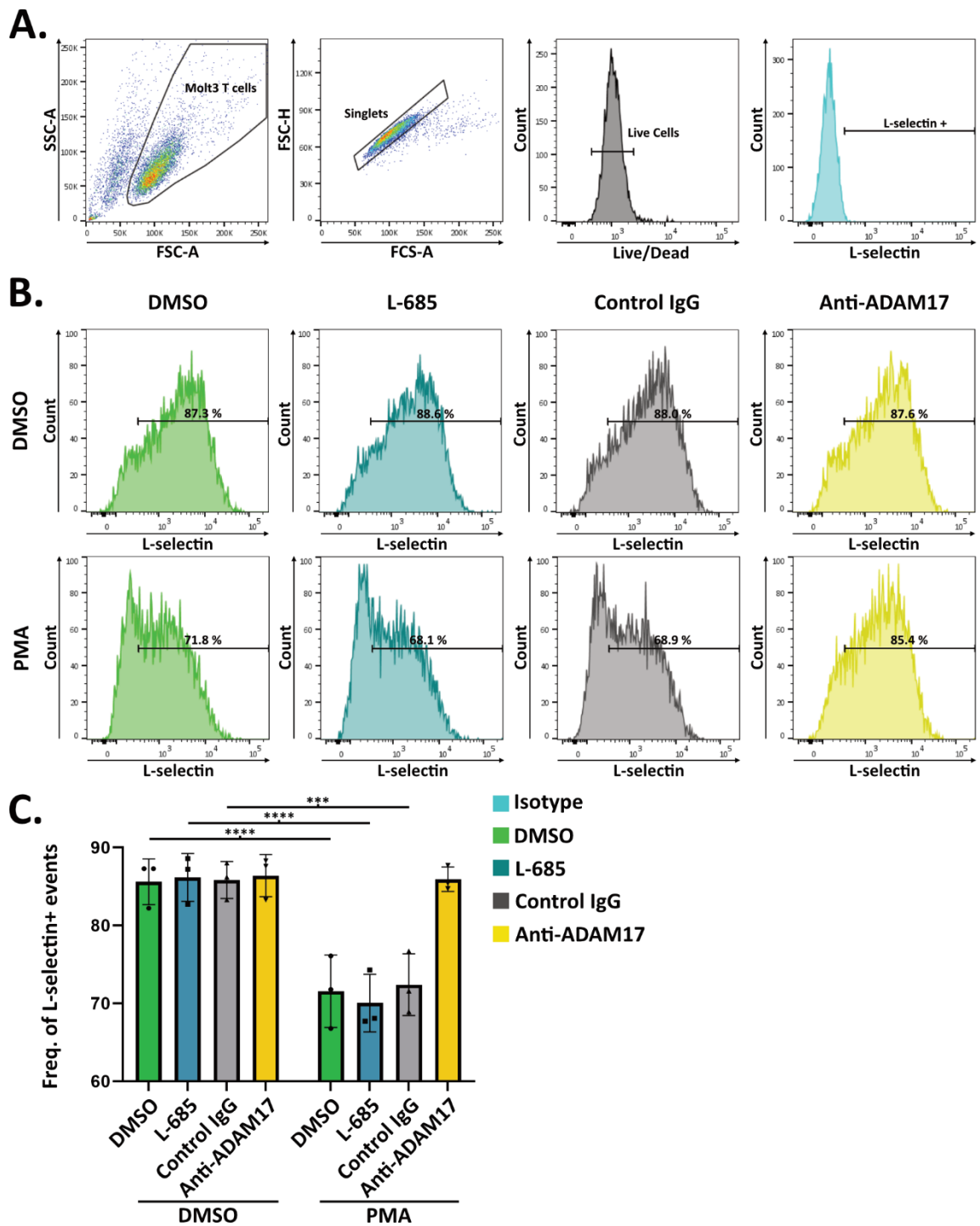


Figure 3.3. L-selectin undergoes sequential proteolysis of its Ecto- and Intra- cellular domains following PMA treatment which can be abrogated by anti-ADAM17 and L-685 respectively. Molt3 T cells were pre-treated with DMSO, L685, control IgG or anti-ADAM17 prior to treatment with PMA (or DMSO control) for 15 minutes to induce L-selectin proteolysis. **(A)** The gating strategy by which L-selectin⁺, Live, Single, Molt3 T cells were defined and **(B)** representative histograms of L-selectin expression are shown. **(C)** The quantified frequency of L-selectin⁺ events under all treatment conditions. n=3 from 3 independent experiments. Statistical Tests: Two-way ANOVA with Fisher's LSD test was performed. *** = p 0.0001, **** = p<0.0001.

Full-length (FL) V5/His tagged L-selectin has a predicted molecular weight of 45.6 kDa and on the western blot, this appeared around the 62 kDa marker (Fig. 3.3D). At the time of this experiment, it was unknown if the intermediate MRF could be detected by flow cytometry, so western blotting was used to detect the proteolysed products of L-selectin. Following ADAM-17 proteolysis, the MRF has a predicted molecular weight of 8.5 kDa and can be seen on the western blot between the 6 and 14 kDa markers (Fig. 3.3D). Of all the conditions, only the γ -secretase inhibitor L-685 was able to increase the blot intensity of the MRF following PMA treatment; it increased from 4792.2 to 14,909.5 (3.1-fold increase; Fig. 3.3D, E), indicating that γ -secretase is involved in proteolysis of the MRF after PMA stimulation of Molt3 T cells. Following further γ -secretase proteolysis, the released tail of L-selectin has a predicted molecular weight of 5.6 kDa, which was not observed by western blotting.

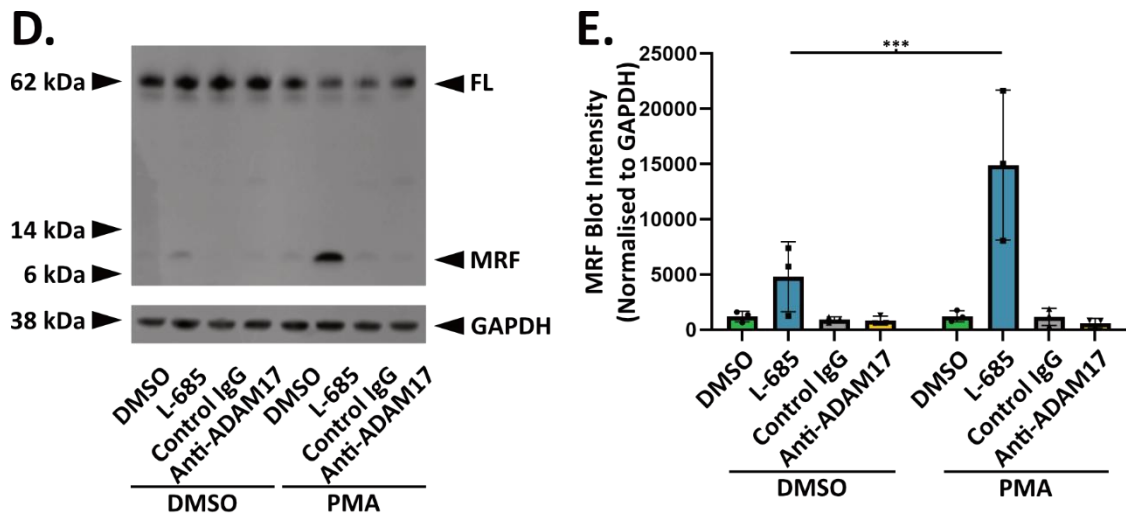


Figure 3.3. continued. L-selectin undergoes sequential proteolysis of its Ecto- and Intra-cellular domains following PMA treatment which can be abrogated by anti-ADAM17 and L-685 respectively. (D) Cells were treated as before but lysates prepared and immunoblotted for L-selectin's V5/His tagged tail. An example blot is shown and **(E)** the intensity of the MRF quantified for all treatment conditions. $n=3$ from 3 independent experiments. Statistical Tests: Two-way ANOVA with Fisher's LSD test was performed. *** = $p < 0.0001$, **** = $p < 0.0001$.

3.2.3. L-selectin's ectodomain and cytoplasmic tail proteolysis can be limited by genetically modified Δ MN and I Δ W L-selectin, respectively

WT, Δ MN or I Δ W Molt3 T cells were treated with PMA to induce L-selectin proteolysis. Ectodomain proteolysis occurred in both the WT and I Δ W Molt3 T cells, reducing the number of L-selectin positive events by 14.3 and 26.5 % respectively (Fig. 3.4A, B, C). A small, significant reduction of 1.7 % for Δ MN Molt3 T cells was observed in the number of L-selectin positive events (Fig. 3.4A, B, C).

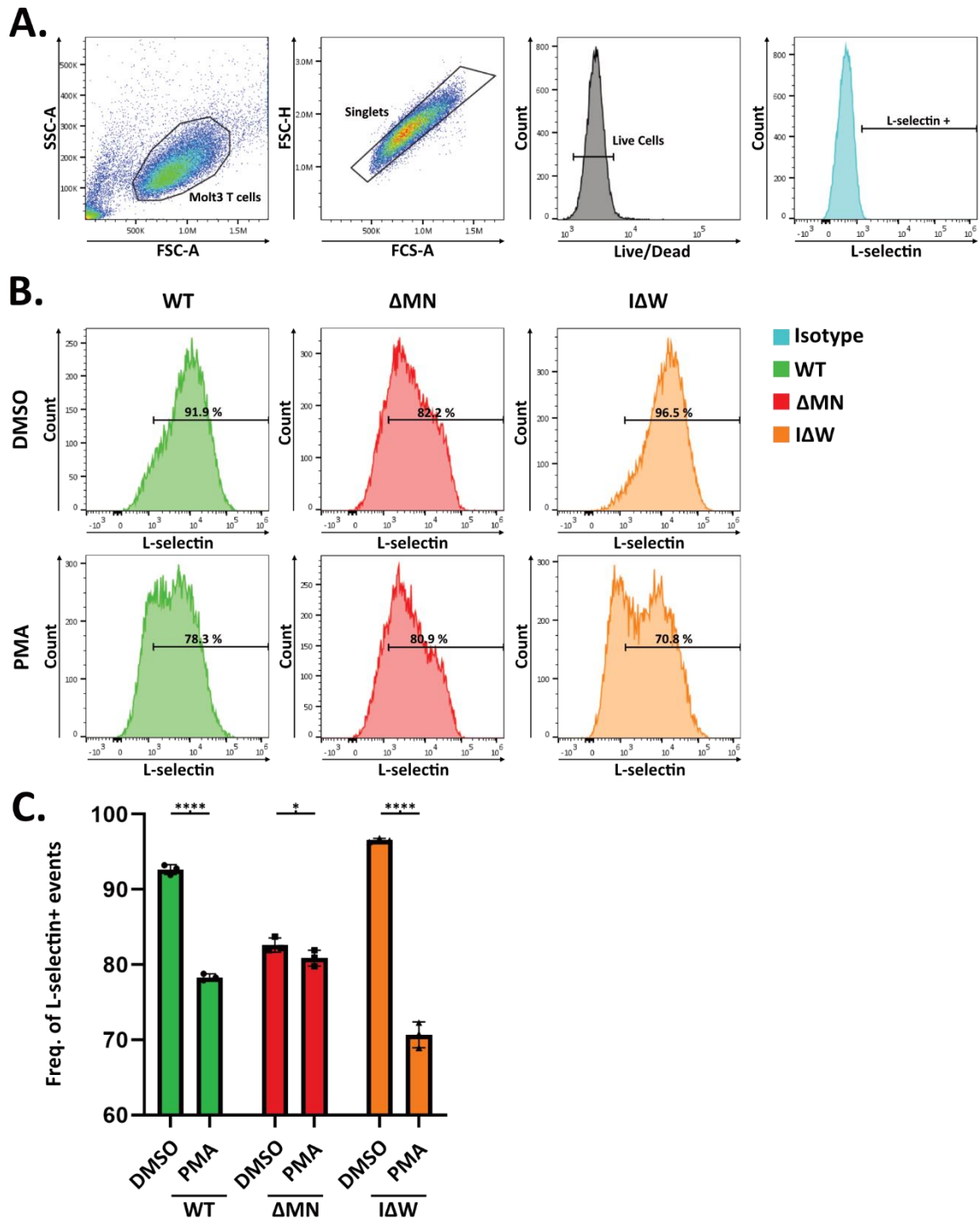


Figure 3.4. PMA induced L-selectin sequential proteolysis of its Ecto- and Intra- cellular domains is limited by genetic variants of L-selectin Δ MN, and I Δ W respectively. Molt3 T cells expressing a L-selectin variant were treated with PMA (or DMSO control) for 15 minutes to induce L-selectin proteolysis. **(A)** The gating strategy by which L-selectin⁺, Live, Single, Molt3 T cells were defined and **(B)** representative histograms of L-selectin expression are shown. **(C)** The quantified frequency of L-selectin⁺ events under each treatment conditions for each L-selectin variant expressed by Molt3 T cells. n=3 from 3 independent experiments. Statistical Tests: Two-way ANOVA with Fisher's LSD test was performed. ** = p 0.005, **** = p<0.0001.

A doublet of full-length IΔW L-selectin was observed and was not altered by PMA addition (Fig. 3.4D). Following PMA addition, no increase was observed in the blot intensity of the MRF for PMA-treated WT Molt3 T cells. The MRF blot intensity for IΔW Molt3 T cells increased from 2630.2 to 7574.5 (2.88-fold increase; Fig. 3.4D, E) in a similar manner to when WT Molt3 T cells were treated with the γ -secretase inhibitor L-685 prior to PMA-induced proteolysis (3.1-fold increase; Fig. 3.3D, E).

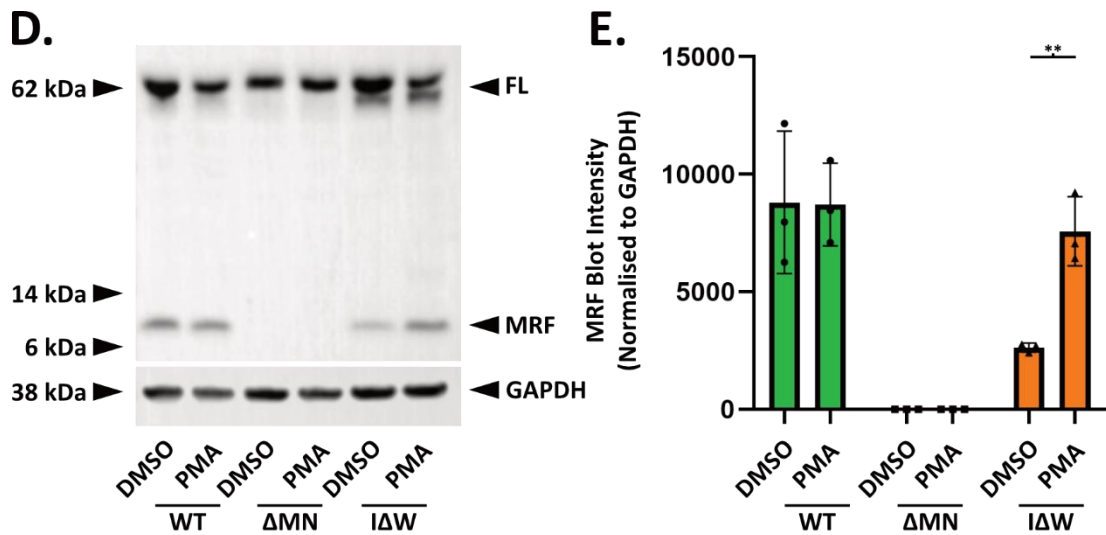
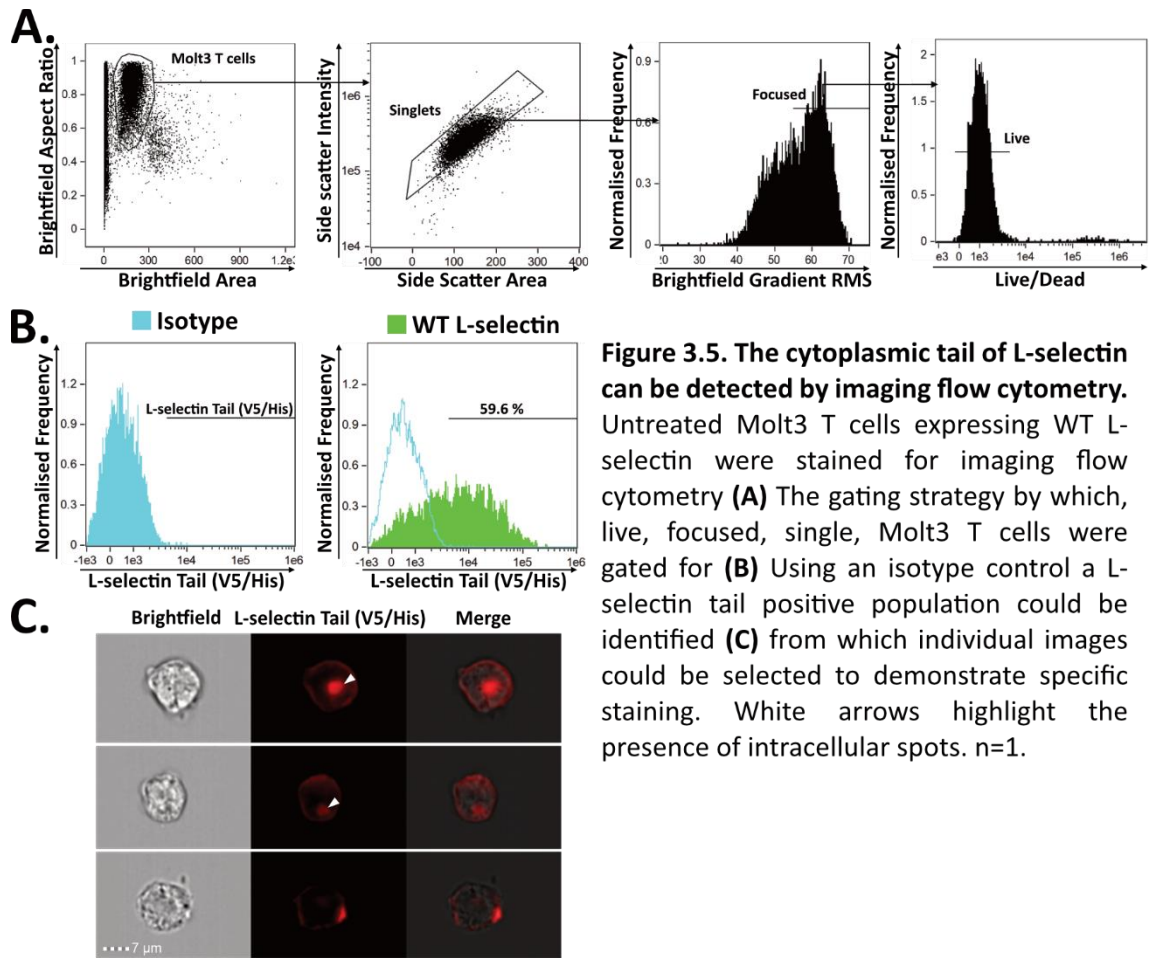


Figure 3.4. continued. PMA induced L-selectin sequential proteolysis of its Ecto- and Intra-cellular domains is limited by genetic variants of L-selectin ΔMN , and $I\Delta W$ respectively. (D) Cells were treated as before but lysates prepared and immunoblotted for L-selectin's V5/His tagged tail. An example blot is shown and **(E)** the intensity of the MRF quantified for each condition. n=3 from 3 independent experiments. Statistical Tests: Two-way ANOVA with Fisher's LSD test was performed. ** = p 0.005, **** = p<0.0001.

3.2.4. Defining parameters to assess the distribution of the tail of L-selectin using imaging flow cytometry

Six antibodies were tested by flow cytometry for their ability to stain the V5/His-tagged tail of L-selectin above the background staining of untransduced Molt3 T cells by conventional flow cytometry. The best of these was selected for further use in imaging flow cytometry experiments (Supp. Fig. 3.1A, B). In imaging flow cytometry, using a conventional gating strategy (with the additional parameter to select focused images; Brightfield Gradient RMS), I showed that 59.6 % of events were positive for L-selectin's cytoplasmic tail by imaging flow cytometry (Fig. 3.5B). Positive events were selected and showed staining at the membrane and intracellular spots, highlighted in the graphic by white arrows (Fig. 3.5C).



The goal of this chapter is to determine the distribution of the tail of L-selectin following proteolysis. By staining sub-cellular compartments (membrane, nucleus, and the lysosome) and the tail of L-selectin, I first sought to determine how these fluorescent signals co-localise. The imaging flow cytometry software package uses a log-transformed Pearson's correlation co-efficient to evaluate the similarity in the distribution of fluorescence between two probes. The software reports this as a 'similarity score', and the example provided by Luminex of how this varies is shown in the materials and methods. The similarity score feature within the software package is designed for use within user-defined sub-cellular compartments or 'masks'. At the time of writing, a quantitative method to generate a 'membrane mask' on cells within a dataset based on membrane-associated fluorescence has not been described. Additionally, as the intracellular region of T cells is dominated by the nucleus, its important the membrane mask is stringent.

The adaptive erode feature within the analysis software is a mask which covers the brightfield image when set at a value of 100/100, as the user-set value decreases, the mask gets smaller according to the shape of the cell toward its centre. This feature can be used to generate concentric ring masks throughout the cell, where each ring is one pixel thick and corresponds to 0.3 μm (Fig. 3.6B). The median intensity values for membrane-associated fluorophores in each concentric ring mask were extracted and plotted against the mask number (mask 1 – 40; Fig. 3.6B, C left).

The median fluorescence intensity values of extracellularly stained CD69 and intracellularly stained L-selectin tail were normalised to the sum intensity for each fluorophore and plotted against the mask number (Fig. 3.6C middle). Peaks were apparent, and the sum of two Lorentzian curves was plotted to these data (Fig. 3.6C right). The width of first Lorentzian curve peak corresponded to masks on the x-axis which contained membrane-associated fluorescence (grey bar on Fig. 3.6C right). The second peak width corresponded to either background cellular fluorescence or intracellular staining. The masks within the grey region were merged to create a

quantitatively defined membrane mask which, when subtracted from the whole cell image, not including regions beyond the membrane mask, generated an intracellular mask (Fig. 3.6D). This method was developed in collaboration with Stephen Cobbold (Emeritus professor, Oxford University).

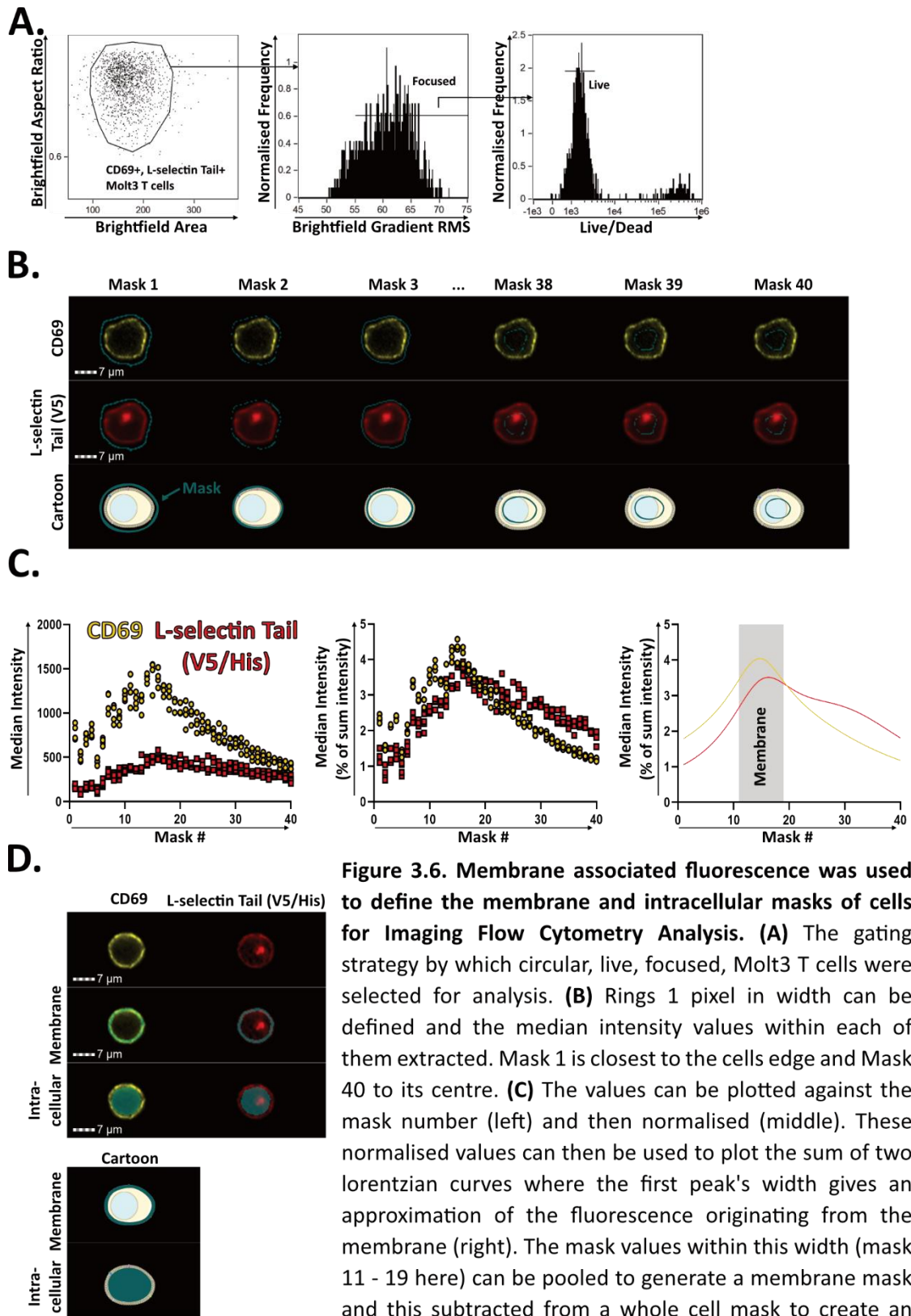


Figure 3.6. Membrane associated fluorescence was used to define the membrane and intracellular masks of cells for Imaging Flow Cytometry Analysis. (A) The gating strategy by which circular, live, focused, Molt3 T cells were selected for analysis. (B) Rings 1 pixel in width can be defined and the median intensity values within each of them extracted. Mask 1 is closest to the cells edge and Mask 40 to its centre. (C) The values can be plotted against the mask number (left) and then normalised (middle). These normalised values can then be used to plot the sum of two lorentzian curves where the first peak's width gives an approximation of the fluorescence originating from the membrane (right). The mask values within this width (mask 11 - 19 here) can be pooled to generate a membrane mask and this subtracted from a whole cell mask to create an intracellular mask. (D) A membrane fluorophore positive cell with and without the defined masks. $n = 3$ of 3 independent experiments.

These masks appeared accurate by eye (Fig. 3.6D), and when this method was applied to another independent preliminary experiment, in which WT L-selectin positive Molt3 T cells were stained for CD107a, L-selectin's ectodomain and V5/His-tagged tail (Fig. 3.7A), extracellular staining of L-selectin was located predominantly in the membrane mask and intracellular staining of CD107a was predominantly within the intracellular mask, so these masks appeared accurate (Fig. 3.7B).

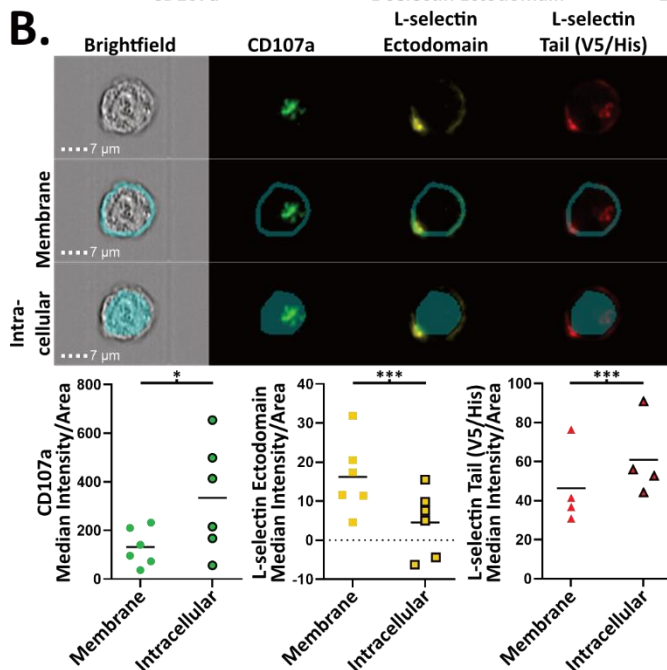
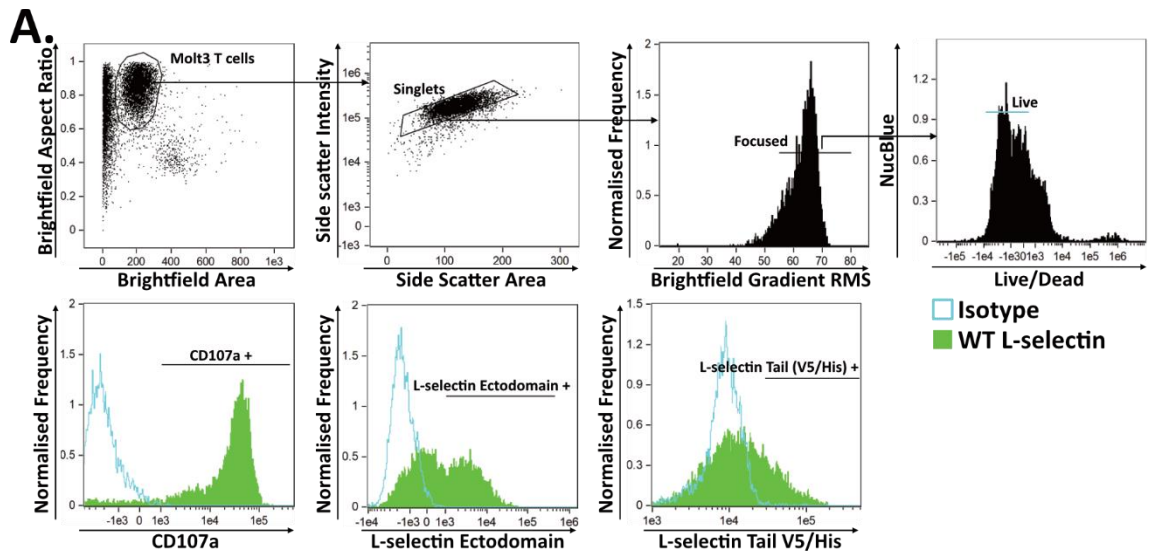


Figure 3.7. Membrane and intracellular masks can be used to quantitate fluorophores. (A) The gating strategy by which live, focused, single, Molt3 T cells can be isolated for analysis and WT L-selectin positive Molt3 T cells stained together for CD107a, L-selectin ectodomain and V5/His tagged tail to show specific staining. **(B)** Specifically stained cell images are shown here to qualitatively demonstrate the distribution of various fluorophore's intensities and the masking strategy. The quantitative median intensity/area as defined by the masking strategy is

shown and aligns with the images. $n = 6$ from 3 independent experiments with two technical replicates, except for V5/His staining where $n = 4$. Statistical Tests: Paired two-tailed parametric t-test. * = $p < 0.05$, *** = $p < 0.001$.

During preliminary experiments, spots were apparent when staining for the L-selectin tail (Fig. 3.5C). The spot counting feature within the imaging flow cytometry software package enables the user to distinguish bright regions of a cell from background fluorescence. It does this using a user-defined spot-to-cell background ratio and enables the user to set a minimum and maximum spot radius. These spots can then be counted and further investigated for their size. If the tail of L-selectin is released from the membrane following proteolysis, intracellular spots may become apparent in experiments. Using the same dataset in Fig. 3.7, L-selectin tail positive events can be selected, and from these, the frequency of spot positive events quantified and selected (Fig. 3.8A, B). These spot positive events can then have their number of spots quantified (Fig. 3.8B).

Spot counting can be conducted across the whole cell, but by doing so includes L-selectin tail fluorescence within the membrane mask, which I did not seek to quantify. In the imaging flow cytometry analysis software, I could perform spot counting within the intracellular mask to exclude membrane-associated fluorescence (full length and MRF L-selectin) and in future experiments spot counting and analysis is performed within the intracellular mask (Fig. 3.8).

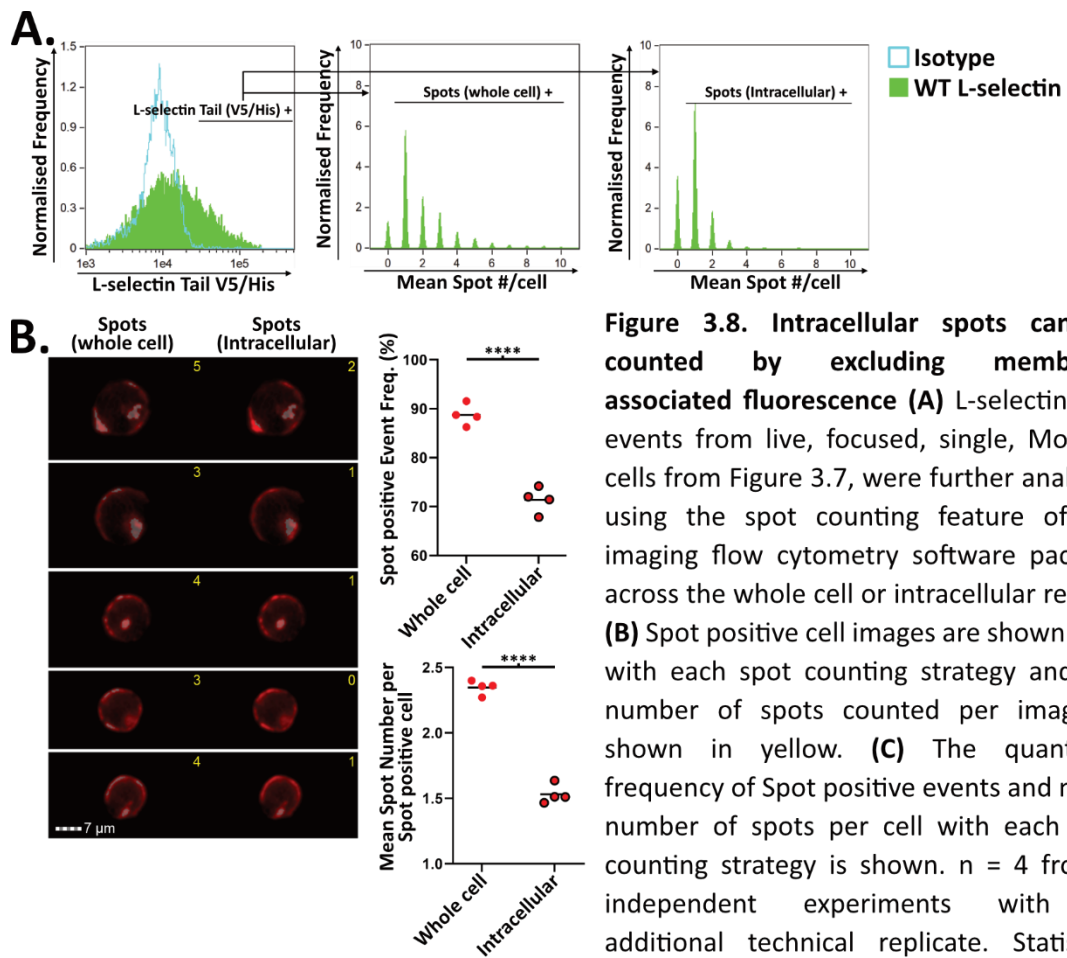


Figure 3.8. Intracellular spots can be counted by excluding membrane associated fluorescence (A) L-selectin tail⁺ events from live, focused, single, Molt3 T cells from Figure 3.7, were further analysed using the spot counting feature of the imaging flow cytometry software package across the whole cell or intracellular region. **(B)** Spot positive cell images are shown here with each spot counting strategy and the number of spots counted per image is shown in yellow. **(C)** The quantified frequency of Spot positive events and mean number of spots per cell with each spot counting strategy is shown. n = 4 from 3 independent experiments with an additional technical replicate. Statistical Tests: Paired two-tailed parametric t-test . **** = p<0.0001.

Using the spot counting feature within the intracellular mask, 70 % of the L-selectin tail positive events have at least one spot and the mean number of spots per cell is approximately 1.5 (Fig. 3.8B)

Within both membrane and intracellular masks, co-localisation scores between the L-selectin tail and other sub-cellular compartments could now be evaluated. In addition, each masked region's median fluorescence intensity for a given marker and intracellular spot counting could be quantified. I used these analyses to investigate the fate of the L-selectin tail following PMA-induced shedding by imaging flow cytometry.

3.2.5. The L-selectin tail is lost from the membrane following PMA-induced sequential proteolysis and does not co-localise with lysosomes or the nucleus

The experiments demonstrating sequential proteolysis of L-selectin by flow cytometry and western blotting in 3.2.2 were repeated for imaging flow cytometry. Accordingly, WT Molt3 T cells were pre-treated with either DMSO, L-685, control IgG or blocking anti-ADAM17 for 1 hour prior to PMA-induced ectodomain proteolysis in the continued presence of inhibitors. Using the γ -secretase inhibitor in the western blotting experiment in 3.2.2 revealed the MRF of L-selectin had been further proteolysed by 15 minutes. Therefore, imaging flow cytometry was used to track L-selectin's cytoplasmic tail at 0, 5, 10 and 15-minutes post-PMA stimulation relative to its vehicle control (DMSO) to detect the released tail of L-selectin. Molt3 T cells were stained with an antibody against L-selectin's tail, NucBlue to stain the nuclear compartment and an antibody against CD107a to label the lysosomal compartment. This was done as a preliminary investigation to determine if the tail of L-selectin migrated to the nucleus, where it may have roles in transcriptional regulation alike the γ -secretase product of amyloid precursor protein (Kimberly et al. 2001), or the lysosomal compartment, where it may be degraded alike the γ -secretase product of Met (a receptor tyrosine kinase; Ancot et al. 2012). The gating strategy used to evaluate median fluorescence intensities is shown in Fig. 3.9A, and representative positively stained histograms at 15 minutes post-PMA treatment relative to DMSO are shown to demonstrate successful staining (Fig. 3.9B).

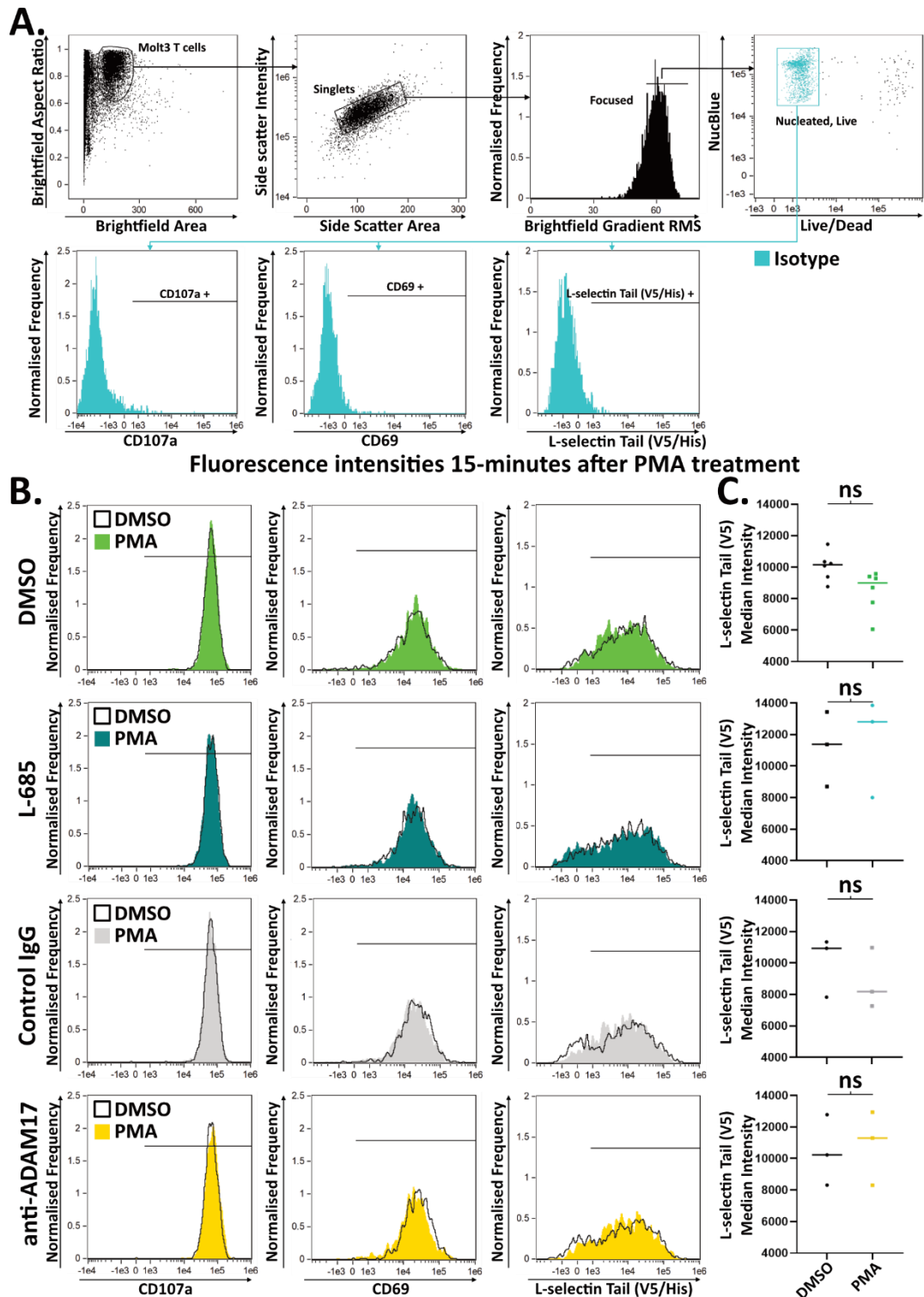


Figure 3.9. PMA induced sequential proteolysis of L-selectin's tail does not cause significant changes to L-selectin's tail median fluorescence intensity values across the whole cell. Molt3 T cells were pre-treated with either L-685, anti-ADAM17 or the relevant controls (DMSO and hlgG respectively) before incubation with PMA. **(A)** The gating strategy by which, live, nucleated, focused, single, Molt3 T cells had their median fluorescence intensities assessed. **(B)** Representative histograms of stained Molt3 T cells after the indicated treatments. **(C)** The quantification of L-selectin's tail median fluorescence intensity at 15 minutes after PMA addition. $n = 3$ from 3 independent experiments except for DMSO pre-treated Molt3 T cells where each experiment contained two technical replicates. Statistical Tests: two-way ANOVA with Fisher's LSD test was performed. ns = non-significant.

Evaluation of whole cell median fluorescence intensity values was first used to determine if the fluorescence corresponding to the L-selectin tail changed following PMA treatment. In the absence of PMA, DMSO (as a control for L-685), L-685, hIgG and anti-ADAM17 did not induce any changes in fluorescence (Fig. 3.10).

Additionally, at 15 minutes following PMA addition, there were no significant changes to whole cell median intensity values for the tail of L-selectin under any pre-treatments (Fig. 3.10).

Except for one statistically significant decrease in CD107a median intensity at 5 minutes post-PMA treatment in L-685 pre-treated cells, no other changes in median intensity values were observed (Fig. 3.10). This decrease in CD107a appears to be an outlier. I had sought to use CD69 as an activation marker in an attempt to gate on cells which proteolyse L-selectin. However, in Molt3 T cells, CD69 is constitutively expressed at the cell membrane and is unchanged by treatment with PMA (Fig. 3.10). This consistency of intensity means I was able to use CD69 as a constant membrane marker rather than an activation marker and determine the similarity score between the tail of L-selectin and the membrane.

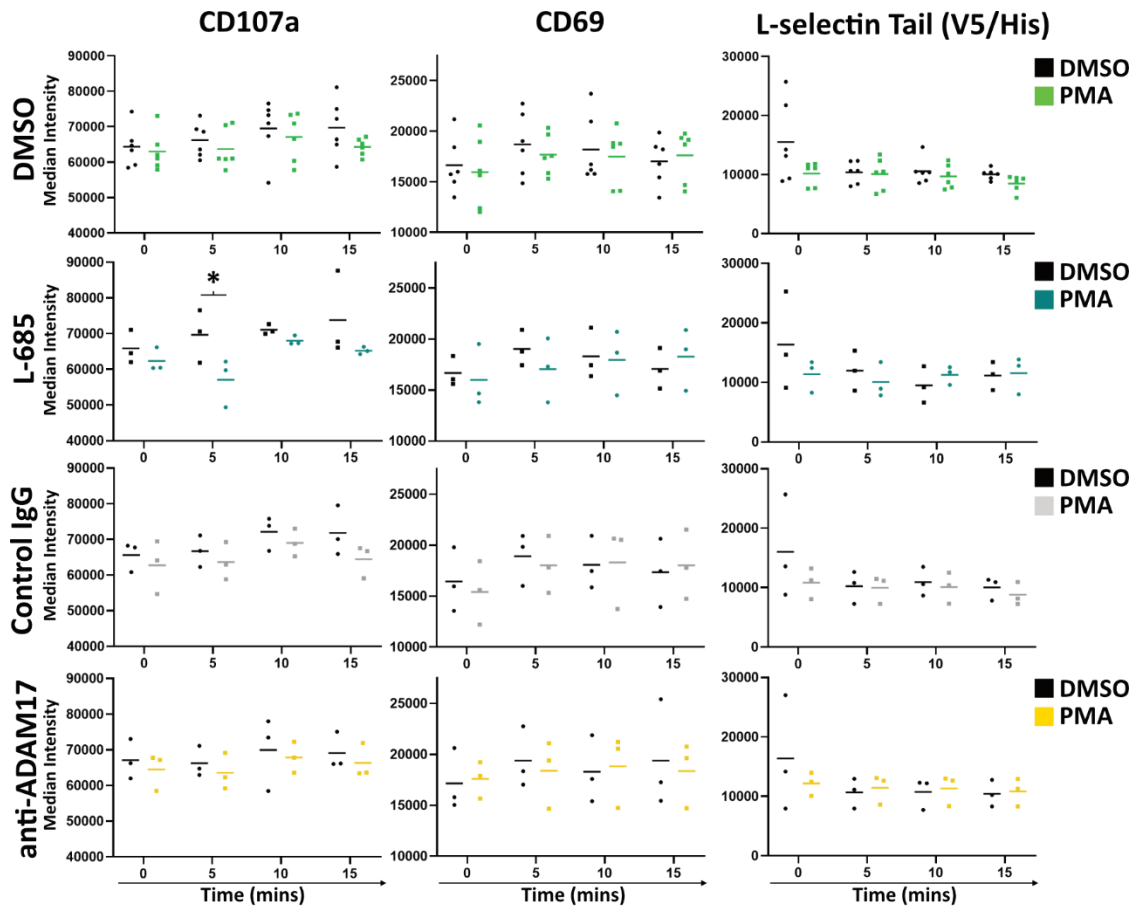


Figure 3.10. The median fluorescence intensity values across the whole cell for CD107a, CD69 or the tail of L-selectin did not change at any time points assayed. Molt3 T cells were pre-treated with either L-685, anti-ADAM17 or the relevant controls (DMSO and IgG respectively) before incubation with PMA. Events were assayed for median fluorescence intensities of the indicated stained markers using the gating strategy in Fig 3.9, A. and the values plotted against time since PMA addition. $n = 3$ from 3 independent experiments except for DMSO pre-treated Molt3 T cells where each experiment contained two technical replicates. Statistical Tests: two-way ANOVA with Fisher's LSD test was performed. * = $p < 0.05$.

Cells that were positive for CD69 (membrane marker), CD107a (lysosome marker) and the L-selectin tail (by V5/His tag staining) relative to the isotype control (Fig. 3.9A) were 'AND-gated' and triple positive events were assessed for their median similarity scores between pairs of markers within the relevant cellular compartments (Fig. 3.11A). Representative staining (Fig. 3.11A) and similarity score histograms (Fig. 3.11B) are shown for the 15-minute time point post-PMA addition. The similarity score between the L-selectin tail and CD69 in the membrane mask decreased at 15 minutes after PMA addition if the cells were pre-treated with DMSO, as the histogram shifted to the left (black arrows; Fig. 3.11B). Molt3 T cells pre-treated with hIgG had a similar trend, but this was not significant. For cells pre-treated with either L-685 or anti-ADAM17, similarity was stable following PMA treatment (Fig. 3.11B). Interestingly, a shift to the right was observed in the similarity score between the L-selectin tail and the nucleus of control IgG pre-treated Molt3 T cells in this replicate. However, this was not significant.

The decrease in similarity between CD69 and the L-selectin tail for DMSO pre-treated Molt3 T cells is a significant decrease of 0.11 from 1.87 to 1.69 (Fig. 3.11C). There were no significant decreases in similarity to CD69 observed at any other time points before 15 minutes, and no increases in similarity with CD107a in the intracellular mask or increases in similar morphology with the nucleus were observed at any time points post-PMA addition under any pre-treatment condition (Fig. 3.12). The CD107a stain is also commonly used as a degranulation marker, but I observed no changes in the distribution of its fluorescence during my experiments with the Molt3 T cell line.

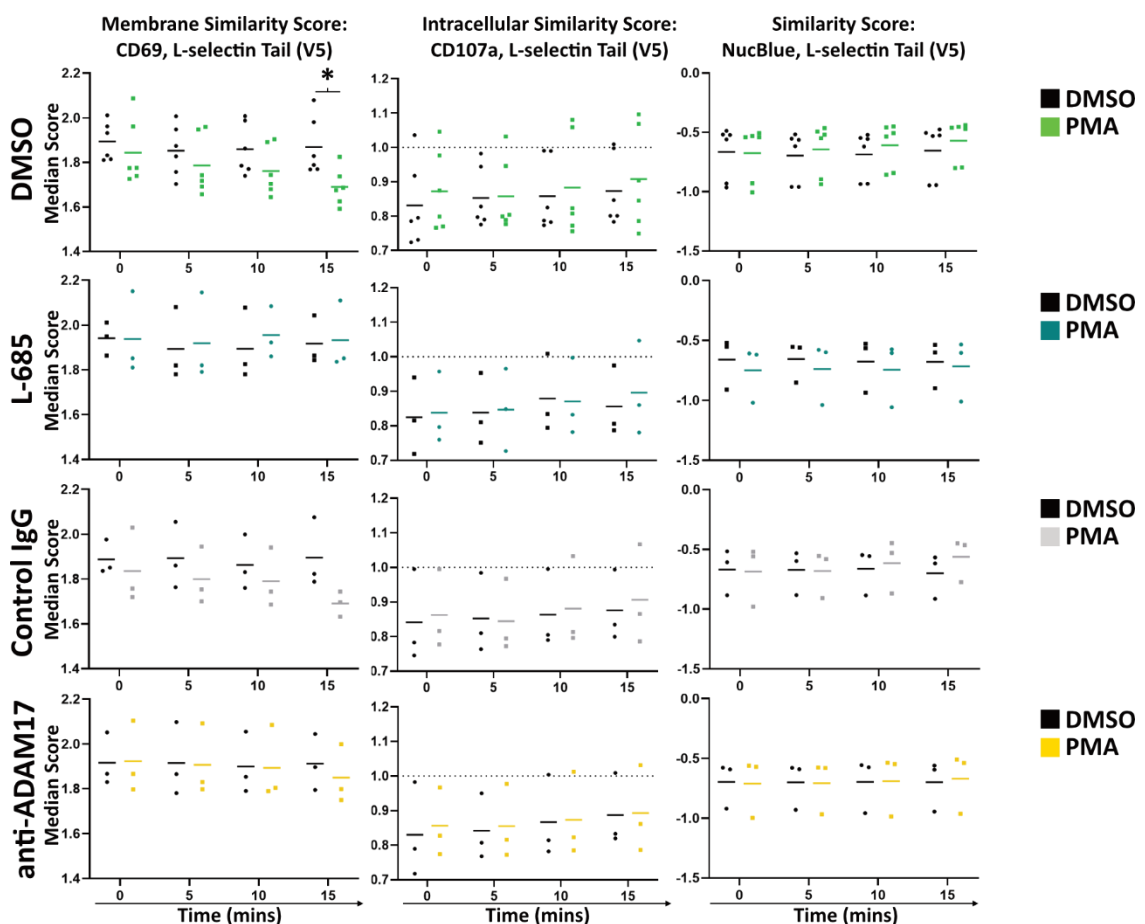


Figure 3.12. The similarity score between the tail of L-selectin, the lysosomal marker (CD107a) or the nucleus did not change at any time point following PMA treatment. Molt3 T cells were pre-treated with either L-685, anti-ADAM17 or the relevant controls (DMSO and hlgG respectively) before incubation with PMA. AND-gated triple positive events as defined in Fig. 3.9, A were assessed for similarity scores. The median similarity scores between the indicated pairs of fluorophores within the relevant masks as in Fig. 3.11, A were plotted against time since PMA addition. $n = 3$ from 3 independent experiments except for DMSO pre-treated Molt3 T cells where each experiment contained two technical replicates. Statistical Tests: two-way ANOVA with Fisher's LSD test was performed. * = $p < 0.05$.

I reasoned, if the L-selectin tail similarity with the membrane marker CD69 decreased at 15 minutes, but no increase was seen in the similarity scores with CD107a or the nucleus, the number of spots per cell should increase as the cytosolic tail is proteolysed and moves away from the membrane. However, no increases in the number of spots per cell could be seen at 15-minutes post PMA addition (Fig. 3.13A), nor any time points prior regardless of pre-treatment or treatment with PMA (Fig. 3.13B). The mean spot area and number of spot positive events was also assessed, but no increases were seen (data not shown).

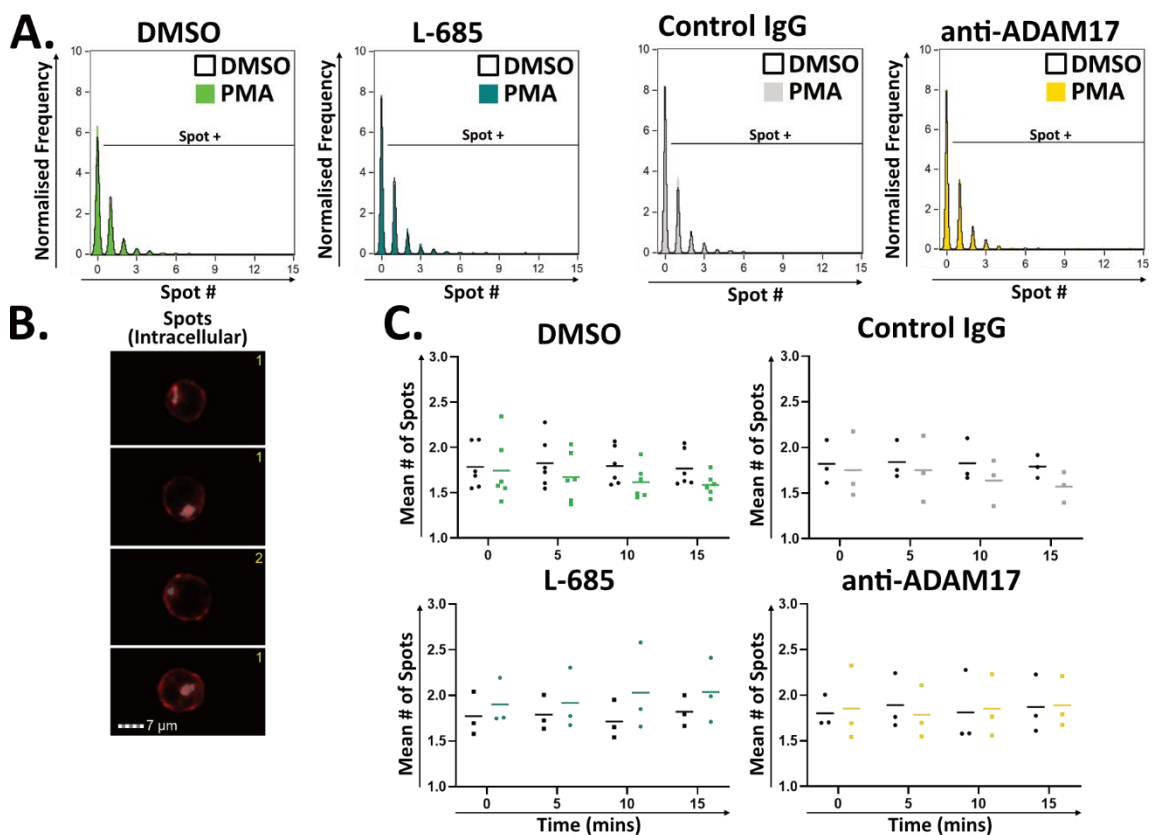


Figure 3.13. The number of spots per cell observed did not change at any timepoints following PMA treatment. Molt3 T cells were pre-treated with either L-685, anti-ADAM17 or the relevant controls (DMSO and hIgG respectively) before incubation with PMA. **(A)** L-selectin tail⁺ events as defined in Fig. 3.9, A according to isotype gating were assessed by **(B)** spot counting on spot⁺ events. Images of representative spot positive events are shown and the yellow text indicates the number of spots in the image. **(C)** The mean number of spots was plotted against time since PMA addition. n = 3 from 3 independent experiments except for DMSO pre-treated Molt3 T cells where each experiment contained two technical replicates. Statistical Tests: two-way ANOVA with Fisher's LSD test was performed.

If the spot parameters did not change, and signal is lost from the membrane, I further reasoned L-selectin tail-associated fluorescence intensity should increase within the intracellular compartment as diffuse signal intensity.

Therefore, I examined the intensity of the L-selectin tail V5/His staining within the membrane and intracellular masks. At 15-minutes following PMA stimulation, a decrease in staining intensity per unit area at the membrane for the L-selectin tail was observed in DMSO pre-treated Molt3 T cells (Fig. 3.14), despite no significant decrease in total cell intensity (Fig. 3.9B).

The L-selectin tail median fluorescence intensity per unit area decreased from 72.59 to 54.48 within the membrane mask. However, no increase in fluorescence intensity per unit area was observed in the intracellular mask following PMA-induced L-selectin proteolysis.

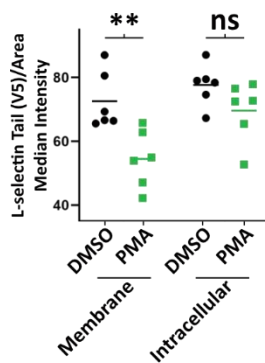


Figure 3.14. PMA induces a decrease in L-selectin's tail fluorescence intensity within the membrane mask. Molt3 T cells expressing WT L-selectin were pre-treated with DMSO before incubation with PMA or DMSO control. **(A)** Live, focused, single, Molt3 T cells as defined in Fig. 3.9. A were assessed for median fluorescence intensity/area of L-selectin's tail (by V5/His staining) using the gating strategy in Fig 3.9, A and areas were defined as in 3.11, A. n = 6 from 3 independent experiments with 2 technical replicates. Statistical Tests: two-way ANOVA with Fisher's LSD test was performed. ** = $p < 0.001$, ns = non-significant.

Together, these data indicate L-selectin tail proteolysis can be detected by imaging flow cytometry as its similarity to the CD69 membrane marker decreases and staining intensity is lost specifically from the membrane of the cell following PMA treatment. However, fluorescence signal corresponding to the tail is lost altogether rather than as a function of redistribution within the cell, because it was not detected in the intracellular compartment. In initial experiments, only 15 % of events shed the ectodomain of L-selectin and became L-selectin negative by flow cytometry (Fig. 3.3). Here, the loss of signal intensity corresponding to L-selectin's tail was not

significant on a whole cell basis. Further, imaging flow cytometry cannot distinguish between full-length L-selectin and the MRF by size like western blotting. Therefore, it is unsurprising the changes in similarity score to the membrane marker are minute. However, they are significant and can be detected.

I hypothesised that the loss of L-selectin tail staining from the membrane mask specifically was either due to: (1) improper fixation and permeabilisation, which caused leakage of the proteolysed tail; (2) an intracellular binding partner blocking the antibody used to detect the V5/His tag upon the tail of L-selectin; (3) and/or degradation of the tail.

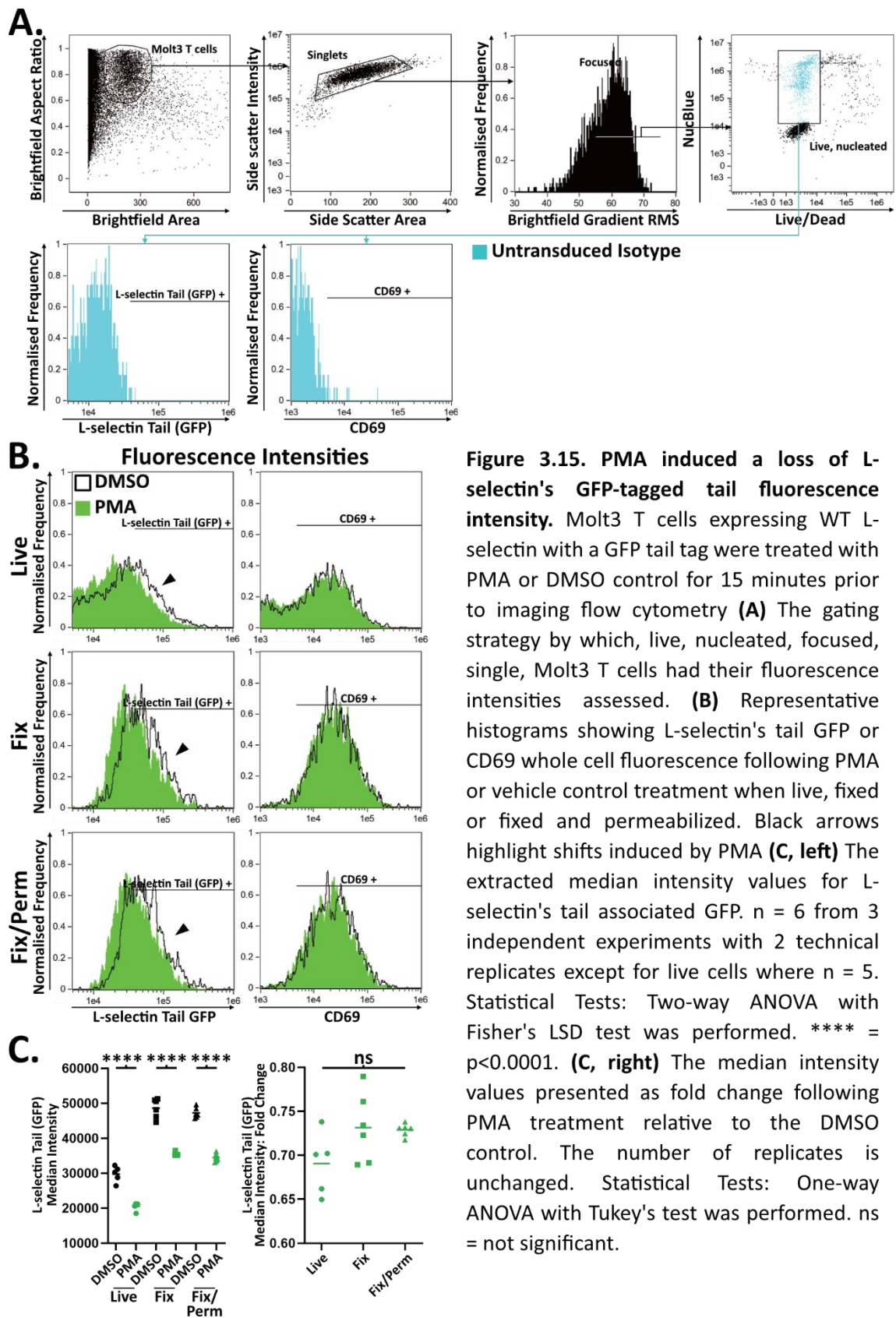
3.2.6. Molt3 T cells expressing WT L-selectin with a cytosolic GFP tag lose GFP signal following PMA-induced L-selectin proteolysis

To address the above hypotheses, a lentiviral vector encoding WT L-selectin with a cytosolic tail GFP tag was obtained from Alexander Ivetic (King's College London; Rzeniewicz et al., 2015). I generated a Molt3 T cell line expressing this construct and treated these cells with PMA for 15 minutes before analysis by imaging flow cytometry. The L-selectin tail was now pre-tagged and therefore enabled me to test the hypothesis that an intracellular binding partner was blocking the antibody I used to detect the V5/His-tagged L-selectin tail. In addition, I performed this experiment with live cells, fixed cells and cells which had undergone fixation and permeabilisation to test the hypothesis that improper fixation or permeabilisation induced leakage of the L-selectin tail following proteolysis resulting in the loss of signal in my previous analysis.

PMA treatment was sufficient to reduce whole-cell GFP fluorescence whilst CD69 again remained stable (Fig. 3.15B). For PMA-treated cells, the GFP median intensity significantly decreased regardless of whether the cells were live, fixed, or fixed and then permeabilised (Fig. 3.15C). The live cells appeared dimmer by median

fluorescence intensity relative to cells either fixed, or fixed and then permeabilised, but the histograms showed this was due to the presence of GFP^{dim} cells, and not the loss of GFP^{bright} cells (Fig. 3.15B). As shown in the representative histograms, CD69 remained stable following PMA treatment and could again be used as a membrane marker in experiments with this Molt3 cell line expressing GFP-tagged L-selectin.

To normalise the median fluorescence intensities to account for the differences between cells imaged when live relative to those which were fixed or fixed and then permeabilised, I expressed the data as fold change (normalised to DMSO treated controls). No significant difference could be seen between any of the post-experiment cell treatments (Fig. 3.15C) i.e. live cells vs fixed vs fixed/permeabilised.



To confirm that the GFP-tagged tail of L-selectin moved away from the membrane like the V5/His-tagged tail of L-selectin, double positive AND-gated events were selected for further analysis (Fig. 3.15A, B). The similarity score of L-selectin's GFP-tagged tail and the CD69 membrane marker within the membrane mask was compared (Fig. 3.16A). PMA-induced a decrease in median similarity score between the two markers of approximately 0.19 (Fig. 3.16C top). This was approximately 0.1 for V5/His tagged L-selectin. When expressed as fold-change in median similarity (normalised to DMSO controls), a small difference between live and fixed cells was detected but not between live cells and those which had been fixed then permeabilised cells (Fig. 3.16C bottom).

Together, these data indicate the loss of fluorescence of the tail of L-selectin at the membrane is not due to a binding partner preventing antibody binding, or loss of the cytoplasmic tail during fixation and permeabilisation. Rather, the PMA-induced loss in fluorescence must be due to degradation.

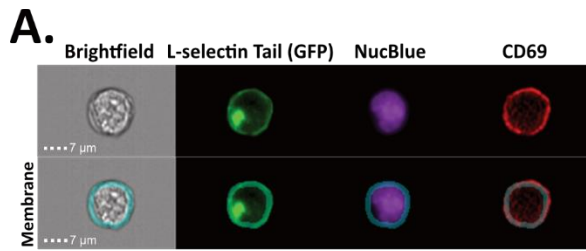
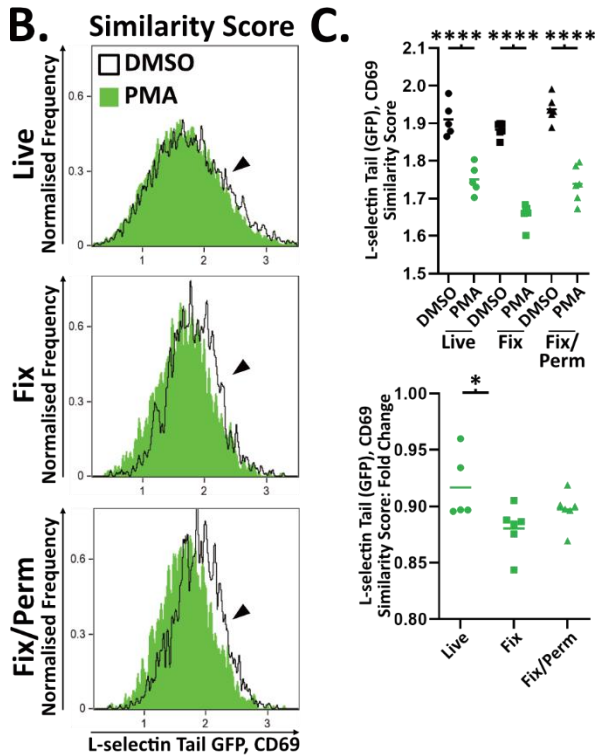


Figure 3.16. PMA induced a decrease in similarity between L-selectin's GFP-tagged tail and the membrane marker. Double positive, AND-gated events as determined by untransduced isotype staining in 3.14, A were assessed for the similarity in the membrane between L-selectin's GFP tagged tail and CD69. **(A)** A double positive event is shown with the masking strategy to analyse similarity scores within the membrane overlaid. **(B)** Representative histograms of the similarity score between the indicated markers after 15 minutes of PMA or DMSO control. Black arrows indicate PMA induced shifts. **(C)** Cellular compartments were defined and co-localisation scores between fluorescent markers assessed within them. **(C, top)** The extracted median similarity scores for the indicated markers. $n = 6$ from 3 independent experiments with 2 technical replicates except for live cells where $n = 5$. Statistical Tests: Two-way ANOVA with Fisher's LSD test was performed. **** = $p < 0.0001$. **(C, bottom)** The median similarity scores are presented as fold change following PMA treatment relative to the DMSO control. The number of replicates is unchanged. Statistical Tests: One-way ANOVA with Tukey's test was performed. * = $p < 0.05$.



3.2.7. Proteasomal inhibition of WT Molt3 T cells stabilises L-selectin's MRF following PMA-induced sequential proteolysis

Due to the PMA-induced loss of L-selectin tail fluorescence at the membrane independent of its tag or permeabilisation, I sought to determine if its loss was due to protein degradation. I pre-treated WT Molt3 T cells with a range of inhibitors prior to PMA stimulation, including MG132, which inhibits the proteasome (Mroczkiewicz et al., 2010), bafilomycin A1 (BafA1), which prevents autophagosome-lysosome fusion and deacidifies intracellular compartments by inhibiting ATPase (Yamamoto et al., 1998), chloroquine (ChQ), which also prevents autophagosome-lysosome fusion (Mauthe et al., 2018), pepstatin and leupeptin, which are broad protease inhibitors (P&L; Maeda et al., 1971; Marcinişzyn et al., 1977), and MRT68921 (MRT), which prevents autophagy in cells by inhibiting ULK-1 and -2 (Petherick et al., 2015).

Under basal conditions, BafA1 caused an accumulation of the MRF, unlike the other inhibitors, but no further increase was seen after PMA treatment. Following 15 minutes of PMA stimulation, only MG132 caused a clear increase in the intensity of the MRF fragment of L-selectin, which was a 3.23-fold increase in signal (Fig. 3.17A, B). Surprisingly, no additional 5.6 kDa band which could be attributed to the γ -secretase released MRF cleavage product (L-selectin's cytoplasmic tail) was observed by western blotting.

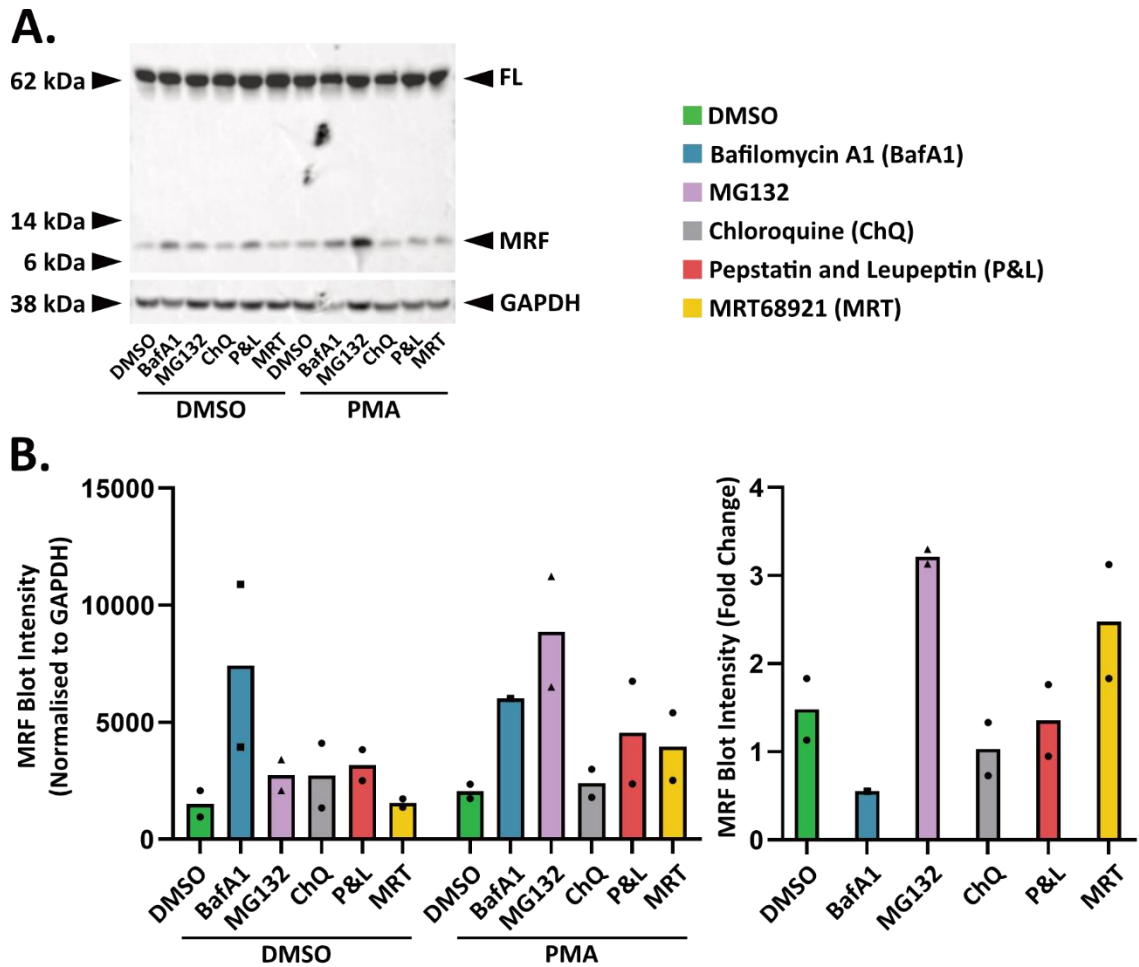


Figure 3.17. The proteasomal inhibitor MG132 stabilises the L-selectin MRF. Molt3 T cells were treated with the indicated inhibitors or DMSO control prior to PMA induced proteolysis or DMSO control before lysis and immunoblotting for L-selectin's V5/His tagged cytosolic tail. **(A)** A representative immunoblot for L-selectin's intracellular domain and **(B)** the quantification of this relative to GAPDH control and presentation as fold change following PMA treatment. n=2 from two independent experiments.

3.2.8. Proteasome Inhibition-induced accumulation of the MRF following PMA-induced sequential proteolysis of L-selectin could not be detected by imaging flow cytometry

To determine whether the accumulated MRF remained in the membrane when the proteasome was inhibited, I performed the same experiment but analysed the samples by imaging flow cytometry. As in the previous experiment, WT Molt3 T cells were stimulated with PMA to induce shedding following pre-treatment with either MG132, or DMSO as a vehicle control. To provide context for changes to similarity scores and median fluorescence intensities induced by PMA treatment, L-selectin's ectodomain was stained in these experiments, which was obviously lost from the cell surface in preliminary experiments (Fig. 3.2 and Fig. 3.2). Regrettably, it was not included in the previous imaging flow cytometry experiments due to the unique set-up of the ImageStream's optics, which limited the number of fluorophores that could be used in a single experiment, preventing its inclusion alongside intracellular markers.

Assessment of the Molt3 T cell whole-cell median fluorescence intensities demonstrated a significant decrease in L-selectin ectodomain intensity from approximately 16700 to 9150 (approximately 55 %) regardless of pre-treatment with MG132 (Fig. 3.18A, B, C). In conventional flow cytometry experiments (Fig. 3.3), this could be abrogated by anti-ADAM-17, and so is due to ectodomain shedding. The L-selectin tail fluorescence tail intensity also significantly decreased with PMA stimulation; with DMSO treated Molt3 T cells this was 19.6 %, if treated with MG132 a lower decrease of 17.4 % was observed (Fig. 3.18B, C). A surprising, but small, increase in CD69 median fluorescence intensity of approximately 6.5 % following PMA stimulation was also observed regardless of pre-treatment, which was not observed in previous experiments (Fig. 3.18B, C). γ -secretase intensity remained constant throughout the experiment (Fig. 3.18B, C). This was included to determine whether co-localisation with γ -secretase and the tail of L-selectin increased with proteasome inhibition. The staining was elevated above the isotype control but upon inspection did not appear specific and so was excluded from further analyses.

Due to the subtle abrogation by MG132 on the decrease of the L-selectin tail whole-cell intensity, I transformed the data to fold-change induced by PMA and compared the two pre-treatments directly, but found no significant difference between DMSO and MG132 pre-treated Molt3 T cells (Fig. 3.18D).

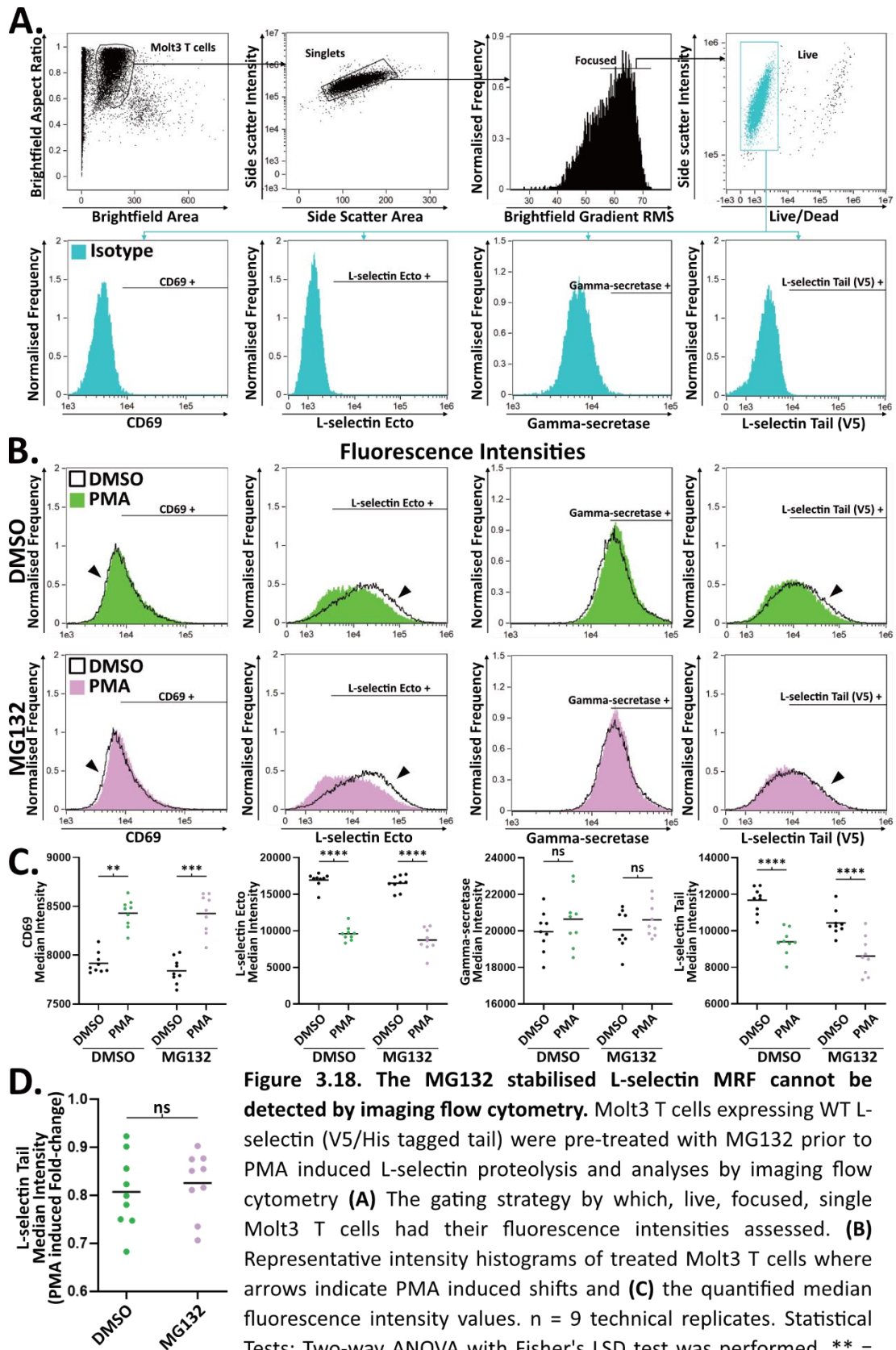


Figure 3.18. The MG132 stabilised L-selectin MRF cannot be detected by imaging flow cytometry. Molt3 T cells expressing WT L-selectin (V5/His tagged tail) were pre-treated with MG132 prior to PMA induced L-selectin proteolysis and analyses by imaging flow cytometry **(A)** The gating strategy by which, live, focused, single Molt3 T cells had their fluorescence intensities assessed. **(B)** Representative intensity histograms of treated Molt3 T cells where arrows indicate PMA induced shifts and **(C)** the quantified median fluorescence intensity values. $n = 9$ technical replicates. Statistical Tests: Two-way ANOVA with Fisher's LSD test was performed. ** = $p < 0.005$, *** = $p < 0.001$, **** = $p < 0.0001$, ns = non-significant. **(D)** To compare pre-treatments, PMA induced fold-change in L-selectin's tail intensity was calculated and compared. The number of replicates remains unchanged. Statistical Tests: One-way ANOVA with Tukey's test was performed.

Cells which were AND-gated as triple positive for CD69 (membrane marker), γ -secretase and the L-selectin tail (by V5/His tag staining) as determined by the isotype control (3.18A) were assessed for their median similarity scores within the relevant compartments (Fig. 3.19A).

As shown previously, PMA induced a loss of L-selectin's ectodomain from the surface of Molt3 T cells, which corresponds to a decrease in similarity score with the CD69 membrane marker of 0.107 and 0.099 following PMA stimulation if pre-treated with DMSO or MG132, respectively (Fig. 3.19B, C). The similarity score between CD69 and the L-selectin tail decreased by 0.1 for DMSO pre-treated Molt3 T cells whilst MG132 pre-treated cells saw a decrease of half this (decrease of 0.041; Fig. 3.19B, C).

To compare data between different treatments, I transformed the data as fold-change induced by PMA and compared the two pre-treatments directly but found no significant difference between DMSO and MG132 pre-treated Molt3 T cells (Fig. 3.19D). This is likely due to the technique not being able to distinguish between full-length and MRF L-selectin within the membrane mask.

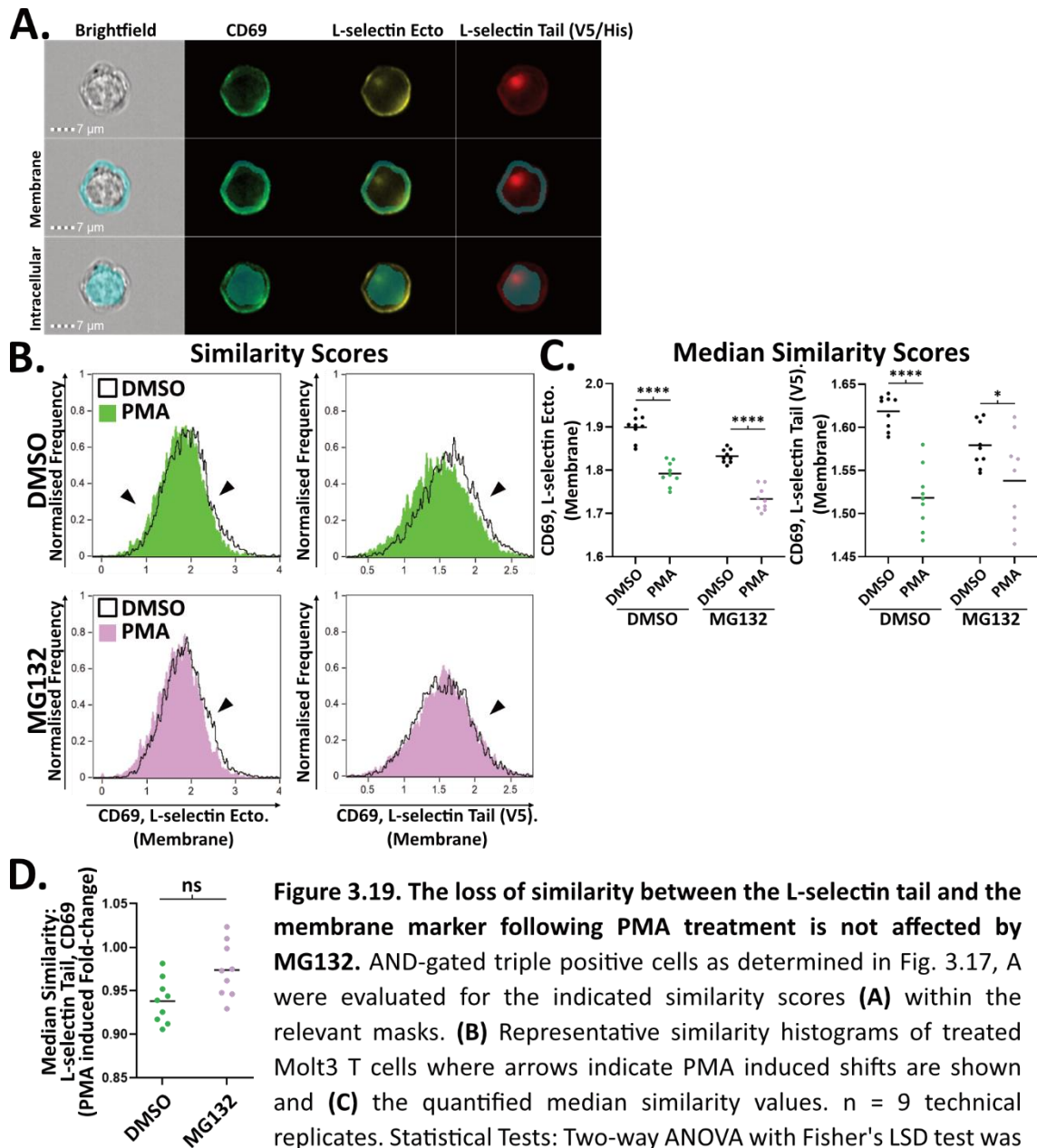


Figure 3.19. The loss of similarity between the L-selectin tail and the membrane marker following PMA treatment is not affected by MG132. AND-gated triple positive cells as determined in Fig. 3.17, A were evaluated for the indicated similarity scores (A) within the relevant masks. (B) Representative similarity histograms of treated Molt3 T cells where arrows indicate PMA induced shifts are shown and (C) the quantified median similarity values. $n = 9$ technical replicates. Statistical Tests: Two-way ANOVA with Fisher's LSD test was performed. * = $p < 0.05$, ** = $p < 0.005$, *** = $p < 0.001$, **** = $p < 0.0001$, ns = non-significant. (D) To compare pre-treatments, PMA induced fold-change in L-selectin's tail intensity was calculated and compared. The number of replicates remains unchanged. Statistical Tests: One-way ANOVA with Tukey's test was performed.

3.2.9 Of the L-selectin variants, only Δ MN L-selectin expressing Molt3 T cells retain the L-selectin tail at the membrane following PMA stimulation

DMSO pre-treated Δ MN and I Δ W Molt3 T cells were evaluated in the same way as WT Molt3 T cells pre-treated with either DMSO or MG132. As stated in the previous section, a small but significant increase in CD69 membrane marker intensity was observed for WT L-selectin expressing Molt3 T cells. Of interest, the DMSO control and PMA-treated cells had elevated median fluorescence intensity values for CD69 if they expressed either mutant form of L-selectin (Fig. 3.20B). Nonetheless, PMA induced a similar increase of approximately 4.5 % upon Molt3 T cells expressing either Δ MN or I Δ W L-selectin (Fig. 3.20A, B). As expected, Δ MN Molt3 T cells did not undergo loss of L-selectin ectodomain-linked fluorescence intensity following PMA stimulation (Fig. 3.20A, B), whilst WT and I Δ W Molt3 T cells did. Interestingly, whilst WT Molt3 T cells saw a 43.3 % decrease in their median fluorescence intensity value of L-selectin's ectodomain, I Δ W Molt3 T cells saw a larger decrease of 71.7 % of their median fluorescence intensity (Fig. 3.20A, B). This agrees with the conventional flow cytometry experiment (Fig. 3.3B, C). Similar patterns were seen for the L-selectin tail intensity, which decreased from 11672.3 to 9387.7 for WT Molt3 T cells (19.6 %) and from 22730.44 to 15664.55 for I Δ W Molt3 T cells (31.1 %), whilst no decrease was seen for Δ MN Molt3 T cells (Fig. 3.20A, B). γ -secretase intensity remained consistent throughout the experiment for all comparisons (3.20A, B). This was again excluded from further analyses due to the aforementioned reasoning.

To directly compare the difference in shedding behaviour between the WT and I Δ W L-selectin variants, I expressed the change in fluorescence associated with L-selectin's ectodomain and tail as PMA-induced fold change (Fig. 3.18C). This demonstrated that whilst Δ MN L-selectin does not change for either L-selectin domain, the fold change in the ectodomain fluorescence for WT L-selectin was 0.57 (Fig. 3.20C). The loss of the ectodomain through shedding for I Δ W L-selectin was much greater, as its fold change was 0.12 (Fig. 3.20C). Despite this, the loss of fluorescence associated with L-selectin's tail between WT and I Δ W L-selectin were

similar. The fold change for WT L-selectin was 0.81 and for IΔW L-selectin this was 0.69 (Fig. 3.20C).

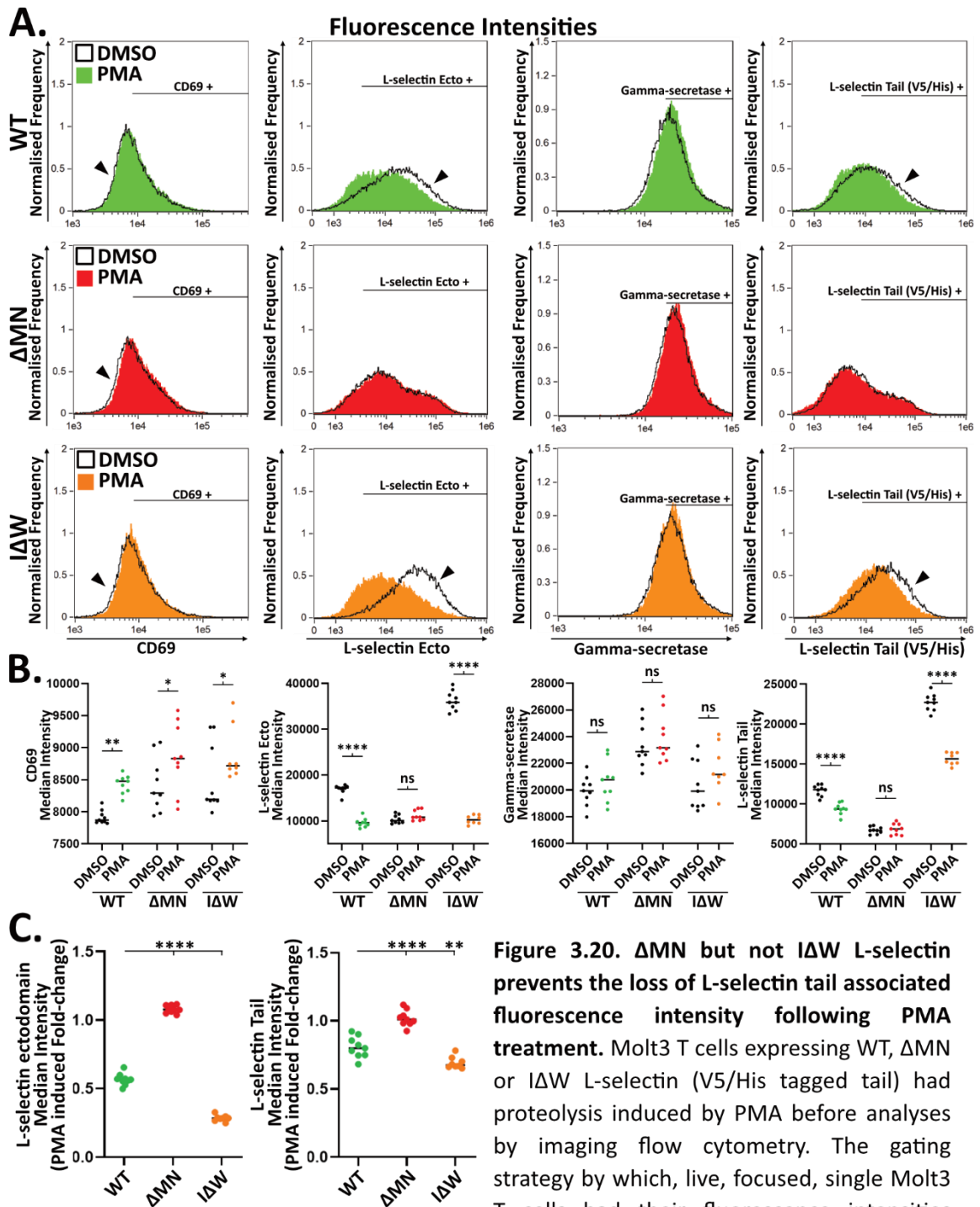


Figure 3.20. ΔMN but not ΔIW L-selectin prevents the loss of L-selectin tail associated fluorescence intensity following PMA treatment. Molt3 T cells expressing WT, ΔMN or ΔIW L-selectin (V5/His tagged tail) had proteolysis induced by PMA before analyses by imaging flow cytometry. The gating strategy by which, live, focused, single Molt3 T cells had their fluorescence intensities assessed is shown in Fig 3.17. A. (A)

Representative intensity histograms of Molt3 T cells where arrows indicate PMA induced shifts are shown and (B) the quantified median fluorescence intensity values are presented. n = 9 technical replicates. Statistical Tests: Two-way ANOVA with Fisher's LSD test was performed. * = p<0.05, ** = p<0.005, **** = p<0.0001, ns = non-significant. (D) To compare L-selectin variants, PMA induced fold-change in L-selectin's ectodomain and tail intensity were calculated and compared. The number of replicates remains unchanged. Statistical Tests: One-way ANOVA with Tukey's test was performed. ** = p<0.005, **** = p<0.0001.

Cells which were positive for CD69 (membrane marker), γ -secretase and the L-selectin tail (by V5/His tag staining) as determined by isotype control gating (3.18A) were AND-gated and assessed for their median similarity scores within their relevant compartments (Fig. 3.19A). L-selectin's ectodomain similarity score to CD69 decreased from 1.90 to 1.79 for WT Molt3 T cells and decreased further from 2.08 to 1.77 for ΔW Molt3 T cells (Fig. 3.21B). A similar trend was observed for the L-selectin tail and its similarity to CD69 (Fig. 3.21B).

To further evaluate the difference in shedding behaviour between the WT and ΔW L-selectin variants, I calculated the PMA-induced fold change in median similarity score between both domains of L-selectin investigated and the membrane marker CD69. ΔMN L-selectin exhibited no drastic fold changes following PMA addition whilst WT L-selectin's ectodomain reduced in similarity to CD69 (fold change of 0.915; Fig. 3.21D). Again, the fold change in similarity between L-selectin's ectodomain and CD69 for ΔW L-selectin ectodomain was greater (fold change of 0.79). However, for L-selectin's tail and CD69 the fold change in similarity scores were more alike for WT and ΔW L-selectin, being 0.94 and 0.86, respectively (Fig. 3.21D).

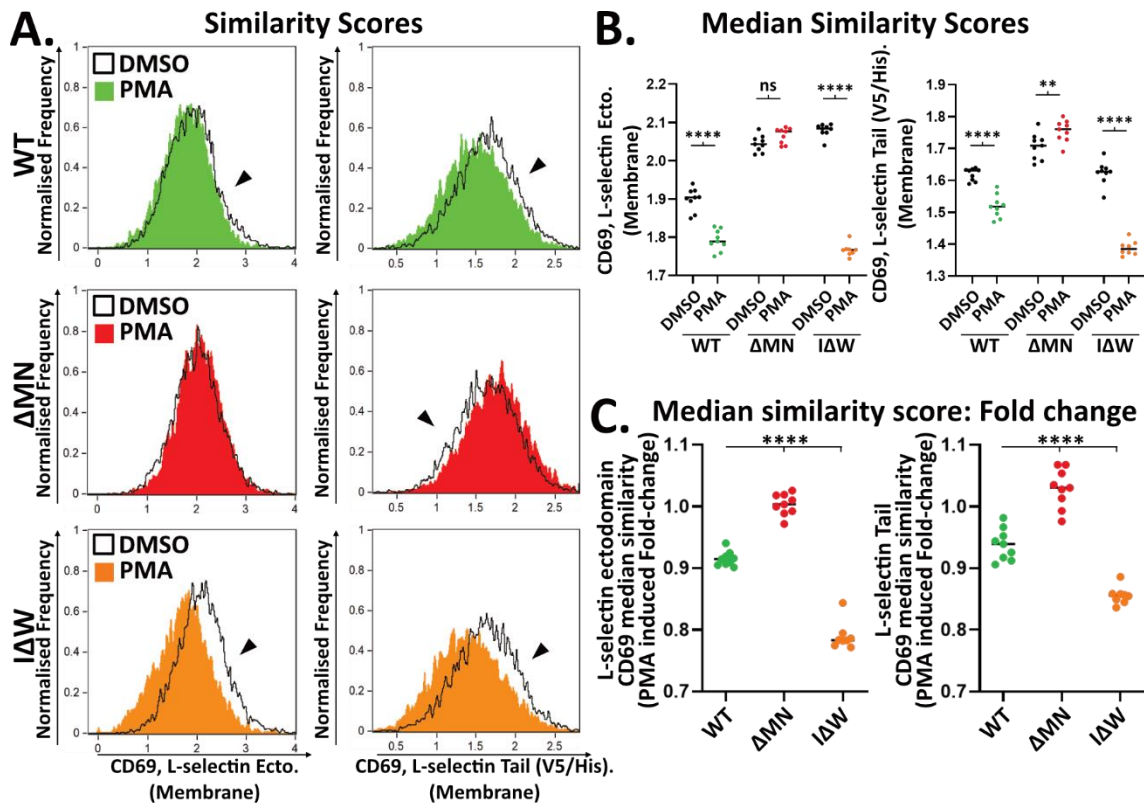


Figure 3.21. Δ MN but not I Δ W L-selectin prevents the decrease in similarity score between L-selectin Tail (V5/His) and CD69 following PMA treatment. Molt3 T cells expressing WT, Δ MN or I Δ W L-selectin (V5/His tagged tail) had proteolysis induced before analyses by imaging flow cytometry. The gating strategy by which AND-gated triple positive, live, focused, single Molt3 T cells had their similarity scores assessed is shown in Fig 3.17. A. and the masking strategy in which similarities were assessed is presented in Fig. 3.18. A. **(A)** Representative similarity histograms of Molt3 T cells where arrows indicate PMA induced shifts are shown and **(B)** the quantified median similarity values are presented. $n = 9$ technical replicates. Statistical Tests: Two-way ANOVA with Fisher's LSD test was performed. * = $p < 0.05$, ** = $p < 0.005$, *** = $p < 0.001$, **** = $p < 0.0001$, ns = non-significant. **(C)** To compare L-selectin variants, PMA induced fold-change in L-selectin's ectodomain and tail similarity to CD69 were calculated and compared. The number of replicates remains unchanged. Statistical Tests: One-way ANOVA with Tukey's test was performed. **** = $p < 0.0001$.

3.3.0 Discussion

In this body of work, I set out to determine the fate of the L-selectin tail following sequential proteolysis by ADAM-17 and γ -secretase. First, I generated three Molt3 T cell lines, each expressing matched levels of either WT, Δ MN or I Δ W L-selectin with an extreme C-terminal V5/His tag at the cytoplasmic tail. However, in later experiments new cell lines were generated which were not matched. Through lentiviral transduction and consequent FACS I was able to generate cell lines with equal levels of L-selectin on the cell surface, which underwent maximal ectodomain shedding in response to PMA (with the exception of ectodomain proteolysis-resistant Δ MN L-selectin as expected). Importantly, the shedding of the ectodomain was mediated by ADAM-17. Following a 1-hour pre-treatment with a γ -secretase inhibitor and 15 minutes of PMA stimulation, WT Molt3 T cells still underwent ectodomain proteolysis as we have previously observed following γ -secretase inhibitor pre-treatment and anti-CD3/CD28 stimulation (Andrew Newman; unpublished observations). γ -secretase inhibitor pre-treatment and PMA stimulation of Molt3 T cells caused an accumulation of the MRF by western blotting. Curiously, when stimulating with anti-CD3/CD28, Andrew Newman was able to see an increase in the level of MRF without γ -secretase inhibition which was increased further upon inhibition. Here, upon treatment with PMA, despite seeing ectodomain proteolysis, an accumulation of the MRF was not seen unless cells were pre-incubated with γ -secretase inhibitor. Nonetheless, an accumulation of the MRF following L-685 pre-treatment and PMA stimulation confirms γ -secretase's role in PMA-induced sequential proteolysis of wildtype L-selectin.

In a similar experiment, ADAM17 shedding-resistant Δ MN L-selectin in Molt3 T cells and a I Δ W L-selectin mutant that is proposed to resist γ -secretase dependent tail proteolysis were tested alongside WT Molt3 T cells. PMA was able to induce ectodomain shedding in WT and I Δ W Molt3 T cells. Further, I Δ W Molt3 T cells appeared to more readily undergo ectodomain proteolysis. Recently, the expression of CD53 (a tetraspannin) has been implicated in stabilising L-selectin in the membrane of murine T cells by limiting ADAM17 proteolysis (Demaria et al. 2020). It

may be that the ΔW mutation interferes with these interactions and enables a higher rate of ADAM-17 proteolysis. Following PMA treatment, WT Molt3 T cells saw no detectable increase in MRF by western blotting presumably due to rapid degradation. Conversely, ΔW Molt3 T cells saw an approximately 3-fold increase in MRF, as was the case with WT Molt3 T cells pre-treated with γ -secretase inhibitor. Of interest, the basal level of MRF in ΔW Molt3 was approximately half that of WT Molt3 T cells, which could indicate lower levels of constitutive shedding (Mohammed et al. 2019). However, this has not been studied or investigated here. The ΔMN L-selectin expressing Molt3 T cells had no detectable MRF due to a lack of ectodomain proteolysis as anticipated. Interestingly, the ΔW L-selectin full length band appeared as a doublet, with a lower kDa band appearing. This may represent a change in this variant's ability to undergo post-translational modification such as ubiquitination.

Content that PMA was able to induce ADAM17- and γ -secretase-mediated sequential proteolysis of WT L-selectin in Molt3 T cells, I moved onto the imaging flow cytometry assays, which were designed to enable me to track the L-selectin tail following shedding. In this assay, I was able to look at whole cell intensity values, much like in conventional flow cytometry, as well as the similarity score between specific fluorophore pairs used to determine colocalisation within cellular compartments. However, T cells have a notoriously small cytoplasm, and at the time of writing, a quantitative imaging flow cytometry method of defining the membrane and intracellular region containing the cytoplasm had not been described in the literature. Using the Molt3 T cell membrane markers, two of which are on the outer leaflet (CD69, L-selectin ectodomain) of the membrane and another on the inner leaflet (L-selectin's tagged tail), I was able to accurately define the region in which membrane-associated fluorescence was located. Using these regions, I could evaluate whole cell median fluorescence, similarity scores, the number of intracellular spots per cell in cells which contained spots, and the median fluorescence intensity per unit area of the cell regions if the whole cell intensity did not show obvious changes.

Using these analyses, I was able to show that the similarity of fluorescence associated with the L-selectin tail and a membrane marker (CD69) significantly decreased at 15 minutes after PMA stimulation. A similar trend was observed for cells treated with hIgG but not for those treated with either L685 or anti-ADAM17. However, these were not significant, likely due to the study being underpowered. At the 15-minute time point, I was able to show that L-selectin tail fluorescence is specifically lost from the membrane, and as it does not increase in the intracellular compartment, the cells despite the whole-cell intensity not significantly decreasing. Despite this, a trend toward decreased whole-cell intensity was observed and further replicates may have demonstrated a significant loss. Therefore, imaging flow cytometry can be used to track L-selectin sequential cleavage. I hypothesised that there were several reasons for the loss of fluorescence rather than a redistribution within the cell: (1) the small 5.6 kDa tagged intracellular tail was not suitably fixed prior to permeabilisation and was washed away (Heinen et al. 2014), despite use of fresh methanol-free formaldehyde for fixation; (2) a PMA-induced L-selectin tail binding partner was effectively blocking the V5/His epitope tag, making it appear as though the tail was being lost; and/or (3) L-selectin was being rapidly degraded by another intracellular organelle, such as the proteasome.

To rule out the first and second possibilities I generated Molt3 T cells expressing WT L-selectin, with a GFP tagged tail, and performed a PMA-induced proteolysis study by imaging flow cytometry. Due to its pre-tagged nature, the loss of fluorescence ruled out the possibility that a binding partner prevented antibody-mediated detection of L-selectin's tail. In the same study, I used live cells, fixed cells, and cells which had been fixed and then permeabilised. As these all lost the same amount of fluorescence. This ruled out the possibility that the tail was improperly fixed prior to permeabilisation. Thus, antibody-mediated detection was successful, and the signal was lost by other means.

To test the remaining hypothesis that L-selectin's tail was degraded by another mechanism, I pre-treated the WT Molt3 T cells with a range of cellular inhibitors targeting autophagy, autophagosome-lysosomal fusion, protease and proteasome activity and found that only the proteasome inhibitor (MG132) could cause an accumulation of the MRF by western blotting following PMA stimulation. Interestingly, BafA1 caused an accumulation of this fragment in the absence of PMA stimulation, which indicates a potential role for endosomal/lysosomal fusion in the basal turn-over of L-selectin, which we have demonstrated to be independent of ADAM-17 (Mohammed et al. 2019). However, as no additional MRF or other V5/His tag signal was observed following BafA1 pre-treatment and PMA stimulation, it is unlikely the route of sequential proteolysis-associated degradation. The pre-treatment inducing proteasome inhibition (MG132) revealed an accumulation of the MRF by western blotting and was used again in an imaging flow cytometry experiment. When pre-treated with vehicle control before PMA stimulation, there was the same loss of the L-selectin tail fluorescence intensity and similarity to the membrane marker as observed in the previous imaging flow cytometry experiment. However, pre-treatment with the proteasome inhibitor decreased loss of L-selectin's tail intensity and halved the decrease in similarity with the membrane marker following PMA treatment. However, when these data were converted to fold change and compared directly, no significant differences could be seen. The inability to detect this by imaging flow cytometry may be due to only 15 % of Molt3 T cells shedding all surface L-selectin and the inability of the technique to distinguish full-length L-selectin from the MRF by size, as can be done in western blotting. Overall, in combination with the western blotting data, this indicates the L-selectin MRF did not migrate to endosomes and is degraded by the proteasome.

It is curious that no new proteolysis product corresponding to the γ -secretase cleaved cytoplasmic tail could be observed by either western blotting or imaging flow cytometry, which may indicate that these are two independent pathways, i.e. proteasome degradation or further proteolysis by γ -secretase. An alternative

suggestion is that γ -secretase migrates alongside L-selectin to the proteasome, where it is immediately proteolysed and degraded.

Imaging flow cytometry analysis of the variants of L-selectin in Molt3 T cells revealed that ΔW L-selectin, which was proposed to resist γ -secretase proteolysis, is still subject to loss of tail-associated fluorescence from the membrane following PMA T cell stimulation. The fluorescence intensity associated with the L-selectin ectodomain and tail at the membrane was lost to an even greater extent than by WT L-selectin following PMA treatment. However, when directly compared, it appears ΔW L-selectin had an increased rate of ADAM-17 ectodomain proteolysis and a rate of γ -secretase proteolysis more alike WT L-selectin, which together causes an accumulation of the MRF seen upon western blots. Therefore, rather than resist L-selectin tail proteolysis, the ΔW L-selectin variant is more readily proteolysed by ADAM-17, which overwhelms γ -secretases ability to turn over the MRF. However, this explanation does not account for the redundancy of γ -secretase inhibition on ΔW L-selectin Molt3 T cells following anti-CD3/CD28 stimulation observed via western blotting by Andrew Newman (Andrew Newman; unpublished observations). To address the observed redundancy, a side-by-side comparison of PMA and anti-CD3/CD28 both with and without L685 pre-treatment could be used prior to western blotting. This would address whether it is the mode of inducing sequential proteolysis which determines resistance of ΔW L-selectin to γ -secretase. However, this is unlikely, as PMA-induced proteolysis of WT L-selectin is still mediated by γ -secretase in Molt3 T cells. Further, both mechanisms are arguably artificial, and the best approach to address this problem would be to use the high-content screening confocal microscope for an experiment using peptide-loaded APCs stained with a cell tracker fluorophore for distinction from Molt3 T cells expressing wild-type, ΔMN and ΔW L-selectins with a GFP pre-tagged tail. All inhibitors and L-selectin variants could be assayed in the 96-well plate set up at much higher resolution to observe proteolysis in real time in response to physiological engagement of the TCR by peptide-MHC.

Another observation from imaging flow cytometry was the subtle but significant increase of CD69 in all three of L-selectin variant-expressing Molt3 T cells in response to PMA. Importantly, the increased basal level of CD69 in those cells expressing Δ MN and I Δ W L-selectin may be important due to our recent finding that primary mouse T cells transgenic for mouse ADAM17-resistant L-selectin express higher levels of CD69 compared to their wild-type counter parts following activation via engagement of their TCR by tumour antigens (Ruben Rex Peter Durairaj; unpublished observations). This, along with the delay of CD25 expression in murine T cells following activation (Mohammed et al. 2019), indicate roles for L-selectin proteolysis in T cell activation. To study this, Molt3 T cells transduced with either mock virus or virus driving expression of each variant of L-selectin could be investigated by qPCR of CD69 and CD25 before and both after transduction and exposure to peptide stimulus to further our understanding of L-selectin's role in T cell activation.

4.0.0. Generation and use of cancer-specific murine CD8 T cells for adoptive immunotherapy of melanoma.

4.1.1. Introduction

Cancer-specific CD8 T cells expressing an ectodomain proteolysis-resistant form of L-selectin (L Δ P) were able to control tumour growth in solid and disseminated models of adoptive cell therapy better than T cells expressing wildtype L-selectin (WT) or no L-selectin (Watson et al. 2019). Further, this increased control of tumour growth by L Δ P T cells synergised with anti-PD-1 therapy and makes the use of L-selectin as a therapeutic transgene in adoptive T cell therapy an exciting prospect, especially when considering it could be paired with any currently developed CAR or TCR used in the clinic.

In the model used by Watson et al, the B16-F10 melanoma cell line (derived from a spontaneous murine melanoma; Olson et al., 2018) was transduced to express the NP68 influenza peptide as a surrogate tumour antigen. This cell line was used as a target tumour and is recognised by T cells expressing the F5 TCR as a surrogate tumour-specific TCR. Expression levels of NP68 were not quantified in this paper, and the recognition of this peptide by the F5 receptor is a high-affinity interaction (Levelt et al. 1999), making this an artificial system. Further, the CD8 T cell donor mice used by Watson et al were transgenic for the F5 TCR alone, the F5 TCR and L-selectin null or the F5 TCR and L Δ P L-selectin (Fig 4.1A). Therefore, the donor T cells did not require *ex vivo* modification to confer cancer specificity or L-selectin variant expression and so were naïve upon delivery to tumour-bearing mice (Fig 4.1B).

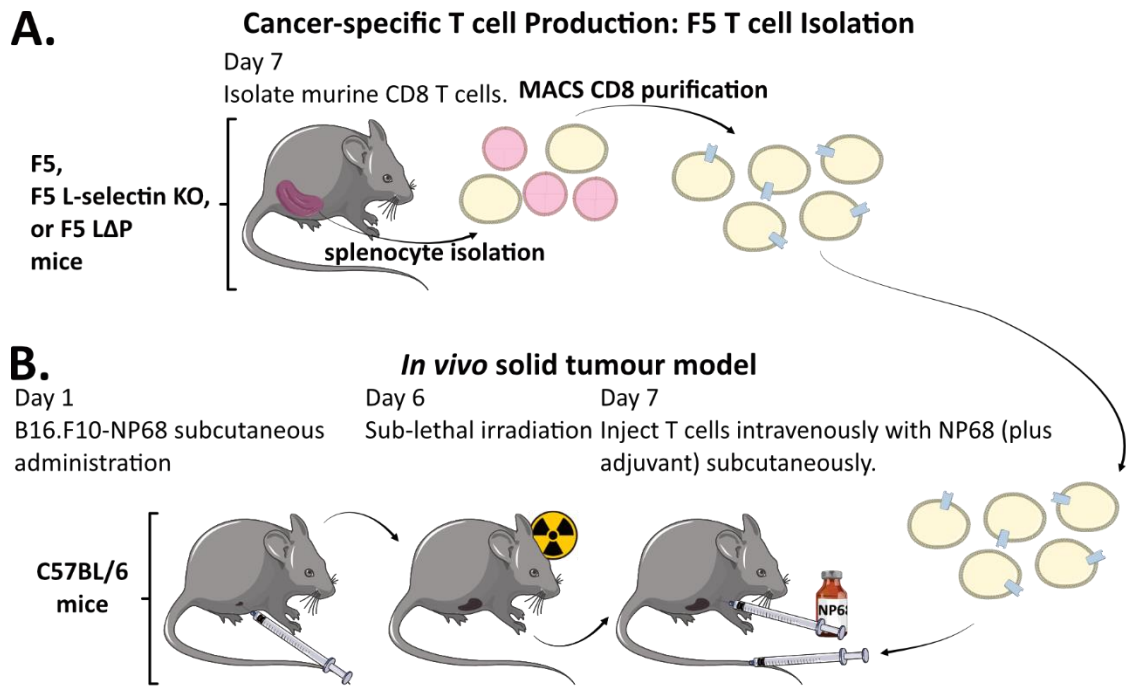


Figure 4.1. Solid tumour model used by Watson et al to demonstrate the benefits of ΔP in T cell mediated control of tumour growth. (A) The extraction and purification of naive murine CD8 T cells bearing the F5 TCR and either, no L-selectin, WT or ΔP L-selectin. **(B)** The protocol by which C57BL/6 mice were subcutaneously injected with B16.F10-NP68 melanoma cells, sub-lethally irradiated and administered NP68 peptide (with adjuvant) and F5 T cells before tumour growth was monitored for a further 23 days (until day 30).

This is a situation not reflected in the clinic, where patients' T cells are isolated, expanded via activation and modified by viral transduction (Wang and Rivière 2016). Therefore, I sought to test the hypothesis that L-selectin variants can be delivered to murine T cells alongside a cancer-specific CAR or TCR to confer the benefits demonstrated by Watson et al.

Watson et al administered their antigen-bearing melanoma cell line subcutaneously to an in-bred immune-competent strain of mice (C57BL/6; Fig. 4.1A; Watson et al., 2019). This is a syngeneic murine model and is therefore fully immunocompetent, which is important when evaluating immunotherapeutic reagents like cancer-specific CAR-T or TCR T cells (Olson et al. 2018). However, the use of a melanoma cell line avoids important aspects of tumorigenesis, such as intratumoral cell heterogeneity, which arises from co-development of the tumour alongside the immune system (Olson et al. 2018). This can be achieved by using chemically induced tumours (i.e. methylcholanthrene) or mice with tissue-specific promoters that drive oncogenesis (i.e. tissue-specific recombinases that drive loss of tumour suppressor genes like

PTEN). However, while these autochthonous models more faithfully recapitulate the tumour microenvironment, they can lack expression of CAR or TCR targets, which can be introduced into cell lines with ease. Therefore, induced tumour models would require extensive characterisation to identify reliable CAR/TCR target antigens, which may not be relevant to human cancers.

Syngeneic murine models can also be criticised as they are entirely murine in nature, and consequently somewhat removed from human cancer immunity. NSG (non-obese diabetic, severe combined immune deficient, gamma-chain knockout) mice lack T, B and NK cells and are sufficiently immuno-deficient to allow engraftment of human CAR-T or TCR-T cells and primary cells from human cancers (Olson et al. 2018). These patient-derived xenograft models recapitulate the complexity of tumour cell heterogeneity, but recruited innate immune cells are murine. Additionally, NSG mice have been shown to lack fully developed lymph nodes (Chappaz and Finke 2010; Olson et al. 2018). Indeed, mice with two of the three genetic alterations present in NSG mice had <20 % of the lymph nodes present in immunocompetent mice (Chappaz and Finke 2010). This is an important consideration for the work presented here, which focuses on the modification of L-selectin, traditionally a lymph node-homing molecule, which was an important factor in the studies by Gattinoni and colleagues (Gattinoni et al. 2005). Therefore, I used a syngeneic tumour model comparable to that used by Watson et al (Fig. 4.2B).

Here, I sought to isolate polyclonal L-selectin KO T cells from mice and transduce them with viral constructs encoding a cancer-specific CAR or TCR, either alone or with variants of L-selectin (Fig 4.2A). These variants included murine WT and Δ P L-selectin (mWT and m Δ P respectively) as tested by Watson et al, as well as their functional human equivalents WT, Δ MN L-selectin in addition to Δ W L-selectin (hWT, h Δ MN and h Δ W respectively; introduced in Chapter 3). Δ P L-selectin has its cleavage region replaced with that of P-selectin and therefore resists ADAM17 proteolysis and is the Δ MN L-selectin functional equivalent (Galkina et al. 2003). I aimed to test human variants of L-selectin to begin their pre-clinical characterisation for later work in human T cells. The transduced murine T cells were then characterised *in vitro* before being delivered to tumour-bearing mice (Fig. 4.2B) to

determine if virally delivered murine and human variants of cleavage-resistant L-selectin can confer improved control of tumour growth.

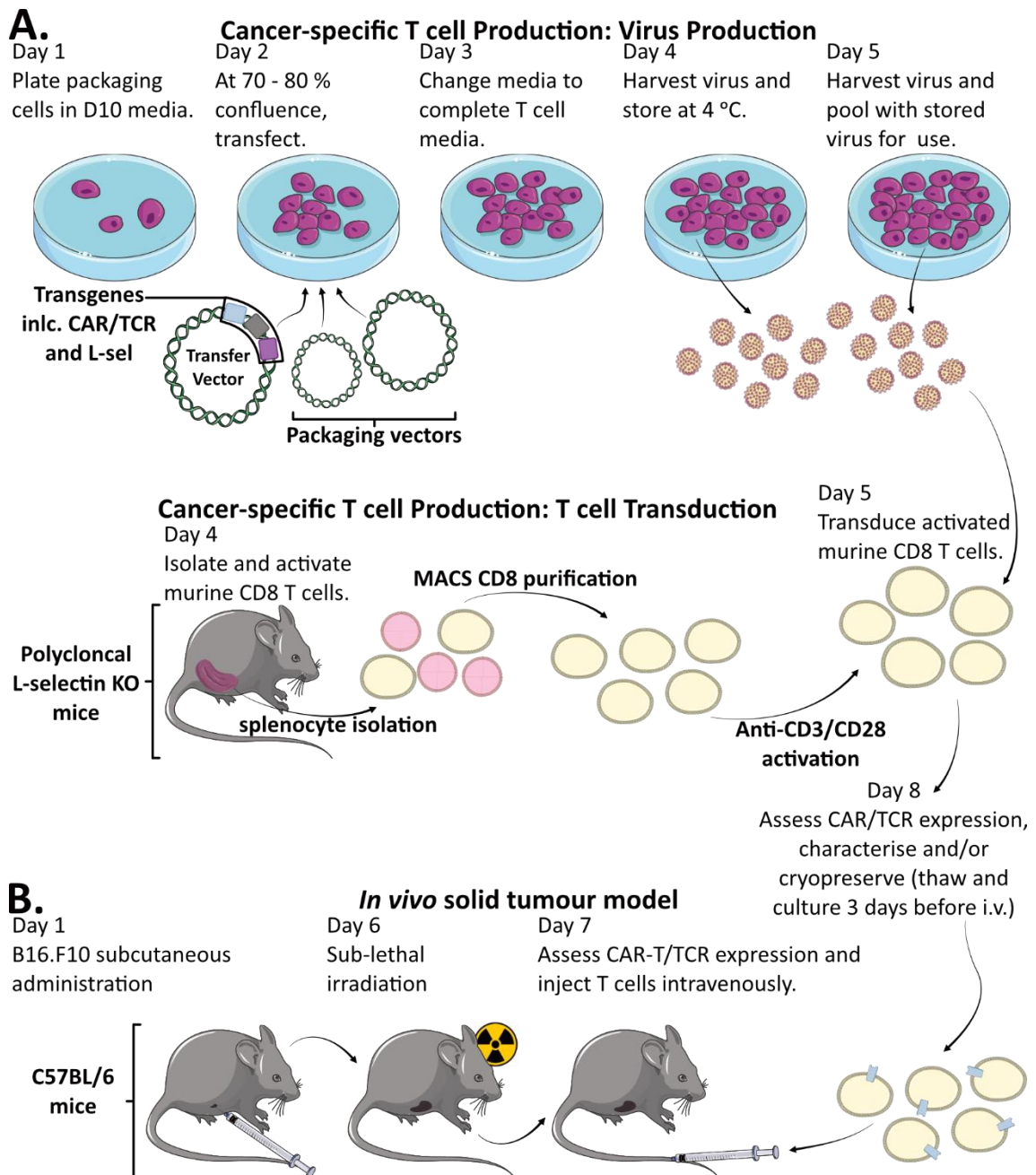


Figure 4.2. Solid tumour model used by Watson et al adapted to test the benefits of virally delivered CAR/TCR alongside L-selectin variants to mediate control of tumour growth. The timelines shown in A and B are independent of one another. **(A)** The production of virus able to deliver both CAR/TCR and variants of L-selectin as well as the extraction, purification, *ex vivo* activation and transduction of murine CD8 T cells. **(B)** The protocol by which C57BL/6 mice were subcutaneously injected with B16.F10, sub-lethally irradiated and administered transduced T cells before tumour growth was monitored for a further 23 days (until day 30).

4.1.2. Chapter aims

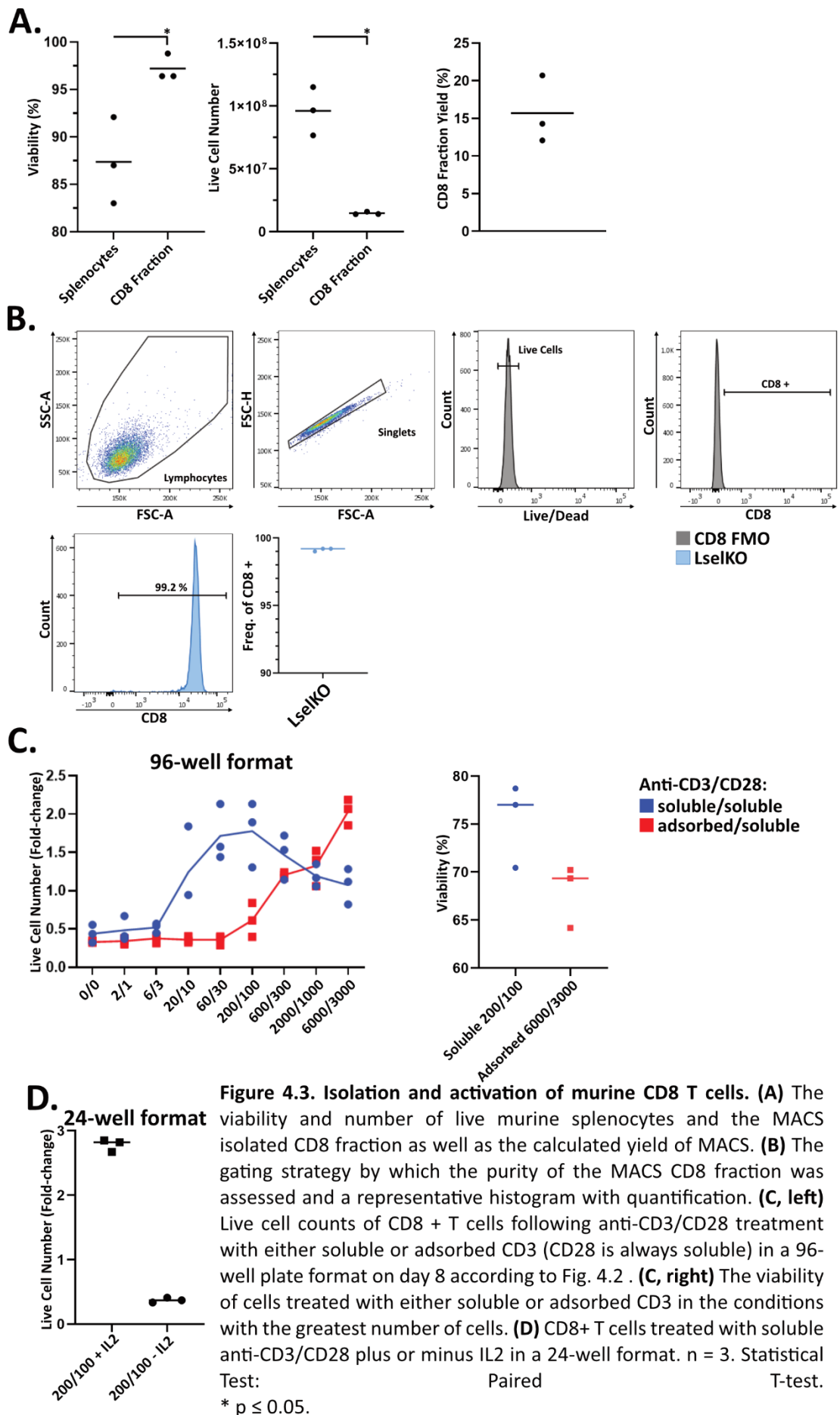
1. Develop a protocol capable of delivering expression of virally encoded genes to murine CD8 T cells in a clinically applicable manner.
2. Produce cancer-specific murine T cells using the above protocol that express murine or human variants of L-selectin.
3. Assess the phenotype of these cells *in vitro* via killing and flow cytometry assays.
4. Determine if cleavage-resistant L-selectin improves T cell-mediated control of tumour growth *in vivo*.

4.2.0 Results

4.2.1 Isolated murine CD8 T cells can be activated *ex vivo* and transduced to express GFP

Human primary T cell transduction has been commonplace for many years, but murine primary T cell transduction is less common and had not been done in our laboratory previously. There are several factors that can influence the efficiency of murine T cell transduction, one of which is the pre-requisite for activation-induced proliferation and the relative timing of transduction (Zhang et al. 2003b).

To optimise activation-induced proliferation and later transduction, CD8 T cells needed to be purified from murine splenocytes. A single polyclonal L-selectin KO spleen yielded 9.60×10^7 splenocytes, which could undergo MACS to give 1.45×10^7 CD8 T cells, providing an average yield of 15.7 % (Fig. 4.3A). MACS additionally improved cell viability from 87.4 % (unsorted) to 97.2 % (sorted) and gave a population of CD8 positive splenocytes that was 99.1 % pure (Fig. 4.3A, B). To assess the ability of anti-CD3 and anti-CD28 to induce proliferation in the presence of IL-2, fold-increase in live T cell numbers was recorded 4 days after activation. This time point is commonly used to assess activated and transduced T cells via *in vitro* killing assays and *in vivo* adoptive cell transfer experiments (Golumba-Nagy et al. 2017). The activating antibodies were titrated to determine the concentration able to induce maximal proliferation with minimal activation-induced cell death (Fig. 4.3C). This was done in a 96-well format to limit the number of donor spleens required in accordance with the refinement, replacement, and reduction of animal use (3Rs). For soluble anti-CD3 and anti-CD28, the optimal doses were 200 and 100 ng/ml, respectively, and for adsorbed anti-CD3 and soluble anti-CD28, the optimal doses were 6000 and 3000 ng/ml, respectively (Fig. 4.3C). The soluble antibody cocktail was chosen as it used a factor of ten less antibody relative to the adsorbed condition, and because cells appeared more viable, although this was not statistically significant (Fig. 4.3C). T cell proliferation was replicated in a 24-well format, as would be required to generate large numbers of transduced T cells for *in vivo* adoptive cell transfer studies and was dependent on IL-2 (Fig. 4.3D).



To demonstrate whether L-selectin KO CD8 T cells could be transduced with virus, I sought out colleagues who had GFP-expressing viruses I could use as a reporter transduction system. Professor Richard Darley provided two viruses derived from two constructs (pRV-Ampho-CMV-GFP and pLV-VSVG-EphA1-eGFP), and Dr Robert Jenkins provided another (pLV-VSVG-SFFV-eGFP), as detailed in Table 4.1.

Designation	Virus Type	Pseudotype	Promoter	Gene
pRV-Ampho-CMV-GFP	Retrovirus (pRV)	Ampho (Mammalian)	CMV	GFP
pLV-VSVG-EphA1-eGFP	Lentivirus (pLV)	VSVG (Mammalian)	EphA1	eGFP
pLV-VSVG-SFFV-eGFP	Lentivirus (pLV)	VSVG (Mammalian)	SFFV	eGFP

Table 4.1. The nomenclature of eGFP constructs used in this work.

Activated polyclonal L-selectin KO CD8 T cells were transduced with variable success, depending on the constructs used (Fig. 4.4A, B). The constructs pRV-Ampho-CMV-GFP and pLV-VSVG-EphA1-eGFP induced expression of their reporter genes at cell frequencies of 15.3 % and 23.0 %, respectively (Fig. 4.4A). However, they presented as small shifts in GFP expression rather than as distinct populations. Conversely, pLV-VSVG-SFFV-eGFP induced a shift of at least 1 log to produce a distinct population, despite comparable transduction efficiency (19.1 %; Fig. 4.4B). pLV-VSVG-EphA1-eGFP and pLV-VSVG-SFFV-eGFP were produced in different laboratories, but both induced comparable increases to the frequency of positive events. Despite this, pLV-VSVG-SFFV-eGFP induced a much greater shift, indicating that the promoter is an important consideration for transgene expression in murine CD8 T cells.

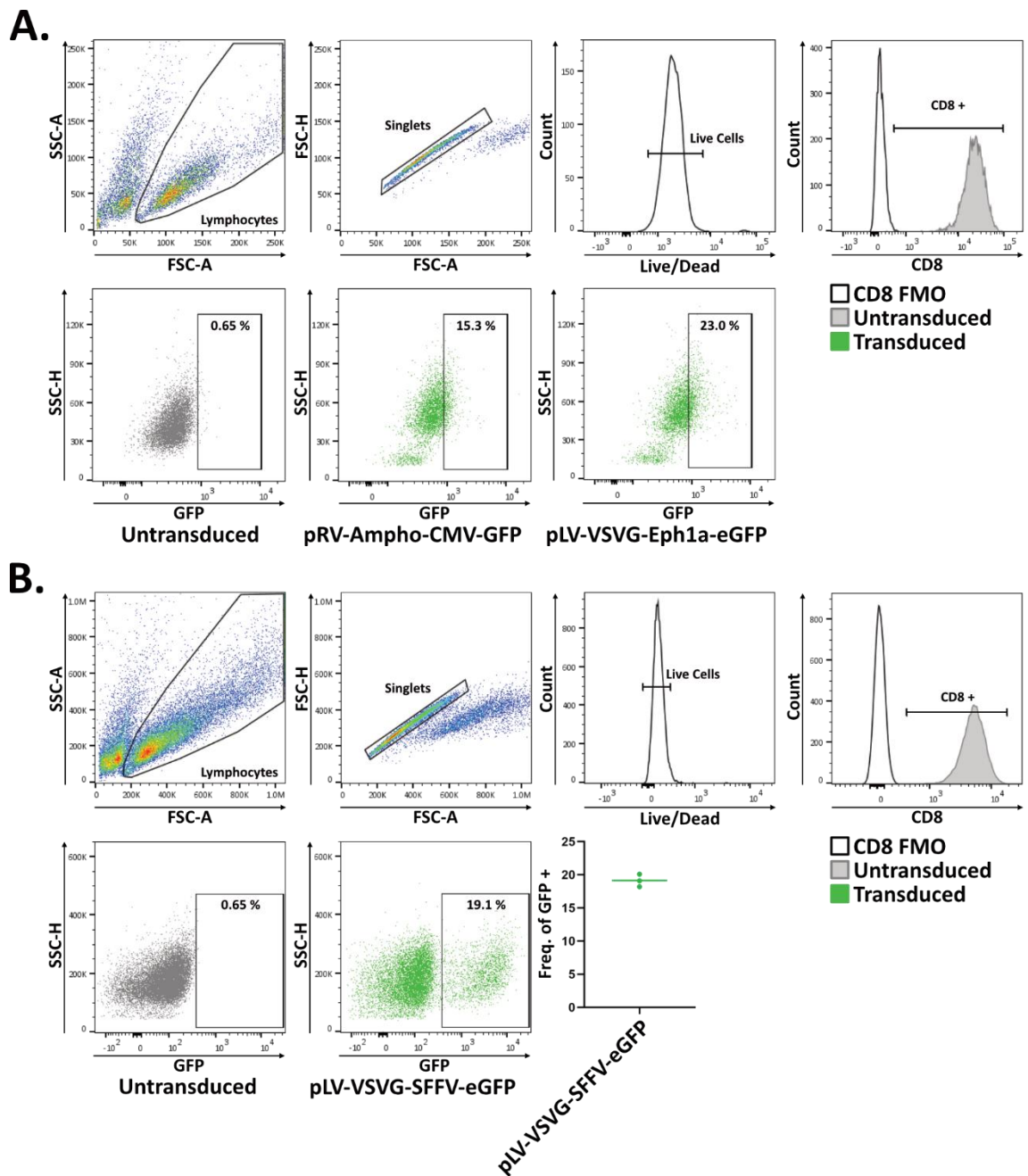


Figure 4.4. *In vitro* activated murine CD8 T cells were virally transduced to express GFP. GFP encoding transfer vectors in Table 4.1 were used to produce viruses in the respective labs they were acquired from and this virus used in the transduction protocol as in Fig. 4.2A. **(A)** The gating strategy by which CD8+, live, single, lymphocytes were assessed for GFP or eGFP expression following transduction in a 24-well format. **(B)** The gating strategy by which CD8+, live, single, lymphocytes were assessed for eGFP expression following transduction in a 96-well format. n = 1.

4.2.2 Retroviruses using their 5' LTR promoter drive expression of a transgenic cancer-specific TCR

To confer cancer-specificity to murine CD8 T cells, a CAR or TCR would need to be delivered by lentiviral or retroviral transduction. Professor Hinrich Abken kindly gave us a murine CAR against human carcinoembryonic antigen (CEA-CAR). If we virally delivered CEA-CAR to murine CD8 T cells, I would need to use CEA transgenic (CEAtg) mice to study their function (Chmielewski et al. 2012), because B16-F10 cells transduced to express human CEA may be rejected by C57BL/6 mice prior to adoptive cell transfer of CEA-specific CAR-T cells.

The detection of the CEA-CAR following transduction of CD8 T cells relies on an anti-IgG F(ab)₂ fragment, which binds a murine IgG marker domain within the CAR construct. In preliminary stains, this antibody cross-reacted with anti-CD8 (data not shown; BioLegend; 53-6.7), so it was only used in single stains for flow cytometry. T cells were isolated and activated as in Fig. 4.3, but CD8 staining was not included in the gating strategy (Fig. 4.5A). CD8 purity was demonstrated in a separate stain (Fig. 4.5C).

Professor Abken's vector was a pBullet retroviral vector that drives transgene expression via a CMV promoter. I trialled two different methods of transfection on an ecotropic cell line (which produces viruses with murine and rattus tropism; Wang et al., 1991) to produce virus. These methods were calcium phosphate and PEIpro transfection, the latter as used in Professor Abken's laboratory. Viruses produced via these methods were used to transduce activated T cells. Mock transduction was used throughout as an experimental control. This mock treatment comprised all steps of the protocol barring the transfer vector and controlled for the effects of the transduction protocol and virus particles on T cell phenotype. Virus produced via the calcium phosphate protocol yielded a small number of CEA-CAR positive cells (19.6%), whereas virus produced via the PEIpro protocol yielded even fewer CEA-CAR positive cells in the 96-well format (9.87%), but more in the 24-well format (23.0%);

Fig 4.5 B). However, as there were no repeats, these differences may be due to variability between replicates.

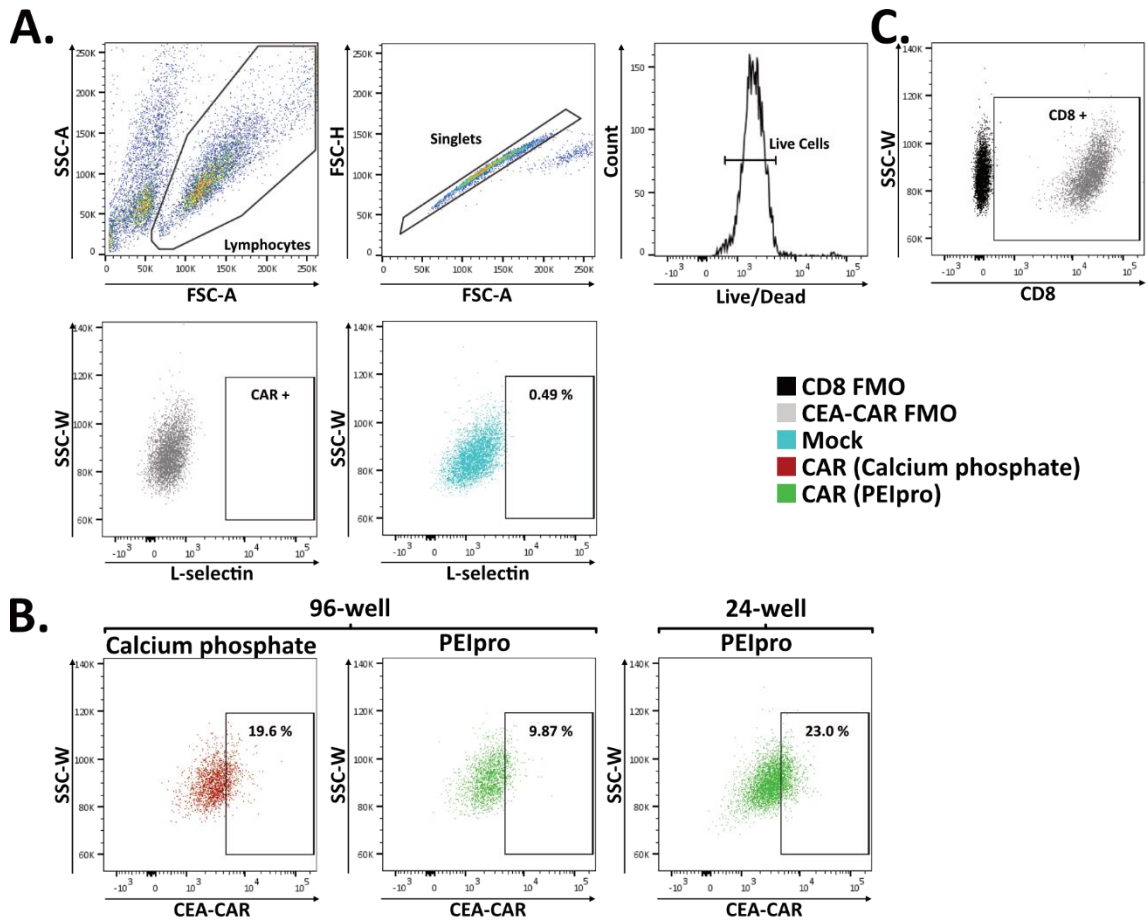


Figure 4.5. *In vitro* activated murine CD8 T cells were retrovirally transduced to express human CEA-specific CAR. Murine CD8 T cells were transduced as in Fig. 4.2A. **(A)** The gating strategy by which live, single, lymphocytes were assessed for CAR expression. **(B)** CAR expression by activated and transduced murine T cells with different viral vector transfection methods and transduction formats. **(C)** FMO staining was conducted on a mixed population of the experimental conditions. To demonstrate that the populations tested are CD8 positive the CD8 FMO and CEA-CAR FMO were compared. $n = 1$.

The small shifts in expression induced by CEA-CAR viral transduction indicated that, if I wanted to use this as my model of adoptive cancer immunotherapy, I would need to express the construct in an alternate vector. However, poor expression may also have been due to poor staining using the antibody fragment needed to detect the CAR. Further, the cross-reactivity of this antibody fragment with other antibodies would be a problem for later planned characterisation by flow cytometry. Finally, the CEAtg mice required for *in vivo* studies were no longer available.

Through a series of fortunate events, I was able to set-up a collaboration with Dr Clare Bennett to secure a retrovirally encoded TCR that recognises tyrosinase-related protein (TRP) -2, an antigen expressed in B16-F10 melanoma cells. The TCR that recognises TRP2 is hereafter referred to as TRP2. Using this TCR, I would be able to use standard C57BL/6 mice as tumour-bearing mice, circumventing hurdles associated with importing a new colony of mice. The vector also encoded a tailless CD19 marker (tICD19; Fig. 4.6A). Additionally, recognition of TRP2 TCR can be mediated via an anti-V β 3 antibody, which I found does not cross-react with anti-CD8 (unlike the anti-IgG F(ab)₂ fragment used to detect the CEA-CAR), mitigating potential future issues with multiparameter flow cytometry. Throughout this chapter, V β 3 positive events are used to define TRP2 positive cells, which have begun expressing transgenes as a result of transduction. During my next transduction, I used FuGene HD, as recommended by Dr Bennett. Transduction using the TRP2-encoding construct induced at least a single log shift in TRP2 positive events (62.3 %) to produce a distinct population. Furthermore, I performed MACS for tICD19 expression to enrich transduced cells, which yielded a TRP2 positive population of 94.8 % (Fig. 4.6B, C). The levels of tICD19 positive events were also enriched from 31.4 % to 67.1 % (Fig. 4.6B, C). The high efficiency of this transduction, indicated by readily detectable levels of transgene (a 2-log shift), as well as the ability to perform MACS enrichment, led me to select this as a candidate TCR and selectable marker for the B16-F10 melanoma model and switch my transfection reagent to FuGene HD.

A.

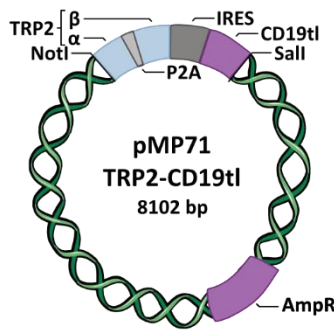
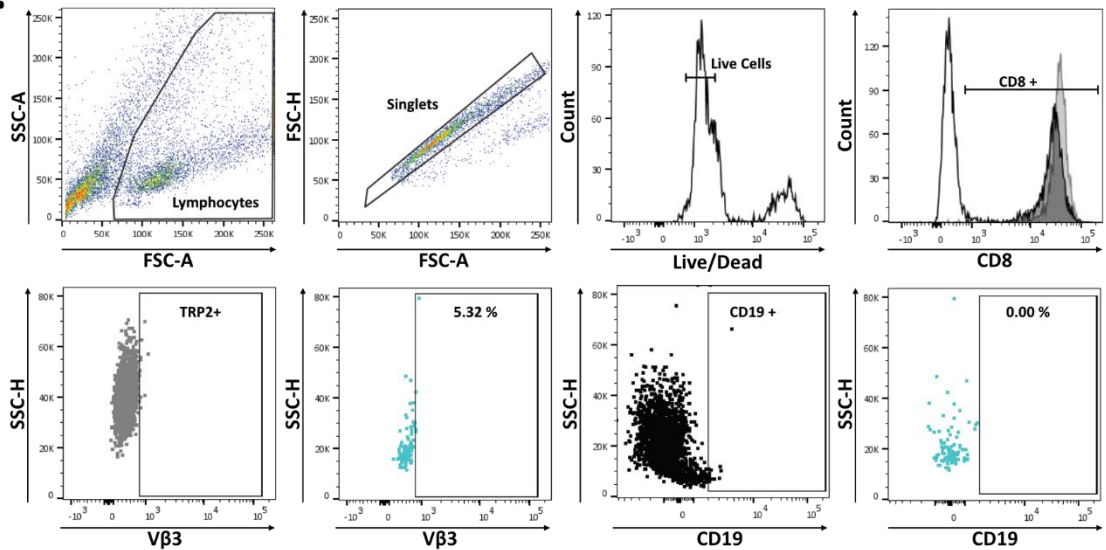
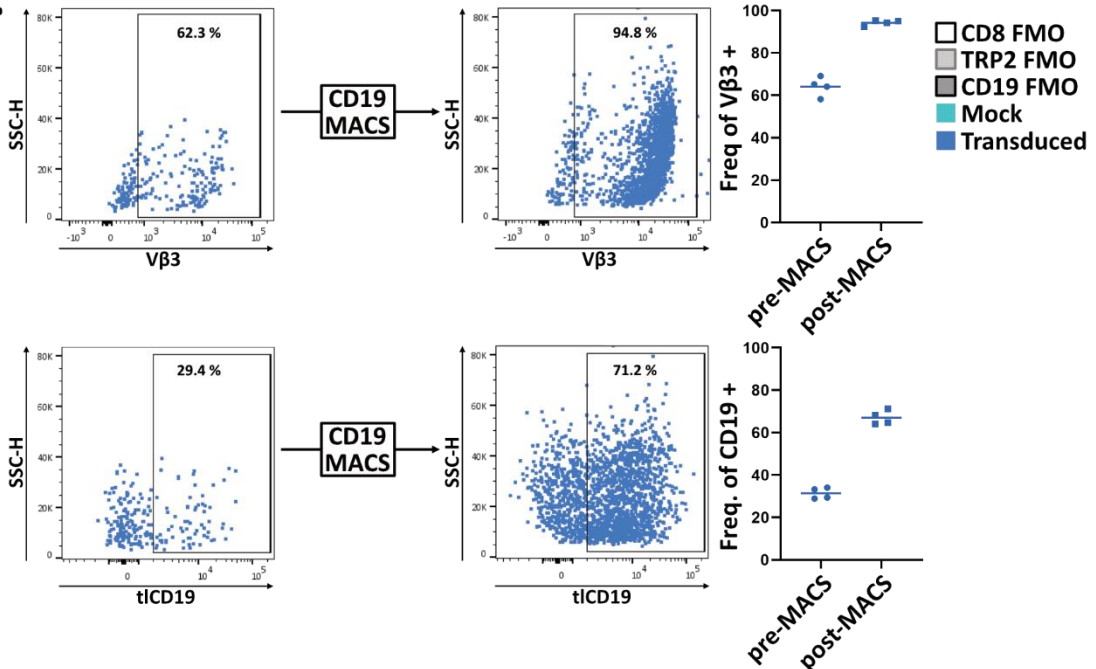


Figure 4.6. *In vitro* activated murine CD8 T cells were retrovirally transduced to express the melanoma-specific TRP2 TCR and enriched via MACS. **(A)** The vector containing the melanoma specific TRP2 TCR and tailless CD19 selection marker was used to produce virus and this used to transduce activated T cells as in Fig. 4.2A. **(B)** The gating strategy by which CD8+, live, single, lymphocytes were assessed for TRP2 and tCD19 expression following retroviral transduction and **(C)** the transduced cells before and after MACS purification in a 24-well format as well as quantification. n = 2, 2 technical replicates.

B.



C.



4.2.3 Retroviruses using their 5' LTR promoter drive expression of transgenic human and murine L-selectin variants

Prior to generating constructs encoding TRP2 alongside each L-selectin variant, it was important to confirm that each L-selectin variant could be virally delivered and expressed, in particular the human L-selectin variants, because they originate from a different species. Therefore, I generated primers that overlapped with the L-selectin mRNA sequence, including NotI and Sall restrictions sites, as well as the MMLV vector (excluding the SNAP and mCherry tags). These primers were used in PCRs with MMLV vectors encoding SNAP- and mCherry-tagged L-selectin variants to produce untagged L-selectin variants (Fig. 4.7A). The SNAP- and mCherry-tagged L-selectin encoding MMLV vectors (Fig. 4.7A) were restriction-digested with NotI and Sall, and the linearised MMLV backbone was purified. The purified MMLV backbone and untagged L-selectin variant PCR products were run on an analytical gel before purification, ligation, and transformation into *E. coli* (Fig. 4.7B). Transformed colonies were selected, mini-prepped, and restriction-digested to confirm insertion of the untagged L-selectin variants (Fig. 4.7C). Colony #2 for hWT, #1 for h Δ MN and #4 for h Δ W L-selectin were sequenced and confirmed to have been successfully cloned (Fig. 4.7D; Appendix).

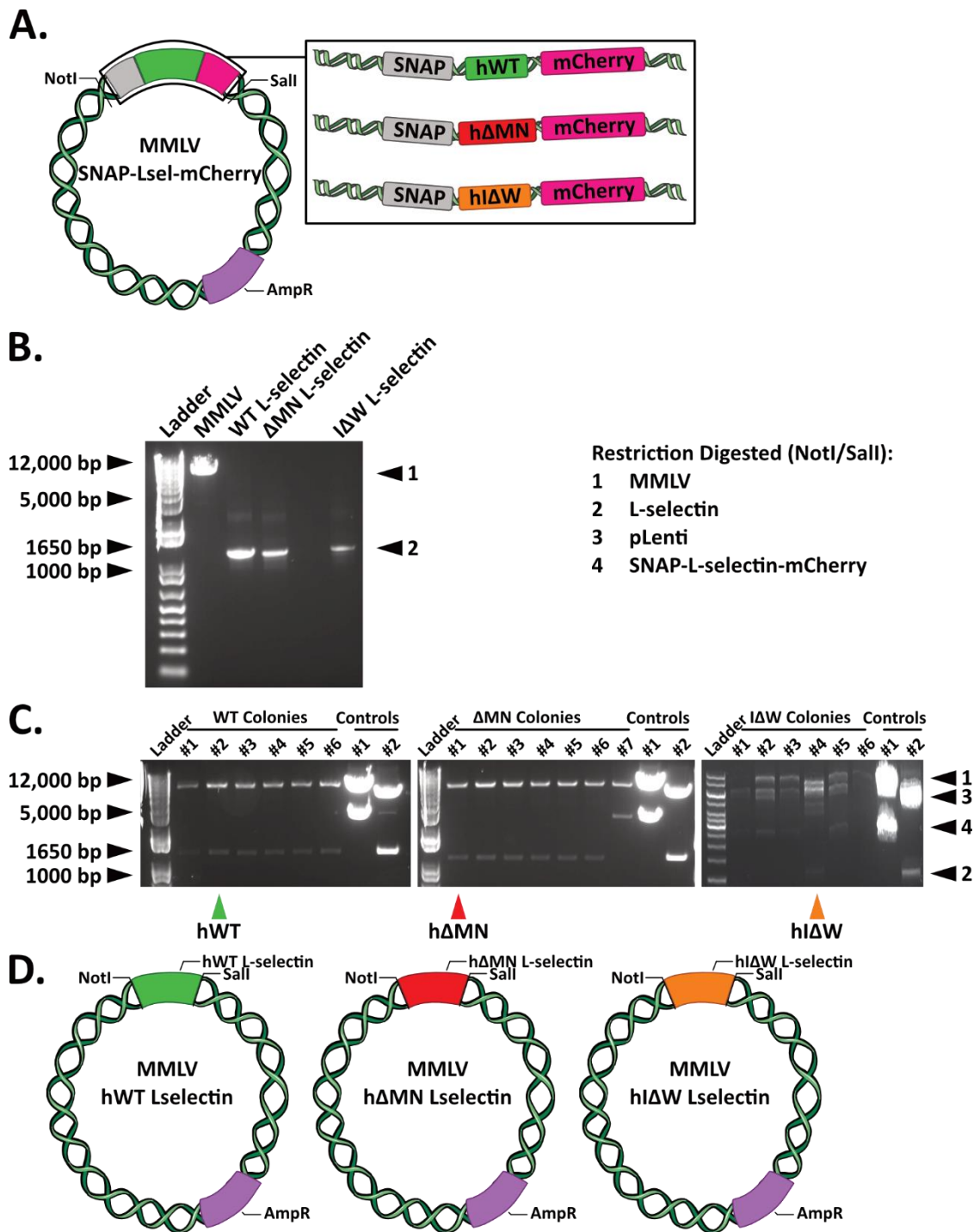


Figure 4.7. Construction of MMLV retroviral vectors encoding human L-selectin variants. (A) The starting materials from which untagged L-selectin variants and linearised MMLV were generated. (B) An analytical gel of restriction digested (NotI/Sall) MMLV and PCR products which are untagged L-selectin variants. (C) Restriction digested (NotI/Sall) mini-prep DNA from transformed *E. coli* clones containing MMLV vectors relative to negative (MMLV-SNAP-Lselectin-mCherry) and positive (pLenti-L-selectin) controls. Coloured arrows indicate colonies selected for sequencing and downstream use. (D) The final sequenced constructs.

These vectors were used to produce virus and these viruses used to transduce activated murine CD8 T cells. All three viruses delivered expression of L-selectin at the T cell surface. The frequency of positive events for hWT, hΔMN and hIΔW L-selectin was 14.1, 28.9 and 14.0 %, respectively. The mock control had <0.5 % positive events (Fig. 4.8B). It is likely that all efficiencies were comparable to hΔMN, which resists TCR-dependent activation-induced ectodomain proteolysis. However, as hWT and hIΔW L-selectin undergo ectodomain proteolysis, they have reduced surface expression. This cannot be confirmed without a non-variable transduction marker or treating the cells with ADAM17 inhibitors throughout transduction (Mohammed et al. 2019).

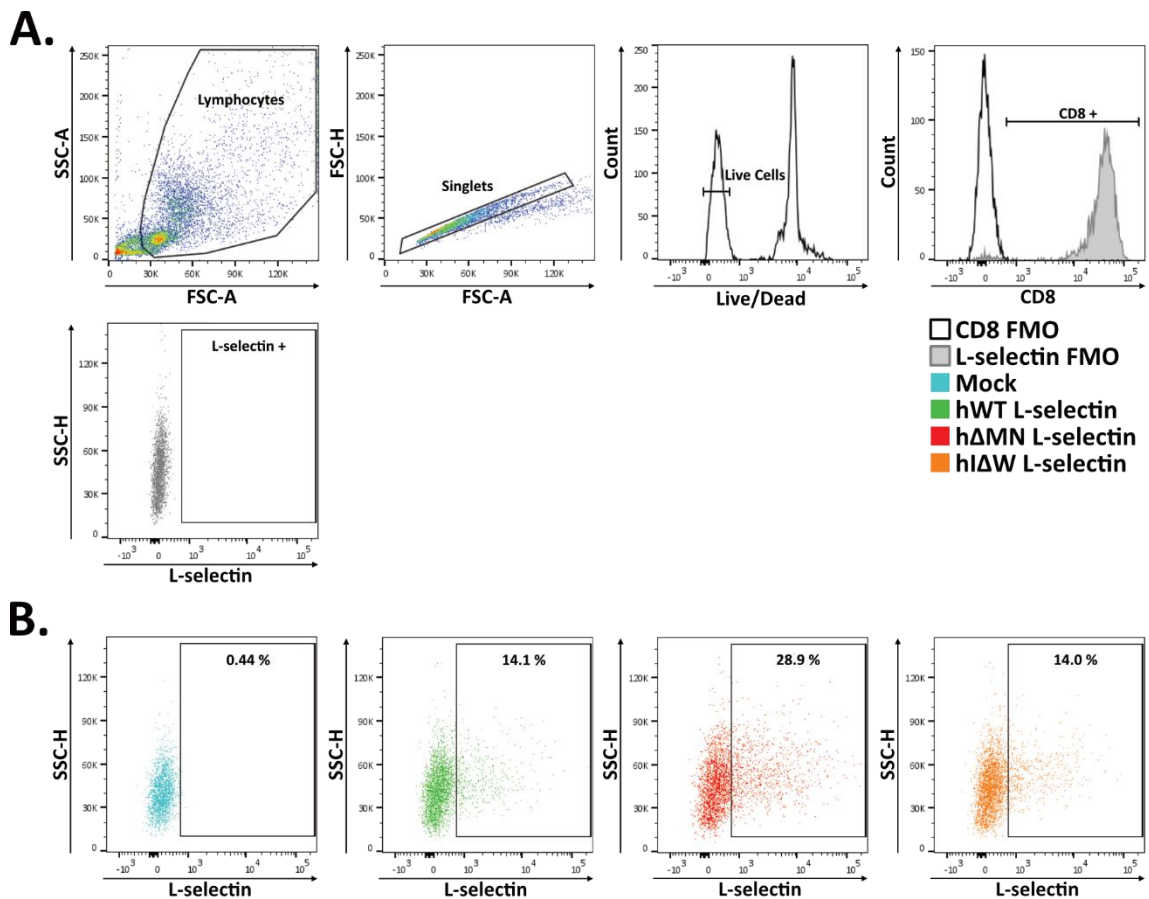


Figure 4.8. *In vitro* activated murine CD8 T cells were retrovirally transduced to express human L-selectin variants. Murine T cells were transduced as in Fig. 4.2A using the vectors in Fig. 4.7D. **(A)** The gating strategy by which CD8+, live, single, lymphocytes were assessed for L-selectin expression following retroviral transduction in a 24-well format. **(B)** T cells transduced with vectors encoding each L-selectin variant relative to a mock transduced control. n = 1.

Following the above experiment, I came across another retroviral vector which has been used to drive CAR and TCR expression at very high levels in both murine and human T cells (Hughes et al. 2005; Kochenderfer et al. 2010; Kerkar et al. 2011). Therefore, in an attempt to improve transgene expression, and if future work beyond this thesis were to investigate mutants in the context of human T cells, I inserted the murine L-selectin variants into pMSGV1. If this improved transgene expression dramatically, human variants would also be inserted into pMSGV1, and this would become my vector for future constructs.

Ly22-negative L-selectin variants lack a particular antibody epitope, enabling distinction from endogenous L-selectin, if present. I generated primers for conventional restriction digestion and T4 ligation that overlapped with the Ly22-negative L-selectin mRNA sequence and included HindIII and Sall restrictions sites. These primers were used in PCRs with SVA positive vectors, which encode Ly22-negative L-selectin variants and were originally used to produce L Δ P L-selectin mice (Fig. 4.9A; Galkina et al., 2003). The pMSGV1 vector encoding a murine CD19-targeting human CAR (from Addgene; Fig. 4.9A) was restriction-digested with HindIII and Sall to produce a linearised backbone. The Ly22-negative L-selectin variant PCR products were also restriction-digested with HindIII and Sall and run on an analytical gel before purification, ligation, and transformation into *E. coli* (Fig. 4.9B).

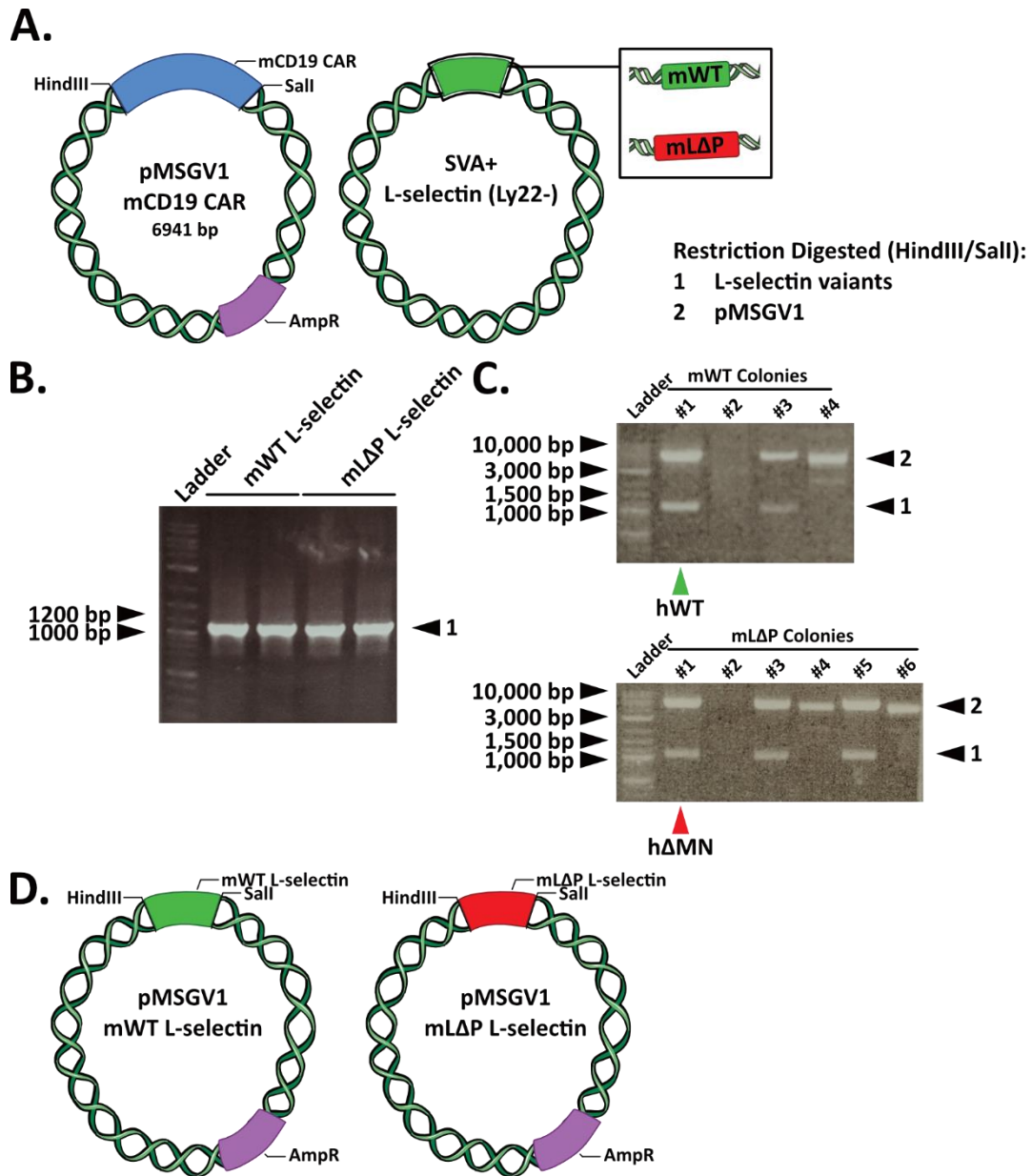


Figure 4.9. Construction of pMSGV1 retroviral vectors encoding murine L-selectin variants. (A) The starting materials from which Ly22 negative L-selectin was generated and put into linearised pMSGV1. (B) An analytical gel of restriction digested (HindIII/Sall) PCR products which are Ly22 negative L-selectin variants. (C) Restriction digested (HindIII/Sall) mini-prep DNA from transformed *E. coli* clones containing pMSGV1 vectors. Coloured arrows indicate colonies selected for sequencing and downstream use. (D) The final sequenced constructs.

Transformed colonies were selected, mini-prepped and restriction-digested to confirm insertion of the Ly22-negative L-selectin variants (Fig. 4.9C). Colony #1 for mWT and mLAP were sent for sequencing and were confirmed to have been successfully cloned (Fig. 4.9D; Appendix).

These vectors were used to produce virus and these viruses used to transduce activated murine CD8 T cells. Both L-selectin variants were expressed at the T cell surface with 7.4 and 29.2 % positive events for mWT and m Δ P L-selectin, respectively. The mock control had 0.87 % positive events (Fig. 4.10B). For L-selectin variant transduced cells, a 1 – 2 log shift in L-selectin expression was seen, indicating higher expression than seen with the MMLV-based constructs (Fig. 4.10B). Again, the cleavage-resistant variant demonstrated a higher level of transduction relative to constructs encoding WT L-selectin, which is likely due to L-selectin ectodomain proteolysis in activated T cells.

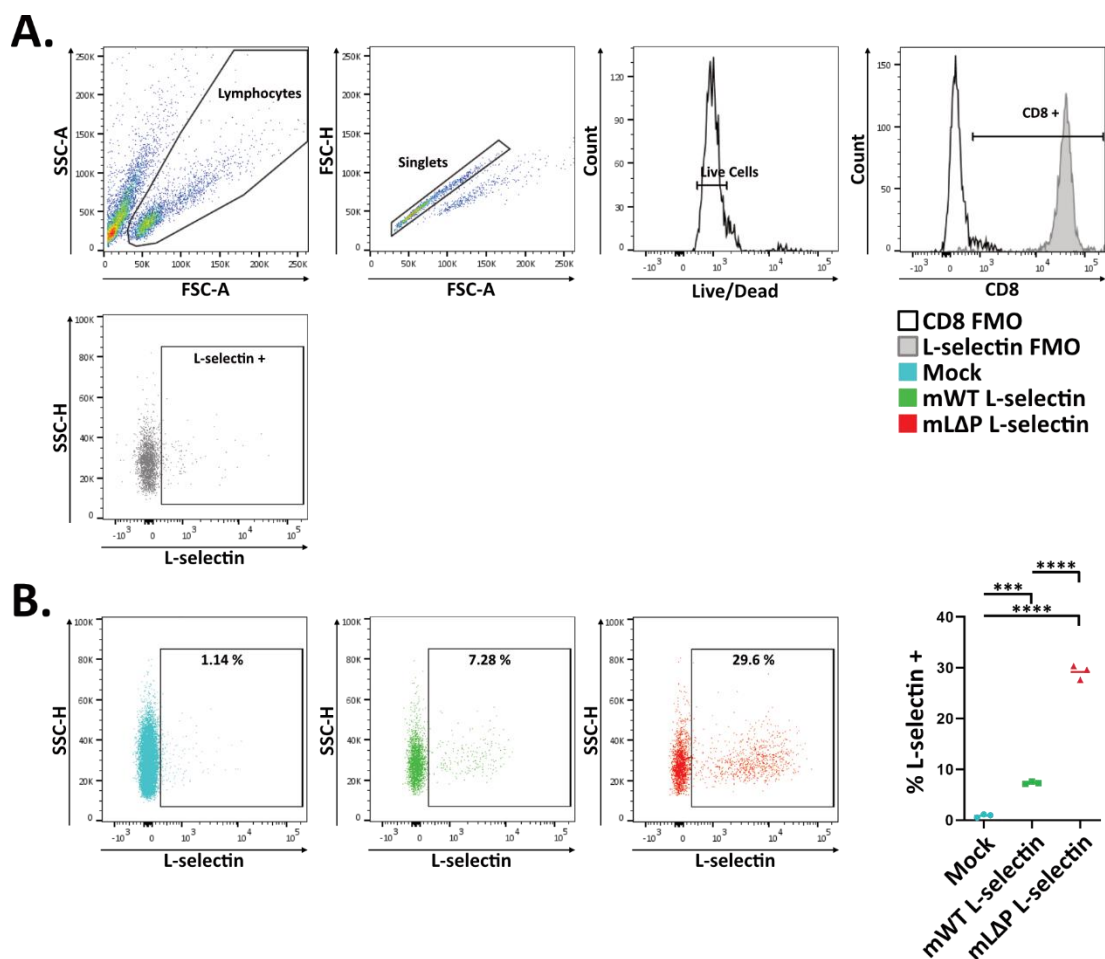


Figure 4.10. *In vitro* activated murine CD8 T cells were retrovirally transduced to express murine L-selectin variants. Murine T cells were transduced as in Fig. 4.2A using the vectors in Fig. 4.9D. **(A)** The gating strategy by which CD8+, live, single lymphocytes were assessed for L-selectin expression following retroviral transduction in a 24-well format. **(B)** T cells transduced with mock control and each construct encoding a L-selectin variant with quantification. n = 3. Statistical Test: One-way ANOVA with Tukey test. *** p \leq 0.0002, **** p < 0.0001.

4.2.4 Retrovirus using the 5' LTR promoter drives co-expression of a transgenic cancer-specific TCR and human and murine L-selectin variants

Content that pMP71 could drive expression of TRP2 and MMLV and pMSGV1 could drive expression of human and murine L-selectin in murine CD8 T cells, respectively, I designed vectors capable of delivering them in a single construct (Fig. 4.11). Looking over the previous transduction experiments, pMSGV1 gave a more distinct population of cleavage-resistant L-selectin positive cells than MMLV. However, neither drove transgene expression as highly as the pMP71 vector. I therefore used this retroviral vector for further development. To retain the CD19-selectable marker for MACS enrichment, I joined tICD19 to each L-selectin mutant via a T2A skip sequence (Fig. 4.11; Liu et al., 2017).

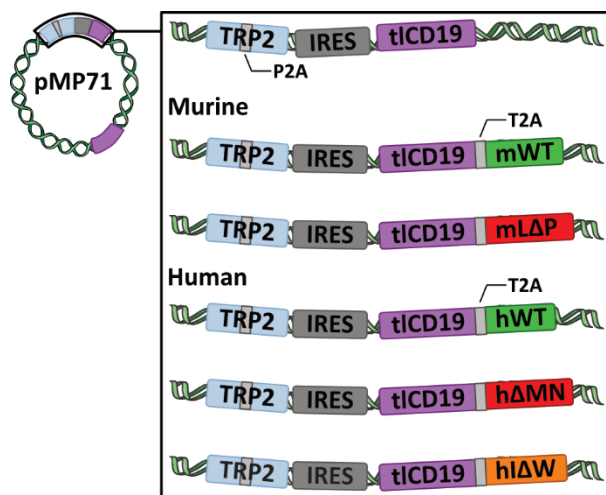


Figure 4.11. Quadricistronic constructs to deliver expression of TRP2, tICD19 marker and a L-selectin variant. These vectors were designed in-house and synthesised by Genewiz. Viruses were produced as in Fig. 4.2A.

Transduction using viruses with transgenes encoding TRP2 and tICD19 (TRP2-tICD19), or these transgenes with an additional murine L-selectin variant, either mWT or mLAP, yielded 56.6 %, 30.1 % and 29.5 % Vβ3 positive events respectively. Each transduction was significantly elevated relative to mock controls, which had 4.9 % positive events (Fig. 4.12B, C). The mock and the TRP2-tICD19 transduction yielded < 0.45 % events double positive for Vβ3 and L-selectin. Vectors additionally containing mWT or mLAP delivered 12.5 % and 18.8 % double positive events, respectively (Fig. 4.12B, C).

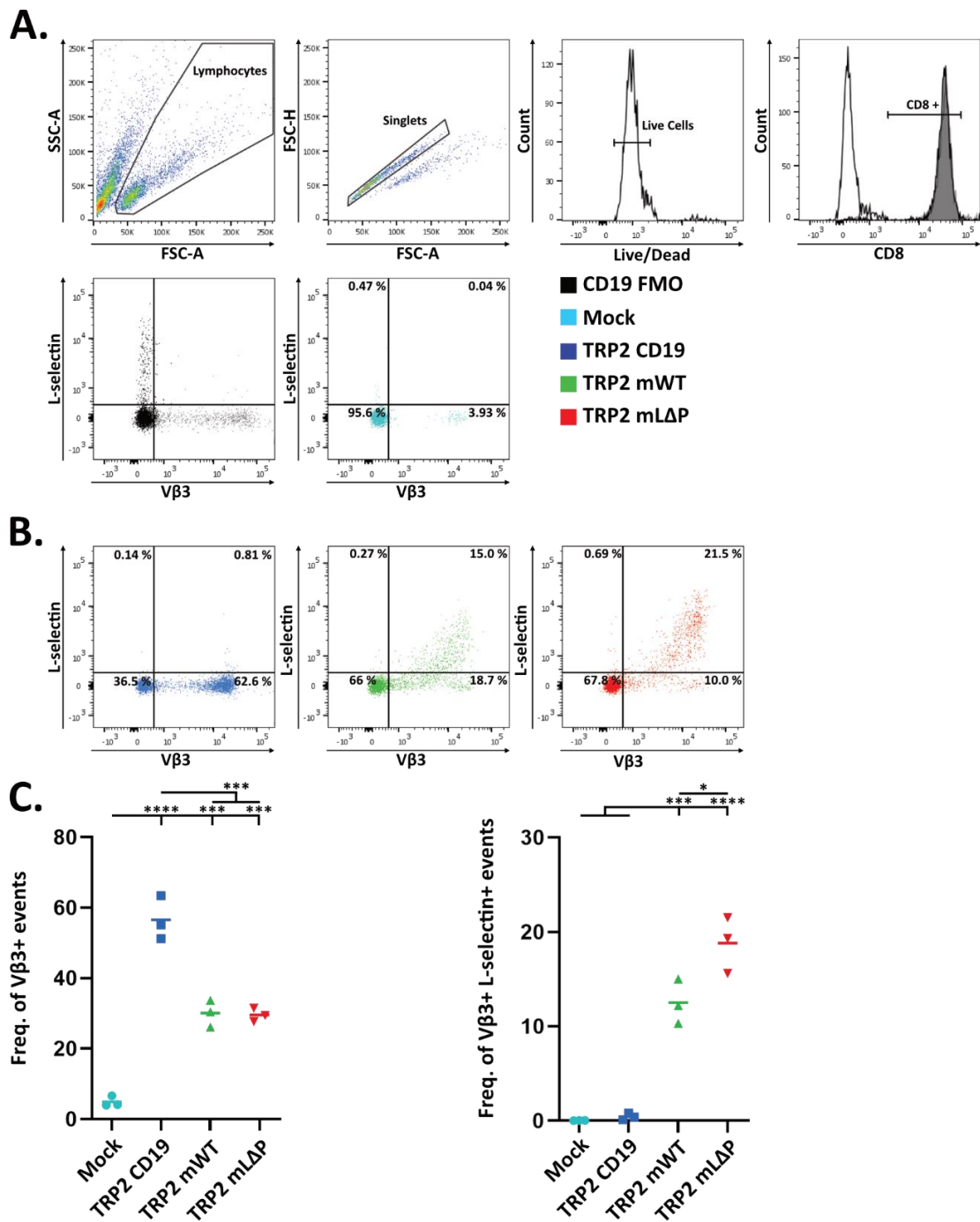


Figure 4.12. Quadricistronic constructs deliver expression of TRP2 and murine L-selectin variants. Murine CD8 T cells were transduced as in Fig. 4.2A using viruses encoding transgenes as in Fig. 4.11. **(A)** The gating strategy by which CD8, live, single, lymphocytes were assessed for transgenic TRP2 and L-selectin expression following transduction. **(B)** Representative plots showing expression of TRP2 and L-selectin by cells transduced with each construct. **(C)** The quantified freq. of TRP2 and L-selectin positive events. $n=3$. Statistical Test: One-way ANOVA with Tukey test. * $p < 0.05$, *** $p < 0.002$, **** $p < 0.0001$.

Transduction using viruses with transgenes encoding either TRP2-tlCD19, or these transgenes with an additional human L-selectin variant, hWT, h Δ MN or h Δ W, yielded 55.1 %, 34.1 %, 38.1% and 15.2 % V β 3 positive events, respectively. The mock control had 5.80 % positive events (Fig. 4.13B). All transductions except the transduction with virus delivering co-expression of h Δ W L-selectin had significantly elevated frequencies of V β 3 positive events above mock controls (Fig. 4.13B, C). Transductions using viruses containing hWT or h Δ MN transgenes induced 12.3 % and 19.9 % double positive events for V β 3 and L-selectin, respectively. These were significantly increased compared to mock (0.08 %) and vectors containing either TRP2-tlCD19 (1.31 %) or these genes alongside h Δ W (2.7 %) were not significantly elevated (Fig. 4.13B, C).

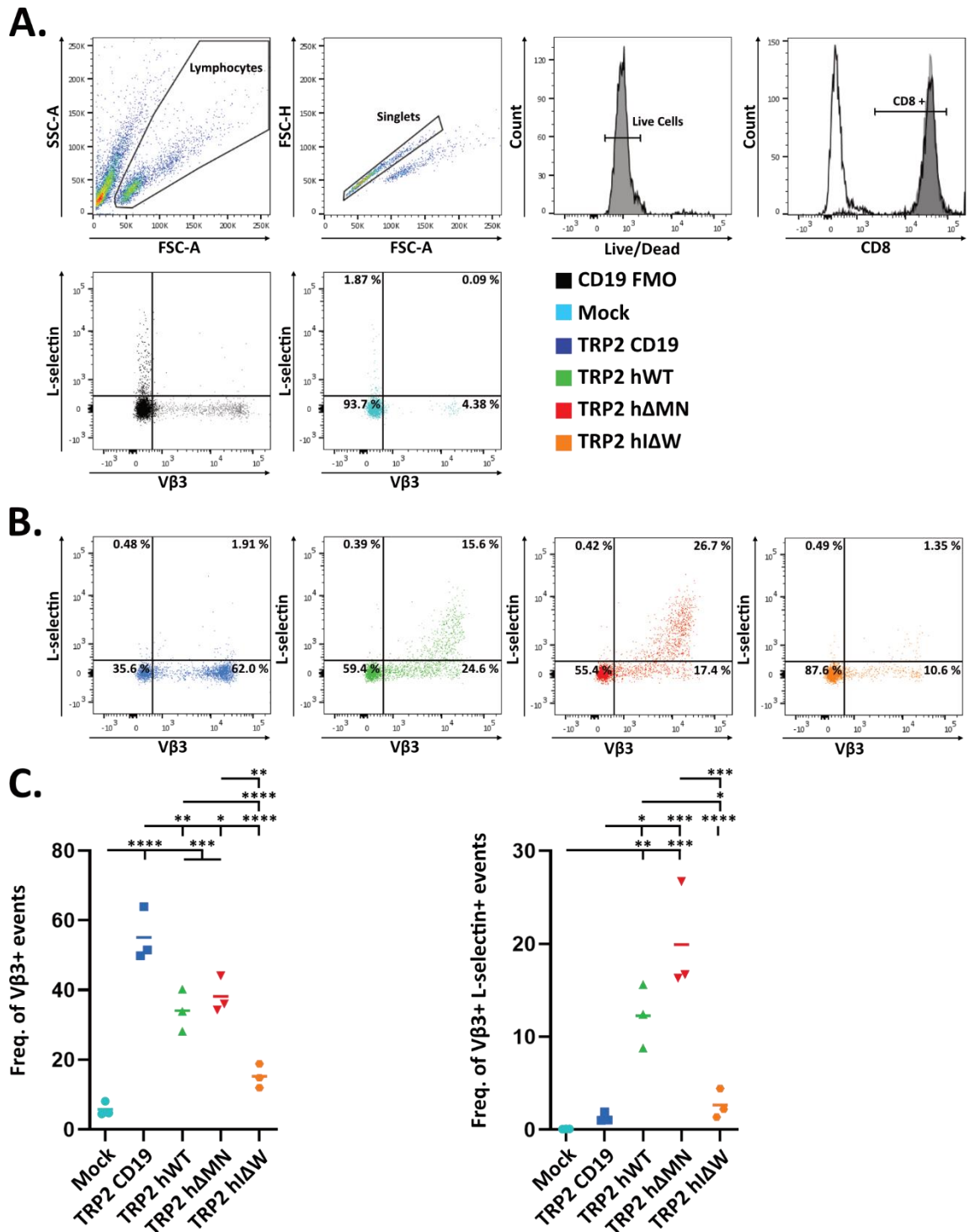


Figure 4.13. Quadricstronic constructs deliver expression of TRP2 and human L-selectin variants. Murine CD8 T cells were transduced as in Fig. 4.2A using viruses encoding transgenes as in Fig. 4.11. **(A)** The gating strategy by which CD8, live, single, lymphocytes were assessed for transgenic TRP2 and L-selectin expression following transduction. **(B)** Representative plots showing expression of TRP2 and L-selectin by cells transduced with each construct. **(C)** The quantified freq. of TRP2 and L-selectin positive events. $n=3$. Statistical Test: One-way ANOVA with Tukey test. * $p<0.05$, *** $p<0.002$, **** $p<0.0001$.

In the same antibody panel, the level of tICD19 was assessed to ensure these cells could be sorted by MACS, which had worked for the original vector containing TRP2-tICD19 (Fig. 4.6). However, across all constructs containing an L-selectin transgene, no transductions exceeded approximately 2.0 % tICD19 positive events. Only the TRP2-tICD19 viral transduction was significantly different to the mock control, with approximately 30 % positive events (Fig. 4.14A, B, C). The same number of live V β 3 positive T cells (by flow cytometry) per transduced population (different numbers of total T cells depending on transduction efficiency) were taken and lysates prepared. The greatest total number of cells across the conditions expressing V β 3 was used as the amount of mock transduced T cells lysed. These lysates were western blotted for the CD19 ectodomain. A faint band was observed in the mock control, but this was clearly much less distinct than bands for each transduced T cell lysate (Fig. 4.14D). Importantly, the TRP2-tICD19 transduced cells had a comparable band to T cells transduced with these genes and an additional L-selectin gene, indicating they still expressed tICD19, but it did not reach the cell surface.

It is also worth noting that the addition of L-selectin to these constructs reduced the number of V β 3 positive events by approximately 40 % relative to the original vector (excluding hI Δ W). This is likely due to the insert size reaching the virus' packaging limit (Fig. 4.13 and 4.14C; Kumar et al., 2001).

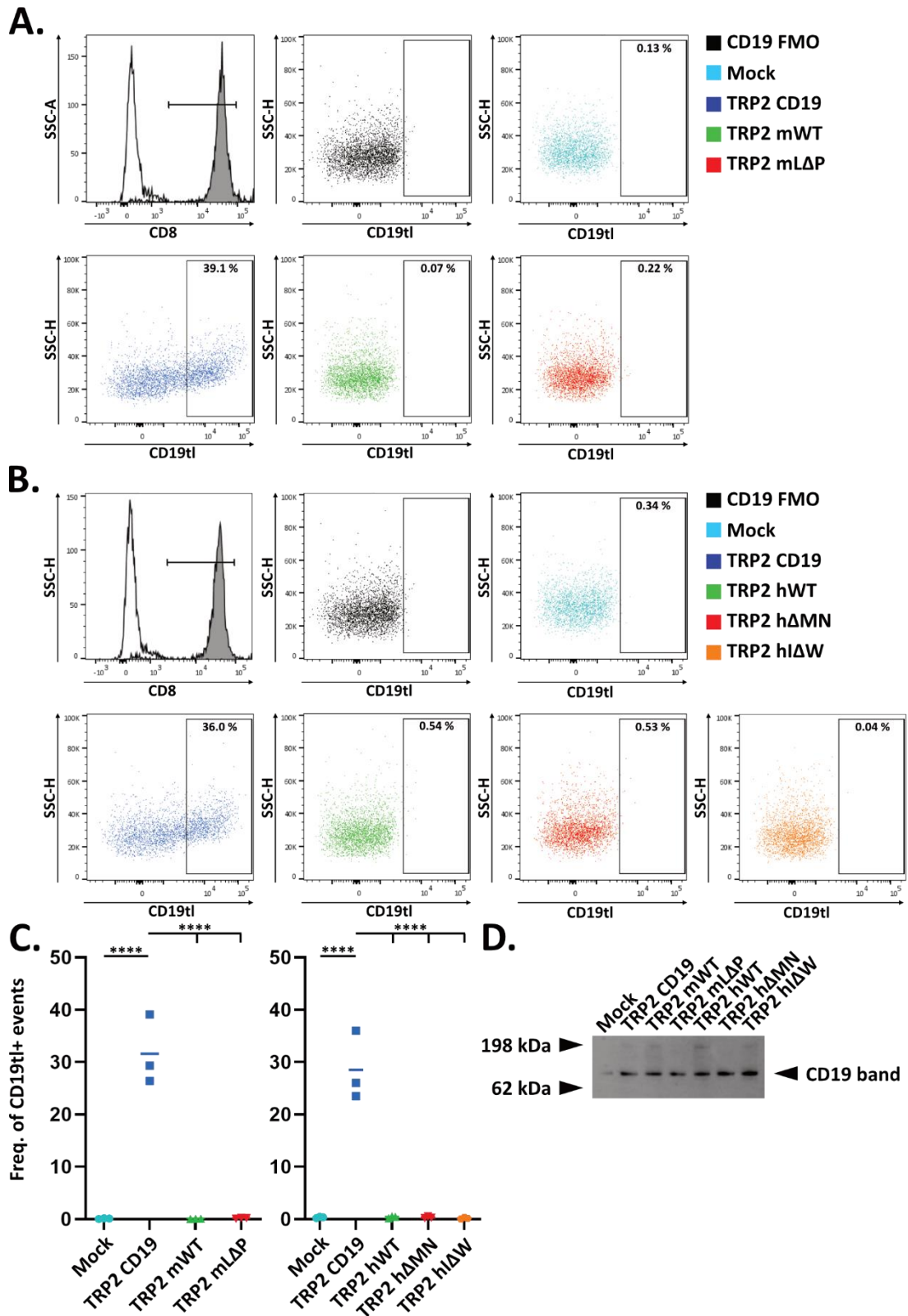


Figure 4.14. Quadricstronic constructs deliver expression of tICD19, but not at the cell surface. Live, single, lymphocytes in Fig. 4.12 and 4.13 were alternatively assessed for expression of tICD19. The gating strategy by which CD8⁺ events were assessed for tICD19 expression and representative plots are shown for **(A)** murine and **(B)** human L-selectin constructs. **(C)** The quantified freq. of tICD19 positive events. $n=3$. Statistical Test: One-way ANOVA with Tukey test. * $p<0.05$, *** $p<0.002$, **** $p<0.0001$. **(D)** Cell lysates prepared from transduced T cells previous assayed by flow cytometry were western blotted for the CD19 ectodomain.

Due to time constraints, rather than investigate the inability of the quadcistronic vectors to express tLCD19 for CD8 T cell MACS enrichment, I redesigned the vectors to remove tLCD19 (Fig. 4.15). This would mean any vectors now containing L-selectin variants would do so in place of tLCD19 and would no longer be approaching the LTR packaging limit (Fig. 4.14), which should restore viral titres and transduction efficiency.

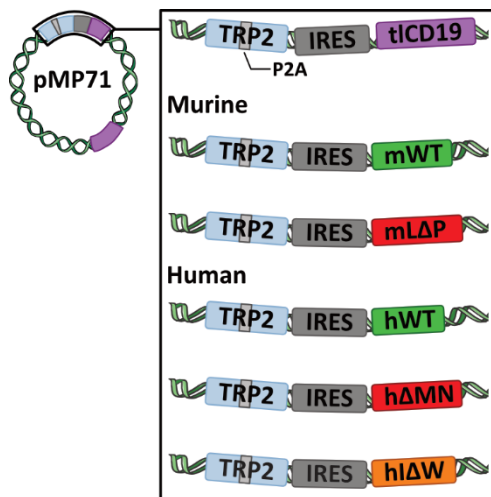


Figure 4.15. Tricistronic constructs to deliver expression of TRP2 and a L-selectin variant. These vectors were designed in-house and synthesised by Genewiz. Viruses were produced as in Fig. 4.2A.

The transduction using viruses with transgenes encoding TRP2 alongside tLCD19, mWT or mLAP yielded 62.5 %, 55.7 % and 53.0 % V β 3 positive events, respectively. These were each significantly elevated relative to the mock control, which had 7.58 % positive events (Fig. 4.16B, C). Both the mock and TRP2-tLCD19 conditions had < 2.6 % events positive for both V β 3 and L-selectin. Viruses encoding transgenes containing mWT or mLAP had 12.6 % and 40.9 % double positive events, respectively. These were significantly elevated relative to mock and TRP2-tLCD19 conditions (Fig. 4.16B, C).

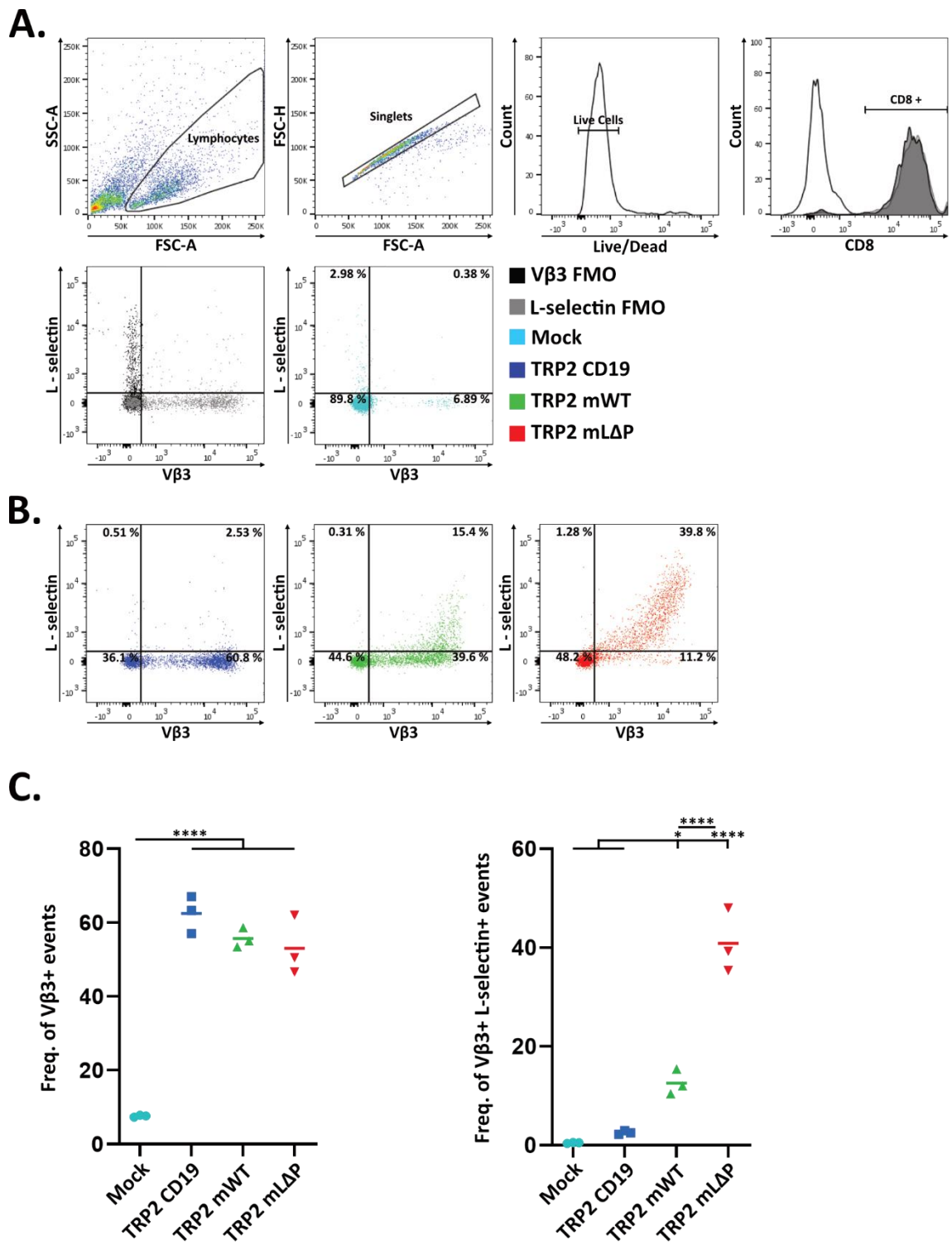


Figure 4.16. Tricistronic constructs deliver expression of TRP2 and murine L-selectin variants. Murine CD8 T cells were transduced as in Fig. 4.2A using viruses encoding transgenes as in Fig. 4.15. **(A)** The gating strategy by which CD8, live, single lymphocytes were assessed for transgenic TRP2 and L-selectin expression. **(B)** Representative plots of expression of TRP2 and L-selectin by cells following transduction with each construct and **(C)** the quantified freq. of positive events. n=3. Statistical Test: One-way ANOVA with Tukey test. * p<0.05, **** p<0.0001.

The transduction using viruses with transgenes encoding TRP2-tlCD19, or these genes alongside hWT, hΔMN or hΔW yielded 62.6 %, 61.3 %, 61.7 % and 52.3 % Vβ3 positive events, respectively. These were elevated relative to the mock control which had 6.85 % positive events (Fig. 4.17B, C). Transductions using viruses encoding TRP2-tlCD19 had significantly greater Vβ3 positive events than the construct additionally containing hΔW (Fig. 4.17B, C). The viruses containing hWT or hΔMN delivered 8.9 % and 43.9 % double positive events for Vβ3 and L-selectin, which were significantly increased compared to mock (0.24 %) and the TRP2-tlCD19 conditions (1.96 %). The virus encoding hΔW delivered 4.2 % double positive events and did not have a significantly elevated frequency of double positive events than mock transductions (Fig. 4.17B, C).

Again, the lower levels of L-selectin on T cells expressing variants susceptible to ectodomain proteolysis were likely due to the anti-CD3/CD28-mediated activation necessary for transduction, as this causes ectodomain proteolysis. Importantly, expression of TRP2 by Vβ3 staining was now equal between vectors containing tlCD19 and L-selectin variants, indicating that the previous lower transduction efficiencies from viruses produced with quadcistronic vectors were likely due to the transgene size approaching the packaging limit of viral vectors.

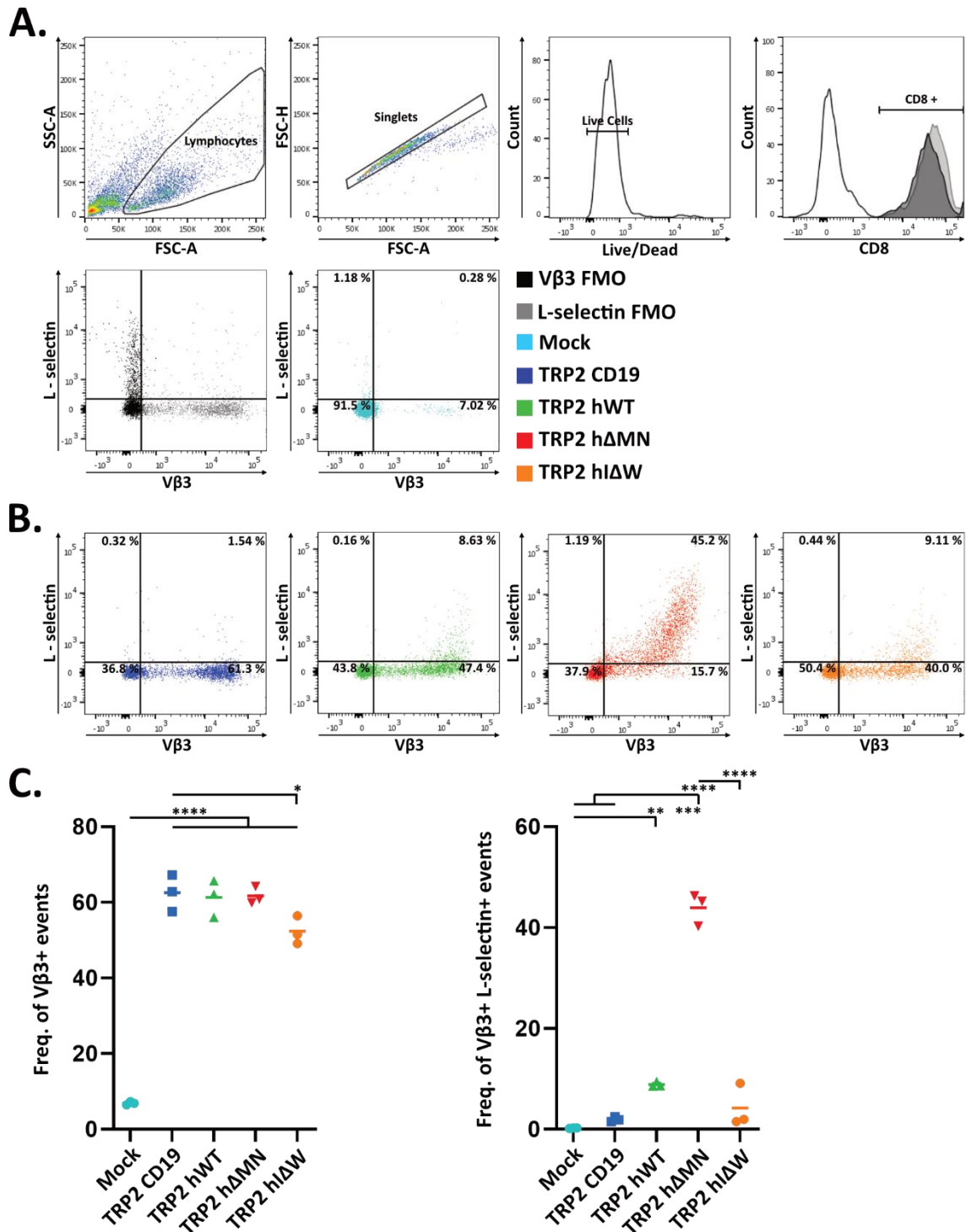


Figure 4.17. Tricistronic constructs deliver expression of TRP2 and human L-selectin variants. Murine CD8 T cells were transduced as in Fig. 4.2A using viruses encoding transgenes as in Fig. 4.15. **(A)** The gating strategy by which CD8, live, single lymphocytes were assessed for transgenic TRP2 and L-selectin expression. **(B)** Representative plots of expression of TRP2 and L-selectin by cells following transduction with each construct and **(C)** the quantified freq. of positive events. n=3. Statistical Test: One-way ANOVA with Tukey test. * p<0.05, ***p<0.002, **** p<0.0001.

4.2.5 Retrovirally delivered L-selectin undergoes sequential proteolysis in transduced murine CD8 T cells

To ensure retrovirally delivered L-selectin underwent ADAM17-mediated proteolysis in murine T cells, on day 9 of the transduction protocol (Fig. 4.2A), which was the day following the testing of transduction efficiency (Fig. 4.16 and 4.17), cells were taken and treated with either PMA or a vehicle control (DMSO) to induce ADAM17 proteolysis. These cells underwent flow cytometry assays to confirm ectodomain shedding. To determine whether human ΔW L-selectin in murine T cells was susceptible to γ -secretase proteolysis western blotting for the human L-selectin tail was performed on T cells expressing human L-selectin variants.

Live CD8 murine T cells (Fig. 4.18A) transduced with viruses encoding murine L-selectin lost the ectodomain of L-selectin when treated with PMA. For wildtype L-selectin, the number of L-selectin positive events fell from 46.2 % to 20.0 % (2.31-fold decrease), whereas for ΔP L-selectin, the number of L-selectin positive events fell from 59.7 % to 52.11 % (1.15-fold increase), indicating that this variant resisted ectodomain proteolysis (Fig. 4.18B, C; Galkina et al., 2003).

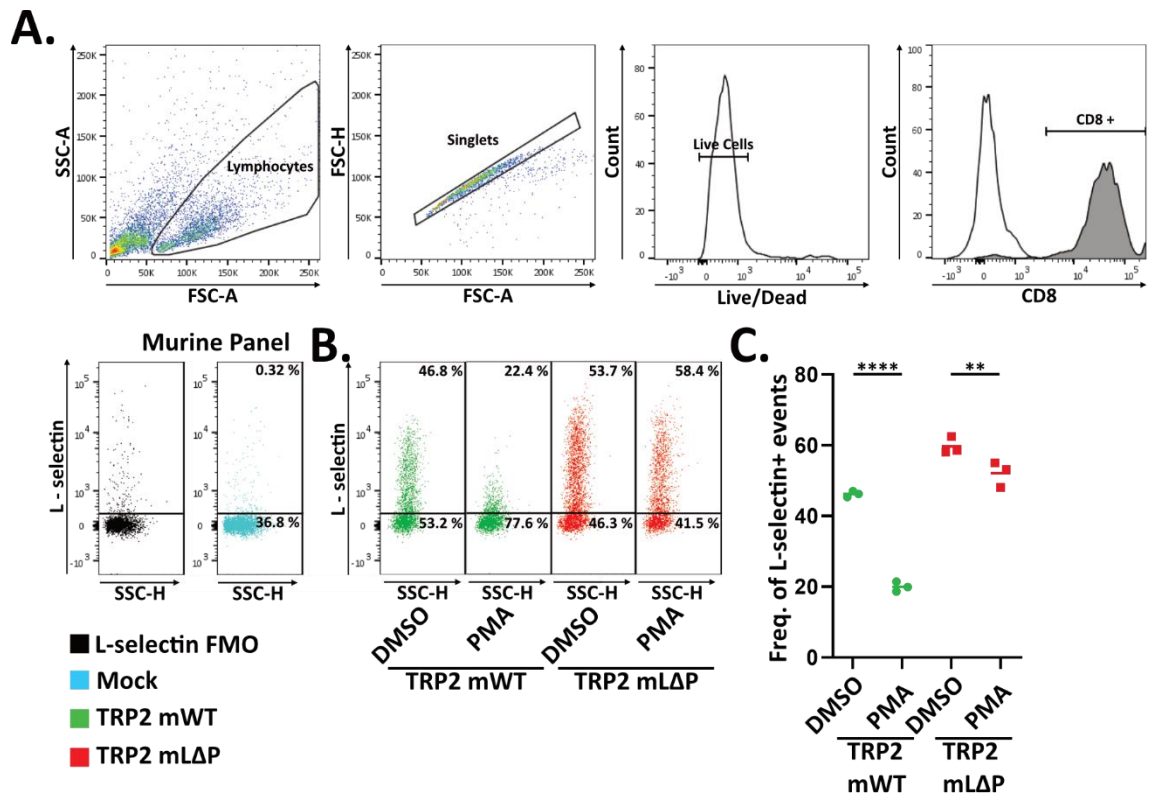


Figure 4.18. Proteolysis of transgenic murine L-selectin can be induced by PMA treatment in murine CD8 T cells. On day 9 according to Fig. 4.2A, the day after transgene levels were assessed (Day 8), transduced T cells were treated with PMA (or vehicle control) prior to flow cytometry. **(A)** The gating strategy by which CD8, live, single lymphocytes were assessed for L-selectin expression. **(B)** Representative plots after 15 minutes of PMA or DMSO treatment and **(C)** the quantified freq. of positive events. n=3. Statistical Test: One-way ANOVA with Tukey test. **p<0.01, **** p<0.0001.

Live CD8 murine T cells (Fig. 4.17A) transduced with viruses encoding human L-selectin constructs also lost the ectodomain of L-selectin when treated with PMA. For wildtype L-selectin, the number of L-selectin positive events fell from 46.6 % to 18.0 % (2.58-fold decrease), whereas for Δ MN L-selectin, the number of L-selectin positive events only fell from 60.8 % to 52.8 % (1.15-fold decrease), indicating that this variant resisted ectodomain proteolysis (Fig. 4.19B, C; Chen et al., 1995). The number of positive events in Δ W L-selectin expressing T cells fell from 29.0 % to 8.92 % (Fig 4.19B, C; 3.25-fold decrease).

To test γ -secretase-mediated proteolysis of L-selectin's tail, western blotting for this domain (which was not tagged with V5/His like L-selectin expressed by Molt3 T cell in chapter 3) was performed on cell lysates. A band was visible between the 6 - 14 kDa markers, like the MRF seen in Chapter 3 following L-selectin proteolysis (Fig. 4.19D). PMA treatment altered the intensity of this band similarly to the MRF from L-selectin expressing Molt3 T cells (Chapter 3). Here, for WT L-selectin, the MRF band intensity decreased with PMA treatment, although not significantly (Fig. 4.19D, E). For Δ W L-selectin expressing T cells, the MRF band intensity increased significantly following proteolysis (Fig. 4.19D, E) from 3776.8 to 8262.3 (2.18-fold increase). The full-length (FL) L-selectin and assumed MRF bands were visible where I would expect on the membrane, although there were several additional bands. I labelled the most distinct as 'unknown', which was comparable in intensity to L-selectin's FL and MRF bands. Its weight was approximately 16 – 17 kDa and may represent a ubiquitinated form of the MRF (Fig. 4.19D).

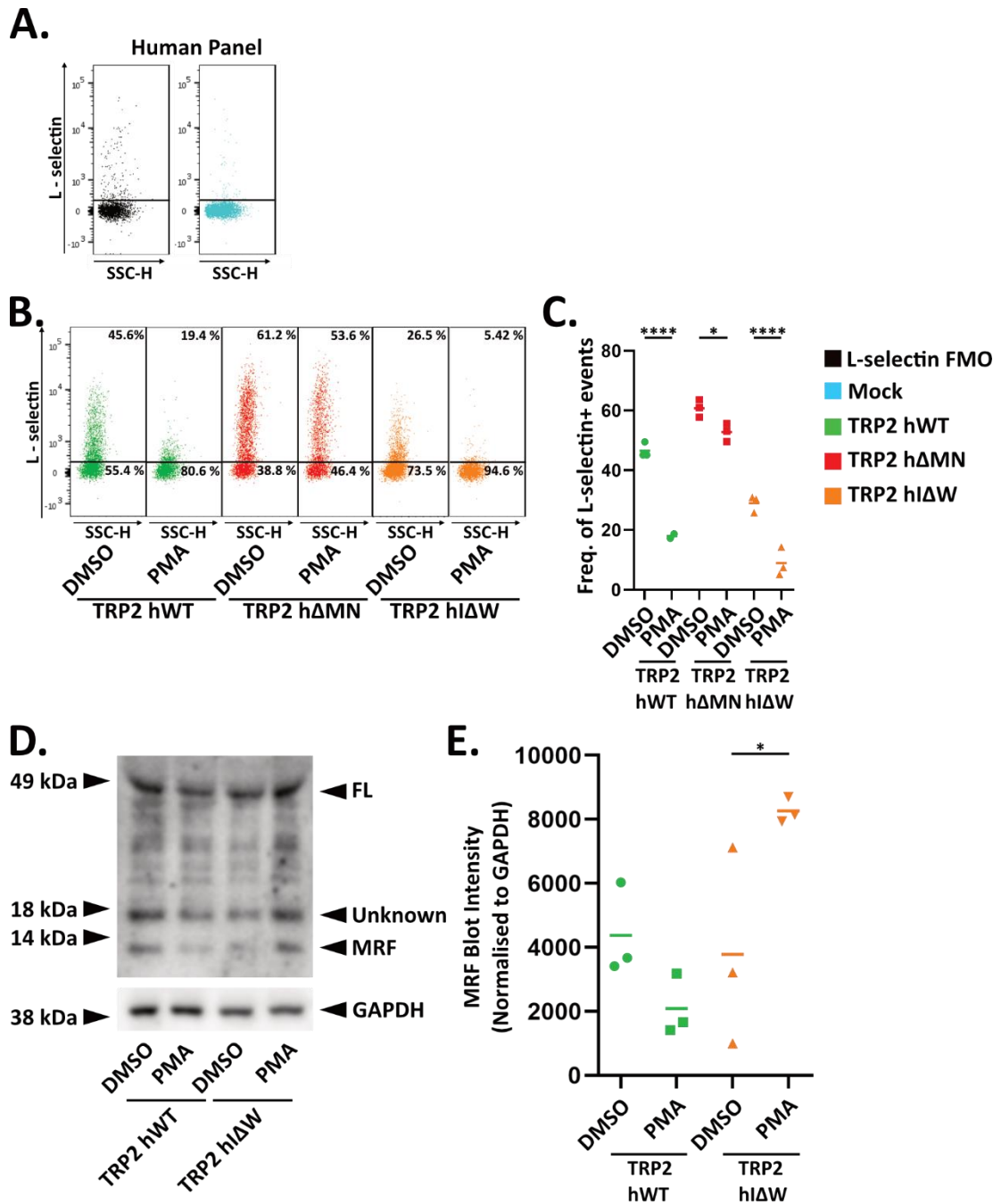


Figure 4.19. Sequential proteolysis of transgenic human L-selectin was induced by PMA treatment in murine CD8 T cells. On day 9 according to Fig. 4.2A, the day after transgene levels were assessed (Day 8), transduced T cells were treated with PMA (or vehicle control) prior to flow cytometry or western blotting for L-selectin's tail (untagged). **(A)** The gating strategy by which lymphocytes were gated is shown in Fig. 4.18A and the controls shown here. **(B)** Representative plots after 15 minutes of PMA or DMSO treatment and **(C)** the quantified freq. of positive events are shown. **(D)** Alternatively to flow cytometry, cell lysates were western blotted for L-selectin's tail and **(E)** the MRF of L-selectin quantified. $n=3$. Statistical Test: One-way ANOVA with Tukey test. * $p<0.05$, **** $p<0.0001$.

4.2.6 TRP2-expressing T cells kill target cancer cells *in vitro*.

To determine if TRP2-expressing T cells could kill target cancer cells, I used the xCELLigence platform to assess B16.F10 cell growth curves alone or with V β 3 positive (TRP2 TCR) transduced T cells at a 1:1 or 2:1 effector-to-target cell ratio (Fig 4.20A). Adherent target cells were plated on a 96-well gold-plated plate, and the xCELLigence sent an electric current through each well every 15 minutes. The resistance increased as target cells grew and decreased when they underwent T cell-mediated cytotoxicity. Resistance was reported as a 'cell index' value, which could be normalised (normalised cell index) to account for variance in target cell seeding and plotted against time to provide growth curves. Normalised cell index values could be further normalised relative to a full lysis control to provide '% cytotoxicity' values, all of which are defined in Chapter 2 (Section 2.6.1; Fig. 2.6).

The number of mock-transduced T cells added to the control condition was the maximum number of total T cells added in any of the given transduced T cell conditions (dotted line, max T cells; Fig. 4.20A). For example, to achieve a 1:1 ratio of V β 3 positive T cells where 10 target cells were present, but transduction efficiency was 50 % for V β 3, 20 transduced T cells were added to the well (10 V β 3 positive T cells). In a control well, 20 mock-transduced T cells were added to target cells to account for the total number of T cells added in the transduced condition. This assay was initiated on the day 8 of the transduction protocol (Fig. 4.2A), which was 3 days following transduction, the same day transduction efficiency was assessed, and PMA-induced shedding induced (Fig. 4.16 and 4.17).

Time 0 in the killing assay corresponds to -15 minutes prior to addition of transduced T cells, after which B16.F10 cell growth was monitored with and without mock-transduced T cells (Fig. 4.20B). When transduced T cells were added, the normalised cell index decreased, indicating TRP2-mediated killing of the cancer target cells, reaching a normalised cell index equivalent to full lysis of target cells over time (Fig. 4.20B). However, at both ratios tested (from approximately 30 hr at 1:1 and 24 hr at 2:1) growth slowed in mock T cell-treated B16.F10 cells relative to B16.F10 cells alone. This was presumably due to the additional T cells causing premature acidification of the medium, in turn inducing B16.F10 cell death, or killing mediated by the endogenous TCR in untransduced T cells.

The normalised cell index relative to the full-lysis control (Triton-x-100) was expressed as % lysis mediated by T cells (Fig 4.20C). It is clear in these graphs, and more so at 1:1 E:T ratio, that T cells mediated killing in two phases: one from 0 – 12 hr and one from 24 – 48 hr. These were separated by a plateau, where either T cell-mediated killing and B16.F10 growth were paused or killing was reduced to the same rate as B16.F10 growth (Fig. 4.20C). The plateau was also seen in the mock control, most clearly at the 2:1 ratio, suggesting that the slowed increase in cell index relative to B16.F10 alone was likely due to endogenous TCR-mediated killing.

All TRP2 TCR-transduced T cells mediated significantly more killing at all ratios and time points than mock controls (Fig. 4.20D). There were no statistical differences between any of the transduced T cells containing TRP2 at any tested ratios or time points (Fig. 4.20D).

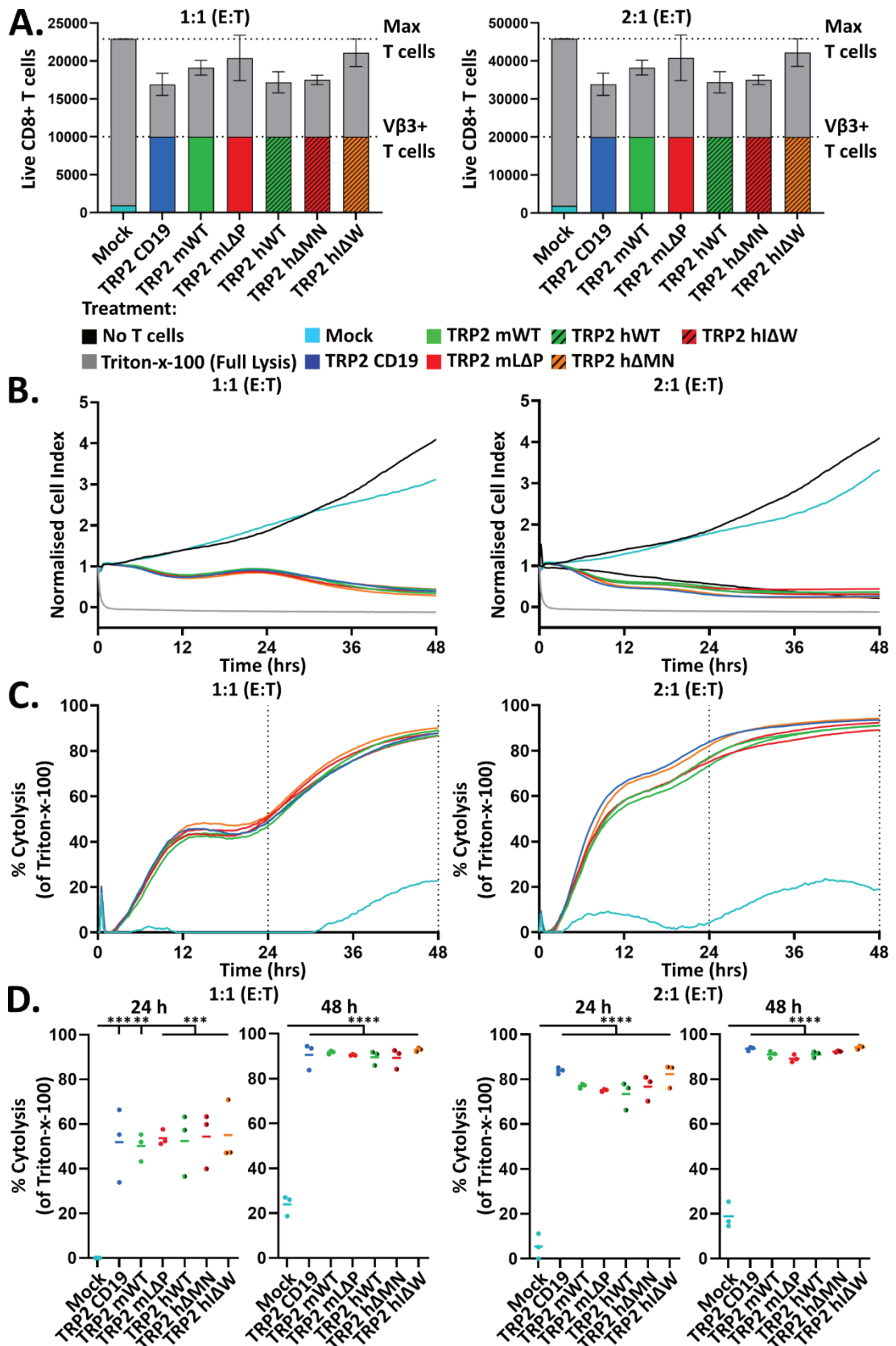
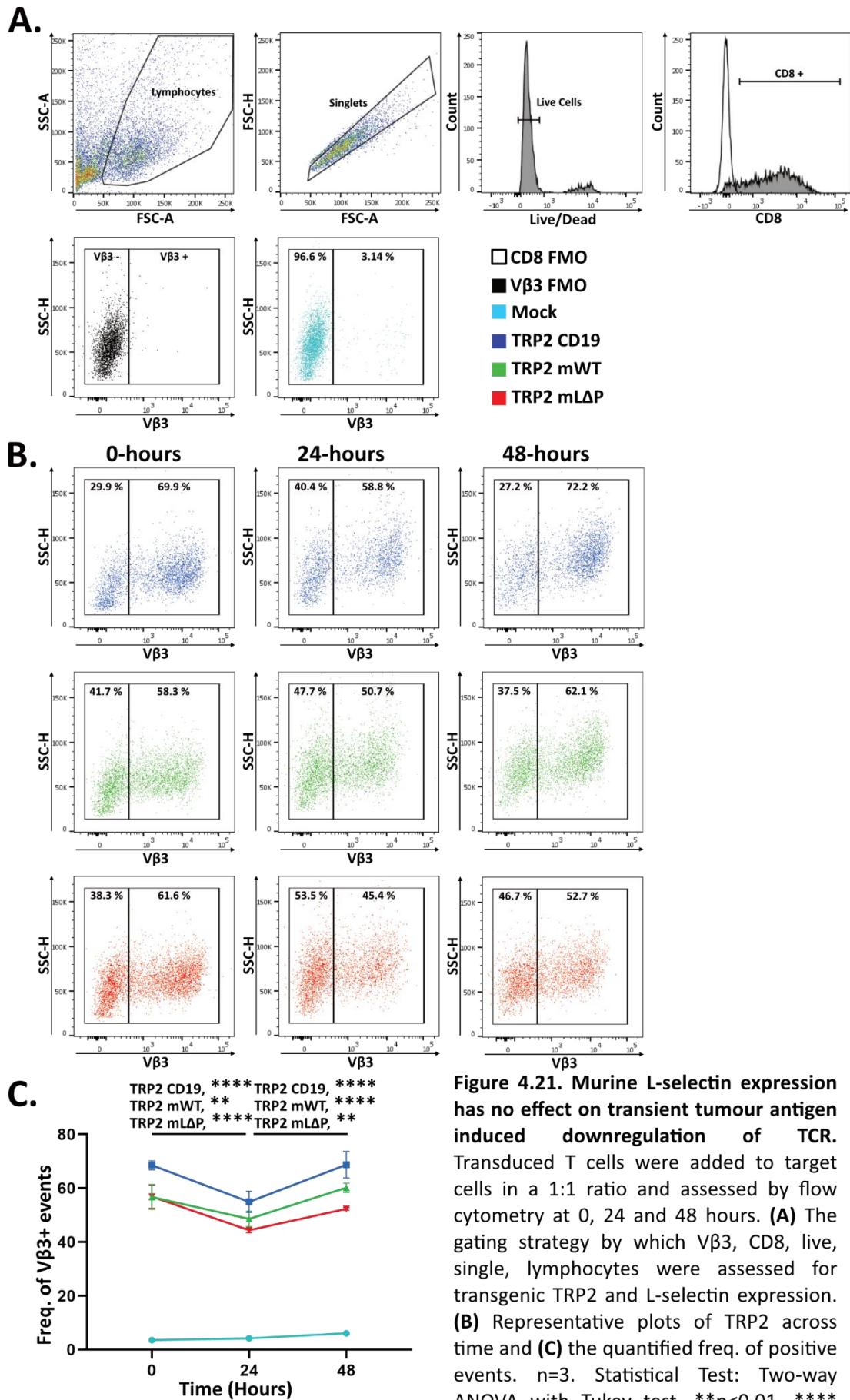
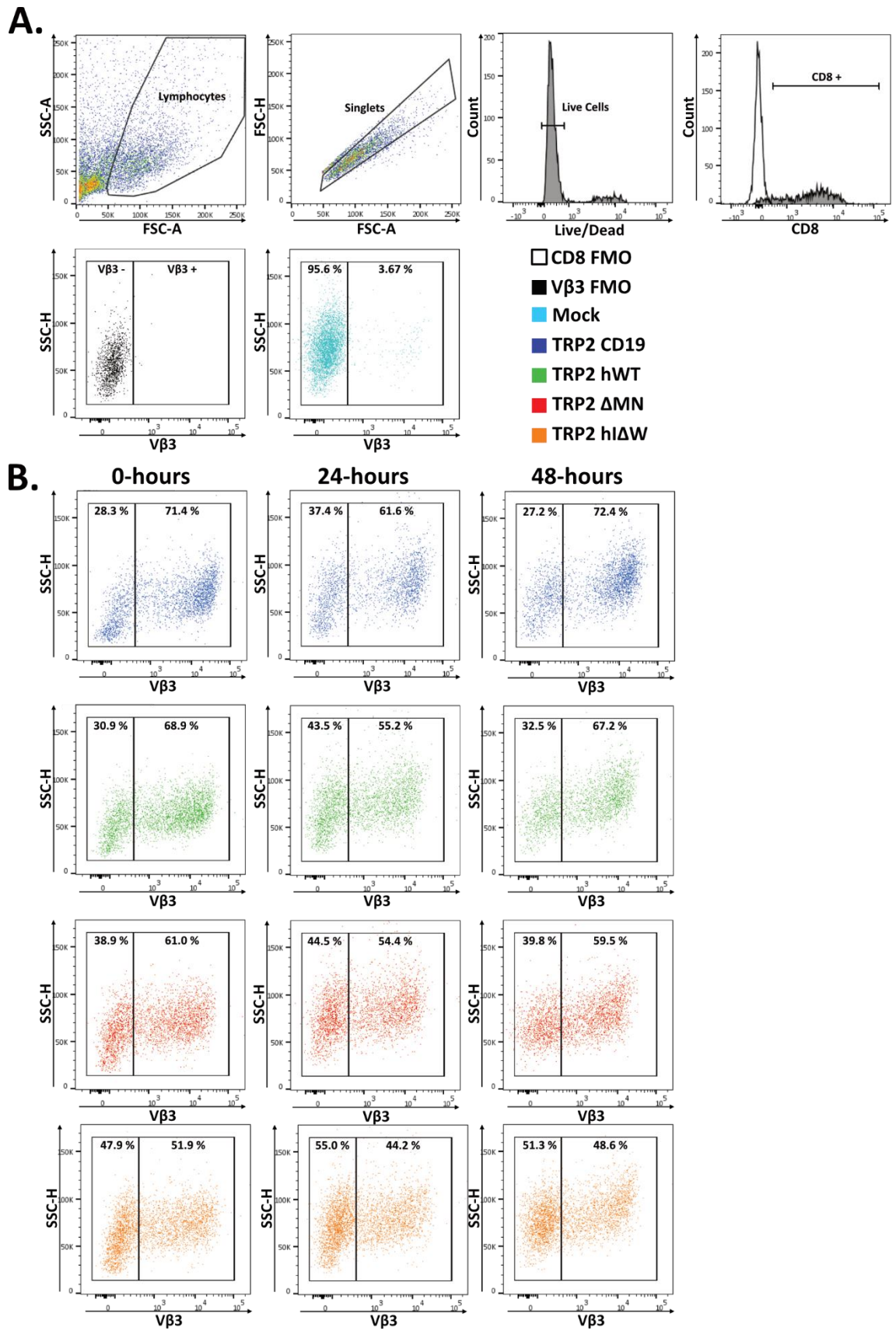


Figure 4.20. TRP2 expressing murine T cells killed target tumour cells *in vitro* (A) T cells were added to target cells at indicated ratios according to Vβ3 levels and the number of mock transduced T cells added accounts for the maximum number of total T cells added. (B) Normalised cell growth indices of B16.F10 under different treatments at each ratio and (C) as % cytolysis. (D) Quantification of % cytolysis at 24 and 48 hours post treatment at both ratios. n=3. Statistical Test: One-way ANOVA with Tukey test. ** p<0.005, ***p<0.001, **** p<0.0001.

Transduced T cells were assessed by flow cytometry for expression of activation markers, including L-selectin, CD27 and CD44. CD69, CD25 and Ki67 were also measured, because they have been linked to L-selectin shedding in murine T cells (Mohammed et al. 2019; Watson et al. 2019), alongside the exhaustion markers TIM-3, LAG-3 and PD-1. Not all markers are shown in this chapter, but the frequency of positive events for each marker across time are shown in the supplementary information (Supp. Fig 4.1). T cells were analysed prior to their addition to plated target cells (0 hr) and at 24 and 48 hr after addition to tumour targets. For each condition, frequencies of positive events were compared between time points, and at each time point, frequencies of positive events were compared between conditions (e.g. Fig. 4.28C).

Following addition to target cells, TRP2-expressing T cells showed a decrease in frequency of 10 % at 24 hr (Fig. 4.21 and 4.22A, B, C), unless they also expressed ΔW L-selectin (Fig. 4.22A, B, C). The number of TRP2 positive T cells recovered to original levels by 48 hr, indicating target-specific T cell activation and TCR downregulation (Lauritsen et al. 1998). For further analysis at each time-point, V β 3 positive events were selected. As the frequency of V β 3 positive events in the mock-transduced condition was only 3 % (Fig. 4.21 and 4.22A), V β 3 positive, TRP2-transduced T cells were compared with V β 3-negative mock-transduced cells for expression of activation markers.





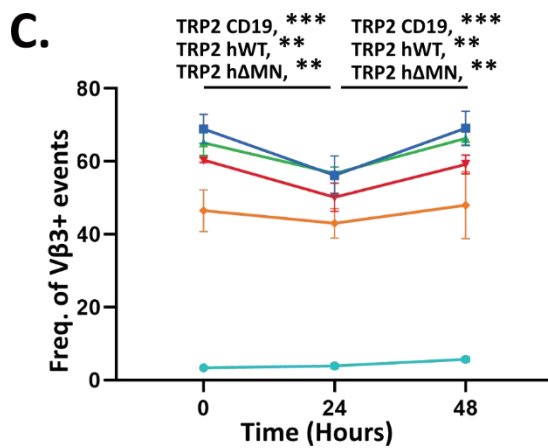


Figure 4.22. Human L-selectin expression has no effect on transient tumour antigen induced downregulation of TCR. Transduced T cells were added to target cells in a 1:1 ratio and assessed by flow cytometry at 0, 24 and 48 hours. **(A)** The gating strategy by which V β 3, CD8, live, single, lymphocytes were assessed for transgenic TRP2 and L-selectin expression. **(B)** Representative plots of TRP2 across time and **(C)** the quantified freq. of positive events. n=3. Statistical Test: Two-way ANOVA with Tukey test. **p<0.01, *** p<0.0005.

Expression of TRP2 alone increased the frequency of PD-1 positive events at 24 hr and 48 hr (Fig. 4.23 and 4.24B, C). Co-expression of WT murine L-selectin had no impact on PD-1 expression at either time point. However, co-expression of shedding-resistant murine Δ P L-selectin prevented further increases in PD-1 positive event frequency beyond 24 hr (Fig. 4.23C). At 48 hr, T cells co-expressing Δ P L-selectin had significantly fewer PD-1 positive events than T cells transduced to express TRP2 alone or alongside WT L-selectin (Fig. 4.23C).

For comparison of conditions containing human L-selectin variants, again, expression of TRP2 alone increased the frequency of PD-1 expression at 24 hr and 48 hr (Fig. 4.24). Co-expression of WT human L-selectin also had no effect on PD-1 expression at 24 and 48 hr relative to T cells transduced to express TRP2 alone (Fig. 4.24C). Δ MN and Δ W L-selectin prevented a further increase in PD-1 positive event frequency beyond 24 hr (Fig. 4.24C). However, this may have been due to the greater variance in these data points at 24 hr. Unlike Δ P L-selectin, Δ MN and Δ W L-selectin bearing T cells did not have significantly fewer PD-1 positive events than T cells transduced to express TRP2 alone (Fig. 4.24C).

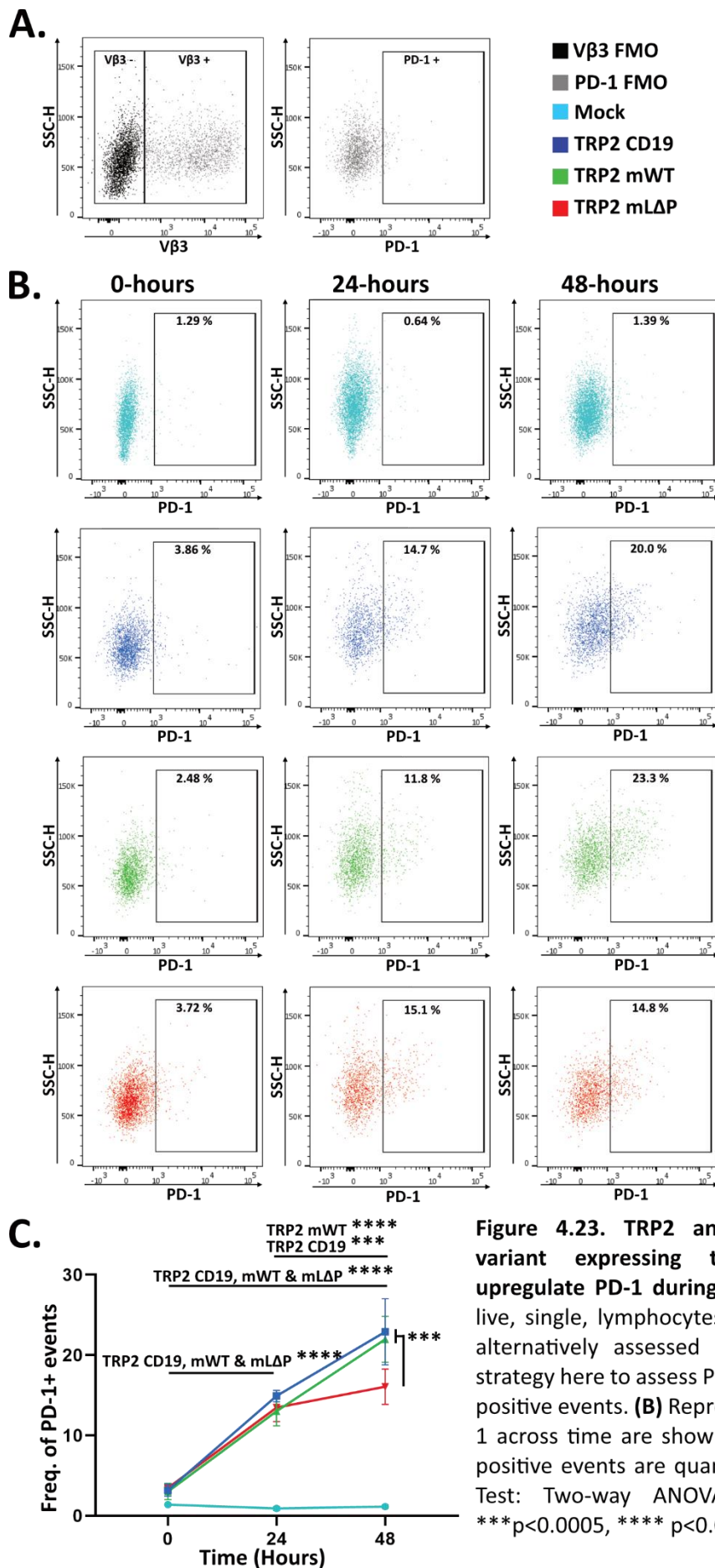
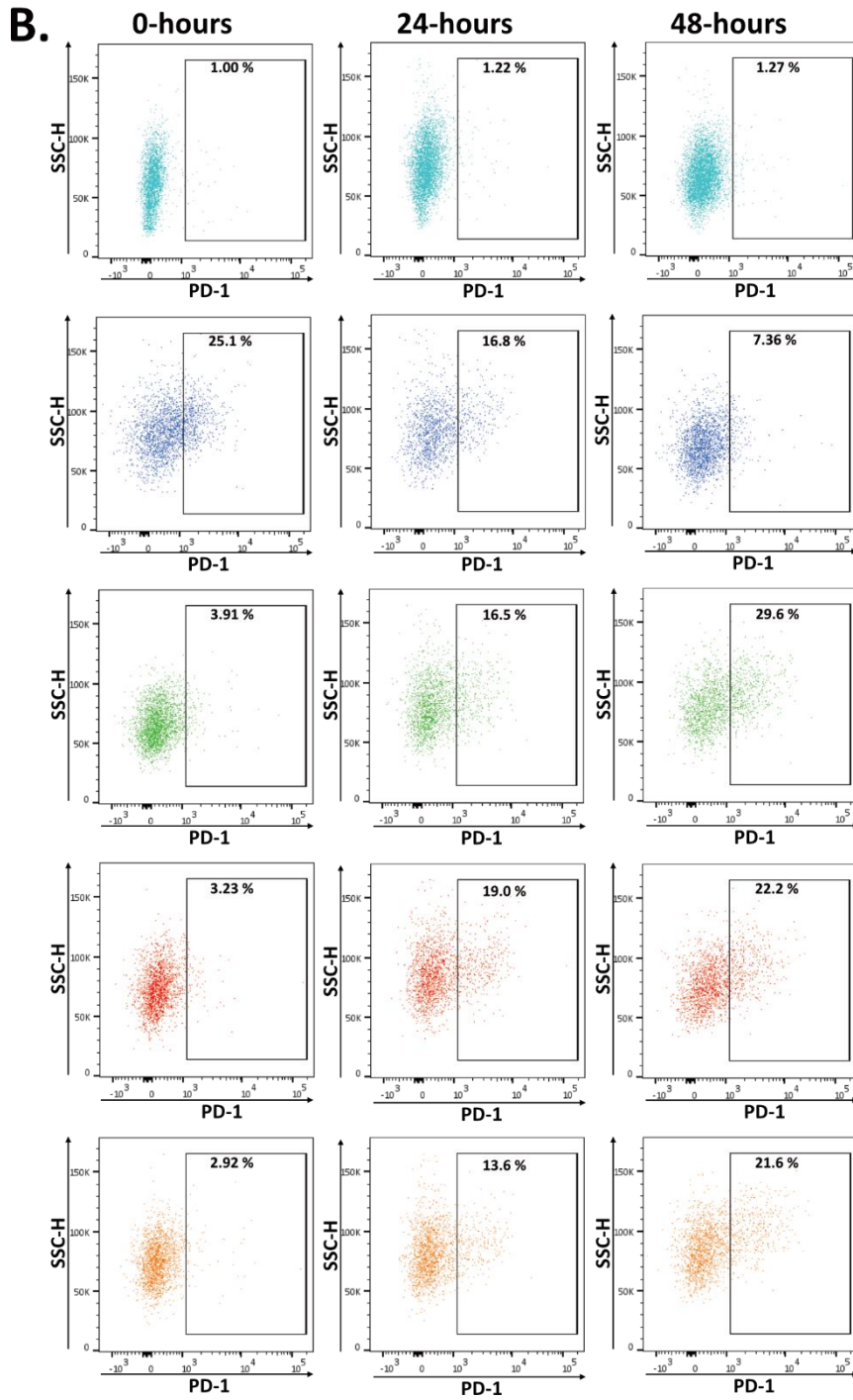
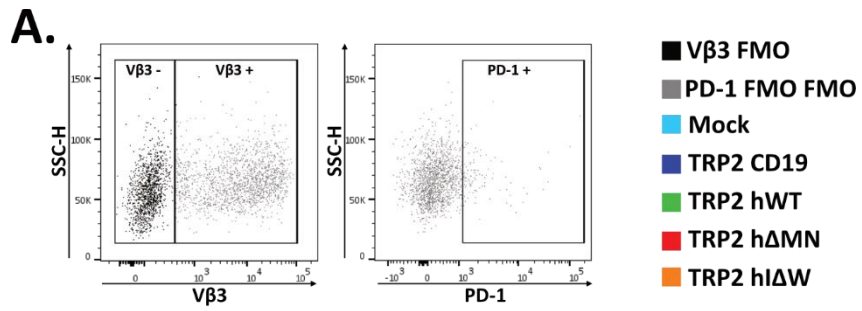


Figure 4.23. TRP2 and murine L-selectin variant expressing transduced T cells upregulate PD-1 during *in vitro* killing. CD8, live, single, lymphocytes from Fig. 4.21 were alternatively assessed using (A) the gating strategy here to assess PD-1 expression on Vβ3 positive events. (B) Representative plots of PD-1 across time are shown and (C) the freq. of positive events are quantified. n=3. Statistical Test: Two-way ANOVA with Tukey test. ***p<0.0005, **** p<0.0001.



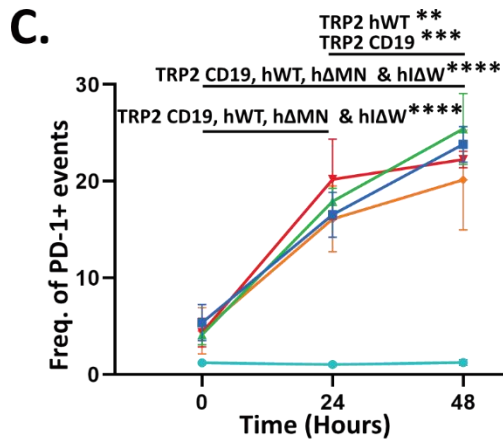


Figure 4.24. TRP2 and human L-selectin variant expressing transduced T cells upregulate PD-1 during *in vitro* killing. CD8, live, single, lymphocytes from Fig. 4.22 were alternatively assessed using **(A)** the gating strategy here to assess PD-1 expression on Vβ3 positive events. **(B)** Representative plots of PD-1 across time are shown and **(C)** the freq. of positive events are quantified. n=3. Statistical Test: Two-way ANOVA with Tukey test. **p<0.01, ***p<0.0005, ****p<0.0001.

Surprisingly, following addition to target cells, TRP2 T cells co-expressing murine and human L-selectin variants showed an increased frequency of L-selectin positive T cells during the 48-hr killing assay (Fig. 4.25 and 4.26A, B, C).

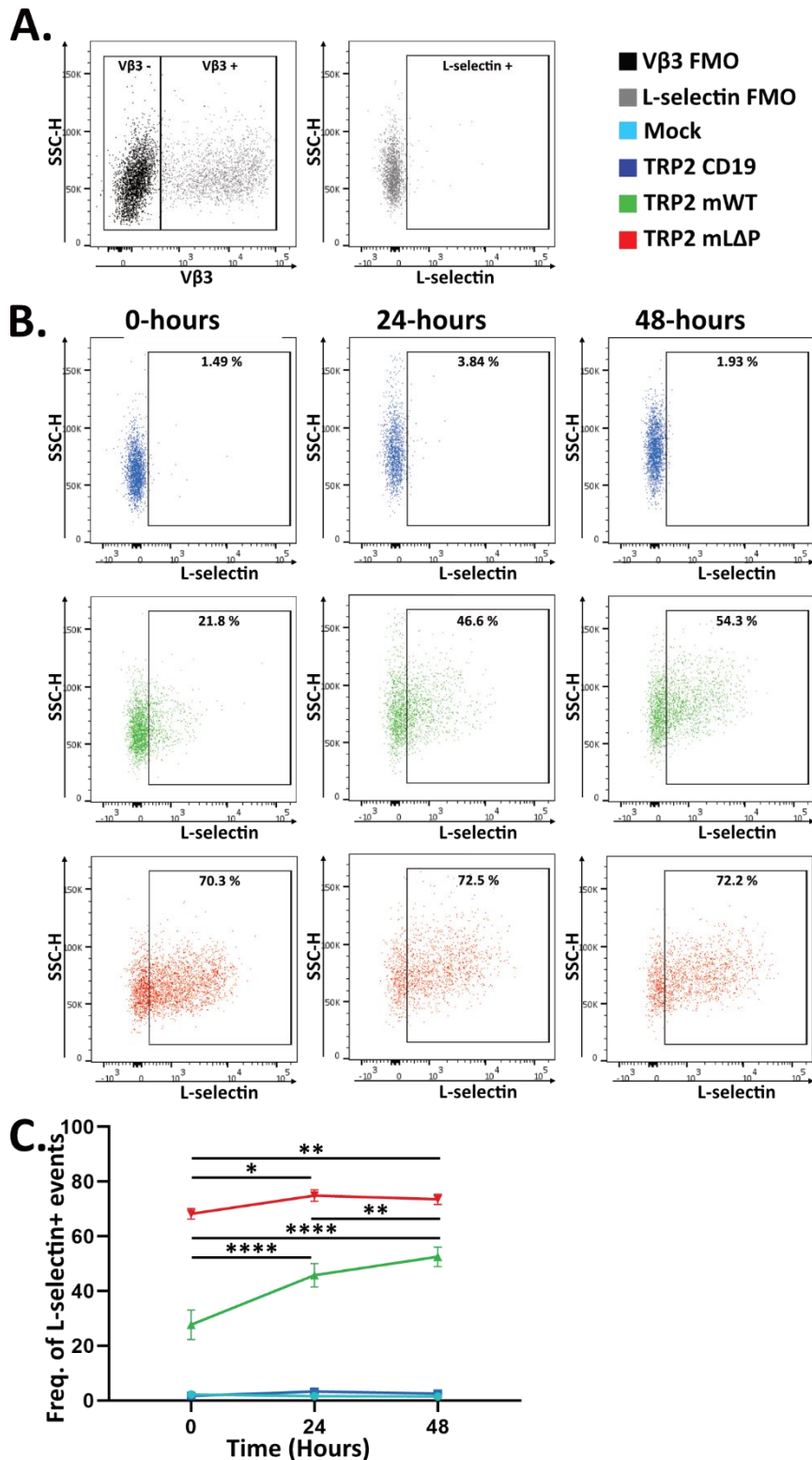
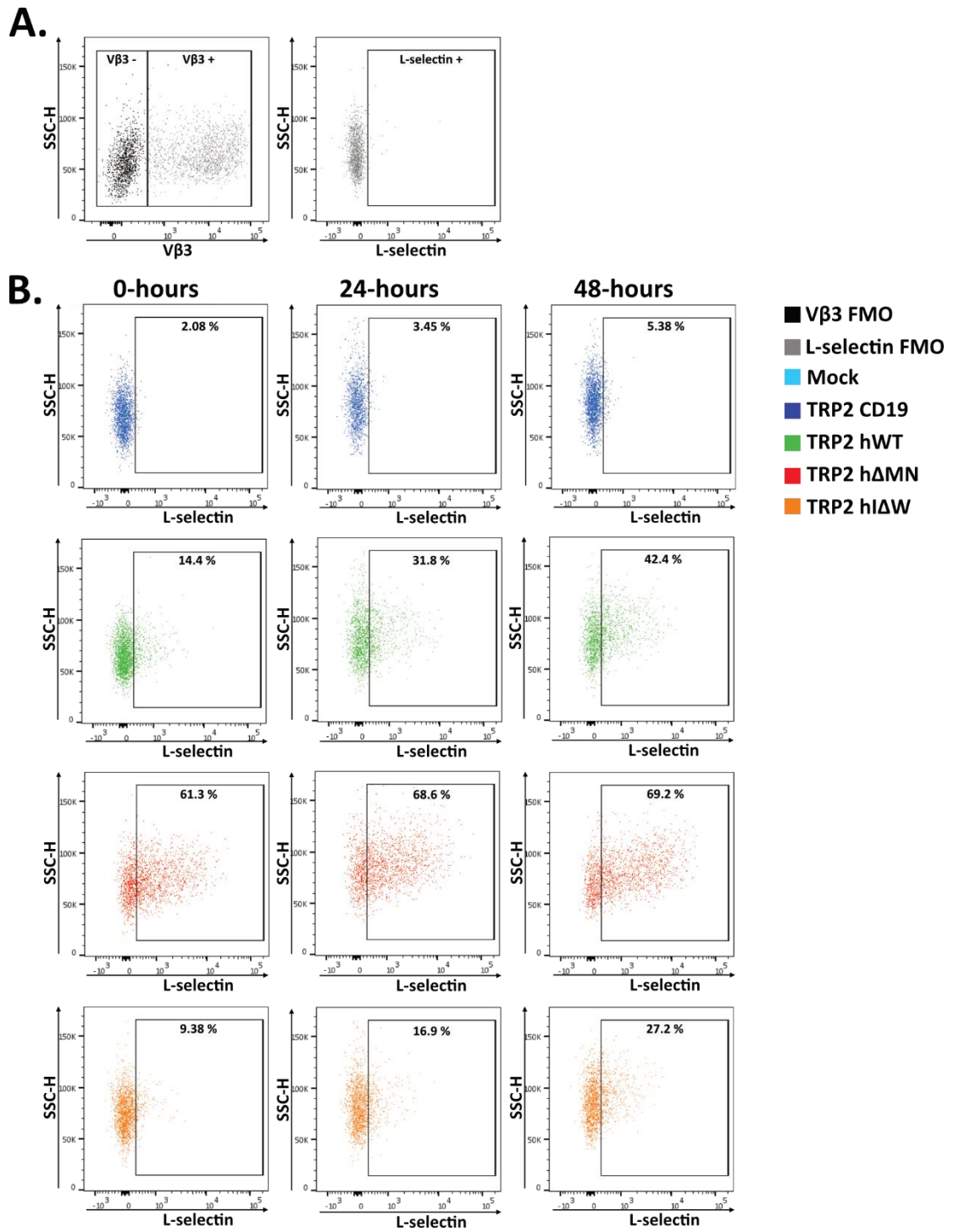


Figure 4.25. Murine L-selectin levels continually rise whilst killing target cells. CD8, live, single, lymphocytes from Fig. 4.21 were alternatively assessed using **(A)** the gating strategy here to assess L-selectin expression on V β 3 positive events. **(B)** Representative plots of L-selectin expression across time and **(C)** the freq. of positive events quantification. n=3. Statistical Test: Two-way ANOVA with Tukey test. *p<0.05, **p<0.01, **** p<0.0001.



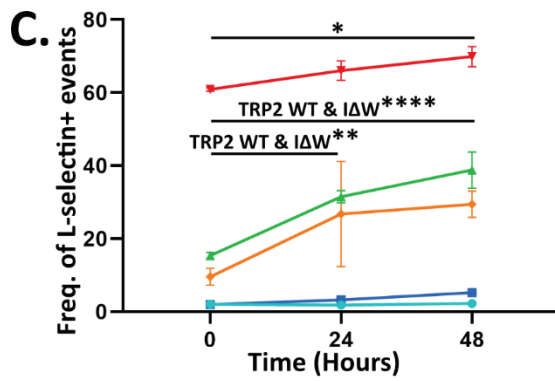


Figure 4.26. Human L-selectin levels continually rise whilst killing target cells. CD8, live, single, lymphocytes from Fig. 4.22 were alternatively assessed using **(A)** the gating strategy here to assess L-selectin expression on V β 3 positive events. **(B)** Representative plots of L-selectin expression across time and **(C)** the freq. of positive events quantification. n=3. Statistical Test: Two-way ANOVA with Tukey test. *p<0.05, **p<0.01, **** p<0.0001.

However, co-expression of L-selectin alongside TRP2 affected T cell activation prior to incubation with tumour targets, because the frequency of CD25 positive events was increased by WT and L Δ P murine L-selectin expression (0-hr; Fig. 4.27B, C). Following addition to target cells, these differences in CD25 positive cell frequency were no longer detectable. This was due to a decrease in the number of CD25 positive events among L-selectin expressing T cells (Fig. 4.27C).

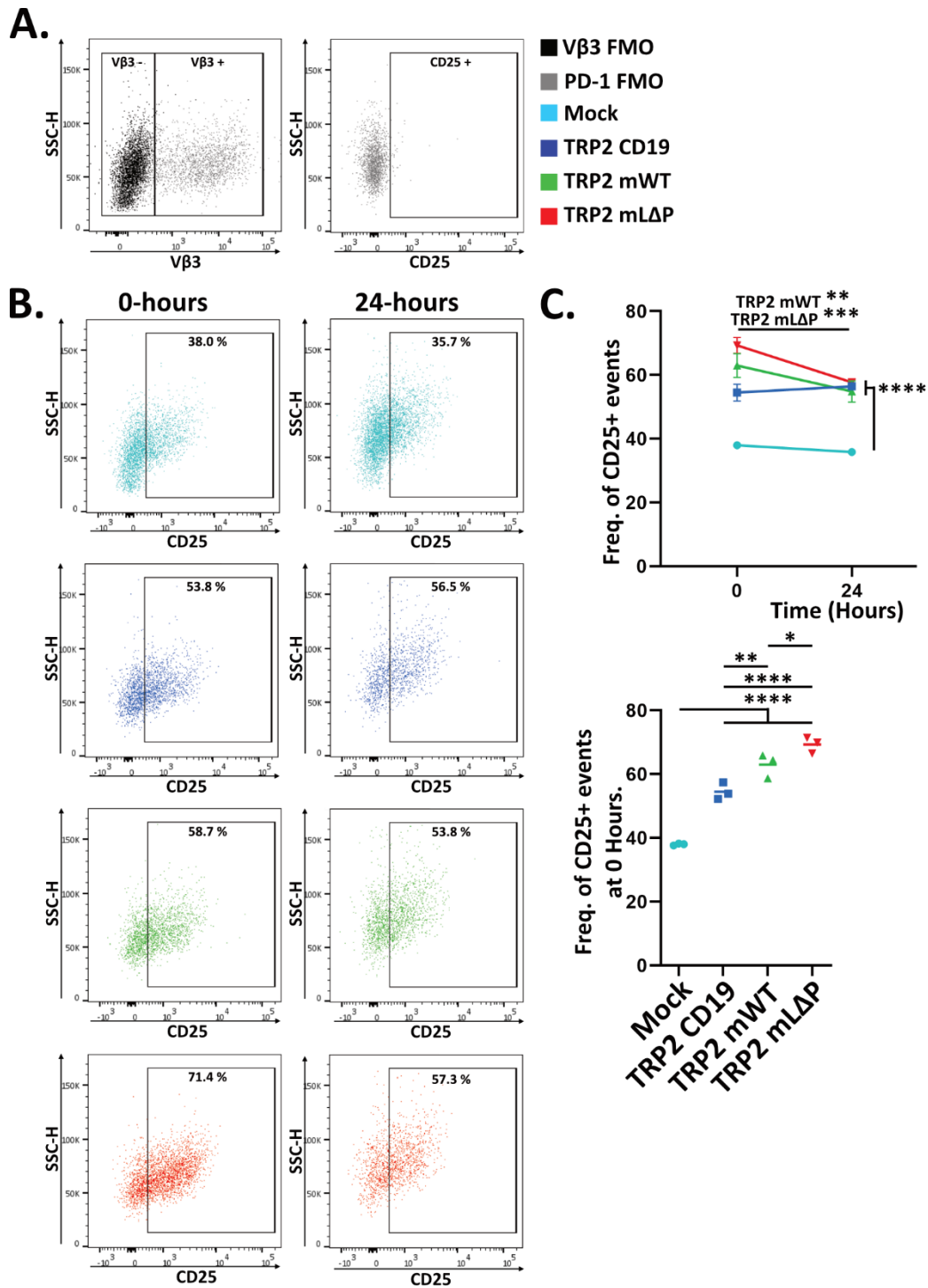
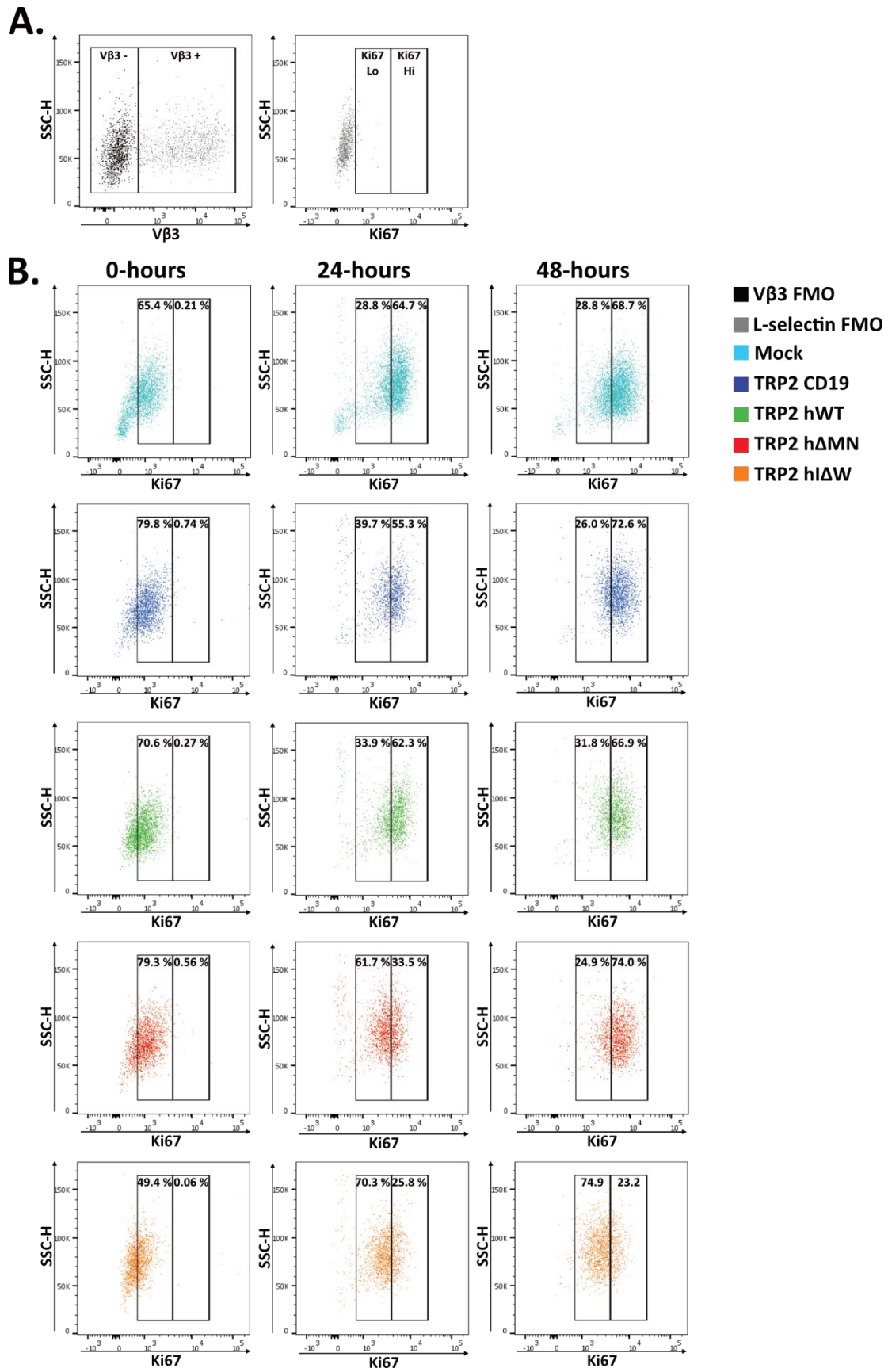


Figure 4.27. TRP2 mLΔP expressing transduced T cells have aberrant expression of CD25 prior to *in vitro* killing. CD8, live, single, lymphocytes from Fig. 4.21 were alternatively assessed using **(A)** the gating strategy here to assess CD25 expression on Vβ3 positive events. **(B)** Representative plots of CD25 expression across time and **(C)** the quantified freq. of CD25 positive events. n=3. Statistical Test: Two-way ANOVA with Tukey test. * p<0.05, ***p<0.002, ****p<0.0005, ***** p<0.0001.

Ki67 expression was not affected by co-expression of murine WT or L Δ P L-selectin, either before or after target cell killing (Supp. Fig. 4.1). However, co-expression of hI Δ W L-selectin, but not WT or Δ MN human L-selectin, reduced the frequency of Ki67-hi events compared to TCR- or mock-transduced T cells during the 48-hr killing assay (Fig. 4.28B, C).



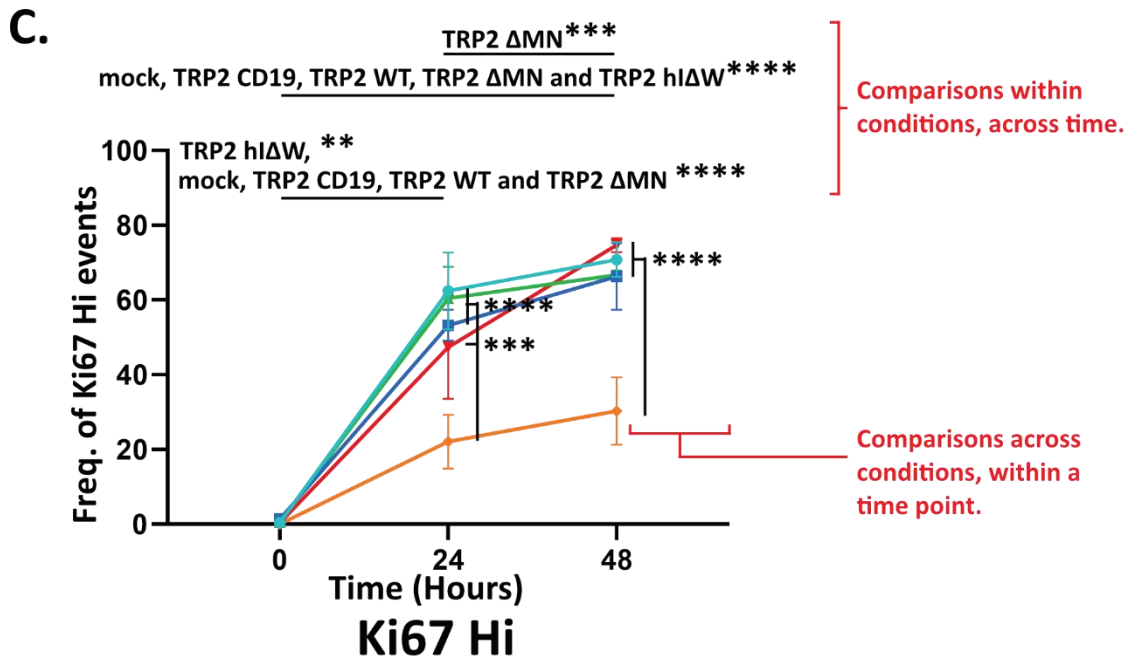


Figure 4.28. Human h Δ W L-selectin causes aberrant Ki67 expression whilst killing target cells. CD8, live, single, lymphocytes from Fig. 4.22 were alternatively assessed using **(A)** the gating strategy to assess Ki67 expression on V β 3 positive events. **(B)** Representative plots of Ki67 expression across time and **(C)** the quantified freq. of Ki67 Hi events n=3. Statistical Test: Two-way ANOVA with Tukey test. *p<0.05, **p<0.01, *** p<0.0005, **** p<0.0001.

At time 0, TRP2-expressing T cells that did not co-express L-selectin were mostly Ki67-lo (80 % of events), and at 24 hr after addition to target cells, approximately 40 % of events were Ki67-lo and 55 % of events were Ki67-hi (Fig. 4.28B). At 48 hr after addition to target cells, the majority (approximately 73 % of events) of T cells were Ki67-hi (Fig. 4.28B, C). Except for h Δ W L-selectin, co-expression of L-selectin had no effect on the frequency of Ki67 -lo or -hi events relative to TRP2 T cells that were L-selectin null (Fig. 4.28B, C). Interestingly, mock-transduced T cells expressed Ki67 similarly to T cells transduced with TRP2 (Fig. 4.28B, C).

Co-expression of h Δ W L-selectin reduced the number of Ki67-lo events prior to the addition T cells to target cells. At 24 and 48 hr after addition to target cells, h Δ W L-selectin reduced the number of Ki67-hi events and prevented an increase in Ki67 expression between 24 and 48 hr (Fig. 4.28B).

4.2.7 Murine CD8 T cells transduced to express TRP2 do not control tumour growth *in vivo*

On day 12 since the beginning of the transduction protocol (Fig. 4.2A), prior to cryopreservation, I again assessed transduction efficiency and cell viability. This was done to determine if the cells continued to expand *in vitro* and if transgene expression was elevated at a later time point. If so, fewer cells would be needed for future *in vivo* experiments, in accordance with the 3Rs.

There were increases in the frequencies of V β 3 positive events from 51.2 % to 74.1 % between day 8 and day 12 (Fig. 4.29A). Further, despite a decrease in viability of 12.6 % (Fig. 4.29B), there were increased numbers of live V β 3 positive events (Fig. 4.29C).

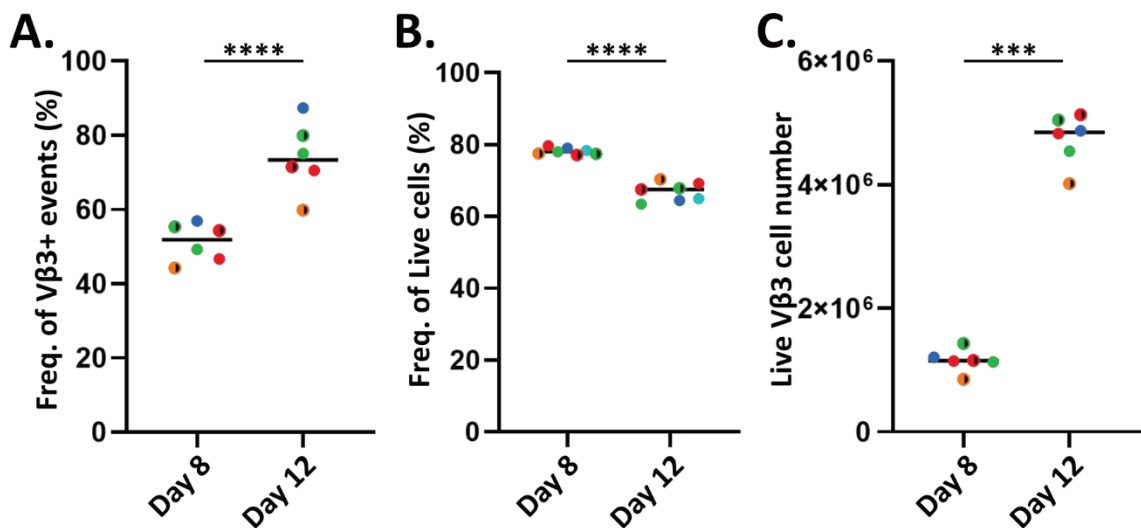


Figure 4.29. The number of live V β 3+ T cells increases throughout *in vitro* cell culture from 8 to 12 days after the transduction protocol began. The mean values from each transduced T cell population are evaluated as a single dataset to determine average frequencies and numbers of V β 3+ live cells. **(A)** The freq. of V β 3+ CD8 T cells identified by flow cytometry via gating strategies like those in Fig. 4.16 and 4.17. **(B)** The number of live cells identified by automated fluorescent cell counting. **(C)** The calculated number of live V β 3 cells. n=3 per transduced T cell population of which there are 6. Mean of means shown. Statistical Test: Paired, two-tailed t-test. ***p<0.0005, ****p<0.0001.

These cells were cryopreserved until mice could have B16.F10 cells subcutaneously administered (Fig. 4.2B), after which the remaining T cells expressing TRP2 (by V β 3 expression) and either murine WT or Δ P L-selectin were pooled 1:1 and administered intravenously to B16.F10 tumour-bearing mice. In this pilot study, I sought to gain insight into the number of T cells required for tumour control during future *in vivo* studies. In the study by Watson et al, the B16.F10-expressed NP68 peptide was injected subcutaneously into tumour-bearing mice, which were then treated with 5×10^5 F5 TCR-expressing T cells administered by tail-vein injection (Fig. 4.1). Our collaborators who gave us the TRP2 TCR constructs had previously trialled 2×10^6 TRP2-transduced T cells, and so I tested T cell doses within this range: PBS (control), 0.2×10^6 , 1×10^6 and 2×10^6 .

All mice showed steady weight loss between day 6 and day 22, which did not exceed 20% of their starting weight. After day 22, all mice steadily gained weight and appeared healthy (Fig. 4.30A). Transfers of TRP2 T-cells had no effect on tumour growth (Fig. 4.30B, C). Although 1×10^6 TRP2 positive cells appeared to control tumour growth relative to the PBS control, the study was underpowered by the endpoint, so normality tests could not be performed (Fig. 4.30B). Further, 2×10^6 T cells did not control tumour growth, so the lower growth rate observed in the 1×10^6 group was likely due to variance and the low power of this study (Fig. 4.30C).

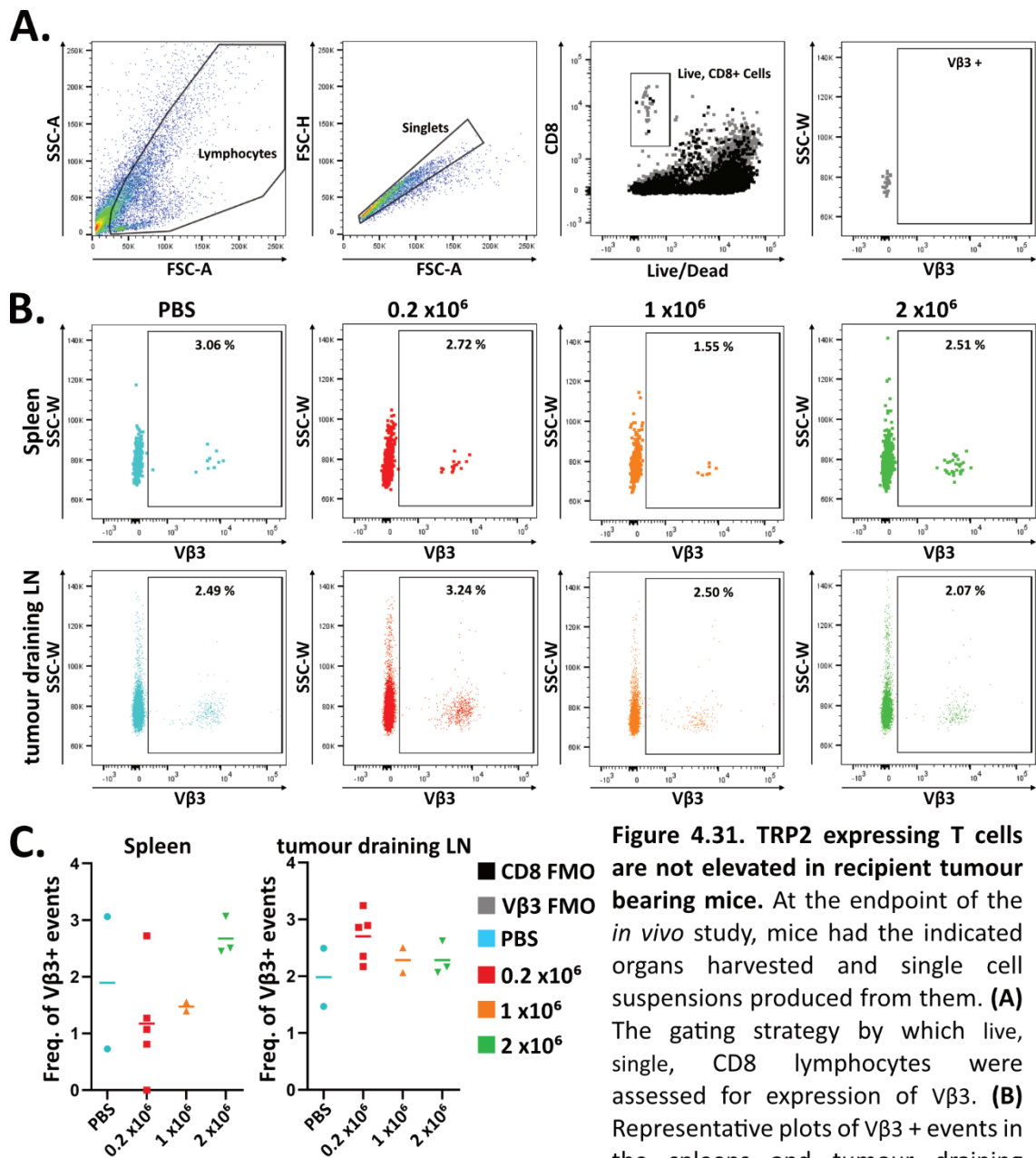


Figure 4.31. TRP2 expressing T cells are not elevated in recipient tumour bearing mice. At the endpoint of the *in vivo* study, mice had the indicated organs harvested and single cell suspensions produced from them. **(A)** The gating strategy by which live, single, CD8 lymphocytes were assessed for expression of Vβ3. **(B)** Representative plots of Vβ3+ events in the spleens and tumour draining lymph nodes of tumour bearing mice who received various doses of TRP2 expressing T cells and **(C)** the quantified freq. of Vβ3 events.

At the end of the study, the tumour, tumour-draining inguinal lymph node (tdLN) and spleen were harvested and analysed for live, Vβ3 positive CD8 positive events by flow cytometry to determine whether the lack of tumour control by TRP2 T cells was due to improper engraftment or homing (Fig. 4.31A). I reasoned the levels of Vβ3 positive CD8 T cells should be higher in mice receiving adoptive cell transfer.

CD8 positive cells were not detected in the tumours, irrespective of V β 3 expression, which would explain the lack of tumour control (data not shown). However, V β 3 CD8 double positive events were found in the spleen and the tdLN (Fig. 4.31B, C). In the spleen, between 1.2 – 2.7 % of the CD8 compartment was V β 3 positive, and there appeared to be a dose-dependent effect, although this was not significant. Similarly, in the tdLN, mice that received TRP2-expressing T cells appeared to have slightly elevated levels of V β 3 CD8 double positive events compared to PBS control (Fig. 4.31C). However, due to the low power of the study and variance in the data, no conclusions could be drawn.

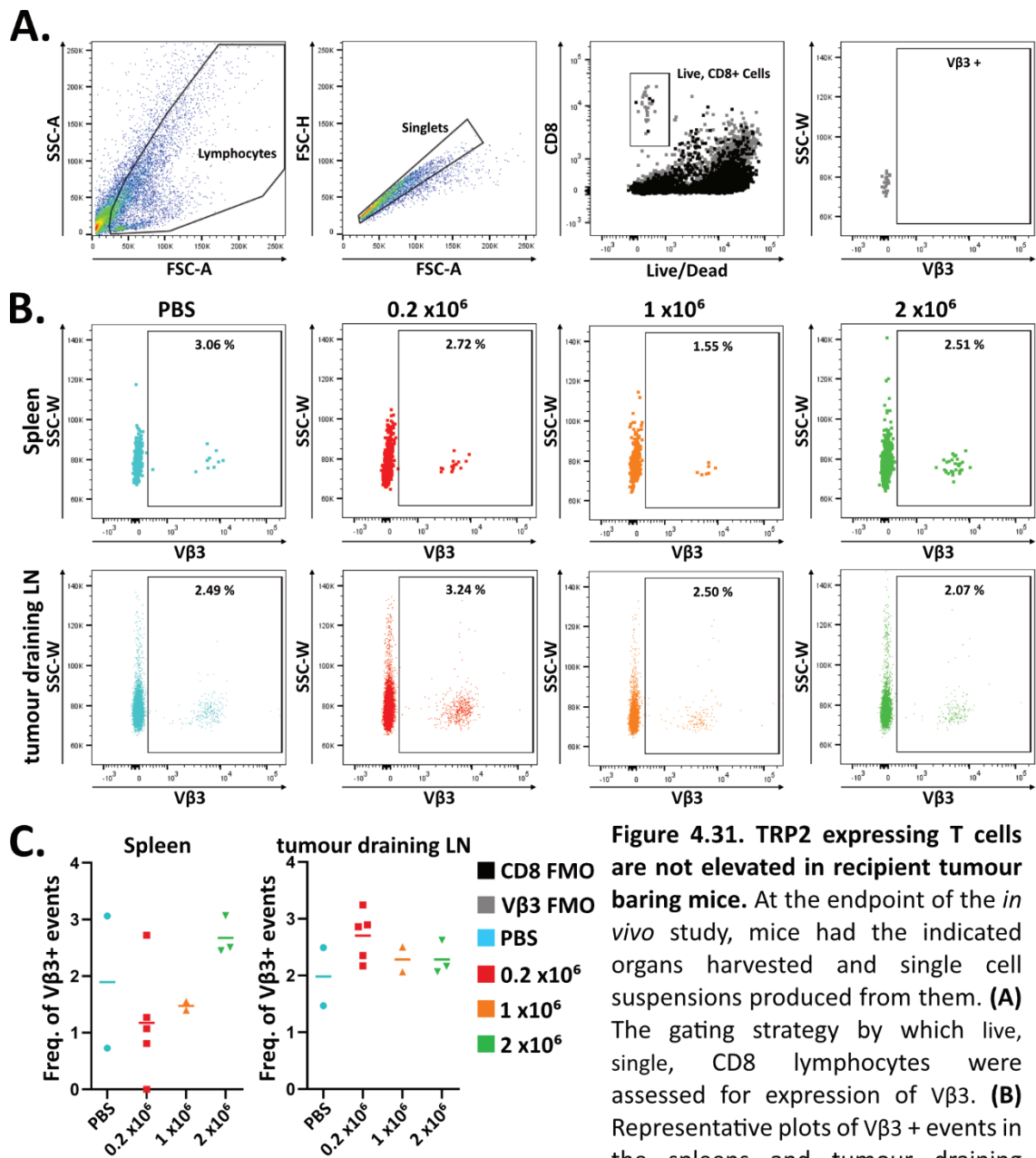


Figure 4.31. TRP2 expressing T cells are not elevated in recipient tumour bearing mice. At the endpoint of the *in vivo* study, mice had the indicated organs harvested and single cell suspensions produced from them. **(A)** The gating strategy by which live, single, CD8 lymphocytes were assessed for expression of Vβ3. **(B)** Representative plots of Vβ3+ events in the spleens and tumour draining lymph nodes of tumour bearing mice who received various doses of TRP2 expressing T cells and **(C)** the quantified freq. of Vβ3 events.

4.3.0 Discussion

In this chapter, I first generated murine cancer-specific T cells expressing variants of L-selectin. The purpose of this work was to evaluate whether L-selectin variants conferred phenotypic changes to T cells *in vitro* and *in vivo* that could be beneficial for the control of tumour growth in a clinically relevant model.

I was able to demonstrate that polyclonal CD8 T cells lacking L-selectin could be extracted, purified, and activated in 96-well and 24-well experiments, as well as transduced to express GFP. During the preliminary GFP transductions, it became clear that not all viruses are created equal and that high transgene expression is dependent on several factors. Although I never intended to seek out these factors, one particular vector expressing eGFP via an SFFV promoter gave at least a one-log shift in transgene expression by flow cytometry. Conversely, the other vectors only gave weak expression of GFP variants despite similar transduction efficiencies. The SFFV promoter has previously been used in a lentivirus to transduce CD4 positive T cell hybridomas to express GFP in a direct comparison with the CMV promoter. The SFFV promoter containing virus gave a frequency of 54 % positive events, and the CMV promoter could not induce expression (Gilham et al. 2010).

Having demonstrated that I could transduce primary murine T cells, I moved on to expressing molecules able to confer cancer specificity. Our collaborators in Cologne provided us with a human CEA-specific murine CAR construct under the control of a CMV promoter. In accordance with Gilham et al, and with GFP expression in a construct driven by the CMV promoter, the CMV-driven CEA-CAR transduction gave only weak expression. This persisted despite multiple methods of virus production and transduction being attempted to boost titres and increase the MOI, respectively. Of note, in our collaborator's published work using this construct, the CEA-CAR T cells were derived from transgenic mice (Chmielewski et al. 2012) rather than *ex vivo* production, as attempted here.

While conducting the above experiments, I performed molecular cloning to insert various L-selectin constructs into retroviral vectors, which use their LTR regions as promoter and enhancer elements to drive efficient transgene expression (Halene et al. 1999).

The human constructs were initially inserted into a readily available vector based on the Moloney murine leukaemia virus (MMLV). After making these vectors and transducing T cells, human L-selectin levels were low, with a transduction efficiency of approximately 30 %. Subsequently, I came across another retroviral vector based on murine stem cell virus (pMSGV1), which delivered high expression of murine melanoma-reactive pmel-1 and TRP-1 to murine T cells at efficiencies of 63 and 81 %, respectively (Kerkar et al. 2011). Additionally, it had also been used to deliver an anti-murine CD19 CAR to murine CD8 T cells at efficiencies of 57 % (Kochenderfer et al., 2010). Therefore, when making the murine L-selectin constructs, I used this vector. Using pMSGV1, transduction efficiency was still approximately 30 %, but the transgene expression was much higher than when delivered using MMLV vectors. However, due to human and murine L-selectin expression being delivered by two different vectors in T cells (MMLV and pMSGV1, respectively), I could not determine if this increased amount of expression was due to the vector or human proteins being poorly expressed in murine T cells. Therefore, I began preparing the reagents to clone and insert human L-selectin into pMSGV1 for direct comparison, after which I would modify these vectors to insert a molecule capable of conferring cancer specificity to T cells.

Fortunately, I was able to foster a collaboration with Claire Bennett's group in UCL to obtain a molecule able to confer cancer specificity. This was a TCR recognising TRP2 in B16.F10, which was provided in a third retroviral vector. Throughout this work, the TRP2 TCR is referred to as TRP2. This vector is based on an improved myeloproliferative sarcoma virus (pMP71), which expresses GFP in murine lymphocytes at 10-fold higher levels than MMLV vectors (Engels et al. 2004). During a preliminary test, transduction yielded 62.3 % TRP2 positive murine T cells (by V β 3 beta chain detection), which after subtracting the endogenous V β 3 staining (mock condition), meant a transduction efficiency of 57 %. This was the best efficiency yet seen, and positive events expressed the protein highly. Further, I was able to enrich these positive cells via MACS for theoretical downstream use, and so this became my new candidate vector.

To retain the ability to enrich successfully transduced T cells, I designed vectors which were quadcistronic for TRP2 (α and β chains), tICD19 and each of the L-selectin variants. However, although the transduced T cells expressed the TCR and L-selectin variants, tICD19 could not be detected at the cell surface. Further, in western blots of these cells, the intensity of the tICD19 band was comparable in T cells transduced with the original TRP2 vector and those also encoding variants of L-selectin. This indicated that the protein was being expressed but was not detectable at the cell surface. One hypothesis to address this was that the 2A sequence was not mediating cleavage and that a fusion product of tICD19 and L-selectin was generated. The bands were all of comparable weight by western blotting, so this did not explain the lack of expression. Instead, it is possible the retained 2A tail added to CD19 prevents protein transport to the cell surface. Additionally, the addition of L-selectin to these vectors caused a reduction in TRP2 expression. I hypothesised this was due to the transgenes now approaching the viruses' packaging limit (Kumar et al. 2001). Therefore, I made tricistronic constructs that replaced tICD19 with each L-selectin variant. In these experiments, V β 3 detection returned to the levels of the original vector, indicating that it was the packaging limit that lowered transduction efficiency. Importantly, these vectors also expressed L-selectin variants, although detection of I Δ W L-selectin was not significantly elevated initially.

Characterisation using PMA to induce ADAM17-dependent ectodomain shedding took place 1 day after (day 9) the initial assessment of transduction efficiencies (day 8). Interestingly, after an additional day in culture, L-selectin variants susceptible to ectodomain proteolysis appeared to have a greater number of L-selectin positive events. In murine T cells, both species of transgenic WT L-selectin underwent ectodomain shedding as reported previously (Galkina et al. 2003; Mohammed et al. 2019). Additionally, both mL Δ P and h Δ MN L-selectin resisted ectodomain proteolysis and retained high levels of surface L-selectin. Expression of hI Δ W mutant ectodomain was downregulated to a greater extent than hWT L-selectin, in agreement with findings in human Molt3 T cells (Chapter 3). In addition, tracking the

proteolysed tail of L-selectin by western blotting also mirrored the findings with Molt3 T cells. Following PMA activation, a band of comparable weight to the MRF in Molt3 T cells (Chapter 3) increased in h Δ W L-selectin expressing T cells, indicating an accumulation of a MRF. However, the level of background binding by the antibody against the tail of L-selectin in these western bands was high, and non-specific or unknown bands were seen. To confirm that these bands were non-specific, mock-transduced (L-selectin KO) T cells and h Δ MN L-selectin expressing murine T cells should be run as negative controls alongside PMA- or vehicle control-treated hWT and h Δ W L-selectin expressing cells.

On the same day that transduction efficiency was assessed (Day 8; Fig. 4.2A), transduced T cells expressing TRP2 alongside each L-selectin variant were added to target cells. These transduced T cells killed target cells *in vitro* at effector-to-target ratios of 1:1 and 2:1, regardless of the expressed L-selectin variant. In 2D culture then, L-selectin expression does not impact the ability of T cells to kill target cells, at least at these time points. Some killing was mediated by mock-transduced cells, but this was significantly lower (approximately 70 %) than T cells expressing TRP2.

In a parallel assay, transduced T cells were assessed for several markers by flow cytometry on each day of killing. In TRP2-expressing T cells, all but those cells expressing h Δ W L-selectin had a transient downregulation of TRP2, which was a result of T cell antigen engagement (Lauritsen et al. 1998). However, as TRP2 h Δ W L-selectin expressing T cells were able to mediate T cell killing, the absence of TRP2 downregulation was likely due to variance in the data and lack of statistical power, as an insignificant decrease in TRP2 positive events was still observed at 24 hr. In all TRP2-expressing constructs, expression of PD-1 increased over time relative to mock controls, indicating specific TCR-mediated activation. Importantly, if proteolysis-resistant forms of L-selectin do exhibit improved tumour control *in vivo* in this more clinically relevant model, it is again likely to synergise with PD-1 blockade (Watson et al. 2019). Of interest, T cells expressing TRP2 m Δ P L-selectin did not exhibit an

increased frequency of PD-1 positive events between 24 and 48 hr. As a result, they had less PD-1 positive events than T cells without L-selectin or with mWT L-selectin. Similar trends were observed for T cells expressing TRP2 and h Δ MN or h Δ W L-selectin, but the variance of the data made it difficult to draw conclusions. However, if cleavage-resistant forms of L-selectin can limit T cell exhaustion *in vitro*, this is an exciting prospect that should be investigated over a longer time course at a higher statistical power.

Prior to addition of T cells to target cells, the expression of WT L-selectin increased the frequency of T cells expressing CD25 relative to T cells transduced to express just TRP2. Further, T cells transduced with m Δ P L-selectin had a significantly higher number of CD25 expressing T cells than those transduced with mWT L-selectin or TRP2-tlCD19 alone. However, 24 hr after application to target cancer cells, the number of m Δ -selectin T cells saw a reduction in frequency of T cells expressing CD25. This resulted in no differences between any TRP2 expressing conditions 24 h after addition to target cells. Previously, we showed that CD25 expression is delayed in virus-specific CD8 positive T cells expressing m Δ P L-selectin following activation *in vitro* and *in vivo* (Mohammed et al. 2019). I hypothesise that the increased number of CD25 positive events in transduced T cells expressing TRP2 and m Δ P L-selectin (before addition to target cells) is due to delayed up- and then down-regulation of CD25 following the anti-CD3/CD28 stimulation necessary for T cell transduction. To address this in a future transduction experiment, CD25 levels should be tracked by flow cytometry on each day of the transduction protocol.

Unlike other transduced T cells, those transduced with h Δ W L-selectin exhibited a delayed appearance of a Ki67-lo population, which did not become a Ki67-hi population by 48 hr. We have previously demonstrated that m Δ P L-selectin causes *in vitro*-activated T cells to have a lower amount of Ki67-lo cells due to their high expression of Ki67 (Watson et al, 2019). The differential level of Ki67 expression in T cells which express h Δ W L-selectin variants further links L-selectin and Ki67,

although no effect of m Δ P L-selectin was observed. If what I hypothesised in Chapter 3 is true, and I Δ W L-selectin is more readily proteolysed by ADAM17 rather than resists γ -secretase mediated cleavage, then it might be expected to have an opposing phenotype to m Δ P and h Δ MN L-selectin. Of the human L-selectin expressing T cells, only T cells bearing h Δ MN L-selectin increase the number of Ki67-hi cells between 24 and 48 hr, which lends credit to the idea that these mutants have opposing phenotypes. It is important to note that even the mock-transduced cells displayed elevated levels of Ki67 expression over time, moving from the Ki67-negative to the Ki67-lo and then the Ki67-hi gates. This indicates that anti-CD3/CD28 was still inducing proliferation. In a future transduction, Ki67 should be monitored throughout the protocol alongside CD25. This experiment would seek to determine the kinetics of these markers following stimulation with anti-CD3/CD28 during transduction, so the effects of target cell recognition can be delineated.

Finally, all T cells expressing TRP2 and a variant of L-selectin exhibited increased frequencies of L-selectin positive events during the killing assay. Thus, no shedding was seen to be induced by exposure to target cells. I hypothesise that this unexpected observation is due to viral transgene expression not having reached maximal protein levels at the cell surface when the cytotoxicity assay was conducted. Therefore, without a potent ADAM17 activator like PMA, TCR-mediated L-selectin downregulation was smaller than the increased expression of virally encoded L-selectin at the cell surface. Support for this comes from the increased frequency of V β 3 positive events 4 days after the initial transduction assessment. This assessment showed that the number of live, positive cells increases by 23 % despite the lower frequency of live cells. I hypothesise, if killing assays had been performed when surface expression of L-selectin had reached maximal levels, TCR-mediated shedding would have been observed. Further, conducting these assays at a later time point may reveal L-selectin variant-mediated differences in the kinetics of tumour cell killing and multiparameter flow cytometry-defined phenotypes. Alternatively, the same exact protocol could be carried out, but the supernatant collected, and ELISA performed for the soluble L-selectin ectodomain, which could demonstrate TCR-

mediated activation and L-selectin shedding, despite elevated transgene surface expression. Alternatively, T cell activation could induce an increase in LTR driven gene expression (Swaims et al. 2010).

Following the second assessment of transgene levels on day 12 since the beginning of the transduction protocol, TRP2 L-selectin expressing T cells were cryopreserved. These were then used in a preliminary *in vivo* study to determine the number of TRP2-expressing T cells needed to mediate tumour control. This number of T cells could then be used in a study evaluating the impact of L-selectin variants on cancer-specific T cell mediated tumour control. Prior to the use of cryopreserved T cells *in vivo*, T cells were cultured for 3 days, transgene levels reassessed to determine the total number of T cells to administer intravenously, and their ability to mediate *in vitro* killing confirmed (data not shown). Unfortunately, no control of tumour growth was seen at any doses tested. For this study, I used a 1:1 mixture of WT or Δ P L-selectin expressing TRP2 T cells. This mixing was pragmatic and done to use the remaining T cells productively. However, despite the presence of Δ P L-selectin, the curves were comparable to those generated by our collaborators using TRP2 cells, which also failed to mediate control of tumour growth alone (Alsaieedi et al. 2018). Following extraction and isolation of the tumours, I sought to determine the number of infiltrating CD8 T cells and whether TRP2-expressing cells were present. However, no CD8 T cells had infiltrated the tumour. Further, the number of V β 3 positive events in the spleen and the tDLN appeared to be only marginally elevated, if at all.

In future experiments, several approaches could be taken to improve engraftment. For example, exogenous IL-2 and a viral vaccination of tumour bearing mice has previously been demonstrated as necessary for control of tumour growth by L-selectin positive T cells (Gattinoni et al. 2005). Another approach could be to administer a greater number of T cells, as in solid tumour therapy of competent mice bearing pancreatic tumours, 1×10^7 CAR-T cells were administered (Chmielewski and Abken 2017). Alternatively, as subcutaneous B16.F10 melanoma is easily accessible,

and we have previously shown that the benefits of L Δ P L-selectin are independent of tumour homing (Watson et al. 2019), the same number of T cells could be administered intratumorally as is currently being done in human trials for head and neck cancer (Larcombe-Young et al. 2020).

5.0.0. General discussion

In this thesis, I have demonstrated that the tail of L-selectin is lost from the cell membrane following T cell stimulation and sequential proteolysis before being degraded. Only ectodomain proteolysis-resistant mutants of L-selectin retain the tail of L-selectin at the cell surface following T cell stimulation. Therefore, it is likely that the retention of the L-selectin tail at the membrane during T cell activation, and consequent intracellular protein interactions, are responsible for the observed phenotypes of cancer-specific T cells bearing cleavage-resistant forms of L-selectin.

5.1.0. Determining the sub-cellular distribution of the tail of L-selectin following γ -secretase proteolysis

L-selectin undergoes ectodomain proteolysis by ADAM17 following *in vitro* and *in vivo* T cell activation (Mohammed et al., 2019). Here, I used the potent activator of ADAM17, PMA, to stimulate T cells and induce sequential proteolysis of L-selectin by ADAM17 and γ -secretase (Lorenzen et al. 2016). I demonstrated that 15 % of WT L-selectin expressing T cells shed enough of the ectodomain of L-selectin to become L-selectin negative following PMA treatment. The tail of L-selectin can interact with several proteins: PKC (Kilian et al. 2004), Lck (Xu et al. 2008), Grb-SOS (Brenner et al. 1996), ezrin, moesin (Ivetic et al. 2002) and calmodulin (Matala et al. 2001). The membrane proteins NOTCH and amyloid precursor protein (APP) also have intracellular domains released by γ -secretase proteolysis, and these migrate to the nucleus to regulate transcription (Schroeter et al. 1998; Kimberly et al. 2001).

Therefore, I sought to determine the spatiotemporal location of the proteolysed cytoplasmic tail of L-selectin following PMA treatment and whether it was involved in the signalling of activated T cells. I used imaging flow cytometry, in combination with a novel, quantitative, method of determining the membrane region, to demonstrate loss of the tail of L-selectin from the membrane of T cells following PMA stimulation. Live cell experiments with a GFP-tagged variant of L-selectin revealed that the tail of L-selectin is degraded following PMA-induced proteolysis. The use of several inhibitors demonstrated lysosome/autophagosome dependent degradation of the V5/His-tagged membrane-retained fragment (MRF) of L-selectin

during homeostatic ADAM17-independent shedding (Mohammed et al., 2019). The proteasome was implicated in the degradation of the MRF of L-selectin following PMA-induced ADAM17-dependent shedding of L-selectin. I was unable to identify inhibitors that could stabilise the γ -secretase released tail of L-selectin. My findings are summarised in Fig. 5.1.

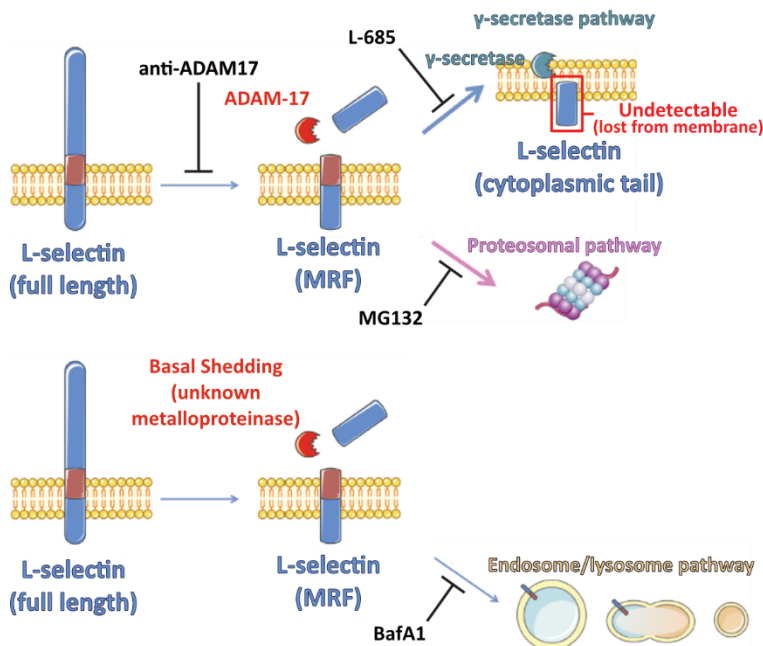


Figure 5.1. The proposed pathways involved in proteolysis or degradation of WT L-selectin. A schematic representation of the proposed L-selectin proteolysis and degradation pathways. L-selectin ectodomain shedding by ADAM-17 produces a MRF. This can be prevented using an anti-ADAM17 antibody. The MRF is either further proteolysed by γ -secretase. This can be prevented using L-685 which stabilises the MRF. The released tail is

undetectable. The MRF is also degraded via the proteasome which can be abrogated by MG132 which stabilises the MRF similarly to L-685. Basal ectodomain proteolysis of L-selectin produces a MRF which is stabilised by BafA1 and therefore degraded via the endosome/lysosome pathway.

Previous experiments by Andrew Newman in the Ager and Knäuper laboratories showed that TCR engagement induces sequential proteolysis of L-selectin by ADAM-17 and γ -secretase. Here, using conventional flow cytometry, western blotting and specific inhibitors, I showed that sequential proteolysis can be induced using PMA. However, both modes of activation were unable to induce detectable amounts of the released cytoplasmic tail of L-selectin assessed by western blotting following γ -secretase proteolysis.

Imaging flow cytometry analysis showed PMA induced a loss of L-selectin tail-associated fluorescence from the cell membrane. Loss of the L-selectin tail-associated fluorescence could have been due to improper fixation of cells prior to

permeabilisation and antibody staining. This possibility was addressed by Heinen et al, who found that 2% fresh formaldehyde was sufficient for preservation of cytosolic and nuclear proteins for detection by flow cytometry (Heinen et al. 2014). Although I used the same fixative and a permeabilising agent designed to detect nuclear proteins, I addressed this possibility by performing imaging flow cytometry with live, fixed, and fixed and permeabilised Molt3 T cells expressing a GFP-tagged tail variant of WT L-selectin (Rzeniewicz et al. 2015). ADAM17-dependent shedding of L-selectin still occurred, and a loss of fluorescence intensity associated with the tail of L-selectin regardless of whether the cells were live, fixed, or fixed then permeabilised was detectable. PMA reduced membrane localisation of the GFP-tagged tail of L-selectin, as found for V5/His-tagged L-selectin, indicating degradation of the released tail.

The γ -secretase product of L-selectin may be degraded by the proteasome as shown for other proteins undergoing sequential proteolysis by ADAMs and γ -secretase (Kisselev and Goldberg 2001; Oberg et al. 2001). Alternatively, the L-selectin MRF could be internalised and degraded via the lysosome/autophagosome pathway as shown for Met, a receptor tyrosine kinase (Ancot et al., 2012). Moreover, Evrard et al demonstrated APP can have several fates depending on which protein mediated ectodomain proteolysis to generate the MRF (Evrard et al. 2018). I used several inhibitors and found an increase in the stability of the MRF following PMA-induced activation when the cells were treated with the proteasome inhibitor MG132 (Mroczkiewicz et al., 2010). Interestingly, BafA1 stabilised the MRF in the absence of PMA-induced shedding and no additional effect upon PMA treatment was observed, indicating that autophagosome/lysosomal degradation of the MRF may be involved in homeostatic turnover of L-selectin, which is independent of ADAM17 (Mohammed et al., 2019). The finding that MG132 stabilised the MRF following PMA treatment suggests that the proteasomal degradation pathway relies on ectodomain proteolysis of L-selectin by ADAM-17. Stabilisation of the MRF could be detected by western blotting, but the imaging flow cytometry data were inconclusive. This was likely due to only 15 % of L-selectin positive T cells fully shedding L-selectin, and the inability of imaging flow cytometry to distinguish full-length L-selectin from the MRF

in the membrane. Western blotting was able to distinguish these by size. Therefore, western blotting was more sensitive for detection of L-selectin's MRF when no subcellular redistribution occurs. To confirm that degradation of the L-selectin MRF following ADAM-17 ectodomain proteolysis occurs via the proteasome, the tail of L-selectin could be immunoprecipitated and probed for ubiquitin, as used for other proteins, such as NOTCH (Oberg et al. 2001).

Therefore, L-selectin proteolysis by ADAM-17 produces the MRF which may be either directly degraded by the proteasome or further proteolysed by γ -secretase, which is then degraded. However, the γ -secretase product was not stabilised by any tested inhibitors, and the mechanism by which the released tail of L-selectin is degraded is unknown. Further, imaging could not detect the γ -secretase-released tail of L-selectin, so its spatiotemporal location prior to degradation could not be determined. As only 15 % of events fully shed the ectodomain of L-selectin, the abundance of the γ -secretase-released tail in the intracellular compartment may limit detection. Previous attempts to detect the γ -secretase product of APP by imaging have required its direct expression to bypass the need for proteolysis, and co-expression of a stabilising partner (Kimberly et al. 2001). Similarly, another study evaluating nuclear localisation signal peptides directly tagged them with GFP and delivered them to cells via 'nano-capsules'. Similar approaches could be taken with the 17-amino-acid tail of L-selectin (Ray et al. 2015).

5.2.0. Fate of the cytoplasmic tail of L-selectin for human variants

In this thesis, I compared WT, Δ MN and I Δ W L-selectin following ADAM-17 and γ -secretase proteolysis in human Molt3 T cells. The Δ MN and I Δ W mutants of L-selectin were described in Chapter 3. Briefly, Δ MN L-selectin has been demonstrated to resist PMA- or TCR-induced ectodomain proteolysis (Chen et al., 1995; Mohammed et al., 2019). The I Δ W L-selectin variant was developed by the Ager and Knäuper labs in collaboration with Pierre Rizkallah (Cardiff University) and was predicted not to be recognised by γ -secretase and undergo consequent secondary proteolysis.

As discussed in 5.1.0, WT L-selectin underwent sequential proteolysis following treatment with PMA, and the tail of L-selectin moved away from the membrane. As expected, the Δ MN L-selectin variant resisted PMA-induced ectodomain proteolysis, as determined by flow cytometry and western blotting (Chen et al., 1995; Mohammed et al., 2019). Unsurprisingly, the cleavage-resistant variant retained L-selectin tail-associated fluorescence at the membrane following PMA treatment, when assessed by imaging flow cytometry. Through conventional flow cytometry, I demonstrated that the level of PMA-induced ectodomain proteolysis of Δ W L-selectin from Molt3 T cells was greater than that of WT L-selectin, which had not been tested previously. Through western blotting, I demonstrated that PMA treatment of T cells did not cause an increase in the amount of WT L-selectin MRF, unless cells were pre-treated with a γ -secretase inhibitor. Conversely, PMA-induced shedding of Δ W L-selectin caused an increase in the amount of the MRF detected by western blotting, and the fold increase in detectable MRF was comparable to WT L-selectin if cells were treated with a γ -secretase inhibitor. Through comparison of WT and Δ W L-selectin by imaging flow cytometry, I again demonstrated that Δ W L-selectin exhibited a greater amount of ectodomain shedding following PMA treatment of T cells. However, Δ W L-selectin lost tail-associated fluorescence from the cell membrane to a similar extent as WT L-selectin.

Therefore, I hypothesise that rather than resist γ -secretase dependent cleavage, Δ W L-selectin is more prone to ectodomain proteolysis and degradation or γ -secretase proteolysis of the MRF is a rate-limiting step. This causes an accumulation of Δ W L-selectin MRF that is detectable by western blotting. In contrast, this cannot be detected by imaging flow cytometry due to an inability to distinguish between full-length L-selectin and its MRF in the membrane. Recently, CD53 (a tetraspannin) has been implicated in regulating the proteolytic activity of ADAM-17 on L-selectin ectodomain shedding, and perhaps the Δ W mutation interferes with this process, rather than abrogation of γ -secretase recognition of the L-selectin cleavage site (Demaria et al. 2020). The study by Demaria was conducted in murine T cells both sufficient and deficient for CD53. In my thesis, I was able to introduce human variants of L-selectin into murine T cells, and PMA-induced proteolysis still occurred,

so ΔW L-selectin could be introduced similarly into these cells to test whether the ΔW mutation interferes with CD53 regulation of ADAM-17 dependent proteolysis of L-selectin. However, evaluation of the MRF by western blotting in murine T cells is confounded by background signals, and I have proposed experiments to address this in the discussion of Chapter 4.

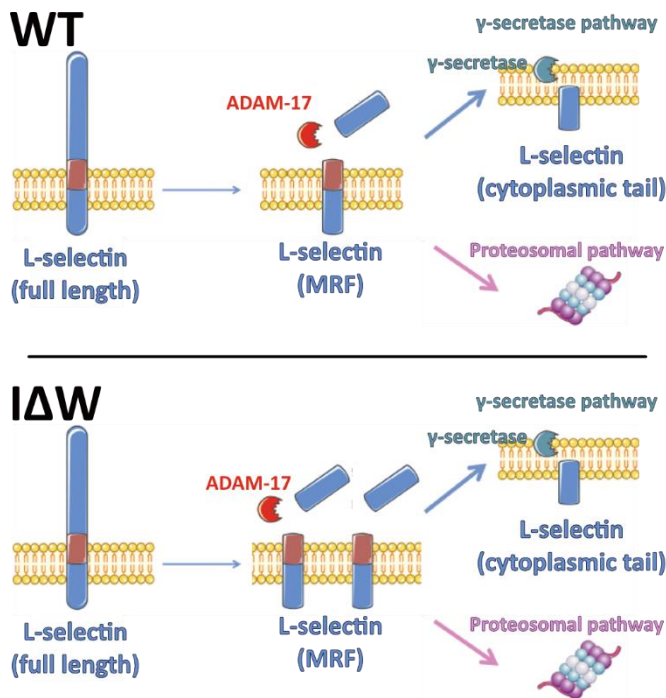


Figure 5.2. The proposed pathways involved in proteolysis or degradation of WT and ΔW L-selectin following T cell treatment with PMA. (WT) A schematic representation of the proposed L-selectin proteolysis and degradation pathways. L-selectin ectodomain shedding by ADAM-17 produces a MRF which is either further proteolysed by γ -secretase (and the released tail is undetectable) or degraded via the proteasome. (**ΔW**) The ΔW mutation causes this variant of L-selectin to be proteolysed to a greater extent than WT L-selectin and the MRF degraded similarly to WT L-selectin.

5.3.0. Impact of L-selectin variants on cancer-specific T cells *in vitro*

The imaging flow cytometry experiments showed that both the ectodomain and tail of ΔMN L-selectin remained at the membrane. The retention of the tail of ΔMN L-selectin at the membrane would enable altered interactions of the L-selectin tail after T cell activation with binding partners such as Moesin (Ivetic et al. 2002), PKC isozymes (Kilian et al. 2004), Grb2-SOS (Brenner et al. 2002), Lck (Xu et al. 2008). My live cell imaging flow cytometry demonstrates loss of the tail of WT L-selectin following PMA-induced activation. Additionally, ΔP L-selectin resisted ectodomain proteolysis like ΔMN L-selectin in murine T cells. Therefore, the continued association of cleavage-resistant forms of L-selectin (ΔMN in human and ΔP in mice) with their intracellular binding partners at the membrane may be what confers altered phenotypes to ΔP L-selectin bearing CD8 T cells in mouse models of cancer immunity (Watson et al. 2019).

Here, I was able to show several impacts of different L-selectin variants on cancer-specific T cells, following delivery of expression using a clinically relevant method. An overview of these impacts is shown in Table 5.1.

Murine variants	Human variants	
LΔP	ΔMN	IΔW
Cleavage-resistant L-selectin bearing T cells mediate target cell lysis as efficiently as WT L-selectin bearing cancer-specific T cells.	Cleavage-resistant L-selectin bearing T cells mediate target cell lysis as efficiently as WT L-selectin bearing cancer-specific T cells.	
3 days after transduction (prior to addition to wells containing target cells), the frequency of CD25 positive events was elevated above T cells solely transduced to express the cancer-specific TCR and T cells co-expressing WT L-selectin.		
No increased frequency of PD-1 positive T cells from 24 hr to 48 hr of T cell-mediated killing unlike cancer-specific T cells that were L-selectin null or co-expressed WT L-selectin. Significantly less PD-1-positive T cells at 48 hr relative to other cancer-specific T cells.	No increased frequency of PD-1 positive T cells from 24 hr to 48 hr of T cell-mediated killing unlike cancer-specific T cells that were L-selectin null or co-expressed WT L-selectin.	No increased frequency of PD-1 positive T cells from 24 hr to 48 hr of T cell-mediated killing unlike cancer-specific T cells that were L-selectin null or co-expressed WT L-selectin.
		Lower expression of Ki67 3 days following transduction and delayed expression of Ki67 during target cell killing relative to all other conditions, including mock-transduced T cells.

Table 5.1. The effects of L-selectin variant co-expression on cancer-specific T cells.
Findings recapped from Chapter 4.

The lack of L-selectin ectodomain proteolysis has been implicated in the degranulation of effector CD8 T cells and consequent target cell killing in 4-hour killing assays (Yang et al. 2011). However, ΔMN and LΔP L-selectin bearing T cells

mediated target cell killing equally as efficiently as L-selectin null, WT or IΔW L-selectin bearing T cells *in vitro* up to the 48 hr time point (Table 5.1).

In addition, lack of ectodomain proteolysis delays expression of the CD25 sub-unit of the high-affinity IL-2R, which consequently delays T cell proliferation (Mohammed et al., 2019). I observed that cleavage-resistant murine L-selectin (LΔP) variants had a significantly greater frequency of CD25 positive cells compared to cancer-specific T cells expressing WT L-selectin. In turn, cancer-specific T cells expressing WT L-selectin had a greater frequency of CD25 positive events than L-selectin null cancer-specific T cells (Table 5.1). This was not conserved during *in vitro* killing. T_{REGS} suppress TILs by sequestering IL-2 from CD8 effector T cells via their constant expression of the high-affinity IL-2 receptor (McNally et al. 2011). Therefore, increased expression of CD25 by LΔP L-selectin bearing T cells warrants further investigation. However, enhanced expression of CD25 may skew LΔP L-selectin T cell populations to short-lived effector cells following *in vivo* administration, negatively impacting long-term engraftment (Pipkin et al. 2010).

The efficacy of PD-1 blockade has been demonstrated in clinical trials to improve patient survival (Larkin et al. 2015), and several approaches to incorporate the effects of PD-1 blockade into CAR-T cell design have been attempted. Ankari et al co-expressed a PD-1/CD28 chimera that competes with PD-1 for ligands and provides CAR-T cells with co-stimulation rather than immunosuppression (Ankari et al. 2013). Another group generated CAR-T cells that secrete PD-1 blocking scFv fragments to provide immune checkpoint blockade within the tumour microenvironment (Li et al. 2017). Both pre-clinical studies demonstrated improved CAR-T function *in vitro* and efficacy *in vivo*. In this thesis, an effect observed over the course of T cell killing *in vitro* was the increase in expression of PD-1 by all cancer-specific T cells. However, this was limited for T cells bearing LΔP, ΔMN or IΔW L-selectin (Table 5.1). The effect of L-selectin expression on PD-1 upregulation should be investigated further because it represents a novel strategy to curb immunosuppression of administered engineered T cells in the tumour microenvironment.

Previously, during repeated *in vitro* stimulation, Ki67 expression was elevated on ΔP L-selectin bearing T cells relative to WT L-selectin or L-selectin null T cells on days 3, 7 and 17 (Watson et al. 2019). I did not observe any increases in Ki67-hi frequencies for cancer-specific T cells bearing ectodomain proteolysis-resistant variants of L-selectin after addition to target cells *in vitro* relative to other cancer-specific T cells. However, a significant and drastic effect on Ki67 expression was introduced to cancer-specific T cells by ΔW L-selectin (Table 5.1). This provides a further link between L-selectin proteolysis and cell proliferation, demarcated by the expression of Ki67. Indeed, Ki67 was recently found to exclude large cytosolic proteins from clustering chromosomes during anaphase (Cuylen-Haering et al. 2020).

The delivery of human L-selectin variants into murine T cells will enable the evaluation of clinically relevant human L-selectin modifications in syngeneic mouse models, but the impact of these mutants in human T cells *in vitro* and *in vivo* has not yet been determined.

5.4.0. *In vivo* evaluation of L-selectin variants in T cells

During the preliminary *in vivo* experiment, cancer-specific T cells could not control tumour growth. Further, no T cells could be detected by flow cytometry in the tumour on termination of the study. In addition, the frequency of $V\beta 3$ positive (cancer-specific) CD8 T cells was not significantly elevated in the spleen or tdLN relative to mice that received PBS.

It has been demonstrated previously that *in vitro*-activated T cells cultured in high concentrations of IL-2 upregulate proteins associated with effector function (gzm B and perforin) and mediate target cell lysis (Pipkin et al. 2010). Indeed, my cancer-specific T cells killed tumour cells *in vitro*. Pipkin et al were able to transfer virus-specific T cells cultured in high concentrations of IL-2 into mice and demonstrate specific T cell proliferation 35 days later in response to viral challenge (Pipkin et al. 2010). This demonstrates T cells cultured in high IL-2 can be engrafted *in vivo*. Early work by Kjaergaard and Shu indicated that L-selectin expression by cancer-specific T cells causes their accumulation in the lymph nodes (LN) of tumour-bearing mice and

prevents their accumulation in tumour sites (Kjaergaard and Shu 1999). However, as I saw no increase of adoptively transferred cancer-specific T cell frequency in the tdLN, my data more likely indicate a lack of T cell engraftment.

CD8 T cells from pmel-TCR and TRP2-TCR mice possess TCRs that recognise the gp100 and TRP-2 antigens expressed by B16.F10 melanoma cells, respectively. T cells from pmel mice have been used in adoptive cell therapy transfer models to evaluate the role of L-selectin. Adoptive transfer of *in vitro*-activated splenocytes into tumour-bearing mice induced tumour regression irrespective of L-selectin expression (Díaz-Montero et al. 2013). However, a greater number of T cells was administered by Díaz-Montero et al (5×10^6) than in my preliminary *in vivo* study (up to 2×10^6). Additionally, CD8 T cells were not isolated, and T cells were cultured in IL-12 rather than IL-2 as done in this body of work. Conversely, in studies where pmel splenocytes were cultured in IL-2 before adoptive transfer into tumour-bearing mice, 1×10^6 T cells mediated tumour control (Gattinoni et al. 2005; Klebanoff et al. 2005). However, in these studies, mice were also administered exogenous IL-2 and a viral vaccine encoding gp100. Both Gattinoni et al and Klebanoff et al demonstrated a dependence on $\beta 2m$ sufficiency in tumour-bearing mice and therefore MHC I and CD8 T cell interactions with APCs in mice was necessary for tumour control (Gattinoni et al. 2005; Klebanoff et al. 2005). Additionally, Gattinoni et al demonstrated that L-selectin sufficient T cells, in contrast to L-selectin deficient T cells, eradicated tumours (Gattinoni et al. 2005). This indicates that despite being capable of inducing target cell cytolysis *in vitro*, T cell activation by APCs is required for effector T cell control of tumours *in vivo*, and L-selectin is required for *in vivo* T cell activation.

In future experiments, either infusion of a greater number of cancer-specific T cells should be administered following culture in IL-12, or exogenous IL-2 and a TRP2 vaccine administered to induce tumour control following T cell priming *in vivo* at the draining LN. Importantly, a viral vaccine delivering expression of the TRP-2 epitope for use with adoptively transferred T cells expressing the TRP-2 T cell receptor has been generated and shown to be effective (Chinnasamy et al. 2013), although this is

not commercially available. Alternatively, the TRP2-TCR peptide has been elucidated as TRP₁₈₀₋₁₈₈ (VYDFFVWL), which can be administered alongside incomplete Freund's adjuvant (IFA), as done with NP68 in previous studies by members of our laboratory (Bloom et al. 1997; Watson et al. 2019).

No T cells could be identified in the tumour following disaggregation, and in a previous study by members of the Ager lab, the benefits conferred to T cells by ΔP L-selectin did not include enhanced tumour homing at the beginning of the therapy (Watson et al. 2019). Considering the altered *in vitro* phenotypes independent of homing, others (Mohammed et al., 2019; Watson et al., 2019; Yang et al., 2011) and now myself have observed, intratumoural delivery of cancer-specific T cells may represent an alternate strategy to evaluate whether cleavage-resistant forms of L-selectin confer a benefit to cancer-specific T cells *in vivo*. Additionally, this method of delivery is currently being trialled in humans, and so is clinically relevant (Larcombe-Young et al. 2020).

5.5.0. Conclusion

ADAM17-dependent proteolysis of L-selectin can be detected via imaging flow cytometry and western blotting, and the MRF or released tail of L-selectin is degraded either directly via the proteasome or following γ -secretase proteolysis. Using specific inhibitors, both pathways were implicated, although detection of the γ -secretase proteolysis product of the L-selectin MRF remains elusive.

Delivery of L-selectin variants to murine T cells in a clinically relevant manner for evaluation in syngeneic models has been achieved. Cleavage-resistant forms of L-selectin alter the phenotype of cancer-specific T cells *in vitro*, and while the consequences of this are undetermined, it warrants further investigation. The tail of L-selectin is rapidly degraded, and so altered phenotypes of cancer-specific T cells bearing cleavage-resistant variants of L-selectin are due to the retention of L-selectin at the cell membrane following T cell receptor stimulation and subsequent protein-protein interactions.

Due to the lack of engraftment of cancer-specific T cells in my preliminary *in vivo* experiments, I cannot draw conclusions as to whether L-selectin proteolysis is beneficial or detrimental to cancer immunity in adoptive cell transfer pre-clinical murine models.

5.6.0. Future work

5.6.1. Experiments not conducted due to the COVID-19 laboratory shut-down

A kinetic study of L-selectin, CD25, Ki67 and PD-1 expression by cancer-specific T cells throughout transduction and *in vitro* killing assays

As discussed, the modified L-selectin mutants delivered to T cells alongside a cancer-specific TCR altered the expression of CD25, Ki67 and PD-1. However, CD25 was altered in murine L-selectin expressing T cells prior to the addition of target cells. Additionally, Ki67 expression increased in mock-transduced cells throughout killing becoming a Ki67-hi population by 48 hrs. Together, these data indicate that the process of transduction, which includes anti-CD3/CD28 treatment, is still mediating an effect on transduced T cells. Additionally, the frequency of L-selectin positive events were increasing during the killing assay. Therefore, these markers should be evaluated throughout transduction, and only once expression is stabilised should cells be cryogenically stored and then used for further *in vitro* and *in vivo* evaluation.

During the killing assay, all T cells except cancer-specific T cells bearing ΔW L-selectin upregulated Ki67. Between 24 and 48 hours of the killing assay, cancer-specific T cells either L-selectin null or transduced to express WT L-selectin had an elevated frequency of PD-1 positive events. At 48 hours, cancer-specific T cells transduced to express ΔP L-selectin had significantly fewer PD-1 positive events. Killing should be assessed via the xCELLigence assay across either a 3-day period or following repeated exposure to target cells and expansion alongside flow cytometric analysis of L-selectin, PD-1 and Ki67 expression. This study would have been performed at a greater power to ensure the observed phenotypes were not due to data variance.

Evaluating modifications to the *in vivo* tumour model to induce tumour control by adoptively transduced T cells

As stated in the COVID19 impact statement, L-selectin KO mice were ready for a follow-up *in vivo* experiment at the onset of the laboratory shutdown. If laboratory access were enabled, I would have generated another batch of cancer-specific murine CD8 T cells during the above kinetic study. Due to the greater statistical power conducted in the kinetic study, a greater number of cancer-specific T cells would have been generated and the excess cryopreserved, to enable a detailed *in vivo* study of L-selectin variants in cancer-specific T cells.

Cryogenically preserved LΔP L-selectin expressing T cells would be adoptively transferred to tumour-bearing mice under the conditions listed in Table 5.2 to determine which mode of delivery would exhibit control of tumour growth for later *in vivo* studies comparing the effects of L-selectin variants on cancer-specific T cells and their control of tumour growth.

# of cancer-specific T cells	Route of administration	Additional treatments
None (PBS)	Intravenous	None
None (PBS)	Intravenous	Exogenous IL-2 and TRP ₁₈₀₋₁₈₈ in IFA
2 x10 ⁶	Intravenous	None
2 x10 ⁶	Intravenous	Exogenous IL-2 and TRP ₁₈₀₋₁₈₈ in IFA
10 x10 ⁶	Intravenous	None
10 x10 ⁶	Intravenous	Exogenous IL-2 and TRP ₁₈₀₋₁₈₈ in IFA
PBS	Intratumoural	None
2 x10 ⁶	Intratumoural	None
10 x10 ⁶	Intratumoural	None

Table 5.2. Proposed adoptive cell therapy treatment groups for B16.F10 melanoma-bearing mice. Exogenous IL-2 would be administered as done by Gattinoni et al, and the TRP₁₈₀₋₁₈₈ in IFA would be administered as done by Watson et al (Gattinoni et al. 2005; Watson et al. 2019).

To maintain feasibility of the study, PBS would have been used as a control rather than mock transduced T cells at each administered dose of cancer-specific T cells. A follow-up study comparing mock-transduced T cells with LΔP L-selectin expressing

cancer specific T cells would then be conducted to affirm the beneficial treatment group (Table 5.2).

5.6.2. Proposed experiments to develop both the conducted experiments, and the studies not conducted due to the laboratory shutdown

Comparison of L-selectin variant-bearing cancer-specific murine L-selectin KO CD8 T cells *in vivo*

Following the above study to determine which *in vivo* model would allow my cancer-specific T cells to control tumour growth, the murine and human variants of L-selectin would be expressed in murine L-selectin KO T cells and compared to mock-transduced T cells in two independent studies (Table 5.3).

Experiment 1 – evaluation of murine L-selectin variants
Mock transduced T cells
TRP2 transduced T cells
TRP2 + mWT L-selectin transduced T cells
TRP2 + m Δ P L-selectin transduced T cells
Experiment 2 – evaluation of human L-selectin variants
Mock transduced T cells
TRP2 transduced T cells
TRP2 + hWT L-selectin transduced T cells
TRP2 + h Δ MN L-selectin transduced T cells
TRP2 + h Δ W L-selectin transduced T cells

Table 5.3. Proposed adoptive cell therapy treatment groups for B16.F10 melanoma bearing mice to evaluate L-selectin variants. The route of administration and number of adoptively transferred T cells would depend on the outcome of the experiment outlined in Table 5.2.

As conducted in my preliminary experiment, tumour growth would be assessed, and end-point analyses of the spleen, tdLN and tumour would be performed using flow cytometry to determine the extent of T cell engraftment, tumour homing and T cell phenotype.

Comparison of L-selectin variant-bearing cancer-specific murine C57BL/6J CD8 T cells *in vivo*

When I began this program of work, my first objective was to emulate the mode of transgene delivery commonly used in the clinic for adoptive cell therapy of solid tumours. I was able to deliver a cancer-specific TCR and variants of L-selectin to murine T cells and have proposed experiments for their use in syngeneic murine cancer models. However, the T cells used in this body of work were L-selectin null T cells. This was useful for determining the effects of transgenic L-selectin without the confounding impact of endogenous L-selectin proteolysis, but patients' naïve T cells would not be L-selectin null prior to *ex vivo* expansion and modification. Therefore, beneficial conditions from experiments 1 and 2 (Table 5.3) should again be tested using naïve murine CD8 T cells from standard C57BL/6 mice, which express endogenous L-selectin.

Determination of L-selectin tail residues that induce the observed murine T cell phenotypes

In this thesis, I was able to deliver a TCR and variants of L-selectin to L-selectin null T cells and demonstrate phenotypes following exposure to target cells *in vitro*. Owing to the degradation of the tail of L-selectin following PMA-induced stimulation, and the retention of the tail of the human cleavage-resistant (Δ MN) form of L-selectin at the T cell surface, I hypothesised that sustained protein-protein interactions between the tail of L-selectin and intracellular proteins cause the phenotypic differences.

To investigate this, Δ MN and Δ P L-selectin transgenes with alanine point mutations at each of the 17 amino acid residues within the tail of L-selectin could be introduced into the pMP71 transgene transfer vector. Viruses produced for each of these mutants could be delivered to murine L-selectin KO CD8 T cells to evaluate the effect each residue has on T cell phenotype following exposure to target cells. T cell phenotype could be evaluated by xCELLigence and flow cytometry as conducted in this thesis. A similar approach was taken previously by Ivetič and colleagues to

determine the contribution of each residue to leukocyte rolling in flow chamber assays (Ivetič et al. 2004).

Generation and characterisation of human variants of L-selectin in human CD8 T cells

Over the course of the laboratory shutdown, Professor Ager and I successfully applied for an internal Institutional Strategic Support Fund Translational Kickstarter Award. We wrote a project addressing the criticism that syngeneic models, although fully immunocompetent, are fundamentally not human. The proposal will use the same transfer vector with pan-mammalian packaging vectors for transgene delivery to human peripheral blood mononuclear cells.

The transgenes will consist of a cancer-specific CD19-targeting CAR (2nd generation; 28z) and either WT L-selectin, Δ MN L-selectin or a CAR with L-selectin's intracellular tail as a CAR signalling domain (3rd generation; L-selectin tail28z). The target cancer will consist of NALM-6 leukemic cells for use during *in vitro* killing assays and flow cytometry. NALM-6 leukemic cells will be engrafted into NSG-mice for an *in vivo* proof of concept study. The following treatment groups will be compared (Table 5.4).

Experiment 1
Mock-transduced T cells
2 nd generation CD19 CAR-transduced T cells
2 nd generation CD19 CAR + hWT L-selectin transduced T cells
2 nd generation CD19 CAR + h Δ MN L-selectin transduced T cells
2 nd generation CD19 CAR + h Δ W L-selectin transduced T cells
Experiment 2
Mock-transduced T cells
2 nd generation CD19 CAR-transduced T cells
3 rd generation CD19 CAR-transduced T cells (incorporating L-selectin tail domain)

Table 5.4. Proposed adoptive cell therapy treatment groups for NALM-6 engrafted NSG mice. The number of CAR-T cells to be engrafted via intravenous administration will be advised by our industrial partner as part of the ISSF Award.

Treatment groups with better control of NALM-6 cells will be evaluated further in ovarian cancer models with our industrial partner, as L-selectin correlated with improved patient prognosis (Fig. 5.3).

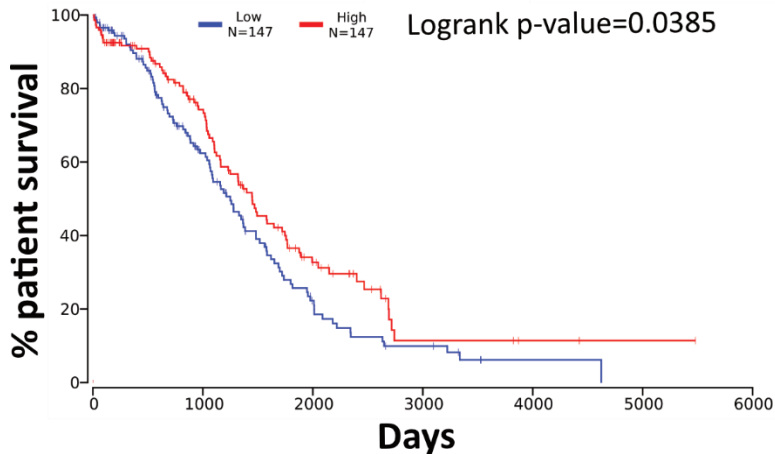


Figure 5.3. L-selectin mRNA (SELL) expression correlates with patient survival in ovarian cancer. The publicly available TCGA dataset was used to evaluate Ovarian serious cystadenocarcinoma patient survival. Cut-off for high (red) and low (blue) SELL is 50 % of the median.

<https://www.cancer.gov/tcga>.

References

- Abbas, A.K. and Lichtman, A.H. 2011. *Basic immunology: functions and disorders of the immune system* ; 3rd ed., updated. Philadelphia, Pa: Elsevier, Saunders.
- Abbott, M. and Ustoyev, Y. 2019. Cancer and the Immune System: The History and Background of Immunotherapy. *Seminars in Oncology Nursing* 35(5), p. 150923. doi: 10.1016/j.soncn.2019.08.002.
- Adachi, K. et al. 2018. IL-7 and CCL19 expression in CAR-T cells improves immune cell infiltration and CAR-T cell survival in the tumor. *Nature Biotechnology* 36(4), pp. 346–351. doi: 10.1038/nbt.4086.
- Ager, A. et al. 2016. Homing to solid cancers: a vascular checkpoint in adoptive cell therapy using CAR T-cells. *Biochemical Society Transactions* 44(2), pp. 377–385. doi: 10.1042/BST20150254.
- Akdis, M. et al. 2016. Interleukins (from IL-1 to IL-38), interferons, transforming growth factor β , and TNF- α : Receptors, functions, and roles in diseases. *The Journal of Allergy and Clinical Immunology* 138(4), pp. 984–1010. doi: 10.1016/j.jaci.2016.06.033.
- Alarcón, B. et al. 2006. T-cell antigen-receptor stoichiometry: pre-clustering for sensitivity. *EMBO Reports* 7(5), pp. 490–495. doi: 10.1038/sj.embor.7400682.
- Ali, H.R. et al. 2014. Association between CD8+ T-cell infiltration and breast cancer survival in 12,439 patients. *Annals of Oncology: Official Journal of the European Society for Medical Oncology* 25(8), pp. 1536–1543. doi: 10.1093/annonc/mdu191.

- Alsaieedi, A. et al. 2018. Safety and efficacy of Tet-regulated IL-12 expression in cancer-specific T cells. *Oncoimmunology* 8(3). Available at: <https://www.ncbi.nlm.nih.gov/pmc/articles/PMC6350686/> [Accessed: 7 July 2020].
- Ancot, F. et al. 2012. Shedding-Generated Met Receptor Fragments can be Routed to Either the Proteasomal or the Lysosomal Degradation Pathway. *Traffic* 13(9), pp. 1261–1272. doi: 10.1111/j.1600-0854.2012.01384.x.
- Ankri, C. et al. 2013. Human T cells engineered to express a programmed death 1/28 costimulatory retargeting molecule display enhanced antitumor activity. *Journal of Immunology (Baltimore, Md.: 1950)* 191(8), pp. 4121–4129. doi: 10.4049/jimmunol.1203085.
- Arbonés, M. et al. 1994. Lymphocyte homing and leukocyte rolling and migration are impaired in L-selectin-deficient mice. *Immunity* 1(4), pp. 247–260. doi: 10.1016/1074-7613(94)90076-0.
- Aspord, C. et al. 2013. Plasmacytoid dendritic cells support melanoma progression by promoting Th2 and regulatory immunity through OX40L and ICOSL. *Cancer Immunology Research* 1(6), pp. 402–415. doi: 10.1158/2326-6066.CIR-13-0114-T.
- Baekkevold, E.S. et al. 2001. The Ccr7 Ligand ELC (Ccl19) Is Transcytosed in High Endothelial Venues and Mediates T Cell Recruitment. *The Journal of Experimental Medicine* 193(9), pp. 1105–1112.
- Baixeras, E. 1992. Characterization of the lymphocyte activation gene 3-encoded protein. A new ligand for human leukocyte antigen class II antigens. *The Journal of Experimental Medicine* 176(2), pp. 327–337.
- Barber, E.K. et al. 1989. The CD4 and CD8 antigens are coupled to a protein-tyrosine kinase (p56lck) that phosphorylates the CD3 complex. *Proceedings of the National Academy of Sciences of the United States of America* 86(9), pp. 3277–3281.
- Bates, G.J. et al. 2006. Quantification of regulatory T cells enables the identification of high-risk breast cancer patients and those at risk of late relapse. *Journal of Clinical Oncology: Official Journal of the American Society of Clinical Oncology* 24(34), pp. 5373–5380. doi: 10.1200/JCO.2006.05.9584.
- Baumhater, S. et al. 1993. Binding of L-selectin to the vascular sialomucin CD34. *Science* 262(5132), pp. 436–438. doi: 10.1126/science.7692600.
- Beadling, C. et al. 1994. Activation of JAK kinases and STAT proteins by interleukin-2 and interferon alpha, but not the T cell antigen receptor, in human T lymphocytes. *The EMBO Journal* 13(23), pp. 5605–5615.
- Beel, A.J. and Sanders, C.R. 2008. Substrate specificity of gamma-secretase and other intramembrane proteases. *Cellular and molecular life sciences: CMLS* 65(9), pp. 1311–1334. doi: 10.1007/s00018-008-7462-2.

- Beresford, P.J. et al. 1999. Granzyme A loading induces rapid cytolysis and a novel form of DNA damage independently of caspase activation. *Immunity* 10(5), pp. 585–594. doi: 10.1016/s1074-7613(00)80058-8.
- Berg, E.L. et al. 1993. L-selectin-mediated lymphocyte rolling on MAdCAM-1. *Nature* 366(6456), pp. 695–698. doi: 10.1038/366695a0.
- Berger, C. et al. 2008. Adoptive transfer of effector CD8+ T cells derived from central memory cells establishes persistent T cell memory in primates. *The Journal of Clinical Investigation* 118(1), pp. 294–305. doi: 10.1172/JCI32103.
- Bhat, P. et al. 2017. Interferon- γ derived from cytotoxic lymphocytes directly enhances their motility and cytotoxicity. *Cell Death & Disease* 8(6), p. e2836. doi: 10.1038/cddis.2017.67.
- Blank, C. et al. 2006. Blockade of PD-L1 (B7-H1) augments human tumor-specific T cell responses in vitro. *International Journal of Cancer* 119(2), pp. 317–327. doi: 10.1002/ijc.21775.
- Bloom, M.B. et al. 1997. Identification of Tyrosinase-related Protein 2 as a Tumor Rejection Antigen for the B16 Melanoma. *The Journal of Experimental Medicine* 185(3), pp. 453–460.
- Böhm, W. et al. 1998. T Cell-Mediated, IFN- γ -Facilitated Rejection of Murine B16 Melanomas. *The Journal of Immunology* 161(2), pp. 897–908.
- Boland, B. et al. 2010. Macroautophagy Is Not Directly Involved in the Metabolism of Amyloid Precursor Protein. *Journal of Biological Chemistry* 285(48), pp. 37415–37426. doi: 10.1074/jbc.M110.186411.
- Bouzin, C. et al. 2007. Effects of vascular endothelial growth factor on the lymphocyte-endothelium interactions: identification of caveolin-1 and nitric oxide as control points of endothelial cell energy. *Journal of Immunology (Baltimore, Md.: 1950)* 178(3), pp. 1505–1511. doi: 10.4049/jimmunol.178.3.1505.
- Brenner, B. et al. 1996. I-Selectin activates the Ras pathway via the tyrosine kinase p56lck. *Proceedings of the National Academy of Sciences of the United States of America* 93(26), pp. 15376–15381.
- Brenner, B.C. et al. 2002. Mechanisms of L-Selectin-Induced Activation of the Nuclear Factor of Activated T Lymphocytes (NFAT). *Biochemical and Biophysical Research Communications* 291(2), pp. 237–244. doi: 10.1006/bbrc.2002.6451.
- Brocker, T. and Karjalainen, K. 1995. Signals through T cell receptor-zeta chain alone are insufficient to prime resting T lymphocytes. *The Journal of Experimental Medicine* 181(5), pp. 1653–1659.
- Bronte, V. et al. 2016. Recommendations for myeloid-derived suppressor cell nomenclature and characterization standards. *Nature Communications* 7(1), p. 12150. doi: 10.1038/ncomms12150.

- Broz, M.L. et al. 2014. Dissecting the tumor myeloid compartment reveals rare activating antigen-presenting cells critical for T cell immunity. *Cancer Cell* 26(5), pp. 638–652. doi: 10.1016/j.ccell.2014.09.007.
- Buscher, K. et al. 2010. The transmembrane domains of L-selectin and CD44 regulate receptor cell surface positioning and leukocyte adhesion under flow. *Journal of Biological Chemistry*, p. jbc.M110.102640. doi: 10.1074/jbc.M110.102640.
- Canault, M. et al. 2006. FHL2 interacts with both ADAM-17 and the cytoskeleton and regulates ADAM-17 localization and activity. *Journal of Cellular Physiology* 208(2), pp. 363–372. doi: 10.1002/jcp.20671.
- Carlsen, H.S. et al. 2005. Disparate lymphoid chemokine expression in mice and men: no evidence of CCL21 synthesis by human high endothelial venules. *Blood* 106(2), pp. 444–446. doi: 10.1182/blood-2004-11-4353.
- Castellino, F. et al. 2006. Chemokines enhance immunity by guiding naive CD8+ T cells to sites of CD4+ T cell-dendritic cell interaction. *Nature* 440(7086), pp. 890–895. doi: 10.1038/nature04651.
- Chao, C.C. et al. 1997. Mechanisms of L-selectin regulation by activated T cells. *The Journal of Immunology* 159(4), pp. 1686–1694.
- Chappaz, S. and Finke, D. 2010. The IL-7 signaling pathway regulates lymph node development independent of peripheral lymphocytes. *Journal of Immunology (Baltimore, Md.: 1950)* 184(7), pp. 3562–3569. doi: 10.4049/jimmunol.0901647.
- Chen, A. et al. 1995. Structural requirements regulate endoproteolytic release of the L-selectin (CD62L) adhesion receptor from the cell surface of leukocytes. *The Journal of Experimental Medicine* 182(2), pp. 519–530.
- Chen, D.S. and Mellman, I. 2013. Oncology meets immunology: the cancer-immunity cycle. *Immunity* 39(1), pp. 1–10. doi: 10.1016/j.immuni.2013.07.012.
- Chen, M.-L. et al. 2005. Regulatory T cells suppress tumor-specific CD8 T cell cytotoxicity through TGF- β signals in vivo. *Proceedings of the National Academy of Sciences* 102(2), pp. 419–424. doi: 10.1073/pnas.0408197102.
- Chinnasamy, D. et al. 2013. Simultaneous Targeting of Tumor Antigens and the Tumor Vasculature using T Lymphocyte Transfer Synergize to Induce Regression of Established Tumors in Mice. *Cancer research* 73(11), pp. 3371–3380. doi: 10.1158/0008-5472.CAN-12-3913.
- Chmielewski, M. et al. 2012. T Cells That Target Carcinoembryonic Antigen Eradicate Orthotopic Pancreatic Carcinomas Without Inducing Autoimmune Colitis in Mice. *Gastroenterology* 143(4), pp. 1095-1107.e2. doi: 10.1053/j.gastro.2012.06.037.

- Chmielewski, M. and Abken, H. 2017. CAR T Cells Releasing IL-18 Convert to T-Bethigh FoxO1low Effectors that Exhibit Augmented Activity against Advanced Solid Tumors. *Cell Reports* 21(11), pp. 3205–3219. doi: 10.1016/j.celrep.2017.11.063.
- Cho, B.K. et al. 1999. Functional differences between memory and naive CD8 T cells. *Proceedings of the National Academy of Sciences* 96(6), pp. 2976–2981. doi: 10.1073/pnas.96.6.2976.
- Chuang, E. et al. 1999. Regulation of cytotoxic T lymphocyte-associated molecule-4 by Src kinases. *Journal of Immunology (Baltimore, Md.: 1950)* 162(3), pp. 1270–1277.
- Clambey, E.T. et al. 2014. Molecules in medicine mini review: the $\alpha\beta$ T cell receptor. *Journal of molecular medicine (Berlin, Germany)* 92(7), pp. 735–741. doi: 10.1007/s00109-014-1145-2.
- Clayton, K.L. et al. 2014. T Cell Ig and Mucin Domain–Containing Protein 3 Is Recruited to the Immune Synapse, Disrupts Stable Synapse Formation, and Associates with Receptor Phosphatases. *The Journal of Immunology* 192(2), pp. 782–791. doi: 10.4049/jimmunol.1302663.
- Colbeck, E.J. et al. 2017. Treg Depletion Licenses T Cell–Driven HEV Neogenesis and Promotes Tumor Destruction. *Cancer Immunology Research* 5(11), pp. 1005–1015. doi: 10.1158/2326-6066.CIR-17-0131.
- Constantin, G. et al. 2000. Chemokines Trigger Immediate $\beta 2$ Integrin Affinity and Mobility Changes: Differential Regulation and Roles in Lymphocyte Arrest under Flow. *Immunity* 13(6), pp. 759–769. doi: 10.1016/S1074-7613(00)00074-1.
- Craddock, J.A. et al. 2010. Enhanced tumor trafficking of GD2 chimeric antigen receptor T cells by expression of the chemokine receptor CCR2b. *Journal of Immunotherapy (Hagerstown, Md.: 1997)* 33(8), pp. 780–788. doi: 10.1097/CJI.0b013e3181ee6675.
- Crowther, M.D. et al. 2020. Genome-wide CRISPR–Cas9 screening reveals ubiquitous T cell cancer targeting via the monomorphic MHC class I-related protein MR1. *Nature Immunology* 21(2), pp. 178–185. doi: 10.1038/s41590-019-0578-8.
- Cuylen-Haering, S. et al. 2020. Chromosome clustering by Ki-67 excludes cytoplasm during nuclear assembly. *Nature* , pp. 1–6. doi: 10.1038/s41586-020-2672-3.
- De Strooper, B. et al. 1999. A presenilin-1-dependent γ -secretase-like protease mediates release of Notch intracellular domain. *Nature* 398(6727), pp. 518–522. doi: 10.1038/19083.
- Demaison, C. et al. 2002. High-level transduction and gene expression in hematopoietic repopulating cells using a human immunodeficiency [correction of imunodeficiency] virus type 1-based lentiviral vector containing an internal spleen focus forming virus promoter. *Human Gene Therapy* 13(7), pp. 803–813. doi: 10.1089/10430340252898984.

- Demaria, M.C. et al. 2020. Tetraspanin CD53 Promotes Lymphocyte Recirculation by Stabilizing L-Selectin Surface Expression. *iScience* 23(5), p. 101104. doi: 10.1016/j.isci.2020.101104.
- Díaz-Montero, C.M. et al. 2013. Understanding the biology of ex vivo-expanded CD8 T cells for adoptive cell therapy: role of CD62L. *Immunologic Research* 57(1–3), pp. 23–33. doi: 10.1007/s12026-013-8456-1.
- Dib, K. et al. 2017. The cytoplasmic tail of L-selectin interacts with the adaptor-protein complex AP-1 subunit μ 1A via a novel basic binding motif. *Journal of Biological Chemistry* 292(16), pp. 6703–6714. doi: 10.1074/jbc.M116.768598.
- Dieterich, L.C. et al. 2017. Tumor-Associated Lymphatic Vessels Upregulate PDL1 to Inhibit T-Cell Activation. *Frontiers in Immunology* 8. Available at: <https://www.ncbi.nlm.nih.gov/pmc/articles/PMC5289955/> [Accessed: 3 August 2020].
- Dios-Esponera, A. et al. 2019. Pak1 Kinase Promotes Activated T Cell Trafficking by Regulating the Expression of L-Selectin and CCR7. *Frontiers in Immunology* 10, p. 370. doi: 10.3389/fimmu.2019.00370.
- Duraiswamy, J. et al. 2013. Dual blockade of PD-1 and CTLA-4 combined with tumor vaccine effectively restores T-cell rejection function in tumors. *Cancer Research* 73(12), pp. 3591–3603. doi: 10.1158/0008-5472.CAN-12-4100.
- Ebnet, K. et al. 1995. Granzyme A-deficient mice retain potent cell-mediated cytotoxicity. *The EMBO Journal* 14(17), pp. 4230–4239.
- Engels, B. et al. 2004. Retroviral Vectors for High-Level Transgene Expression in T Lymphocytes. Available at: <https://www.liebertpub.com/doi/abs/10.1089/104303403322167993> [Accessed: 7 July 2020].
- Erbe, D.V. et al. 1992. Identification of an E-selectin region critical for carbohydrate recognition and cell adhesion. *The Journal of Cell Biology* 119(1), pp. 215–227. doi: 10.1083/jcb.119.1.215.
- Evrard, C. et al. 2018. Contribution of the Endosomal-Lysosomal and Proteasomal Systems in Amyloid- β Precursor Protein Derived Fragments Processing. *Frontiers in Cellular Neuroscience* 12, p. 435. doi: 10.3389/fncel.2018.00435.
- Facciabene, A. et al. 2011. Tumour hypoxia promotes tolerance and angiogenesis via CCL28 and T(reg) cells. *Nature* 475(7355), pp. 226–230. doi: 10.1038/nature10169.
- Ferguson, A.R. and Engelhard, V.H. 2010. CD8 T cells activated in distinct lymphoid organs differentially express adhesion proteins and co-express multiple chemokine receptors. *Journal of immunology (Baltimore, Md. : 1950)* 184(8), pp. 4079–4086. doi: 10.4049/jimmunol.0901903.

- Finlay, D.K. et al. 2012. PDK1 regulation of mTOR and hypoxia-inducible factor 1 integrate metabolism and migration of CD8+ T cells. *The Journal of Experimental Medicine* 209(13), pp. 2441–2453. doi: 10.1084/jem.20112607.
- Fisher, D.T. et al. 2014. The two faces of IL-6 in the tumor microenvironment. *Seminars in Immunology* 26(1), pp. 38–47. doi: 10.1016/j.smim.2014.01.008.
- Förster, R. et al. 1999. CCR7 Coordinates the Primary Immune Response by Establishing Functional Microenvironments in Secondary Lymphoid Organs. *Cell* 99(1), pp. 23–33. doi: 10.1016/S0092-8674(00)80059-8.
- Fraser, J.H. et al. 1999. CTLA4 ligation attenuates AP-1, NFAT and NF-kappaB activity in activated T cells. *European Journal of Immunology* 29(3), pp. 838–844. doi: 10.1002/(SICI)1521-4141(199903)29:03<838::AID-IMMU838>3.0.CO;2-P.
- Freeman, G.J. et al. 2000. Engagement of the PD-1 immunoinhibitory receptor by a novel B7 family member leads to negative regulation of lymphocyte activation. *The Journal of Experimental Medicine* 192(7), pp. 1027–1034. doi: 10.1084/jem.192.7.1027.
- Galkina, E. et al. 2003. L-Selectin Shedding Does Not Regulate Constitutive T Cell Trafficking but Controls the Migration Pathways of Antigen-activated T Lymphocytes. *The Journal of Experimental Medicine* 198(9), pp. 1323–1335. doi: 10.1084/jem.20030485.
- Galon, J. et al. 2006. Type, density, and location of immune cells within human colorectal tumors predict clinical outcome. *Science (New York, N.Y.)* 313(5795), pp. 1960–1964. doi: 10.1126/science.1129139.
- Gattinoni, L. et al. 2005. Acquisition of full effector function in vitro paradoxically impairs the in vivo antitumor efficacy of adoptively transferred CD8+ T cells. *The Journal of Clinical Investigation* 115(6), pp. 1616–1626. doi: 10.1172/JCI24480.
- Gentles, A.J. et al. 2015. The prognostic landscape of genes and infiltrating immune cells across human cancers. *Nature Medicine* 21(8), pp. 938–945. doi: 10.1038/nm.3909.
- Gerlach, C. et al. 2010. One naive T cell, multiple fates in CD8+ T cell differentiation. *The Journal of Experimental Medicine* 207(6), pp. 1235–1246. doi: 10.1084/jem.20091175.
- Gilham, D.E. et al. 2010. Cytokine stimulation and the choice of promoter are critical factors for the efficient transduction of mouse T cells with HIV-1 vectors. *The Journal of Gene Medicine* 12(2), pp. 129–136. doi: 10.1002/jgm.1421.
- Golumba-Nagy, V. et al. 2017. Genetic Modification of T Cells with Chimeric Antigen Receptors: A Laboratory Manual. *Human Gene Therapy Methods* 28(6), pp. 302–309. doi: 10.1089/hgtb.2017.083.
- Gondek, D.C. et al. 2005. Cutting Edge: Contact-Mediated Suppression by CD4+CD25+ Regulatory Cells Involves a Granzyme B-Dependent, Perforin-Independent Mechanism. *The Journal of Immunology* 174(4), pp. 1783–1786. doi: 10.4049/jimmunol.174.4.1783.

- Gonzalez, H. et al. 2018. Roles of the immune system in cancer: from tumor initiation to metastatic progression. *Genes & Development* 32(19–20), pp. 1267–1284. doi: 10.1101/gad.314617.118.
- Goping, I.S. et al. 2003. Granzyme B-Induced Apoptosis Requires Both Direct Caspase Activation and Relief of Caspase Inhibition. *Immunity* 18(3), pp. 355–365. doi: 10.1016/S1074-7613(03)00032-3.
- Gunderson, A.J. et al. 2020. TGF β suppresses CD8 + T cell expression of CXCR3 and tumor trafficking. *Nature Communications* 11(1), p. 1749. doi: 10.1038/s41467-020-15404-8.
- Gupta-Rossi, N. et al. 2001. Functional Interaction between SEL-10, an F-box Protein, and the Nuclear Form of Activated Notch1 Receptor. *Journal of Biological Chemistry* 276(37), pp. 34371–34378. doi: 10.1074/jbc.M101343200.
- Haas, A.R. et al. 2019. Phase I Study of Lentiviral-Transduced Chimeric Antigen Receptor-Modified T Cells Recognizing Mesothelin in Advanced Solid Cancers. *Molecular Therapy* 27(11), pp. 1919–1929. doi: 10.1016/j.ymthe.2019.07.015.
- Halene, S. et al. 1999. Improved Expression in Hematopoietic and Lymphoid Cells in Mice After Transplantation of Bone Marrow Transduced With a Modified Retroviral Vector. *Blood* 94(10), pp. 3349–3357. doi: 10.1182/blood.V94.10.3349.422k05_3349_3357.
- Halle, S. et al. 2016. In Vivo Killing Capacity of Cytotoxic T Cells Is Limited and Involves Dynamic Interactions and T Cell Cooperativity. *Immunity* 44(2), pp. 233–245. doi: 10.1016/j.immuni.2016.01.010.
- Hamilton, M.J. et al. 2014. Macrophages are more potent immune suppressors ex vivo than immature myeloid-derived suppressor cells induced by metastatic murine mammary carcinomas. *Journal of Immunology (Baltimore, Md.: 1950)* 192(1), pp. 512–522. doi: 10.4049/jimmunol.1300096.
- Han, X. et al. 2019. Multi-antigen-targeted chimeric antigen receptor T cells for cancer therapy. *Journal of Hematology & Oncology* 12(1), p. 128. doi: 10.1186/s13045-019-0813-7.
- Hanson, E.M. et al. 2009. Myeloid-Derived Suppressor Cells Down-Regulate L-Selectin Expression on CD4+ and CD8+ T Cells. *The Journal of Immunology* 183(2), pp. 937–944. doi: 10.4049/jimmunol.0804253.
- Heinen, A.P. et al. 2014. Improved method to retain cytosolic reporter protein fluorescence while staining for nuclear proteins. *Cytometry Part A* 85(7), pp. 621–627. doi: 10.1002/cyto.a.22451.
- Heusel, J.W. et al. 1994. Cytotoxic lymphocytes require granzyme B for the rapid induction of DNA fragmentation and apoptosis in allogeneic target cells. *Cell* 76(6), pp. 977–987. doi: 10.1016/0092-8674(94)90376-X.

- Hickman, H.D. et al. 2008. Direct priming of antiviral CD8+ T cells in the peripheral interfollicular region of lymph nodes. *Nature Immunology* 9(2), pp. 155–165. doi: 10.1038/ni1557.
- Hodi, F.S. et al. 2010. Improved Survival with Ipilimumab in Patients with Metastatic Melanoma. *The New England journal of medicine* 363(8), pp. 711–723. doi: 10.1056/NEJMoa1003466.
- Hor, J.L. et al. 2015. Spatiotemporally Distinct Interactions with Dendritic Cell Subsets Facilitates CD4+ and CD8+ T Cell Activation to Localized Viral Infection. *Immunity* 43(3), pp. 554–565. doi: 10.1016/j.immuni.2015.07.020.
- Huang, P.-W. and Chang, J.W.-C. 2019. Immune checkpoint inhibitors win the 2018 Nobel Prize. *Biomedical Journal* 42(5), pp. 299–306. doi: 10.1016/j.bj.2019.09.002.
- Hughes, M.S. et al. 2005. Transfer of a TCR Gene Derived from a Patient with a Marked Antitumor Response Conveys Highly Active T-Cell Effector Functions. *Human gene therapy* 16(4), pp. 457–472. doi: 10.1089/hum.2005.16.457.
- Hui, E. et al. 2017. T cell costimulatory receptor CD28 is a primary target for PD-1-mediated inhibition. *Science (New York, N.Y.)* 355(6332), pp. 1428–1433. doi: 10.1126/science.aaf1292.
- Hwang, J.-R. et al. 2020. Recent insights of T cell receptor-mediated signaling pathways for T cell activation and development. *Experimental & Molecular Medicine* 52(5), pp. 750–761. doi: 10.1038/s12276-020-0435-8.
- Imboden, J. and Stobo, J. 1985. Transmembrane signalling by the T cell antigen receptor. Perturbation of the T3-antigen receptor complex generates inositol phosphates and releases calcium ions from intracellular stores. *The Journal of Experimental Medicine* 161(3), pp. 446–456.
- Ishida, Y. et al. 1992. Induced expression of PD-1, a novel member of the immunoglobulin gene superfamily, upon programmed cell death. *The EMBO Journal* 11(11), pp. 3887–3895.
- Ishikura, S. et al. 2016. The Nuclear Zinc Finger Protein Zfat Maintains FoxO1 Protein Levels in Peripheral T Cells by Regulating the Activities of Autophagy and the Akt Signaling Pathway. *The Journal of Biological Chemistry* 291(29), pp. 15282–15291. doi: 10.1074/jbc.M116.723734.
- Ivetic, A. et al. 2002. The Cytoplasmic Tail of L-selectin Interacts with Members of the Ezrin-Radixin-Moesin (ERM) Family of Proteins CELL ACTIVATION-DEPENDENT BINDING OF MOESIN BUT NOT EZRIN. *Journal of Biological Chemistry* 277(3), pp. 2321–2329. doi: 10.1074/jbc.M109460200.
- Ivetič, A. et al. 2004. Mutagenesis of the Ezrin-Radixin-Moesin Binding Domain of L-selectin Tail Affects Shedding, Microvillar Positioning, and Leukocyte Tethering. *Journal of Biological Chemistry* 279(32), pp. 33263–33272. doi: 10.1074/jbc.M312212200.

- Janas, M.L. et al. 2005. IL-2 regulates perforin and granzyme gene expression in CD8+ T cells independently of its effects on survival and proliferation. *Journal of Immunology (Baltimore, Md.: 1950)* 175(12), pp. 8003–8010. doi: 10.4049/jimmunol.175.12.8003.
- Johnson, L.A. et al. 2009. Gene therapy with human and mouse T-cell receptors mediates cancer regression and targets normal tissues expressing cognate antigen. *Blood* 114(3), pp. 535–546. doi: 10.1182/blood-2009-03-211714.
- Jung, D. and Alt, F.W. 2004. Unraveling V(D)J Recombination: Insights into Gene Regulation. *Cell* 116(2), pp. 299–311. doi: 10.1016/S0092-8674(04)00039-X.
- Jung, Y. et al. 2016. Three-dimensional localization of T-cell receptors in relation to microvilli using a combination of superresolution microscopies. *Proceedings of the National Academy of Sciences of the United States of America* 113(40), pp. E5916–E5924. doi: 10.1073/pnas.1605399113.
- Kahn, J. et al. 1994. Membrane proximal cleavage of L-selectin: identification of the cleavage site and a 6-kD transmembrane peptide fragment of L-selectin. *Journal of Cell Biology* 125(2), pp. 461–470. doi: 10.1083/jcb.125.2.461.
- Kaiserman, D. et al. 2006. The major human and mouse granzymes are structurally and functionally divergent. *The Journal of Cell Biology* 175(4), pp. 619–630. doi: 10.1083/jcb.200606073.
- Kang, C.-W. et al. 2015. Apoptosis of tumor infiltrating effector TIM-3+CD8+ T cells in colon cancer. *Scientific Reports* 5, p. 15659. doi: 10.1038/srep15659.
- Kansagra, A.J. et al. 2019. Clinical utilization of Chimeric Antigen Receptor T-cells (CAR-T) in B-cell acute lymphoblastic leukemia (ALL)—an expert opinion from the European Society for Blood and Marrow Transplantation (EBMT) and the American Society for Blood and Marrow Transplantation (ASBMT). *Bone Marrow Transplantation* 54(11), pp. 1868–1880. doi: 10.1038/s41409-019-0451-2.
- Kansas, G.S. et al. 1991. Molecular mapping of functional domains of the leukocyte receptor for endothelium, LAM-1. *The Journal of Cell Biology* 114(2), pp. 351–358. doi: 10.1083/jcb.114.2.351.
- Kasahara, T. et al. 1983. Interleukin 2-mediated immune interferon (IFN-gamma) production by human T cells and T cell subsets. *The Journal of Immunology* 130(4), pp. 1784–1789.
- Kerker, S.P. et al. 2011. Genetic engineering of murine CD8+ and CD4+ T cells for pre-clinical adoptive immunotherapy studies. *Journal of immunotherapy (Hagerstown, Md. : 1997)* 34(4), pp. 343–352. doi: 10.1097/CJI.0b013e3182187600.
- Kilian, K. et al. 2004. The interaction of protein kinase C isozymes alpha, iota, and theta with the cytoplasmic domain of L-selectin is modulated by phosphorylation of the receptor. *The Journal of Biological Chemistry* 279(33), pp. 34472–34480. doi: 10.1074/jbc.M405916200.

- Killock, D.J. et al. 2009. In Vitro and in Vivo Characterization of Molecular Interactions between Calmodulin, Ezrin/Radixin/Moesin, and L-selectin. *Journal of Biological Chemistry* 284(13), pp. 8833–8845. doi: 10.1074/jbc.M806983200.
- Killock, D.J. and Ivetić, A. 2010. The cytoplasmic domains of TNF α -converting enzyme (TACE/ADAM17) and L-selectin are regulated differently by p38 MAPK and PKC to promote ectodomain shedding. *Biochemical Journal* 428(2), pp. 293–304. doi: 10.1042/BJ20091611.
- Kim, H.R. et al. 2019. Tumor microenvironment dictates regulatory T cell phenotype: Upregulated immune checkpoints reinforce suppressive function. *Journal for Immunotherapy of Cancer* 7. Available at: <https://www.ncbi.nlm.nih.gov/pmc/articles/PMC6894345/> [Accessed: 6 August 2020].
- Kimberly, W.T. et al. 2001. The intracellular domain of the beta-amyloid precursor protein is stabilized by Fe65 and translocates to the nucleus in a notch-like manner. *The Journal of Biological Chemistry* 276(43), pp. 40288–40292. doi: 10.1074/jbc.C100447200.
- Kisselev, A.F. and Goldberg, A.L. 2001. Proteasome inhibitors: from research tools to drug candidates. *Chemistry & Biology* 8(8), pp. 739–758. doi: 10.1016/S1074-5521(01)00056-4.
- Kjaergaard, J. and Shu, S. 1999. Tumor infiltration by adoptively transferred T cells is independent of immunologic specificity but requires down-regulation of L-selectin expression. *Journal of Immunology (Baltimore, Md.: 1950)* 163(2), pp. 751–759.
- Klebanoff, C.A. et al. 2005. Central memory self/tumor-reactive CD8+ T cells confer superior antitumor immunity compared with effector memory T cells. *Proceedings of the National Academy of Sciences of the United States of America* 102(27), pp. 9571–9576. doi: 10.1073/pnas.0503726102.
- Klinger, A. et al. 2009. Cyclical expression of L-selectin (CD62L) by recirculating T cells. *International Immunology* 21(4), pp. 443–455. doi: 10.1093/intimm/dxp012.
- Kochenderfer, J.N. et al. 2010. Adoptive transfer of syngeneic T cells transduced with a chimeric antigen receptor that recognizes murine CD19 can eradicate lymphoma and normal B cells. *Blood* 116(19), pp. 3875–3886. doi: 10.1182/blood-2010-01-265041.
- Kouo, T. et al. 2015. Galectin-3 shapes antitumor immune responses by suppressing CD8+ T cells via LAG-3 and inhibiting expansion of plasmacytoid dendritic cells. *Cancer immunology research* 3(4), pp. 412–423. doi: 10.1158/2326-6066.CIR-14-0150.
- Krummel, M. and Allison, J.P. 1996. CTLA-4 engagement inhibits IL-2 accumulation and cell cycle progression upon activation of resting T cells. *The Journal of Experimental Medicine* 183(6), pp. 2533–2540.
- Ku, A.W. et al. 2016. Tumor-induced MDSC act via remote control to inhibit L-selectin-dependent adaptive immunity in lymph nodes. *eLife* 5. doi: 10.7554/eLife.17375.
- Kumar, M. et al. 2001. Systematic Determination of the Packaging Limit of Lentiviral Vectors. *Human Gene Therapy* 12(15), pp. 1893–1905. doi: 10.1089/104303401753153947.

- Lahdenpohja, N. et al. 1998. Pre-Exposure to Oxidative Stress Decreases the Nuclear Factor- κ B-Dependent Transcription in T Lymphocytes. *The Journal of Immunology* 160(3), pp. 1354–1358.
- Larcombe-Young, D. et al. 2020. PanErbB-targeted CAR T-cell immunotherapy of head and neck cancer. *Expert Opinion on Biological Therapy* 20(9), pp. 965–970. doi: 10.1080/14712598.2020.1786531.
- Larkin, J. et al. 2015. Combined Nivolumab and Ipilimumab or Monotherapy in Previously Untreated Melanoma. *The New England journal of medicine* 373(1), pp. 23–34. doi: 10.1056/NEJMoa1504030.
- Lauritsen, J.P.H. et al. 1998. Two Distinct Pathways Exist for Down-Regulation of the TCR. *The Journal of Immunology* 161(1), pp. 260–267.
- Law, R.H.P. et al. 2010. The structural basis for membrane binding and pore formation by lymphocyte perforin. *Nature* 468(7322), pp. 447–451. doi: 10.1038/nature09518.
- Le Gall, S.M. et al. 2010. ADAM17 is regulated by a rapid and reversible mechanism that controls access to its catalytic site. *Journal of Cell Science* 123(22), pp. 3913–3922. doi: 10.1242/jcs.069997.
- Legut, M. et al. 2018. CRISPR-mediated TCR replacement generates superior anticancer transgenic T cells. *Blood* 131(3), pp. 311–322. doi: 10.1182/blood-2017-05-787598.
- Letourneur, F. and Klausner, R.D. 1992. Activation of T cells by a tyrosine kinase activation domain in the cytoplasmic tail of CD3 epsilon. *Science (New York, N.Y.)* 255(5040), pp. 79–82. doi: 10.1126/science.1532456.
- Levelt, C.N. et al. 1999. High- and low-affinity single-peptide/MHC ligands have distinct effects on the development of mucosal CD8 $\alpha\alpha$ and CD8 $\alpha\beta$ T lymphocytes. *Proceedings of the National Academy of Sciences of the United States of America* 96(10), pp. 5628–5633.
- Li, S. et al. 2017. Enhanced Cancer Immunotherapy by Chimeric Antigen Receptor-Modified T Cells Engineered to Secrete Checkpoint Inhibitors. *Clinical Cancer Research: An Official Journal of the American Association for Cancer Research* 23(22), pp. 6982–6992. doi: 10.1158/1078-0432.CCR-17-0867.
- Linsley, P.S. et al. 1994. Human B7-1 (CD80) and B7-2 (CD86) bind with similar avidities but distinct kinetics to CD28 and CTLA-4 receptors. *Immunity* 1(9), pp. 793–801. doi: 10.1016/s1074-7613(94)80021-9.
- Liu, Y. et al. 2009. Regulation of arginase I activity and expression by both PD-1 and CTLA-4 on the myeloid-derived suppressor cells. *Cancer immunology, immunotherapy: CII* 58(5), pp. 687–697. doi: 10.1007/s00262-008-0591-5.
- Liu, Z. et al. 2017. Systematic comparison of 2A peptides for cloning multi-genes in a polycistronic vector. *Scientific Reports* 7(1), p. 2193. doi: 10.1038/s41598-017-02460-2.

- Long, A.H. et al. 2015. 4-1BB costimulation ameliorates T cell exhaustion induced by tonic signaling of chimeric antigen receptors. *Nature Medicine* 21(6), pp. 581–590. doi: 10.1038/nm.3838.
- Lorenzen, I. et al. 2016. Control of ADAM17 activity by regulation of its cellular localisation. *Scientific Reports* 6, p. 35067. doi: 10.1038/srep35067.
- Lou, J. et al. 2006. Flow-enhanced adhesion regulated by a selectin interdomain hinge. *The Journal of Cell Biology* 174(7), pp. 1107–1117. doi: 10.1083/jcb.200606056.
- Lozano, E. et al. 2012. The TIGIT/CD226 axis regulates human T cell function. *Journal of Immunology (Baltimore, Md.: 1950)* 188(8), pp. 3869–3875. doi: 10.4049/jimmunol.1103627.
- Lu, Y. et al. 1998. Phosphatidylinositol 3-Kinase Is Required for CD28 But Not CD3 Regulation of the TEC Family Tyrosine Kinase EMT/ITK/TSK: Functional and Physical Interaction of EMT with Phosphatidylinositol 3-Kinase. *The Journal of Immunology* 161(10), pp. 5404–5412.
- MacLachlan, B.J. et al. 2020. Molecular characterization of HLA class II binding to the LAG-3 T cell co-inhibitory receptor. *European Journal of Immunology* n/a(n/a). Available at: <https://onlinelibrary.wiley.com/doi/abs/10.1002/eji.202048753> [Accessed: 9 November 2020].
- Maeda, K. et al. 1971. THE STRUCTURE AND ACTIVITY OF LEUPEPTINS AND RELATED ANALOGS. *The Journal of Antibiotics* 24(6), pp. 402–404. doi: 10.7164/antibiotics.24.402.
- Maher, J. et al. 2002. Human T-lymphocyte cytotoxicity and proliferation directed by a single chimeric TCRzeta /CD28 receptor. *Nature Biotechnology* 20(1), pp. 70–75. doi: 10.1038/nbt0102-70.
- Marciniszyn, J. et al. 1977. Pepstatin inhibition mechanism. *Advances in Experimental Medicine and Biology* 95, pp. 199–210. doi: 10.1007/978-1-4757-0719-9_12.
- Marincola, F.M. et al. 1996. Analysis of expression of the melanoma-associated antigens MART-1 and gp100 in metastatic melanoma cell lines and in in situ lesions. *Journal of Immunotherapy with Emphasis on Tumor Immunology: Official Journal of the Society for Biological Therapy* 19(3), pp. 192–205. doi: 10.1097/00002371-199605000-00004.
- Martinet, L. et al. 2011a. Human solid tumors contain high endothelial venules: association with T- and B-lymphocyte infiltration and favorable prognosis in breast cancer. *Cancer Research* 71(17), pp. 5678–5687. doi: 10.1158/0008-5472.CAN-11-0431.
- Martinet, L. et al. 2011b. Human Solid Tumors Contain High Endothelial Venules: Association with T- and B-Lymphocyte Infiltration and Favorable Prognosis in Breast Cancer. *Cancer Research* 71(17), pp. 5678–5687. doi: 10.1158/0008-5472.CAN-11-0431.
- Martinet, L. et al. 2012. High endothelial venules (HEVs) in human melanoma lesions. *Oncoimmunology* 1(6), pp. 829–839. doi: 10.4161/onci.20492.

- Matala, E. et al. 2001. The Cytoplasmic Domain of L-Selectin Participates in Regulating L-Selectin Endoproteolysis. *The Journal of Immunology* 167(3), pp. 1617–1623. doi: 10.4049/jimmunol.167.3.1617.
- Matsumura, R. et al. 2000. Interferon gamma and tumor necrosis factor alpha induce Fas expression and anti-Fas mediated apoptosis in a salivary ductal cell line. *Clinical and Experimental Rheumatology* 18(3), pp. 311–318.
- Maude, S.L. et al. 2018. Tisagenlecleucel in Children and Young Adults with B-Cell Lymphoblastic Leukemia. *New England Journal of Medicine* 378(5), pp. 439–448. doi: 10.1056/NEJMoa1709866.
- Mauthe, M. et al. 2018. Chloroquine inhibits autophagic flux by decreasing autophagosome-lysosome fusion. *Autophagy* 14(8), pp. 1435–1455. doi: 10.1080/15548627.2018.1474314.
- Mazzoni, A. et al. 2002. Myeloid suppressor lines inhibit T cell responses by an NO-dependent mechanism. *Journal of Immunology (Baltimore, Md.: 1950)* 168(2), pp. 689–695. doi: 10.4049/jimmunol.168.2.689.
- McGranahan, N. et al. 2016. Clonal neoantigens elicit T cell immunoreactivity and sensitivity to immune checkpoint blockade. *Science (New York, N.Y.)* 351(6280), pp. 1463–1469. doi: 10.1126/science.aaf1490.
- McNally, A. et al. 2011. CD4+CD25+ regulatory T cells control CD8+ T-cell effector differentiation by modulating IL-2 homeostasis. *Proceedings of the National Academy of Sciences* 108(18), pp. 7529–7534. doi: 10.1073/pnas.1103782108.
- Mebius, R.E. et al. 1993. Expression of GlyCAM-1, an endothelial ligand for L-selectin, is affected by afferent lymphatic flow. *The Journal of Immunology* 151(12), pp. 6769–6776.
- Migaki, G.I. et al. 1995. Mutational analysis of the membrane-proximal cleavage site of L-selectin: relaxed sequence specificity surrounding the cleavage site. *Journal of Experimental Medicine* 182(2), pp. 549–557. doi: 10.1084/jem.182.2.549.
- Mittal, D. et al. 2014. New insights into cancer immunoediting and its three component phases--elimination, equilibrium and escape. *Current Opinion in Immunology* 27, pp. 16–25. doi: 10.1016/j.coi.2014.01.004.
- Miyazaki, T. et al. 1994. Functional activation of Jak1 and Jak3 by selective association with IL-2 receptor subunits. *Science* 266(5187), pp. 1045–1047. doi: 10.1126/science.7973659.
- Mohammed, R.N. et al. 2016. L-selectin Is Essential for Delivery of Activated CD8+ T Cells to Virus-Infected Organs for Protective Immunity. *Cell Reports* 14(4), pp. 760–771. doi: 10.1016/j.celrep.2015.12.090.
- Mohammed, R.N. et al. 2019a. ADAM17-dependent proteolysis of L-selectin promotes early clonal expansion of cytotoxic T cells. *Scientific Reports* 9(1), p. 5487. doi: 10.1038/s41598-019-41811-z.

- Mohammed, R.N. et al. 2019b. ADAM17-dependent proteolysis of L-selectin promotes early clonal expansion of cytotoxic T cells. *Scientific Reports* 9. Available at: <https://www.ncbi.nlm.nih.gov/pmc/articles/PMC6445073/> [Accessed: 5 May 2020].
- Mohammed, S. et al. 2017. Improving Chimeric Antigen Receptor-Modified T Cell Function by Reversing the Immunosuppressive Tumor Microenvironment of Pancreatic Cancer. *Molecular Therapy: The Journal of the American Society of Gene Therapy* 25(1), pp. 249–258. doi: 10.1016/j.ymthe.2016.10.016.
- Moriggl, R. et al. 1999. Stat5 is required for IL-2-induced cell cycle progression of peripheral T cells. *Immunity* 10(2), pp. 249–259. doi: 10.1016/s1074-7613(00)80025-4.
- Motz, G.T. et al. 2014. Tumor endothelium FasL establishes a selective immune barrier promoting tolerance in tumors. *Nature Medicine* 20(6), pp. 607–615. doi: 10.1038/nm.3541.
- Moussion, C. and Girard, J.-P. 2011. Dendritic cells control lymphocyte entry to lymph nodes through high endothelial venules. *Nature* 479(7374), pp. 542–546. doi: 10.1038/nature10540.
- Mroczkiewicz, M. et al. 2010. Studies of the synthesis of all stereoisomers of MG-132 proteasome inhibitors in the tumor targeting approach. *Journal of Medicinal Chemistry* 53(4), pp. 1509–1518. doi: 10.1021/jm901619n.
- Nakanishi, Y. et al. 2009. CD8 + T lymphocyte mobilization to virus-infected tissue requires CD4 + T-cell help. *Nature* 462(7272), pp. 510–513. doi: 10.1038/nature08511.
- Noguchi, T. et al. 2017. Temporally Distinct PD-L1 Expression by Tumor and Host Cells Contributes to Immune Escape. *Cancer Immunology Research* 5(2), pp. 106–117. doi: 10.1158/2326-6066.CIR-16-0391.
- Nolz, J.C. 2015. Molecular Mechanisms of CD8+ T cell Trafficking and Localization. *Cellular and molecular life sciences : CMLS* 72(13), pp. 2461–2473. doi: 10.1007/s00018-015-1835-0.
- Noman, M.Z. et al. 2014. PD-L1 is a novel direct target of HIF-1 α , and its blockade under hypoxia enhanced MDSC-mediated T cell activation. *The Journal of Experimental Medicine* 211(5), pp. 781–790. doi: 10.1084/jem.20131916.
- Oberg, C. et al. 2001. The Notch intracellular domain is ubiquitinated and negatively regulated by the mammalian Sel-10 homolog. *The Journal of Biological Chemistry* 276(38), pp. 35847–35853. doi: 10.1074/jbc.M103992200.
- Olson, B. et al. 2018. Mouse Models for Cancer Immunotherapy Research. *Cancer Discovery* 8(11), pp. 1358–1365. doi: 10.1158/2159-8290.CD-18-0044.
- Park, J.H. et al. 2018. Long-Term Follow-up of CD19 CAR Therapy in Acute Lymphoblastic Leukemia. *New England Journal of Medicine* 378(5), pp. 449–459. doi: 10.1056/NEJMoa1709919.

- Park, S.-G. et al. 2009. The kinase PDK1 integrates T cell antigen receptor and CD28 coreceptor signaling to induce NF- κ B and activate T cells. *Nature Immunology* 10(2), pp. 158–166. doi: 10.1038/ni.1687.
- Parry, R.V. et al. 2005. CTLA-4 and PD-1 receptors inhibit T-cell activation by distinct mechanisms. *Molecular and Cellular Biology* 25(21), pp. 9543–9553. doi: 10.1128/MCB.25.21.9543-9553.2005.
- Petherick, K.J. et al. 2015. Pharmacological Inhibition of ULK1 Kinase Blocks Mammalian Target of Rapamycin (mTOR)-dependent Autophagy. *Journal of Biological Chemistry* 290(18), pp. 11376–11383. doi: 10.1074/jbc.C114.627778.
- Pinazza, M. et al. 2018. Histone deacetylase 6 controls Notch3 trafficking and degradation in T-cell acute lymphoblastic leukemia cells. *Oncogene* 37(28), pp. 3839–3851. doi: 10.1038/s41388-018-0234-z.
- Pipkin, M.E. et al. 2010. Interleukin-2 and Inflammation Induce Distinct Transcriptional Programs that Promote the Differentiation of Effector Cytolytic T Cells. *Immunity* 32(1), pp. 79–90. doi: 10.1016/j.immuni.2009.11.012.
- Preston, G.C. et al. 2013. The Impact of KLF2 Modulation on the Transcriptional Program and Function of CD8 T Cells. *PLOS ONE* 8(10), p. e77537. doi: 10.1371/journal.pone.0077537.
- Prokopchuk, O. et al. 2005. Interleukin-4 enhances proliferation of human pancreatic cancer cells: evidence for autocrine and paracrine actions. *British Journal of Cancer* 92(5), pp. 921–928. doi: 10.1038/sj.bjc.6602416.
- Purbhoo, M.A. et al. 2004. T cell killing does not require the formation of a stable mature immunological synapse. *Nature Immunology* 5(5), pp. 524–530. doi: 10.1038/ni1058.
- Puri, K.D. et al. 1995. Sialomucin CD34 is the major L-selectin ligand in human tonsil high endothelial venules. *Journal of Cell Biology* 131(1), pp. 261–270. doi: 10.1083/jcb.131.1.261.
- Qureshi, O.S. et al. 2011. Trans-endocytosis of CD80 and CD86: a molecular basis for the cell-extrinsic function of CTLA-4. *Science (New York, N.Y.)* 332(6029), pp. 600–603. doi: 10.1126/science.1202947.
- Rafiq, S. et al. 2020. Engineering strategies to overcome the current roadblocks in CAR T cell therapy. *Nature Reviews. Clinical Oncology* 17(3), pp. 147–167. doi: 10.1038/s41571-019-0297-y.
- Ramos, C.A. et al. 2018. In Vivo Fate and Activity of Second- versus Third-Generation CD19-Specific CAR-T Cells in B Cell Non-Hodgkin's Lymphomas. *Molecular Therapy* 26(12), pp. 2727–2737. doi: 10.1016/j.ymthe.2018.09.009.
- Ray, M. et al. 2015. Quantitative tracking of protein trafficking to the nucleus using cytosolic protein delivery by nanoparticle-stabilized nanocapsules. *Bioconjugate chemistry* 26(6), pp. 1004–1007. doi: 10.1021/acs.bioconjchem.5b00141.

- Robbins, P.F. et al. 2011. Tumor regression in patients with metastatic synovial cell sarcoma and melanoma using genetically engineered lymphocytes reactive with NY-ESO-1. *Journal of Clinical Oncology: Official Journal of the American Society of Clinical Oncology* 29(7), pp. 917–924. doi: 10.1200/JCO.2010.32.2537.
- Rodriguez, P.C. et al. 2002. Regulation of T cell receptor CD3zeta chain expression by L-arginine. *The Journal of Biological Chemistry* 277(24), pp. 21123–21129. doi: 10.1074/jbc.M110675200.
- Romeo, C. et al. 1992. Sequence requirements for induction of cytolysis by the T cell antigen Fc receptor ζ chain. *Cell* 68(5), pp. 889–897. doi: 10.1016/0092-8674(92)90032-8.
- Roose, J.P. et al. 2005. A Diacylglycerol-Protein Kinase C-RasGRP1 Pathway Directs Ras Activation upon Antigen Receptor Stimulation of T Cells. *Molecular and Cellular Biology* 25(11), pp. 4426–4441. doi: 10.1128/MCB.25.11.4426-4441.2005.
- Ross, S.H. et al. 2016. Phosphoproteomic Analyses of Interleukin 2 Signaling Reveal Integrated JAK Kinase-Dependent and -Independent Networks in CD8(+) T Cells. *Immunity* 45(3), pp. 685–700. doi: 10.1016/j.immuni.2016.07.022.
- Ross, S.H. and Cantrell, D.A. 2018. Signaling and Function of Interleukin-2 in T Lymphocytes. *Annual review of immunology* 36, pp. 411–433. doi: 10.1146/annurev-immunol-042617-053352.
- Rzeniewicz, K. et al. 2015. L-selectin shedding is activated specifically within transmigrating pseudopods of monocytes to regulate cell polarity in vitro. *Proceedings of the National Academy of Sciences* 112(12), pp. E1461–E1470. doi: 10.1073/pnas.1417100112.
- Saito, T. and Germain, R.N. 1987. Predictable acquisition of a new MHC recognition specificity following expression of a transfected T-cell receptor β -chain gene. *Nature* 329(6136), pp. 256–259. doi: 10.1038/329256a0.
- Sato, E. et al. 2005. Intraepithelial CD8+ tumor-infiltrating lymphocytes and a high CD8+/regulatory T cell ratio are associated with favorable prognosis in ovarian cancer. *Proceedings of the National Academy of Sciences of the United States of America* 102(51), pp. 18538–18543. doi: 10.1073/pnas.0509182102.
- Savoldo, B. et al. 2011. CD28 costimulation improves expansion and persistence of chimeric antigen receptor-modified T cells in lymphoma patients. *The Journal of Clinical Investigation* 121(5), pp. 1822–1826. doi: 10.1172/JCI46110.
- Sawant, D.V. et al. 2019. Adaptive plasticity of IL-10 + and IL-35 + T reg cells cooperatively promotes tumor T cell exhaustion. *Nature Immunology* 20(6), pp. 724–735. doi: 10.1038/s41590-019-0346-9.
- Scarlett, U.K. et al. 2012. Ovarian cancer progression is controlled by phenotypic changes in dendritic cells. *The Journal of Experimental Medicine* 209(3), pp. 495–506. doi: 10.1084/jem.20111413.

- Schrama, D. et al. 2001. Targeting of lymphotoxin-alpha to the tumor elicits an efficient immune response associated with induction of peripheral lymphoid-like tissue. *Immunity* 14(2), pp. 111–121. doi: 10.1016/s1074-7613(01)00094-2.
- Schroeter, E.H. et al. 1998. Notch-1 signalling requires ligand-induced proteolytic release of intracellular domain. *Nature* 393(6683), pp. 382–386. doi: 10.1038/30756.
- Simon, M.M. et al. 2000. Cytotoxic T Cells Specifically Induce Fas on Target Cells, Thereby Facilitating Exocytosis-Independent Induction of Apoptosis. *The Journal of Immunology* 165(7), pp. 3663–3672. doi: 10.4049/jimmunol.165.7.3663.
- Sinicrope, F.A. et al. 2009. Intraepithelial effector (CD3+)/regulatory (FoxP3+) T-cell ratio predicts a clinical outcome of human colon carcinoma. *Gastroenterology* 137(4), pp. 1270–1279. doi: 10.1053/j.gastro.2009.06.053.
- Smith-Garvin, J.E. et al. 2009. T Cell Activation. *Annual Review of Immunology* 27(1), pp. 591–619. doi: 10.1146/annurev.immunol.021908.132706.
- Song, D.-G. et al. 2012. CD27 costimulation augments the survival and antitumor activity of redirected human T cells in vivo. *Blood* 119(3), pp. 696–706. doi: 10.1182/blood-2011-03-344275.
- Sousa, S. et al. 2015. Human breast cancer cells educate macrophages toward the M2 activation status. *Breast cancer research: BCR* 17, p. 101. doi: 10.1186/s13058-015-0621-0.
- Spranger, S. et al. 2017. Tumor-residing Batf3 dendritic cells are required for effector T cell trafficking and adoptive T cell therapy. *Cancer cell* 31(5), pp. 711–723.e4. doi: 10.1016/j.ccell.2017.04.003.
- Streeter, P.R. et al. 1988. Immunohistologic and functional characterization of a vascular addressin involved in lymphocyte homing into peripheral lymph nodes. *Journal of Cell Biology* 107(5), pp. 1853–1862. doi: 10.1083/jcb.107.5.1853.
- Swaims, A.Y. et al. 2010. Immune activation induces immortalization of HTLV-1 LTR-Tax transgenic CD4+ T cells. *Blood* 116(16), pp. 2994–3003. doi: 10.1182/blood-2009-07-231050.
- Tape, C.J. et al. 2011. Cross-domain inhibition of TACE ectodomain. *Proceedings of the National Academy of Sciences of the United States of America* 108(14), pp. 5578–5583. doi: 10.1073/pnas.1017067108.
- Tedder, T.F. et al. 1989. Isolation and chromosomal localization of cDNAs encoding a novel human lymphocyte cell surface molecule, LAM-1. Homology with the mouse lymphocyte homing receptor and other human adhesion proteins. *The Journal of Experimental Medicine* 170(1), pp. 123–133. doi: 10.1084/jem.170.1.123.
- Terabe, M. et al. 2000. NKT cell-mediated repression of tumor immunosurveillance by IL-13 and the IL-4R-STAT6 pathway. *Nature Immunology* 1(6), pp. 515–520. doi: 10.1038/82771.

The complement binding-like domains of the murine homing receptor facilitate lectin activity. 1991. *The Journal of Cell Biology* 115(1), pp. 235–243.

Thomas, D.A. and Massagué, J. 2005. TGF- β directly targets cytotoxic T cell functions during tumor evasion of immune surveillance. *Cancer Cell* 8(5), pp. 369–380. doi: 10.1016/j.ccr.2005.10.012.

Topham, D.J. et al. 1997. CD8+ T cells clear influenza virus by perforin or Fas-dependent processes. *The Journal of Immunology* 159(11), pp. 5197–5200.

Tsukamoto, S. et al. 2014. Tetraspanin CD9 modulates ADAM17-mediated shedding of LR11 in leukocytes. *Experimental & Molecular Medicine* 46(4), p. e89. doi: 10.1038/emm.2013.161.

Varela-Rohena, A. et al. 2008. Control of HIV-1 immune escape by CD8 T-cells expressing enhanced T-cell receptor. *Nature medicine* 14(12), pp. 1390–1395. doi: 10.1038/nm.1779.

Vasconcelos, Z. et al. 2015. Individual Human Cytotoxic T Lymphocytes Exhibit Intracloonal Heterogeneity during Sustained Killing. *Cell Reports* 11(9), pp. 1474–1485. doi: 10.1016/j.celrep.2015.05.002.

Voron, T. et al. 2015. VEGF-A modulates expression of inhibitory checkpoints on CD8+ T cells in tumors. *The Journal of Experimental Medicine* 212(2), pp. 139–148. doi: 10.1084/jem.20140559.

Walunas, T.L. et al. 1994. CTLA-4 can function as a negative regulator of T cell activation. *Immunity* 1(5), pp. 405–413. doi: 10.1016/1074-7613(94)90071-x.

Wang, H. et al. 1991. Cell-surface receptor for ecotropic murine retroviruses is a basic amino-acid transporter. *Nature* 352(6337), pp. 729–731. doi: 10.1038/352729a0.

Wang, J. et al. 2019. Fibrinogen-like protein 1 is a major immune inhibitory ligand of LAG3. *Cell* 176(1–2), pp. 334–347.e12. doi: 10.1016/j.cell.2018.11.010.

Wang, R. et al. 2009. Structural Basis of the CD8 $\alpha\beta$ /MHC Class I Interaction: Focused Recognition Orients CD8 β to a T Cell Proximal Position. *The Journal of Immunology* 183(4), pp. 2554–2564. doi: 10.4049/jimmunol.0901276.

Wang, X. and Rivière, I. 2016. Clinical manufacturing of CAR T cells: foundation of a promising therapy. *Molecular Therapy - Oncolytics* 3, p. 16015. doi: 10.1038/mto.2016.15.

Watson, H.A. et al. 2019. L-Selectin Enhanced T Cells Improve the Efficacy of Cancer Immunotherapy. *Frontiers in Immunology* 10. Available at: <https://www.ncbi.nlm.nih.gov/pmc/articles/PMC6582763/> [Accessed: 8 September 2019].

Wedepohl, S. et al. 2017. Reducing Macro- and Microheterogeneity of N-Glycans Enables the Crystal Structure of the Lectin and EGF-Like Domains of Human L-Selectin To Be Solved at 1.9 Å Resolution. *ChemBioChem* 18(13), pp. 1338–1345. doi: 10.1002/cbic.201700220.

van de Weyer, P.S. et al. 2006. A highly conserved tyrosine of Tim-3 is phosphorylated upon stimulation by its ligand galectin-9. *Biochemical and Biophysical Research Communications* 351(2), pp. 571–576. doi: 10.1016/j.bbrc.2006.10.079.

Wing, K. et al. 2008. CTLA-4 Control over Foxp3+ Regulatory T Cell Function. *Science* 322(5899), pp. 271–275. doi: 10.1126/science.1160062.

Wolchok, J.D. et al. 2016. Updated results from a phase III trial of nivolumab (NIVO) combined with ipilimumab (IPI) in treatment-naive patients (pts) with advanced melanoma (MEL) (CheckMate 067). *Journal of Clinical Oncology* 34(15_suppl), pp. 9505–9505. doi: 10.1200/JCO.2016.34.15_suppl.9505.

Wooldridge, L. et al. 2005. Interaction between the CD8 Coreceptor and Major Histocompatibility Complex Class I Stabilizes T Cell Receptor-Antigen Complexes at the Cell Surface. *The Journal of biological chemistry* 280(30), pp. 27491–27501. doi: 10.1074/jbc.M500555200.

Worbs, T. et al. 2007. CCR7 ligands stimulate the intranodal motility of T lymphocytes in vivo. *The Journal of Experimental Medicine* 204(3), pp. 489–495. doi: 10.1084/jem.20061706.

Xu, F. et al. 2014. LSECtin expressed on melanoma cells promotes tumor progression by inhibiting antitumor T-cell responses. *Cancer Research* 74(13), pp. 3418–3428. doi: 10.1158/0008-5472.CAN-13-2690.

Xu, T. et al. 2008. Critical role of Lck in L-selectin signaling induced by sulfatides engagement. *Journal of Leukocyte Biology* 84(4), pp. 1192–1201. doi: 10.1189/jlb.0208084.

Yamamoto, A. et al. 1998. Bafilomycin A1 prevents maturation of autophagic vacuoles by inhibiting fusion between autophagosomes and lysosomes in rat hepatoma cell line, H-4-II-E cells. *Cell Structure and Function* 23(1), pp. 33–42. doi: 10.1247/csf.23.33.

Yáñez-Muñoz, R.J. et al. 2006. Effective gene therapy with nonintegrating lentiviral vectors. *Nature Medicine* 12(3), pp. 348–353. doi: 10.1038/nm1365.

Yang, S. et al. 2011a. The Shedding of CD62L (L-Selectin) Regulates the Acquisition of Lytic Activity in Human Tumor Reactive T Lymphocytes. *PLOS ONE* 6(7), p. e22560. doi: 10.1371/journal.pone.0022560.

Yang, S. et al. 2011b. The Shedding of CD62L (L-Selectin) Regulates the Acquisition of Lytic Activity in Human Tumor Reactive T Lymphocytes. *PLOS ONE* 6(7), p. e22560. doi: 10.1371/journal.pone.0022560.

Ying, Z. et al. 2019. Parallel Comparison of 4-1BB or CD28 Co-stimulated CD19-Targeted CAR-T Cells for B Cell Non-Hodgkin's Lymphoma. *Molecular Therapy - Oncolytics* 15, pp. 60–68. doi: 10.1016/j.omto.2019.08.002.

Youn, J.-I. et al. 2008. Subsets of Myeloid-Derived Suppressor Cells in Tumor Bearing Mice. *Journal of immunology (Baltimore, Md. : 1950)* 181(8), pp. 5791–5802.

Zaynagetdinov, R. et al. 2015. Interleukin-5 Facilitates Lung Metastasis by Modulating the Immune Microenvironment. *Cancer research* 75(8), pp. 1624–1634. doi: 10.1158/0008-5472.CAN-14-2379.

Zhang, L. et al. 2003a. Intratumoral T cells, recurrence, and survival in epithelial ovarian cancer. *The New England Journal of Medicine* 348(3), pp. 203–213. doi: 10.1056/NEJMoa020177.

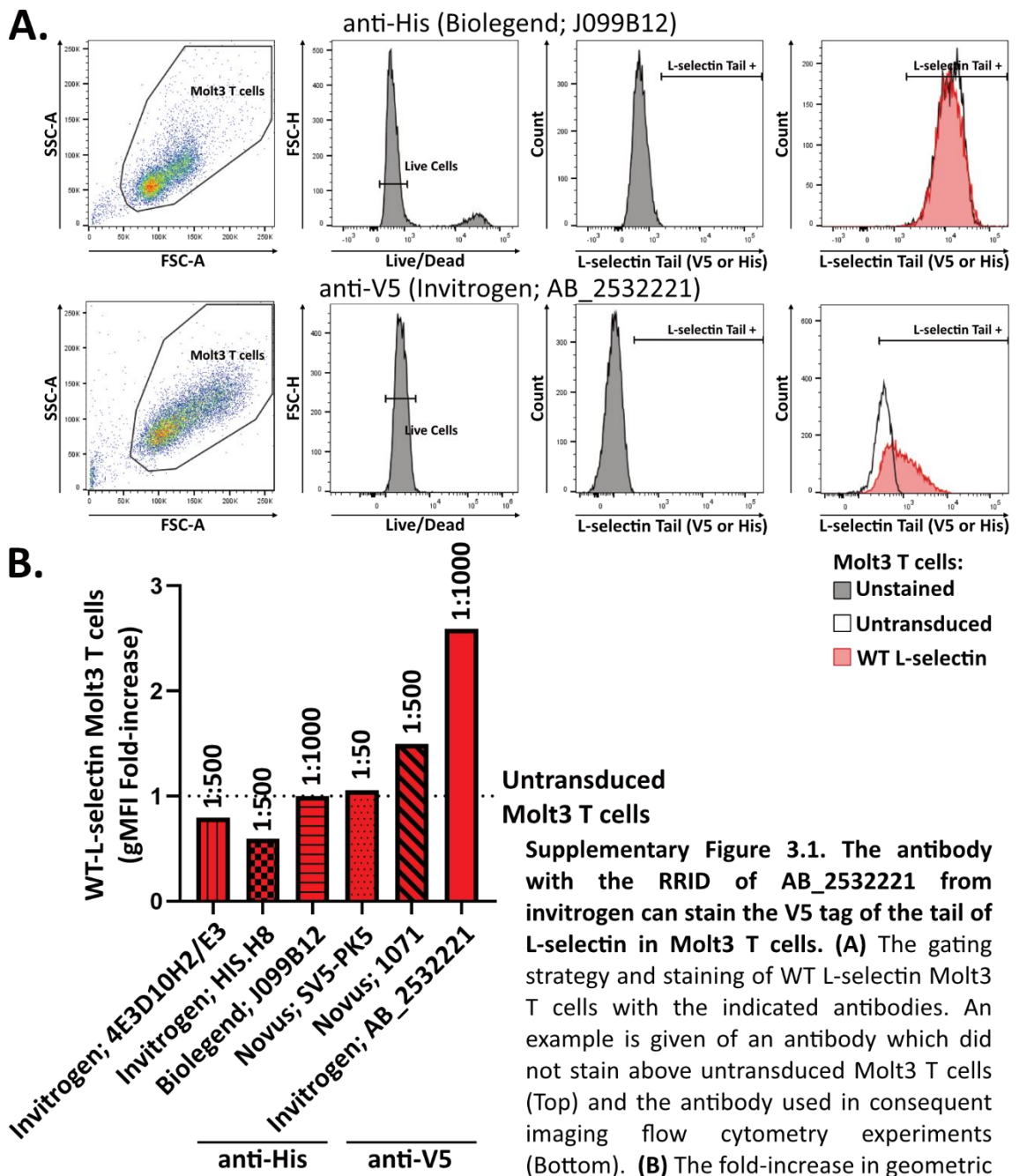
Zhang, Q. et al. 2012. Prognostic Significance of Tumor-Associated Macrophages in Solid Tumor: A Meta-Analysis of the Literature. *PLoS ONE* 7(12). Available at: <https://www.ncbi.nlm.nih.gov/pmc/articles/PMC3532403/> [Accessed: 5 August 2020].

Zhang, T. et al. 2003b. Efficient Transduction of Murine Primary T Cells Requires a Combination of High Viral Titer, Preferred Tropism, and Proper Timing of Transduction. *Journal of Hematotherapy & Stem Cell Research* 12(1), pp. 123–130. doi: 10.1089/152581603321210208.

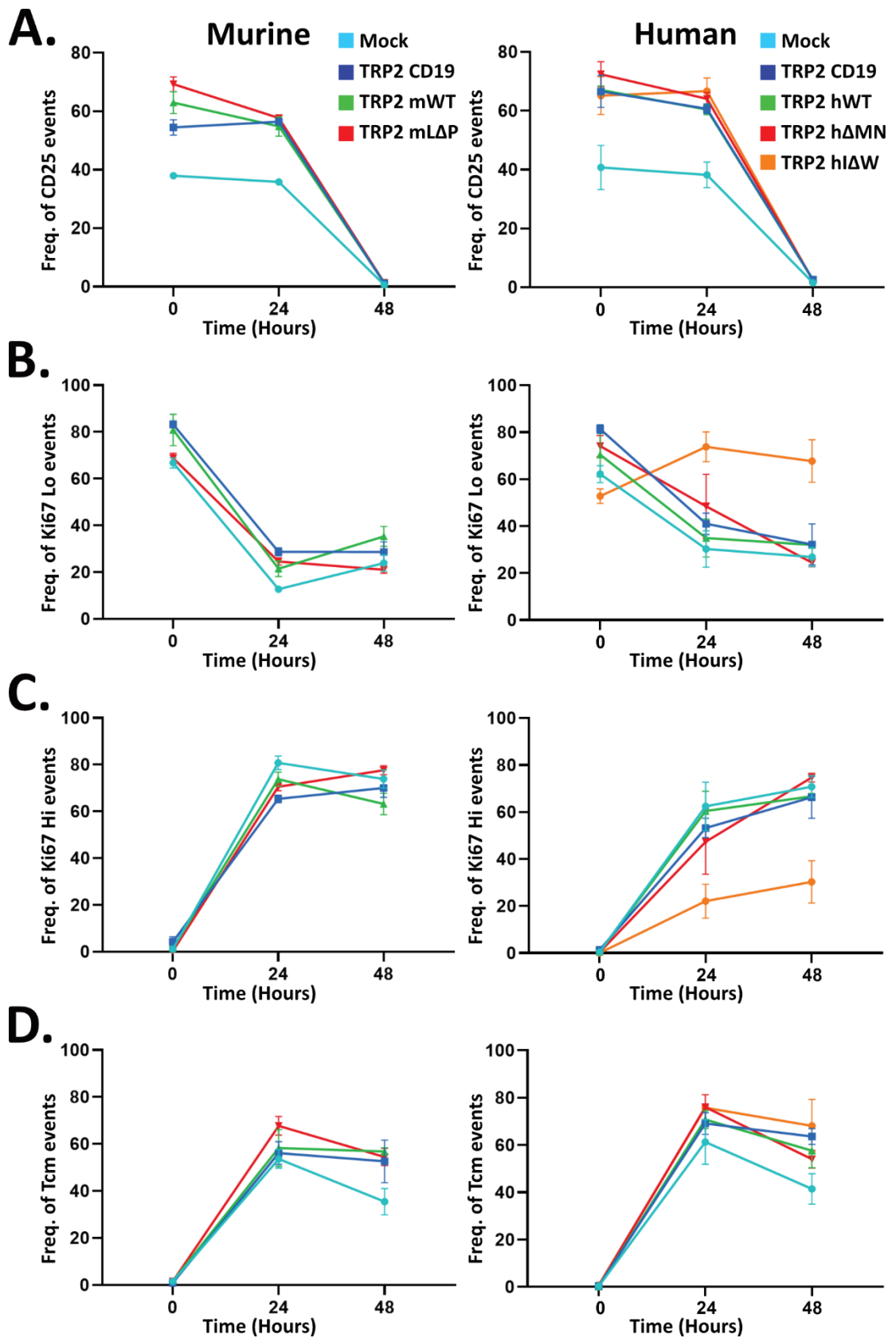
Zhang, W. et al. 1998. LAT: The ZAP-70 Tyrosine Kinase Substrate that Links T Cell Receptor to Cellular Activation. *Cell* 92(1), pp. 83–92. doi: 10.1016/S0092-8674(00)80901-0.

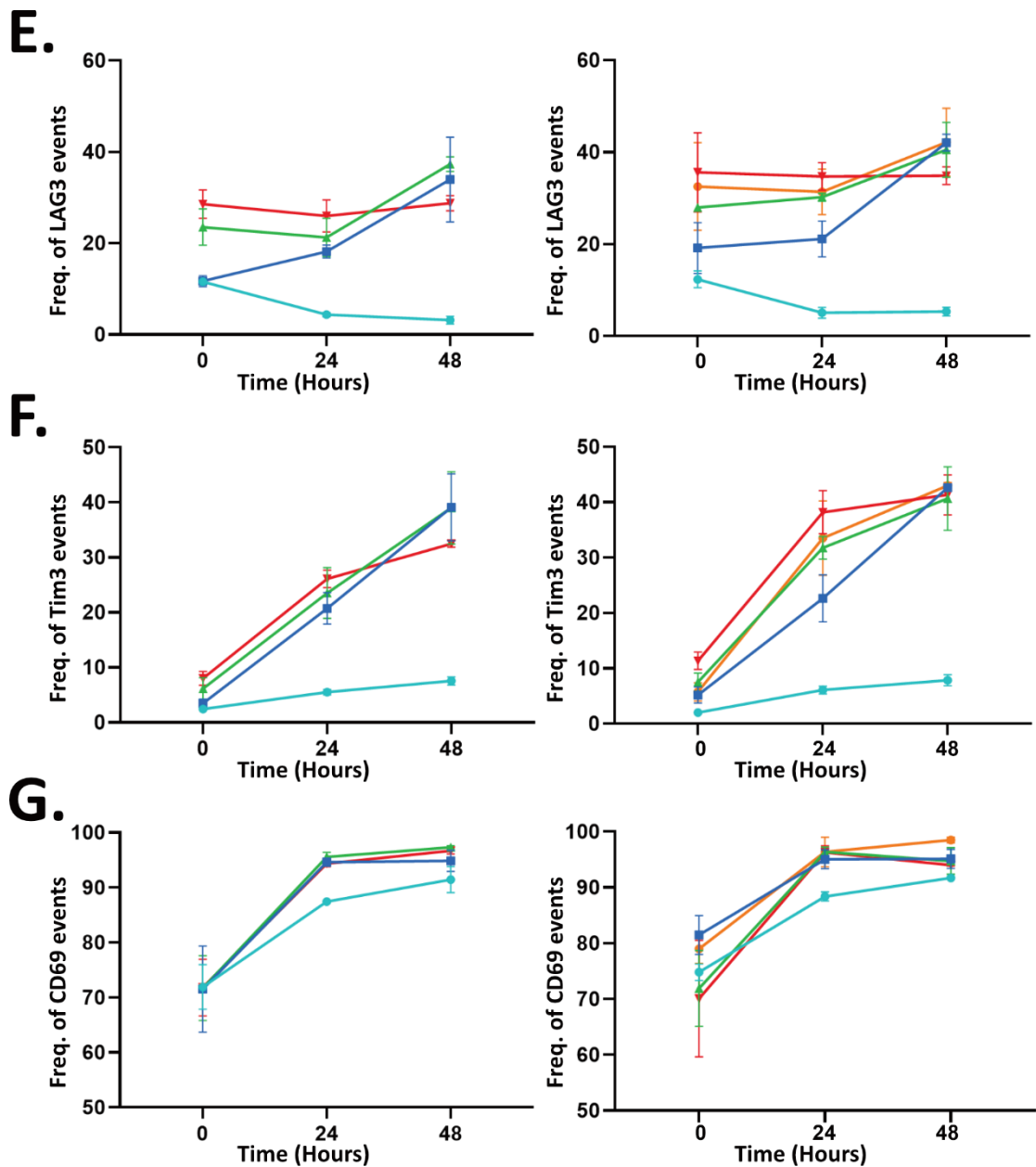
Zhao, L. et al. 2001. Regulation of Membrane Metalloproteolytic Cleavage of L-selectin (CD62L) by the Epidermal Growth Factor Domain. *Journal of Biological Chemistry* 276(33), pp. 30631–30640. doi: 10.1074/jbc.M103748200.

Appendix I: Supplementary figures



Supplementary Figure 3.1. The antibody with the RRID of AB_2532221 from invitrogen can stain the V5 tag of the tail of L-selectin in Molt3 T cells. (A) The gating strategy and staining of WT L-selectin Molt3 T cells with the indicated antibodies. An example is given of an antibody which did not stain above untransduced Molt3 T cells (Top) and the antibody used in consequent imaging flow cytometry experiments (Bottom). (B) The fold-increase in geometric mean fluorescence intensity (gMFI) of each tested antibody in Molt3 T cells expressing WT L-selectin over untransduced cells. Dilutions are shown above each bar and are the best result for each antibody in the range of 1:10 to 1:5000. n=1.





Supplementary Figure 4.1. Multi-parameter flow cytometry phenotype markers of TRP2 expressing T cells during target cell killing. In the main text for murine CD8 T cells expressing TRP2 and L-selectin, if a marker was not shown for both species of L-selectin or at all, it is shown here. The populations plotted are: **(A)** CD25 +, **(B)** Ki67 Lo, **(C)** Ki67 Hi, **(D)** Tcm (CD44 +, CD27 +), **(E)** LAG3 +, **(F)** Tim3 + **(G)** CD69 +. n=3.

Appendix II: Vector sequences

The sequences which encode untagged and tagged variants of L-selectin are highlighted in red. The sequences which encode a molecule that confers cancer-specificity to T cells is highlighted in blue.

pLenti-hWT-L-selectin

CTTTAAGACCAATGACTTACAAGGCAGCTGTAGATCTTAGCCACTTTTTAAAAGAAAAGGGG
GGACTGGAAGGGCTAATCACTCCCAACGAAGACAAGATCTGCTTTTTGCTTGTACTGGGTC
TCTCTGGTTAGACCAGATCTGAGCCTGGGAGCTCTCTGGCTAACTAGGGAACCCACTGCTTA
AGCCTCAATAAAGCTTGCCTTGAGTGCTTCAAGTAGTGTGTGCCCGTCTGTTGTGTGACTCT
GGTAACTAGAGATCCCTCAGACCCTTTTAGTCAGTGTGGAAAATCTCTAGCAGCATCTAGAA
TTAATTCCGTGTATTCTATAGTGTACCTAAATCGTATGTGTATGATACATAAGGTTATGTAT
TAATTGTAGCCGCGTTCTAACGACAATATGTACAAGCCTAATTGTGTAGCATCTGGCTTACT
GAAGCAGACCCTATCATCTCTCTCGTAAACTGCCGTCAGAGTCGGTTTGGTTGGACGAACCT
TCTGAGTTTCTGGTAACGCCGTCGCCGACCCGGAATGGTCAGCGAACCAATCAGCAGGGT
CATCGCTAGCCAGATCCTCTACGCCGACGCATCGTGGCCGGCATCACCGGCGCCACAGGT
GCGGTTGCTGGCGCCTATATCGCCGACATCACCGATGGGGAAGATCGGGCTCGCCACTTCG
GGCTCATGAGCGCTTGTTTCGGCGTGGGTATGGTGGCAGGCCCGTGGCCGGGGGACTGT
TGGGCGCCATCTCCTTGCATGCACCATTCTTGCGGCGGCGGTGCTCAACGGCCTCAACCTA
CTACTGGGCTGCTTCTAATGCAGGAGTCGCATAAGGGAGAGCGTCAATGGTGCCTCTC
AGTACAATCTGCTCTGATGCCGCATAGTTAAGCCAGCCCCGACACCCGCCAACACCCGCTGA
CGCGCCCTGACGGGCTTGTCTGCTCCCGCATCCGCTTACAGACAAGCTGTGACCGTCTCCG
GGAGCTGCATGTGTCAGAGGTTTTACCGTCATCACCGAAACGCGCGAGACGAAAGGGCCT
CGTGATACGCCTATTTTTATAGGTTAATGTCATGATAATAATGGTTTCTTAGACGTCAGGTG
GCACTTTTCGGGGAATGTGCGCGGAACCCCTATTTGTTATTTTTCTAAATACATTCAAATA
TGTATCCGCTCATGAGACAATAACCCTGATAAATGCTTCAATAATATTGAAAAAGGAAGAGT
ATGAGTATTCAACATTTCCGTGTCGCCCTTATCCCTTTTTGCGGCATTTTGCCTTCTGTTT
TTGCTCACCCAGAAACGCTGGTGAAAGTAAAAGATGCTGAAGATCAGTTGGGTGCACGAGT
GGGTTACATCGAACTGGATCTCAACAGCGGTAAGATCCTTGAGAGTTTTCGCCCCGAAGAA
CGTTTTCCAATGATGAGCACTTTTAAAGTTCTGCTATGTGGCGCGGTATTATCCCGTATTGAC
GCCGGCAAGAGCAACTCGGTCGCCGCATACACTATTCTCAGAATGACTTGGTTGAGTACT
CACCAGTCACAGAAAAGCATCTTACGGATGGCATGACAGTAAGAGAATTATGCAGTGCTGC

CATAACCATGAGTGATAAACTGCGGCCAACTTACTTCTGACAACGATCGGAGGACCGAAG
GAGCTAACCGCTTTTTTGCACAACATGGGGGATCATGTAACCTCGCCTTGATCGTTGGGAACC
GGAGCTGAATGAAGCCATACCAAACGACGAGCGTGACACCACGATGCCTGTAGCAATGGC
AACAAACGTTGCGCAAACCTATTAACCTGGCGAACTACTTACTCTAGCTTCCCGGCAACAATTA
TAGACTGGATGGAGGCGGATAAAGTTGCAGGACCACTTCTGCGCTCGGCCCTCCGGCTGG
CTGGTTTATTGCTGATAAATCTGGAGCCGGTGAGCGTGGGTCTCGCGGTATCATTGCAGCA
CTGGGGCCAGATGGTAAGCCCTCCCGTATCGTAGTTATCTACACGACGGGGAGTCAGGCAA
CTATGGATGAACGAAATAGACAGATCGCTGAGATAGGTGCCTCACTGATTAAGCATTGGTA
ACTGTCAGACCAAGTTTACTCATATATACTTTAGATTGATTTAAACTTCATTTTTAATTTAA
AGGATCTAGGTGAAGATCCTTTTTGATAATCTCATGACCAAATCCCTAACGTGAGTTTTC
GTTCCACTGAGCGTCAGACCCCGTAGAAAAGATCAAAGGATCTTCTTGAGATCCTTTTTTTCT
GCGCGTAATCTGCTGCTTGCAAACAAAAAACCACCGCTACCAGCGGTGGTTTGTGGCCG
GATCAAGAGCTACCAACTCTTTTTCCGAAGGTAACCTGGCTTCAGCAGAGCGCAGATACCAA
ATACTGTCCTTCTAGTGTAGCCGTAGTTAGGCCACCACTTCAAGAACTCTGTAGCACCGCCT
ACATACCTCGCTCTGCTAATCCTGTTACCAGTGGCTGCTGCCAGTGGCGATAAGTCGTGTCT
TACCGGGTTGGACTCAAGACGATAGTTACCGGATAAGGCGCAGCGGTCCGGCTGAACGGG
GGGTTTCGTGCACACAGCCAGCTTGGAGCGAACGACCTACACCGAACTGAGATACCTACAG
CGTGAGCATTGAGAAAGCGCCACGCTTCCCGAAGGGAGAAAGGCGGACAGGTATCCGGTA
AGCGGCAGGGTCCGGAACAGGAGAGCGCACGAGGGAGCTTCCAGGGGGAAACGCCTGGTA
TCTTTATAGTCCTGTCCGGTTTTCGCCACCTCTGACTTGAGCGTCGATTTTTGTGATGCTCGTC
AGGGGGGCGGAGCCTATGGAAAAACGCCAGCAACGCGGCCTTTTTACGGTTCCTGGCCTTT
TGCTGGCCTTTTGCTCACATGTTCTTTCCTGCGTTATCCCCTGATTCTGTGGATAACCGTATTA
CCGCCTTTGAGTGAGCTGATACCGCTCGCCGACCCGAACGACCGAGCGCAGCGAGTCAGT
GAGCGAGGAAGCGGAAGAGCGCCCAATACGCAAACCGCCTCTCCCCGCGGTTGGCCGAT
TCATTAATGCAGCTGTGGAATGTGTGTCAGTTAGGGTGTGGAAAGTCCCCAGGCTCCCCAG
CAGGCAGAAGTATGCAAAGCATGCATCTCAATTAGTCAGCAACCAGGTGTGGAAAGTCCCC
AGGCTCCCCAGCAGGCAGAAGTATGCAAAGCATGCATCTCAATTAGTCAGCAACCATAGTC
CCGCCCTAACTCCGCCCATCCCGCCCCTAACTCCGCCAGTTCGCCCATTTCTCCGCCCAT
GGCTGACTAATTTTTTTTATTTATGCAGAGGCCGAGGCCGCCTCGGCCTCTGAGCTATTCCA
GAAGTAGTGAGGAGGCTTTTTTGGAGGCCTAGGCTTTTGCAAAAAGCTTGGACACAAGACA
GGCTTGCGAGATATGTTTGAGAATAACCACTTTATCCCGCGTCAGGGAGAGGCAGTGCGTAA
AAAGACGCGGACTCATGTGAAATACTGGTTTTTATGTCGCCAGATCTCTATAATCTCGCGCA

ACCTATTTTCCCCTCGAACACTTTTTAAGCCGTAGATAAACAGGCTGGGACACTTCACATGA
GCGAAAAATACATCGTCACCTGGGACATGTTGCAGATCCATGCACGTAAACTCGCAAGCCG
ACTGATGCCTTCTGAACAATGGAAAGGCATTATTGCCGTAAGCCGTGGCGGTCTGTACCGG
GTGCGTTACTGGCGCGTGAAGTGGGTATTCGTCATGTCGATACCGTTTGTATTTCCAGCTAC
GATCACGACAACCAGCGCGAGCTTAAAGTGCTGAAACGCGCAGAAGGCGATGGCGAAGGC
TTCATCGTTATTGATGACCTGGTGGATACCGGTGGTACTGCGGTTGCGATTCTGTAAATGTA
TCCAAAAGCGCACTTTGTCACCATCTTCGAAAACCGGCTGGTCGTCGCTGGTTGATGACT
ATGTTGTTGATATCCC GCAAGATACCTGGATTGAACAGCCGTGGGATATGGGCGTCGTATT
CGTCCCGCCAATCTCCGGTCGTAATCTTTTCAACGCCTGGCACTGCCGGGCGTTGTTCTTTT
TAACTTCAGGCGGGTTACAATAGTTTCCAGTAAGTATTCTGGAGGCTGCATCCATGACACAG
GCAAACCTGAGCGAAACCCTGTTCAAACCCCGCTTTAAACATCCTGAAACCTCGACGCTAGT
CCGCCGCTTTAATCACGGCGCACAACCGCCTGTGCAGTCGGCCCTTGATGGTAAAACCATCC
CTCACTGGTATCGCATGATTAACCGTCTGATGTGGATCTGGCGCGGCATTGACCCACGCGA
AATCCTCGACGTCCAGGCACGTATTGTGATGAGCGATGCCGAACGTACCGACGATGATTTA
TACGATACGGTGATTGGCTACCGTGGCGGCAACTGGATTTATGAGTGGGCCCCGGATCTTT
GTGAAGGAACCTTACTTCTGTGGTGTGACATAATTGGACAAACTACCTACAGAGATTTAAAG
CTCTAAGGTAAATATAAAATTTTTAAGTGTATAATGTGTTAAACTACTGATTCTAATTGTTTG
TGTATTTTAGATTCCAACCTATGGAACCTGATGAATGGGAGCAGTGGTGAATGCCTTTAATG
AGGAAAACCTGTTTTGCTCAGAAGAAATGCCATCTAGTGATGATGAGGCTACTGCTGACTCT
CAACATTCTACTCCTCCAAAAAAGAAGAGAAAGGTAGAAGACCCCAAGGACTTTTCTTCAG
AATTGCTAAGTTTTTTGAGTCATGCTGTGTTTAGTAATAGAACTCTTGCTTGCTTTGCTATTTA
CACCACAAAGGAAAAAGCTGCACTGCTATAACAAGAAAATTATGGAAAAATATTCTGTAACC
TTTATAAGTAGGCATAACAGTTATAATCATAACATACTGTTTTTTTCTTACTCCACACAGGCAT
AGAGTGTCTGCTATTAATAACTATGCTCAAAAATTGTGTACCTTTAGCTTTTTAATTTGTAAA
GGGGTTAATAAGGAATATTTGATGTATAGTGCCTTGACTAGAGATCATAATCAGCCATACCA
CATTTGTAGAGGTTTTACTTGCTTTAAAAAACCTCCCACACCTCCCCCTGAACCTGAAACATA
AAATGAATGCAATTGTTGTTGTTAACTTGTTTATTGCAGCTTATAATGGTTACAAATAAAGCA
ATAGCATCACAAATTTACAAATAAAGCATTTTTTTTCACTGCATTCTAGTTGTGGTTTGTCCA
AACTCATCAATGTATCTTATCATGTCTGGATCAACTGGATAACTCAAGCTAACCAAAAATCATC
CCAAACTCCCACCCCATACCCTATTACCACTGCCAATTACCTAGTGGTTTCATTTACTCTAAA
CCTGTGATTCTCTGAATTATTTTCATTTTAAAGAAATTGTATTTGTTAAATATGTACTACAAA
CTTAGTAGTTGGAAGGGCTAATCACTCCCAAAGAAGACAAGATATCCTTGATCTGTGGATC

TACCACACACAAGGCTACTTCCCTGATTAGCAGAACTACACACCAGGGCCAGGGGTCAGAT
ATCCACTGACCTTTGGATGGTGCTACAAGCTAGTACCAGTTGAGCCAGATAAGGTAGAAGA
GGCCAATAAAGGAGAGAACACCAGCTTGTACACCCTGTGAGCCTGCATGGGATGGATGAC
CCGGAGAGAGAAGTGTTAGAGTGGAGGTTTGACAGCCGCCTAGCATTTCATCACGTGGCCC
GAGAGCTGCATCCGGAGTACTTCAAGAAGTCTGATATCGAGCTTGCTACAAGGGACTTTC
CGCTGGGGACTTTCCAGGGAGGCGTGGCCTGGGCGGGACTGGGGAGTGCGAGCCCTCA
GATCCTGCATATAAGCAGCTGCTTTTTGCCTGTACTGGGTCTCTCTGGTTAGACCAGATCTG
AGCCTGGGAGCTCTCTGGCTAACTAGGGAACCCACTGCTTAAGCCTCAATAAAGCTTGCCTT
GAGTGCTTCAAGTAGTGTGTGCCCGTCTGTTGTGTGACTCTGGTAACTAGAGATCCCTCAGA
CCCTTTTAGTCAGTGTGAAAATCTCTAGCAGTGGCGCCCGAACAGGGACTTGAAAGCGAA
AGGGAAACCAGAGGAGCTCTCTGACGCAGGACTCGGCTTGCTGAAGCGCGCACGGCAAG
AGGCGAGGGGCGGCGACTGGTGAGTACGCCAAAATTTTACTAGCGGAGGCTAGAAGG
AGAGAGATGGGTGCGAGAGCGTCAGTATTAAGCGGGGAGAATTAGATCGCGATGGGAA
AAAATTCGGTTAAGGCCAGGGGAAAGAAAAAATATAAATTAAAACATATAGTATGGGCA
AGCAGGGAGCTAGAACGATTCGCAGTTAATCCTGGCCTGTTAGAAACATCAGAAGGCTGTA
GACAAATACTGGGACAGCTACAACCATCCCTTCAGACAGGATCAGAAGAACTTAGATCATT
ATATAACAGTAGCAACCCTCTATTGTGTGCATCAAAGGATAGAGATAAAAGACACCAAG
GAAGCTTTAGACAAGATAGAGGAAGAGCAAAACAAAAGTAAGACCACCGCACAGCAAGCG
GCCGCTGATCTTCAGACCTGGAGGAGGAGATATGAGGGACAATTGGAGAAGTGAATTATA
TAAATATAAAGTAGTAAAAATTGAACCATTAGGAGTAGCACCCACCAAGGCAAAGAGAAGA
GTGGTGCAGAGAGAAAAAGAGCAGTGGGAATAGGAGCTTTGTTCCCTGGGTTCTTGGGA
GCAGCAGGAAGCACTATGGGCGCAGCGTCAATGACGCTGACGGTACAGGCCAGACAATTA
TTGTCTGGTATAGTGCAGCAGCAGAACAATTTGCTGAGGGCTATTGAGGCGCAACAGCATC
TGTTGCAACTCACAGTCTGGGGCATCAAGCAGCTCCAGGCAAGAATCCTGGCTGTGGAAAG
ATACCTAAAGGATCAACAGCTCCTGGGGATTTGGGGTTGCTCTGGAAAACCTATTTGCACCA
CTGCTGTGCCTTGAATGCTAGTTGGAGTAATAAATCTCTGGAACAGATTTGGAATCACACG
ACCTGGATGGAGTGGGACAGAGAAATTAACAATTACACAAGCTTAATACACTCCTTAATTG
AAGAATCGCAAACCAGCAAGAAAAGAATGAACAAGAATTATTGGAATTAGATAAATGGG
CAAGTTTGTGGAATTGGTTTAAACATAACAAATTGGCTGTGGTATATAAAATTATTCATAATG
ATAGTAGGAGGCTTGGTAGGTTTAAAGAATAGTTTTTGTGCTGTACTTTCTATAGTGAATAGAGT
TAGGCAGGGATATTCACCATTATCGTTTCAGACCCACCTCCCAACCCGAGGGGACCCGACA
GGCCCGAAGGAATAGAAGAAGAAGGTGGAGAGAGAGACAGAGACAGATCCATTCGATTA

GTGAACGGATCTCGACGGTCGCCAAATGGCAGTATTCATCCACAATTTTAAAAGAAAAGGG
GGGATTGGGGGTACAGTGCAGGGGAAAGAATAGTAGACATAATAGCAACAGACATACA
AACTAAAGAATTACAAAAACAAATTACAAAAATTCAAAATTTTCGGGTTTATTACAGGGACA
GCAGAGATCCAGTTTGGATCGATAAGCTTGATATCGAATTCCTGCAGCCCCGATAAAATAAA
AGATTTTATTTAGTCTCCAGAAAAAGGGGGGAATGAAAGACCCACCTGTAGGTTTGGCAA
GCTAGCTGCAGTAACGCCATTTTGAAGGCATGGAAAAATACCAACCAAGAATAGAGAAG
TTCAGATCAAGGGCGGGTACATGAAAATAGCTAACGTTGGGCCAAACAGGATATCTGCGGT
GAGCAGTTTCGGCCCCGGCCGGGGCCAAGAACAGATGGTCACCGCAGTTTCGGCCCCGG
CCCGAGGCCAAGAACAGATGGTCCCCAGATATGGCCCAACCCTCAGCAGTTTCTTAAGACC
CATCAGATGTTTCCAGGCTCCCCAAGGACCTGAAATGACCCTGCGCCTTATTTGAATTAAC
CAATCAGCCTGCTTCTCGCTTCTGTTGCGCGCTTCTGCTTCCCGAGCTCTATAAAAGAGCTC
ACAACCCCTCACTCGGCGCGCCAGTCTCCGACAGACTGAGTCGCCGGGGGGGATCCAAA
GCCATGATATTTCCATGGAAATGTCAGAGCACCCAGAGGGACTTATGGAACATCTTCAAGTT
GTGGGGGTGGACAATGCTCTGTTGTGATTTCTGGCACATCATGGAACCGACTGCTGGACT
TACCATTATTCTGAAAAACCCATGAACTGGCAAAGGGCTAGAAGATTCTGCCGAGACAATT
ACACAGATTTAGTTGCCATACAAAACAAGGCGGAAATTGAGTATCTGGAGAAGACTCTGCC
TTTCAGTCGTTCTTACTACTGGATAGGAATCCGGAAGATAGGAGGAATATGGACGTGGGTG
GGAACCAACAAATCTCTCACTGAAGAAGCAGAGAAGTGGGGAGATGGTGAGCCCAACAAC
AAGAAGAACAAGGAGGACTGCGTGGAGATCTATATCAAGAGAAACAAAGATGCAGGCAAA
TGGAACGATGACGCTGCCACAACTAAAGGCAGCCCTCTGTTACACAGCTTCTTGCCAGCC
CTGGTCATGCAGTGGCCATGGAGAATGTGTAGAAATCATCAATAATTACACCTGCAACTGT
GATGTGGGGTACTATGGGCCCCAGTGTGAGTTTGTGATTCAGTGTGAGCCTTTGGAGGCC
CAGAGCTGGGTACCATGGACTGTACTIONCACCCTTTGGGAACTTCAGCTTCAGCTCACAGTGT
GCCTTCAGCTGCTCTGAAGGAACAACTTAACTGGGATTGAAGAAACCACCTGTGGACCAT
TTGGAACTGGTCATCTCCAGAACCAACCTGTCAAGTGATTGAGTGTGAGCCTCTATCAGCA
CCAGATTTGGGGATCATGAACTGTAGCCATCCCCTGGCCAGCTTCAGCTTTACCTCTGCATG
TACCTTCATCTGCTCAGAAGGAACTGAGTTAATTGGGAAGAAGAAAACCATTTGTGAATCAT
CTGGAATCTGGTCAAATCCTAGTCCAATATGTCAAAAATTGGACAAAAGCTTCTCAATGATT
AAGGAGGGTGATTATAACCCCTCTTCATTCCAGTGGCAGTCATGGTTACTGCATTCTCTGG
GTTGGCATTATCATTTGGCTGGCAAGGAGATTAAGAAAAGGCAAGAAATCCAAGAGAAGT
ATGAATGACCCATATCTCGAGTCTAGAGGGCCCTTCGAAGGTAAGCCTATCCCTAACCCCTCT
CCTCGGTCTCGATTCTACGCGTACCGGTTCATCATCACCATCACCATTGAGGATCCCGGGCTC

GAGAGGCCTGGTACCACGCGTGCGGCCGCGACTCTAGAGTCGACCTGCAGGCATGCAAGC
TTGATATCAAGCTTATCGATAATCAACCTCTGGATTACAAAATTTGTGAAAGATTGACTGGT
ATTCTTAACTATGTTGCTCCTTTTACGCTATGTGGATACGCTGCTTTAATGCCTTTGTATCATG
CTATTGCTTCCCGTATGGCTTTCATTTTCTCCTCCTTGATAAATCCTGGTTGCTGTCTCTTTAT
GAGGAGTTGTGGCCCGTTGTCAGGCAACGTGGCGTGGTGTGCACTGTGTTTGCTGACGCAA
CCCCACTGGTTGGGGCATTGCCACCACCTGTCAGCTCCTTCCGGGACTTTCGCTTTCCCC
TCCCTATTGCCACGGCGGAACTCATCGCCGCTGCCTTGCCCGCTGCTGGACAGGGGCTCG
GCTGTTGGGCACTGACAATTCCGTGGTGTGTCGGGGAAATCATCGTCCTTTCCTGGCTGC
TCGCCTGTGTTGCCACCTGGATTCTGCGCGGGACGTCCTTCTGCTACGTCCCTTCGGCCCTCA
ATCCAGCGGACCTTCTTCCCGCGGCTGCTGCCGGCTCTGCGGCCTTCCCGGTCTTCGCC
TTCGCCCTCAGACGAGTCGGATCTCCCTTTGGGCCGCTCCCCGCATCGATACCGTCGACCT
CGACTTTAAGACCA

pLenti-hΔMN-L-selectin

CTTTAAGACCAATGACTTACAAGGCAGCTGTAGATCTTAGCCACTTTTTAAAAGAAAAGGGG
GGACTGGAAGGGCTAATTCCTCCCAACGAAGACAAGATCTGCTTTTTGCTTGTACTGGGTC
TCTCTGGTTAGACCAGATCTGAGCCTGGGAGCTCTCTGGCTAACTAGGGAACCCACTGCTTA
AGCCTCAATAAAGCTTGCCTTGAGTGCTTCAAGTAGTGTGTGCCCGTCTGTTGTGTGACTCT
GGTAACTAGAGATCCCTCAGACCCTTTAGTCAGTGTGGAAAATCTCTAGCAGCATCTAGAA
TTAATTCGTGTATTCTATAGTGTACCTAAATCGTATGTGTATGATACATAAGGTTATGTAT
TAATTGTAGCCGCGTTCTAACGACAATATGTACAAGCCTAATTGTGTAGCATCTGGCTTACT
GAAGCAGACCCTATCATCTCTCGTAACTGCCGTCAGAGTCGGTTTGGTTGGACGAACCT
TCTGAGTTTCTGGTAACGCCGTCCCGCACCCGGAATGGTCAGCGAACCAATCAGCAGGGT
CATCGCTAGCCAGATCCTCTACGCCGACGCATCGTGGCCGGCATCACCGGCCGCCACAGGT
GCGGTTGCTGGCGCCTATATCGCCGACATCACCGATGGGGAAGATCGGGCTCGCCACTTCG
GGCTCATGAGCGCTTGTTCGGCGTGGGTATGGTGGCAGGCCCGTGGCCGGGGGACTGT
TGGGCGCCATCTCCTTGCATGCACCATTCTTGCGGCGGCGGTGCTCAACGGCCTCAACCTA
CTACTGGGCTGCTTCTAATGCAGGAGTCGCATAAGGGAGAGCGTCGAATGGTGCCTCTC
AGTACAATCTGCTCTGATGCCGCATAGTTAAGCCAGCCCCGACACCCGCCAACACCCGCTGA
CGCGCCCTGACGGGCTTGTCTGCTCCCGCATCCGCTTACAGACAAGCTGTGACCGTCTCCG
GGAGCTGCATGTGTCAGAGGTTTTACCGTCATCACCGAAACGCGCGAGACGAAAGGGCCT
CGTGATACGCCTATTTTTATAGGTTAATGTCATGATAATAATGGTTTCTTAGACGTCAGGTG

GCACTTTTCGGGGAAATGTGCGCGGAACCCCTATTTGTTTATTTTTCTAAATACATTCAAATA
TGTATCCGCTCATGAGACAATAACCCTGATAAATGCTTCAATAATATTGAAAAAGGAAGAGT
ATGAGTATTCAACATTTCCGTGTCGCCCTTATTCCCTTTTTTTCGCGGCATTTTGCCTTCCTGTTT
TTGCTCACCCAGAAACGCTGGTGAAAGTAAAGATGCTGAAGATCAGTTGGGTGCACGAGT
GGGTTACATCGAACTGGATCTCAACAGCGGTAAGATCCTTGAGAGTTTTTCGCCCCGAAGAA
CGTTTTCCAATGATGAGCACTTTTAAAGTTCTGCTATGTGGCGCGGTATTATCCCGTATTGAC
GCCGGGCAAGAGCAACTCGGTGCGCCGATACACTATTCTCAGAATGACTTGGTTGAGTACT
CACCAGTCACAGAAAAGCATCTTACGGATGGCATGACAGTAAGAGAATTATGCAGTGCTGC
CATAACCATGAGTGATAAACTGCGGCCAACTTACTTCTGACAACGATCGGAGGACCGAAG
GAGCTAACCGCTTTTTTGCACAACATGGGGGATCATGTAACCTGCCTTGATCGTTGGGAACC
GGAGCTGAATGAAGCCATACCAAACGACGAGCGTGACACCACGATGCCTGTAGCAATGGC
AACACGTTGCGCAAACCTATTAACCTGGCGAACTACTTACTCTAGCTTCCCGGCAACAATTA
TAGACTGGATGGAGGCGGATAAAGTTGCAGGACCACTTCTGCGCTCGGCCCTCCGGCTGG
CTGGTTTATTGCTGATAAATCTGGAGCCGGTGAGCGTGGGTCTCGCGGTATCATTGCAGCA
CTGGGGCCAGATGGTAAGCCCTCCCGTATCGTAGTTATCTACACGACGGGGAGTCAGGCAA
CTATGGATGAACGAAATAGACAGATCGCTGAGATAGGTGCCTCACTGATTAAGCATTGGTA
ACTGTCAGACCAAGTTTACTCATATATACTTTAGATTGATTTAAAACCTCATTTTTAATTTAAA
AGGATCTAGGTGAAGATCCTTTTTGATAATCTCATGACCAAATCCCTTAACGTGAGTTTTT
GTTCCACTGAGCGTCAGACCCCGTAGAAAAGATCAAAGGATCTTCTTGAGATCCTTTTTTTCT
GCGCGTAATCTGCTGCTTGCAAACAAAAAAACCACCGCTACCAGCGGTGGTTTGTGGCCG
GATCAAGAGCTACCAACTCTTTTTCCGAAGGTAACCTGGCTTCAGCAGAGCGCAGATACCAA
ATACTGTCCTTCTAGTGTAGCCGTAGTTAGGCCACCACTTCAAGAACTCTGTAGCACCGCCT
ACATACCTCGCTCTGCTAATCCTGTTACCAGTGGCTGCTGCCAGTGGCGATAAGTCGTGTCT
TACCGGGTTGGACTCAAGACGATAGTTACCGGATAAGGCGCAGCGGTGCGGGCTGAACGGG
GGGTTTCGTGCACACAGCCCAGCTTGGAGCGAACGACCTACACCGAACTGAGATACCTACAG
CGTGAGCATTGAGAAAGCGCCACGCTTCCCGAAGGGAGAAAGGCGGACAGGTATCCGGTA
AGCGGCAGGGTCGGAACAGGAGAGCGCACGAGGGAGCTTCCAGGGGGAAACGCCTGGTA
TCTTTATAGTCTGTGCGGTTTTGCCACCTCTGACTTGAGCGTCGATTTTTGTGATGCTCGTC
AGGGGGGCGGAGCCTATGGAAAAACGCCAGCAACGCGGCCTTTTTACGGTTCCTGGCCTTT
TGCTGGCCTTTTCTCACATGTTCTTTCTGCGTTATCCCTGATTCTGTGGATAACCGTATTA
CCGCCTTTGAGTGAAGCTGATACCGCTCGCCGACCGAACGACCGAGCGCAGCGAGTCAGT
GAGCGAGGAAGCGGAAGAGCGCCCAATACGCAAACCGCCTCTCCCGCGCGTTGGCCGAT

TCATTAATGCAGCTGTGGAATGTGTGTCAGTTAGGGTGTGGAAAGTCCCCAGGCTCCCCAG
CAGGCAGAAGTATGCAAAGCATGCATCTCAATTAGTCAGCAACCAGGTGTGGAAAGTCCCC
AGGCTCCCCAGCAGGCAGAAGTATGCAAAGCATGCATCTCAATTAGTCAGCAACCATAGTC
CCGCCCTAACTCCGCCATCCCGCCCCTAACTCCGCCAGTTCCGCCATTCTCCGCCCAT
GGCTGACTAATTTTTTTTATTTATGCAGAGGCCGAGGCCGCCTCGGCCTCTGAGCTATTCCA
GAAGTAGTGAGGAGGCTTTTTTGGAGGCCTAGGCTTTTGCAAAAAGCTTGGACACAAGACA
GGCTTGCGAGATATGTTTGAGAATACCACTTTATCCCGCGTCAGGGAGAGGCAGTGCGTAA
AAAGACGCGGACTCATGTGAAATACTGGTTTTTATGTCGCCAGATCTCTATAATCTCGCGCA
ACCTATTTTCCCCTCGAACACTTTTTAAGCCGTAGATAAACAGGCTGGGACACTTCACATGA
GCGAAAAATACATCGTCACCTGGGACATGTTGCAGATCCATGCACGTAAACTCGCAAGCCG
ACTGATGCCTTCTGAACAATGGAAAGGCATTATTGCCGTAAGCCGTGGCGGTCTGTACCGG
GTGCGTTACTGGCGCGTGAAGTGGGTATTCGTCATGTCGATACCGTTTGTATTTCCAGCTAC
GATCACGACAACCAGCGCGAGCTTAAAGTGCTGAAACGCGCAGAAGGCGATGGCGAAGGC
TTCATCGTTATTGATGACCTGGTGGATACCGGTGGTACTGCGGTTGCGATTTCGTGAAATGTA
TCCAAAAGCGCACTTTGTCACCATCTTCGCAAAACCGGCTGGTCGTCCGCTGGTTGATGACT
ATGTTGTTGATATCCCGCAAGATACCTGGATTGAACAGCCGTGGGATATGGGCGTCGTATT
CGTCCCGCAATCTCCGGTTCGTAATCTTTTCAACGCCTGGCACTGCCGGGCGTTGTTCTTTT
TAACTTCAGGCGGGTTACAATAGTTTCCAGTAAGTATTCTGGAGGCTGCATCCATGACACAG
GCAAACCTGAGCGAAACCCTGTTCAAACCCCGCTTTAAACATCCTGAAACCTCGACGCTAGT
CCGCCGCTTTAATCACGGCGCACAACCGCCTGTGCAGTCGGCCCTTGATGGTAAAACCATCC
CTCACTGGTATCGCATGATTAACCGTCTGATGTGGATCTGGCGCGGCATTGACCCACGCGA
AATCCTCGACGTCCAGGCACGTATTGTGATGAGCGATGCCGAACGTACCGACGATGATTTA
TACGATACGGTGATTGGCTACCGTGGCGGCAACTGGATTTATGAGTGGGCCCCGGATCTTT
GTGAAGGAACCTTACTTCTGTGGTGTGACATAATTGGACAAACTACCTACAGAGATTTAAAG
CTCTAAGGTAAATATAAAATTTTTAAGTGTATAATGTGTTAAACTACTGATTCTAATTGTTTG
TGTATTTTAGATTCCAACCTATGGAACCTGATGAATGGGAGCAGTGGTGGAAATGCCTTTAATG
AGGAAAACCTGTTTTGCTCAGAAGAAATGCCATCTAGTGATGATGAGGCTACTGCTGACTCT
CAACATTCTACTCCTCCAAAAAAGAAGAGAAAGGTAGAAGACCCCAAGGACTTTCCTTCAG
AATTGCTAAGTTTTTTGAGTCATGCTGTGTTTAGTAATAGAACTCTTGCTTGCTTTGCTATTTA
CACCACAAAGGAAAAAGCTGCACTGCTATACAAGAAAATTATGGAAAAATATTCTGTAACC
TTTATAAGTAGGCATAACAGTTATAATCATAACATACTGTTTTTTCTTACTCCACACAGGCAT
AGAGTGTCTGCTATTAATAACTATGCTCAAAAATTGTGTACCTTAGCTTTTTAATTTGTA

GGGGTTAATAAGGAATATTTGATGTATAGTGCCTTGACTAGAGATCATAATCAGCCATACCA
CATTGTAGAGGTTTTACTTGCTTTAAAAAACCTCCCACACCTCCCCCTGAACCTGAAACATA
AAATGAATGCAATTGTTGTTGTTAACTTGTTTATTGCAGCTTATAATGGTTACAAATAAAGCA
ATAGCATCACAAATTCACAAATAAAGCATTTTTTCTACTGCATTCTAGTTGTGGTTTGTCCA
AACTCATCAATGTATCTTATCATGTCTGGATCAACTGGATAACTCAAGCTAACCAAAATCATC
CCAAACTTCCCACCCCATACCCTATTACCACTGCCAATTACCTAGTGGTTTCATTTACTCTAAA
CCTGTGATTCTCTGAATTATTTTCATTTTAAAGAAATTGTATTTGTTAAATATGACTACAAA
CTTAGTAGTTGGAAGGGCTAATTCACTCCCAAAGAAGACAAGATATCCTTGATCTGTGGATC
TACCACACACAAGGCTACTTCCCTGATTAGCAGAACTACACACCAGGGCCAGGGGTCAGAT
ATCCACTGACCTTTGGATGGTGCTACAAGCTAGTACCAGTTGAGCCAGATAAGGTAGAAGA
GGCCAATAAAGGAGAGAACACCAGCTTGTTACACCCTGTGAGCCTGCATGGGATGGATGAC
CCGGAGAGAGAAGTGTTAGAGTGGAGGTTTGACAGCCGCCTAGCATTTCATCACGTGGCCC
GAGAGCTGCATCCGGAGTACTTCAAGAAGCTGCTGATATCGAGCTTGCTACAAGGGACTTTC
CGCTGGGGACTTTCCAGGGAGGCGTGGCCTGGGCGGGACTGGGGAGTGGCGAGCCCTCA
GATCCTGCATATAAGCAGCTGCTTTTTGCCTGTAAGTGGTCTCTCTGGTTAGACCAGATCTG
AGCCTGGGAGCTCTCTGGCTAACTAGGGAACCCACTGCTTAAGCCTCAATAAAGCTTGCCTT
GAGTGCTTCAAGTAGTGTGTGCCGTCTGTTGTGTGACTCTGGTAACTAGAGATCCCTCAGA
CCCTTTTAGTCAGTGTGGAAAATCTCTAGCAGTGGCGCCCGAACAGGGACTTGAAAGCGAA
AGGGAAACCAGAGGAGCTCTCTGACGCAGGACTCGGCTTGCTGAAGCGCGCACGGCAAG
AGGCGAGGGGCGGCGACTGGTGAGTACGCCAAAATTTTACTAGCGGAGGCTAGAAGG
AGAGAGATGGGTGCGAGAGCGTCAGTATTAAGCGGGGAGAATTAGATCGCGATGGGAA
AAAATTCGGTTAAGGCCAGGGGGAAAGAAAAAATATAAATTAACATATAGTATGGGCA
AGCAGGGAGCTAGAACGATTCGCAGTTAATCCTGGCCTGTTAGAAACATCAGAAGGCTGTA
GACAAATACTGGGACAGCTACAACCATCCCTTCAGACAGGATCAGAAGAACTTAGATCATT
ATATAATACAGTAGCAACCCTCTATTGTGTGCATCAAAGGATAGAGATAAAAGACACCAAG
GAAGCTTTAGACAAGATAGAGGAAGAGCAAAACAAAAGTAAGACCACCGCACAGCAAGCG
GCCGCTGATCTTCAGACCTGGAGGAGGAGATATGAGGGACAATTGGAGAAGTGAATTATA
TAAATATAAAGTAGTAAAAATTGAACCATTAGGAGTAGCACCCACCAAGGCAAAGAGAAGA
GTGGTGCAGAGAGAAAAAGAGCAGTGGGAATAGGAGCTTTGTTCCCTGGGTTCTTGGGA
GCAGCAGGAAGCACTATGGGCGCAGCGTCAATGACGCTGACGGTACAGGCCAGACAATTA
TTGTCTGGTATAGTGCAGCAGCAGAACAATTTGCTGAGGGCTATTGAGGCGCAACAGCATC
TGTTGCAACTCACAGTCTGGGGCATCAAGCAGCTCCAGGCAAGAATCCTGGCTGTGGAAAG

ATACCTAAAGGATCAACAGCTCCTGGGGATTTGGGGTTGCTCTGGAAAACCTCATTTGCACCA
CTGCTGTGCCTTGGAATGCTAGTTGGAGTAATAAATCTCTGGAACAGATTTGGAATCACACG
ACCTGGATGGAGTGGGACAGAGAAATTAACAATTACACAAGCTTAATACACTCCTTAATTG
AAGAATCGCAAACCAGCAAGAAAAGAATGAACAAGAATTATTGGAATTAGATAAATGGG
CAAGTTTGTGGAATTGGTTTAAACATAACAAATTGGCTGTGGTATATAAAATTATTCATAATG
ATAGTAGGAGGCTTGGTAGGTTTAAAGAATAGTTTTTGGCTGTACTTTCTATAGTGAATAGAGT
TAGGCAGGGATATTCACCATTATCGTTTCAGACCCACCTCCCAACCCCGAGGGGACCCGACA
GGCCCGAAGGAATAGAAGAAGAAGGTGGAGAGAGAGACAGAGACAGATCCATTTCGATTA
GTGAACGGATCTCGACGGTCGCCAAATGGCAGTATTCATCCACAATTTTAAAAGAAAAGGG
GGGATTGGGGGTACAGTGCAGGGGAAAGAATAGTAGACATAATAGCAACAGACATACA
AACTAAAGAATTACAAAAACAAATTACAAAAATTCAAATTTTCGGGTTTATTACAGGGACA
GCAGAGATCCAGTTTGGATCGATAAGCTTGATATCGAATTCCTGCAGCCCCGATAAAATAAA
AGATTTTATTTAGTCTCCAGAAAAAGGGGGGAATGAAAGACCCACCTGTAGGTTTGGCAA
GCTAGCTGCAGTAACGCCATTTTGAAGGCATGGAAAAATACCAAACCAAGAATAGAGAAG
TTCAGATCAAGGGCGGGTACATGAAAATAGCTAACGTTGGGCCAAACAGGATATCTGCGGT
GAGCAGTTTCGGCCCCGGCCGGGGCCAAGAACAGATGGTCACCGCAGTTTCGGCCCCGG
CCCGAGGCCAAGAACAGATGGTCCCCAGATATGGCCCAACCCTCAGCAGTTTCTTAAGACC
CATCAGATGTTTCCAGGCTCCCCAAGGACCTGAAATGACCCTGCGCCTTATTTGAATTAAC
CAATCAGCCTGCTTCTCGCTTCTGTTGCGCGCTTCTGCTTCCCGAGCTCTATAAAAGAGCTC
ACAACCCTCACTCGGCGCGCCAGTCCTCCGACAGACTGAGTCGCCCGGGGGGATCCAAA
GCCATGATATTTCCATGGAAATGTCAGAGCACCCAGAGGGACTTATGGAACATCTTCAAGTT
GTGGGGGTGGACAATGCTCTGTTGTGATTTCTGGCACATCATGGAACCGACTGCTGGACT
TACCATTATTCTGAAAAACCCATGAACTGGCAAAGGGCTAGAAGATTCTGCCGAGACAATT
ACACAGATTTAGTTGCCATACAAAACAAGGCGGAAATTGAGTATCTGGAGAAGACTCTGCC
TTTCAGTCGTTCTTACTACTGGATAGGAATCCGGAAGATAGGAGGAATATGGACGTGGGTG
GGAACCAACAAATCTCTCACTGAAGAAGCAGAGAAGTGGGGAGATGGTGAGCCCAACAAC
AAGAAGAACAAGGAGGACTGCGTGGAGATCTATATCAAGAGAAACAAAGATGCAGGCAA
TGGAACGATGACGCTGCCACAACTAAAGGCAGCCCTCTGTTACACAGCTTCTTGCCAGCC
CTGGTCATGCAGTGGCCATGGAGAATGTGTAGAAATCATCAATAATTACACCTGCAACTGT
GATGTGGGGTACTATGGGCCCCAGTGTGAGTTTGTGATTCAGTGTGAGCCTTTGGAGGCC
CAGAGCTGGGTACCATGGACTGTAICTACCCTTTGGGAACTTCAGCTTCAGCTCACAGTGT
GCCTTCAGCTGCTCTGAAGGAACAACTTAACTGGGATTGAAGAAACCACCTGTGGACCAT

TTGGAAACTGGTCATCTCCAGAACCAACCTGTCAAGTGATTAGTGTGAGCCTCTATCAGCA
CCAGATTTGGGGATCATGAACTGTAGCCATCCCCTGGCCAGCTTCAGCTTTACCTCTGCATG
TACCTTCATCTGCTCAGAAGGAACTGAGTTAATTGGGAAGAAGAAAACCATTTGTGAATCAT
CTGGAATCTGGTCAAATCCTAGTCCAATATGTCAAAAATTGGACAAAAGCTTCTCACCCCTCT
TCATTCCAGTGGCAGTCATGGTTACTGCATTCTCTGGGTTGGCATTATCATTGGCTGGCAA
GGAGATTAATAAAGGCAAGAAATCCAAGAGAAGTATGAATGACCCATATCTCGAGTCTA
GAGGGCCCTTCGAAGGTAAGCCTATCCCTAACCTCTCCTCGGTCTCGATTCTACGCGTACC
GGTCATCATCACCATCACCAATTGAGGATCCCAGGCTCGAGAGGCCTGGTACCACGCGTGCG
GCCGCGACTCTAGAGTCGACCTGCAGGCATGCAAGCTTGATATCAAGCTTATCGATAATCAA
CCTCTGGATTACAAAATTTGTGAAAGATTGACTGGTATTCTTAACTATGTTGCTCCTTTTACG
CTATGTGGATACGCTGCTTTAATGCCTTTGTATCATGCTATTGCTTCCCGTATGGCTTTCATTT
TCTCCTCCTGTATAAATCCTGGTTGCTGTCTTTATGAGGAGTTGTGGCCCGTTGTCAGGC
AACGTGGCGTGGTGTGCACTGTGTTGCTGACGCAACCCCCACTGGTTGGGGCATTGCCAC
CACCTGTCAGCTCCTTCCGGGACTTTCGCTTTCCCCCTCCCTATTGCCACGGCGGAACTCAT
CGCCGCTGCCTTGCCCGCTGCTGGACAGGGGCTCGGCTGTTGGGCACTGACAATTCCGTG
GTGTTGTCGGGGAAATCATCGTCCTTTCCTGGCTGCTCGCCTGTGTTGCCACCTGGATTCT
GCGCGGGACGTCCTTCTGCTACGTCCCTTCGGCCCTCAATCCAGCGGACCTTCTTCCCGCG
GCCTGCTGCCGGCTCTGCGGCCTTTCGCGTCTTCGCCTTCGCCCTCAGACGAGTCGGATC
TCCCTTTGGGCCGCTCCCCGCATCGATACCGTCGACCTCGACTTTAAGACCA

pLenti-IDW-L-selectin

CTTTAAGACCAATGACTTACAAGGCAGCTGTAGATCTTAGCCACTTTTTAAAAGAAAAGGGG
GGACTGGAAGGGCTAATCACTCCCAACGAAGACAAGATCTGCTTTTTGCTTGTACTGGGTC
TCTCTGGTTAGACCAGATCTGAGCCTGGGAGCTCTCTGGCTAACTAGGGAACCCACTGCTTA
AGCCTCAATAAAGCTTGCCTTGAGTGCTTCAAGTAGTGTGTGCCCGTCTGTTGTGTGACTCT
GGTAACTAGAGATCCCTCAGACCCTTTTAGTCAGTGTGGAAAATCTCTAGCAGCATCTAGAA
TTAATTCCGTGTATTCTATAGTGTACCTAAATCGTATGTGTATGATACATAAGGTTATGTAT
TAATTGTAGCCGCTTCTAACGACAATATGTACAAGCCTAATTGTGTAGCATCTGGCTTACT
GAAGCAGACCCTATCATCTCTCTCGTAAACTGCCGTCAGAGTCGGTTTGGTTGGACGAACCT
TCTGAGTTTCTGGTAACGCCGTCCCGCACCCGGAAATGGTCAGCGAACCAATCAGCAGGGT
CATCGCTAGCCAGATCCTCTACGCCGACGCATCGTGGCCGGCATCACCGGCCGCCACAGGT

GCGGTTGCTGGCGCCTATATCGCCGACATCACCGATGGGGAAGATCGGGCTCGCCACTTCCG
GGCTCATGAGCGCTTGTTCGGCGTGGGTATGGTGGCAGGCCCGTGGCCGGGGGACTGT
TGGGCGCCATCTCCTTGCATGCACCATTCTTTCGGGCGGCGGTGCTCAACGGCCTCAACCTA
CTACTGGGCTGCTTCTAATGCAGGAGTCGCATAAGGGAGAGCGTCGAATGGTGCCTCTC
AGTACAATCTGCTCTGATGCCGCATAGTTAAGCCAGCCCCGACACCCGCCAACACCCGCTGA
CGCGCCCTGACGGGCTTGTCTGCTCCCGGCATCCGCTTACAGACAAGCTGTGACCGTCTCCG
GGAGCTGCATGTGTCAGAGGTTTTACCGTCATCACCGAAACGCGCGAGACGAAAGGGCCT
CGTGATACGCCTATTTTTATAGGTTAATGTCATGATAATAATGGTTTCTTAGACGTCAGGTG
GCACTTTTCGGGAAATGTGCGCGGAACCCCTATTTGTTATTTTTCTAAATACATTCAAATA
TGTATCCGCTCATGAGACAATAACCCTGATAAATGCTTCAATAATATTGAAAAAGGAAGAGT
ATGAGTATTCAACATTTCCGTGTCGCCCTTATTCCCTTTTTGCGGCATTTTGCCTCCTGTTT
TTGCTCACCCAGAAACGCTGGTGAAAGTAAAAGATGCTGAAGATCAGTTGGGTGCACGAGT
GGGTTACATCGAACTGGATCTCAACAGCGGTAAGATCCTTGAGAGTTTTCGCCCCGAAGAA
CGTTTTCCAATGATGAGCACTTTTAAAGTTCTGCTATGTGGCGCGGTATTATCCCGTATTGAC
GCCGGGCAAGAGCAACTCGGTCGCCGCATACACTATTCTCAGAATGACTTGGTTGAGTACT
CACCAGTCACAGAAAAGCATCTTACGGATGGCATGACAGTAAGAGAATTATGCAGTGCTGC
CATAACCATGAGTGATAAACTGCGGCCAACTTACTTCTGACAACGATCGGAGGACCGAAG
GAGCTAACCGCTTTTTTGACAACATGGGGGATCATGTAACCTGCCTTGATCGTTGGGAACC
GGAGCTGAATGAAGCCATACCAAACGACGAGCGTGACACCACGATGCCTGTAGCAATGGC
AACACGTTGCGCAAACCTATTAACCTGGCGAACTACTTACTCTAGCTTCCCGGCAACAATTAA
TAGACTGGATGGAGGCGGATAAAGTTGCAGGACCACTTCTGCGCTCGGCCCTCCGGCTGG
CTGGTTTATTGCTGATAAATCTGGAGCCGGTGAGCGTGGGTCTCGCGGTATCATTGCAGCA
CTGGGGCCAGATGGTAAGCCCTCCCGTATCGTAGTTATCTACACGACGGGGAGTCAGGCAA
CTATGGATGAACGAAATAGACAGATCGCTGAGATAGGTGCCTCACTGATTAAGCATTGGTA
ACTGTCAGACCAAGTTTACTCATATATACTTTAGATTGATTTAAAACCTCATTTTTAATTTAAA
AGGATCTAGGTGAAGATCCTTTTTGATAATCTCATGACCAAATCCCTTAACGTGAGTTTTC
GTTCCACTGAGCGTCAGACCCCGTAGAAAAGATCAAAGGATCTTCTTGAGATCCTTTTTTTCT
GCGCGTAATCTGCTGCTTGC AAACAAAAAACCACCGCTACCAGCGGTGGTTTGTTCGG
GATCAAGAGCTACCAACTCTTTTTCCGAAGGTAACCTGGCTTCAGCAGAGCGCAGATACCAA
ATACTGTCCTTCTAGTGTAGCCGTAGTTAGGCCACCACTTCAAGAACTCTGTAGCACCGCCT
ACATACCTCGCTCTGCTAATCCTGTTACCAAGTGGCTGCTGCCAGTGGCGATAAGTCGTGTCT
TACCGGGTTGGACTCAAGACGATAGTTACCGGATAAGGCGCAGCGGTGGGCTGAACGGG

GGGTTTCGTGCACACAGCCCAGCTTGGAGCGAACGACCTACACCGAACTGAGATACCTACAG
CGTGAGCATTGAGAAAGCGCCACGCTTCCCGAAGGGAGAAAGGCGGACAGGTATCCGGTA
AGCGGCAGGGTCGGAACAGGAGAGCGCACGAGGGAGCTTCCAGGGGGAAACGCCTGGTA
TCTTTATAGTCCTGTCGGGTTTTGCCACCTCTGACTTGAGCGTCGATTTTTGTGATGCTCGTC
AGGGGGGCGGAGCCTATGGAAAAACGCCAGCAACGCGGCCTTTTTACGGTTCCTGGCCTTT
TGCTGGCCTTTTGCTCACATGTTCTTTCCTGCGTTATCCCCTGATTCTGTGGATAACCGTATTA
CCGCCTTTGAGTGAGCTGATACCGCTCGCCGAGCCGAACGACCGAGCGCAGCGAGTCAGT
GAGCGAGGAAGCGGAAGAGCGCCAATACGCAAACCGCCTCTCCCCGCGCGTTGGCCGAT
TCATTAATGCAGCTGTGGAATGTGTGTCAGTTAGGGTGTGGAAAGTCCCCAGGCTCCCCAG
CAGGCAGAAGTATGCAAAGCATGCATCTCAATTAGTCAGCAACCAGGTGTGGAAAGTCCCC
AGGCTCCCCAGCAGGCAGAAGTATGCAAAGCATGCATCTCAATTAGTCAGCAACCATAGTC
CCGCCCTAACTCCGCCCATCCCGCCCCTAACTCCGCCAGTTCCGCCATTCTCCGCCCAT
GGCTGACTAATTTTTTTTATTTATGCAGAGGCCGAGGCCGCCTCGGCCTCTGAGCTATTCCA
GAAGTAGTGAGGAGGCTTTTTTTGGAGGCCTAGGCTTTTGCAAAAAGCTTGGACACAAGACA
GGCTTGCGAGATATGTTTGAGAATACTACTTTATCCCGCGTCAGGGAGAGGCAGTGCGTAA
AAAGACGCGGACTCATGTGAAATACTGGTTTTTAGTGCGCCAGATCTCTATAATCTCGCGCA
ACCTATTTTCCCCTCGAACACTTTTTAAGCCGTAGATAAACAGGCTGGGACACTTCACATGA
GCGAAAAATACATCGTCACCTGGGACATGTTGCAGATCCATGCACGTAAACTCGCAAGCCG
ACTGATGCCTTCTGAACAATGGAAAGGCATTATTGCCGTAAGCCGTGGCGGTCTGTACCGG
GTGCGTACTGGCGCGTGAACCTGGGTATTTCGTCATGTCGATACCGTTTGTATTTCCAGCTAC
GATCACGACAACCAGCGCGAGCTTAAAGTGCTGAAACGCGCAGAAGGCGATGGCGAAGGC
TTCATCGTTATTGATGACCTGGTGGATACCGGTGGTACTGCGGTTGCGATTTCGTGAAATGTA
TCCAAAAGCGCACTTTGTCACCATCTTCGCAAACCGGCTGGTCGTCGCTGGTTGATGACT
ATGTTGTTGATATCCCGCAAGATACCTGGATTGAACAGCCGTGGGATATGGGCGTCGTATT
CGTCCCGCCAATCTCCGGTCGTAATCTTTTCAACGCCTGGCACTGCCGGGCGTTGTTCTTTT
TAACTTCAGGCGGGTTACAATAGTTTCCAGTAAGTATTCTGGAGGCTGCATCCATGACACAG
GCAAACCTGAGCGAAACCCTGTTCAAACCCCGCTTTAAACATCCTGAAACCTCGACGCTAGT
CCGCCGCTTTAATCACGGCGCACAACCGCCTGTGCAGTCGGCCCTTGATGGTAAAACCATCC
CTCACTGGTATCGCATGATTAACCGTCTGATGTGGATCTGGCGCGGCATTGACCCACGCGA
AATCCTCGACGTCCAGGCACGTATTGTGATGAGCGATGCCGAACGTACCGACGATGATTTA
TACGATACGGTGATTGGCTACCGTGGCGGCAACTGGATTTATGAGTGGGCCCGGATCTTT
GTGAAGGAACCTTACTTCTGTGGTGTGACATAATTGGACAAACTACCTACAGAGATTTAAAG

CTCTAAGGTAAATATAAAATTTTTAAGTGTATAATGTGTTAAACTACTGATTCTAATTGTTTG
TGTATTTTAGATTCCAACCTATGGAAGTATGAATGGGAGCAGTGGTGGAAATGCCTTTAATG
AGGAAAACCTGTTTTGCTCAGAAGAAATGCCATCTAGTGATGATGAGGCTACTGCTGACTCT
CAACATTCTACTCCTCCAAAAAGAAGAGAAAGGTAGAAGACCCCAAGGACTTTCCTTCAG
AATTGCTAAGTTTTTTGAGTCATGCTGTGTTTAGTAATAGAAGTCTTGCTTGCTTTGCTATTTA
CACCACAAAGGAAAAAGCTGCACTGCTATAACAAGAAAATTATGGAAAAATATTCTGTAACC
TTTATAAGTAGGCATAACAGTTATAATCATAACTGTTTTTTCTTACTCCACACAGGCAT
AGAGTGTCTGCTATTAATAACTATGCTCAAAAATTGTGTACCTTAGCTTTTTAATTTGTAAA
GGGGTTAATAAGGAATATTTGATGTATAGTGCCTTGACTAGAGATCATAATCAGCCATACCA
CATTTGTAGAGGTTTTACTTGCTTTAAAAACCTCCACACCTCCCCCTGAACCTGAAACATA
AAATGAATGCAATTGTTGTTGTTAACTTGTTTATTGCAGCTTATAATGGTTACAAATAAAGCA
ATAGCATCACAAATTTACAAATAAAGCATTTTTTTCACTGCATTCTAGTTGTGGTTTGTCCA
AACTCATCAATGTATCTTATCATGTCTGGATCAACTGGATAACTCAAGCTAACCAAAATCATC
CCAAACTTCCCACCCCATACCCTATTACCACTGCCAATTACCTAGTGGTTTTCATTTACTCTAAA
CCTGTGATTCTCTGAATTATTTTCATTTTAAAGAAATTGTATTTGTTAAATATGTAATAAAA
CTTAGTAGTTGGAAGGGCTAATCACTCCCAAAGAAGACAAGATATCCTTGATCTGTGGATC
TACCACACACAAGGCTACTTCCCTGATTAGCAGAACTACACACCAGGGCCAGGGGTCAGAT
ATCCACTGACCTTTGGATGGTGCTACAAGCTAGTACCAGTTGAGCCAGATAAGGTAGAAGA
GGCCAATAAAGGAGAGAACACCAGCTTGTTACACCCTGTGAGCCTGCATGGGATGGATGAC
CCGGAGAGAGAAGTGTTAGAGTGGAGGTTTGACAGCCGCCTAGCATTTTCATCACGTGGCCC
GAGAGCTGCATCCGGAGTACTTCAAGAACTGCTGATATCGAGCTTGCTACAAGGGACTTTC
CGCTGGGGACTTTCCAGGGAGGCGTGGCCTGGGCGGGACTGGGGAGTGGCGAGCCCTCA
GATCCTGCATATAAGCAGCTGCTTTTTGCCTGTAAGTGGTCTCTCTGGTTAGACCAGATCTG
AGCCTGGGAGCTCTCTGGCTAACTAGGGAACCCACTGCTTAAGCCTCAATAAAGCTTGCCTT
GAGTGCTTCAAGTAGTGTGTGCCGTCTGTTGTGTGACTCTGGTAACTAGAGATCCCTCAGA
CCTTTTTAGTCAGTGTGGAAAATCTCTAGCAGTGGCGCCCGAACAGGGACTTGAAAGCGAA
AGGGAAACCAGAGGAGCTCTCTCGACGCAGGACTCGGCTTGCTGAAGCGCGCACGGCAAG
AGGCGAGGGGCGGCGACTGGTGAGTACGCCAAAATTTTACTAGCGGAGGCTAGAAGG
AGAGAGATGGGTGCGAGAGCGTCAGTATTAAGCGGGGAGAATTAGATCGCGATGGGAA
AAAATTCGGTTAAGGCCAGGGGAAAGAAAAAATAAATTAACATATAGTATGGGCA
AGCAGGGAGCTAGAACGATTCGAGTTAATCCTGGCCTGTTAGAAACATCAGAAGGCTGTA
GACAAATACTGGGACAGCTACAACCATCCCTTCAGACAGGATCAGAAGAACTTAGATCATT

ATATAATACAGTAGCAACCCTCTATTGTGTGCATCAAAGGATAGAGATAAAAGACACCAAG
GAAGCTTTAGACAAGATAGAGGAAGAGCAAAACAAAAGTAAGACCACCGCACAGCAAGCG
GCCGCTGATCTTCAGACCTGGAGGAGGAGATATGAGGGACAATTGGAGAAGTGAATTATA
TAAATATAAAGTAGTAAAAATTGAACCATTAGGAGTAGCACCCACCAAGGCAAAGAGAAGA
GTGGTGCAGAGAGAAAAAGAGCAGTGGGAATAGGAGCTTTGTTCCCTGGGTTCTTGGGA
GCAGCAGGAAGCACTATGGGCGCAGCGTCAATGACGCTGACGGTACAGGCCAGACAATTA
TTGTCTGGTATAGTGCAGCAGCAGAACAATTTGCTGAGGGCTATTGAGGCGCAACAGCATC
TGTTGCAACTCACAGTCTGGGGCATCAAGCAGCTCCAGGCAAGAATCCTGGCTGTGGAAAG
ATACCTAAAGGATCAACAGCTCCTGGGGATTTGGGGTTGCTCTGGAAAACCTATTTGCACCA
CTGCTGTGCCTTGAATGCTAGTTGGAGTAATAAATCTCTGGAACAGATTTGGAATCACACG
ACCTGGATGGAGTGGGACAGAGAAATTAACAATTACACAAGCTTAATACTCCTTAATTG
AAGAATCGCAAACCAGCAAGAAAAGAATGAACAAGAATTATTGGAATTAGATAAATGGG
CAAGTTTGTGAATTGGTTAACATAACAAATTGGCTGTGGTATATAAAATTATTCATAATG
ATAGTAGGAGGCTTGGTAGGTTAAGAATAGTTTTTGCTGTACTTTCTATAGTGAATAGAGT
TAGGCAGGGATATTCACCATTATCGTTTCAGACCCACCTCCCAACCCCGAGGGGACCCGACA
GGCCCGAAGGAATAGAAGAAGAAGGTGGAGAGAGAGACAGAGACAGATCCATTCGATTA
GTGAACGGATCTCGACGGTCGCCAAATGGCAGTATTCATCCACAATTTTAAAAGAAAAGGG
GGGATTGGGGGTACAGTGCAGGGGAAAGAATAGTAGACATAATAGCAACAGACATACA
AACTAAAGAATTACAAAAACAATTACAAAAATTCAAATTTTTCGGGTTTATTACAGGGACA
GCAGAGATCCAGTTTGGATCGATAAGCTTGATATCGAATTCCTGCAGCCCCGATAAAATAAA
AGATTTTATTTAGTCTCCAGAAAAAGGGGGGAATGAAAGACCCACCTGTAGGTTTGGCAA
GCTAGCTGCAGTAACGCCATTTTGAAGGCATGGAAAAATACCAAACCAAGAATAGAGAAG
TTCAGATCAAGGGCGGGTACATGAAAATAGCTAACGTTGGGCCAAACAGGATATCTGCGGT
GAGCAGTTTCGGCCCCGGCCGGGGCCAAGAACAGATGGTCACCGCAGTTTCGGCCCCGG
CCCGAGGCCAAGAACAGATGGTCCCCAGATATGGCCCAACCCTCAGCAGTTTCTTAAGACC
CATCAGATGTTTCCAGGCTCCCCAAGGACCTGAAATGACCCTGCGCCTTATTTGAATTAAC
CAATCAGCCTGCTTCTCGCTTCTGTTTCGCGCGCTTCTGCTTCCCGAGCTCTATAAAAGAGCTC
ACAACCCTCACTCGGCGCGCCAGTCTCCGACAGACTGAGTCGCCCGGGGGGATCCAAA
GCCATGATATTTCCATGGAAATGTCAGAGCACCCAGAGGGACTTATGGAACATCTTCAAGTT
GTGGGGGTGGACAATGCTCTGTTGTGATTTCTGGCACATCATGGAACCGACTGCTGGACT
TACCATTATTCTGAAAAACCCATGAACTGGCAAAGGGCTAGAAGATTCTGCCGAGACAATT
ACACAGATTTAGTTGCCATACAAAACAAGGCGGAAATTGAGTATCTGGAGAAGACTCTGCC

TTTCAGTCGTTCTTACTACTGGATAGGAATCCGGAAGATAGGAGGAATATGGACGTGGGTG
GGAACCAACAAATCTCTCACTGAAGAAGCAGAGAAGTGGGGAGATGGTGAGCCCAACAAC
AAGAAGAACAAGGAGGACTGCGTGGAGATCTATATCAAGAGAAACAAAGATGCAGGCAA
TGGAACGATGACGCCTGCCACAACTAAAGGCAGCCCTCTGTTACACAGCTTCTTGCCAGCC
CTGGTCATGCAGTGGCCATGGAGAATGTGTAGAAATCATCAATAATTACACCTGCAACTGT
GATGTGGGGTACTATGGGCCCCAGTGTGAGTTTGTGATTCAGTGTGAGCCTTTGGAGGCC
CAGAGCTGGGTACCATGGACTGTACTCACCTTTGGGAACTTCAGCTTCAGCTCACAGTGT
GCCTTCAGCTGCTCTGAAGGAACAACTTAAGTGGGATTGAAGAAACCACCTGTGGACCAT
TTGGAACTGGTCATCTCCAGAACCAACCTGTCAAGTATTGAGTGTGAGCCTCTATCAGCA
CCAGATTTGGGGATCATGAACTGTAGCCATCCCCTGGCCAGCTTCAGCTTTACCTCTGCATG
TACCTTCATCTGCTCAGAAGGAACTGAGTTAATTGGGAAGAAGAAAACCATTTGTGAATCAT
CTGGAATCTGGTCAAATCCTAGTCCAATATGTCAAAAATTGGACAAAAGCTTCTCAATGATT
AAGGAGGGTATTATAACCCCTCTTCATTCCAGTGGCAGTCATGGTTACTGCATTCTCTGG
GTTGGCATTGTTGGATTGGCTGGCAAGGAGATTAAGGCAAGAAATCCAAGAGAAG
TATGAATGACCCATATCTCGAGTCTAGAGGGCCCTTCGAAGGTAAGCCTATCCCTAACCTC
TCCTCGGTCTCGATTCTACGCGTACCGGTATCATCACCATCACCATTGAGGATCCCGGGCT
CGAGAGGCCTGGTACCACGCGTGC GGCCGCGACTCTAGAGTCGACCTGCAGGCATGCAAG
CTTGATATCAAGCTTATCGATAATCAACCTCTGGATTACAAAATTTGTGAAAGATTGACTGG
TATTCTTAACTATGTTGCTCCTTTACGCTATGTGGATACGCTGCTTTAATGCCTTTGTATCAT
GCTATTGCTTCCCGTATGGCTTTCATTTCTCCTCCTGTATAAATCCTGGTTGCTGTCTCTT
ATGAGGAGTTGTGGCCGTTGTCAGGCAACGTGGCGTGGTGTGCACTGTGTTTGCTGACGC
AACCCCACTGGTTGGGGCATTGCCACCACCTGTCAGCTCCTTTCCGGGACTTTGCTTTCCC
CCTCCCTATTGCCACGCGGAACTCATCGCCGCTGCCTTGCCCGCTGCTGGACAGGGGCTC
GGCTGTTGGGCACTGACAATTCCGTGGTGTGTCGGGGAAATCATCGTCCTTTCTTGCTG
CTCGCCTGTGTTGCCACCTGGATTCTGCGGGGACGTCCTTCTGCTACGTCCTTCCGGCCCTC
AATCCAGCGGACCTTCTTCCCGCGGCTGCTGCCGGCTCTGCGGCCTTCCCGGTCTTCG
CCTTCGCCCTCAGACGAGTCGGATCTCCCTTTGGGCCGCTCCCGCATCGATACCGTCGAC
CTCGACTTTAAGACCA

pMMLV-hWT-L-selectin

TGACATATACATGTGAAAGACCCACCTGTAGGTTTGGCAAGCTAGCTTAAGTACGCCATTT
TGCAAGGCATGGAAAAATACATAACTGAGAATAGAAAAGTTCAGATCAAGGTCAGGAACA

GATGGAACAGCTGAATATGGGCCAAACAGGATATCTGTGGTAAGCAGTTCCTGCCCCGGCT
CAGGGCCAAGAACAGATGGAACAGCTGAATATGGGCCAAACAGGATATCTGTGGTAAGCA
GTTCTGCCCCGGCTCAGGGCCAAGAACAGATGGTCCCAGATGCGGTCCAGCCCTCAGCA
GTTTCTAGAGAACCATCAGATGTTTCCAGGGTGCCCCAAGGACCTGAAATGACCCTGTGCCT
TATTTGAACTAACCAATCAGTTCGCTTCTCGCTTCTGTTTCGCGCGCTTCTGCTCCCCGAGCTC
AATAAAAGAGCCCAACCCCTCACTCGGCGCGCCAGTCTCCGATTGACTGAGTCGCCCG
GGTACCCGTGTATCCAATAAACCCCTCTTGCAGTTGCATCCGACTTGTGGTCTCGCTGTTCTT
GGGAGGGTCTCCTCTGAGTGATTGACTACCCGTCAGCGGGGGTCTTTCATTTGGGGGCTCG
TCCGGGATCGGGAGACCCCTGCCAGGGACCACCGACCCACCACCGGGAGGTAAGCTGGC
CAGCAACTTATCTGTGTCTGTCCGATTGTCTAGTGTCTATGACTGATTTTATGCGCCTGCGTC
GGTACTAGTTAGCTAACTAGCTCTGTATCTGGCGGACCCGTGGTGGAAGTACGAGTTCGG
AACACCCGGCCGCAACCCTGGGAGACGTCCCAGGGACTTCGGGGGCGTTTTTGTGGCCCC
ACCTGAGTCCAAAATCCCGATCGTTTTGGACTCTTTGGTGCACCCCCCTTAGAGGAGGGAT
ATGTGGTTCTGGTAGGAGACGAGAACCTAAAACAGTTCGCCCTCCGTCTGAATTTTTGCTT
TCGGTTTGGGACCGAAGCCGCGCCGCGCTTGTCTGCTGCAGCATCGTTCTGTGTTGTCT
CTGTCTGACTGTGTTTCTGTATTTGTCTGAAAATATGGGCCCGCCGCGGGCCAGACTGT
TACCACTCCCTTAAGTTTGACCTTAGGTCAGTGGAAAGATGTGAGCGGATCGCTCACAACC
AGTCGGTAGATGTCAAGAAGAGACGTTGGGTTACCTTCTGCTCTGCAGAATGGCCAACCTT
TAACGTCGGATGGCCGCGAGACGGCACCTTTAACCGAGACCTCATACCCAGGTTAAGATC
AAGGTCTTTTACCTGGCCCGCATGGACACCCAGACCAGGTCCCCTACATCGTGACCTGGGA
AGCCTTGGCTTTTACCCCCCTCCCTGGGTCAAGCCCTTTGTACACCCTAAGCCTCCGCCTCC
TCTTCTCCATCCGCCCCGTCTCTCCCCCTTGAACCTCCTCGTTGACCCCGCCTCGATCCTCC
CTTTATCCAGCCCTCACTCCTTCTAGGGCCCCCATATGAGATCTTATATGGGGCACCCCC
GCCCTTGTAAACTTCCCTGACCTGACATGACAAGAGTTACTAACAGCCCCTCTCTCCAAGC
TCACTTACAGGCTCTCTACTTAGTCCAGCACGAAGTCTGGAGACCTCTGGCGGCAGCCTACC
AAGAACAACCTGGACCGACCGGTGGTACCTCACCTTACCGAGTCGGCGACACAGTGTGGGT
CCGCCGACACCAGACTAAGAACCTTGAACCTCGCTGGAAAGGACCTTACACAGTCCTGCTG
ACCACCCCAACCGCCCTCAAAGTAGACGGCATCGCAGCTTGGATACACGCCGCCACGTAA
ACAATTGAAGATCTAGTCGAAATTAACCCTCACTAAAGGGAACAAAAGCTGGAGCTCCAC
CGCGGTGGCGGCCGCCACCATGGGCTGCAGAAGAACTAGAGAAGGACCAAGCAAAGCCAT
GATATTTCCATGGAAATGTCAGAGCACCCAGAGGGACTTATGGAACATCTTCAAGTTGTGG
GGGTGGACAATGCTCTGTTGTGATTTCTGGCACATCATGGAACCGACTGCTGGACTTACCA

TTATTCTGAAAAACCCATGAACTGGCAAAGGGCTAGAAGATTCTGCCGAGACAATTACACA
GATTTAGTTGCCATACAAAACAAGGCGGAAATTGAGTATCTGGAGAAGACTCTGCCTTTCA
GTCGTTCTTACTACTGGATAGGAATCCGGAAGATAGGAGGAATATGGACGTGGGTGGGAA
CCAACAATCTCTTACTGAAGAAGCAGAGAACTGGGGAGATGGTGAGCCCAACAACAAGA
AGAACAAGGAGGACTGCGTGGAGATCTATATCAAGAGAAACAAAGATGCAGGCAAATGGA
ACGATGACGCCTGCCACAACTAAAGGCAGCCCTCTGTTACACAGCTTCTTGCCAGCCCTGG
TCATGCAGTGGCCATGGAGAATGTGTAGAAATCATCAATAATTACACCTGCAACTGTGATGT
GGGGTACTATGGGCCCCAGTGTGAGTTTGTGATTGAGTGTGAGCCTTTGGAGGCCCCAGAG
CTGGGTACCATGGACTGTACTIONCACCCTTTGGGAACTTCAGCTTCAGCTCACAGTGTGCCTT
CAGCTGCTCTGAAGGAACAACTTAACTGGGATTGAAGAAACCACCTGTGGACCATTTGGA
AACTGGTCATCTCCAGAACCAACCTGTCAAGTGATTGAGTGTGAGCCTCTATCAGCACCAGA
TTTGGGGATCATGAACTGTAGCCATCCCCTGGCCAGCTTCAGCTTTACCTCTGCATGTACCTT
CATCTGCTCAGAAGGAACTGAGTTAATTGGGAAGAAGAAAACCATTTGTGAATCATCTGGA
ATCTGGTCAAATCCTAGTCCAATATGTCAAAAATTGGACAAAAGTTTCTCAATGATTAAGGA
GGGTGATTATAACCCCTCTTCATTCCAGTGGCAGTCATGGTTACTGCATTCTCTGGGTTGG
CATTTATCATTGGCTGGCAAGGAGATTAAGGCAAGAAATCCAAGAGAAGTATGAA
TGACCCATATTAAGTCGACGGTACCGCGGGCCCGGGATCCACCGGATCTAGATAACTGAGA
TCCGGATTAGTCCAATTTGTTAAAGACAGGATATCAGTGGTCCAGGCTCTAGTTTTGACTCA
ACAATATCACCAGCTGAAGCCTATAGAGTACGAGCCATAGATAAAAATAAAAGATTTTTATTTA
GTCTCCAGAAAAAGGGGGGAATGAAAGACCCACCTGTAGGTTTGGCAAGCTAGCTTAAGT
AACGCCATTTTGAAGGCATGGAAAAATACATAACTGAGAATAGAGAAGTTCAGATCAAGG
TCAGGAACAGATGGAACAGCTGAATATGGGCCAAACAGGATATCTGTGGTAAGCAGTTCCT
GCCCCGGCTCAGGGCCAAGAACAGATGGAACAGCTGAATATGGGCCAAACAGGATATCTG
TGTAAGCAGTTCCTGCCCCGGCTCAGGGCCAAGAACAGATGGTCCCCAGATGCGGTCCAG
CCCTCAGCAGTTTCTAGAGAACCATCAGATGTTTCCAGGGTCCCCAAGGACCTGAAATGAC
CCTGTGCCTTATTTGAACTAACCAATCAGTTCGCTTCTCGCTTCTGTTGCGCGCTTCTGCTCC
CCGAGCTCAATAAAAGAGCCCACAACCCCTCACTCGGGGCGCCAGTCCCTCCGATTGACTGA
GTCGCCCCGGGTACCCGTGTATCCAATAAACCTCTTGCAAGTTCATCCGACTTGTGGTCTCG
CTGTTCCCTGGGAGGGTCTCCTCTGAGTGATTGACTACCCGTCAGCGGGGGTCTTTCACATG
CAGCATGTATCAAATAATTTGGTTTTTTTTCTTAAGTATTTACATTAATGGCCATAGTACT
TAAAGTTACATTGGCTTCCTTGAAATAAACATGGAGTATTCAGAATGTGCATAAATATTTCT
AATTTAAGATAGTATCTCCATTGGCTTCTACTTTTTCTTTATTTTTTTTTGTCTCTGTCTTC

ATACTTTAGATTGATTTAAACTTCATTTTTAATTTAAAAGGATCTAGGTGAAGATCCTTTTT
GATAATCTCATGACCAAATCCCTTAACGTGAGTTTTCGTTCCACTGAGCGTCAGACCCCGT
AGAAAAGATCAAAGGATCTTCTTGAGATCCTTTTTTTCTGCGCGTAATCTGCTGCTTGCAAAC
AAAAAAACCACCGCTACCAGCGGTGGTTTGTTGCCGGATCAAGAGCTACCAACTCTTTTTTC
CGAAGGTAACCTGGCTTCAGCAGAGCGCAGATACCAAATACTGTTCTTCTAGTGTAGCCGTA
GTTAGGCCACCACTTCAAGAACTCTGTAGCACCGCTACATACCTCGCTCTGCTAATCCTGTT
ACCAGTGGCTGCTGCCAGTGGCGATAAGTCGTGTCTTACCGGGTTGGACTCAAGACGATAG
TTACCGGATAAGGCGCAGCGGTCTGGGCTGAACGGGGGGTTCGTGCACACAGCCCAGCTTG
GAGCGAACGACCTACACCGAACTGAGATACCTACAGCGTGAGCTATGAGAAAGCGCCACG
CTTCCCGAAGGGAGAAAGGCGGACAGGTATCCGGTAAGCGGCAGGGTCGGAACAGGAGA
GCGCACGAGGGAGCTTCCAGGGGGAAACGCCTGGTATCTTTATAGTCCTGTCTGGGTTTTCGC
CACCTCTGACTTGAGCGTCGATTTTTGTGATGCTCGTCAGGGGGGCGGAGCCTATGGAAAA
ACGCCAGCAACGCGCCTTTTTACGGTTCCTGGCCTTTTGCTGGCCTTTTGCTCACATGTTCT
TTCCTGCGTTATCCCCTGATTCTGTGGATAACCGTATTACCGCCTTTGAGTGAGCTGATACCG
CTCGCCGACGCCGAACGACCGAGCGCAGCGAGTCAGTGAGCGAGGAAGCGGAAGAGCGC
CCAATACGCAAACCGCCTCTCCCCGCGGTTGGCCGATTCATTAATGCAGCTGGCACGACAG
GTTTCCCGACTGGAAAGCGGGCAGTGAGCGCAACGCAATTAATGTGAGTTAGCTCACTCAT
TAGGCACCCCAGGCTTTACACTTTATGCTTCCGGCTCGTATGTTGTGTGGAATTGTGAGCGG
ATAACAATTTACACAGGAAACAGCTATGACCATGATTACGCCAAGCTTTGCTCTTAGGAGT
TTCCTAATACATCCCAAACCTCAAATATATAAAGCATTGACTTGTTCTATGCCCTAGGGGGCG
GGGGGAAGCTAAGCCAGCTTTTTTTAACATTTAAAATGTTAATTCATTTTAAATGCACAGA
TGTTTTTATTTACATAAGGGTTTCAATGTGCATGAATGCTGCAATATCCTGTTACCAAAGCTA
GTATAAATAAAAATAGATAAACGTGGAAATTAAGTTAGAGTTTCTGTCATTAACGTTTCCTTCC
TCAGTTGACAACATAAATGCGCTGCTGAGAAGCCAGTTTGCATCTGTCAGGATCAATTTCCC
ATTATGCCAGTCATATTAATTAAGTCAATTAGTTGATTTTTATTTT

pMMLV-hΔMN-L-selectin

TGACATATACATGTGAAAGACCCACCTGTAGGTTTGGCAAGCTAGCTTAAGTACGCCATTT
TGCAAGGCATGGAAAAATACATAACTGAGAATAGAAAAGTTCAGATCAAGGTCAGGAACA
GATGGAACAGCTGAATATGGGCCAAACAGGATATCTGTGGTAAGCAGTTCCTGCCCCGGCT
CAGGGCCAAGAACAGATGGAACAGCTGAATATGGGCCAAACAGGATATCTGTGGTAAGCA
GTTCTGCCCCGGCTCAGGGCCAAGAACAGATGGTCCCCAGATGCGGTCCAGCCCTCAGCA

GTTTCTAGAGAACCATCAGATGTTTCCAGGGTGCCCAAGGACCTGAAATGACCCTGTGCCT
TATTTGAACTAACCAATCAGTTCGCTTCTCGCTTCTGTTTCGCGCGCTTCTGCTCCCCGAGCTC
AATAAAAGAGCCCACAACCCCTCACTCGGCGCGCCAGTCCTCCGATTGACTGAGTCGCCCCG
GGTACCCGTGTATCCAATAAACCTCTTGCAAGTTGCATCCGACTTGTGGTCTCGCTGTTCTT
GGGAGGGTCTCCTCTGAGTGATTGACTACCCGTCAGCGGGGGTCTTTCATTTGGGGGCTCG
TCCGGGATCGGGAGACCCCTGCCAGGGACCACCGACCCACCACCGGGAGGTAAGCTGGC
CAGCAACTTATCTGTGTCTGTCCGATTGTCTAGTGTCTATGACTGATTTTATGCGCCTGCGTC
GGTACTAGTTAGCTAACTAGCTCTGTATCTGGCGGACCCGTGGTGGAAGTACGAGTTCGG
AACACCCGGCCGCAACCCTGGGAGACGTCCAGGGACTTCGGGGGCGTTTTTGTGGCCCCG
ACCTGAGTCCAAAATCCCGATCGTTTTGGACTCTTTGGTGCACCCCCCTTAGAGGAGGGAT
ATGTGGTTCTGGTAGGAGACGAGAACCTAAAACAGTTCGCCCTCCGTCTGAATTTTTGCTT
TCGGTTTGGGACCGAAGCCGCGCCGCGCTTGTCTGCTGCAGCATCGTCTGTGTTGTCT
CTGTCTGACTGTGTTTCTGTATTTGTCTGAAAATATGGGCCCCGCGCGGGCCAGACTGT
TACCACTCCCTTAAGTTTGACCTTAGGTCACTGGAAAGATGTCGAGCGGATCGCTCACAACC
AGTCGGTAGATGTCAAGAAGAGACGTTGGGTTACCTTCTGCTCTGCAGAATGGCCAACCTT
TAACGTCGGATGGCCGCGAGACGGCACCTTAACCGAGACCTCATCACCCAGGTTAAGATC
AAGGTCTTTTACCTGGCCCGCATGGACACCCAGACCAGGTCCCCTACATCGTGACCTGGGA
AGCCTTGGCTTTTTGACCCCCCTCCCTGGGTCAAGCCCTTGTACACCCTAAGCCTCCGCCTCC
TCTTCTCCATCCGCCCGTCTCTCCCCCTGAACCTCCTCGTTCGACCCCGCTCGATCCTCC
CTTTATCCAGCCCTCACTCCTTCTCTAGGGCCCCCATATGAGATCTTATATGGGGCACCCCC
GCCCCTTGTAACCTCCCTGACCCTGACATGACAAGAGTTACTAACAGCCCCTCTCTCAAGC
TCACTTACAGGCTCTCTACTTAGTCCAGCACGAAGTCTGGAGACCTCTGGCGGCAGCCTACC
AAGAACAACCTGGACCGACCGGTGGTACCTCACCTTACCGAGTCGGCGACACAGTGTGGGT
CCGCCGACACCAGACTAAGAACCTTGAACCTCGCTGGAAAGGACCTTACACAGTCCTGCTG
ACCACCCCAACCGCCCTCAAAGTAGACGGCATCGCAGCTTGGATACACGCCGCCACGTAA
AACAAATTGAAGATCTAGTCGAAATTAACCCTCACTAAAGGGAACAAAAGCTGGAGCTCCAC
CGCGGTGGCGGCCGCCACCATGGGCTGCAGAAGAACTAGAGAAGGACCAAGCAAAGCCAT
GATATTTCCATGGAAATGTCAGAGCACCCAGAGGGACTTATGGAACATCTTCAAGTTGTGG
GGGTGGACAATGCTCTGTTGTGATTTCTGGCACATCATGGAACCGACTGCTGGACTTACCA
TTATTCTGAAAAACCCATGAACTGGCAAAGGGCTAGAAGATTCTGCCGAGACAATTACACA
GATTTAGTTGCCATACAAAACAAGGCGGAAATTGAGTATCTGGAGAAGACTCTGCCTTTCA
GTCGTTCTTACTACTGGATAGGAATCCGGAAGATAGGAGGAATATGGACGTGGGTGGGAA

CCAACAAATCTCTTACTGAAGAAGCAGAGAACTGGGGAGATGGTGAGCCCAACAACAAGA
AGAACAAGGAGGACTGCGTGGAGATCTATATCAAGAGAAACAAGATGCAGGCAAATGGA
ACGATGACGCCTGCCACAACTAAAGGCAGCCCTCTGTTACACAGCTTCTTGCCAGCCCTGG
TCATGCAGTGGCCATGGAGAATGTGTAGAAATCATCAATAATTACACCTGCAACTGTGATGT
GGGGTACTATGGGCCCCAGTGTGAGTTTGTGATTGAGTGTGAGCCTTTGGAGGCCCCAGAG
CTGGGTACCATGGACTGTACTIONCACCCTTTGGGAACTTCAGCTTCAGCTCACAGTGTGCCTT
CAGCTGCTCTGAAGGAACAACTTAACTGGGATTGAAGAAACCACCTGTGGACCATTGGA
AACTGGTCATCTCCAGAACCAACCTGTCAAGTGATTGAGTGTGAGCCTCTATCAGCACCAGA
TTTGGGGATCATGAACTGTAGCCATCCCCTGGCCAGCTTCAGCTTTACCTCTGCATGTACCTT
CATCTGCTCAGAAGGAACTGAGTTAATTGGGAAGAAGAAAACCATTTGTGAATCATCTGGA
ATCTGGTCAAATCCTAGTCCAATATGTCAAAAATTGGACAAAAGTTTCTCACCCCTCTTCATT
CCAGTGGCAGTCATGGTTACTGCATTCTCTGGGTTGGCATTATCATTGGCTGGCAAGGAG
ATTAATAAAGGCAAGAAATCCAAGAGAAGTATGAATGACCCATATTAAGTCGACGGTACC
GCGGGCCCGGGATCCACCGGATCTAGATAACTGAGATCCGGATTAGTCCAATTTGTTAAAG
ACAGGATATCAGTGGTCCAGGCTCTAGTTTTGACTCAACAATATCACCAGCTGAAGCCTATA
GAGTACGAGCCATAGATAAAATAAAAGATTTTATTTAGTCTCCAGAAAAGGGGGGAATGA
AAGACCCACCTGTAGTTTGGCAAGCTAGCTTAAGTAACGCCATTTTGAAGGCATGGAA
AAATACATAACTGAGAATAGAGAAGTTCAGATCAAGGTCAGGAACAGATGGAACAGCTGA
ATATGGGCCAAACAGGATATCTGTGGTAAGCAGTTCCTGCCCGGCTCAGGGCCAAGAACA
GATGGAACAGCTGAATATGGGCCAAACAGGATATCTGTGGTAAGCAGTTCCTGCCCGGCT
CAGGGCCAAGAACAGATGGTCCCCAGATGCGGTCCAGCCCTCAGCAGTTTCTAGAGAACCA
TCAGATGTTTCCAGGGTGCCCCAAGGACCTGAAATGACCCTGTGCCTTATTTGAACTAACCA
ATCAGTTCGCTTCTCGCTTCTGTTGCGCGCTTCTGCTCCCCGAGCTCAATAAAAGAGCCCAC
AACCCCTCACTCGGGGCGCCAGTCCCGATTGACTGAGTCGCCCGGGTACCCGTGTATCCA
ATAAACCCCTCTTGCAGTTGCATCCGACTTGTGGTCTCGCTGTTCCCTGGGAGGGTCTCCTCTG
AGTGATTGACTACCCGTCAGCGGGGGTCTTTCACATGCAGCATGTATCAAAATTAATTTGGT
TTTTTTTCTTAAGTATTTACATTAATGGCCATAGTACTTAAAGTTACATTGGCTTCCTTGAAA
TAAACATGGAGTATTCAGAATGTGTCATAAATATTTCTAATTTAAGATAGTATCTCCATTGG
CTTTCTACTTTTTCTTTATTTTTTTTTGTCTCTGTCTTCCATTTGTTGTTGTTGTTGTTGTT
GTTTGTGTTGTTGGTTGGTTGGTTAATTTTTTTTTAAAGATCCTACACTATAGTTCAAGCTAGA
CTATTAGCTACTCTGTAACCCAGGGTGACCTGAAGTCATGGGTAGCCTGCTGTTTTAGCCT
TCCCACATCTAAGATTACAGGTATGAGCTATCATTTTTGGTATATTGATTGATTGATTGATTG

ATGTGTGTGTGTGATTGTGTTTGTGTGTGTGATTGTGTATATGTGTGTATGGTTGTGTGT
GATTGTGTGTATGTATGTTTGTGTGTGATTGTGTGTGTGTGATTGTGCATGTGTGTGTGTGT
GATTGTGTTTATGTGTATGATTGT
GTGTGTTGTGTATATATATTTTATGGTAGTGAGAGGCAACGCTCCGGCTCAGTGTGAGGTTG
GTTTTGAGACAGAGTCTTTCACTTAGCTTGAATTCACTGGCCGTCGTTTTACAACGTCGTG
ACTGGGAAAACCCTGGCGTTACCCAACCTAATCGCCTTGACGACATCCCCCTTTCGCCAGC
TGCGTAATAGCGAAGAGGCCCGCACCGATCGCCCTTCCAACAGTTGCGCAGCCTGAATG
GCGAATGGCGCCTGATGCGGTATTTTCTCCTTACGCATCTGTGCGGTATTTACACCCGCATA
TGGTGCACTCTCAGTACAATCTGCTCTGATGCCGCATAGTTAAGCCAGCCCCGACACCCGCC
AACACCCGCTGACGCGCCCTGACGGGCTTGTCTGCTCCCGGCATCCGCTTACAGACAAGCT
GTGACCGTCTCCGGGAGCTGCATGTGTCAGAGGTTTTACCGTCATCACCGAAACGCGCGA
GACGAAAGGGCCTCGTGATACGCCTATTTTTATAGGTTAATGTCATGATAATAATGGTTTCT
TAGACGTCAGGTGGCACTTTTCGGGAAATGTGCGCGGAACCCCTATTTGTTTATTTTTCTA
AATACATTCAAATATGTATCCGCTCATGAGACAATAACCCTGATAAATGCTTCAATAATATTG
AAAAAGGAAGAGTATGAGTATTCAACATTTCCGTGTCGCCCTTATTCCCTTTTTTGCGGCATT
TTGCCTCCTGTTTTTGCTCACCCAGAAACGCTGGTGAAAGTAAAAGATGCTGAAGATCAGT
TGGGTGCACGAGTGGGTTACATCGAACTGGATCTCAACAGCGGTAAGATCCTTGAGAGTTT
TCGCCCCGAAGAACGTTTTCCAATGATGAGCACTTTTAAAGTTCTGCTATGTGGCGCGGTAT
TATCCCGTATTGACGCCGGGCAAGAGCAACTCGGTCGCCGCATACACTATTCTCAGAATGAC
TTGTTGAGTACTCACCAGTCACAGAAAAGCATCTTACGGATGGCATGACAGTAAGAGAAT
TATGCAGTGCTGCCATAACCATGAGTGATAACACTGCGGCCAACTTACTTCTGACAACGATC
GGAGGACCGAAGGAGCTAACCGCTTTTTTGACAACATGGGGGATCATGTAACCTGCCTTG
ATCGTTGGGAACCGGAGCTGAATGAAGCCATACCAAACGACGAGCGTGACACCACGATGC
CTGTAGCAATGGCAACAACGTTGCGCAAACCTATTAACCTGGCGAACTACTTACTTAGCTTCC
CGGCAACAATTAAGACTGGATGGAGGCGGATAAAGTTGCAGGACCACTTCTGCGCTCGG
CCCTTCCGGCTGGCTGGTTTATTGCTGATAAATCTGGAGCCGGTGAGCGTGGGTCTCGCGG
TATCATTGCAGCACTGGGGCCAGATGGTAAGCCCTCCCGTATCGTAGTTATCTACACGACGG
GGAGTCAGGCAACTATGGATGAACGAAATAGACAGATCGCTGAGATAGGTGCCTCACTGA
TTAAGCATTGGTAACTGTCAGACCAAGTTTACTCATATATACTTTAGATTGATTTAAACTTC
ATTTTTAATTTAAAGGATCTAGGTGAAGATCCTTTTTGATAATCTCATGACCAAAATCCCTT
AACGTGAGTTTTCGTTCCACTGAGCGTCAGACCCCGTAGAAAAGATCAAAGGATCTTCTTGA
GATCCTTTTTTTCTGCGCGTAATCTGCTGCTTGCAAACAAAAAAACCACCGCTACCAGCGGT

GGTTTGGTTGCCGGATCAAGAGCTACCAACTCTTTTTCCGAAGGTAAGTGGCTTCAGCAGAG
CGCAGATACCAAATACTGTTCTTCTAGTGTAGCCGTAGTTAGGCCACCACTTCAAGAACTCT
GTAGCACCGCCTACATACTCGCTCTGCTAATCCTGTTACCAGTGGCTGCTGCCAGTGGCGA
TAAGTCGTGTCTTACCGGGTTGGACTCAAGACGATAGTTACCGGATAAGGCGCAGCGGTCTG
GGCTGAACGGGGGGTTCGTGCACACAGCCCAGCTTGGAGCGAACGACCTACACCGAACTG
AGATACCTACAGCGTGAGCTATGAGAAAGCGCCACGCTTCCCGAAGGGAGAAAGGCGGAC
AGGTATCCGGTAAGCGGCAGGGTTCGGAACAGGAGAGCGCACGAGGGAGCTTCCAGGGGG
AAACGCCTGGTATCTTTATAGTCCTGTCGGGTTTCGCCACCTCTGACTTGAGCGTCGATTTTT
GTGATGCTCGTCAGGGGGGCGGAGCCTATGGAAAAACGCCAGCAACGCGGCCTTTTTACG
GTTCTGGCCTTTTGCTGGCCTTTGCTCACATGTTCTTTCCTGCGTTATCCCCTGATTCTGTG
GATAACCGTATTACCGCCTTTGAGTGAGCTGATACCGCTCGCCGAGCCGAACGACCGAGC
GCAGCGAGTCAGTGAGCGAGGAAGCGGAAGAGCGCCCAATACGCAAACCGCCTCTCCCCG
CGCGTTGGCCGATTCATTAATGCAGCTGGCACGACAGGTTTCCCGACTGGAAAGCGGGCAG
TGAGCGCAACGCAATTAATGTGAGTTAGCTCACTCATTAGGCACCCCAGGCTTTACACTTTA
TGCTTCGGGCTCGTATGTTGTGTGGAATTGTGAGCGGATAACAATTTACACAGGAAACAG
CTATGACCATGATTACGCCAAGCTTTGCTCTTAGGAGTTTCTAATACATCCCAAACCTCAAT
ATATAAAGCATTGACTTGTTCTATGCCCTAGGGGGCGGGGGGAAGCTAAGCCAGCTTTTTT
TAACATTTAAAATGTTAATTCATTTTAAATGCACAGATGTTTTTATTTACATAAGGGTTTCAAT
GTGCATGAATGCTGCAATATTCCTGTTACCAAAGCTAGTATAAATAAAAATAGATAAACGTG
GAAATTACTTAGAGTTTCTGTCATTAACGTTTCTTCTCAGTTGACAACATAAATGCGCTGC
TGAGAAGCCAGTTTGCATCTGTCAGGATCAATTTCCATTATGCCAGTCATATTAATTAAG
TCAATTAGTTGATTTTTATTTT

pMMLV- Δ W-L-selectin

TGACATATACATGTGAAAGACCCACCTGTAGGTTTGGCAAGCTAGCTTAAGTACGCCATTT
TGCAAGGCATGGAAAAATACATAACTGAGAATAGAAAAGTTCAGATCAAGGTCAGGAACA
GATGGAACAGCTGAATATGGGCCAAACAGGATATCTGTGGTAAGCAGTTCCTGCCCCGGCT
CAGGGCCAAGAACAGATGGAACAGCTGAATATGGGCCAAACAGGATATCTGTGGTAAGCA
GTTCTGCCCCGGCTCAGGGCCAAGAACAGATGGTCCCAGATGCGGTCCAGCCCTCAGCA
GTTTCTAGAGAACCATCAGATGTTTCCAGGGTCCCCAAGGACCTGAAATGACCCTGTGCCT
TATTTGAACTAACCAATCAGTTCGCTTCTCGCTTCTGTTTCGCGCGCTTCTGCTCCCCGAGCTC
AATAAAAGAGCCCAACCCCTCACTCGGCGCGCCAGTCCTCCGATTGACTGAGTCGCCCCG

GGTACCCGTGTATCCAATAAACCCCTCTTGCAGTTGCATCCGACTTGTGGTCTCGCTGTTCCCT
GGGAGGGTCTCCTCTGAGTGATTGACTACCCGTCAGCGGGGGTCTTTCATTTGGGGGCTCG
TCCGGGATCGGGAGACCCCTGCCAGGGACCACCGACCCACCACCGGGAGGTAAGCTGGC
CAGCAACTTATCTGTGTCTGTCCGATTGTCTAGTGTCTATGACTGATTTTATGCGCCTGCGTC
GGTACTAGTTAGCTAACTAGCTCTGTATCTGGCGGACCCGTGGTGGAAGTACGAGTTCGG
AACACCCGGCCGCAACCCTGGGAGACGTCCCAGGGACTTCGGGGGCGTTTTTGTGGCCCG
ACCTGAGTCCAAAATCCCGATCGTTTTGGACTCTTTGGTGCACCCCCCTTAGAGGAGGGAT
ATGTGGTTCTGGTAGGAGACGAGAACCTAAAACAGTTCCTCCGCTCGTCTGAATTTTTGCTT
TCGGTTTGGGACCGAAGCCGCGCCGCGCGTCTTGTCTGCTGCAGCATCGTTCTGTGTTGTCT
CTGTCTGACTGTGTTTCTGTATTTGTCTGAAAATATGGGCCCGCCGCGGGCCAGACTGT
TACCACTCCCTTAAGTTTGACCTTAGGTCACTGGAAAGATGTGAGCGGATCGCTCACAACC
AGTCGGTAGATGTCAAGAAGAGACGTTGGGTTACCTTCTGCTCTGCAGAATGGCCAACCTT
TAACGTCGGATGGCCGCGAGACGGCACCTTTAACCGAGACCTCATCACCAGGTTAAGATC
AAGGTCTTTTACCTGGCCCGCATGGACACCCAGACCAGGTCCCCTACATCGTGACCTGGGA
AGCCTTGGCTTTTGACCCCCCTCCCTGGGTCAAGCCCTTGTACACCCTAAGCCTCCGCTCC
TCTTCTCCATCCGCCCCGTCTCTCCCCCTTGAACCTCCTCGTTGACCCCGCCTCGATCCTCC
CTTTATCCAGCCCTCACTCCTTCTCTAGGCGCCCCATATGAGATCTTATATGGGGCACCCCC
GCCCCTTGTAACCTCCCTGACCCTGACATGACAAGAGTTACTAACAGCCCCTCTCTCCAAGC
TCACTTACAGGCTCTCTACTTAGTCCAGCACGAAGTCTGGAGACCTCTGGCGGCAGCCTACC
AAGAACAACCTGGACCGACCGGTGGTACCTCACCTTACCGAGTCGGCGACACAGTGTGGGT
CCGCCGACACCAGACTAAGAACCTTGAACCTCGCTGGAAAGGACCTTACACAGTCCTGCTG
ACCACCCCAACCGCCCTCAAAGTAGACGGCATCGCAGCTTGGATACACGCCGCCACGTAA
ACAATTGAAGATCTAGTCGAAATTAACCCTCACTAAAGGGAACAAAAGCTGGAGCTCCAC
CGCGGTGGCGGCCGCCACCATGGGCTGCAGAAGAACTAGAGAAGGACCAAGCAAAGCCAT
GATATTTCCATGGAAATGTCAGAGCACCCAGAGGGACTTATGGAACATCTTCAAGTTGTGG
GGGTGGACAATGCTCTGTTGTGATTTCTGGCACATCATGGAACCGACTGCTGGACTTACCA
TTATTCTGAAAAACCCATGAACTGGCAAAGGGCTAGAAGATTCTGCCGAGACAATTACACA
GATTTAGTTGCCATACAAAACAAGGCGGAAATTGAGTATCTGGAGAAGACTCTGCCTTCA
GTCGTTCTTACTACTGGATAGGAATCCGGAAGATAGGAGGAATATGGACGTGGGTGGGAA
CCAACAATCTCTTACTGAAGAAGCAGAGAAGTGGGGAGATGGTGGAGCCCAACAACAAGA
AGAACAAGGAGGACTGCGTGGAGATCTATATCAAGAGAAAACAAGATGCAGGCAAATGGA
ACGATGACGCCTGCCACAACTAAAGGCAGCCCTCTGTTACACAGCTTCTTGCCAGCCCTGG

ACCAGTGGCTGCTGCCAGTGGCGATAAGTCGTGTCTTACCGGGTTGGACTCAAGACGATAG
TTACCGGATAAAGGCGCAGCGGTCTGGGCTGAACGGGGGGTTCGTGCACACAGCCCAGCTTG
GAGCGAACGACCTACACCGAACTGAGATACCTACAGCGTGAGCTATGAGAAAGCGCCACG
CTTCCCGAAGGGAGAAAGGCGGACAGGTATCCGGTAAGCGGCAGGGTCGGAACAGGAGA
GCGCACGAGGGAGCTTCCAGGGGGAAACGCCTGGTATCTTTATAGTCCTGTCTGGGTTTCGC
CACCTCTGACTTGAGCGTCGATTTTTGTGATGCTCGTCAGGGGGGCGGAGCCTATGGAAAA
ACGCCAGCAACGCGGCCTTTTTACGGTTCCTGGCCTTTTGCTGGCCTTTTGCTCACATGTTCT
TTCCTGCGTTATCCCCTGATTCTGTGGATAACCGTATTACCGCCTTTGAGTGAGCTGATACCG
CTCGCCGACGCCGAACGACCGAGCGCAGCGAGTCAGTGAGCGAGGAAGCGGAAGAGCGC
CCAATACGCAAACCGCCTCTCCCCGCGCGTTGGCCGATTCAATTAATGCAGCTGGCACGACAG
GTTTCCCGACTGGAAAGCGGGCAGTGAGCGCAACGCAATTAATGTGAGTTAGCTCACTCAT
TAGGCACCCCAGGCTTTACACTTTATGCTTCCGGCTCGTATGTTGTGTGGAATTGTGAGCGG
ATAACAATTTACACAGGAAACAGCTATGACCATGATTACGCCAAGCTTTGCTCTTAGGAGT
TTCCTAATACATCCCAAACCTCAAATATATAAAGCATTGACTTGTTCTATGCCCTAGGGGGCG
GGGGGAAGCTAAGCCAGCTTTTTTTAACATTTAAAATGTTAATTCATTTTAAATGCACAGA
TGTTTTTATTTACATAAGGGTTTCAATGTGCATGAATGCTGCAATATCCTGTTACCAAAGCTA
GTATAAATAAAAATAGATAAACGTGGAAATTAAGTACTTAGAGTTTCTGTCATTAACGTTTCCTCC
TCAGTTGACAACATAAATGCGCTGCTGAGAAGCCAGTTTGCATCTGTCAGGATCAATTTCCC
ATTATGCCAGTCATATTAATTAAGTCAATTAGTTGATTTTTATTT

pMSGV1-mWT-L-selectin

AATGAAAGACCCACCTGTAGGTTTGGCAAGCTAGCTTAAGTAACGCCATTTTGCAAGGCAT
GGAAAATACATAACTGAGAATAGAGAAGTTCAGATCAAGGTTAGGAACAGAGAGACAGCA
GAATATGGGCCAAACAGGATATCTGTGGTAAGCAGTTCCTGCCCCGGCTCAGGGCCAAGAA
CAGATGGTCCCAGATGCGGTCCCGCCCTCAGCAGTTTCTAGAGAACCATCAGATGTTTCCA
GGGTGCCCCAAGGACCTGAAATGACCCTGTGCCTTATTTGAACTAACCAATCAGTTCGCTTC
TCGCTTCTGTTGCGCGCTTCTGCTCCCCGAGCTCAATAAAAGAGCCCACAACCCCTCACTCG
GCGCGCCAGTCTCCGATAGACTGCGTCGCCCGGGTACCCGTATTCCAATAAAGCCTCTTG
CTGTTTGCATCCGAATCGTGACTCGCTGATCCTTGGGAGGGTCTCCTCAGATTGATTGACT
GCCACCTCGGGGGTCTTTCATTTGGAGGTTCCACCGAGATTTGGAGACCCCTGCCAGGG
ACCACCGACCCCCCGCCGGGAGGTAAGCTGGCCAGCGGTTCGTTTCGTGTCTGTCTGTCT
TTGTGCGTGTTTGTGCCGGCATCTAATGTTTGCGCCTGCGTCTGTACTAGTTAGCTAACTAGC

TCTGTATCTGGCGGACCCGTGGTGGAACTGACGAGTTCGGAACACCCGGCCGCAACCCTGG
GAGACGTCCCAGGGACTTCGGGGGCCGTTTTTGTGGCCCGACCTGAGTCCTAAAATCCCGA
TCGTTTAGGACTCTTTGGTGCACCCCCCTTAGAGGAGGGATATGTGGTTCTGGTAGGAGAC
GAGAACCTAAAACAGTTCCTCGCCTCCGTCTGAATTTTTGCTTTCGGTTTGGGACCGAAGCCG
CGCCGCGCGTCTTGTCTGCTGCAGCATCGTTCTGTGTTGTCTCTGTCTGACTGTGTTTCTGTA
TTTGTCTGAAAATATGGGCCCGGGCTAGCCTGTTACCACTCCCTTAAGTTTGACCTTAGGTC
ACTGGAAGATGTCGAGCGGATCGCTACAACAGTCGGTAGATGTCAAGAAGAGACGTT
GGGTTACCTTCTGCTCTGCAGAATGGCCAACCTTTAACGTCGGATGGCCGCGAGACGGCAC
CTTTAACCGAGACCTCATCACCCAGGTTAAGATCAAGGTCTTTTACCTGGCCCGCATGGAC
ACCCAGACCAGGTCCCCTACATCGTGACCTGGGAAGCCTTGGCTTTTGACCCCCCTCCCTGG
GTCAAGCCCTTTGTACACCCTAAGCCTCCGCCTCCTTCTCCATCCGCCCGTCTCTCCCC
TTGAACCTCCTCGTTCGACCCCGCCTCGATCCTCCCTTATCCAGCCCTCACTCCTTCTTAGG
CGCCCCATATGGCCATATGAGATCTTATATGGGGCACCCCCGCCCTTGTAACCTCCCTG
ACCCTGACATGACAAGAGTTACTAACAGCCCCTCTCTCCAAGCTCACTTACAGGCTCTCTACT
TAGTCCAGCACGAAGTCTGGAGACCTCTGGCGGCAGCCTACCAAGAACAACCTGGACCGACC
GGTGGTACCTCACCTTACCGAGTCGGCGACACAGTGTGGGTCCGCCGACACCAGACTAAG
AACCTAGAACCTCGCTGGAAAGGACCTTACACAGTCCTGCTGACCACCCCCACCGCCCTCAA
AGTAGACGGCATCGCAGCTTGGATACACGCCGCCACGTGAAGGCTGCCGACCCCGGGGG
TGGACCATCCTCTAGCCCTCGAGAAGCTTGCCGCCATGGTGTTCATGGAGATGTGAGGG
TACTTACTGGGGCTCGAGGAACATCCTGAAGCTGTGGGTCTGGACACTGCTCTGTTGTGACT
TCCTGATACACCATGGAACCTCACTGTTGGACTTACCATTATTCTGAAAAGCCCATGAACTGG
GAAAATGCTAGAAAGTTCTGCAAGCAAATTACACAGATTTAGTCGCCATACAAAACAAGA
GAGAAATTGAGTATTTAGAGAATACATTGCCAAAAGCCCTTACTACTGGATAGGAATC
AGGAAAATTGGGAAAATGTGGACATGGGTGGGAACCAACAAAACCTCACTAAAGAAGCA
GAGAACTGGGGTGCTGGGGAGCCCAACAACAAGAAGTCCAAGGAGGACTGTGTGGAGAT
CTATATCAAGAGGGAACGAGACTCTGGGAAATGGAACGATGACGCCTGTCACAAACGAAA
GGCAGCTCTCTGCTACACAGCCTTGGCCAGCCAGGGTCTTGCAATGGCCGTGGAGAATGT
GTGGAAACTATCAACAATCACACGTGCATATGTGATGAAGGGTATTACGGGCCCCAGTGTC
AGTATGTGGTCCAGTGTGAGCCTTTGGAGGCCCTGAGTTGGGTACCATGGACTGCATCCA
CCCCTTGGGAAACTTCACTTCCAGTCCAAGTGTGCTTTCACTGTTCTGAGGGAAAGAGAGC
TACTTGGGACTGCAGAAACACAGTGTGGAGCATCTGGAAACTGGTCATCTCCAGAGCCAAT
CTGCCAAGTGGTCCAGTGTGAGCCTTTGGAGGCCCTGAGTTGGGTACCATGGACTGCATC

CACCCCTGGGAACTTCAGCTTCCAGTCCAAGTGTGCTTTCAACTGTTCTGAGGGAAGAGA
GCTACTTGGGACTGCAGAAACACAGTGTGGAGCATCTGGAACTGGTCATCTCCAGAGCCA
ATCTGCCAAGAGACAAACAGAAGTTTCTCAAAGATCAAAGAAGGTGACTACAACCCCTCTT
CATTCTGTAGCCGTCATGGTCACCGCATTCTCGGGGCTGGCATTCTCATTGGCTGGCAA
GGCGGTTAAAAAAGGCAAGAAATCTCAAGAAAGGATGGATGATCCTTACTAAGGTCGAC
GGTACCGCGGGCCCGGGATCCGATAAAATAAAAGATTTTATTTAGTCTCCAGAAAAAGGGG
GGAATGAAAGACCCACCTGTAGGTTTGGCAAGCTAGCTTAAGTAACGCCATTTTGAAGG
CATGGAATAACATAACTGAGAATAGAGAAGTTCAGATCAAGGTTAGGAACAGAGAGACA
GCAGAATATGGGCCAAACAGGATATCTGTGGTAAGCAGTTCCTGCCCCGGCTCAGGGCCAA
GAACAGATGGTCCCAGATGCGGTCCCGCCCTCAGCAGTTTCTAGAGAACCATCAGATGTTT
CCAGGGTGCCCCAAGGACCTGAAATGACCCTGTGCCTTATTTGAACTAACCAATCAGTTCGC
TTCTCGCTTCTGTTTCGCGCGCTTCTGCTCCCCGAGCTCAATAAAAGAGCCCACAACCCCTCAC
TCGGCGCGCCAGTCTCCGATAGACTGCGTCGCCCGGGTACCCGTGTATCCAATAAACCCCTC
TTGCAGTTGCATCCGACTTGTGGTCTCGCTGTTCCCTGGGAGGGTCTCCTCTGAGTGATTGA
CTACCCGTCAGCGGGGGTCTTTCATGGGTAACAGTTTCTTGAAGTTGGAGAACAACATTCTG
AGGGTAGGAGTCGAATATTAAGTAATCCTGACTCAATTAGCCACTGTTTTGAATCCACATAC
TCCAATACTCCTGAAATCCATCGATGGAGTTCATTATGGACAGCGCAGAAAGAGCTGGGGA
GAATTGTGAAATTGTTATCCGCTCACAATTCCACACAACATACGAGCCGGAAGCATAAAGTG
TAAAGCCTGGGGTGCCTAATGAGTGAGCTAACTCACATTAATTGCGTTGCGCTCACTGCCCC
CTTCCAGTCGGGAAACCTGTCGTGCCAGCTGCATTAATGAATCGGCCAACGCGCGGGGAG
AGGCGGTTTTCGTATTGGGCGCTCTTCCGCTTCTCGCTCACTGACTCGCTGCGCTCGGTTCG
TTCGGCTGCGGCGAGCGGTATCAGCTCACTCAAAGGCGGTAATACGGTTATCCACAGAATC
AGGGGATAACGCAGGAAAGAACATGTGAGCAAAAGGCCAGCAAAAGGCCAGGAACCGTA
AAAAGGCCGCGTTGCTGGCGTTTTTCCATAGGCTCCGCCCCCTGACGAGCATCACAAAAAT
CGACGCTCAAGTCAGAGGTGGCGAAACCCGACAGGACTATAAAGATACCAGGCGTTTCCCC
CTGGAAGCTCCCTCGTGCCTCTCCTGTTCCGACCCTGCCGCTTACCGGATACCTGTCCGCCT
TTCTCCCTTCGGGAAGCGTGGCGCTTCTCATAGCTCACGCTGTAGGTATCTCAGTTCGGTG
TAGGTCGTTTCGCTCCAAGCTGGGCTGTGTGCACGAACCCCCGTTACGCCGACCGCTGCG
CCTTATCCGGTAACTATCGTCTTGAGTCCAACCCGGTAAGACACGACTTATCGCCACTGGCA
GCAGCCACTGGTAACAGGATTAGCAGAGCGAGGTATGTAGGCGGTGCTACAGAGTTCTTG
AAGTGGTGGCCTAACTACGGCTACACTAGAAGAACAGTATTTGGTATCTGCGCTCTGCTGA
AGCCAGTTACCTTCGGAAAAAGAGTTGGTAGCTCTTGATCCGGCAAACAAACCACCGCTGG

TAGCGGTGGTTTTTTTTGTTTGCAAGCAGCAGATTACGCGCAGAAAAAAGGATCTCAAGAA
GATCCTTTGATCTTTTCTACGGGGTCTGACGCTCAGTGGAACGAAAACCTCACGTTAAGGGAT
TTTGGTCATGAGATTATCAAAAAGGATCTTCACCTAGATCCTTTTAAATTA AAAATGAAGTTT
TAAATCAATCTAAAGTATATATGAGTAACTTGGTCTGACAGTTACCAATGCTTAATCAGTG
AGGCACCTATCTCAGCGATCTGTCTATTTGTTTCATCCATAGTTGCCTGACTCCCCGTCGTGT
AGATAACTACGATACGGGAGGGCTTACCATCTGGCCCCAGTGCTGCAATGATACCGCGAGA
CCCACGCTCACGGGCTCCAGATTTATCAGCAATAAACCAGCCAGCCGGAAGGGCCGAGCGC
AGAAGTGGTCCTGCAACTTTATCCGCCTCCATCCAGTCTATTAATTGTTGCCGGGAAGCTAG
AGTAAGTAGTTCGCCAGTTAATAGTTTTCGCAACGTTGTTGCCATTGCTACAGGCATCGTGG
TGTCACGCTCGTCGTTTGGTATGGCTTCATTCAGCTCCGGTCCCAACGATCAAGGCGAGTT
ACATGATCCCCATGTTGTGCAAAAAGCGGTTAGCTCCTTCGGTCTCCGATCGTTGTCAG
AAGTAAGTTGGCCGAGTGTTATCACTCATGGTTATGGCAGCACTGCATAATTCTCTTACTG
TCATGCCATCCGTAAGATGCTTTTCTGTGACTGGTGAGTACTCAACCAAGTCATTCTGAGAA
TAGTGTATGCGGCGACCGAGTTGCTCTTGCCCGCGTCAATACGGGATAATACCGCGCCAC
ATAGCAGAACTTTAAAAGTGCTCATCATTGGAAAACGTTCTTCGGGGCGAAAACCTCTCAAG
GATCTTACCGCTGTTGAGATCCAGTTCGATGTAACCCACTCGTGCACCCAACCTGATCTTCAG
CATCTTTTACTTTCACCAGCGTTTCTGGGTGAGCAAAAACAGGAAGGCAAAATGCCGCAAA
AAAGGGAATAAGGGCGACACGGAAATGTTGAATACTCATACTCTTCCTTTTTCAATATTATT
GAAGCATTTATCAGGGTATTGTCTCATGAGCGGATACATATTTGAATGTATTTAGAAAAAT
AAACAAATAGGGGTCCGCGCACATTTCCCCGAAAAGTGCCACCTGACGTCTAAGAAACCA
TTATTATCATGACATTAACCTATAAAAATAGGCGTATCACGAGGCCCTTTCGTCTCGCGCGTT
TCGGTGATGACGGTGAAAACCTCTGACACATGCAGCTCCCGGAGACGGTACAGCTTGTCT
GTAAGCGGATGCCGGGAGCAGACAAGCCCGTCAGGGCGCGTCAGCGGGTGTGGCGGGT
GTCGGGGCTGGCTTAACTATGCGGCATCAGAGCAGATTGTA CTGAGAGTGCACCATATGCG
GTGTGAAATACCGCACAGATGCGTAAGGAGAAAATACCGCATCAGGCGCCATTGCCATTC
AGGCTGCGCAACTGTTGGGAAGGGCGATCGGTGCGGGCCTCTTCGCTATTACGCCAGCTGG
CGAAAGGGGGATGTGCTGCAAGGCGATTAAGTTGGGTAACGCCAGGGTTTTCCAGTCAC
GACGTTGTAAAACGACGGCGCAAGGAATGGTGCATGCAAGGAGATGGCGCCCAACAGTCC
CCCGGCCACGGGGCCTGCCACCATACCCACGCCGAAACAAGCGCTCATGAGCCCGAAGTGG
CGAGCCCGATCTTCCCATCGGTGATGTCGGCGATATAGGCGCCAGCAACCGCACCTGTGG
CGCCGGTGATGCCGGCCACGATGCGTCCGGCGTAGAGGCGATTAGTCCAATTTGTTAAAGA

CAGGATATCAGTGGTCCAGGCTCTAGTTTTGACTCAACAATATCACCAGCTGAAGCCTATAG
AGTACGAGCCATAGATAAAAATAAAAAGATTTTATTTAGTCTCCAGAAAAAGGGGGG

pMSGV1-mLAP-L-selectin

AATGAAAGACCCACCTGTAGGTTTGGCAAGCTAGCTTAAGTAACGCCATTTTGCAAGGCAT
GGAAAATACATAACTGAGAATAGAGAAGTTCAGATCAAGGTTAGGAACAGAGAGACAGCA
GAATATGGGCCAAACAGGATATCTGTGGTAAGCAGTTCCTGCCCGGCTCAGGGCCAAGAA
CAGATGGTCCCAGATGCGGTCCCGCCCTCAGCAGTTTCTAGAGAACCATCAGATGTTTCCA
GGGTGCCCCAAGGACCTGAAATGACCCTGTGCCTTATTTGAACTAACCAATCAGTTCGCTTC
TCGCTTCTGTTGCGCGCTTCTGCTCCCCGAGCTCAATAAAAGAGCCCACAACCCCTCACTCG
GCGCGCCAGTCCCTCCGATAGACTGCGTCGCCCGGGTACCCGTATTCCAATAAAGCCTCTTG
CTGTTTGCATCCGAATCGTGGACTCGCTGATCCTGGGAGGGTCTCCTCAGATTGATTGACT
GCCACCTCGGGGGTCTTTCATTTGGAGGTTCCACCGAGATTTGGAGACCCCTGCCAGGG
ACCACCGACCCCCCGCCGGGAGGTAAGCTGGCCAGCGGTCTGTTTCGTGTCTGTCTCTGTCT
TTGTGCGTGTTTGTGCCGGCATCTAATGTTTGCGCCTGCGTCTGTACTAGTTAGCTAACTAGC
TCTGTATCTGGCGGACCCGTGGTGGAACTGACGAGTTCGGAACACCCGGCCGCAACCCTGG
GAGACGTCCCAGGGACTTCGGGGGCGTTTTTGTGGCCCGACCTGAGTCCTAAAATCCCGA
TCGTTTAGGACTCTTTGGTGCACCCCCCTTAGAGGAGGGATATGTGGTTCTGGTAGGAGAC
GAGAACCTAAAACAGTTCCTCGCTCGTGAATTTTTGCTTTCGTTTTGGGACCGAAGCCG
CGCCGCGGTCTTGTCTGCTGCAGCATCGTTCTGTGTTGTCTCTGTCTGACTGTGTTTCTGTA
TTTGTCTGAAAATATGGGCCCGGGCTAGCCTGTTACCACTCCCTTAAGTTTGACCTTAGGTC
ACTGGAAGATGTGCGAGCGGATCGCTCACAACCAGTCGGTAGATGTCAAGAAGAGACGTT
GGGTTACCTTCTGCTCTGCAGAATGGCCAACCTTTAACGTCCGATGGCCGCGAGACGGCAC
CTTTAACCGAGACCTCATCACCCAGGTTAAGATCAAGGTCTTTTACCTGGCCCCGCATGGAC
ACCCAGACCAGGTCCCCTACATCGTGACCTGGGAAGCCTTGGCTTTTGACCCCCCTCCCTGG
GTCAAGCCCTTTGTACACCCTAAGCCTCCGCCTCCTCTTCCATCCGCCCCGTCTCTCCCC
TTGAACCTCCTCGTTCGACCCCGCCTCGATCCTCCCTTATCCAGCCCTCACTCCTTCTCTAGG
CGCCCCATATGGCCATATGAGATCTTATATGGGGCACCCCCGCCCTTGTAACCTCCCTG
ACCCTGACATGACAAGAGTTACTAACAGCCCCTCTCTCCAAGCTCACTTACAGGCTCTCTACT
TAGTCCAGCACGAAGTCTGGAGACCTCTGGCGGCAGCCTACCAAGAACAACCTGGACCGACC
GGTGGTACCTCACCTTACCGAGTCGGCGACACAGTGTGGGTCCGCCGACACCAGACTAAG
AACCTAGAACCTCGCTGGAAAGGACCTTACACAGTCTGCTGACCACCCCCACCGCCCTCAA

AGTAGACGGCATCGCAGCTTGGATACACGCCGCCACGTGAAGGCTGCCGACCCCGGGG
TGGACCATCCTCTAGCCCTCGAGAAGCTTGCCGCCATGGTGTTCATGGAGATGTGAGGG
TACTTACTGGGGCTCGAGGAACATCCTGAAGCTGTGGGTCTGGACACTGCTCTGTTGTGACT
TCCTGATACACCATGGAACACTGTTGGACTTACCATTATTCTGAAAAGCCCATGAACTGG
GAAAATGCTAGAAAGTTCTGCAAGCAAATTACACAGATTTAGTCGCCATACAAAACAAGA
GAGAAATTGAGTATTTAGAGAATACATTGCCCAAAGCCCTTATTACTACTGGATAGGAATC
AGGAAAATTGGGAAAATGTGGACATGGGTGGGAACCAACAAAACACTCTACTAAAGAAGCA
GAGAACTGGGGTGCTGGGGAGCCCAACAACAAGAAGTCCAAGGAGGACTGTGTGGAGAT
CTATATCAAGAGGGAACGAGACTCTGGGAAATGGAACGATGACGCCTGTCACAAACGAAA
GGCAGCTCTCTGCTACACAGCCTCTTGCCAGCCAGGGTCTTGCAATGGCCGTGGAGAATGT
GTGGAAACTATCAACAATCACACGTGCATCTGTGATGCAGGGTATTACGGGCCCCAGTGTC
AGTATGTGGTCCAGTGTGAGCCTTTGGAGGCCCTGAGTTGGGTACCATGGACTGCATCCA
CCCCTTGGGAAACTTCAGCTTCCAGTCCAAGTGTGCTTTCAACTGTTCTGAGGGAAGAGAGC
TACTTGGGACTGCAGAAACACAGTGTGGAGCATCTGGAAACTGGTCATCTCCAGAGCCAAT
CTGCCAAGTGGTCCAGTGTGAGCCTTTGGAGGCCCTGAGTTGGGTACCATGGACTGCATC
CACCCCTTGGGAAACTTCAGCTTCCAGTCCAAGTGTGCTTTCAACTGTTCTGAGGGAAGAGA
GCTACTTGGGACTGCAGAAACACAGTGTGGAGCATCTGGAAACTGGTCATCTCCAGAGCCA
ATCTGCCAAGCAGGGACACTGACAATCCAGGAAGCTCCCCTCTTCATTCTGTAGCCGTCAT
GGTACC GCATTCTCGGGGCTGGCATTCTCATTTGGCTGGCAAGGCGGTTAAAAAAGGC
AAGAAATCTCAAGAAAGGATGGATGATCCATACTAAGGTCGACGGTACCGCGGGCCCGGG
ATCCGATAAAATAAAAGATTTTATTTAGTCTCCAGAAAAAGGGGGGAATGAAAGACCCAC
CTGTAGGTTTGGCAAGCTAGCTTAAGTAACGCCATTTTGCAAGGCATGGAAAATACATAACT
GAGAATAGAGAAGTTCAGATCAAGGTTAGGAACAGAGAGACAGCAGAATATGGGCCAAAC
AGGATATCTGTGGTAAGCAGTTCCTGCCCGGCTCAGGGCCAAGAACAGATGGTCCCCAGA
TGCGGTCCCGCCCTCAGCAGTTTCTAGAGAACCATCAGATGTTTCCAGGGTGCCCCAAGGA
CCTGAAATGACCCTGTGCCTTATTTGAACTAACCAATCAGTTCGCTTCTCGCTTCTGTTGCGG
CGCTTCTGCTCCCCGAGCTCAATAAAAGAGCCACAACCCCTCACTCGGCGCGCCAGTCCTC
CGATAGACTGCGTCGCCCGGGTACCCGTGTATCCAATAAACCCCTTGCAGTTGCATCCGAC
TTGTGGTCTCGCTGTTCTTGGGAGGGTCTCCTCTGAGTGATTGACTACCCGTCAGCGGGGG
TCTTTCATGGGTAACAGTTTCTTGAAGTTGGAGAACAACATTCTGAGGGTAGGAGTCGAAT
ATTAAGTAATCCTGACTCAATTAGCCACTGTTTTGAATCCACATACTCCAATACTCCTGAAAT
CCATCGATGGAGTTCATTATGGACAGCGCAGAAAGAGCTGGGGAGAATTGTGAAATTGTTA

TCCGCTCACAATTCCACACAACATACGAGCCGGAAGCATAAAGTGTAAGCCTGGGGTGCC
TAATGAGTGAGCTAACTCACATTAATTGCGTTGCGCTCACTGCCCGCTTTCCAGTCGGGAAA
CCTGTCGTGCCAGCTGCATTAATGAATCGGCCAACGCGCGGGGAGAGGCGTTTTGCGTATT
GGGCGCTCTCCGCTTCTCGCTCACTGACTCGCTGCGCTCGGTCGTTGCGGTGCGGCGAGC
GGTATCAGCTCACTCAAAGGCGGTAATACGGTTATCCACAGAATCAGGGGATAACGCAGGA
AAGAACATGTGAGCAAAAGGCCAGCAAAAGGCCAGGAACCGTAAAAAGGCCGCGTTGCTG
GCGTTTTTTCATAGGCTCCGCCCCCTGACGAGCATCAGAAAATCGACGCTCAAGTCAGAG
GTGGCGAAACCCGACAGGACTATAAAGATACCAGGCGTTTTCCCCTGGAAGCTCCCTCGTG
CGCTCTCCTGTTCCGACCCTGCCGCTTACCGGATACCTGTCCGCCTTTCTCCCTTCGGGAAGC
GTGGCGCTTTCTCATAGCTCACGCTGTAGGTATCTCAGTTCGGTGTAGGTCGTTGCTCCAA
GCTGGGCTGTGTGCACGAACCCCCGTTACGCCGACCGCTGCGCCTTATCCGTAACCTATC
GTCTTGAGTCCAACCCGGTAAGACACGACTTATCGCCACTGGCAGCAGCCACTGGTAACAG
GATTAGCAGAGCGAGGTATGTAGGCGGTGCTACAGAGTTCTTGAAGTGGTGGCCTAACTAC
GGCTACACTAGAAGAACAGTATTTGGTATCTGCGCTCTGCTGAAGCCAGTTACCTTCGGAAA
AAGAGTTGGTAGCTCTTGATCCGGCAAACAACCACCGCTGGTAGCGGTGGTTTTTTTTGTTT
GCAAGCAGCAGATTACGCGCAGAAAAAAGGATCTCAAGAAGATCCTTTGATCTTTTCTAC
GGGGTCTGACGCTCAGTGGAACGAAAACCTCACGTTAAGGGATTTTGGTCATGAGATTATCA
AAAAGGATCTTACCTAGATCCTTTTAAATTAATAAATGAAGTTTTAAATCAATCTAAAGTATA
TATGAGTAACTTGGTCTGACAGTTACCAATGCTTAATCAGTGAGGCACCTATCTCAGCGAT
CTGTCTATTTGTTTCATCCATAGTTGCCTGACTCCCCGTCGTGTAGATAACTACGATACGGGA
GGGCTTACCATCTGGCCCCAGTGCTGCAATGATACCGCGAGACCCACGCTCACCGGCTCCA
GATTTATCAGCAATAAACCAGCCAGCCGGAAGGGCCGAGCGCAGAAGTGGTCCTGCAACTT
TATCCGCCTCCATCCAGTCTATTAATTGTTGCCGGAAGCTAGAGTAAGTAGTTCGCCAGTT
AATAGTTTGCGCAACGTTGTTGCCATTGCTACAGGCATCGTGGTGTACGCTCGTCGTTTGG
TATGGCTTCATTAGCTCCGTTCCCAACGATCAAGGCGAGTTACATGATCCCCATGTTGT
GCAAAAAGCGGTTAGCTCCTTCGGTCTCCGATCGTTGTCAGAAGTAAGTTGGCCGCAGT
GTTATCACTCATGGTTATGGCAGCACTGCATAATTCTTTACTGTCATGCCATCCGTAAGATG
CTTTTCTGTGACTGGTGAAGTACTCAACCAAGTCATTCTGAGAATAGTGTATGCGGCGACCGA
GTTGCTCTTGCCCGCGTCAATACGGGATAATACCGCGCCACATAGCAGAACTTTAAAAGT
GCTCATCATTGGAAAACGTTCTTCGGGGCGAAAACCTCAAGGATCTTACCGCTGTTGAGAT
CCAGTTCGATGTAACCCACTCGTGCACCCAAGTATCTTACGATCTTTTACTTTACCCAGCG
TTTCTGGGTGAGCAAAAACAGGAAGGCCAAAATGCCGCAAAAAGGGAATAAGGGCGACAC

GGAAATGTTGAATACTCATACTCTTCTTTTTCAATATTATTGAAGCATTATCAGGGTTATT
GTCTCATGAGCGGATACATATTTGAATGTATTTAGAAAAATAAACAAATAGGGGTTCCGCG
CACATTTCCCCGAAAAGTGCCACCTGACGTCTAAGAAACCATTATTATCATGACATTAACCTA
TAAAAATAGGCGTATCACGAGGCCCTTTCGTCTCGCGCGTTTCGGTGATGACGGTGAAAAC
CTCTGACACATGCAGCTCCCGGAGACGGTCACAGCTTGTCTGTAAGCGGATGCCGGGAGCA
GACAAGCCCGTCAGGGCGCGTCAGCGGGTGTGGCGGGTGTGGGGGCTGGCTTAACTATG
CGGCATCAGAGCAGATTGTACTGAGAGTGCACCATATGCGGTGTGAAATACCGCACAGATG
CGTAAGGAGAAAATACCGCATCAGGCGCCATTCGCCATTCAGGCTGCGCAACTGTTGGGAA
GGGCGATCGGTGCGGGCCTCTTCGCTATTACGCCAGCTGGCGAAAGGGGGATGTGCTGCA
AGGCGATTAAGTTGGGTAACGCCAGGGTTTTCCAGTCACGACGTTGTA AACGACGGCGC
AAGGAATGGTGCATGCAAGGAGATGGCGCCCAACAGTCCCCCGCCACGGGGCCTGCCAC
CATACCCACGCCGAAACAAGCGCTCATGAGCCGAAGTGGCGAGCCCGATCTTCCCCATCG
GTGATGTCGGCGATATAGGCGCCAGCAACCGCACCTGTGGCGCCGGTGATGCCGGCCACG
ATGCGTCCGGCGTAGAGGCGATTAGTCCAATTTGTTAAAGACAGGATATCAGTGGTCCAGG
CTCTAGTTTTGACTCAACAATATCACCGCTGAAGCCTATAGAGTACGAGCCATAGATAAAA
TAAAAGATTTTATTTAGTCTCCAGAAAAAGGGGGG

pBullet-CMV-CEACAR-28z

GGGTGGACCATCCTCTAGACTGCCATGGATTTTCAGGTGCAGATTTTCAGCTTCTGCTAAT
CAGTGCCTCAGTCATAATGTCTAGAGGTGTCCACTCCCAGGTCCA ACTGCAGGAGTCAGGA
CCTGACCTGGTGAAACCTTCTCAGTCACTTTCACTCACCTGCACTGTCACTGGCTACTCCATC
ACCAGTGGTTATAGCTGGCACTGGATCCGGCAGTTTCCAGGAAACAAACTGGAATGGATGG
GCTACATAACAATACAGTGGTATCACTAACTACAACCCCTCTCTCAA AAGTCGAATCTCTATCA
CTCGAGACACATCCAAGAACCAGTTCTTCTGCGAGTTGAATTCTGTGACTACTGAGGACACA
GCCACATATTACTGTGCAAGAGAAGACTATGATTACCACTGGTACTTCGATGTCTGGGGCCA
AGGGACCACGGTCACCGTCTCCTCAGGAGGTGGTGGATCGGGCGGTGGCGGGTCTGGGTG
GCGGCGGATCTGACATCCAGCTGACCCAGTCTCCAGCAATCATGTCTGCATCTCTAGGGGA
GGAGATCACCTAACCTGCAGTGCCAGCTCGAGTGTAAGTTACATGCACTGGTACCAGCAG
AAGTCAGGCACTTCTCCAAACTCTTGATTTATAGCACATCCAACCTGGCTTCTGGAGTCCCT
TCTCGTT CAGTGGCAGTGGGTCTGGGACCTTTTTATTCTCTCACAATCAGCAGTGTGGAGGC
TGAAGATGCTGCCGATTATACTGCCATCAGTGGAGTAGTTATCCACGTTCCGAGGGGGG
ACCAAGCTGGAGATCAAAGTAGATCCTGTGCCAGGGATGGTGGTTGTAAGCCTTGCATAT

GTACAGTCCCAGAAGTATCATCTGTCTTCATCTTCCCCCAAAGCCCAAGGATGTGCTCACCA
TACTCTGACTCCTAAGGTCACGTGTGTTGTGGTAGACATCAGCAAGGATGATCCCGAGGTC
CAGTTCAGCTGGTTTGTAGATGATGTGGAGGTGCACACAGCTCAGACGCAACCCCGGGAG
GAGCAGTTCAACAGCACTTCCGCTCAGTCAGTGAAGTCCCATCATGCACCAGGACTGGCT
CAATGGCAAGGAGTTCAAATGCAGGGTCAACAGTGCAGCTTCCCTGCCCCATCGAGAAA
ACCATCTCCAAAACCAAAGGCAGACCGAAGGCTCCACAGGTGTGCACCATTCCACCTCCCAA
GGAGCAGATGGCCAAGGATAAAGTCAGTCTGACCTGCATGATAACAGACTTCTCCCTGAA
GACATTACTGTGGAGTGGCAGTGGAAATGGGCAGCCAGCGGAGAAGTACAAGAACAAGTCAAG
CCCATCATGGACACAGATGGCTCTTACTTCGTCTACAGCAAGCTCAATGTGCAGAAGAGCAA
CTGGGAGGCAGGAAATACTTTCACCTGCTCTGTGTTACATGAGGGCCTGCACAACCACCATA
CTGAGAAGAGCCTCTCCCACTCTCCTGGTATTGTGTTCTGGCTTGCCTGCTGGGTGGCTCC
TTCGGCTTTCTGGGTTTCTGGGCTCTGCATCCTCTGCTGTGTCAATAGTAGAAGGAACAG
ACTCCTCAAAGTGACTACATGAACATGACTCCCCGGAGGCCTGGGCTCACTCGAAAGCCTT
ACCAGCCCTACGCCCCTGCCAGAGACTTTCAGCGTACCGCCCCCTGAGAGCAAATTCAGC
AGGAGTGCAGAGACTGCTGCCAACCTGCAGGACCCCAACCAGCTCTACAATGAGCTCAATC
TAGGGCGAAGAGAGGAATATGACGTCTTGGAGAAGAAGCGGGCTCGGGATCCAGAGATG
GGAGGCAAACAGCAGAGGAGGAGGAACCCCAAGGCGTATACAATGCACTGCAGAA
AGACAAGATGGCAGAAGCCTACAGTGAGATCGGCACAAAAGGCGAGAGGCGGAGAGGCA
AGGGGCACGATGGCCTTACCAGGGTCTCAGCACTGCCACCAAGGACACCTATGATGCCCT
GCATATGCAGACCCTGGCCCCCTCGCTAAGTCGACGAGTACTCGAGAGATCCGGATTAGTCC
AATTTGTTAAAGACAGGATATCAGTGGTCCAGGCTCTAGTTTTGACTCAACAATATCACCAG
CTGAAGCCTATAGTACGAGCCATAGATAAAATAAAAGATTTTATTTAGTCTCCAGAAAAGG
GGGAATGAAAGACCCACCTGTAGGTTTGGCAAGCTAGCTTAAGTAACGCCATTTTGCAAG
GCATGGAAAAATACATAACTGAGAATAGAGAAGTTCAGATCAAGGTCAGGAACAGATGGA
ACAGCTGAATATGGGCCAAACAGGATATCTGTGGTAAGCAGTTCCTGCCCCGGCTCAGGGC
CAAGAACAGATGGAACAGCTGAATATGGGCCAAACAGGATATCTGTGGTAAGCAGTTCCTG
CCCCGGCTCAGGGCCAAGAACAGATGGTCCCCAGATGCGGTCCAGCCCTCAGCAGTTTCTA
GAGAACCATCAGATGTTTCCAGGGTGCCCAAGGACCTGAAATGACCCTGTGCCTTATTTGA
ACTAACCAATCAGTTCGCTTCTCGCTTCTGTTTCGCGCGCTTCTGCTCCCCGAGCTCAATAAAA
GAGCCACAACCCCTCACTCGGGGCGCCAGTCCCGATTGACTGAGTCGCCCGGGTACCC
GTGTATCCAATAAACCCCTCTTGCAGTTGCATCCGACTTGTGGTCTCGCTGTTCCCTGGGAGG
GTCTCCTCTGAGTGATTGACTACCCGTCAGCGGGGGTCTTTCACACCATGCAGCATGTATCA

AAATTAATTTGGTTTTTTTTCTTAAGTATTTACATTAATGGCCATAGTCTGCTCGATCGAGG
AGCTTTTTGCAAAAGCCTAGGCCTCCAAAAGCCTCTTCACTACTTCTGGAATAGCTCAGAG
GCCGAGGCGGCCTCGGCCTCTGCATAAATAAAATAGAAATTAGTCAGCCATGCATGGGGCG
GAGAATGGGCGGAACTGGGCGGAGTTAGGGGCGGGATGGGCGGAGTTAGGGGCGGGAC
TATGGTTGCTGACTAATTGCTGCATTAATGAATCGGCCAACGCGCGGGGAGAGGCGGTTTG
CGTATTGGGCGCTCTCCGCTTCTCGCTCACTGACTCGCTGCGCTCGGTCGTTCCGGCTGCG
GCGAGCGGTATCAGCTCACTCAAAGGCGGTAATACGGTTATCCACAGAATCAGGGGATAAC
GCAGGAAAGAACATGTGAGCAAAGGCCAGCAAAGGCCAGGAACCGTAAAAAGGCCGC
GTTGCTGGCGTTTTTCCATAGGCTCCGCCCCCTGACGAGCATCACAAAATCGACGCTCAA
GTCAGAGGTGGCGAAACCCGACAGGACTATAAAGATACCAAGGCGTTTCCCCTGGAAGCT
CCCTCGTGCCTCTCCTGTTCCGACCCTGCCGCTTACCGGATACCTGTCCGCTTTCTCCCTC
GGGAAGCGTGGCGCTTCTCATAGCTCACGCTGTAGGTATCTCAGTTCGGTGTAGGTCGTT
GCTCCAAGCTGGGCTGTGTGCACGAACCCCCGTTACGCCGACCGCTGCGCCTTATCCGGT
AACTATCGTCTTGAGTCCAACCCGGTAAGACACGACTTATCGCCACTGGCAGCAGCCACTGG
TAACAGGATTAGCAGAGCGAGGTATGTAGGCGGTGCTACAGAGTTCTTGAAGTGGTGGCC
TAACTACGGCTACACTAGAAGGACAGTATTTGGTATCTGCGCTCTGCTGAAGCCAGTTACCT
TCGGAAAAAGAGTTGGTAGCTCTTGATCCGGCAAACAAACCACCGCTGGTAGCGGTGGTTT
TTTTGTTTGCAAGCAGCAGATTACGCGCAGAAAAAAGGATCTCAAGAAGATCCTTTGATCT
TTTCTACGGGGTCTGACGCTCAGTGAACGAAAACCTCACGTTAAGGGATTTTGGTCATGAG
ATTATCAAAAAGGATCTTACCTAGATCCTTTTAAATTA AAAATGAAGTTTTAAATCAATCTA
AAGTATATATGAGTAACTTGGTCTGACAGTTACCAATGCTTAATCAGTGAGGCACCTATCT
CAGCGATCTGTCTATTTGTTTCATCCATAGTTGCCTGACTCCCCGTCGTGTAGATAACTACGA
TACGGGAGGGCTTACCATCTGGCCCCAGTGCTGCAATGATACCGCGAGACCCACGCTCACC
GGCTCCAGATTTATCAGCAATAAACCAGCCAGCCGGAAGGGCCGAGCGCAGAAGTGGTCC
TGCAACTTTATCCGCTCCATCCAGTCTATTAATTGTTGCCGGAAGCTAGAGTAAGTAGTT
CGCCAGTTAATAGTTTGCGCAACGTTGTTGCCATTGCTACAGGCATCGTGGTGTACGCTCG
TCGTTTGGTATGGCTTCATTCAGCTCCGGTTCCCAACGATCAAGGCGAGTTACATGATCCCC
CATGTTGTGCAAAAAGCGGTTAGCTCCTTCGGTCTCCGATCGTTGTCAGAAGTAAGTTGG
CCGAGTGTTATCACTCATGGTTATGGCAGCACTGCATAATTCTTACTGTCATGCCATCCG
TAAGATGCTTTTCTGTGACTGGTGAGTACTCAACCAAGTCATTCTGAGAATAGTGTATGCGG
CGACCGAGTTGCTCTTGCCCGCGTCAACACGGGATAATACCGCGCCACATAGCAGA ACTT
TAAAAGTGCTCATCATTGGAAAACGTTCTTCGGGGCGAAAACCTCTCAAGGATCTTACCGCTG

TTGAGATCCAGTTCGATGTAACCCACTCGTGCACCCAAGTATCTTCAGCATCTTTACTTTC
ACCAGCGTTTCTGGGTGAGCAAAAACAGGAAGGCAAAATGCCGCAAAAAGGGAATAAGG
GCGACACGGAAATGTTGAATACTCATACTCTTCTTTTTCAATATTATTGAAGCATTATCAG
GGTTATTGTCTCATGAGCGGATACATATTTGAATGTATTTAGAAAAATAAACAAATAGGGGT
TCCGCGCACATTTCCCGAAAAGTGCCACCTGACGTCTAAGAAACCATTATTATCATGACATT
AACCTATAAAAATAGGCGTATCACGAGGCCCTTTCGTCTCGCGGTTTCGGTGATGACGGT
GAAAACCTCTGACACATGCAGCTCCCGGAGACGGTACAGCTTGTCTGTAAGCGGATGCCG
GGAGCAGACAAGCCCGTCAGGGCGCGTCAGCGGGTGTGGCGGGTGTGCGGGCTGGCTT
AACTATGCGGCATCAGAGCAGATTGTAAGTACTGAGAGTGCACCATTGACGCTCTCCCTTATGCG
ACTCCTGCATAGGAAGCAGCCAGTAGTAGGTTGAGGCCGTTGAGCACCGCCGCCGCAAG
GAATGGTCTGGCTTATCGAAATTAATACGACTCACTATAGGGAGACCGGAATTCCCATCGAT
ATCGATGGGCTAGAGTCCGTTACATAACTTACGGTAAATGGCCCGCCTGGCTGACCGCCCA
ACGACCCCGCCATTGACGTCAATAATGACGTATGTTCCCATAGTAACGCCAATAGGGACT
TTCCATTGACGTCAATGGGTGGAGTATTTACGGTAAACTGCCCACTTGGCAGTACATCAAGT
GTATCATATGCCAAGTCCGCCCCCTATTGACGTCAATGACGGTAAATGGCCCGCCTGGCATT
ATGCCCAGTACATGACCTTACGGGACTTTCCTACTTGGCAGTACATCTACGTATTAGTCATCG
CTATTACCATGCATGGTGTGATGCGGTTTTGGCAGTACACCAATGGGCGTGGATAGCGGTTTG
ACTCACGGGGATTTCCAAGTCTCCACCCCATGACGTCAATGGGAGTTTGTGGTGGCACCAA
AATCAACGGGACTTTCCAAAATGTCGTAACAACCTCCGCCCCATTGACGCAATGGGCGGTA
GGCGTGTACGGTGGGAGGTCTATATAAGCAGAGCTCGTTTAGTGAACCGGCGCCAGTCCTC
CGATTGACTGAGTCGCCCCGGGTACCCGTGTATCCAATAAACCTCTTGCAGTTGCATCCGAC
TTGTGGTCTCGCTGTTCTTGGGAGGGTCTCCTCTGAGTGATTGACTACCCGTCAGCGGGGG
TCTTTCATTTGGGGGCTCGTCCGGGATCGGGAGACCCCTGCCAGGACCACCGACCCACCA
CCGGGAGGTAAGCTGGCCAGCAACTTATTCTGTGTCTGTCCGATTGTCTAGTGTCTATGACT
GATTTTATGCGCCTGCGTCCGTTACTAGTTAGCTAACTAGCTCTGTATCTGGCGGACCCGTGG
TGGAAGTACGAGTTCGGAACACCCGGCCGCAACCCTGGGAGACGTCCCAGGGACTTTGG
GGCCGTTTTTGTGGCCCGACCTGAGTCCTAAAATCCCGATCGTTTAGGACTCTTTGGTGCA
CCCCCTTAGAGGAGGGATATGTGGTTCTGGTAGGAGACGAGAACCTAAAACAGTTCCCGC
CTCCGTCTGAATTTTTGCTTTCGGTTTGGGACCGAAGCCGCGCGTCTTGTCTGCTGCAGCATC
GTTCTGTGTTGTCTGTCTGACTGTGTTTCTGTATTTGTCTGAAAATATGGGCCCGGGCTAG
CCTGTTACCACTCCCTTAAGTTTGACCTTAGGTCACTGGAAAGATGTCGAGCGGATCGCTCA
CAACCAGTCGGTAGATGTCAAGAAGAGACGTTGGGTTACCTTCTGCTCTGCAGAATGGCCA

ACCTTTAACGTGGATGGCCGCGAGACGGCACCTTTAACCGAGACCTCATCACCCAGGTAA
GATCAAGGTCTTTTACCTGGCCCGCATGGACACCCAGACCAGGTCCCCTACATCGTGACCT
GGGAAGCCTTGGCTTTTGACCCCCCTCCCTGGGTCAAGCCCTTTGTACACCCTAAGCCTCCG
CCTCCTCTCCTCCATCCGCCCCGTCTCTCCCCCTTGAACCTCCTCGTTCGACCCCGCCTCGAT
CCTCCCTTTATCCAGCCCTCACTCCTTCTCTAGGCGCCCCATATGGCCATATGAGATCTTATA
TGGGGCACCCCGCCCTTGTAACTTCCCTGACCCTGACATGACAAGAGTTACTAACAGCC
CCTCTCTCCAACCTCACTTACAGGCTCTCTACTTAGTCCAGCACGAAGTCTGGAGACCTCTGGC
GGCAGCCTACCAAGAACAACCTGGACCGACCGGTGGTACCTCACCTTACCGAGTCGGCGAC
ACAGTGTGGGTCCGCCGACACCAGACTAAGAACCTAGAACCTCGCTGGAAAGGACCTTACA
CAGTCTGCTGACCACCCACCGCCCTCAAAGTAGACGGCATCGCAGCTTGGATACACGCC
GCCACGTGAAGGCTGCCGACCCCGG

pMP71-TRP2

AGCATCGTTCTGTGTTGTCTCTGTCTGACTGTGTTTCTGTATTTGTCTGAAAATTAGCTCGAC
AAAGTTAAGTAATAGTCCCTCTCTCCAAGCTCACTTACAGGCGCCGCATGGCCCCGCGGCT
GCTGTGCTACACCGTGCTGTGCCTGCTGGGCGCCAGAATCCTGAACAGCAAGGTGATCCAG
ACCCCCAGATACCTGGTGAAGGGCCAGGGCCAGAAAGCCAAGATGAGATGCATCCCCGAG
AAGGGCCACCCCGTGGTGTCTGGTATCAGCAGAACAAGAACAACGAGTTCAAGTTCCTGA
TCAACTCCAGAACCAGGAAGTGCTGCAGCAGATCGACATGACCGAGAAGAGGTTTCAGCG
CCGAGTGCCCCAGCAACAGCCCCTGCAGCCTGAAATCCAGAGCAGCGAGGCCGGCGACA
GCGCCCTGTACCTGTGCGCCAGCAGCCTGACAGGCGGCGAGCAGTACTTCGGCCCTGGCAC
CAGGCTGACCGTGCTCGAGGACCTGAGGAACGTGACCCCCCAAGGTGTCCCTGTTTCGAG
CCCAGCAAGGCCGAGATCGCCAACAAGCAGAAGGCCACCCTGGTGTGCCTGGCCAGGGGC
TTCTTCCCCGACCACGTGGAGCTGTCTGGTGGGTGAACGGCAAGGAGGTGCACAGCGGC
GTGTGCACCGACCCCGAGCCTACAAGGAGAGCAACTACAGCTACTGCCTGAGCAGCAGGC
TGAGAGTGAGCGCCACCTTCTGGCACAACCCAGGAACCACTTCCGCTGTCAGGTGCAGTT
CCACGGCCTGAGCGAGGAGGACAAGTGGCCCCGAGGGCAGCCCCAAGCCCGTGACCCAGAA
CATCAGCGCCGAGGCCTGGGGCAGAGCCGACTGCGGCATCACCAGCGCCAGCTACCACCA
GGGCGTGCTGTCCGCCACCATCTGTACGAGATCCTGCTGGGCAAGGCCACACTGTACGCC
GTGCTGGTGTCCGGCCTGGTGTGATGGCCATGGTGAAGAAGAAGAACAGCAGCGGCAGC
GGCGCCACCAACTTCAGCCTGCTGAAGCAGGCCGGCGACGTGGAGGAAAACCTGGGCCC
ATGAGGCCCGTGACCTGCAGCGTGCTGGTGTGCTGCTGATGCTGCGGAGAAGCAACGGC

GACGGCGACAGCGTGACCCAGACCGAGGGCCTGGTGACCCTGACAGAGGGACTGCCCGTG
ATGCTGAACTGCACCTACCAGACCATCTACAGCAACCCCTTCTGTTTTGGTACGTGCAGCA
CCTGAACGAGAGCCCCAGACTGCTGCTGAAGAGCTTCACGACAACAAGAGGACCGAGCA
CCAGGGCTTCCACGCCACCCTGCACAAGAGCAGCAGCAGCTTCCACCTGCAAAAGTCCAGC
GCCAGCTGTCCGACAGCGCCCTGTACTACTGCGCCCTGAGGGGCAGCAACAACAGGATCT
TCTTCGGCGACGGCACCCAGCTGGTCGTGAAGCCCGACATCCAGAACCCCGAGCCCGCCGT
GTACCAGCTGAAGGACCCAGAAGCCAGGACAGCACCCCTGTGCCTGTTACCGACTTCGAC
AGCCAGATCAACGTGCCAAGACCATGGAGAGCGGCACCTTCATCACCGACAAGTGCGTGC
TGGACATGAAGGCCATGGACAGCAAGAGCAACGGCGCCATCGCCTGGTCCAACCAGACCA
GCTTCACATGCCAGGACATCTTCAAGGAGACCAACGCCACCTACCCAGCAGCGACGTGCC
CTGCGACGCCACCCTGACCGAGAAGAGCTTCGAGACCGACATGAACCTGAACTTCCAGAAC
CTGAGCGTGATGGGCCTGAGAATCCTGCTGCTGAAGGTGGCCGGCTTCAACCTGCTGATGA
CCCTGAGGCTGTGGAGCAGCTGAGTCGACACGCGTACGTCGCGACCGCGGACATGTACAG
AGCTCGAGCGGGATCAATTCCGCCCCCCCCCTAACGTTACTGGCCGAAGCCGCTTGGAATA
AGGCCGGTGTGCGTTTGTCTATATGTTATTTTCCACCATATTGCCGTCTTTGGCAATGTGAG
GGCCCGAAACCTGGCCCTGTCTTCTTGACGAGCATTCTAGGGGTCTTCCCTCTCGCCA
AAGGAATGCAAGGTCTGTTGAATGTCGTGAAGGAAGCAGTTCCTCTGGAAGCTTCTGAAG
ACAAACAACGTCTGTAGCGACCCTTTGCAGGCAGCGGAACCCCCACCTGGCGACAGGTGC
CTCTGCGGCCAAAAGCCACGTGTATAAGATACACCTGCAAAGGCGGCACAACCCAGTGCC
ACGTTGTGAGTTGGATAGTTGTGGAAAGAGTCAAATGGCTCTCCTCAAGCGTATTCAACAA
GGGGCTGAAGGATGCCAGAAGGTACCCATTGTATGGGATCTGATCTGGGGCCTCGGTG
CACATGCTTTACATGTGTTTAGTCGAGGTTAAAAACGTCTAGGCCCCCGAACCACGGGG
ACGTGGTTTTCTTTGAAAAACACGATAATAATGCCACCATGCCATCTCCTCTCCCTGTCTCC
TTCTCCTCTTTCTTACCTTAGTAGGAGGCAGGCCCCAGAAGTCCTTACTGGTGGAGGTAGA
AGAGGGAGGCAATGTTGTGCTGCCATGCCTCCCGACTCCTCACCTGTCTCTTCTGAGAAGC
TGGCTTGGTATCGAGGTAACCAGTCAACACCCTTCTGGAGCTGAGCCCCGGGTCCCCTGG
CCTGGGATTGCACGTGGGGTCCCTGGGCATCTTGCTAGTGATTGTCAATGTCTCAGACCATA
TGGGGGGCTTCTACCTGTGCCAGAAGAGGCCCCCTTCAAGGACATCTGGCAGCCTGCCTG
GACAGTGAACGTGGAGGATAGTGGGGAGATGTTCCGGTGAATGCTTCAGACGTCAGGGA
CCTGGACTGTGACCTAAGGAACAGGTCCTCTGGGAGCCACAGGTCCACTTCTGGTTCCCAG
CTGTATGTGTGGGCTAAAGACCATCCTAAGGTCTGGGGAAACAAAGCCTGTATGTGCCCTC
GGGGGAGCAGTTTGAATCAGAGTCTAATCAACCAAGACCTCACTGTGGCACCCGGCTCCAC

ACTTTGGCTGTCTGTGGGGTACCCCTGTCCCAGTGGCCAAAGGCTCCATCTCCTGGACCC
ATGTGCATCCTAGGAGACCTAATGTTTCACTACTGAGCCTAAGCCTTGGGGGAGAGCACCC
GGTCAGAGAGATGTGGGTTTGGGGTCTCTTCTGCTTCTGCCCAAGCCACAGCTTTAGAT
GAAGGCACCTATTATTGTCTCCGAGGAAACCTGACCATCGAGAGGCACGTGAAGGTCATTG
CAAGGTCAGCAGTGTGGCTCTGGCTGTTGAGAACTGGTGGATGGATAGTCCCAGTGGTGA
CTTTAGTATATGTCATCTTCTGTATGGTTTCTCTGGTGGCTTTTCTCTATTGTCAAAGAGCCTT
TATCCTGAGAAGGAAAAGGAAGCGAATGACTGACCCCGCCAGGAGATTCTTCAAAGTGAC
GTGATCCGGATTAGTCCAATTTGTTAAAGACAGGATATCAGTGGTCCAGGCTCTAGTTTTGA
CTCAACAATATCACCAGCTGAAGCCTATAGAGTGAATTCGGATCCAAGCTTAGGCCTGCTCG
CTTTCTTGCTGTCCATTTCTATTAAAGGTTCCCTTGTCCCTAAGTCCAACTACTAAACTGGG
GGATATTATGAAGGGCCTTGAGCATCTGGATTCTGCCTAGCGCTAAGCTTCTAACACGAGC
CATAGATAGAATAAAAGATTTTATTTAGTCTCCAGAAAAAGGGGGGAATGAAAGACCCAC
CTGTAGGTTTGGCAAGCTAGCTTAAGTAAGCATTTTGCAAGGCATGGAAAAATACATAACT
GAGAATAGAGAAGTTCAGATCAAGGTTAGGAACAGAGAGACAGGAGAATATGGGCCAAA
CAGGATATCTGTGGTAAGCAGTTCCTGCCCCGGCTCAGGGCCAAGAACAGTTGGAACAGCA
GAATATGGGCCAACAGGATATCTGTGGTAAGCAGTTCCTGCCCCGGCTCAGGGCCAAGAA
CAGATGGTCCCAGATGCGGTCCCGCCCTCAGCAGTTTCTAGAGAACCATCAGATGTTTCCA
GGGTGCCCCAAGGACCTGAAATGACCCTGTGCCTTATTTGAACTAACCAATCAGTTCGCTTC
TCGTTCTGTTGCGCGCTTCTGCTCCCCGAGCTCAATAAAAGAGCCACAACCCCTCACTCG
GCGCGCCAGTCTCCGATAGACTGCGTCGCCCCGGGTACCCGTATTCCAATAAAGCCTCTT
GCTGTTTGCATCCGAATCGTGGACTCGCTGATCCTTGGGAGGGTCTCCTCAGATTGATTGAC
TGCCACCTCGGGGGTCTTTCATTCTCGAGAGCTTTGGCGTAATCATGGTCATAGCTGTTTCC
TGTGTGAAATTGTTATCCGCTCACAATTCCACACAACATACGAGCCGGAAGCATAAAGTGTA
AAGCCTGGGGTGCCTAATGAGTGAGCTAACTCACATTAATTGCGTTGCGCTCACTGCCCCGCT
TTCCAGTCGGGAAACCTGTCGTGCCAGCTGCATTAATGAATCGGCCAACGCGCGGGGAGA
GGCGGTTTGCATATTGGGCGCTCTTCCGCTTCCCTCGCTCACTGACTCGCTGCGCTCGGTGCT
TCGGCTGCGGCGAGCGGTATCAGCTCACTCAAAGGCGGTAATACGGTTATCCACAGAATCA
GGGGATAACGCAGGAAAGAACATGTGAGCAAAAGGCCAGCAAAAGGCCAGGAACCGTAA
AAAGGCCGCGTTGCTGGCGTTTTTCCATAGGCTCCGCCCCCTGACGAGCATCACAAAATC
GACGCTCAAGTCAGAGGTGGCGAAACCCGACAGGACTATAAAGATACCAGGCGTTTTCCCC
TGGAAGCTCCCTCGTGCCTCTCCTGTTCCGACCCTGCCGCTTACCGGATACCTGTCCGCCTT
TCTCCCTTCGGGAAGCGTGGCGCTTTCTCAATGCTCACGCTGTAGGTATCTCAGTTCGGTGT

AGGTCGTTGCTCCAAGCTGGGCTGTGTGCACGAACCCCCGTTAGCCCGACCGCTGCGC
CTTATCCGGTAACTATCGTCTTGAGTCCAACCCGGTAAGACACGACTTATCGCCACTGGCAG
CAGCCACTGGTAACAGGATTAGCAGAGCGAGGTATGTAGGCGGTGCTACAGAGTTCTTGA
AGTGGTGGCCTAACTACGGCTACACTAGAAGGACAGTATTTGGTATCTGCGCTCTGCTGAA
GCCAGTTACCTTCGGAAAAAGAGTTGGTAGCTCTTGATCCGGCAAACAAACCACCGCTGGT
AGCGGTGGTTTTTTTTGTTTGAAGCAGCAGATTACGCGCAGAAAAAAGGATCTCAAGAAG
ATCCTTTGATCTTTTCTACGGGGTCTGACGCTCAGTGGAACGAAAACCTCACGTTAAGGGATT
TTGGTCATGAGATTATCAAAAAGGATCTTACCTAGATCCTTTTAAATTA AAAATGAAGTTTT
AAATCAATCTAAAGTATATATGAGTAACTTGGTCTGACAGTTACCAATGCTTAATCAGTGA
GGCACCTATCTCAGCGATCTGTCTATTTGTTTCATCCATAGTTGCCTGACTCCCCGTCGTGTA
GATAACTACGATACGGGAGGGCTTACCATCTGGCCCCAGTGCTGCAATGATACCGCGAGAC
CCACGCTCACCGGCTCCAGATTTATCAGCAATAAACCAGCCAGCCGGAAGGGCCGAGCGCA
GAAGTGGTCTGCAACTTTATCCGCCTCCATCCAGTCTATTAATTGTTGCCGGAAGCTAGA
GTAAGTAGTTCGCCAGTTAATAGTTTGCGCAACGTTGTTGCCATTGCTGCTGGCATCGTGGT
GTCACGCTCGTCGTTTGGTATGGCTTCATTCAGCTCCGGTTCCCAACGATCAAGGCGAGTTA
CATGATCCCCATGTTGTGCAAAAAGCGGTTAGCTCCTTCGGTCTCCGATCGTTGTCAGA
AGTAAGTTGGCCGAGTGTTATCACTCATGGTTATGGCAGCACTGCATAATTCTCTTACTGT
CATGCCATCCGTAAGATGCTTTTCTGTGACTGGTGAGTACTCAACCAAGTCATTCTGAGAAT
AGTGTATGCGGCGACCGAGTTGCTCTTGCCCGCGTCAATACGGGATAATACCGCGCCACA
TAGCAGAACTTTAAAAGTGCTCATCATTGAAAACGTTCTTCGGGGCGAAAACCTCTCAAGG
ATCTTACCGCTGTTGAGATCCAGTTCGATGTAACCCACTCGTGACCCAACTGATCTTCAGCA
TCTTTTACTTTCACCAGCGTTTCTGGGTGAGCAAAAACAGGAAGGCAAAATGCCGCAAAAA
AGGGAATAAGGGCGACACGGAAATGTTGAATACTCATACTCTTCCTTTTTCAATATTATTGA
AGCATTATCAGGGTTATTGTCTCATGAGCGGATACATATTTGAATGTATTTAGAAAAATAA
ACAAATAGGGGTTCCGCGCACATTTCCCCGAAAAGTGCCACCTGACGTCTAAGAAACCATTA
TTATCATGACATTAACCTATAAAAATAGGCGTATCACGAGGCCCTTTTCGTCTTCAAGCTGCCT
CGCGCGTTTTCGGTGATGACGGTGAAAACCTCTGACACATGCAGCTCCCGGAGACGGTCACA
GCTTGTCTGTAAGCGGATGCCGGGAGCAGACAAGCCCGTCAGGGCGCGTCAGCGGGTGT
GGCGGGTGTGCGGGCGCAGCCATGACCCAGTCACGTAGCGATAGTTACTATGCGGCATCA
GAGCAGATTGTACTGAGAGTGCACCATATGCGGTGTGAAATACCGCACAGATGCGTAAGG
AGAAAATACCGCATCAGGCGCCATTCGCCATTCAGGCTGCGCAACTGTTGGGAAGGGCGAT
CGGTGCGGGCCTCTTCGCTATTACGCCAGCTGGCGAAAAGGGGGATGTGCTGCAAGGCGAT

TAAGTTGGGTAACGCCAGGGTTTTCCAGTCACGACGTTGTAAAACGACGGCCAGTGAATT
AGTACTCTAGCTTAAGTAAGCCATTTTGAAGGCATGGAAAAATACATAACTGAGAATAGA
GAAGTTCAGATCAAGGTTAGGAACAGAGAGACAGGAGAATATGGGCCAAACAGGATATCT
GTGGTAAGCAGTTCCTGCCCGGCTCAGGGCCAAGAACAGTTGGAACAGCAGAATATGGG
CCAAACAGGATATCTGTGGTAAGCAGTTCCTGCCCGGCTCAGGGCCAAGAACAGATGGTC
CCCAGATGCGGTCCCGCCCTCAGCAGTTTCTAGAGAACCATCAGATGTTTCCAGGGTGCCCC
AAGGACCTGAAATGACCCTGTGCCTTATTTGAACTAACCAATCAGTTCGCTTCTCGCTTCTGT
TCGCGCGCTTCTGCTCCCGAGCTCAATAAAAGAGCCCAACAACCCCTCACTCGGCGCGCCAG
TCCTCCGATTGACTGCGTCGCCCCGGGTACCCGTATTCCAATAAAGCCTCTTGCTGTTTGCAT
CCGAATCGTGGACTCGCTGATCCTTGGGAGGGTCTCCTCAGATTGATTGACTGCCACCTCG
GGGGTCTTTCAATTTGGAGGTTCCACCGAGATTTGGAGACCCCTGCCAGGGACCACCGACC
CCCCGCCGGGAGGTAAGCTGGCCAGCGGTGTTTTCGTGTCTGTCTGTCTTTGGGCGTGT
TTGTGCCGGCATCTAATGTTTGCCTGCGTCTGTACTAGTTGGCTAACTAGATCTGTATCTG
GCGGTCCCGCGGAAGAAGTACGAGTTCGTATTCCCGGCCGAGCCCTGGGAGACGTCCC
AGCGGCCTCGGGGGCCCGTTTTGTGGCCATTCTGTATCAGTTAACCTACCCGAGTCGGACT
TTTTGGAGCTCCGCCACTGTCCGAGGGGTACGTGGCTTTGTTGGGGACGAGAGACAGAG
ACACTTCCCGCCCCCGTCTGAATTTTTGCTTTCGGTTTTACGCCGAAACCGCGCCGCGCTCT
TGTCTGCTGC

pMP71-TRP2-hWT-L-selectin

AGCATCGTTCTGTGTTGTCTCTGTCTGACTGTGTTTCTGTATTTGTCTGAAAATTAGCTCGAC
AAAGTTAAGTAATAGTCCCTCTCTCAAGCTCACTTACAGGCGGCCGCATGGCCCCGCGGCT
GCTGTGCTACACCGTGCTGTGCCTGCTGGGCGCCAGAATCCTGAACAGCAAGGTGATCCAG
ACCCCCAGATACTGGTGAAGGGCCAGGGCCAGAAAGCCAAGATGAGATGCATCCCCGAG
AAGGGCCACCCCGTGGTGTCTGGTATCAGCAGAACAAGAACAACGAGTTCAAGTTCCTGA
TCAACTTCCAGAACCAGGAAGTGCTGCAGCAGATCGACATGACCGAGAAGAGGTTTCAGCG
CCGAGTGCCCCAGCAACAGCCCCTGCAGCCTGGAATCCAGAGCAGCGAGGCCGGCGACA
GCGCCCTGTACCTGTGCGCCAGCAGCCTGACAGGCGGCGAGCAGTACTTCGGCCCTGGCAC
CAGGCTGACCGTGCTCGAGGACCTGAGGAACGTGACCCCCCAAGGTGTCCCTGTTTCGAG
CCCAGCAAGGCCGAGATCGCCAACAAGCAGAAGGCCACCCTGGTGTGCCTGGCCAGGGGC
TTCTTCCCGACCACGTGGAGCTGTCTTGGTGGGTGAACGGCAAGGAGGTGCACAGCGGC
GTGTGCACCGACCCCAGGCCTACAAGGAGAGCAACTACAGCTACTGCCTGAGCAGCAGGC

TGAGAGTGAGCGCCACCTTCTGGCACAACCCCAGGAACCACTTCCGCTGTCAGGTGCAGTT
CCACGGCCTGAGCGAGGAGGACAAGTGGCCCGAGGGCAGCCCCAAGCCCGTGACCCAGAA
CATCAGCGCCGAGGCCTGGGGCAGAGCCGACTGCGGCATCACCAGCGCCAGCTACCACCA
GGGCGTGCTGTCCGCCACCATCCTGTACGAGATCCTGCTGGGCAAGGCCACACTGTACGCC
GTGCTGGTGTCCGGCCTGGTGTGATGGCCATGGTGAAGAAGAAGAACAGCAGCGGCAGC
GGCGCCACCAACTTCAGCCTGCTGAAGCAGGCCGGCGACGTGGAGGAAAACCTGGGCCC
ATGAGGCCCGTGACCTGCAGCGTGCTGGTGTGCTGCTGATGCTGCGGAGAAGCAACGGC
GACGGCGACAGCGTGACCCAGACCGAGGGCCTGGTGACCCTGACAGAGGGACTGCCCGTG
ATGCTGAACTGCACCTACCAGACCATCTACAGCAACCCCTTCTGTTTTGGTACGTGCAGCA
CCTGAACGAGAGCCCCAGACTGCTGCTGAAGAGCTTCACCGACAACAAGAGGACCGAGCA
CCAGGGCTTCCACGCCACCCTGCACAAGAGCAGCAGCAGCTTCCACCTGCAAAAGTCCAGC
GCCAGCTGTCCGACAGCGCCCTGTACTACTGCGCCCTGAGGGGCAGCAACAACAGGATCT
TCTTCGGCGACGGCACCCAGCTGGTCGTGAAGCCCGACATCCAGAACCCCGAGCCCGCCGT
GTACCAGCTGAAGGACCCCAAGAAGCCAGGACAGCACCCCTGTGCCTGTTACCGACTTCGAC
AGCCAGATCAACGTGCCAAGACCATGGAGAGCGGCACCTTCATCACCGACAAGTGCGTGC
TGGACATGAAGGCCATGGACAGCAAGAGCAACGGCGCCATCGCCTGGTCCAACCAGACCA
GCTTCACATGCCAGGACATCTTCAAGGAGACCAACGCCACCTACCCAGCAGCGACGTGCC
CTGCGACGCCACCCTGACCGAGAAGAGCTTCGAGACCGACATGAACCTGAACTTCCAGAAC
CTGAGCGTGATGGGCCTGAGAATCCTGCTGCTGAAGGTGGCCGGCTTCAACCTGCTGATGA
CCCTGAGGCTGTGGAGCAGCTGAGTCGACACGCGTACGTGCGGACCGCGGACATGTACAG
AGCTCGAGCGGGATCAATTCCGCCCCCCCCCTAACGTTACTGGCCGAAGCCGCTTGAATA
AGGCCGGTGTGCGTTTGTCTATATGTTATTTTCCACCATATTGCCGTCTTTGGCAATGTGAG
GGCCCGGAAACCTGGCCCTGTCTTCTTGACGAGCATTCTAGGGGTCTTCCCTCTCGCCA
AAGGAATGCAAGGTCTGTTGAATGTCGTGAAGGAAGCAGTTCCTCTGGAAGCTTCTGAAG
ACAAACAACGTCTGTAGCGACCCTTTCAGGCAGCGGAACCCCCACCTGGCGACAGGTGC
CTCTGCGGCCAAAAGCCACGTGTATAAGATACACCTGCAAAGGCGGCACAACCCCAAGTCC
ACGTTGTGAGTTGGATAGTTGTGGAAAGAGTCAAATGGCTCTCCTCAAGCGTATTCAACAA
GGGGCTGAAGGATGCCAGAAGGTACCCATTGTATGGGATCTGATCTGGGGCCTCGGTG
CACATGCTTTACATGTGTTTAGTCGAGGTTAAAAACGTCTAGGCCCCCCGAACCACGGGG
ACGTGGTTTTCTTTGAAAAACACGATAATAATGCCACCATGCCATCTCCTCTCCCTGTCTCC
TTCCTCCTCTTCTTACCTTAGTAGGAGGCAGGCCCCAGAAGTCCTTACTGGTGGAGGTAGA
AGAGGGAGGCAATGTTGTGCTGCCATGCCTCCCGGACTCCTCACCTGTCTCTTCTGAGAAGC

TGGCTTGGTATCGAGGTAACCAGTCAACACCCTTCCTGGAGCTGAGCCCCGGGTCCCCTGG
CCTGGGATTGCACGTGGGGTCCCTGGGCATCTTGCTAGTGATTGTCAATGTCTCAGACCATA
TGGGGGGCTTCTACCTGTGCCAGAAGAGGCCCCCTTCAAGGACATCTGGCAGCCTGCCTG
GACAGTGAACGTGGAGGATAGTGGGGAGATGTTCCGGTGAATGCTTCAGACGTCAGGGA
CCTGGACTGTGACCTAAGGAACAGGTCCTCTGGGAGCCACAGGTCCACTTCTGGTTCCCAG
CTGTATGTGTGGGCTAAAGACCATCCTAAGGTCTGGGGAACAAAGCCTGTATGTGCCCTC
GGGGGAGCAGTTTGAATCAGAGTCTAATCAACCAAGACCTCACTGTGGCACCCGGCTCCAC
ACTTTGGCTGTCTGTGGGGTACCCCTGTCCCAGTGGCCAAAGGCTCCATCTCCTGGACCC
ATGTGCATCCTAGGAGACCTAATGTTTCACTACTGAGCCTAAGCCTTGGGGGAGAGCACCC
GGTCAGAGAGATGTGGGTTTGGGGTCTCTTCTGCTTCTGCCCAAGCCACAGCTTTAGAT
GAAGGCACCTATTATTGTCTCCGAGGAAACCTGACCATCGAGAGGCACGTGAAGGTCATTG
CAAGGTCAGCAGTGTGGCTCTGGCTGTTGAGAACTGGTGGATGGATAGTCCCAGTGGTGA
CTTTAGTATATGTCATCTTCTGTATGGTTTCTCTGGTGGCTTTTCTCTATTGTCAAAGAGCCTT
TATCCTGAGAAGGAAAAGGAAGCGAATGACTGACCCCGCCAGGAGATTCTTCAAAGTGAC
GGGCAGCGGCGAAGGCCGCGGCAGCCTGCTGACCTGCGGCGATGTGGAAGAAAACCCTG
GCCCGATGGGCTGCAGAAGAACTAGAGAAGGACCAAGCAAAGCCATGATATTTCCATGGA
AATGTCAGAGCACCCAGAGGGACTTATGGAACATCTTCAAGTTGTGGGGGTGGACAATGCT
CTGTTGTGATTTCTGGCACATCATGGAACCGACTGCTGGACTTACCATTATTCTGAAAAAC
CCATGAACTGGCAAAGGGCTAGAAGATTCTGCCGAGACAATTACACAGATTTAGTTGCCAT
ACAAAACAAGGCGGAAATTGAGTATCTGGAGAAGACTCTGCCTTTCAGTCGTTCTTACTACT
GGATAGGAATCCGGAAGATAGGAGGAATATGGACGTGGGTGGGAACCAACAAATCTCTCA
CTGAAGAAGCAGAGAACTGGGGAGATGGTGAGCCCAACAACAAGAAGAACAAGGAGGAC
TGC GTGGAGATCTATATCAAGAGAAACAAGATGCAGGCAAATGGAACGATGACGCCTGC
CACAACTAAAGGCAGCCCTCTGTTACACAGCTTCTTGCCAGCCCTGGTCATGCAGTGGCCA
TGGAGAATGTGTAGAAATCATCAATAATTACACCTGCAACTGTGATGTGGGGTACTATGGG
CCCCAGTGTGAGTTTGTGATTCAGTGTGAGCCTTTGGAGGCCCCAGAGCTGGGTACCATGG
ACTGTACTCACCTTTGGGAACTTCAGCTTCAGCTCACAGTGTGCCTTCAGCTGCTCTGAA
GGAACAACTTAACTGGGATTGAAGAAACCACCTGTGGACCATTTGGAACCTGGTCATCTC
CAGAACCAACCTGTCAAGTGATTCAGTGTGAGCCTCTATCAGCACCAGATTTGGGGATCATG
AACTGTAGCCATCCCCTGGCCAGCTTCAGCTTTACCTCTGCATGTACCTTCATCTGCTCAGAA
GGAACCTGAGTTAATTGGGAAGAAGAAAACCATTTGTGAATCATCTGGAATCTGGTCAAATC
CTAGTCCAATATGTCAAAAATTGGACAAAAGTTTCTCAATGATTAAGGAGGGTGATTATAAC

CCCTCTTCATTCCAGTGGCAGTCATGGTTACTGCATTCTCTGGGTTGGCATTATCATTGG
CTGGCAAGGAGATTAAAAAAGGCAAGAAATCCAAGAGAAGTATGAATGACCCATATTAAT
CCGATTAGTCCAATTTGTTAAAGACAGGATATCAGTGGTCCAGGCTCTAGTTTTGACTCAA
CAATATCACCAGCTGAAGCCTATAGAGTGAATTCGGATCCAAGCTTAGGCCTGCTCGCTTTC
TTGCTGTCCCATTCTATTAAAGGTTCCCTTTGTTCCCTAAGTCCAACACTAACTGGGGGAT
ATTATGAAGGGCCTTGAGCATCTGGATTCTGCCTAGCGCTAAGCTTCTAACACGAGCCATA
GATAGAATAAAAGATTTTATTTAGTCTCCAGAAAAAGGGGGAATGAAAGACCCACCTGT
AGGTTTGGCAAGCTAGCTTAAGTAAGCCATTTTGCAAGGCATGGAAAAATACATAACTGAG
AATAGAGAAGTTCAGATCAAGGTTAGGAACAGAGAGACAGGAGAATATGGGCCAAACAG
GATATCTGTGGTAAGCAGTTCCTGCCCCGGCTCAGGGCCAAGAACAGTTGGAACAGCAGAA
TATGGGCCAAACAGGATATCTGTGGTAAGCAGTTCCTGCCCCGGCTCAGGGCCAAGAACAG
ATGGTCCCAGATGCGGTCCCGCCCTCAGCAGTTTCTAGAGAACCATCAGATGTTTCCAGGG
TGCCCAAGGACCTGAAATGACCCTGTGCCTTATTTGAACTAACCAATCAGTTCGCTTCTCG
TTCTGTTGCGCGCTTCTGCTCCCCGAGCTCAATAAAAGAGCCACAACCCCTCACTCGGCG
CGCCAGTCTCCGATAGACTGCGTCGCCCCGGGTACCCGTATTCCCAATAAAGCCTCTTGCT
GTTTGCATCCGAATCGTGGACTCGCTGATCCTGGGAGGGTCTCCTCAGATTGATTGACTGC
CCACCTCGGGGGTCTTTCATTCTCGAGAGCTTTGGCGTAATCATGGTCATAGCTGTTTCTGT
GTGAAATTGTTATCCGCTCACAAATCCACACAACATACGAGCCGGAAGCATAAAGTGTA
GCCTGGGGTGCCTAATGAGTGAGCTAACTCACATTAATTGCGTTGCGCTCACTGCCCCGTTT
CCAGTCGGGAAACCTGTCGTGCCAGCTGCATTAATGAATCGGCCAACGCGCGGGGAGAGG
CGGTTTGCATATTGGGCGCTTCCGCTTCTCGCTCACTGACTCGCTGCGCTCGGTCTGTTG
GCTGCGGCGAGCGGTATCAGCTCACTCAAAGGCGGTAATACGGTTATCCACAGAATCAGGG
GATAACGCAGGAAAGAACATGTGAGCAAAAGGCCAGCAAAAGGCCAGGAACCGTAAAAA
GGCCGCGTTGCTGGCGTTTTTCCATAGGCTCCGCCCCCTGACGAGCATCACAAAAATCGAC
GCTCAAGTCAGAGGTGGCGAAACCCGACAGGACTATAAAGATACCAGGCGTTTCCCCCTGG
AAGCTCCCTCGTGCCTCTCCTGTTCCGACCCTGCCGCTTACCGGATACCTGTCCGCTTTCT
CCCTTCGGGAAGCGTGGCGCTTCTCAATGCTCACGCTGTAGGTATCTCAGTTCGGTGTAGG
TCGTTGCTCCAAGCTGGGCTGTGTGCACGAACCCCCGTTACGCCGACCGCTGCGCCTTA
TCCGGTAACTATCGTCTTGAGTCCAACCCGGTAAGACACGACTTATCGCCACTGGCAGCAGC
CACTGGTAACAGGATTAGCAGAGCGAGGTATGTAGGCGGTGCTACAGAGTTCTTGAAGTG
GTGGCCTAACTACGGCTACACTAGAAGGACAGTATTTGGTATCTGCGCTCTGCTGAAGCCA
GTTACCTTCGGAAAAAGAGTTGGTAGCTCTTGATCCGGCAAACAAACCACCGCTGGTAGCG

GTGGTTTTTTTTGTTTGAAGCAGCAGATTACGCGCAGAAAAAAGGATCTCAAGAAGATCC
TTTGATCTTTTCTACGGGGTCTGACGCTCAGTGGAACGAAAACCTCACGTTAAGGGATTTTGG
TCATGAGATTATCAAAAAGGATCTTACCTAGATCCTTTTAAATTAATAAATGAAGTTTTAAAT
CAATCTAAAGTATATATGAGTAACTTGGTCTGACAGTTACCAATGCTTAATCAGTGAGGCA
CCTATCTCAGCGATCTGTCTATTTGTTTCATCCATAGTTGCCTGACTCCCCGTCGTGTAGATA
ACTACGATACGGGAGGGCTTACCATCTGGCCCCAGTGCTGCAATGATACCGCGAGACCCAC
GCTCACCGGCTCCAGATTTATCAGCAATAAACCAGCCAGCCGGAAGGGCCGAGCGCAGAA
GTGGTCTGCAACTTTATCCGCCTCCATCCAGTCTATTAATTGTTGCCGGGAAGCTAGAGTA
AGTAGTTCGCCAGTTAATAGTTTGCGCAACGTTGTTGCCATTGCTGCTGGCATCGTGGTGTG
ACGCTCGTCGTTTGGTATGGCTTCATTCAGCTCCGGTCCCAACGATCAAGGCGAGTTACAT
GATCCCCATGTTGTGCAAAAAAGCGTTAGCTCCTTCGGTCTCCGATCGTTGTCAGAAGT
AAGTTGGCCGAGTGTTATCACTCATGGTTATGGCAGCACTGCATAATTCTTACTGTCAT
GCCATCCGTAAGATGCTTTTCTGTGACTGGTGAGTACTCAACCAAGTCATTCTGAGAATAGT
GTATGCGGCGACCGAGTTGCTCTTGCCCGGCGTCAATACGGGATAATACCGCGCCACATAG
CAGAACTTTAAAAGTGCTCATCATTGGAAAACGTTCTTCGGGGCGAAAACCTCAAGGATCT
TACCGCTGTTGAGATCCAGTTCGATGTAACCCACTCGTGCACCCAACTGATCTTCAGCATCTT
TTACTTTCACCAGCGTTTCTGGGTGAGCAAAAACAGGAAGGCAAATGCCGCAAAAAAGGG
AATAAGGGCGACACGGAAATGTTGAATACTCATACTCTTCTTTTTCAATATTATTGAAGCAT
TTATCAGGGTTATTGTCTCATGAGCGGATACATATTTGAATGTATTTAGAAAAATAACAAA
TAGGGGTTCCGCGCACATTTCCCCGAAAAGTGCCACCTGACGTCTAAGAAACCATTATTATC
ATGACATTAACCTATAAAAATAGGCGTATCACGAGGCCCTTTCGTCTTCAAGCTGCCTCGCG
CGTTTCGGTGATGACGGTGAAAACCTCTGACACATGCAGCTCCCGGAGACGGTCACAGCTT
GTCTGTAAGCGGATGCCGGGAGCAGACAAGCCCGTCAGGGCGCGTCAGCGGGTGTGGCG
GGTGTGCGGGGCGCAGCCATGACCCAGTCACGTAGCGATAGTTACTATGCGGCATCAGAGC
AGATTGTAAGTGCAGAGTGCACCATATGCGGTGTGAAATACCGCACAGATGCGTAAGGAGAA
AATACCGCATCAGGCGCCATTCGCCATTCAGGCTGCGCAACTGTTGGGAAGGGCGATCGGT
GCGGGCCTCTTCGCTATTACGCCAGCTGGCGAAAGGGGGATGTGCTGCAAGGCGATTAAG
TTGGGTAACGCCAGGGTTTTCCAGTCACGACGTTGTAAAACGACGGCCAGTGAATTAGTA
CTCTAGCTTAAGTAAGCCATTTTGAAGGCATGGAAAAATACATAACTGAGAATAGAGAAG
TTCAGATCAAGGTTAGGAACAGAGAGACAGGAGAATATGGGCCAAACAGGATATCTGTGG
TAAGCAGTTCCTGCCCCGGCTCAGGGCCAAGAACAGTTGGAACAGCAGAATATGGGCCAA
ACAGGATATCTGTGGTAAGCAGTTCCTGCCCCGGCTCAGGGCCAAGAACAGATGGTCCCCA

GATGCGGTCCCGCCCTCAGCAGTTTCTAGAGAACCATCAGATGTTTCCAGGGTGCCCCAAG
GACCTGAAATGACCCTGTGCCTTATTTGAACTAACCAATCAGTTCGCTTCTCGCTTCTGTTCC
CGCGCTTCTGCTCCCCGAGCTCAATAAAAGAGCCCACAACCCCTCACTCGGGCGGCCAGTCC
TCCGATTGACTGCGTCGCCCCGGGTACCCGTATTCCCAATAAAGCCTCTTGCTGTTTGCATCCG
AATCGTGGACTCGCTGATCCTTGGGAGGGTCTCCTCAGATTGATTGACTGCCACCTCGGG
GGTCTTTCATTTGGAGGTTCCACCGAGATTTGGAGACCCCTGCCAGGGACCACCGACCCCC
CCGCCGGGAGGTAAGCTGGCCAGCGGTCGTTTCGTGTCTGTCTGTCTTTGGGCGTGTGTTG
TGCCGGCATCTAATGTTTGCCTGCGTCTGTAAGTTGGCTAACTAGATCTGTATCTGGC
GGTCCCGCGGAAGAACTGACGAGTTCGTATTCCCGGCCGAGCCCCTGGGAGACGTCCAG
CGGCCTCGGGGGCCCGTTTTGTGGCCATTCTGTATCAGTTAACCTACCCGAGTCGGACTTT
TTGGAGCTCCGCCACTGTCCGAGGGGTACGTGGCTTTGTTGGGGACGAGAGACAGAGAC
ACTTCCCGCCCCGTCTGAATTTTTGCTTTCGGTTTTACGCCGAAACCGCGCCGCGCTTTG
TCTGCTGC

pMP71-TRP2-hΔMN-L-selectin

AGCATCGTTCTGTGTTGTCTCTGTCTGACTGTGTTTCTGTATTTGTCTGAAAATTAGCTCGAC
AAAGTTAAGTAATAGTCCCTCTCTCCAAGCTCACTTACAGGCGCCGCATGGCCCCGCGGCT
GCTGTGCTACACCGTGCTGTGCCTGCTGGGCGCCAGAATCCTGAACAGCAAGGTGATCCAG
ACCCCCAGATACTGGTGAAGGGCCAGGGCCAGAAAGCCAAGATGAGATGCATCCCCGAG
AAGGGCCACCCCGTGGTGTCTGGTATCAGCAGAACAAGAACAACGAGTTCAAGTTCCTGA
TCAACTTCCAGAACCAGGAAGTGCTGCAGCAGATCGACATGACCGAGAAGAGGTTTCAGCG
CCGAGTGCCCCAGCAACAGCCCCTGCAGCCTGAAATCCAGAGCAGCGAGGCCGGCGACA
GCGCCCTGTACCTGTGCGCCAGCAGCCTGACAGGCGGCGAGCAGTACTTCGGCCCTGGCAC
CAGGCTGACCGTGCTCGAGGACCTGAGGAACGTGACCCCCCAAGGTGTCCCTGTTTCGAG
CCCAGCAAGGCCGAGATCGCCAACAAGCAGAAGGCCACCCTGGTGTGCCTGGCCAGGGGC
TTCTTCCCGACCACGTGGAGCTGTCTTGGTGGGTGAACGGCAAGGAGGTGCACAGCGGC
GTGTGCACCGACCCCCAGGCCTACAAGGAGAGCAACTACAGCTACTGCCTGAGCAGCAGGC
TGAGAGTGAGCGCCACCTTCTGGCACAACCCAGGAACCACTTCCGCTGTCAGGTGCAGTT
CCACGGCCTGAGCGAGGAGGACAAGTGGCCCGAGGGCAGCCCCAAGCCCGTGACCCAGAA
CATCAGCGCCGAGGCCTGGGGCAGAGCCGACTGCGGCATCACCAGCGCCAGCTACCACCA
GGGCGTGCTGTCCGCCACCATCCTGTACGAGATCCTGCTGGGCAAGGCCACACTGTACGCC
GTGCTGGTGTCCGGCCTGGTGTGATGGCCATGGTGAAGAAGAAGAACAGCAGCGGCAGC

GGCGCCACCAACTTCAGCCTGCTGAAGCAGGCCGGCGACGTGGAGGAAAACCTGGGCCC
ATGAGGCCCGTGACCTGCAGCGTGCTGGTGCTGCTGCTGATGCTGCGGAGAAGCAACGGC
GACGGCGACAGCGTGACCCAGACCGAGGGCCTGGTGACCCTGACAGAGGGACTGCCCGTG
ATGCTGAACTGCACCTACCAGACCATCTACAGCAACCCCTTCTGTTTTGGTACGTGCAGCA
CCTGAACGAGAGCCCCAGACTGCTGCTGAAGAGCTTCACCGACAACAAGAGGACCGAGCA
CCAGGGCTTCCACGCCACCCTGCACAAGAGCAGCAGCAGCTTCCACCTGCAAAAGTCCAGC
GCCAGCTGTCCGACAGCGCCCTGTACTACTGCGCCCTGAGGGGCAGCAACAACAGGATCT
TCTTCGGCGACGGCACCCAGCTGGTCGTGAAGCCCGACATCCAGAACCCCGAGCCCGCCGT
GTACCAGCTGAAGGACCCCAAGCCAGGACAGCACCCCTGTGCCTGTTACCGACTTCGAC
AGCCAGATCAACGTGCCCAAGACCATGGAGAGCGGCACCTTCATCACCGACAAGTGCGTGC
TGGACATGAAGGCCATGGACAGCAAGAGCAACGGCGCCATCGCCTGGTCCAACCAGACCA
GCTTCACATGCCAGGACATCTTCAAGGAGACCAACGCCACCTACCCAGCAGCGACGTGCC
CTGCGACGCCACCCTGACCGAGAAGAGCTTCGAGACCGACATGAACCTGAACTCCAGAAC
CTGAGCGTGATGGGCCTGAGAATCCTGCTGCTGAAGGTGGCCGGCTTCAACCTGCTGATGA
CCCTGAGGCTGTGGAGCAGCTGAGTCGACACGCGTACGTGCGGACCGCGGACATGTACAG
AGCTCGAGCGGGATCAATTCCGCCCCCCCCCTAACGTTACTGGCCGAAGCCGCTTGAATA
AGGCCGGTGTGCGTTTGTCTATATGTTATTTCCACCATATTGCCGTCTTTGGCAATGTGAG
GGCCCGAAACCTGGCCCTGTCTTCTTGACGAGCATTCCCTAGGGGTCTTCCCTCTCGCCA
AAGGAATGCAAGGTCTGTTGAATGTCGTGAAGGAAGCAGTTCCTCTGGAAGCTTCTGAAG
ACAAACAACGTCTGTAGCGACCCTTTCGAGGCAGCGGAACCCCCACCTGGCGACAGGTGC
CTCTGCGGCCAAAAGCCACGTGTATAAGATACACCTGCAAAGGCGGCACAACCCAGTGCC
ACGTTGTGAGTTGGATAGTTGTGAAAGAGTCAAATGGCTCTCCTCAAGCGTATTCAACAA
GGGGCTGAAGGATGCCAGAAGGTACCCATTGTATGGGATCTGATCTGGGGCCTCGGTG
CACATGCTTTACATGTGTTTAGTCGAGGTTAAAAACGTCTAGGCCCCCCGAACCACGGGG
ACGTGGTTTTCTTTGAAAAACACGATAATAATGCCACCATGCCATCTCCTCTCCCTGTCTCC
TTCCTCCTCTTTCTTACCTTAGTAGGAGGCAGGCCCCAGAAGTCCTTACTGGTGGAGGTAGA
AGAGGGAGGCAATGTTGTGCTGCCATGCCTCCCGGACTCCTCACCTGTCTCTTCTGAGAAGC
TGGCTTGGTATCGAGGTAACCAGTCAACACCCTTCTGGAGCTGAGCCCCGGTCCCCTGG
CCTGGGATTGCACGTGGGGTCCCTGGGCATCTTGCTAGTGATTGTCAATGTCTCAGACCATA
TGGGGGGCTTCTACCTGTGCCAGAAGAGGCCCCCTTCAAGGACATCTGGCAGCCTGCCTG
GACAGTGAACGTGGAGGATAGTGGGGAGATGTTCCGGTGAATGCTTCAGACGTCAGGGA
CCTGGACTGTGACCTAAGGAACAGGTCTCTGGGAGCCACAGGTCCACTTCTGGTTCCCAG

CTGTATGTGTGGGCTAAAGACCATCCTAAGGTCTGGGGAACAAAGCCTGTATGTGCCCTC
GGGGGAGCAGTTTGAATCAGAGTCTAATCAACCAAGACCTCACTGTGGCACCCGGCTCCAC
ACTTTGGCTGTCCTGTGGGGTACCCCTGTCCCAGTGGCCAAAGGCTCCATCTCCTGGACCC
ATGTGCATCCTAGGAGACCTAATGTTTCACTACTGAGCCTAAGCCTTGGGGGAGAGCACCC
GGTCAGAGAGATGTGGGTTTGGGGTCTCTTCTGCTTCTGCCCAAGCCACAGCTTTAGAT
GAAGGCACCTATTATTGTCTCCGAGGAAACCTGACCATCGAGAGGCACGTGAAGGTCATTG
CAAGGTCAGCAGTGTGGCTCTGGCTGTTGAGAACTGGTGGATGGATAGTCCCAGTGGTGA
CTTTAGTATATGTCATCTTCTGTATGGTTTCTCTGGTGGCTTTTCTCTATTGTCAAAGAGCCTT
TATCCTGAGAAGGAAAAGGAAGCGAATGACTGACCCCGCCAGGAGATTCTTCAAAGTGAC
GGGCAGCGGCGAAGGCCGCGGCAGCCTGCTGACCTGCGGCGATGTGGAAGAAAACCTG
GCCCGATGGGCTGCAGAAGAACTAGAGAAGGACCAAGCAAAGCCATGATATTTCCATGGA
AATGTCAGAGCACCCAGAGGGACTTATGGAACATCTTCAAGTTGTGGGGGTGGACAATGCT
CTGTTGTGATTTCTGGCACATCATGGAACCGACTGCTGGACTTACCATTATTCTGAAAAAC
CCATGAACTGGCAAAGGGCTAGAAGATTCTGCCGAGACAATTACACAGATTTAGTTGCCAT
ACAAAACAAGGCGGAAATTGAGTATCTGGAGAAGACTCTGCCTTTCAGTCGTTCTTACTACT
GGATAGGAATCCGGAAGATAGGAGGAATATGGACGTGGGTGGGAACCAACAATCTCTcA
CTGAAGAAGCAGAGAACTGGGGAGATGGTGAGCCCAACAACAAGAAGAACAAGGAGGAC
TGC GTGGAGATCTATATCAAGAGAAACAAGATGCAGGCAAATGGAACGATGACGCCTGC
CACAACTAAAGGCAGCCCTCTGTTACACAGCTTCTTGCCAGCCCTGGTCATGCAGTGGCCA
TGGAGAATGTGTAGAAATCATCAATAATTACACCTGCAACTGTGATGTGGGGTACTATGGG
CCCCAGTGTCAGTTTGTGATTCAGTGTGAGCCTTTGGAGGCCCCAGAGCTGGGTACCATGG
ACTGTACTCACCTTTGGGAACTTCAGCTTCAGCTCACAGTGTGCCTTCAGCTGCTCTGAA
GGAACAACTTAACTGGGATTGAAGAAACCACCTGTGGACCATTTGGAACTGGTCATCTC
CAGAACCAACCTGTCAAGTGATTCAGTGTGAGCCTCTATCAGCACCAGATTTGGGGATCATG
AACTGTAGCCATCCCCTGGCCAGCTTCAGCTTACCTCTGCATGTACCTTCATCTGCTCAGAA
GGA ACTGAGTTAATTGGGAAGAAGAAAACCATTTGTGAATCATCTGGAATCTGGTCAAATC
CTAGTCCAATATGTCAAAAATTGGACAAAAGcTTCTACCCCTCTTCATTCCAGTGGCAGTCA
TGGTACTGCATTCTCTGGGTTGGCATTATCATTGGCTGGCAAGGAGATTA AAAAAAGGC
AAGAAATCCAAGAGAAGTATGAATGACCCATATTAATCCGGATTAGTCCAATTTGTTAAAGA
CAGGATATCAGTGGTCCAGGCTCTAGTTTTGACTCAACAATATCACCAGCTGAAGCCTATAG
AGTGAATTCGGATCCAAGCTTAGGCCTGCTCGCTTCTTGCTGTCCATTTCTATTAAGGTT
CCTTTGTTCCCTAAGTCCA ACTACTAACTGGGGGATATTATGAAGGGCCTTGAGCATCTGG

ATTCTGCCTAGCGCTAAGCTTCCTAACACGAGCCATAGATAGAATAAAAAGATTTTATTTAGT
CTCCAGAAAAAGGGGGGAATGAAAGACCCACCTGTAGGTTTGGCAAGCTAGCTTAAGTA
AGCCATTTTGAAGGCATGGAAAAATACATAACTGAGAATAGAGAAGTTCAGATCAAGGT
AGGAACAGAGAGACAGGAGAATATGGGCCAAACAGGATATCTGTGGTAAGCAGTTCCTGC
CCCGGCTCAGGGCCAAGAACAGTTGGAACAGCAGAATATGGGCCAAACAGGATATCTGTG
GTAAGCAGTTCCTGCCCCGGCTCAGGGCCAAGAACAGATGGTCCCAGATGCGGTCCCCC
CTCAGCAGTTTCTAGAGAACCATCAGATGTTTCCAGGGTGCCCCAAGGACCTGAAATGACCC
TGTGCCTTATTTGAACTAACCAATCAGTTCGCTTCTCGCTTCTGTTGCGCGCTTCTGCTCCCC
GAGCTCAATAAAAAGAGCCCACAACCCCTCACTCGGCGCGCCAGTCTCCGATAGACTGCGT
CGCCCGGGGTACCCGTATCCCAATAAAGCCTCTTGCTGTTTGCATCCGAATCGTGGACTCG
CTGATCCTTGGGAGGGTCTCCTCAGATTGATTGACTGCCACCTCGGGGGTCTTTCATTCTC
GAGAGCTTTGGCGTAATCATGGTCATAGCTGTTTCTGTGTGAAATTGTTATCCGCTCACAA
TTCCACACAACATACGAGCCGGAAGCATAAAGTGTAAGCCTGGGGTGCCTAATGAGTGAG
CTAACTCACATTAATTGCGTTGCGCTCACTGCCCGCTTCCAGTCGGGAAACCTGTCGTGCC
AGCTGCATTAATGAATCGGCCAACGCGCGGGGAGAGGGCGTTTGCATTTGGGCGCTCTTC
CGCTTCTCGCTCACTGACTCGCTGCGCTCGGTGTTCCGGCTGCGGCGAGCGGTATCAGCTC
ACTCAAAGGCGGTAATACGGTTATCCACAGAATCAGGGGATAACGCAGGAAAGAACATGT
GAGCAAAAGGCCAGCAAAAGGCCAGGAACCGTAAAAAGGCCGCGTTGCTGGCGTTTTTCC
ATAGGCTCCGCCCCCTGACGAGCATCACAAAAATCGACGCTCAAGTCAGAGGTGGCGAAA
CCCGACAGGACTATAAAGATAACCAGGCGTTTTCCCCTGGAAGCTCCCTCGTGCGCTCTCCTG
TTCCGACCCTGCCGTTACCGGATACCTGTCCGCCTTCTCCCTTCGGGAAGCGTGGCGCTTT
CTCAATGCTCACGCTGTAGGTATCTCAGTTCGGTGTAGGTCGTTGCTCCAAGCTGGGCTGT
GTGCACGAACCCCCGTTTCAGCCCGACCGCTGCGCCTTATCCGGTAACTATCGTCTTGAGTC
CAACCCGGTAAGACACGACTTATCGCCACTGGCAGCAGCCACTGGTAACAGGATTAGCAGA
GCGAGGTATGTAGGCGGTGCTACAGAGTCTTGAAGTGGTGGCCTAACTACGGCTACACTA
GAAGGACAGTATTTGGTATCTGCGCTCTGCTGAAGCCAGTTACCTTCGGAAAAAGAGTTGG
TAGCTCTTGATCCGGCAAACAAACCACCGCTGGTAGCGGTGGTTTTTTTTGTTTGCAAGCAGC
AGATTACGCGCAGAAAAAAGGATCTCAAGAAGATCCTTTGATCTTTTCTACGGGGTCTGAC
GCTCAGTGGAACGAAAACACTCACGTTAAGGGATTTTGGTCATGAGATTATCAAAAAGGATCT
TCACCTAGATCCTTTTAAATTAATAAATGAAGTTTTAAATCAATCTAAAGTATATATGAGTAAA
CTTGGTCTGACAGTTACCAATGCTTAATCAGTGAGGCACCTATCTCAGCGATCTGTCTATTT
GTTTCATCCATAGTTGCCTGACTCCCCGTCGTGTAGATAACTACGATACGGGAGGGCTTACCA

TCTGGCCCCAGTGCTGCAATGATACCGCGAGACCCACGCTCACCGGCTCCAGATTTATCAGC
AATAAACCCAGCCAGCCGGAAGGGCCGAGCGCAGAAGTGGTCCTGCAACTTTATCCGCCTCC
ATCCAGTCTATTAATTGTTGCCGGAAGCTAGAGTAAGTAGTTCGCCAGTTAATAGTTTGGC
CAACGTTGTTGCCATTGCTGCTGGCATCGTGGTGTACGCTCGTCGTTTGGTATGGCTTCAT
TCAGCTCCGGTCCCAACGATCAAGGCGAGTTACATGATCCCCATGTTGTGCAAAAAAGCG
GTTAGCTCCTTCGGTCCTCCGATCGTTGTCAGAAGTAAGTTGGCCGAGTGTTATCACTCAT
GGTTATGGCAGCACTGCATAATTCTTACTGTCATGCCATCCGTAAGATGCTTTTCTGTGAC
TGGTGAGTACTCAACCAAGTCATTCTGAGAATAGTGTATGCGGCGACCGAGTTGCTCTTGCC
CGGCGTCAATACGGGATAATACCGCGCCACATAGCAGAACTTTAAAAGTGCTCATCATTGG
AAAACGTTCTTCGGGGCGAAAACCTCAAGGATCTTACCGCTGTTGAGATCCAGTTCGATGT
AACCCACTCGTGCACCCAAGTATCTTACGATCTTTACTTTACCCAGCGTTTCTGGGTGAG
CAAAAACAGGAAGGCAAAATGCCGCAAAAAGGGAATAAGGGCGACACGGAAATGTTGA
ATACTCATACTCTTCTTTTTCAATATTATTGAAGCATTATCAGGGTTATTGTCTCATGAGCG
GATACATATTTGAATGTATTTAGAAAAATAACAAATAGGGGTCCGCGCACATTTCCCCGA
AAAGTGCCACCTGACGTCTAAGAAACCATTATTATCATGACATTAACCTATAAAAATAGGCG
TATCACGAGGCCCTTTCGTCTTCAAGCTGCCTCGCGCGTTTCGGTGATGACGGTGAAAACCT
CTGACACATGCAGCTCCCGGAGACGGTCACAGCTTGTCTGTAAGCGGATGCCGGGAGCAG
ACAAGCCCGTCAGGGCGCGTCAGCGGGTGTGGCGGGTGTGGGGCGCAGCCATGACCCA
GTCACGTAGCGATAGTTACTATGCGGCATCAGAGCAGATTGTAAGTACTGAGAGTGCACCATATG
CGGTGTGAAATACCGCACAGATGCGTAAGGAGAAAATACCGCATCAGGCGCCATTCGCCAT
TCAGGCTGCGCAACTGTTGGGAAGGGCGATCGGTGCGGGCCTCTTCGCTATTACGCCAGCT
GGCGAAAGGGGGATGTGCTGCAAGGCGATTAAGTTGGGTAACGCCAGGGTTTTCCAGTC
ACGACGTTGTAACCGACGGCCAGTGAATTAGTACTCTAGCTTAAGTAAGCCATTTTGAAG
GCATGGAAAAATACATAACTGAGAATAGAGAAGTTCAGATCAAGGTTAGGAACAGAGAGA
CAGGAGAATATGGGCCAAACAGGATATCTGTGGTAAGCAGTTCCTGCCCCGGCTCAGGGCC
AAGAACAGTTGGAACAGCAGAATATGGGCCAAACAGGATATCTGTGGTAAGCAGTTCCTGC
CCCGGCTCAGGGCCAAGAACAGATGGTCCCCAGATGCGGTCCCGCCCTCAGCAGTTTCTAG
AGAACCATCAGATGTTTCCAGGGTGCCCAAGGACCTGAAATGACCCTGTGCCTTATTTGAA
CTAACCAATCAGTTCGCTTCTCGCTTCTGTTGCGCGCTTCTGCTCCCCGAGCTCAATAAAAG
AGCCACAACCCCTCACTCGGCGCGCCAGTCTCCGATTGACTGCGTGCAGGGGTACCCGT
ATTCCAATAAAGCCTCTTGCTGTTTGCATCCGAATCGTGGACTCGCTGATCCTTGGGAGGG
TCTCCTCAGATTGATTGACTGCCACCTCGGGGGTCTTTCATTTGGAGGTTCCACCGAGATT

GGAGACCCCTGCCAGGGACCACCGACCCCCCGCCGGGAGGTAAGCTGGCCAGCGGTCTG
TTTCGTGTCTGTCTCTGTCTTTGGGCGTGTTTGTGCCGGCATCTAATGTTTGGCCTGCGTCT
GTAAGTGGCTAACTAGATCTGTATCTGGCGGTCCCGCGGAAGAACTGACGAGTTCGTA
TTCCCGGCCGAGCCCCTGGGAGACGTCCAGCGGCCTCGGGGGCCCCTTTTGTGGCCAT
TCTGTATCAGTTAACCTACCCGAGTCGGACTTTTTGGAGCTCCGCCACTGTCCGAGGGGTAC
GTGGCTTTGTTGGGGACGAGAGACAGAGACACTTCCCGCCCCGTCTGAATTTTTGCTTTC
GTTTTACGCCGAAACCGCGCCGCGCTTGTCTGCTGC

pMP71-TRP2- Δ W-L-selectin

AGCATCGTTCTGTGTTGTCTCTGTCTGACTGTGTTTCTGTATTTGTCTGAAAATTAGCTCGAC
AAAGTTAAGTAATAGTCCCTCTCTCCAAGCTCACTTACAGGCGGCCGCATGGCCCCGCGGCT
GCTGTGCTACACCGTGCTGTGCCTGCTGGGCGCCAGAATCCTGAACAGCAAGGTGATCCAG
ACCCCAGATACCTGGTGAAGGGCCAGGGCCAGAAAGCCAAGATGAGATGCATCCCCGAG
AAGGGCCACCCCGTGGTGTCTGGTATCAGCAGAACAAGAACAACGAGTTCAAGTTCCTGA
TCAACTCCAGAACCAGGAAGTGCTGCAGCAGATCGACATGACCGAGAAGAGGTTTCAGCG
CCGAGTGCCCCAGCAACAGCCCCTGCAGCCTGAAATCCAGAGCAGCGAGGCCGGCGACA
GCGCCCTGTACCTGTGCGCCAGCAGCCTGACAGGCGGCGAGCAGTACTTCGGCCCTGGCAC
CAGGCTGACCGTGCTCGAGGACCTGAGGAACGTGACCCCCCAAGGTGTCCCTGTTTCGAG
CCCAGCAAGGCCGAGATCGCCAACAAGCAGAAGGCCACCCTGGTGTGCCTGGCCAGGGGC
TTCTTCCCGACCACGTGGAGCTGTCTTGGTGGGTGAACGGCAAGGAGGTGCACAGCGGC
GTGTGCACCGACCCCCAGGCCTACAAGGAGAGCAACTACAGCTACTGCCTGAGCAGCAGGC
TGAGAGTGAGCGCCACCTTCTGGCACAACCCAGGAACCACTTCCGCTGTCAGGTGCAGTT
CCACGGCCTGAGCGAGGAGGACAAGTGGCCCGAGGGCAGCCCCAAGCCCGTGACCCAGAA
CATCAGCGCCGAGGCCTGGGGCAGAGCCGACTGCGGCATCACCAGCGCCAGCTACCACCA
GGGCGTGCTGTCCGCCACCATCCTGTACGAGATCCTGCTGGGCAAGGCCACACTGTACGCC
GTGCTGGTGTCCGGCCTGGTGTGATGGCCATGGTGAAGAAGAAGAACAGCAGCGGCAGC
GGCGCCACCAACTTCAGCCTGCTGAAGCAGGCCGGCGACGTGGAGGAAAACCTGGGCCC
ATGAGGCCCGTGACCTGCAGCGTGCTGGTGTGCTGCTGATGCTGCGGAGAAGCAACGGC
GACGGCGACAGCGTGACCCAGACCGAGGGCCTGGTGACCCTGACAGAGGGACTGCCCGTG
ATGCTGAACTGCACCTACCAGACCATCTACAGCAACCCCTTTCTGTTTTGGTACGTGCAGCA
CCTGAACGAGAGCCCCAGACTGCTGCTGAAGAGCTTACCGACAACAAGAGGACCGAGCA
CCAGGGCTTCCACGCCACCCTGCACAAGAGCAGCAGCAGCTTCCACCTGCAAAAGTCCAGC

GCCCAGCTGTCCGACAGCGCCCTGTACTACTGCGCCCTGAGGGGCAGCAACAACAGGATCT
TCTTCGGCGACGGCACCCAGCTGGTCGTGAAGCCCCGACATCCAGAACCCCGAGCCCGCCGT
GTACCAGCTGAAGGACCCCAAGCCAGGACAGCACCTGTGCCTGTTACCGACTTCGAC
AGCCAGATCAACGTGCCAAGACCATGGAGAGCGGCACCTTCATCACCGACAAGTGCGTGC
TGGACATGAAGGCCATGGACAGCAAGAGCAACGGCGCCATCGCCTGGTCCAACCAGACCA
GCTTCACATGCCAGGACATCTTCAAGGAGACCAACGCCACCTACCCAGCAGCGACGTGCC
CTGCGACGCCACCCTGACCGAGAAGAGCTTCGAGACCGACATGAACCTGAACTCCAGAAC
CTGAGCGTGATGGGCCTGAGAATCCTGCTGCTGAAGGTGGCCGGCTTCAACCTGCTGATGA
CCCTGAGGCTGTGGAGCAGCTGAGTCGACACGCGTACGTGCGACCGCGGACATGTACAG
AGCTCGAGCGGGATCAATTCCGCCCCCCCCCTAACGTTACTGGCCGAAGCCGCTTGAATA
AGGCCGGTGTGCGTTTGTCTATATGTTATTTCCACCATATTGCCGTCTTTGGCAATGTGAG
GGCCCGAAACCTGGCCCTGTCTTCTTGACGAGCATTCTAGGGGTCTTCCCTCTCGCCA
AAGGAATGCAAGGTCTGTTGAATGTCGTGAAGGAAGCAGTTCCTCTGGAAGCTTCTGAAG
ACAAACAACGTCTGTAGCGACCCTTTCAGGCAGCGGAACCCCCACCTGGCGACAGGTGC
CTCTGCGGCCAAAAGCCACGTGTATAAGATACACCTGCAAAGGCGGCACAACCCCAAGTCC
ACGTTGTGAGTTGGATAGTTGTGGAAAGAGTCAAATGGCTCTCCTCAAGCGTATTCAACAA
GGGGCTGAAGGATGCCAGAAGGTACCCATTGTATGGGATCTGATCTGGGGCCTCGGTG
CACATGCTTTACATGTGTTTAGTCGAGGTTAAAAACGTCTAGGCCCCCCGAACCACGGGG
ACGTGGTTTTCTTTGAAAAACACGATAATAATGCCACCATGCCATCTCCTCTCCCTGTCTCC
TTCCTCCTCTTCTTACCTTAGTAGGAGGCAGGCCCCAGAAGTCCTTACTGGTGGAGGTAGA
AGAGGGAGGCAATGTTGTGCTGCCATGCCTCCCGACTCCTCACCTGTCTCTTCTGAGAAGC
TGGCTTGGTATCGAGGTAACCAGTCAACACCCTTCTGGAGCTGAGCCCCGGTCCCCTGG
CCTGGGATTGCACGTGGGGTCCCTGGGCATCTTGCTAGTGATTGTCAATGTCTCAGACCATA
TGGGGGGCTTCTACCTGTGCCAGAAGAGGCCCCCTTCAAGGACATCTGGCAGCCTGCCTG
GACAGTGAACGTGGAGGATAGTGGGGAGATGTTCCGGTGAATGCTTCAGACGTCAGGGA
CCTGGACTGTGACCTAAGGAACAGGTCCTCTGGGAGCCACAGGTCCACTTCTGGTTCCCAG
CTGTATGTGTGGGCTAAAGACCATCCTAAGGTCTGGGGAACAAAGCCTGTATGTGCCCTC
GGGGGAGCAGTTTGAATCAGAGTCTAATCAACCAAGACCTCACTGTGGCACCCGGCTCCAC
ACTTTGGCTGTCTGTGGGGTACCCCTGTCCCAGTGGCCAAAGGCTCCATCTCCTGGACCC
ATGTGCATCCTAGGAGACCTAATGTTTCACTACTGAGCCTAAGCCTTGGGGGAGAGCACCC
GGTCAGAGAGATGTGGGTTTGGGGTCTCTTCTGCTTCTGCCCAAGCCACAGCTTTAGAT
GAAGGCACCTATTATTGTCTCCGAGGAAACCTGACCATCGAGAGGCACGTGAAGGTCATTG

CAAGGTCAGCAGTGTGGCTCTGGCTGTTGAGAACTGGTGGATGGATAGTCCCAGTGGTGA
CTTTAGTATATGTCATCTTCTGTATGGTTTCTCTGGTGGCTTTTCTCTATTGTCAAAGAGCCTT
TATCCTGAGAAGGAAAAGGAAGCGAATGACTGACCCCGCCAGGAGATTCTTCAAAGTGAC
GGGCAGCGGCGAAGGCCGCGGCAGCCTGCTGACCTGCGGCGATGTGGAAGAAAACCTG
GCCCGATGGGCTGCAGAAGAACTAGAGAAGGACCAAGCAAAGCCATGATATTTCCATGGA
AATGTCAGAGCACCCAGAGGGACTTATGGAACATCTTCAAGTTGTGGGGGTGGACAATGCT
CTGTTGTGATTTCTGGCACATCATGGAACCGACTGCTGGACTTACCATTATTCTGAAAAAC
CCATGAACTGGCAAAGGGCTAGAAGATTCTGCCGAGACAATTACACAGATTTAGTTGCCAT
ACAAAACAAGGCGGAAATTGAGTATCTGGAGAAGACTCTGCCTTTCAGTCGTTCTTACTACT
GGATAGGAATCCGGAAGATAGGAGGAATATGGACGTGGGTGGGAACCAACAATCTCTcA
CTGAAGAAGCAGAGAACTGGGGAGATGGTGAGCCCAACAACAAGAAGAACAAGGAGGAC
TGC GTGGAGATCTATATCAAGAGAAACAAGATGCAGGCAAATGGAACGATGACGCCTGC
CACAACTAAAGGCAGCCCTCTGTTACACAGCTTCTTGCCAGCCCTGGTCATGCAGTGGCCA
TGGAGAATGTGTAGAAATCATCAATAATTACACCTGCAACTGTGATGTGGGGTACTATGGG
CCCCAGTGTCAGTTTGTGATTCAGTGTGAGCCTTTGGAGGCCCCAGAGCTGGGTACCATGG
ACTGTACTCACCTTTGGGAACTTCAGCTTCAGCTCACAGTGTGCCTTCAGCTGCTCTGAA
GGAACAACTTAACTGGGATTGAAGAAACCACCTGTGGACCATTTGAAACTGGTCATCTC
CAGAACCAACCTGTCAAGTGATTCAGTGTGAGCCTCTATCAGCACCAGATTTGGGGATCATG
AACTGTAGCCATCCCCTGGCCAGCTTCAGCTTACCTCTGCATGTACCTTCATCTGCTCAGAA
GAACTGAGTTAATTGGGAAGAAGAAAACCATTTGTGAATCATCTGGAATCTGGTCAAATC
CTAGTCCAATATGTCAAAAATTGGACAAAAGTTTCTCAATGATTAAGGAGGGTGATTATAAC
CCCCTCTCATTCCAGTGGCAGTCATGTTACTGCATTCTCTGGGTTGGCATTTTGGATTTGG
CTGGCAAGGAGATTAATAAAGGCAAGAAATCCAAGAGAAGTATGAATGACCCATATTAAT
CCGGATTAGTCCAATTTGTTAAAGACAGGATATCAGTGGTCCAGGCTCTAGTTTTGACTCAA
CAATATCACCAGCTGAAGCCTATAGAGTGAATTCGGATCCAAGCTTAGGCCTGCTCGCTTTC
TTGCTGTCCCATTTCTATTAAAGGTTCCCTTTGTTCCCTAAGTCCAACACTAAACTGGGGGAT
ATTATGAAGGGCCTTGAGCATCTGGATTCTGCCTAGCGCTAAGCTTCTAACACGAGCCATA
GATAGAATAAAAGATTTTATTTAGTCTCCAGAAAAGGGGGGAATGAAAGACCCACCTGT
AGGTTTGGCAAGCTAGCTTAAGTAAGCCATTTTGCAAGGCATGGAAAAATACATAACTGAG
AATAGAGAAGTTCAGATCAAGGTTAGGAACAGAGAGACAGGAGAATATGGGCCAAACAG
GATATCTGTGGTAAGCAGTTCCTGCCCCGGCTCAGGGCCAAGAACAGTTGGAACAGCAGAA
TATGGGCCAAACAGGATATCTGTGGTAAGCAGTTCCTGCCCCGGCTCAGGGCCAAGAACAG

ATGGTCCCAGATGCGGTCCCGCCCTCAGCAGTTTCTAGAGAACCATCAGATGTTCCAGGG
TGCCCAAGGACCTGAAATGACCCTGTGCCTTATTTGAACTAACCAATCAGTTCGCTTCTCGC
TTCTGTTGCGCGCTTCTGCTCCCGAGCTCAATAAAAGAGCCCAACCCCTCACTCGGCG
CGCCAGTCTCCGATAGACTGCGTCGCCCAGGGTACCCGTATTCCAATAAAGCCTCTTGCT
GTTTGCATCCGAATCGTGGACTCGCTGATCCTTGGGAGGGTCTCCTCAGATTGATTGACTGC
CCACCTCGGGGGTCTTTCATTCTCGAGAGCTTTGGCGTAATCATGGTCATAGCTGTTTCCTGT
GTGAAATTGTTATCCGCTACAATCCACACAACATACGAGCCGGAAGCATAAAGTGTA
GCCTGGGGTGCCTAATGAGTGAGCTAACTCACATTAATTGCGTTGCGCTCACTGCCCGCTT
CCAGTCGGGAAACCTGTCGTGCCAGCTGCATTAATGAATCGGCCAACGCGCGGGGAGAGG
CGGTTTGCATATTGGGCGCTTCCGCTTCTCGCTCACTGACTCGCTGCGCTCGGTGCTTCG
GCTGCGGCGAGCGGTATCAGCTCACTCAAAGGCGGTAATACGGTTATCCACAGAATCAGGG
GATAACGCAGGAAAGAACATGTGAGCAAAGGCCAGCAAAGGCCAGGAACCGTAAAAA
GGCCGCGTTGCTGGCGTTTTTCCATAGGCTCCGCCCCCTGACGAGCATCACAAAAATCGAC
GCTCAAGTCAGAGGTGGCGAAACCCGACAGGACTATAAAGATACCAGGCGTTTCCCCCTGG
AAGCTCCCTCGTGCGCTCTCCTGTTCCGACCCTGCCGCTTACCGGATACCTGTCCGCCTTCT
CCCTTCGGGAAGCGTGGCGCTTCTCAATGCTCACGCTGTAGGTATCTCAGTTCGGTGTAGG
TCGTTGCTCCAAGCTGGGCTGTGTGCACGAACCCCCGTTACGCCGACCGCTGCGCCTTA
TCCGGTAACTATCGTCTTGAGTCCAACCCGTAAGACACGACTTATCGCCACTGGCAGCAGC
CACTGGTAACAGGATTAGCAGAGCGAGGTATGTAGGCGGTGCTACAGAGTTCTTGAAGTG
GTGGCCTAACTACGGCTACACTAGAAGGACAGTATTTGGTATCTGCGCTCTGCTGAAGCCA
GTTACCTTCGGAAAAAGAGTTGGTAGCTCTTGATCCGGCAAACAAACCACCGCTGGTAGCG
GTGGTTTTTTTTGTTTGAAGCAGCAGATTACGCGCAGAAAAAAGGATCTCAAGAAGATCC
TTTGATCTTTTCTACGGGGTCTGACGCTCAGTGGAACGAAAACCTCACGTTAAGGGATTTTGG
TCATGAGATTATCAAAAAGGATCTTACCTAGATCCTTTTAAATTAATAAATGAAGTTTTAAAT
CAATCTAAAGTATATATGAGTAACTTGGTCTGACAGTTACCAATGCTTAATCAGTGAGGCA
CCTATCTCAGCGATCTGTCTATTTGTTTCATCCATAGTTGCCTGACTCCCCGTCGTGTAGATA
ACTACGATACGGGAGGGCTTACCATCTGGCCCCAGTGCTGCAATGATACCGCGAGACCCAC
GCTCACCGGCTCCAGATTTATCAGCAATAAACCAGCCAGCCGGAAGGGCCGAGCGCAGAA
GTGGTCTGCAACTTTATCCGCCTCCATCCAGTCTATTAATTGTTGCCGGGAAGCTAGAGTA
AGTAGTTCGCCAGTTAATAGTTTGCACAACGTTGTTGCCATTGCTGCTGGCATCGTGGTGTG
ACGCTCGTCTTTGGTATGGCTTCATTCAGCTCCGGTCCCAACGATCAAGGCGAGTTACAT
GATCCCCATGTTGTGCAAAAAAGCGGTTAGCTCCTTCGGTCTCCGATCGTTGTCAGAAGT

AAGTTGGCCG CAGTGTTATCACTCATGGTTATGGCAGCACTGCATAATTCTTACTGTCAT
GCCATCCGTAAGATGCTTTTCTGTGACTGGTGAGTACTCAACCAAGTCATTCTGAGAATAGT
GTATGCGGGCACCAGATTGCTCTTGCCCGGGCGTCAATACGGGATAATACCGCGCCACATAG
CAGAACTTTAAAAGTGCTCATCATTGGAAAACGTTCTTCGGGGCGAAAACCTCAAGGATCT
TACCGCTGTTGAGATCCAGTTCGATGTAACCCACTCGTGCACCCAAGTATCTTCAGCATCTT
TTACTTTACCAGCGTTTCTGGGTGAGCAAAAACAGGAAGGCAAATGCCGCAAAAAAGGG
AATAAGGGCGACACGGAAATGTTGAATACTCATACTCTTCTTTTTCAATATTATTGAAGCAT
TTATCAGGGTTATTGTCTCATGAGCGGATACATATTTGAATGTATTTAGAAAAATAACAAA
TAGGGGTTCCGCGCACATTTCCCCGAAAAGTGCCACCTGACGTCTAAGAAACCATTATTATC
ATGACATTAACCTATAAAAATAGGCGTATCACGAGGCCCTTTCGTCTTCAAGCTGCCTCGCG
CGTTTCGGTGATGACGGTGAAAACCTCTGACACATGCAGCTCCCGGAGACGGTCACAGCTT
GTCTGTAAGCGGATGCCGGGAGCAGACAAGCCCGTCAGGGCGCGTCAGCGGGTGTGGCG
GGTGTGCGGGCGCAGCCATGACCCAGTCACGTAGCGATAGTTACTATGCGGCATCAGAGC
AGATTGTAAGTGCAGAGTGCACCATATGCGGTGTGAAATACCGCACAGATGCGTAAGGAGAA
AATACCGCATCAGGCGCCATTCGCCATTCAGGCTGCGCAACTGTTGGGAAGGGCGATCGGT
GCGGGCCTCTTCGCTATTACGCCAGCTGGCGAAAGGGGGATGTGCTGCAAGGCGATTAAG
TTGGGTAACGCCAGGGTTTTCCAGTCACGACGTTGTAAAACGACGGCCAGTGAATTAGTA
CTCTAGCTTAAGTAAGCCATTTTGCAAGGCATGGAAAAATACATAACTGAGAATAGAGAAG
TTCAGATCAAGGTTAGGAACAGAGAGACAGGAGAATATGGGCCAACAGGATATCTGTGG
TAAGCAGTTCCTGCCCGGCTCAGGGCCAAGAACAGTTGGAACAGCAGAATATGGGCCAA
ACAGGATATCTGTGGTAAGCAGTTCCTGCCCGGCTCAGGGCCAAGAACAGATGGTCCCCA
GATGCGGTCCCGCCCTCAGCAGTTTCTAGAGAACCATCAGATGTTTCCAGGGTGCCCCAAG
GACCTGAAATGACCCTGTGCCTTATTTGAACTAACCAATCAGTTCGCTTCTCGCTTCTGTTG
CGCGCTTCTGCTCCCCGAGCTCAATAAAAGAGCCACAACCCCTCACTCGGCGCGCCAGTCC
TCCGATTGACTGCGTCGCCCCGGGTACCCGTATTCCCAATAAAGCCTCTTGCTGTTTGCATCCG
AATCGTGGACTCGCTGATCCTTGGGAGGGTCTCCTCAGATTGATTGACTGCCACCTCGGG
GGTCTTTCATTTGGAGGTTCCACCGAGATTTGGAGACCCCTGCCAGGGACCACCGACCCCC
CCGCCGGGAGGTAAGCTGGCCAGCGGTCGTTTCGTGTCTGTCTCTGTCTTTGGGCGTGTTG
TGCCGGCATCTAATGTTTGCCTGCGTCTGTACTAGTTGGCTAACTAGATCTGTATCTGGC
GGTCCCGCGGAAGAACTGACGAGTTCGATTCCCGGCCGAGCCCTGGGAGACGTCCAG
CGGCCTCGGGGGCCCGTTTTGTGGCCATTCTGTATCAGTTAACCTACCCGAGTCGGACTTT
TTGGAGCTCCGCCACTGTCCGAGGGGTACGTGGCTTTGTTGGGGGACGAGAGACAGAGAC

ACTTCCCGCCCCGTCTGAATTTTTGCTTTCGGTTTTACGCCGAAACCGCGCCGCGGTCTTG
TCTGCTGC

pMP71-TRP2-mWT-L-selectin

AGCATCGTTCTGTGTTGTCTCTGTCTGACTGTGTTTCTGTATTTGTCTGAAAATTAGCTCGAC
AAAGTTAAGTAATAGTCCCTCTCTCCAAGCTCACTTACAGGCGGCCGCATGGCCCCGCGGCT
GCTGTGCTACACCGTGCTGTGCCTGCTGGGCGCCAGAATCCTGAACAGCAAGGTGATCCAG
ACCCCCAGATACCTGGTGAAGGGCCAGGGCCAGAAAGCCAAGATGAGATGCATCCCCGAG
AAGGGCCACCCCGTGGTGTCTGGTATCAGCAGAACAAGAACAACGAGTTCAAGTTCCTGA
TCAACTCCAGAACCAGGAAGTGCTGCAGCAGATCGACATGACCGAGAAGAGGTTTCAGCG
CCGAGTGCCCCAGCAACAGCCCCTGCAGCCTGGAAATCCAGAGCAGCGAGGCCGCGGACA
GCGCCCTGTACCTGTGCGCCAGCAGCCTGACAGGCGGCGAGCAGTACTTCGGCCCTGGCAC
CAGGCTGACCGTGCTCGAGGACCTGAGGAACGTGACCCCCCAAGGTGTCCCTGTTTCGAG
CCCAGCAAGGCCGAGATCGCCAACAAGCAGAAGGCCACCCTGGTGTGCCTGGCCAGGGGC
TTCTTCCCCGACCACGTGGAGCTGTCTTGGTGGGTGAACGGCAAGGAGGTGCACAGCGGC
GTGTGCACCGACCCCCAGGCCTACAAGGAGAGCAACTACAGCTACTGCCTGAGCAGCAGGC
TGAGAGTGAGCGCCACCTTCTGGCACAACCCCAGGAACCACTTCCGCTGTCAGGTGCAGTT
CCACGGCCTGAGCGAGGAGGACAAGTGGCCCCGAGGGCAGCCCCAAGCCCGTGACCCAGAA
CATCAGCGCCGAGGCCTGGGGCAGAGCCGACTGCGGCATCACCAGCGCCAGCTACCACCA
GGGCGTGCTGTCCGCCACCATCCTGTACGAGATCCTGCTGGGCAAGGCCACACTGTACGCC
GTGCTGGTGTCCGGCCTGGTGTGCTGATGGCCATGGTGAAGAAGAAGAACAGCAGCGGCAGC
GGCGCCACCAACTTCAGCCTGCTGAAGCAGGCCGGCGACGTGGAGGAAAACCCTGGGCCC
ATGAGGCCCGTGACCTGCAGCGTGCTGGTGTGCTGCTGATGCTGCGGAGAAGCAACGGC
GACGGCGACAGCGTGACCCAGACCGAGGGCCTGGTGACCCTGACAGAGGGACTGCCCGTG
ATGCTGAACTGCACCTACCAGACCATCTACAGCAACCCCTTCTGTTTTGGTACGTGCAGCA
CCTGAACGAGAGCCCCAGACTGCTGCTGAAGAGCTTCACCGACAACAAGAGGACCGAGCA
CCAGGGCTTCCACGCCACCCTGCACAAGAGCAGCAGCAGCTTCCACCTGCAAAAGTCCAGC
GCCAGCTGTCCGACAGCGCCCTGTACTACTGCGCCCTGAGGGGCAGCAACAACAGGATCT
TCTTCGGCGACGGCACCCAGCTGGTCGTGAAGCCCGACATCCAGAACCCCGAGCCCGCCGT
GTACCAGCTGAAGGACCCCAAGCCAGGACAGCACCCCTGTGCCTGTTACCGACTTCGAC
AGCCAGATCAACGTGCCAAGACCATGGAGAGCGGCACCTTCATCACCGACAAGTGCGTGC
TGGACATGAAGGCCATGGACAGCAAGAGCAACGGCGCCATCGCCTGGTCCAACCAGACCA

GCTTCACATGCCAGGACATCTTCAAGGAGACCAACGCCACCTACCCCAGCAGCGACGTGCC
CTGCGACGCCACCCTGACCGAGAAGAGCTTCGAGACCGACATGAACCTGAACTTCCAGAAC
CTGAGCGTGATGGGCCTGAGAATCCTGCTGCTGAAGGTGGCCGGCTTCAACCTGCTGATGA
CCCTGAGGCTGTGGAGCAGCTGAGTCGACACGCGTACGTGCGACCGCGGACATGTACAG
AGCTCGAGCGGGATCAATTCCGCCCCCCCCCTAACGTTACTGGCCGAAGCCGCTTGAATA
AGGCCGGTGTGCGTTTGTCTATATGTTATTTTCCACCATATTGCCGTCTTTTGGCAATGTGAG
GGCCCGAAACCTGGCCCTGTCTTCTTGACGAGCATTCTAGGGGTCTTTCCCTCTCGCCA
AAGGAATGCAAGGTCTGTTGAATGTCGTGAAGGAAGCAGTTCCTCTGGAAGCTTCTGAAG
ACAAACAACGTCTGTAGCGACCCTTTGCAGGCAGCGGAACCCCCACCTGGCGACAGGTGC
CTCTGCGGCCAAAAGCCACGTGTATAAGATACACCTGCAAAGGCGGCACAACCCCAAGTCC
ACGTTGTGAGTTGGATAGTTGTGGAAAGAGTCAAATGGCTCTCCTCAAGCGTATTCAACAA
GGGGCTGAAGGATGCCAGAAGGTACCCATTGTATGGGATCTGATCTGGGGCCTCGGTG
CACATGCTTTACATGTGTTTAGTCGAGGTTAAAAACGTCTAGGCCCCCCGAACCACGGGG
ACGTGGTTTTCTTTGAAAAACACGATAATAATGCCACCATGCCATCTCCTCTCCCTGTCTCC
TTCCTCCTTTTCTTACCTTAGTAGGAGGCAGGCCCCAGAAGTCCTTACTGGTGGAGGTAGA
AGAGGGAGGCAATGTTGTGCTGCCATGCCTCCCGACTCCTCACCTGTCTCTTCTGAGAAGC
TGGCTTGGTATCGAGGTAACCAGTCAACACCCTTCTGGAGCTGAGCCCCGGGTCCCCTGG
CCTGGGATTGCACGTGGGGTCCCTGGGCATCTTGCTAGTGATTGTCAATGTCTCAGACCATA
TGGGGGGCTTCTACCTGTGCCAGAAGAGGCCCCCTTTCAAGGACATCTGGCAGCCTGCCTG
GACAGTGAACGTGGAGGATAGTGGGGAGATGTTCCGGTGAATGCTTCAGACGTCAGGGA
CCTGGACTGTGACCTAAGGAACAGGTCCTCTGGGAGCCACAGGTCCACTTCTGGTTCCCAG
CTGTATGTGTGGGCTAAAGACCATCCTAAGGTCTGGGGAACAAAGCCTGTATGTGCCCTC
GGGGGAGCAGTTTGAATCAGAGTCTAATCAACCAAGACCTCACTGTGGCACCCGGCTCCAC
ACTTTGGCTGTCTGTGGGGTACCCCTGTCCCAGTGGCCAAAGGCTCCATCTCCTGGACCC
ATGTGCATCCTAGGAGACCTAATGTTTCACTACTGAGCCTAAGCCTTGGGGGAGAGCACCC
GGTCAGAGAGATGTGGGTTTGGGGTCTCTTCTGCTTCTGCCCAAGCCACAGCTTTAGAT
GAAGGCACCTATTATTGTCTCCGAGGAAACCTGACCATCGAGAGGCACGTGAAGGTCATTG
CAAGGTCAGCAGTGTGGCTCTGGCTGTTGAGAACTGGTGGATGGATAGTCCCAGTGGTGA
CTTTAGTATATGTCATCTTCTGTATGGTTTCTCTGGTGGCTTTTCTCTATTGTCAAAGAGCCTT
TATCCTGAGAAGGAAAAGGAAGCGAATGACTGACCCCGCCAGGAGATTCTTCAAAGTGAC
GGGCAGCGGCGAAGGCCGCGGCAGCCTGCTGACCTGCGGCGATGTGGAAGAAAACCTG
GCCCGATGGTGTTCATGGAGATGTGAGGGTACTTACTGGGGCTCGAGGAACATCCTGAA

GCTGTGGGTCTGGACACTGCTCTGTTGTGACTTCTGATACACCATGGAACACTGTTGGA
CTTACCATTATTCTGAAAAGCCCATGAACTGGGAAAATGCTAGAAAGTTCTGCAAGCAAAT
TACACAGATTTAGTCGCCATACAAAACAAGAGAGAAATTGAGTATTTAGAGAATACATTGC
CCAAAAGCCCTTATTACTACTGGATAGGAATCAGGAAAATTGGGAAAATGTGGACATGGGT
GGGAACCAACAAAACACTCTACTAAAGAAGCAGAGAACTGGGGTGCTGGGGAGCCCAACAA
CAAGAAGTCCAAGGAGGACTGTGTGGAGATCTATATCAAGAGGGAACGAGACTCTGGGAA
ATGGAACGATGACGCCTGTCAAAACGAAAGGCAGCTCTCTGCTACACAGCCTTTGCCAG
CCAGGGTCTTGCAATGGCCGTGGAGAATGTGTGGAACTATCAACAATCACACGTGCATAT
GTGATGAAGGGTATTACGGGCCCCAGTGTGAGTATGTGGTCCAGTGTGAGCCTTTGGAGGC
CCCTGAGTTGGGTACCATGGACTGCATCCACCCCTTGGGAACTTCAGCTTCAGTCCAAGT
GTGCTTTCAACTGTTCTGAGGGAAGAGAGCTACTTGGGACTGCAGAAACACAGTGTGGAGC
ATCTGGAACTGGTCATCTCCAGAGCCAATCTGCCAAGTGGTCCAGTGTGAGCCTTTGGAG
GCCCCTGAGTTGGGTACCATGGACTGCATCCACCCCTTGGGAACTTCAGCTTCAGTCCAA
GTGTGCTTTCAACTGTTCTGAGGGAAGAGAGCTACTTGGGACTGCAGAAACACAGTGTGGA
GCATCTGGAACTGGTCATCTCCAGAGCCAATCTGCCAAGAGACAAACAGAAGTTTCTCAA
AGATCAAAGAAGGTGACTACAACCCCTCTTCATTCTGTAGCCGTCATGGTCACCGCATTC
TCGGGGCTGGCATTCTCATTGGCTGGCAAGGCGGTTAAAAAAGGCAAGAAATCTCAAG
AAAGGATGGATGATCCTTACTAATCCGGATTAGTCCAATTTGTTAAAGACAGGATATCAGTG
GTCCAGGCTCTAGTTTTGACTCAACAATATCACCAGCTGAAGCCTATAGAGTGAATTCGGAT
CCAAGCTTAGGCCTGCTCGCTTCTTGCTGTCCATTTCTATTAAGGTTCTTTGTTCCCTAA
GTCCAATACTAACTGGGGGATATTATGAAGGGCCTTGAGCATCTGGATTCTGCCTAGCG
CTAAGCTTCCTAACACGAGCCATAGATAGAATAAAAGATTTTATTTAGTCTCCAGAAAAAGG
GGGAATGAAAGACCCACCTGTAGGTTTGGCAAGCTAGCTTAAGTAAGCCATTTTGCAAG
GCATGGAAAAATACATACTGAGAATAGAGAAGTTCAGATCAAGGTTAGGAACAGAGAGA
CAGGAGAATATGGGCCAAACAGGATATCTGTGGTAAGCAGTTCCTGCCCCGGCTCAGGGCC
AAGAACAGTTGGAACAGCAGAATATGGGCCAAACAGGATATCTGTGGTAAGCAGTTCCTGC
CCCGGCTCAGGGCCAAGAACAGATGGTCCCCAGATGCGGTCCCGCCCTCAGCAGTTTCTAG
AGAACCATCAGATGTTTCCAGGGTGCCCAAGGACCTGAAATGACCCTGTGCCTTATTTGAA
CTAACCAATCAGTTCGCTTCTCGCTTCTGTTGCGCGCTTCTGCTCCCCGAGCTCAATAAAAG
AGCCACAACCCCTCACTCGGCGCGCCAGTCTCCGATAGACTGCGTGCCTCCGGGGTACCC
GTATTCCAATAAAGCCTCTTGCTGTTTGCATCCGAATCGTGGACTCGCTGATCCTTGGGAG
GGTCTCTCAGATTGATTGACTGCCACCTCGGGGGTCTTTCATTCTCGAGAGCTTTGGCGT

AATCATGGTCATAGCTGTTTCCTGTGTGAAATTGTTATCCGCTCACAATTCCACACAACATAC
GAGCCGGAAGCATAAAGTGTAAGCCTGGGGTGCCTAATGAGTGAGCTAACTCACATTAAT
TGCGTTGCGCTCACTGCCCGCTTCCAGTCGGGAAACCTGTCGTGCCAGCTGCATTAATGAA
TCGGCCAACGCGCGGGGAGAGGCGGTTTGC GTATTGGGCGCTCTCCGCTTCCTCGCTCAC
TGA CTGCTGCGCTCGGTGTTCCGGCTGCGGCGAGCGGTATCAGCTCACTCAAAGGCGGTA
ATACGGTTATCCACAGAATCAGGGGATAACGCAGGAAAGAACATGTGAGCAAAGGCCAG
CAAAGGCCAGGAACCGTAAAAAGGCCGCGTTGCTGGCGTTTTTTCATAGGCTCCGCCCC
CTGACGAGCATCACAAAATCGACGCTCAAGTCAGAGGTGGCGAAACCCGACAGGACTAT
AAAGATAACCAGGCGTTTTCCCCTGGAAGCTCCCTCGTGCCTCTCCTGTTCCGACCCTGCCG
CTTACCGGATACCTGTCCGCCTTCTCCCTTCGGGAAGCGTGGCGCTTCTCAATGCTCACGC
TG TAGGTATCTCAGTTCGGTGTAGGTCGTTCCGCTCCAAGCTGGGCTGTGTGCACGAACCCCC
CGTTCAGCCCGACCGCTGCGCCTTATCCGGTAACTATCGTCTTGAGTCCAACCCGGTAAGAC
ACGACTTATCGCCACTGGCAGCAGCCACTGGTAACAGGATTAGCAGAGCGAGGTATGTAG
GCGGTGCTACAGAGTCTTGAAGTGGTGGCCTAACTACGGCTACACTAGAAGGACAGTATT
TGGTATCTGCGCTCTGCTGAAGCCAGTTACCTTCGGAAAAAGAGTTGGTAGCTCTTGATCCG
GCAAACAACCACCGCTGGTAGCGGTGGTTTTTTGTTTGCAAGCAGCAGATTACGCGCAG
AAAAAAGGATCTCAAGAAGATCCTTTGATCTTTTCTACGGGGTCTGACGCTCAGTGGAAC
GAAACTCACGTTAAGGGATTTTGGTCATGAGATTATCAAAAAGGATCTTCACCTAGATCCT
TTAAATTA AAAATGAAGTTTTAAATCAATCTAAAGTATATATGAGTAACTTGGTCTGACA
GTTACCAATGCTTAATCAGTGAGGCACCTATCTCAGCGATCTGTCTATTTTCGTTCCATCCATAG
TTGCCTGACTCCCCGTCGTGTAGATAACTACGATACGGGAGGGCTTACCATCTGGCCCCAGT
GCTGCAATGATACCGCGAGACCCACGCTCACCGGCTCCAGATTTATCAGCAATAAACCAGCC
AGCCGGAAGGGCCGAGCGCAGAAGTGGTCCTGCAACTTTATCCGCCTCCATCCAGTCTATT
AATTGTTGCCGGAAGCTAGAGTAAGTAGTTCGCCAGTTAATAGTTTGC GCAACGTTGTTG
CCATTGCTGCTGGCATCGTGGTGTACGCTCGTCGTTTGGTATGGCTTCATTCAGCTCCGGT
TCCCAACGATCAAGGCGAGTTACATGATCCCCATGTTGTGCAAAAAAGCGGTTAGCTCCTT
CGGTCTCCGATCGTTGTCAGAAGTAAGTTGGCCGAGTGTTATCACTCATGGTTATGGCAG
CACTGCATAATTCTTACTGTCATGCCATCCGTAAGATGCTTTTCTGTGACTGGTGAGTACT
CAACCAAGTCATTCTGAGAATAGTGTATGCGGCGACCGAGTTGCTCTTGCCCGGCGTCAAT
ACGGGATAATACCGCGCCACATAGCAGAACTTTAAAAGTGCTCATCATTGGAAAACGTTCTT
CGGGGCGAAA ACTCTCAAGGATCTTACCGCTGTTGAGATCCAGTTCGATGTAACCCACTCGT
GCACCCA ACTGATCTTCAGCATCTTTTACTTTACCAGCGTTTCTGGGTGAGCAAAAACAGG

AAGGCAAAATGCCGCAAAAAGGGAATAAGGGCGACACGGAAATGTTGAATACTCATACT
CTTCCTTTTTCAATATTATTGAAGCATTATCAGGGTTATTGTCTCATGAGCGGATACATATTT
GAATGTATTTAGAAAAATAACAAATAGGGGTTCCGCGCACATTTCCCCGAAAAGTGCCAC
CTGACGTCTAAGAAACCATTATTATCATGACATTAACCTATAAAAATAGGCGTATCACGAGG
CCCTTCGTCTTCAAGCTGCCTCGCGCTTTCGGTGATGACGGTGAAAACCTCTGACACATG
CAGTCCCGGAGACGGTCACAGCTTGTCTGTAAGCGGATGCCGGGAGCAGACAAGCCCGT
CAGGGCGCGTCAGCGGGTGTGGCGGGTGTGGGGCGCAGCCATGACCCAGTCACGTAGC
GATAGTTACTATGCGGCATCAGAGCAGATTGTAAGTACTGAGAGTGCACCATATGCGGTGTGAAA
TACCGCACAGATGCGTAAGGAGAAAATACCGCATCAGGCGCCATTCGCCATTCAGGCTGCG
CAACTGTTGGGAAGGGCGATCGGTGCGGGCCTCTTCGCTATTACGCCAGCTGGCGAAAGG
GGGATGTGCTGCAAGGCGATTAAGTTGGTAACGCCAGGGTTTTCCAGTCACGACGTTGT
AAAACGACGGCCAGTGAATTAGTACTCTAGCTTAAGTAAGCCATTTTGCAAGGCATGGAAA
AATACATAACTGAGAATAGAGAAGTTCAGATCAAGGTTAGGAACAGAGAGACAGGAGAAT
ATGGGCCAAACAGGATATCTGTGGTAAGCAGTTCCTGCCCGGCTCAGGGCCAAGAACAGT
TGGAACAGCAGAATATGGGCCAAACAGGATATCTGTGGTAAGCAGTTCCTGCCCGGCTCA
GGGCCAAGAACAGATGGTCCCCAGATGCGGTCCCGCCCTCAGCAGTTTCTAGAGAACCATC
AGATGTTTCCAGGGTGCCCCAAGGACCTGAAATGACCCTGTGCCTATTTGAACTAACCAAT
CAGTTCGCTTCTCGCTTCTGTTTCGCGCGCTTCTGCTCCCCGAGCTCAATAAAAGAGCCCACAA
CCCCTCACTCGGCGCGCCAGTCCCGATTGACTGCGTCGCCCCGGGTACCCGTATTCCCAAT
AAAGCCTCTTGCTGTTTGCATCCGAATCGTGGACTCGCTGATCCTTGGGAGGGTCTCCTCAG
ATTGATTGACTGCCACCTCGGGGGTCTTTCATTTGGAGGTTCCACCGAGATTTGGAGACCC
CTGCCAGGGACCACCGACCCCCCGCCGGGAGGTAAGCTGGCCAGCGGTCGTTTCGTGTC
TGCTCTGTCTTTGGGCGTGTTTGTGCCGGCATCTAATGTTTGCCTGCGTCTGTACTAGTT
GGCTAACTAGATCTGTATCTGGCGGTCCCGCGGAAGAACTGACGAGTTCGTATTCCCGGCC
GCAGCCCCTGGGAGACGTCCCAGCGGCCTCGGGGGCCCGTTTTGTGGCCATTCTGTATCA
GTTAACCTACCCGAGTCGGACTTTTTGGAGCTCCGCCACTGTCCGAGGGGTACGTGGCTTTG
TTGGGGGACGAGAGACAGAGACACTTCCCGCCCCGTCTGAATTTTTGCTTTCGGTTTTACG
CCGAAACCGCGCCGCGCTTGTCTGCTGC

pMP71-TRP2-mLAP-L-selectin

AGCATCGTTCTGTGTTGTCTCTGTCTGACTGTGTTTCTGTATTTGTCTGAAAATTAGCTCGAC
AAAGTTAAGTAATAGTCCCTCTCTCCAAGCTCACTTACAGGCGGCCGCATGGCCCCGCGGCT

GCTGTGCTACACCGTGCTGTGCCTGCTGGGCGCCAGAATCCTGAACAGCAAGGTGATCCAG
ACCCCAGATACCTGGTGAAGGGCCAGGGCCAGAAAGCCAAGATGAGATGCATCCCCGAG
AAGGGCCACCCCGTGGTGTCTGGTATCAGCAGAACAAGAACAACGAGTTCAAGTTCCTGA
TCAACTTCCAGAACCAGGAAGTGCTGCAGCAGATCGACATGACCGAGAAGAGGTTTCAGCG
CCGAGTGCCCCAGCAACAGCCCCTGCAGCCTGGAAATCCAGAGCAGCGAGGCCGGCGACA
GCGCCCTGTACCTGTGCGCCAGCAGCCTGACAGGCGGCGAGCAGTACTTCGGCCCTGGCAC
CAGGCTGACCGTGCTCGAGGACCTGAGGAACGTGACCCCCCAAGGTGTCCCTGTTTCGAG
CCCAGCAAGGCCGAGATCGCCAACAAGCAGAAGGCCACCCTGGTGTGCCTGGCCAGGGGC
TTCTTCCCCGACCACGTGGAGCTGTCTTGGTGGGTGAACGGCAAGGAGGTGCACAGCGGC
GTGTGCACCGACCCCCAGGCCTACAAGGAGAGCAACTACAGCTACTGCCTGAGCAGCAGGC
TGAGAGTGAGCGCCACCTTCTGGCACAACCCCAGGAACCACTTCCGCTGTCAGGTGCAGTT
CCACGGCCTGAGCGAGGAGGACAAGTGGCCCCAGGGCAGCCCCAAGCCCGTGACCCAGAA
CATCAGCGCCGAGGCCTGGGGCAGAGCCGACTGCGGCATCACCAGCGCCAGCTACCACCA
GGGCGTGCTGTCCGCCACCATCCTGTACGAGATCCTGCTGGGCAAGGCCACACTGTACGCC
GTGCTGGTGTCCGGCCTGGTGTGCTGATGGCCATGGTGAAGAAGAAGAACAGCAGCGGCAGC
GGCGCCACCAACTTCAGCCTGCTGAAGCAGGCCGGCGACGTGGAGGAAAACCCTGGGCCC
ATGAGGCCCGTGACCTGCAGCGTGCTGGTGTGCTGCTGATGCTGCGGAGAAGCAACGGC
GACGGCGACAGCGTGACCCAGACCGAGGGCCTGGTGACCCTGACAGAGGGACTGCCCGTG
ATGCTGAACTGCACCTACCAGACCATCTACAGCAACCCCTTCTGTTTTGGTACGTGCAGCA
CCTGAACGAGAGCCCCAGACTGCTGCTGAAGAGCTTCACCGACAACAAGAGGACCGAGCA
CCAGGGCTTCCACGCCACCCTGCACAAGAGCAGCAGCAGCTTCCACCTGCAAAAGTCCAGC
GCCAGCTGTCCGACAGCGCCCTGTACTACTGCGCCCTGAGGGGCAGCAACAACAGGATCT
TCTTCGGCGACGGCACCCAGCTGGTCGTGAAGCCCGACATCCAGAACCCCGAGCCCGCCGT
GTACCAGCTGAAGGACCCCAGAAGCCAGGACAGCACCTGTGCCTGTTACCGACTTCGAC
AGCCAGATCAACGTGCCAAGACCATGGAGAGCGGCACCTTCATCACCGACAAGTGCGTGC
TGGACATGAAGGCCATGGACAGCAAGAGCAACGGCGCCATCGCCTGGTCCAACCAGACCA
GCTTCACATGCCAGGACATCTTCAAGGAGACCAACGCCACCTACCCCAGCAGCGACGTGCC
CTGCGACGCCACCCTGACCGAGAAGAGCTTCGAGACCGACATGAACCTGAACTTCCAGAAC
CTGAGCGTGATGGGCCTGAGAATCCTGCTGCTGAAGGTGGCCGGCTTCAACCTGCTGATGA
CCCTGAGGCTGTGGAGCAGCTGAGTCGACACGCGTACGTGCGGACCGCGGACATGTACAG
AGCTCGAGCGGGATCAATTCCGCCCCCCCCCTAACGTTACTGGCCGAAGCCGCTTGAATA
AGGCCGGTGTGCGTTTTGTCTATATGTTATTTTCCACCATATTGCCGTCTTTGGCAATGTGAG

GGCCCGAAACCTGGCCCTGTCTTCTTGACGAGCATTCTAGGGGTCTTCCCTCTCGCCA
AAGGAATGCAAGGTCTGTTGAATGTCGTGAAGGAAGCAGTTCCTCTGGAAGCTTCTGAAG
ACAAACAACGTCTGTAGCGACCCTTTCAGGCAGCGGAACCCCCACCTGGCGACAGGTGC
CTCTGCGGCCAAAAGCCACGTGTATAAGATACACCTGCAAAGGCGGCACAACCCAGTGCC
ACGTTGTGAGTTGGATAGTTGTGGAAAGAGTCAAATGGCTCTCCTCAAGCGTATTCAACAA
GGGGCTGAAGGATGCCAGAAGGTACCCATTGTATGGGATCTGATCTGGGGCCTCGGTG
CACATGCTTTACATGTGTTTAGTCGAGGTTAAAAACGTCTAGGCCCCCGAACCACGGGG
ACGTGGTTTTCTTTGAAAAACACGATAATAATGCCACCATGCCATCTCCTCTCCCTGTCTCC
TTCCTCCTCTTTCTTACCTTAGTAGGAGGCAGGCCCCAGAAGTCCTTACTGGTGGAGGTAGA
AGAGGGAGGCAATGTTGTGCTGCCATGCCTCCCGACTCCTCACCTGTCTCTTCTGAGAAGC
TGGCTTGGTATCGAGGTAACCAGTCAACACCCTTCTGGAGCTGAGCCCCGGGTCCCCTGG
CCTGGGATTGCACGTGGGGTCCCTGGGCATCTTGCTAGTGATTGTCAATGTCTCAGACCATA
TGGGGGGCTTCTACCTGTGCCAGAAGAGGCCCCCTTCAAGGACATCTGGCAGCCTGCCTG
GACAGTGAACGTGGAGGATAGTGGGGAGATGTTCCGGTGAATGCTTCAGACGTCAGGGA
CCTGGACTGTGACCTAAGGAACAGGTCCTCTGGGAGCCACAGGTCCACTTCTGGTTCCCAG
CTGTATGTGTGGGCTAAAGACCATCCTAAGGTCTGGGGAACAAAGCCTGTATGTGCCCTC
GGGGGAGCAGTTTGAATCAGAGTCTAATCAACCAAGACCTCACTGTGGCACCCGGCTCCAC
ACTTTGGCTGTCTGTGGGGTACCCCTGTCCCAGTGGCCAAAGGCTCCATCTCCTGGACCC
ATGTGCATCCTAGGAGACCTAATGTTTCACTACTGAGCCTAAGCCTTGGGGGAGAGCACCC
GGTCAGAGAGATGTGGGTTTGGGGTCTCTTCTGCTTCTGCCCAAGCCACAGCTTTAGAT
GAAGGCACCTATTATTGTCTCCGAGGAAACCTGACCATCGAGAGGCACGTGAAGGTCATTG
CAAGGTCAGCAGTGTGGCTCTGGCTGTTGAGAACTGGTGGATGGATAGTCCCAGTGGTGA
CTTTAGTATATGTCATCTTCTGTATGGTTTCTCTGGTGGCTTTTCTCTATTGTCAAAGAGCCTT
TATCCTGAGAAGGAAAAGGAAGCGAATGACTGACCCCGCCAGGAGATTCTTCAAAGTGAC
GGGCAGCGGCGAAGGCCGCGCAGCCTGCTGACCTGCGGCGATGTGGAAGAAAACCTG
GCCCGATGGTGTTTCCATGGAGATGTGAGGGTACTTACTGGGGCTCGAGGAACATCCTGAA
GCTGTGGGTCTGGACACTGCTCTGTTGTGACTTCTGATACACCATGGAACACTGTTGGA
CTTACCATTATTCTGAAAAGCCCATGAACTGGGAAAATGCTAGAAAATTCTGCAAGCAAAAT
TACACAGATTTAGTCGCCATACAAAACAAGAGAGAAATTGAGTATTTAGAGAATACATTGC
CCAAAAGCCCTTATTACTACTGGATAGGAATCAGGAAAATTGGGAAAATGTGGACATGGGT
GGGAACCAACAAAACCTCTCACTAAAGAAGCAGAGAACTGGGGTGTGGGGAGCCCAACAA
CAAGAAGTCCAAGGAGGACTGTGTGGAGATCTATATCAAGAGGGAACGAGACTCTGGGAA

ATGGAACGATGACGCCTGTCACAAACGAAAGGCAGCTCTCTGCTACACAGCCTCTTGCCAG
CCAGGGTCTTGCAATGGCCGTGGAGAATGTGTGGAACTATCAACAATCACACGTGCATAT
GTGATGAAGGGTATTACGGGCCCCAGTGTCAAGTATGTGGTCCAGTGTGAGCCTTTGGAGGC
CCCTGAGTTGGGTACCATGGACTGCATCCACCCCTTGGGAACTTCAGCTTCCAGTCCAAGT
GTGCTTTCAACTGTTCTGAGGGAAGAGAGCTACTTGGGACTGCAGAAACACAGTGTGGAGC
ATCTGGAACTGGTCATCTCCAGAGCCAATCTGCCAAGTGGTCCAGTGTGAGCCTTTGGAG
GCCCTGAGTTGGGTACCATGGACTGCATCCACCCCTTGGGAACTTCAGCTTCCAGTCCAA
GTGTGCTTTCAACTGTTCTGAGGGAAGAGAGCTACTTGGGACTGCAGAAACACAGTGTGGC
GCCTCAGGAACTGGTCATCTCCGGAGCCAATCTGCCAAGCAGGGACACTGACAATCCAGG
AAGTCCCCTCTTCATTCTGTAGCCGTCATGGTCACCGCATTCTCGGGGCTGGCATTCTCA
TTTGGCTGGCAAGGCGGTTAAAAAAGGCAAGAAATCTCAAGAAAGGATGGATGATCCAT
ACTAA

TCCGGATTAGTCCAATTTGTTAAAGACAGGATATCAGTGGTCCAGGCTCTAGTTTTG
ACTCAACAATATCACCAGCTGAAGCCTATAGAGTGAATTCGGATCCAAGCTTAGGCCTGCTC
GCTTTCTTGCTGTCCCATTTCTATTAAGGTTCTTTGTTCCCTAAGTCCAACTACTAACTGG
GGATATTATGAAGGGCCTTGAGCATCTGGATTCTGCCTAGCGCTAAGCTTCTAACACGA
GCCATAGATAGAATAAAAGATTTTATTTAGTCTCCAGAAAAAGGGGGGAATGAAAGACCCC
ACCTGTAGGTTTGGCAAGCTAGCTTAAGTAAGCCATTTTGAAGGCATGGAAAAATACATA
ACTGAGAATAGAGAAGTTCAGATCAAGGTTAGGAACAGAGAGACAGGAGAATATGGGCCA
AACAGGATATCTGTGGTAAGCAGTTCCTGCCCGGCTCAGGGCCAAGAACAGTTGGAACAG
CAGAATATGGGCCAAACAGGATATCTGTGGTAAGCAGTTCCTGCCCGGCTCAGGGCCAAG
AACAGATGGTCCCAGATGCGGTCCCGCCCTCAGCAGTTTCTAGAGAACCATCAGATGTTTC
CAGGGTGCCCAAGGACCTGAAATGACCCTGTGCCTTATTTGAACTAACCAATCAGTTCGCT
TCTCGCTTCTGTTGCGCGCTTCTGCTCCCCGAGCTCAATAAAAGAGCCCACAACCCCTCACT
CGGCGCGCCAGTCTCCGATAGACTGCGTGCCTCGGGGTACCCGTATTCCCAATAAAGCCT
CTTGCTGTTTGCATCCGAATCGTGGACTCGCTGATCCTTGGGAGGGTCTCCTCAGATTGATT
GACTGCCACCTCGGGGTCTTTATTCTCGAGAGCTTTGGCGTAATCATGGTCATAGCTGT
TTCCTGTGTGAAATTGTTATCCGCTCACAATCCACACAACATACGAGCCGGAAGCATAAAG
TGTAAGCCTGGGGTGCCTAATGAGTGAGCTAACTCACATTAATTGCGTTGCGCTCACTGCC
CGCTTTCCAGTCGGGAAACCTGTCGTGCCAGCTGCATTAATGAATCGGCCAACGCGCGGGG
AGAGGCGGTTTTCGTATTGGGCGCTTCCGCTTCTCGCTCACTGACTCGCTGCGCTCGGT
CGTTCGGCTGCGGCGAGCGGTATCAGCTCACTCAAAGGCGGTAATACGGTTATCCACAGAA
TCAGGGGATAACGCAGGAAAGAACATGTGAGCAAAAGGCCAGCAAAAGGCCAGGAACCG

TAAAAAGCCGCGTTGCTGGCGTTTTTCCATAGGCTCCGCCCCCTGACGAGCATCACAAAA
ATCGACGCTCAAGTCAGAGGTGGCGAAACCCGACAGGACTATAAAGATAACCAGGCGTTTCC
CCCTGGAAGCTCCCTCGTGGCTCTCTGTTCCGACCCTGCCGTTACCGGATACCTGTCCGC
CTTTCTCCCTTCGGGAAGCGTGGCGTTTTCTCAATGCTCACGCTGTAGGTATCTCAGTTCGGT
GTAGGTCGTTGCTCCAAGCTGGGCTGTGTGCACGAACCCCCGTTACGCCGACCGCTGC
GCCTTATCCGGTAACTATCGTCTTGAGTCCAACCCGGTAAGACACGACTTATCGCCACTGGC
AGCAGCCACTGGTAACAGGATTAGCAGAGCGAGGTATGTAGGCGGTGCTACAGAGTTCCT
GAAGTGGTGGCCTAACTACGGCTACACTAGAAGGACAGTATTTGGTATCTGCGCTCTGCTG
AAGCCAGTTACCTTCGGAAAAAGAGTTGGTAGCTCTTGATCCGGCAAACAAACCACCGCTG
GTAGCGGTGGTTTTTTTTGTTTGCAAGCAGCAGATTACGCGCAGAAAAAAGGATCTCAAGA
AGATCCTTTGATCTTTTCTACGGGGTCTGACGCTCAGTGAACGAAAACCTCACGTTAAGGGA
TTTTGGTCATGAGATTATCAAAAAGGATCTTCACCTAGATCCTTTTAAATTAATAAATGAAGTT
TTAAATCAATCTAAAGTATATATGAGTAACTTGGTCTGACAGTTACCAATGCTTAATCAGT
GAGGCACCTATCTCAGCGATCTGTCTATTTTCGTTCCATAGTTGCCTGACTCCCCGTCGTG
TAGATAACTACGATACGGGAGGGCTTACCATCTGGCCCCAGTGCTGCAATGATACCGCGAG
ACCCACGCTCACCGGCTCCAGATTTATCAGCAATAAACCAGCCAGCCGGAAGGGCCGAGCG
CAGAAGTGGTCCCTGCAACTTTATCCGCCTCCATCCAGTCTATTAATTGTTGCCGGGAAGCTA
GAGTAAGTAGTTCGCCAGTTAATAGTTTGCGCAACGTTGTTGCCATTGCTGCTGGCATCGTG
GTGTCACGCTCGTCGTTTGGTATGGCTTCATTCAGCTCCGGTCCCAACGATCAAGGCGAGT
TACATGATCCCCATGTTGTGCAAAAAGCGGTTAGCTCCTTCGGTCCCTCCGATCGTTGTCA
GAAGTAAGTTGGCCGAGTGTTATCACTCATGGTTATGGCAGCACTGCATAATTCTTACT
GTCATGCCATCCGTAAGATGCTTTTCTGTGACTGGTGAGTACTCAACCAAGTCATTCTGAGA
ATAGTGTATGCGGCGACCGAGTTGCTCTTGCCCGCGTCAATACGGGATAATACCGCGCCA
CATAGCAGAACTTTAAAAGTGCTCATCATTGGAAAACGTTCTTCGGGGCGAAAACCTCTCAAG
GATCTTACCGCTGTTGAGATCCAGTTCGATGTAACCCACTCGTGCACCCAAGTATCTTCAG
CATCTTTTACTTTCACCAGCGTTTCTGGGTGAGCAAAAACAGGAAGGCAAAATGCCGCAAA
AAAGGGAATAAGGGCGACACGGAAATGTTGAATACTCATACTCTTCTTTTTCAATATTATT
GAAGCATTTATCAGGGTTATTGTCTCATGAGCGGATACATATTTGAATGTATTTAGAAAAAT
AAACAAATAGGGTTCCGCGCACATTTCCCCGAAAAGTGCCACCTGACGTCTAAGAAACCA
TTATTATCATGACATTAACCTATAAAAATAGGCGTATCACGAGGCCCTTTCGTCTTCAAGCTG
CCTCGCGCGTTTCGGTGTGACGGTGAAAACCTCTGACACATGCAGTCCCGGAGACGGTC
ACAGCTTGTCTGTAAGCGGATGCCGGGAGCAGACAAGCCCGTCAGGGCGCGTCAGCGGGT

GTTGGCGGGTGTCTGGGGCGCAGCCATGACCCAGTCACGTAGCGATAGTTACTATGCGGCAT
CAGAGCAGATTGTAAGTACTGAGAGTGCACCATATGCGGGTGTGAAATACCGCACAGATGCGTAAG
GAGAAAATACCGCATCAGGCGCCATTCGCCATTCAGGCTGCGCAACTGTTGGGAAGGGCG
ATCGGTGCGGGCCTCTTCGCTATTACGCCAGCTGGCGAAAGGGGGATGTGCTGCAAGGCG
ATTAAGTTGGGTAACGCCAGGGTTTTCCAGTCACGACGTTGTAAAACGACGGCCAGTGAA
TTAGTACTCTAGCTTAAGTAAGCCATTTTGAAGGCATGGAAAAATACATAACTGAGAATAG
AGAAGTTCAGATCAAGGTTAGGAACAGAGAGACAGGAGAATATGGGCCAAACAGGATATC
TGTGGTAAGCAGTTCCTGCCCGGCTCAGGGCCAAGAACAGTTGGAACAGCAGAATATGG
GCCAAACAGGATATCTGTGGTAAGCAGTTCCTGCCCGGCTCAGGGCCAAGAACAGATGGT
CCCCAGATGCGGTCCCGCCCTCAGCAGTTTCTAGAGAACCATCAGATGTTTCCAGGGTGCC
CAAGGACCTGAAATGACCCTGTGCCTTATTTGAACTAACCAATCAGTTCGCTTCTCGCTTCTG
TTCGCGCGCTTCTGCTCCCCGAGCTCAATAAAAGAGCCCACAACCCCTCACTCGGCGCGCCA
GTCCTCCGATTGACTGCGTCGCCCGGGTACCCGTATTCCAATAAAGCCTCTTGCTGTTTGCA
TCCGAATCGTGGACTCGCTGATCCTTGGGAGGGTCTCCTCAGATTGATTGACTGCCACCTC
GGGGTCTTTCATTTGGAGGTTCCACCGAGATTTGGAGACCCCTGCCAGGGACCACCGAC
CCCCCGCCGGGAGGTAAGCTGGCCAGCGGTCGTTTCGTGTCTGTCTCTGTCTTTGGGCGT
GTTTGTGCCGGCATCTAATGTTTGCCTGCGTCTGTAAGTGGCTAACTAGATCTGTATC
TGCGGGTCCCGCGGAAGAAGTACGAGTTCGTATTCCCGGCCGAGCCCCTGGGAGACGTC
CCAGCGGCCTCGGGGGCCCGTTTTGTGGCCATTCTGTATCAGTTAACCTACCCGAGTCGGA
CTTTTTGGAGCTCCGCCACTGTCCGAGGGGTACGTGGCTTTGTTGGGGGACGAGAGACAGA
GACTTCCCGCCCCGTCTGAATTTTTGCTTTCGGTTTTACGCCGAAACCGCGCCGCGCGTC
TTGTCTGCTGC

